

# **Investigating the role of the CCL2/CCR2 axis in monocytes and its modulation by extracellular nucleotides**

---

Hinnah Campwala

A Thesis Presented for the Degree of  
Doctor of Philosophy at the University of East Anglia

Faculty of Science, School of Biological Sciences

**March 2015**



© This copy of the thesis has been supplied on condition that anyone who consults it is understood to recognise that its copyright rests with the author and that use of any information derived there from must be in accordance with current UK Copyright Law. In addition, any quotation or extract must include full attribution.

*In the name of God, the most Beneficent, the most Merciful*

## **Declaration**

I hereby declare that the work in this thesis is my own work and has not been previously submitted for any other degree at this or any other university or institution. Where other sources of information have been used, they have been reference and acknowledged.

This thesis contains approximately 99,900 words excluding appendices.

The work in this thesis has previously appeared in the publication below. All of the main figures (Fig. 1 to Fig. 6) are directly attributable to myself and appear in Chapters 4, 5, and 6. Supplementary figure (Fig. S1) is directly attributable to Darren Sexton.

Campwala, H, Sexton, DW, Crossman, DC & Fountain, SJ (2014). P2Y(6) receptor inhibition perturbs CCL2-evoked signalling in human monocytic and peripheral blood mononuclear cells. *J Cell Sci*, **127**, 4964-73.

# Abstract

---

The chemokine CCL2 activates its cognate receptor CCR2 to orchestrate monocyte trafficking towards infected, inflamed, and injured tissues during immune responses and the development of inflammatory disease. However, despite research into this area being plentiful, CCR2 antagonists have lacked clinical efficacy. A possible explanation for this may be that other chemoattractants such as extracellular nucleotides steer monocyte trafficking and compensate for a loss in CCR2 function. This study therefore intended to (i) determine the mechanisms involved in CCL2/CCR2-mediated monocyte signalling and function and (ii), examine the requirement of purinoceptor signalling for CCL2/CCR2-mediated monocyte signalling and function. Human monocytic THP-1 cells and PBMCs were employed as models to assess CCR2 activation indirectly by intracellular  $Ca^{2+}$  release, cell migration, and cell adhesion to vascular endothelium. Techniques such as *lentivirus*-mediated gene-knockdown, RT-PCR, and HPLC complemented these studies. A pharmacological approach indicated a requirement of CCR2,  $Ca^{2+}$ ,  $G\alpha_{i/o}$ -type G-proteins, PI3K, PLC,  $IP_3$ Rs, RyRs, SERCA, DAGL, DAGK, and PKC for CCL2-mediated monocyte signalling and/or function. Initial observations from apyrase studies indicated an involvement of extracellular nucleotides in CCL2/CCR2-mediated monocyte signalling and function. Pharmacological experiments also indicated that although P1, P2X1, P2X4, P2X7, P2Y<sub>1</sub>, P2Y<sub>11</sub>, P2Y<sub>12</sub>, and P2Y<sub>13</sub> purinoceptors were unlikely to play a major role, P2Y<sub>6</sub> and CCR2 engaged in crosstalk. Cross-desensitisation experiments and studies on *P2RY6*-knockdown THP-1 cells supported this finding and indicated that a blockade of P2Y<sub>6</sub> signalling was likely to affect the capacity of monocytes to migrate and adhere in response to CCL2. Moreover, these findings indicated that P2Y<sub>6</sub> and CCR2 crosstalk in monocytes was likely to involve ATP release. The findings in this thesis suggest that the CCL2/CCR2 axis is important for monocyte signalling and function and that P2Y<sub>6</sub> engages in crosstalk with CCR2. Taken together, these findings may prove relevant in the search for future therapies for monocyte-associated inflammatory diseases.

# Table of Contents

---

<b>ABSTRACT</b> .....	<b>4</b>
<b>TABLE OF CONTENTS</b> .....	<b>5</b>
<b>LIST OF FIGURES</b> .....	<b>11</b>
<b>LIST OF TABLES</b> .....	<b>15</b>
<b>ABBREVIATIONS</b> .....	<b>17</b>
<b>PAPERS AND CONFERENCE ABSTRACTS</b> .....	<b>20</b>
<b>ACKNOWLEDGEMENTS</b> .....	<b>21</b>
<b>CHAPTER 1: INTRODUCTION</b> .....	<b>22</b>
<b>1.1 The immune system</b> .....	<b>22</b>
<b>1.2 Monocytes</b> .....	<b>22</b>
1.2.1 Human and mouse monocyte heterogeneity.....	22
1.2.2 Monocyte origins .....	24
1.2.3 Monocyte functions.....	25
1.2.3.1 Recruitment during infection and inflammation.....	25
1.2.3.1.1 Bone marrow egression.....	25
1.2.3.1.2 Sensing of warning signals .....	25
1.2.3.1.3 Trafficking and adhesion.....	25
1.2.3.1.4 Transmigration/Diapedesis .....	26
1.2.3.1.5 Phagocytosis .....	27
1.2.3.2 Precursors for mononuclear phagocytes .....	27
1.2.3.3 Patrolling.....	28
1.2.4 Involvement in sterile inflammation.....	28
<b>1.3 G-protein-coupled receptors (GPCRs)</b> .....	<b>29</b>
1.3.1 General overview.....	29
1.3.2 GPCR structure .....	30
1.3.3 G-protein cycle .....	30
1.3.4 Heterotrimeric G-protein effectors.....	32
1.3.4.1 Main effectors of G $\alpha$ and G $\beta\gamma$ subunits .....	32
1.3.4.1.1 Adenylate cyclase (AC) .....	32
1.3.4.1.2 Phospholipase C (PLC) .....	33
1.3.4.1.3 Phosphoinositide-3-kinases (PI3Ks) .....	34
1.3.5 Regulation of GPCR signalling .....	35
1.3.5.1 Receptor expression and trafficking .....	35
1.3.5.2 Receptor desensitisation.....	35
1.3.5.3 Receptor internalisation/endocytosis.....	36
<b>1.4 Calcium (Ca<sup>2+</sup>) signalling</b> .....	<b>37</b>
1.4.1 General overview.....	37
1.4.2 ON mechanisms.....	38
1.4.2.1 Channel-mediated Ca <sup>2+</sup> influx and release .....	38
1.4.2.2 Store-mediated Ca <sup>2+</sup> release .....	39
1.4.2.3 Ca <sup>2+</sup> -binding proteins/Ca <sup>2+</sup> buffers.....	40
1.4.3 OFF mechanisms .....	40
1.4.3.1 Ca <sup>2+</sup> pumps and exchangers.....	40

<b>1.5</b>	<b>Chemokines</b> .....	<b>41</b>
1.5.1	General overview.....	41
1.5.2	Chemokine receptors and ligand pairings .....	42
<b>1.6</b>	<b>Chemokine (CC-motif) receptor 2 (CCR2)</b> .....	<b>43</b>
1.6.1	General overview and structure .....	43
1.6.2	Homo- and heterodimerisation.....	45
1.6.3	Ligands.....	45
1.6.4	Signalling and involvement in monocyte function.....	45
1.6.5	Involvement in human monocyte pathologies .....	46
<b>1.7</b>	<b>Purinoreceptor Signalling</b> .....	<b>47</b>
1.7.1	General overview.....	47
1.7.2	Purinoreceptors .....	48
1.7.2.1	P1 .....	48
1.7.2.2	P2X.....	48
1.7.2.3	P2Y.....	49
1.7.2.4	Ligands for purinoreceptors.....	50
1.7.2.5	Distribution in immune cells and monocytes.....	50
1.7.5	ATP release.....	52
1.7.6	Ecto-nucleotidases .....	52
1.7.7	Involvement in monocyte function.....	53
1.7.8	Involvement in human monocyte pathologies .....	54
<b>1.8</b>	<b>Aims and project outline</b> .....	<b>57</b>
<b>CHAPTER 2: MATERIALS AND METHODS</b> .....		<b>59</b>
<b>2.1</b>	<b>Materials and reagents</b> .....	<b>59</b>
<b>2.2</b>	<b>Cell culture</b> .....	<b>61</b>
2.2.1	Description of cell lines and passage.....	61
2.2.1.1	THP-1 cells .....	61
2.2.1.2	1321N1 cells .....	62
2.2.1.3	HUVEC cells .....	63
2.2.1.4	HEK293T cells.....	64
<b>2.3</b>	<b>Primary Cell Isolation</b> .....	<b>64</b>
2.3.1	Collection of human peripheral blood and isolation of PBMCs .....	64
2.3.2	Isolation of monocytes and monocyte-depleted PBMCs .....	65
<b>2.4</b>	<b>Reverse transcription-polymerase chain reaction (RT-PCR)</b> .....	<b>65</b>
2.4.1	Total RNA extraction .....	65
2.4.2	Total RNA quantification .....	66
2.4.3	First strand complementary DNA synthesis .....	66
2.4.4	Primer design and preparation.....	67
2.4.5	Polymerase chain reaction (PCR).....	70
2.4.6	Agarose gel electrophoresis .....	71
<b>2.5</b>	<b>Generation of P2Y<sub>6</sub>-knockdown THP-1 cells</b> .....	<b>71</b>
2.5.1	Preparation of plasmid DNA for transfection .....	72
2.5.2	Lentivirus production in HEK293T.....	73
2.5.3	Generation of P2Y <sub>6</sub> -KD cells using lentiviral transduction particles .....	74
2.5.4	Puromycin kill curve.....	75
2.5.5	THP-1 cell transduction and puromycin selection .....	76
2.5.6	Quantitative real-time PCR (qRT-PCR) .....	77
<b>2.6</b>	<b>Calcium mobilisation</b> .....	<b>77</b>

2.6.1	Intracellular Ca <sup>2+</sup> measurements (with extracellular Ca <sup>2+</sup> ) .....	79
2.6.2	Intracellular Ca <sup>2+</sup> measurements (without extracellular Ca <sup>2+</sup> ) .....	79
2.6.3	Intracellular Ca <sup>2+</sup> measurements on Fura-2 AM-loaded 1321N1 cells.....	80
<b>2.7</b>	<b>Transwell chemotaxis assay.....</b>	<b>80</b>
<b>2.8</b>	<b>HUVEC adhesion assay .....</b>	<b>81</b>
<b>2.9</b>	<b>ATP/β-hexosaminidase release studies.....</b>	<b>83</b>
2.9.1	Extracellular nucleotide detection by ion-pair reverse-phase HPLC .....	83
2.9.2	ATP detection by luciferase-luciferin.....	84
2.10	β-hexosaminidase release.....	84
<b>2.11</b>	<b>Nucleotide hydrolysis studies .....</b>	<b>85</b>
2.11.1	Apyrase studies .....	85
2.11.2	THP-1 cell studies .....	85
<b>2.12</b>	<b>THP-1 cell viability assays .....</b>	<b>86</b>
2.12.1	Trypan blue exclusion assay.....	86
2.12.2	Lactate dehydrogenase (LDH) assay.....	86
<b>2.13</b>	<b>Statistical analysis.....</b>	<b>87</b>
<b>CHAPTER 3: COMPARISON OF MRNA EXPRESSION OF MONOCYTE MARKERS, CC CHEMOKINES, CC CHEMOKINE RECEPTORS AND PURINOCEPTORS IN THP-1 CELLS AND HUMAN MONOCYTES .....</b>		<b>88</b>
<b>3.1</b>	<b>Introduction .....</b>	<b>88</b>
<b>3.2</b>	<b>Aims .....</b>	<b>89</b>
<b>3.3</b>	<b>Results .....</b>	<b>89</b>
3.3.1	RT-PCR analysis of monocyte and myeloid markers .....	89
3.3.2	RT-PCR analysis of CC chemokines .....	92
3.3.3	RT-PCR analysis of CC chemokine receptors .....	94
3.3.4	RT-PCR analysis of P1 purinoceptors .....	99
3.3.5	RT-PCR analysis of P2X purinoceptors .....	102
3.3.6	RT-PCR analysis of P2Y purinoceptors .....	107
<b>3.4</b>	<b>Summary.....</b>	<b>111</b>
<b>CHAPTER 4: MECHANISMS INVOLVED IN CCL2/CCR2-MEDIATED MONOCYTE SIGNALLING AND FUNCTION.....</b>		<b>112</b>
<b>4.1</b>	<b>Introduction .....</b>	<b>112</b>
<b>4.2</b>	<b>Aims .....</b>	<b>113</b>
<b>4.3</b>	<b>Results .....</b>	<b>114</b>
4.3.1	CCL2-evoked Ca <sup>2+</sup> responses in THP-1 cells and human PBMCs.....	114
4.3.2	Effect of Ca <sup>2+</sup> removal on CCL2-mediated THP-1 cell signalling and function.....	116
4.3.2.1	Effect Ca <sup>2+</sup> removal on CCL2-evoked Ca <sup>2+</sup> responses in THP-1 cells ...	116
4.3.2.2	Effect of BAPTA-AM on CCL2-mediated THP-1 cell chemotaxis.....	118
4.3.3	Effect of CCR2 antagonism on CCL2-mediated THP-1 cell signalling and function.....	120
4.3.3.1	Effect of BMS-CCR2-22 on CCL2- and CCL5-evoked Ca <sup>2+</sup> responses in THP-1 cells.....	120

4.3.3.2	Effect of BMS-CCR2-22 on CCL2-mediated THP-1 cell chemotaxis and adhesion.....	124
4.3.4	Effect of $G\alpha_{i/o}$ inhibition on CCL2/CCR2-mediated THP-1 cell signalling and function.....	128
4.3.4.1	Effect of PTx on CCL2-, ATP- and ADP-evoked $Ca^{2+}$ responses in THP-1 cells .....	128
4.3.4.2	Effect of PTx on CCL2-mediated THP-1 cell chemotaxis .....	130
4.3.5	Effect of $G\beta\gamma$ inhibition on CCL2-mediated THP-1 cell chemotaxis .....	132
4.3.6	Effect of PI3K inhibition on CCL2/CCR2-mediated THP-1 cell signalling and function.....	134
4.3.6.1	Effect of LY-294002 on CCL2-evoked $Ca^{2+}$ responses in THP-1 cells... ..	134
4.3.6.2	Effect of LY-294002 on CCL2-mediated THP-1 cell chemotaxis .....	135
4.3.7	Effect of PLC inhibition on CCL2/CCR2-mediated THP-1 cell signalling and function.....	137
4.3.7.1	Effect of U-73122 on CCL2-evoked $Ca^{2+}$ responses in THP-1 cells .....	137
4.3.7.2	Effect of U-73122 on CCL2-mediated THP-1 cell chemotaxis .....	138
4.3.8	Effect of $IP_3R$ inhibition on CCL2/CCR2-mediated THP-1 cell signalling and function.....	140
4.3.8.1	Effect of XeC on CCL2-evoked $Ca^{2+}$ responses in THP-1 cells .....	140
4.3.8.2	Effect of XeC on CCL2-mediated THP-1 cell chemotaxis.....	141
4.3.9	Effect of RyR inhibition on CCL2/CCR2-mediated THP-1 cell signalling and function.....	144
4.3.9.1	Effect of dantrolene on CCL2-evoked $Ca^{2+}$ responses in THP-1 cells ...	144
4.3.9.2	Effect of dantrolene on CCL2-mediated THP-1 cell chemotaxis .....	145
4.3.10	Effect of SERCA inhibition on CCL2/CCR2-mediated THP-1 cell signalling and function .....	145
4.3.10.1	Effect of thapsigargin on CCL2-evoked $Ca^{2+}$ responses in THP-1 cells .....	146
4.3.10.2	Effect of thapsigargin on CCL2-mediated THP-1 cell chemotaxis .....	149
4.3.11	Effect of SOCE inhibition on CCL2/CCR2-associated THP-1 cell signalling and function .....	151
4.3.11.1	Effect of SKF-96365 on CCL2-evoked $Ca^{2+}$ responses in THP-1 cells ..	151
4.3.12	Effect of inhibiting DAG metabolism on CCL2/CCR2-mediated THP-1 cell signalling and function.....	154
4.3.12.1	Effect of RHC-80267 on CCL2-evoked $Ca^{2+}$ responses in THP-1 cells .....	154
4.3.12.2	Effect of RHC-80267 on CCL2-mediated THP-1 cell chemotaxis.....	155
4.3.12.3	Effect of R-59-022 on CCL2-evoked $Ca^{2+}$ responses in THP-1 cells..	158
4.3.12.4	Effect of R-59-022 on UDP-evoked $Ca^{2+}$ responses in THP-1 cells ...	159
4.3.12.5	Effect of R-59-022 on CCL2-mediated THP-1 cell chemotaxis.....	159
4.3.13	Effect of PKC inhibition on CCL2/CCR2-mediated THP-1 cell signalling and function.....	164
4.3.13.1	Effect of GF-109203X on CCL2-evoked $Ca^{2+}$ responses in THP-1 cells .....	164
4.3.13.2	Effect of GF-109203X on CCL2-mediated THP-1 cell chemotaxis .....	165
<b>4.4</b>	<b>Summary .....</b>	<b>169</b>

## **CHAPTER 5: MODULATION OF CCL2/CCR2-MEDIATED MONOCYTE SIGNALLING AND FUNCTION BY EXTRACELLULAR NUCLEOTIDES .....**

<b>5.1</b>	<b>Introduction .....</b>	<b>171</b>
<b>5.2</b>	<b>Aims .....</b>	<b>172</b>
<b>5.3</b>	<b>Results .....</b>	<b>173</b>
5.3.1	Chemotactic effects of extracellular nucleotides on THP-1 cells .....	173

5.3.2	Effect of ecto-nucleotidases on CCL2/CCR2-mediated THP-1 cell and PBMC signalling and function .....	175
5.3.2.1	Investigating the selectivity of apyrase .....	175
5.3.2.2	Effect of apyrase on CCL2-evoked Ca <sup>2+</sup> responses in THP-1 cells and human PBMCs .....	178
5.3.2.3	Effect of apyrase on CCL2-mediated THP-1 cell chemotaxis and adhesion.....	183
5.3.2.4	Effect of apyrase isoenzymes on CCL2-evoked Ca <sup>2+</sup> responses in THP-1 cells .....	187
5.3.3	Effect of ADA on CCL2-evoked Ca <sup>2+</sup> responses in THP-1 cells .....	190
5.3.4	Effect of endogenous ecto-nucleotidases on CCL2/CCR2-mediated THP-1 cell signalling.....	191
5.3.4.1	Endogenous ecto-nucleotidases in THP-1 cells .....	191
5.3.4.2	Effect of ecto-nucleotidase inhibitors on CCL2-evoked Ca <sup>2+</sup> responses in THP-1 cells .....	192
5.3.4.2.1	ARL-67156.....	192
5.3.4.2.2	POM-1 .....	197
5.3.5	Effect of P1 receptor antagonism on CCL2-evoked Ca <sup>2+</sup> responses in THP-1 cells.....	200
5.3.6	Effect of P2 receptor antagonists on CCL2/CCR2-mediated THP-1 cell signalling and function .....	204
5.3.6.1	Suramin .....	204
5.3.6.2	PPADS.....	206
5.3.6.3	Effect of P2X receptor antagonists on CCL2/CCR2-mediated THP-1 cell signalling and function .....	209
5.3.6.3.1	P2X1 .....	209
5.3.6.3.2	P2X4 .....	211
5.3.6.3.3	P2X7 .....	213
5.3.6.4	Effect of P2Y receptor antagonism on CCL2/CCR2-mediated THP-1 cell signalling and function .....	217
5.3.6.4.1	P2Y <sub>1</sub> .....	217
5.3.6.4.2	P2Y <sub>11</sub> .....	219
5.3.6.4.3	P2Y <sub>12</sub> .....	221
5.3.6.4.4	P2Y <sub>13</sub> .....	223
<b>5.4</b>	<b>Summary .....</b>	<b>226</b>

**CHAPTER 6: INVESTIGATING THE REQUIREMENT OF THE P2Y<sub>6</sub> RECEPTOR FOR CCL2/CCR2-MEDIATED MONOCYTE SIGNALLING AND FUNCTION .....**

<b>6.1</b>	<b>Introduction .....</b>	<b>227</b>
<b>6.2</b>	<b>Aims .....</b>	<b>229</b>
<b>6.3</b>	<b>Results .....</b>	<b>229</b>
6.3.1	Effect of P2Y <sub>6</sub> antagonism on CCL2/CCR2-mediated THP-1 cell and human PBMC signalling and function .....	229
6.3.1.1	Effect of MRS-2578 on CCL2-evoked Ca <sup>2+</sup> responses in THP-1 cells ...	229
6.3.1.2	Effect of MRS-2578 on CCL2-evoked Ca <sup>2+</sup> responses in human PBMCs .....	234
6.3.1.3	Effect of dual P2Y <sub>6</sub> /CCR2 antagonism on CCL2-evoked Ca <sup>2+</sup> responses in THP-1 cells.....	236
6.3.1.4	Effect of MRS-2578 on CCL2-mediated THP-1 cell and PBMC chemotaxis .....	238
6.3.1.5	Effect of MRS-2578 on CCL2-mediated THP-1 cell adhesion.....	241
6.3.2	Characterisation of P2Y <sub>6</sub> -stable and parental 1321N1 astrocytoma cells..	244

6.3.2.1	Extracellular nucleotide-evoked Ca <sup>2+</sup> responses in P2Y <sub>6</sub> -stable 1321N1 cells.....	244
6.3.2.2	Extracellular nucleotide-evoked Ca <sup>2+</sup> responses in parental 1321N1 cells.....	244
6.3.2.3	Effect of MRS-2578 on ADP and UDP-evoked Ca <sup>2+</sup> responses in P2Y <sub>6</sub> -stable 1321N1 cells.....	245
6.3.3	Effect of P2Y <sub>6</sub> antagonism on extracellular nucleotide-evoked Ca <sup>2+</sup> responses in THP-1 cells.....	249
6.3.4	The functional presence of P2Y <sub>14</sub> in THP-1 cells .....	250
6.3.5	Investigating CCR2 and P2Y <sub>6</sub> crosstalk in THP-1 cells .....	253
6.3.5.1	Effect of CCL2/UDP co-application on Ca <sup>2+</sup> responses in THP-1 cells.....	253
6.3.5.2	Effect of BMS-CCR2-22 on UDP-evoked Ca <sup>2+</sup> responses in THP-1 cells.....	254
6.3.6	Investigating crosstalk between P2Y <sub>6</sub> and FPRs in THP-1 cells.....	257
6.3.6.1	Effect of apyrase and MRS-2578 on fMLP-evoked Ca <sup>2+</sup> responses in THP-1 cells.....	257
6.3.6.2	Effect of apyrase and MRS-2578 on fMLP-mediated THP-1 cell chemotaxis .....	261
6.3.7	Effect of P2Y <sub>6</sub> desensitisation on CCL2-evoked Ca <sup>2+</sup> responses in THP-1 cells.....	263
6.3.7.1	Effect of repeat ADP or UDP challenge on Ca <sup>2+</sup> responses in THP-1 cells.....	263
6.3.7.2	Effect of ADP and UDP challenge on CCL2-evoked Ca <sup>2+</sup> responses in THP-1 cells.....	265
6.3.8	Generation and evaluation of <i>P2RY6</i> -KD THP-1 cells .....	267
6.3.8.1	Generation of <i>P2RY6</i> -KD THP-1 cells with in-house <i>P2RY6</i> -shRNA lentivirus .....	267
6.3.8.1.1	UDP-evoked Ca <sup>2+</sup> responses.....	267
6.3.8.1.2	qRT-PCR analysis of <i>P2RY6</i> expression.....	268
6.3.8.2	Generation of <i>P2RY6</i> -KD THP-1 cells using MISSION <sup>®</sup> <i>P2RY6</i> -shRNA lentivirus.....	269
6.3.8.2.1	UDP-evoked Ca <sup>2+</sup> responses.....	269
6.3.8.2.2	CCL2-evoked Ca <sup>2+</sup> responses .....	270
6.3.8.2.3	qRT-PCR analysis of <i>P2RY6</i> and <i>CCR2</i> expression.....	271
6.3.9	CCL2/ <i>CCR2</i> -mediated function of P2Y <sub>6</sub> -KD cells.....	272
6.3.10	CCL2-mediated extracellular nucleotide release in THP-1 cells.....	276
6.3.10.1	Detecting CCL2-mediated extracellular nucleotide release.....	276
6.3.10.2	Investigating THP-1 cell lysosomes as a source of ATP .....	280
<b>5.4</b>	<b>Summary .....</b>	<b>281</b>
<b>CHAPTER 7: DISCUSSION .....</b>		<b>282</b>
<b>7.1</b>	<b>Overview .....</b>	<b>282</b>
<b>7.2</b>	<b>Concluding Remarks .....</b>	<b>282</b>
<b>7.3</b>	<b>Key Findings.....</b>	<b>284</b>
<b>7.4</b>	<b>Future Directions.....</b>	<b>313</b>
<b>APPENDIX : SUPPLEMENTARY DATA.....</b>		<b>315</b>
<b>REFERENCES .....</b>		<b>341</b>

# List of Figures

---

## Chapter 1

Figure 1.1	Differentiation of monocytes in the bone marrow.....	24
Figure 1.2	The leukocyte adhesion cascade.....	27
Figure 1.3	G-protein-coupled receptor.....	30
Figure 1.4	G-protein cycle.....	31
Figure 1.5	Classical GPCR pathways.....	34
Figure 1.6	Overview of Ca <sup>2+</sup> signalling.....	37
Figure 1.7	Chemokine families.....	42
Figure 1.8	Chemokine receptors and their ligands.....	43
Figure 1.9	Crystal structure of the human CCR2 receptor.....	44
Figure 1.10	Structure of functional P2X purinoceptors.....	49
Figure 1.11	Structures of some naturally-occurring purinoceptor ligands.....	50

## Chapter 2

Figure 2.1	pLKO.1 puro shRNA vector.....	72
Figure 2.2	Detection of plasmid DNA.....	73
Figure 2.3	THP-1 cell puromycin kill curve.....	76
Figure 2.4	Structure and fluorescence spectra of Fluo-4 AM and Fura-2 AM.....	78
Figure 2.5	Cell chemotaxis.....	81
Figure 2.6	Log-log plot of standard curve data for ATP.....	84

## Chapter 3

Figure 3.1	Detection of mRNA for $\beta$ -actin ( <i>ACTB</i> ) and monocyte/myeloid markers in human brain, THP-1 cells, and human monocytes.....	91
Figure 3.2	Detection of mRNA for CC chemokines in human brain, THP-1 cells, and human monocytes.....	93
Figure 3.3	Detection of mRNA for CC chemokine receptors in human brain and human monocyte-depleted PBMCs.....	96
Figure 3.4	Detection of mRNA for CC chemokine receptors in THP-1 cells.....	97
Figure 3.5	Detection of mRNA for CC chemokine receptors in human monocytes.....	98
Figure 3.6	Detection of mRNA for P1 purinoceptors in human brain, THP-1 cells, and human monocytes.....	101
Figure 3.7	Detection of mRNA for P2X purinoceptors in human brain and retina.....	104
Figure 3.8	Detection of mRNA for P2X purinoceptors in THP-1 cells.....	105
Figure 3.9	Detection of mRNA for P2X purinoceptors in human monocytes.....	106
Figure 3.10	Detection of mRNA for P2Y purinoceptors in human brain and THP-1 cells.....	109
Figure 3.11	Detection of mRNA for P2Y purinoceptors in human monocytes.....	110

## Chapter 4

Figure 4.1	Signalling pathways investigated in this chapter.....	113
Figure 4.2	CCL2-evoked Ca <sup>2+</sup> responses in THP-1 cells and PBMCs.....	115
Figure 4.3	Effect of extracellular Ca <sup>2+</sup> removal on CCL2-evoked Ca <sup>2+</sup> responses in THP-1 cells.....	117
Figure 4.4	Effect of BAPTA-AM on CCL2-mediated THP-1 cell chemotaxis.....	119
Figure 4.5	Effect of BMS-CCR2-22 on CCL2-evoked Ca <sup>2+</sup> responses in THP-1 cells.....	122
Figure 4.6	Effect of BMS-CCR2-22 on CCL5-evoked Ca <sup>2+</sup> responses in THP-1 cells.....	123
Figure 4.7	Effect of BMS-CCR2-22 on CCL2-mediated THP-1 cell chemotaxis.....	126
Figure 4.8	Effect of BMS-CCR2-22 on CCL2-mediated THP-1 cell adhesion to quiescent and TNF $\alpha$ -treated HUVEC monolayers.....	127

Figure 4.9	Effect of PTx on CCL2, ATP, and ADP-evoked Ca <sup>2+</sup> responses in THP-1 cells.....	129
Figure 4.10	Effect of PTx on CCL2-mediated THP-1 cell chemotaxis.....	131
Figure 4.11	Effect of gallein on fluo 4-AM Ca <sup>2+</sup> signal detection.....	133
Figure 4.12	Effect of LY-294002 on CCL2-evoked Ca <sup>2+</sup> responses in THP-1 cells.....	136
Figure 4.13	Effect of U-73122 on CCL2-evoked Ca <sup>2+</sup> responses in THP-1 cells.....	139
Figure 4.14	Effect of XeC on CCL2-evoked Ca <sup>2+</sup> responses in THP-1 cells.....	142
Figure 4.15	Effect of XeC on CCL2-mediated THP-1 cell chemotaxis.....	143
Figure 4.16	Effect of thapsigargin on CCL2-evoked Ca <sup>2+</sup> responses in THP-1 cells....	147
Figure 4.17	Effect of thapsigargin on CCL2-evoked Ca <sup>2+</sup> responses in THP-1 cells in the absence of extracellular Ca <sup>2+</sup> .....	148
Figure 4.18	Effect of thapsigargin on CCL2-mediated THP-1 cell chemotaxis.....	150
Figure 4.19	Effect of SKF-96365 on CCL2-evoked Ca <sup>2+</sup> responses in THP-1 cells....	153
Figure 4.20	Effect of RHC-80267 on CCL2-evoked Ca <sup>2+</sup> responses in THP-1 cells....	156
Figure 4.21	Effect of RHC-80267 on CCL2-evoked Ca <sup>2+</sup> responses in THP-1 cells in the absence of extracellular Ca <sup>2+</sup> .....	157
Figure 4.22	Effect of R-59-022 on CCL2-evoked Ca <sup>2+</sup> responses in THP-1 cells.....	161
Figure 4.23	Effect of R-59-022 on CCL2-evoked Ca <sup>2+</sup> responses in THP-1 cells in the absence of extracellular Ca <sup>2+</sup> .....	162
Figure 4.24	Effect of R-59-022 on UDP-evoked Ca <sup>2+</sup> responses in THP-1 cells.....	163
Figure 4.25	Effect of GF-109203X on CCL2-evoked Ca <sup>2+</sup> responses in THP-1 cells...166	
Figure 4.26	Effect of GF-109203X on CCL2-evoked Ca <sup>2+</sup> responses in THP-1 cells in the absence of extracellular Ca <sup>2+</sup> .....	167
Figure 4.27	Effect of signalling inhibitors on CCL2-mediated THP-1 cell chemotaxis.....	168

## Chapter 5

Figure 5.1	THP-1 cell migration towards extracellular nucleotides.....	174
Figure 5.2	Effect of apyrase on CCL2-evoked Ca <sup>2+</sup> responses in THP-1 cells.....	180
Figure 5.3	Effect of apyrase on CCL2-evoked Ca <sup>2+</sup> responses in THP-1 cells in the absence of extracellular Ca <sup>2+</sup> .....	181
Figure 5.4	Effect of apyrase on CCL2-evoked Ca <sup>2+</sup> responses in human PBMCs.....	182
Figure 5.5	Effect of apyrase on CCL2-mediated THP-1 cell chemotaxis.....	184
Figure 5.6	Effect of apyrase on CCL2-mediated human PBMC chemotaxis.....	185
Figure 5.7	Effect of apyrase on THP-1 cell adhesion to quiescent HUVEC monolayers.....	186
Figure 5.8	Effect of apyrase isoenzymes on CCL2-evoked Ca <sup>2+</sup> responses in THP-1 cells.....	189
Figure 5.9	Effect of ARL-67156 on CCL2-evoked Ca <sup>2+</sup> responses in THP-1 cells....	195
Figure 5.10	Effect of ARL-67156 on CCL2-evoked Ca <sup>2+</sup> responses in THP-1 cells in the absence of extracellular Ca <sup>2+</sup> .....	196
Figure 5.11	Effect of POM-1 on CCL2-evoked intracellular Ca <sup>2+</sup> responses in THP-1 cells.....	199
Figure 5.12	Effect of CGS-15943 on CCL2-evoked Ca <sup>2+</sup> responses in THP-1 cells....	202
Figure 5.13	Effect of CGS-15943 on CCL2-evoked Ca <sup>2+</sup> responses in apyrase-treated THP-1 cells.....	203
Figure 5.14	Effect of suramin on CCL2-evoked Ca <sup>2+</sup> responses in THP-1 cells.....	205
Figure 5.15	Effect of PPADS on CCL2-evoked Ca <sup>2+</sup> responses in THP-1 cells.....	207
Figure 5.16	Effect of PPADS on CCL2-mediated THP-1 chemotaxis.....	208
Figure 5.17	Effect of P2X antagonists on CCL2-mediated THP-1 cell chemotaxis....	216
Figure 5.18	Effect of P2Y antagonists on CCL2-mediated THP-1 cell chemotaxis....	225

## Chapter 6

Figure 6.1	Effect of MRS-2578 on CCL2-evoked Ca <sup>2+</sup> responses in THP-1 cells....	232
Figure 6.2	Effect of MRS-2578 on CCL2-evoked Ca <sup>2+</sup> responses in THP-1 cells	

	in the absence of extracellular Ca <sup>2+</sup> .....	233
Figure 6.3	Effect of MRS-2578 on CCL2-evoked Ca <sup>2+</sup> responses in human PBMCs.....	235
Figure 6.4	Effect of MRS-2578 and BMS-CCR2-22 on CCL2-evoked Ca <sup>2+</sup> responses in THP-1 cells.....	237
Figure 6.5	Effect of MRS-2578 on CCL2-mediated THP-1 cell chemotaxis.....	239
Figure 6.6	Effect of MRS-2578 on CCL2-mediated human PBMC chemotaxis.....	240
Figure 6.7	Effect of MRS-2578 on CCL2-mediated THP-1 cell adhesion to quiescent and TNF $\alpha$ -treated HUVEC monolayers.....	243
Figure 6.8	Effect of MRS-2578 on ADP-evoked Ca <sup>2+</sup> responses in P2Y <sub>6</sub> -stable 1321N1 cells.....	247
Figure 6.9	Effect of MRS-2578 on UDP-evoked Ca <sup>2+</sup> responses in P2Y <sub>6</sub> -stable 1321N1 cells.....	248
Figure 6.10	UDP-glucose-evoked Ca <sup>2+</sup> responses in THP-1 cells.....	252
Figure 6.11	Effect of CCL2/UDP co-application on Ca <sup>2+</sup> responses in THP-1 cells.....	255
Figure 6.12	Effect of BMS-CCR2-22 on UDP-evoked Ca <sup>2+</sup> responses in THP-1 cells.....	256
Figure 6.13	Effect of apyrase on fMLP-evoked Ca <sup>2+</sup> responses in THP-1 cells.....	259
Figure 6.14	Effect of MRS-2578 on fMLP-evoked Ca <sup>2+</sup> responses in THP-1 cells.....	260
Figure 6.15	Effect of apyrase and MRS-2578 on fMLP-mediated THP-1 cell chemotaxis.....	262
Figure 6.16	Effect of repeat ADP- or UDP-challenge on Ca <sup>2+</sup> responses in THP-1 cells.....	264
Figure 6.17	Effect of ADP or UDP challenge on CCL2-evoked Ca <sup>2+</sup> responses in THP-1 cells.....	266
Figure 6.18	CCL2-mediated scrambled and P2Y <sub>6</sub> -KD cell chemotaxis.....	274
Figure 6.19	CCL2-mediated adhesion of scrambled and P2Y <sub>6</sub> -KD cells to quiescent and TNF $\alpha$ -treated HUVEC monolayers.....	275
Figure 6.20	Detection of CCL2-mediated ATP release in THP-1 cells by ion-pair reverse-phase HPLC.....	278
Figure 6.21	Detection of CCL2-mediated ATP release in THP-1 cells by luciferase-luciferin.....	279
<b>Chapter 7</b>		
Figure 7.1	CCR2 and P2Y <sub>6</sub> crosstalk in monocytes.....	283
<b>Appendix 1</b>		
Figure A1	Detection of adenine nucleotides and nucleosides by ion-pair reverse-phase HPLC.....	315
Figure A2	Detection of uridine nucleotides and nucleoside by ion-pair reverse-phase HPLC.....	316
Figure A3	Effect of compounds on LDH release from THP-1 cells.....	317
Figure A4	Effect of water-soluble compounds on THP-1 cell viability.....	318
Figure A5	Effect of DMSO-soluble compounds on THP-1 cell viability.....	319
Figure A6	Effect of apyrase on ATP.....	320
Figure A7	Effect of apyrase on ADP.....	321
Figure A8	Effect of apyrase on UTP.....	322
Figure A9	Effect of apyrase on UDP.....	323
Figure A10	Hydrolysis of ATP by SBS and THP-1 cells.....	324
Figure A11	Effect of POM-1 on ATP- and ADP-evoked Ca <sup>2+</sup> responses in THP-1 cells.....	325
Figure A12	Effect of POM-1 on UTP- and UDP-evoked Ca <sup>2+</sup> responses in THP-1 cells.....	326
Figure A13	Effect of Ro-0437626 on CCL2-evoked Ca <sup>2+</sup> responses in THP-1 cells.....	327
Figure A14	Effect of Ro-0437626 on $\alpha,\beta$ -MeATP-evoked Ca <sup>2+</sup> responses in THP-1 cells.....	328
Figure A15	Effect of 5-BDBD on CCL2-evoked Ca <sup>2+</sup> responses in THP-1 cells.....	329
Figure A16	Effect of A 438079 on BzATP-evoked Ca <sup>2+</sup> responses in THP-1 cells.....	330

Figure A17	Effect of apyrase on MRS 2365-evoked Ca <sup>2+</sup> responses in THP-1 cells...	331
Figure A18	Effect of NF-340 on ATP- and βNAD-evoked Ca <sup>2+</sup> responses in THP-1 cells.....	332
Figure A19	Effect of MRS-2211 on CCL2- and ADP-evoked Ca <sup>2+</sup> responses in THP-1 cells.....	333
Figure A20	ATP- and ADP-evoked Ca <sup>2+</sup> responses in P2Y <sub>6</sub> -stable 1321N1 cells.....	334
Figure A21	UTP- and UDP-evoked Ca <sup>2+</sup> responses in P2Y <sub>6</sub> -stable 1321N1 cells.....	335
Figure A22	Extracellular nucleotide-evoked Ca <sup>2+</sup> responses in parental 1321N1 cells.....	336
Figure A23	Effect of MRS-2578 on ATP- and ADP-evoked Ca <sup>2+</sup> responses in THP-1 cells.....	337
Figure A24	Effect of MRS-2578 on UTP and UDP-evoked Ca <sup>2+</sup> responses in THP-1 cells.....	338
Figure A25	UDP-evoked Ca <sup>2+</sup> responses in scrambled and P2RY6-KD THP-1 cells.....	339
Figure A26	CCL2-evoked Ca <sup>2+</sup> responses in scrambled and P2RY6-KD THP-1 cells.....	340

# List of Tables

---

## Chapter 1

Table 1.1	Human and mouse monocyte subsets.....	23
Table 1.2	Frequencies of monocytes in human pathologies.....	29
Table 1.3	Heterotrimeric G $\alpha$ -proteins and their effectors.....	32
Table 1.4	CCR2 antagonists in clinical development (2014).....	47
Table 1.5	Human purinoceptors.....	51
Table 1.6	Major ecto-nucleotidase families.....	53
Table 1.7	P1 ligands in clinical development (2012).....	55
Table 1.8	P2X ligands in clinical development (2012).....	56
Table 1.9	P2Y ligands in clinical development (2012).....	56

## Chapter 2

Table 2.1	Chemoattractants and extracellular nucleotides.....	59
Table 2.2	Purinoceptor agonists.....	60
Table 2.3	Chemokine and purinoceptor antagonists.....	60
Table 2.4	Nucleotide/nucleoside metabolising enzymes.....	60
Table 2.5	Inhibitors and modulators.....	61
Table 2.6	Primer sequences for <i>ACTB</i> (actin, beta) and monocyte markers.....	67
Table 2.7	Primer sequences for CC chemokines and receptors.....	68
Table 2.8	Primer sequences for P1 purinoceptors.....	69
Table 2.9	Primer sequences for P2X purinoceptors.....	69
Table 2.10	Primer sequences for P2Y purinoceptors.....	70
Table 2.11	shRNA sequences for <i>P2RY6</i> .....	72
Table 2.12	Lentivirus <i>P2RY6</i> shRNA sequences.....	74
Table 2.13	Nucleotide retention times.....	83

## Chapter 3

Table 3.1	Detection of mRNA for $\beta$ -actin ( <i>ACTB</i> ) and monocyte/myeloid markers in human brain, THP-1 cells, and human monocytes.....	89
Table 3.2	Detection of mRNA for CC chemokines in human brain, THP-1 cells, and human monocytes.....	92
Table 3.3	Detection of mRNA for CC chemokine receptors in human brain, THP-1 cells and human monocytes.....	95
Table 3.4	Detection of mRNA for P1 purinoceptors in human brain, THP-1 cells and human monocytes.....	99
Table 3.5	Detection of mRNA for P2X purinoceptors in human brain, THP-1 cells and human monocytes.....	102
Table 3.6	Detection of mRNA for P2Y purinoceptors in human brain, THP-1 cells and human monocytes.....	107

## Chapter 4

Table 4.1	Effect of dantrolene on CCL2-evoked Ca <sup>2+</sup> responses in THP-1 cells.....	145
-----------	--	-----

## Chapter 5

Table 5.1	Hydrolysis of nucleotides by apyrase.....	177
Table 5.2	Effect of ADA on CCL2-evoked Ca <sup>2+</sup> responses in THP-1 cells.....	190
Table 5.3	Effect of THP-1 cells and SBS on nucleotide and nucleoside levels.....	192
Table 5.4	Effect of POM-1 on extracellular nucleotide-evoked Ca <sup>2+</sup> responses in THP-1 cells.....	198
Table 5.5	Effect of Ro-0437626 on CCL2- and $\alpha$ , $\beta$ -meATP-evoked Ca <sup>2+</sup> responses in THP-1 cells.....	210
Table 5.6	Effect of 5-BDBD on CCL2-evoked Ca <sup>2+</sup> responses in THP-1 cells.....	212
Table 5.7	Effect of A-438079 on CCL2 and BzATP-evoked Ca <sup>2+</sup> responses in THP-1 cells.....	214

Table 5.8	Effect of MRS-2179 on CCL2- and ADP-evoked Ca <sup>2+</sup> responses in THP-1 cells.....	218
Table 5.9	Effect of apyrase on MRS-2365-evoked Ca <sup>2+</sup> responses in THP-1 cells.....	218
Table 5.10	Effect of NF-340 on CCL2, ATP and β-NAD-evoked Ca <sup>2+</sup> responses in THP-1 cells.....	220
Table 5.11	Effect of AR-C-66096 on CCL2 and ADP-evoked Ca <sup>2+</sup> responses in THP-1 cells.....	222
Table 5.12	Effect of MRS-2211 on CCL2- and ADP-evoked Ca <sup>2+</sup> responses in THP-1 cells.....	223
<b>Chapter 6</b>		
Table 6.1	Nucleotide Ca <sup>2+</sup> responses in P2Y <sub>6</sub> -stable 1321N1 cells.....	244
Table 6.2	Nucleotide Ca <sup>2+</sup> responses in parental 1321N1 cells.....	245
Table 6.3	Effect of MRS-2578 on extracellular nucleotide-evoked Ca <sup>2+</sup> responses in THP-1 cells.....	249
Table 6.4	UDP-evoked Ca <sup>2+</sup> responses in scrambled and <i>P2RY6</i> -KD cell lines.....	267
Table 6.5	Relative quantitation and fold-shift values for scrambled and <i>P2RY6</i> -KD 14075 THP-1 cells.....	268
Table 6.6	UDP-evoked Ca <sup>2+</sup> responses in scrambled and <i>P2RY6</i> -KD cell lines.....	269
Table 6.7	CCL2-evoked Ca <sup>2+</sup> responses in scrambled and <i>P2RY6</i> -KD cell lines.....	270
Table 6.8	Relative quantitation and fold-shift values for scrambled and <i>P2RY6</i> -KD cells.....	271
Table 6.9	β-hexosaminidase in THP-1 cell supernatants.....	280

# Abbreviations

---

Listed below are the meanings to some commonly used abbreviations:

AC	Adenylate cyclase
ADA	Adenosine deaminase
ADP	Adenosine 5'-diphosphate
AMP	Adenosine 5'-monophosphate
ATP	Adenosine 5'-triphosphate
bp	Base pairs
BzATP	2'(3')-O-(4-Benzoylbenzoyl)adenosine-5'-triphosphate
Ca <sup>2+</sup>	Calcium ion
CCL2	Chemokine (CC-motif) ligand 2
CCL5	Chemokine (CC-motif) ligand 5
CCR2	Chemokine (CC-motif) receptor 2
CD14	Cluster of differentiation 14
CD16	Cluster of differentiation 16
DAG	Diacylglycerol
DAGK	Diacylglycerol kinase
DAGL	Diacylglycerol lipase
EC <sub>50</sub>	Half-maximal effective concentration
EGTA	Ethylene glycol tetraacetic acid
E-NPP	Ecto-nucleotide pyrophosphatase/phosphodiesterase
ER	Endoplasmic reticulum
fMLP	Formyl-Methionyl-Leucyl-Phenylalanine

FPR	Formyl-peptide receptor
GPCR	G-protein-coupled receptor
GPN	Glycyl-L-phenylalanine-naphthylamide
HPLC	High-performance liquid chromatography
HUVEC	Human umbilical-cord endothelial cell
IC <sub>50</sub>	Half-maximal inhibitory concentration
ICAM-1	Intercellular adhesion molecule-1
IP <sub>3</sub>	Inositol 1,4,5-trisphosphate
IP <sub>3</sub> R	IP <sub>3</sub> receptor
K <sub>B</sub>	Equilibrium dissociation constant of a ligand (functional assay)
KD	Knockdown
K <sub>i</sub>	Equilibrium dissociation constant of a ligand (inhibition assay)
K <sub>i</sub>	Inhibitor constant, half-maximal inhibitory concentration
K <sub>d</sub>	Equilibrium dissociation constant of a ligand (binding assay)
LDH	Lactate dehydrogenase
α,β-MeATP	α,β-Methyleneadenosine 5'-triphosphate
mRNA	Messenger ribonucleic acid
β-NAD	β-Nicotinamide adenine dinucleotide
NDP	Nucleoside diphosphate
NTP	Nucleoside triphosphate
PBMC	Peripheral blood mononuclear cell
PI3K	Phosphoinositide-3-kinase
pIC <sub>50</sub>	Negative logarithm to base 10 of the IC <sub>50</sub>
PIP <sub>2</sub>	Phosphatidylinositol 4,5 bisphosphate

PKC	Protein kinase C
PLC	Phospholipase C
PRR	Pathogen-recognition receptor
PTx	<i>Bordetella pertussis</i>
RT	Reverse transcriptase
RT-PCR	Reverse transcription-polymerase chain reaction
RyR	Ryanodine receptor
SBS	Salt-buffered solution
SERCA	Sarco/endoplasmic reticulum Ca <sup>2+</sup> ATPase
shRNA	Short-hairpin ribonucleic acid
SOCE	Store-operated calcium entry
TNF $\alpha$	Tumour necrosis factor $\alpha$
UDP	Uridine 5'-diphosphate
UMP	Uridine 5'-monophosphate
UTP	Uridine 5'-triphosphate
VCAM-1	Vascular cell-adhesion molecule-1
XeC	Xestospongine-C

# Papers and Conference Abstracts

---

Listed below are published works resulting from the work in this thesis.

## **Papers**

Campwala, H, Sexton, DW, Crossman, DC & Fountain, SJ (2014). P2Y<sub>6</sub> receptor inhibition perturbs CCL2-evoked signalling in human monocytic and peripheral blood mononuclear cells. *J Cell Sci*, **127**, 4964-73.

## **Conference Abstracts**

Campwala, H & Fountain, SJ (2012). Activation of purinergic P2Y receptors modulates C-C chemokine signalling in human monocytes. *Proceedings of the British Pharmacological Society*, pA2 online, **(10)**, 4.

Campwala, H & Fountain, SJ (2012). C-C chemokine signalling in human monocytes involves a concomitant release of ATP and activation of purinergic receptors. *Proc Physiol Soc*, **27**, PC161

Campwala, H & Fountain, SJ (2013). Activation of purinergic P2Y receptors modulates C-C chemokine signalling in human monocytes. Abstracts of the Fourth (2012) UK Purine Club Annual Symposium. *Purinergic Signalling*, **9(4)**:697-706.

Campwala, H, Sexton, DW, Crossman, DC & Fountain, SJ (2014). Impaired CCL2-dependent signalling in P2Y<sub>6</sub> receptor-deficient monocytes. Abstracts of the Fifth (2013) UK Purine Club Annual Symposium. *Purinergic Signalling*. In Press.

# Acknowledgements

---

I would first like to thank my primary supervisor Samuel Fountain for his continued guidance and dedicated support throughout this process. My special thanks also go to my supervisory committee, David Crossman and Darren Sexton for their guidance and helpful discussions. In addition, I would like to extend my thanks to the University of East Anglia and the John and Pamela Salter charitable trust for supporting this work.

I would also like to thank those who have helped me to acquire the many technical skills, samples, and data that have made this work possible. I wish to thank Samuel, Darren, Charles Brearley, Tracey Swingler, Julie Sanderson, Stefan Bidula, and Venketesh Sivaramakrishnan.

I am also deeply grateful to Mohammad Hajihosseini, Gabriella Kelemen, Charles, and Darren for their guidance, encouragement, and unconditional support.

I would also like to thank my former managers at Pfizer, Steve Liu and Gary Salmon who encouraged me to pursue this degree.

Last but by no means least; I would like to thank my parents and my husband. Every time I was ready to quit, you did not let me and I am forever grateful. This thesis stands as a testament to your unconditional love and encouragement.

# Chapter 1: Introduction

---

## 1.1 The immune system

The immune system is a continuously evolving system that protects human health by acting against a constant onslaught of challenges made by pathogens, tumour cells, and dead cells. The immune system consists of two branches, the innate immune response and the antigen-specific adaptive response, both diverging via a sophisticated network of cellular and chemical effectors (Parkin and Cohen, 2001). The innate branch of the immune system is fixed in germ-line deoxyribonucleic acid (DNA) and consists of various immune cells (e.g. neutrophils, macrophages, and monocytes) and effectors (e.g. complements, cytokines and chemokines) which act collectively to provide a rapid response without the need to adapt to a changing environment. In contrast, the adaptive branch comprises of cells such as T-lymphocytes (thymus-derived), B-lymphocytes (bone-marrow-derived), and dendritic cells. Together, these provide a slow but specific response that increases in speed upon re-exposure due to an ability to remember and learn from past-experiences (Koenderman *et al.*, 2014). Despite the intrinsic differences between the two branches, the cellular custodians of both systems rely on an ability to sense warning signals from specific molecules through the activation of surface pattern recognition receptors (PRRs) that alert them to intruding organisms or cellular damage (Bianchi, 2007). Warning signals detected by PRRs include pathogen/microbial-associated molecular patterns (PAMPs/MAMPs) associated with microbial challenge, and damage-associated molecular-patterns (DAMPs) associated with cellular damage or death.

## 1.2 Monocytes

### 1.2.1 Human and mouse monocyte heterogeneity

Monocytes represent a population of immune cells that are crucial for driving the innate immune response (Ingersoll *et al.*, 2011). Monocytes and their progeny (macrophages and dendritic cells), participate in a wide range of protective activities including the removal of intruding organisms and cell debris, tissue healing, and the initiation of adaptive immune responses (Ingersoll *et al.*, 2011). Although monocytes are a heterogeneous cell population, they are characterised by their expression of specific PRRs. This concept was first introduced by Passlick *et al.* (1989) and Geissmann *et al.* (2003) who observed that human monocytes differed in their expression of cluster of differentiation 14 (CD14; lipopolysaccharide receptor), cluster of differentiation 16 (CD16; low affinity Fc $\gamma$ III receptor), and the chemokine receptors CX<sub>3</sub>C-motif receptor-1

(CX<sub>3</sub>CR1), and CC-motif receptor 2 (CCR2). Based on the information provided in these studies, human monocyte subsets have been divided into classical (CD14<sup>++</sup>/CD16<sup>-</sup>), intermediate (CD14<sup>++</sup>/CD16<sup>+</sup>), and non-classical (CD14<sup>+</sup>/CD16<sup>++</sup>) monocytes (Table 1.1) (Weber *et al.*, 2000; Geissmann *et al.*, 2003; Ziegler-Heitbrock 2007; Yona and Jung, 2010).

Mouse monocyte subsets can be distinguished by differential expression of lymphocyte 6C (Ly6C/Gr1; pro-inflammatory antigen) and cluster of differentiation 43 (CD43; leukosialin), but also differ in their expression of CX<sub>3</sub>CR1, CCR2, and cluster of differentiation 62L (CD62L; L-selectin) (Geissmann *et al.*, 2003). Mouse monocytes are therefore grouped into classical (Ly6C<sup>high</sup>), intermediate (Ly6C<sup>middle</sup>), and non-classical (Ly6C<sup>low</sup>) subsets (Table 1.1) (Geissmann *et al.*, 2003; Sunderkötter *et al.*, 2004; Geissmann *et al.*, 2010; Ziegler-Heitbrock *et al.*, 2010; Yang *et al.*, 2014). Data from gene array studies suggests that mouse subsets closely resemble human subsets (Geissmann *et al.*, 2003; Ingersoll *et al.*, 2010; Cros *et al.*, 2010).

**Table 1.1 Human and mouse monocyte subsets**

Species	Subset	% of MNC	Markers	Possible roles
Human	Classical	80-95	CD14 <sup>++</sup> CD16 <sup>-</sup> CCR2 <sup>high</sup> CX <sub>3</sub> CR1 <sup>low</sup>	Phagocytosis
	Intermediate	2-11	CD14 <sup>++</sup> CD16 <sup>+</sup> CCR2 <sup>mid</sup> CX <sub>3</sub> CR1 <sup>high</sup> CCR5 <sup>+</sup>	Pro-inflammatory
	Non-classical	2-8	CD14 <sup>+</sup> CD16 <sup>++</sup> CCR2 <sup>low</sup> CX <sub>3</sub> CR1 <sup>high</sup>	Patrolling
Mouse	Classical	40-45	CD11b <sup>+</sup> CD115 <sup>+</sup> CD43 <sup>low</sup> CD62L <sup>+</sup> Ly6C <sup>high</sup> CCR2 <sup>high</sup> CX <sub>3</sub> CR1 <sup>low</sup>	Phagocytosis and Pro-inflammatory
	Intermediate	5-32	CD11b <sup>+</sup> CD115 <sup>+</sup> CD43 <sup>high</sup> CD62L <sup>-</sup> Ly6C <sup>middle</sup> CCR2 <sup>high</sup> CX <sub>3</sub> CR1 <sup>low</sup>	Pro-inflammatory
	Non-classical	26-50	CD11b <sup>+</sup> CD115 <sup>+</sup> CD43 <sup>high</sup> CD62L <sup>-</sup> Ly6C <sup>low</sup> CCR2 <sup>low</sup> CX <sub>3</sub> CR1 <sup>high</sup>	Patrolling and Tissue repair

MNC = mononuclear cell. Human intermediate monocytes also express chemokine (CC-motif) receptor 5 (CCR5). Murine monocytes also express cluster of differentiation 115 (CD115; colony stimulating factor receptor 1 (CSF-1R)) and cluster of differentiation 11b (CD11b; integrin αM) (Geissmann *et al.*, 2003; Sunderkötter *et al.*, 2004; Ziegler-Heitbrock., 2010; Yang *et al.*, 2014).

## 1.2.2 Monocyte origins

Our current understanding of the origins of human monocytes has been predicted predominantly from data on mouse monocytes. From these data, we now know that haematopoietic stem cells (HSCs) in the bone marrow differentiate into monocytes via a series of committed steps (Figure 1.1) (Akashi *et al.*, 2000). HSCs give rise to myeloid and lymphoid-committed precursors (MP and LP). While LPs primarily give rise to lymphoid cells, MPs generate monocyte/macrophage and dendritic cell precursors (MDPs) that are responsible for generating common dendritic cell precursors (CDP), some macrophage subsets, and monocytes (Fogg *et al.*, 2006). Generation of monocytes from MDPs requires the growth factor colony-stimulating factor/CSF1-R (Dai *et al.*, 2002). Following their generation, classical monocytes egress from the bone marrow into the bloodstream in a CCR2-dependent manner (Kuziel *et al.*, 1997; Serbina and Pamer, 2006; Tsou *et al.*, 2007). The mechanisms involved in the egression of non-classical monocytes however, remain uncertain. Although the exact mechanisms are unknown, monocytes also emigrate from reservoirs in the spleen and lung (Van Furth and Sluiter, 1986; Swirski *et al.*, 2009).

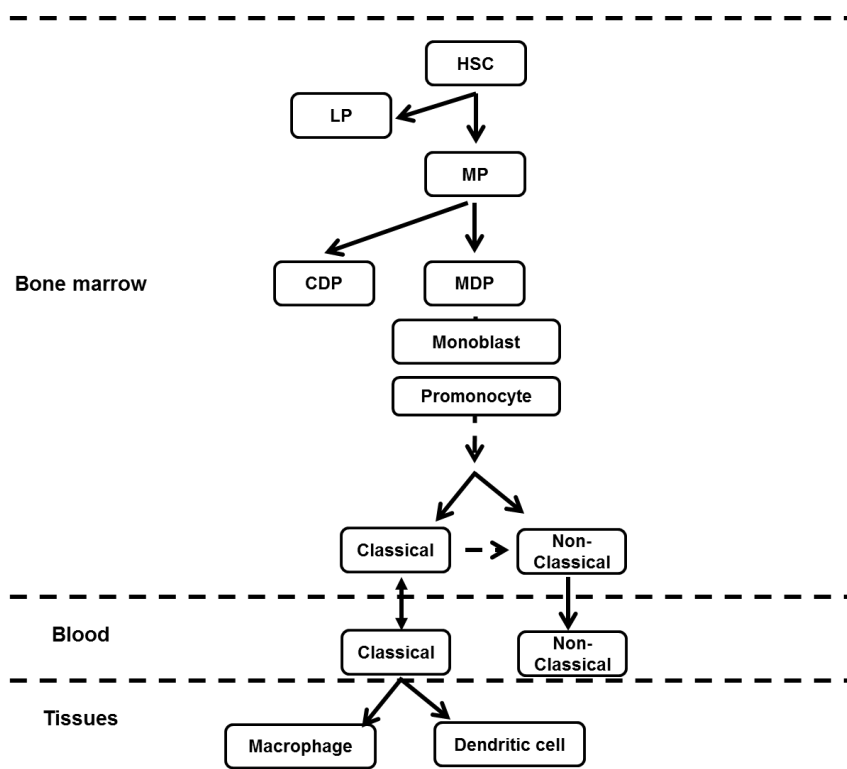


**Figure 1.1** Differentiation of monocytes in the bone marrow

HSCs generate monocytes through MDPs. During inflammation, classical monocytes generate macrophages and dendritic cells; however, in the absence of inflammation, classical monocytes return to the bone marrow where they generate intermediate and non-classical monocytes. Adapted from Geissmann *et al.* (2010).

### **1.2.3 Monocyte functions**

Monocytes roles are orchestrated by their expression of various innate scavenging and sensing receptors PRRs (Lauvau *et al.*, 2014). Some of the main roles undertaken by monocytes are discussed below.

#### **1.2.3.1 Recruitment during infection and inflammation**

##### **1.2.3.1.1 Bone marrow egression**

Classical human monocytes are key players in initiating innate immune responses during pathogen challenge (Lauvau *et al.*, 2014). While the exact functions of human classical monocytes are yet to be defined, studies on their mouse (Ly6C<sup>high</sup>) counterparts suggest that bacterial infection or inflammation drives the rapid egression of these cells from the bone marrow in a CCR2-dependent manner (Serbina and Pamer, 2006; Tsou *et al.*, 2007; Shi *et al.*, 2011). For example, during *Listeria monocytogenes* (LM) infection, increased levels of the CCR2 ligand CCL2 are released by bone marrow mesenchymal stromal cells (MSCs) and their progeny in a bid to drive monocytes towards endothelial cells, and from there, into the bloodstream (Serbina and Pamer 2006; Serbina *et al.*, 2008; Shi *et al.*, 2011). Evidence from other studies also suggests that another CCR2 ligand, CCL7, is equally involved in this process (Jia *et al.*, 2008).

##### **1.2.3.1.2 Sensing of warning signals**

Monocytes rely on a wide array of sensing machineries such as PRRs for the efficient detection of PAMPs or DAMPs associated with cellular damage or death. One example of an important PRR pathway is the Toll-like receptor-myeloid differentiation primary response gene (88) (TLR-MyD88) pathway. Early studies by Serbina *et al.* (2003a) were the first to propose an involvement of TLR-MyD88 in monocyte activation following LM infection. In their studies, the authors observed that LM-infected mouse macrophages activated classical (Ly6C<sup>high</sup>) monocytes by secreting CCL2 in a TLR-MyD88-dependent manner. Other monocyte cytosolic sensing machineries include, dead box polypeptide 41 (DDX41) and stimulator of interferon (IFN) genes (STING), both of which are involved in producing interferon gamma (IFN- $\gamma$ ) and inflammasome complexes for the production of interleukin 1-beta (IL-1 $\beta$ ) (Lauvau *et al.*, 2014).

##### **1.2.3.1.3 Trafficking and adhesion**

Following sensing of warning signals, monocytes rely on trafficking and adhesion molecules to promote their localisation into injured or infected tissues. Crucial to their

trafficking are ligands for CCR2 (Section 1.5.3), CX<sub>3</sub>CR1, CC-motif receptor 1 (CCR1), and CCR5 (Serbina and Pamer, 2006; Auffray *et al.*, 2009; Lauvau *et al.*, 2014).

Monocyte localisation at sites involves the leukocyte-adhesion cascade (Ley *et al.*, 2007), a pathway by which various selectins, arrest chemokines, and integrins mediate monocyte capture, rolling, and transmigration into the endothelium (Figure 1.2). The initial rolling of monocytes along the endothelium involves selectins, such as L-selectin and P-selectin, very late antigen 4 (VLA4;  $\alpha_4\beta_1$ -integrin) which is expressed by monocytes and facilitates their rolling by engaging with endothelial vascular cell-adhesion molecule-1 (VCAM-1) (Berlin *et al.*, 1995). Endothelial cells also induce the expression of intercellular adhesion molecule-1 (ICAM-1) near the foci of infection, which may be important for localising monocyte adhesion (Shi *et al.*, 2010).

Monocyte rolling is followed by their arrest (tethering), a process involving “arrest chemokines”, integrins, and adhesion molecules (Campbell *et al.*, 1998). The slow rolling of monocytes on the endothelium facilitates their arrest/adhesion and subsequent diapedesis (Figure 1.2). A specific example of an arrest chemokine is CCL5, which platelets deposit onto the inflamed endothelium (Von Hundelshausen *et al.*, 2001). The binding of chemokines to glycosaminoglycans (GAGs) located on the endothelial surface are also required for monocyte arrest (Johnson *et al.*, 2005). Arrest chemokines also facilitate monocyte adhesion by altering the affinity of integrins for adhesion molecules from a low-affinity conformation to a high-affinity conformation (Chan *et al.*, 2001). Monocyte adhesion may also involve pathways mediated by the enzyme phospholipase C and formyl peptide receptors which are required by integrins to assume a high-affinity conformation (Hyduk *et al.*, 2007; Wantha *et al.*, 2013).

#### **1.2.3.1.4 Transmigration/Diapedesis**

Monocyte transmigration into the endothelium is a rapid process facilitated by adhesion molecules such as ICAM-1 and VCAM-1 (Figure 1.2). Studies by Schenkel *et al.* (2004) have suggested that human peripheral blood monocytes move from areas of firm adhesion to the nearest preferred junction where they transmigrate. In the absence of adhesion molecules, monocytes are unable to polarise or adhere to the vascular endothelium, suggesting that adhesion molecules are critical for monocyte transmigration (Schenkel *et al.*, 2004).

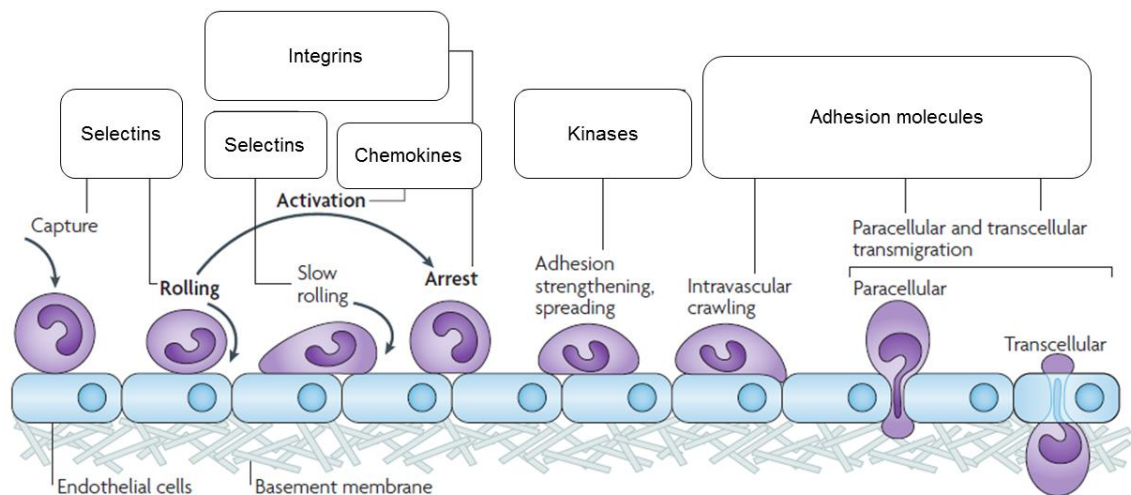


**Figure 1.2 The leukocyte adhesion cascade**

The leukocyte adhesion cascade describes the capture, rolling, activation, arrest, and transmigration of leukocytes. Adapted from Ley *et al.* (2007).

### 1.2.3.1.5 Phagocytosis

Monocytes are efficient phagocytes and produce reactive oxygen species, nitrogen species, and phagolysosomal enzymes in response to bacterial, fungal, parasitic, and viral infections (Serbina *et al.*, 2008). For example, during infection with LM, monocytes are recruited by infected macrophages and differentiate in a CCR2/TLR-MyD88-dependent manner into TNF $\alpha$  and inducible nitric oxide synthase (iNOS) – producing dendritic cells (TipDCs) (Randolph *et al.*, 1999; Serbina *et al.*, 2003a, 2003b). Monocyte differentiation into TipDCs is also facilitated by the synthesis of TNF $\alpha$  and interferon gamma (IFN- $\gamma$ ) by bacteria and recruited natural killer (NK) cells (Pamer, 2004). Following their generation, TipDCs carry phagocytosed particles towards the T-cell area of draining lymph nodes for clearance (Randolph *et al.*, 1999; Serbina *et al.*, 2003a, 2003b). Additional studies have suggested that mouse Ly6C<sup>high</sup> monocytes also contribute to the priming of cluster of differentiation 4 (CD4) T-cells during *Mycobacterium tuberculosis* (Mtb) infection (Samstein *et al.* 2013). The authors discovered that Ly6C<sup>high</sup> monocytes carried antigens towards the lymph nodes and transferred these to classical DCs (cDCs) which then presented these to antigen-specific CD4 T-cells, activating them for Mtb clearance.

### 1.2.3.2 Precursors for mononuclear phagocytes

Classical (CD14<sup>++</sup>/CD16<sup>-</sup>) monocytes are best known for their role as a direct source of tissue macrophages and antigen-presenting dendritic cells (DCs) (Figure 1.1) (Geissmann *et al.*, 2010). The mononuclear phagocyte-system (MPS) is composed of monocytes, macrophages, and DCs, and assumes that commitment of cells to a myeloid lineage is pre-determined in the bone marrow (Van Furth *et al.*, 1972). The MPS also assumes that

monocytes with their short half-life of 20 hours are a transient reservoir for tissue-resident macrophages and DCs since these are terminally differentiated and unable to self-proliferate (Van Furth *et al.*, 1972; Geissmann *et al.*, 2010).

However, the MPS has come under much scrutiny since the discovery of monocyte/macrophage and dendritic cell precursors (MDPs) which are directly responsible for generating monocytes, common dendritic cell precursors (CDP), and some macrophage subsets (Figure 1.1) (Fogg *et al.*, 2006). This suggests that DCs and macrophages do not rely solely on monocyte input for replenishment. Indeed, newer experimental approaches have established that most steady-state macrophages and DCs originate and self-proliferate independent of monocyte input (Hashimoto *et al.*, 2013; Yona *et al.*, 2013). The importance of the MPS has been further questioned following the discovery that tissue-resident macrophages pushed to the M2- (alternative-state) of activation by helminth infection or interleukin-4 (IL-4), can self-proliferate without monocyte input (Jenkins *et al.*, 2011). These findings are important since they suggest that a local proliferation of M2 macrophages may be important for fulfilling M2-associated functions such as wound healing, T-helper type 2 (Th2) lymphocyte responses and the resolution of inflammation (Martinez and Gordon, 2014).

### **1.2.3.3 Patrolling**

Peripheral blood monocytes act as a reservoir of effectors and scavengers that are activated when required. Studies in mice have revealed that non-classical (Ly6C<sup>low</sup>) monocytes participate in immune homeostasis by patrolling blood vessels to monitor PAMPs (Auffray *et al.*, 2007). Through their studies, the authors found that Ly6C<sup>low</sup> monocytes displayed a “crawling-” or “patrolling-” type behaviour along the endothelial lumen independent of the direction of blood-flow, a process facilitated by their high expression of CX<sub>3</sub>CR1 and the integrin, lymphocyte function-associated antigen-1 (LFA-1). Upon infection with LM, Ly6C<sup>low</sup> monocytes respond rapidly by migrating into infected tissues and releasing pro-inflammatory mediators such as TNF $\alpha$ , IL-1 $\beta$ , and chemokines for the recruitment of other cells (Auffray *et al.*, 2007). Studies by Cros *et al.* (2010) have demonstrated that human non-classical (CD14<sup>+</sup>/CD16<sup>++</sup>) monocytes also display a similar behaviour. Further studies (Carlin *et al.*, 2013) have suggested that non-classical monocytes also play a housekeeping role for vasculature and through toll-like receptor-7 (TLR7), recruit neutrophils for repairing endothelial integrity following damage.

### **1.2.4 Involvement in sterile inflammation**

While inflammation is beneficial for restoring organism homeostasis, it can also become detrimental if prolonged or excessive. Studies on mouse and human monocyte subsets

have revealed that excessive monocyte infiltration into tissues in the absence of infection leads to sterile inflammation, a major marker in the onset and progression of chronic inflammatory diseases such as atherosclerosis, rheumatoid arthritis, and stroke (Table 1.2) (Yang *et al.*, 2014).

**Table 1.2**      **Frequencies of monocytes in human pathologies**

Pathology	CD16 <sup>-</sup>	CD16 <sup>+</sup>
Rheumatoid arthritis	No change	↑2.2%
Coronary arterial disease		↑2.2 to 8%
Atherosclerosis	8% ↓	↑8%
Haemophagocytic syndrome		↑31%
Crohn's disease		↑5.7%
Cancer		↑13.3%
Stroke		↑3%
Tuberculosis	↓10%	↑9%
Sepsis	No change to ↓9.5%	↑11.5 to 12%

Adapted from Yang *et al.* (2014)

Although monocyte frequencies in human pathologies seem to be dependent on their expression of CD16, monocyte signalling and function during both innate immune responses and sterile inflammation is also regulated by G-protein-coupled receptors.

## 1.3 G-protein-coupled receptors (GPCRs)

### 1.3.1 General overview

GPCRs are a large family of receptor proteins responsible for mediating extracellular to intracellular signals within a broad range of physiological settings. Comprised of over 1000 genes, GPCRs represent a key therapeutic target for the pharmaceutical industry with almost half of all approved drugs targeting this class of proteins (Garland, 2013). Members of this group are subdivided into six families based on their sequence homology: A (rhodopsin-like), B (secretin-like), C (glutamate/pheromone), F (frizzled), adhesion, and others, with family members sharing up to 25% sequence homology (Pierce *et al.*, 2002). The rhodopsin-like (class A) family is the largest group of GPCRs and includes receptors for light (rhodopsin), chemokine receptors, and P1 and P2Y purinoceptors (Pierce *et al.*, 2002; Abbracchio *et al.*, 2006; Von Kügelgen, 2006; Fredholm *et al.*, 2011; Bachelier *et al.*, 2014).

### 1.3.2 GPCR structure

Our current understanding of the structure of GPCRs comes primarily from high-resolution crystallography structures of rhodopsin and the  $\beta$ 2-adrenergic receptor (Schertler *et al.*, 1993; Palczewski *et al.*, 2000; Rasmussen *et al.*, 2011). Together with the recently published high-resolution crystal structures of the human P2Y<sub>1</sub> and P2Y<sub>12</sub> purinoceptors (Zhang *et al.*, 2014; Zhang *et al.*, 2015), these have provided the molecular models from which most GPCR structures and protein dynamics have been elucidated.

In general, all GPCRs are characterised by a signature seven-transmembrane (7TM)  $\alpha$ -helix configuration, three extracellular loops (ECL1 to ECL3), three intracellular loops (ICL1 to ICL3), an extracellular N-terminal tail, and an intracellular C-terminal tail (Figure 1.3). Functionally, the extracellular domain controls ligand access, the 7TM region forms the main structural core and transduces any extracellular information to the intracellular domain via conformational changes, and the intracellular domain directs cellular signalling and physiological events by interacting with cytosolic effectors (Kobilka, 2007).

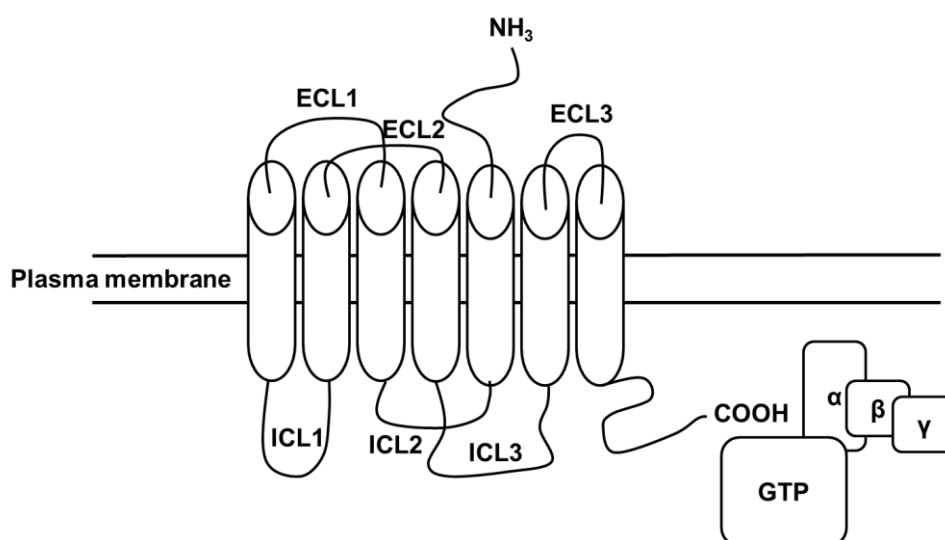


**Figure 1.3 G-protein-coupled receptor**

GPCRs generally comprise of a 7TM helical structure with an extracellular N-terminal domain (ammonia-NH<sub>3</sub>), and an intracellular C-terminal domain (carboxylic acid-COOH). The 7TM helical structures are connected by three extracellular loops (ECL1–ECL3) and three intracellular loops (ICL1–ICL3). Classical GPCR signalling involves a transduction of extracellular signals to an intracellular heterotrimeric G-protein comprising of  $\alpha$ ,  $\beta$ , and  $\gamma$  subunits. Adapted from Bridges and Lindsley (2008).

### 1.3.3 G-protein cycle

Classical GPCR activation involves a ligand-induced conformational change through the stabilisation of effector molecules such as heterotrimeric G-proteins comprising of  $\alpha$ ,  $\beta$ ,

and  $\gamma$  subunits (Pierce *et al.*, 2002) (Figure 1.3). The  $\alpha$  subunit binds to guanine triphosphate (GTP) and guanine diphosphate (GDP), while  $\beta$  and  $\gamma$  associate in an obligatory  $G\beta\gamma$  dimer (Evanko *et al.*, 2001).

The simplest kinetic model proposed for GPCR activation is the two-state model (Figure 1.4). This proposes that a receptor exists in equilibrium between two states, the low-affinity state (R), and the high-affinity state (R\*) (Leff, 1995). Full agonists bind R\*, inverse agonists to R, and partial agonists to R and R\* (Leff, 1995). In the low-affinity (R) state where  $G\alpha\beta\gamma$  has a low affinity for the GPCR,  $G\alpha$  remains tightly bound to  $G\beta\gamma$  and aids in plasma membrane localisation while preventing the spontaneous release of GDP by acting as a guanine-nucleotide dissociation inhibitor (GDI) (Brandt and Ross, 1985). In the high-affinity (R\*) state, the ligand-bound GPCR acts as a guanine-nucleotide exchange factor (GEF), and through its C-terminus, binds to the GDP-bound  $G\alpha\beta\gamma$  causing GDP to be replaced by GTP (Leifert *et al.*, 2005). This causes  $G\alpha$  and  $G\beta\gamma$  to separate, leaving them free to activate downstream effectors. Signalling by  $G\alpha$  and  $G\beta\gamma$  terminates upon hydrolysis of GTP by GTPase, which leads to a re-association of GTP-bound  $G\alpha$  to  $G\beta\gamma$  (Bridges and Lindsley, 2008).

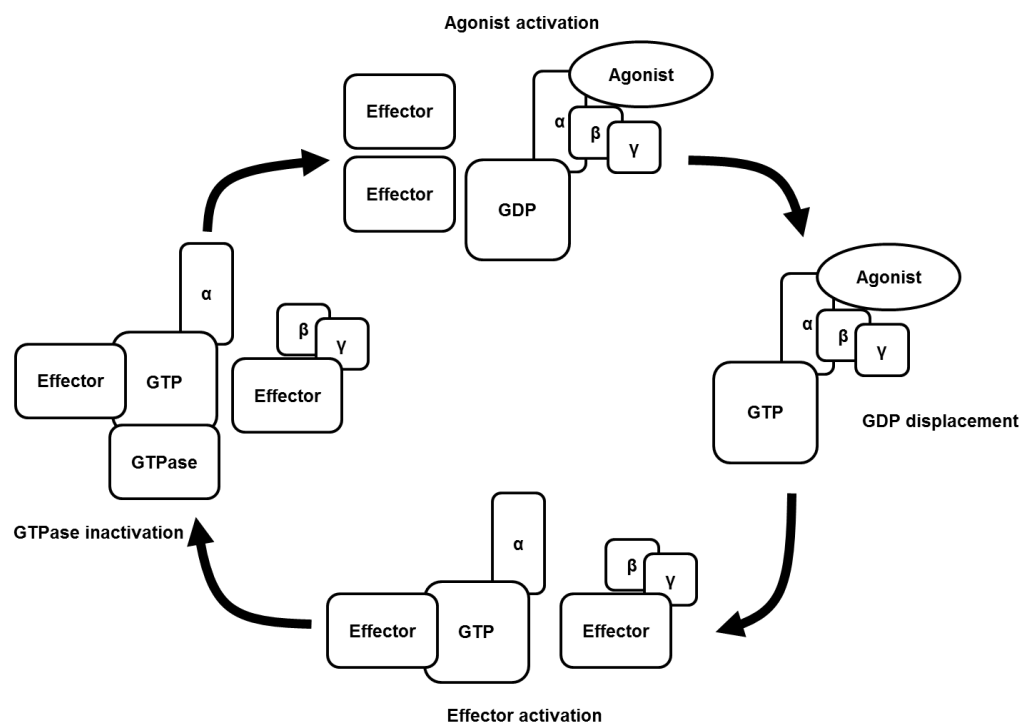


**Figure 1.4 G-protein cycle**

Upon activation, GDP dissociates from  $G\alpha$  and is replaced by GTP, leading to a dissociation of  $G\alpha\beta\gamma$  and effector activation by  $G\alpha$  and  $G\beta\gamma$ . The G-protein cycle is terminated by GTPase leading to a re-association of  $G\alpha\beta\gamma$ . Adapted from Bridges and Lindsley (2008).

### 1.3.4 Heterotrimeric G-protein effectors

The downstream signalling cascades driven by GPCRs depend on the isoforms of  $G\alpha$ ,  $G\beta$ , and  $G\gamma$  activated. In humans, there are 15  $G\alpha$ , 5  $G\beta$ , and 12  $G\gamma$  genes that encode for  $G\alpha$ ,  $G\beta$ , and  $G\gamma$  subunits (Wettschureck and Offermanns, 2005). Heterotrimeric G-proteins are generally referred to by their  $G\alpha$  subunits and are classed into four main families based on their sequence homology and their sensitivity to *Bordetella Pertussis* (PTx), a bacterial toxin able to ribosylate adenosine 5'-diphosphate (ADP) of the GDP-bound heterotrimer (Table 1.3) (Katada, 2012).

**Table 1.3 Heterotrimeric  $G\alpha$ -proteins and their effectors**

<b><math>G\alpha</math>-protein class</b>	<b>Main Effector(s)</b>	<b>PTx sensitive?</b>
$G\alpha_s$ ( $G\alpha_s$ , $G\alpha_{sXL}$ , $G\alpha_{olf}$ )	Activation of adenylylate cyclase	No
$G\alpha_{i/o}$ ( $G\alpha_{i1}$ , $G\alpha_{i2}$ , $G\alpha_{i3}$ , $G\alpha_o$ , $G\alpha_z$ , $G\alpha_{gust}$ , $G\alpha_{t-r}$ , $G\alpha_{t-c}$ )	Inhibition of adenylylate cyclase/ Activation of phospholipase C $\beta$	Yes
$G\alpha_{q/11}$ ( $G\alpha_q$ , $G\alpha_{11}$ , $G\alpha_{14}$ , $G\alpha_{15/16}$ )	Activation of phospholipase C $\beta$	No
$G\alpha_{12/13}$ ( $G\alpha_{12}$ , $G\alpha_{13}$ )	Activation of Rho GTPases	No

Adapted from Wettschureck and Offermanns (2005)

#### 1.3.4.1 Main effectors of $G\alpha$ and $G\beta\gamma$ subunits

##### 1.3.4.1.1 Adenylylate cyclase (AC)

The AC enzymes (E.C. 4.6.1.1) are a well-established effector of  $G\alpha$  subunits of the  $G\alpha_s$  and  $G\alpha_{i/o}$  class of G-proteins, but are also modulated by  $G\beta\gamma$  (when activated by  $G\alpha_s$ ), calcium ions ( $Ca^{2+}$ ), and protein kinases (Hanoune and Defer, 2001).

ACs are important for controlling the synthesis of cyclic adenosine 3',5'-monophosphate (cAMP), a prototypical signalling molecule involved in regulating protein kinase A, phosphodiesterases, cyclic nucleotide-gated ion channels, and small G-protein regulating exchange proteins activated by cAMP (EPACs) (Gancedo, 2013). In mammals, ten AC genes (*AC1-10*) have been cloned and characterised, *AC1-9* encode for transmembrane ACs (tmACs) mainly regulated by GPCRs, and *AC10* encodes for a soluble AC (sAC) mainly activated by adenosine 5'-triphosphate (ATP) and  $Ca^{2+}$  (Sunahara and Taussig, 2002).

Structurally, mammalian ACs comprise of two homologous catalytic domains (C1 and C2) forming a heterodimer. While C1 comprises of only a small amount of catalytic residues, C2 comprises of a complementary set of residues that are essential for AC activity (Krupinski *et al.*, 1989). Although all tmAC structures comprise of bound  $G\alpha_s$  subunits and are activated directly by  $G\alpha_s$ , tmACs 1, 5, and 6 can also be inhibited by  $G\alpha_{i/o}$ -type G-proteins (Sunahara and Taussig, 2002).

#### 1.3.4.1.2 Phospholipase C (PLC)

The PLC enzymes (EC 3.1.4.3) are a family of soluble cytosolic enzymes responsible for the hydrolysis of phosphatidylinositol 4,5-bisphosphate ( $PIP_2$ ) for the generation of inositol 1,4,5-trisphosphate ( $IP_3$ ) and the signalling lipid diacylglycerol (DAG) (Figure 1.5). The PLC family is comprised of thirteen members grouped into six different classes ( $\beta$ ,  $\gamma$ ,  $\delta$ ,  $\epsilon$ ,  $\zeta$ , and  $\eta$ ) depending on their structure and regulatory mechanisms (Fukami *et al.*, 2010). Of these, only PLC $\beta$ , PLC $\epsilon$  and PLC $\eta$  are activated directly by heterotrimeric G-proteins, and are a well-established effector of  $G\alpha$  subunits of the  $G\alpha_{q/11}$  class of G-proteins and  $G\beta\gamma$  subunits of the  $G\alpha_{i/o}$  class of G-proteins (Blank *et al.*, 1992; Boyer *et al.*, 1992; Smrcka *et al.*, 1993; Kadamur and Ross, 2013).

Structurally, PLC isoenzymes comprise of subtype-specific domains and conserved core domains, which include a pleckstrin homology (PH) domain located in the N-terminal domain, a series of EF hands, a catalytic triose phosphate isomerase (TIM) barrel, and a C-terminal C2 domain (Bunney and Katan, 2011). Evidence from fluorescence resonance energy transfer (FRET) assays suggests that PLC activation by the  $G\beta\gamma$  dimer involves a direct binding of  $G\beta\gamma$  to the PH domain during activation (Wang *et al.*, 1999).

As mentioned above, the principle substrate of PLC is  $PIP_2$ . As a signalling molecule,  $PIP_2$  acts a membrane anchor for proteins (Falkenburger *et al.*, 2010).  $PIP_2$  is also utilised as a substrate for the synthesis of phosphatidylinositol 3,4,5-trisphosphate ( $PIP_3$ ), a signalling lipid involved in controlling many cellular processes (Cantley, 2002). Although  $PIP_2$  is important for cellular signalling, the formation of  $IP_3$  and DAG from  $PIP_2$  is essential for mammalian cell signalling and function.  $IP_3$  is required for the release of intracellular  $Ca^{2+}$  from internal  $Ca^{2+}$  stores such as the endoplasmic reticulum (ER) (Figure 1.5) (Berridge, 1983; Streb *et al.*, 1983). This process, which occurs through the activation of  $IP_3$  receptors ( $IP_3Rs$ ), is crucial for the regulation of metabolic and regulatory processes such as cell differentiation, proliferation, exocytosis, and tissue contraction (Berridge, 2009). The signalling lipid DAG is a signalling molecule in its own right but also serves as a precursor for other signalling lipids (Baldanzi, 2014). Signalling cascades regulated by DAG occur typically through the activation of target proteins such as protein

kinase C, Munc13s, protein kinase D, Ras guanyl nucleotide-releasing proteins (RasGRP), and chimaerins (Baldanzi, 2014).

### 1.3.4.1.3 Phosphoinositide-3-kinases (PI3Ks)

The G $\beta\gamma$  subunit can also directly activate PI3Ks (Figure 1.5) (Krugmann *et al.*, 1999; Brock *et al.*, 2003). The PI3Ks are subdivided into three classes (Type IA, IB, and II) based on their substrate requirements and mechanism of action (Katso *et al.*, 2001). Of these, only PI3K $\gamma$  (p110 $\gamma$ ) a Type IB class of PI3Ks, is activated by GPCRs (Krugmann *et al.*, 1999; Brock *et al.*, 2003). Activation of PI3Ks by G $\beta\gamma$  is important for modulating signalling pathways involved in cell growth, survival, and migration (Foster *et al.*, 2003). The requirement of PI3K for efficient immune cell chemotaxis and polarity is also widely accepted. For example, neutrophils and macrophages require PI3K activation at the leading edge for cell polarisation and chemotaxis (Li *et al.*, 2000; Hirsch *et al.*, 2000; Wang *et al.*, 2002).

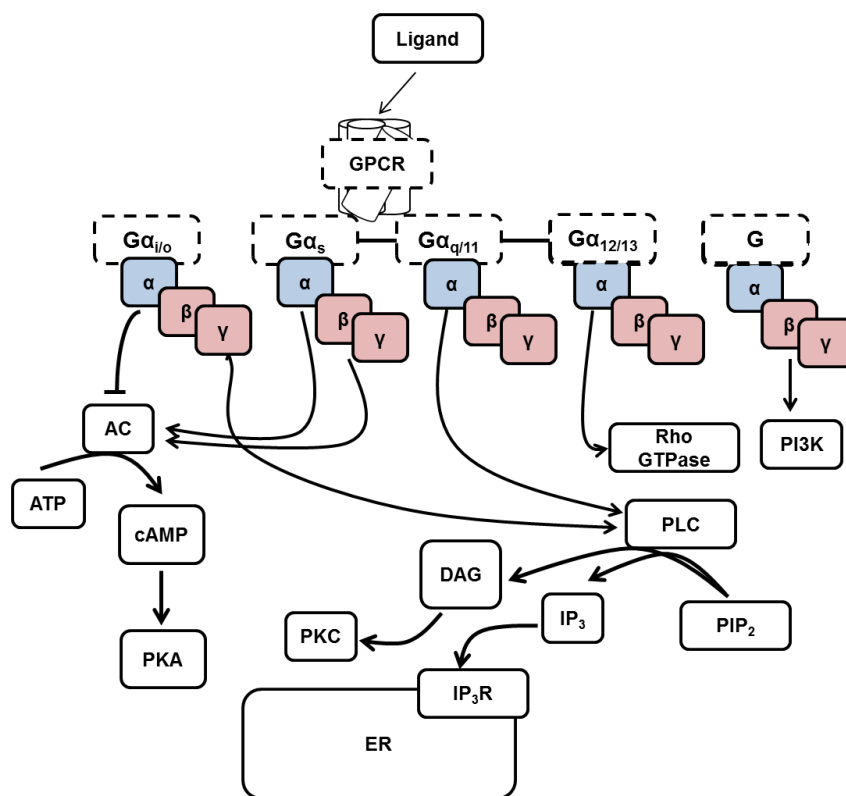


**Figure 1.5 Classical GPCR pathways**

Upon activation, G $\alpha$  and G $\beta\gamma$  activate different downstream effectors. Modulation of AC is achieved by G $\alpha$  subunits of the G $\alpha_s$  and G $\alpha_{i/o}$ -type G-proteins (and G $\beta\gamma$  when activated by G $\alpha_s$ ). PLC is activated by G $\alpha$  subunits of the G $\alpha_{q/11}$ -type G-proteins and G $\beta\gamma$  subunits of the G $\alpha_{i/o}$ -type G-proteins. Rho GTPase is activated by G $\alpha$  subunits of the G $\alpha_{12/13}$  (and G $\alpha_{q/11}$ )-type G-proteins. G $\beta\gamma$  dimers are also involved in activating PI3K. PLC activation is important for Ca $^{2+}$  release from internal Ca $^{2+}$  stores.

### 1.3.5 Regulation of GPCR signalling

Although it is widely accepted that GTPases regulate GPCR activation (Figure 1.4), in recent years, it has become apparent that other mechanisms play a similar role. The purpose of these mechanisms discussed below is to protect GPCRs from over-activation, thereby allowing subsequent GPCR-mediated responses to remain close to the ambient stimulation level.

#### 1.3.5.1 Receptor expression and trafficking

The expression of a GPCR on the cell surface is influenced by how efficiently it is assembled in the ER, packaged in the Golgi complex, and delivered to the plasma membrane (Dong *et al.*, 2007). The primary location for receptor production is the ER. Here, receptors must be correctly synthesised, folded and matured before they can be packaged into coat protein complex II (COPII) transport vesicles and trafficked to the ER-Golgi intermediate complex (ERGIC), the Golgi complex, and to the trans-Golgi network (TGN) for final assembly and maturation prior to trafficking to the plasma membrane (Dong *et al.*, 2007). The individual steps taken by a GPCR from the ER to the plasma membrane are determined by specific GPCR membrane-proximal C-terminal and extracellular N-terminal amino acid motifs (Duvernay *et al.*, 2005). These determine the concentration of components for delivery to the Golgi complex, their rate of delivery, and their packaging in COPII vesicles (Duvernay *et al.*, 2005; Dong *et al.*, 2007).

While motifs can also prevent the export of incorrectly assembled GPCRs, accessory (chaperone) proteins within the ER and at the cell surface also fulfil this role (Margeta-Mitrovic *et al.*, 2000; Ellgaard and Helenius, 2001). Chaperone proteins such as calnexin and calreticulin bind to carbohydrate chains of GPCR intermediates and stabilise correct conformations whilst preventing their misfolding (Williams, 2006). Correct conformations are passed from one chaperone to another until the correct and final conformation is achieved. In the same manner, chaperones can also prevent the export of incorrect conformations and promote their degradation by the cytoplasmic ubiquitin–proteasome system (UPS) (Meusser *et al.*, 2005).

#### 1.3.5.2 Receptor desensitisation

Repeat or prolonged exposure of a GPCR to a ligand can lead to a dampened response due to receptor desensitisation, a mechanism by which GPCRs restore themselves to full functional capacity. At the receptor level, GPCRs can be desensitised through homologous or agonist-specific desensitisation by the G-protein-coupled receptor kinase (GRK)– $\beta$ -arrestin system (Pitcher *et al.*, 1998). Comprised of a family of seven GRK isoenzymes (GRK1–GRK7) and four arrestin isoforms (arrestin1-4), the GRK- $\beta$ -arrestin

system selectively targets the active ( $R^*$ ) ligand-bound state of the receptor (Pitcher *et al.*, 1998; Claing *et al.*, 2002). GRKs specifically phosphorylate the serine and threonine residues in GPCR C-terminal domains thereby preventing ligand interaction. While this is alone capable of desensitising GPCRs, GRK phosphorylation also leads to the recruitment of arrestins that further desensitise GPCRs by displacing heterotrimeric G-proteins (Claing *et al.*, 2002).

GPCRs are also desensitised through negative-feedback signals generated by GPCR-activated kinases (Gainetdinov *et al.*, 2004). For example, PKA and protein PKC can alter the responsiveness of multiple GPCRs by uncoupling these from heterotrimeric G-proteins or by causing GPCRs to switch from one G-protein to another (Daaka *et al.*, 1997).

The recent identification of regulators of G-protein signalling (RGS) proteins has also enhanced our understanding of GPCR desensitisation. Approximately 25 RGS proteins exist, with individual members grouped into four classes (R4, R7, R12 and RZ) based on their sequence homology (Ross and Wilkie, 2000). RGS proteins act as GTPase activating proteins (GAPs), accelerating the hydrolysis of GTP-bound  $G\alpha$  of  $G\alpha_{q/11}$  and  $G\alpha_{i/o}$ -type G-proteins. As a result, receptor signalling is dampened or completely inactivated (Ross and Wilkie, 2000).

### **1.3.5.3 Receptor internalisation/endocytosis**

Prolonged or repeat ligand exposure can also cause GPCRs to draw away from the cell surface (Chuang and Costa, 1979). While receptor internalisation can occur by a number of different mechanisms (Pierce *et al.*, 2002), a well-studied example is via clathrin-coated pits, a process dependent on arrestins and dynamin, and reliant on the GRK- $\beta$ -arrestin system (Ferguson *et al.*, 1996). During this process, arrestins such as  $\beta$ -arrestin and arrestin-3 are recruited by GRK-dependent phosphorylation. These bind to the heavy chain and  $\beta$ 2-adaptin subunit of clathrin, thereby forming a stable interaction with a clathrin-coated pit (Goodman *et al.*, 1996). As a result, the GTPase dynamin oligomerises, leading to the production of a helical extension at the neck of the pit, which facilitates the withdrawal of GPCRs from the cell surface (Claing *et al.*, 2002). Receptors are either internalised into endosomes and dephosphorylated, resensitised and recycled rapidly back to the cell surface, recycled slowly (4 hours) in larger endosomes, or degraded (down-regulated) (Ferguson *et al.*, 2001).

## 1.4 Calcium (Ca<sup>2+</sup>) signalling

### 1.4.1 General overview

Ca<sup>2+</sup> is a highly versatile and ubiquitous second messenger that is released in response to GPCR activation. It is involved in regulating a diverse number of cellular processes such as cell differentiation, migration, death, and neurotransmission (Berridge *et al.*, 2000). Cellular processes regulated by Ca<sup>2+</sup> are initiated by a simple rise in cytosolic levels of Ca<sup>2+</sup> ([Ca<sup>2+</sup>]<sub>i</sub>) from 100 nM to roughly 1 μM in response to external stimuli such as neurotransmitters, hormones, and agonists (Berridge *et al.*, 2000; Patel and Docampo, 2010). However, in order to control the occurrence and magnitude of physiological events dependent on a rise in [Ca<sup>2+</sup>]<sub>i</sub>, its release and influx must be regulated in a time-dependent manner. The system responsible for ensuring this is a sophisticated cell-specific calcium-signalling toolkit that is comprised of a complex network of Ca<sup>2+</sup> channels, organelles, Ca<sup>2+</sup> pumps and signalling components that constantly evolve depending on the circumstances under which they are required (Berridge *et al.*, 2000).

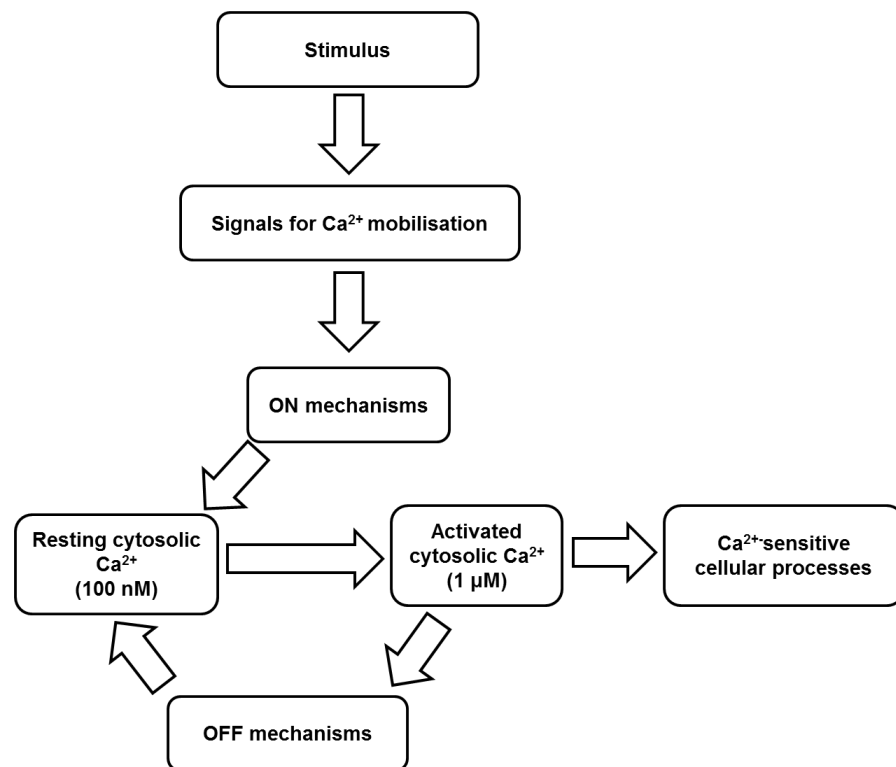


**Figure 1.6 Overview of Ca<sup>2+</sup> signalling**

Stimuli generate signals that activate ON mechanisms to trigger increases in [Ca<sup>2+</sup>]<sub>i</sub> by either releasing Ca<sup>2+</sup> from stores or allowing Ca<sup>2+</sup> influx. Following its release, Ca<sup>2+</sup> levels are rapidly brought down to cytosolic levels by OFF mechanisms. Adapted from Berridge *et al.* (2000).

## 1.4.2 ON mechanisms

Cytosolic  $\text{Ca}^{2+}$  is increased by “ON mechanisms” to enable the relaying of essential information required for inducing downstream signalling events (Berridge *et al.*, 2000; Bootman *et al.*, 2001). ON mechanisms allow  $\text{Ca}^{2+}$  signals to be generated either by allowing  $\text{Ca}^{2+}$  influx from the extracellular space, or by allowing  $\text{Ca}^{2+}$  to be released from internal stores (Bootman *et al.*, 2001; Berridge, 2002). Mechanisms allowing  $\text{Ca}^{2+}$  influx include the receptor-operated (ROCC), voltage-operated (VOCC), and store-operated (SOCC)  $\text{Ca}^{2+}$  channels located in the plasma membrane. Internal stores containing high concentrations of  $\text{Ca}^{2+}$  include the endoplasmic reticulum (ER), sarcoendoplasmic reticulum (SR, muscle cells), mitochondria, and acidic organelles such as acidocalcisomes, lysosomes, and the Golgi apparatus (Bootman *et al.*, 2001; Berridge, 2002; Patel and Docampo, 2010).

### 1.4.2.1 Channel-mediated $\text{Ca}^{2+}$ influx and release

A diverse set of plasma membrane and intracellular ROCCs modulate increases in cytosolic  $\text{Ca}^{2+}$  following external stimuli. Examples of plasma membrane ROCCs include the nicotinic acetylcholine receptor and the P2X purinoceptors (North, 2002; Albuquerque *et al.*, 2009). Other cell surface ROCCs such as GPCRs and protein tyrosine kinase-linked receptors (PTRKs) can raise cytosolic  $\text{Ca}^{2+}$  either by promoting  $\text{Ca}^{2+}$  release through the activation of PLC (Section 1.3.4.2.1), or by allowing  $\text{Ca}^{2+}$  influx via TRPC and SOCCs; the latter an indirect consequence of store-depletion (Hofmann, *et al.*, 1999). The  $\text{Ca}^{2+}$ -induced- $\text{Ca}^{2+}$ -release (CICR) receptors  $\text{IP}_3\text{R}$  and RyR (Section 1.4.2.2) are also ROCCs, and promote the release of  $\text{Ca}^{2+}$  from internal stores such as the ER (Vetter, 2012).

Membrane depolarisation in response to electrical excitation can also lead to  $\text{Ca}^{2+}$  entry through cell surface VOCCs such as  $\text{Ca}_v1$  (L-type),  $\text{Ca}_v2$  (N-, P/Q- and R-type), and  $\text{Ca}_v3$  (T-type) channels (Catterall, 2000; Clapham, 2007). Of these channels, the L-type channels are the most well studied, and are expressed by excitable cells and non-excitable cells such as immune cells where they regulate  $\text{Ca}^{2+}$  signalling, cell activation and survival (Suzuki *et al.*, 2010). VOCCs allow  $\text{Ca}^{2+}$  levels to be increased directly by allowing  $\text{Ca}^{2+}$  influx, but also indirectly by triggering CICR through  $\text{IP}_3\text{R}$  and RyR (Berridge *et al.*, 2000).

The SOCCs are auto-regulatory plasma membrane channels that open in response to internal store depletion. Their simple aim is to raise  $[\text{Ca}^{2+}]_i$  via store-operated calcium entry (SOCE; also known as capacitative calcium entry) so that excess cytosolic  $\text{Ca}^{2+}$  can be sequestered by  $\text{Ca}^{2+}$  pumps and exchangers to allow a refilling of internal  $\text{Ca}^{2+}$  stores

(Putney, 2001; Parekh and Putney, 2005). A well-studied example is the  $\text{Ca}^{2+}$ -release activated  $\text{Ca}^{2+}$  channel (CRAC), which is activated entirely by ER  $\text{Ca}^{2+}$  depletion (Feske, 2010).

#### 1.4.2.2 Store-mediated $\text{Ca}^{2+}$ release

Internal stores (intracellular organelles) such as the ER represent a major source of  $\text{Ca}^{2+}$  from which many cell types generate  $\text{Ca}^{2+}$  signals. As mentioned previously,  $\text{Ca}^{2+}$  release from the ER primarily involves the activation of  $\text{IP}_3\text{Rs}$  by  $\text{IP}_3$ , a product formed from the hydrolysis of  $\text{PIP}_2$  by PLC (Berridge, 1993, 2009). Further increases in  $[\text{Ca}^{2+}]_i$  via the ER are achieved through CICR (Berridge, 2002).

Mitochondria, which are essential for aerobic metabolism and cell survival, are a second type of organelle important for regulating  $[\text{Ca}^{2+}]_i$  (Murchison and Griffith, 2000).  $\text{Ca}^{2+}$  release and uptake by mitochondria involves a sodium ( $\text{Na}^+$ )-dependent  $\text{Ca}^{2+}$  exchanger (mNCX) (Carafoli *et al.*, 1974; Murchison and Griffith, 2000). Mitochondria are also key players in apoptosis, where excessive levels of  $\text{Ca}^{2+}$  sequestered by mitochondria lead to the opening of permeability transition pores (PTP), forcing mitochondria to release  $\text{Ca}^{2+}$  and pro-apoptotic factors such as oxygen species and cytochrome C into the cytoplasm (Hajnóczky *et al.*, 2003).

$\text{Ca}^{2+}$  can also be stored and released from acidic organelles. Acidocalcisomes are a family of organelles represented by examples such as basophilic granules and platelet dense granules (Docampo and Moreno, 2011). These are rich in  $\text{Ca}^{2+}$  and serve several functions including the storage of cations, osmoregulation, and maintenance of cellular pH (Patel and Docampo, 2010; Docampo and Moreno, 2011). Lysosomes are a second type of organelle and are primarily involved in degrading and recycling extracellular particles and apoptotic bodies delivered by endocytic and autophagic routes (Patel and Docampo, 2010). As  $\text{Ca}^{2+}$ -storing organelles, lysosomes can release  $\text{Ca}^{2+}$  into the cytosol upon exposure to the cathepsin-C substrate, glycyl-L-phenylalanine-naphthylamide (GPN) (Berg *et al.*, 1994). The second messenger nicotinic acid–adenine dinucleotide phosphate (NAADP) is also known to mobilise  $\text{Ca}^{2+}$  from lysosomes and other organelles through a modulation of transient receptor potential cation channel, mucolipin subfamily (TRPML) channels and two-pore channels (Zhang *et al.*, 2009; Patel *et al.*, 2010).

The Golgi apparatus (GA) and its associated secretory organelles represent a centralised sorting and processing station concerned with ensuring that proteins synthesised by the ER are correctly glycosylated and packaged into carrier proteins prior to dispatch to their final destinations (Jackson, 2009). However, it is now apparent that the GA, like the ER, is a bona fide  $\text{IP}_3$ -sensitive  $\text{Ca}^{2+}$  store (Pinton *et al.*, 1998). In addition to its sensitivity to  $\text{IP}_3$ , the GA is also NAADP-sensitive (Mitchell *et al.*, 2003).  $\text{Ca}^{2+}$  released by the GA is

required for generating cytosolic  $\text{Ca}^{2+}$  signals and for ensuring the efficient function of enzymes and components involved in protein processing and packaging (Vanoevelen *et al.*, 2005).

#### **1.4.2.3 $\text{Ca}^{2+}$ -binding proteins/ $\text{Ca}^{2+}$ buffers**

Translation of  $\text{Ca}^{2+}$  signals into cellular responses involves the participation of  $\text{Ca}^{2+}$ -binding proteins (CBP), a diverse group of proteins that regulate  $[\text{Ca}^{2+}]_i$  either by transporting  $\text{Ca}^{2+}$  across membranes for participation in cellular functions during ON reactions, or by acting as  $\text{Ca}^{2+}$  sensors and buffers during OFF reactions (Berridge *et al.*, 2003). The CBPs are low-affinity/high-capacity binders of  $\text{Ca}^{2+}$  and can exist either as mobile proteins found in the cytosol or extracellular space (e.g. calmodulin), or non-mobile proteins found in membranes (e.g. calreticulin) (Yáñez *et al.*, 2012).

#### **1.4.3 OFF mechanisms**

Following completion of its signalling functions,  $\text{Ca}^{2+}$  is rapidly removed from the cytosol in order to prevent  $\text{Ca}^{2+}$  overload, which can cause cell necrosis and apoptosis (Berridge, *et al.*, 2000, 2003; Hajnóczky *et al.*, 2003). The calcium signalling toolkit has equipped itself with a number of sophisticated OFF mechanisms that work collectively to return  $[\text{Ca}^{2+}]_i$  to resting levels (100 nM). Components of this system include various  $\text{Ca}^{2+}$  pumps, exchangers, and buffers (latter discussed in Section 1.4.2.3) that facilitate  $\text{Ca}^{2+}$  extrusion or sequestration.

##### **1.4.3.1 $\text{Ca}^{2+}$ pumps and exchangers**

The calcium-signalling toolkit consists of a number of pumps that remove  $\text{Ca}^{2+}$  from the cytosol either by extruding it from the cell, or by sequestering it into intracellular organelles. The contribution of individual pumps depends on the  $[\text{Ca}^{2+}]_i$ , where lower concentrations of  $\text{Ca}^{2+}$  are cleared by higher affinity systems, and higher concentrations are cleared by lower-affinity mechanisms.

The plasma membrane  $\text{Ca}^{2+}$ -ATPases (PMCA) and the  $\text{Na}^+/\text{Ca}^{2+}$  exchanger (NCX) remove excess  $\text{Ca}^{2+}$  by extruding it from the cell (Brini and Carafoli, 2011). The PMCA are encoded by four genes (*PMCA1 to PMCA4*) and are considered high-affinity, low-capacity P-type ATPases since they utilise ATP to produce an aspartyl-phosphate intermediate (Guerini *et al.*, 2005; Brini and Carafoli, 2011). PMCA exist in two conformational states, an E1 state that binds to  $\text{Ca}^{2+}$  in the cytosol with a high-affinity, and a low-affinity E2 state that releases  $\text{Ca}^{2+}$  from the cell (Guerini *et al.*, 2005). PMCA coordinate  $\text{Ca}^{2+}$  extrusion with the low-affinity, high-capacity NCX pumps (Marchand *et al.*, 2012). Encoded by three genes (*NCX1 to NCX3*), the NCX pumps are fully reversible

pumps which remove  $\text{Ca}^{2+}$  from the cytosol using the electrochemical gradient of three sodium ( $\text{Na}^+$ ) ions to remove a single  $\text{Ca}^{2+}$  ion (Brini and Carafoli, 2011).

Intracellular organelles also sequester excess cytosolic  $\text{Ca}^{2+}$ . Sequestration into the ER and NAADP-sensitive lysosomes is through the high-affinity sarco/endoplasmic reticulum  $\text{Ca}^{2+}$  ATPase (SERCA) pump, a P-type ATPase (Periasamy and Kalyanasundaram, 2007). However, unlike other  $\text{Ca}^{2+}$  pumps, SERCA is also important for replenishing the ER following  $\text{Ca}^{2+}$  depletion (Clapham, 2007). To date, three major isoforms of SERCA have been identified (SERCA1 (a-b), SERCA2 (a-d) and SERCA3 (a-f)), which are encoded by the genes *ATP2A1*, *ATP2A2* and *ATP2A3* (Periasamy and Kalyanasundaram, 2007).

Sequestration of cytosolic  $\text{Ca}^{2+}$  by mitochondrion is important for regulating cell processes such as metabolism, respiration, and oxidative phosphorylation (Murchison and Griffith, 2000). However, mitochondrial uptake is also important during  $\text{Ca}^{2+}$  overload (Hajnóczky *et al.*, 2003). Mitochondrial  $\text{Ca}^{2+}$  uptake depends largely on its close proximity to the ER and the activation of voltage dependent anion channels (VDAC) that facilitate  $\text{Ca}^{2+}$  diffusion through the outer mitochondrial membrane (OMM) (Raffaello *et al.*, 2012). Diffusion of  $\text{Ca}^{2+}$  through the inner mitochondrial membrane (IMM) is driven by the mitochondrial  $\text{Ca}^{2+}$  uniporter (MCU), a low-affinity, high-capacity transmembrane protein activated when cytosolic  $\text{Ca}^{2+}$  levels are in excess of levels regulated by other mechanisms (Kirichok *et al.*, 2004; De Stefani *et al.*, 2011).  $\text{Ca}^{2+}$  uptake by the uniporter is driven by an electrochemical gradient generated by the respiratory chain (Kirichok *et al.*, 2004; De Stefani *et al.*, 2011).

## 1.5 Chemokines

### 1.5.1 General overview

The chemokines are a family of low molecular weight (~70 amino acid) chemotactic peptides that stimulate the release of intracellular  $\text{Ca}^{2+}$  from internal stores as a prerequisite to their primary role, which is to direct the polarisation and migration of monocytes and other immune cells (Rollins, 1997). By directing cellular migration, chemokines play a crucial role not only in embryonic development and host defence, but also in the development of inflammatory diseases (Raman *et al.*, 2011). Chemokines can be broadly classified as being either homeostatic, (involved in cell trafficking, e.g. chemokine (CC-motif) ligand 21 (CCL21)), inflammatory (synthesised in response to inflammatory insult, e.g. chemokine (CXC-motif) ligand 8 (CXCL8)), or both (e.g. CCL2).

To date, around 50 chemokines have been identified, with almost all members secreted from the cell upon synthesis (Bachelier *et al.*, 2014). Chemokines are grouped into four

classes (C, CC, CXC and CX<sub>3</sub>C) based on the number and location of their conserved cysteine residues which can either be adjacent or separated by amino acids (Figure 1.6) (Zlotnik and Yoshie, 2000). The current system replaces the previous system where chemokines were given multiple names. For example, CCL2 has many synonyms including, monocyte-chemoattractant protein-1 (MCP-1) and small inducible cytokine A2 (SCYA2) (Zlotnik and Yoshie, 2000).

All chemokines exhibit a highly variable sequence homology but in general, have a conserved tertiary structure consisting of a disordered 6-10aa N-terminal region followed by a long loop (N loop) that ends in a 310 helix, a three-stranded  $\beta$ -sheet, and a C-terminal  $\alpha$ -helical domain (Allen *et al.*, 2007).

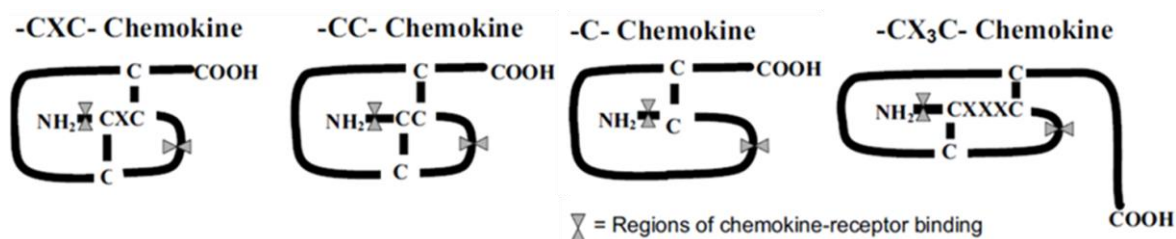


**Figure 1.7 Chemokine families**

CXC chemokines have one amino acid separated by two adjacent conserved cysteine residues, the CC chemokines have two adjacent conserved cysteine residues, the C chemokines have one conserved cysteine residue, and the CX<sub>3</sub>C chemokine CX<sub>3</sub>CL1 (fractalkine), has three amino acids separated by four conserved cysteine residues (Townson and Liptak, 2003).

### 1.5.2 Chemokine receptors and ligand pairings

Chemokines exert their effects through the activation of receptors. However, due to their promiscuous nature, chemokines often activate multiple receptors. To date, 24 mammalian chemokine receptors have been cloned, of which six are atypical G-protein-independent, arrestin-dependent receptors (Figure 1.7) (Bachelier *et al.*, 2014). While the majority of chemokines exert their effects through the activation of class-A GPCRs coupled to G $\alpha_{i/o}$ -type G-proteins (Section 1.3), members of the CXC and CC families can also activate atypical receptors. Studies on human embryonic kidney 293 (HEK293) and 300-19 pre-B cells transfected with G $\alpha_{i/o}$ , G $\alpha_s$ , or G $\alpha_{q/11}$ , have shown that G $\alpha_{i/o}$  and G $\beta\gamma$  are required for chemotaxis (Arai *et al.*, 1997; Neptune and Bourne *et al.*, 1997).

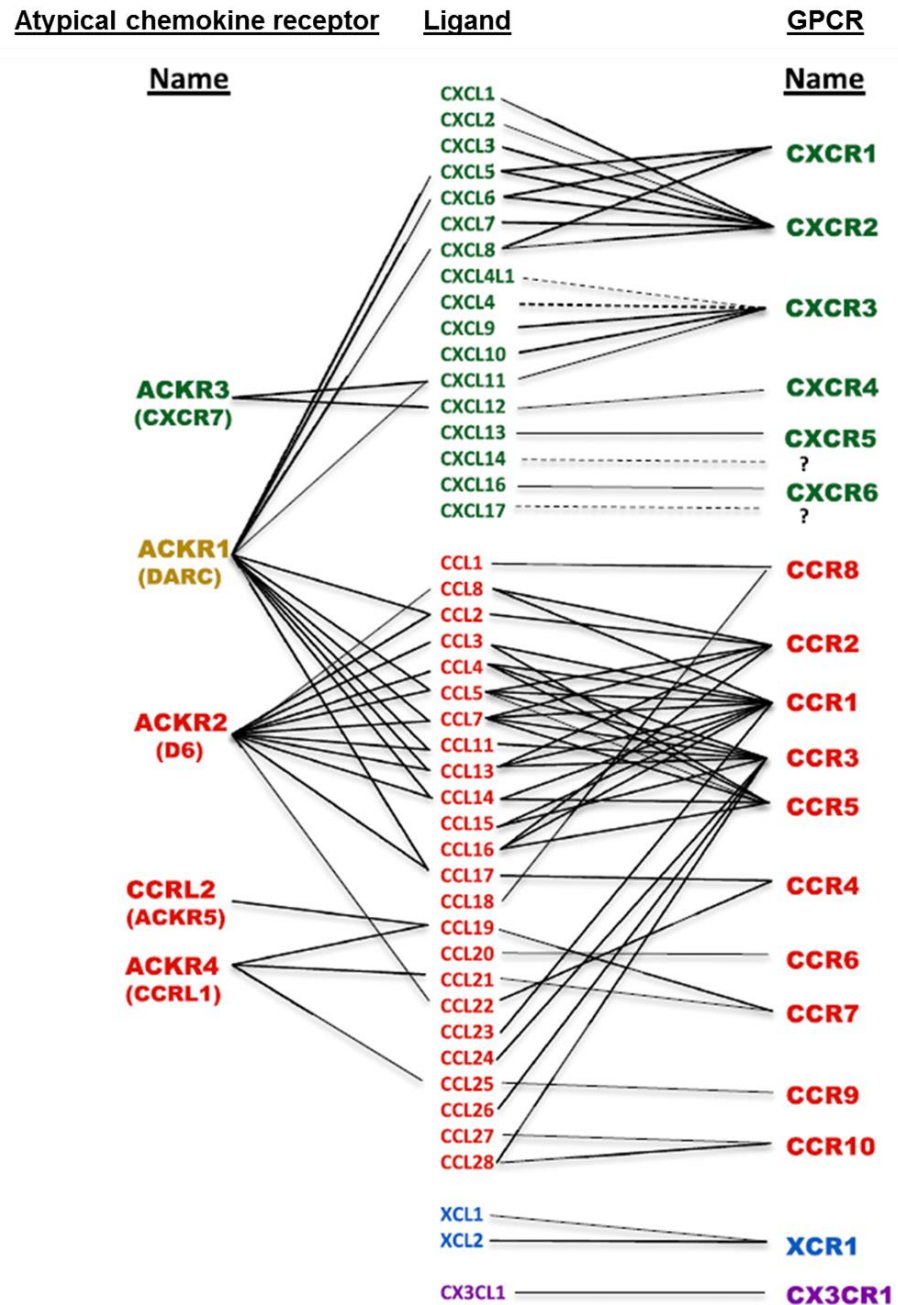


**Figure 1.8 Chemokine receptors and their ligands**

Adapted from Bachelerie *et al.* (2014).

## 1.6 Chemokine (CC-motif) receptor 2 (CCR2)

### 1.6.1 General overview and structure

The human CCR2 receptor (cluster of differentiation 192/CD192) is a chemokine receptor belonging to the class-A family of GPCRs (Section 1.3). The CCR2 receptor is important for immune cell recruitment and is expressed by a wide variety of cells including monocytes, T lymphocytes, and endothelial cells (Loetscher *et al.*, 1996; Sozzani *et al.*, 1997; Weber *et al.*, 1999).

The human CCR2 receptor consists of two isoforms, CCR2A (360 amino acids (aa)) and CCR2B (374 aa) encoded by the *CCR2A* and *CCR2B* genes respectively, which are located on the short arm of chromosome 3 (3p21) (Charo *et al.*, 1994; Yamagami *et al.*, 1994; Samson *et al.*, 1996). Both isoforms are produced from an alternatively spliced C-terminus, where the 47 aa C-terminus of CCR2B is located in the same exon as the 7TM regions of the receptor, while the 61 aa C-terminus of CCR2A lies in a downstream exon (Charo *et al.*, 1994; Wong *et al.*, 1997). These differences appear to determine the surface expression and activation of both isoforms *in vitro* and *in vivo* (Wong *et al.*, 1997; Sanders *et al.*, 2000; Cho *et al.*, 2007). Early studies by Wong *et al.* (1997) showed that CCR2A-transfected HEK293 cells (embryonic kidney) released intracellular  $Ca^{2+}$  less readily than CCR2B-transfected cells due to a lower surface expression caused by a C-termini retention signal. Other more recent studies (Sanders *et al.*, 2000) have shown that CCR2A-transfected Jurkat (T-lymphocyte) cells require 5-fold more CCL2 than CCR2B transfectants for chemotaxis.

Figure 1.8 shows the recently modelled crystal structure of the human CCR2 receptor (Kothandan *et al.*, 2012). While most GPCR structures are based on the bovine rhodopsin and human  $\beta$ 2-adrenergic receptors, the crystal structure of CCR2 is modelled on the closer homolog, chemokine (CXC motif) receptor 4 (CXCR4). The N-terminal region of CCR2 is critical for defining ligand specificity and binding affinity, where studies by Monteclaro and Charo (1996) have shown that replacing this region with the N-terminal region from CCR1 leads to a lower CCL2 binding affinity.

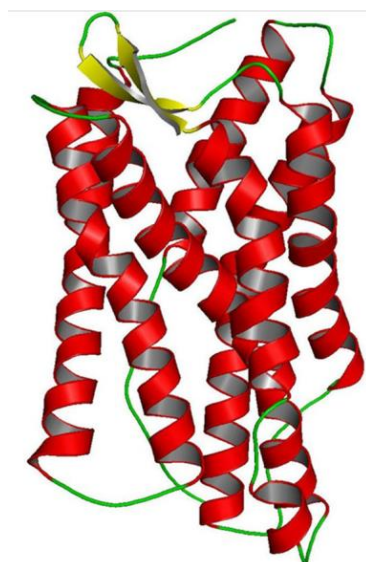


**Figure 1.9** Crystal structure of the human CCR2 receptor

Representation of the crystal structure of CCR2. The 7TM helical domains are shown in red, the extracellular/intracellular loops in green, and  $\beta$ -sheet in yellow (Kothandan *et al.*, 2012).

### 1.6.2 Homo- and heterodimerisation

Similar to other GPCRs, CCR2 may form homo- or heterodimers. The binding of CCL2 to CCR2 favours homodimerisation (Rodríguez-Frade *et al.*, 1999), which may be important for functional responses such as chemotaxis. The CCR2 receptor can also form heterodimers with other chemokine receptors such as CCR5 and CXCR4 (Bachelierie *et al.*, 2014). The CCR2-CCR5 heterodimer is a well-studied example, and favours signalling via  $G\alpha_{q/11}$  rather than  $G\alpha_{i/o}$  (Mellado *et al.*, 2001). Moreover, the ligands for these receptors seem to operate synergistically, inducing intracellular  $Ca^{2+}$  release at concentrations 10- to 100-fold lower than either chemokine alone (Mellado *et al.*, 2001). The formation of CCR2 heterodimers may also be important for receptor activation and cell function. In studies reported by El-Asmar *et al.* (2005), it was seen that CCR2 and CCR5 ligands cross-competed for receptors, where CCR2 ligands blocked the binding of CCR5 ligands, and CCR5 ligands blocked the binding of CCR2 ligands.

### 1.6.3 Ligands

The human CCR2 receptor is a high-affinity receptor for chemokines of the monocyte-chemoattractant protein (MCP) family and is activated by CCL2 (MCP-1), CCL7 (MCP-2), CCL8 (MCP-8), CCL11 (eotaxin-1), and CCL13 (MCP-4) (Bachelierie *et al.*, 2014). The preferred endogenous ligand for CCR2 however, is CCL2 (Bachelierie *et al.*, 2014). The N-terminal regions of ligands are crucial for efficient CCR2 activation. For example, a deletion or truncation of residues in the N-terminal region of CCL2 generates a ligand that is still able to bind to CCR2, but is either inactive, or behaves as an antagonist (Jarnagin *et al.*, 1999).

The formation of heterodimers between ligands may also be relevant for CCR2 activation. For example, reports in literature suggest that CCL2 can form strong heterodimers with CCL8 at the expense of CCL2 homodimers (Crown *et al.*, 2006). Weaker heterodimers between CCL2 and other CCR2 ligands (CCL2-CCL13, CCL2-CCL11), can also be formed (Crown *et al.*, 2006).

### 1.6.4 Signalling and involvement in monocyte function

The CCR2 receptor signals via the activation of  $G\alpha_{i/o}$ -type G-proteins (Section 1.3). Activation of CCR2 leads to an inhibition of AC by  $G\alpha$ , and an activation of PLC and PI3K by  $G\beta\gamma$  (Bizzarri *et al.*, 1995; Myers *et al.*, 1995; Turner *et al.*, 1998).

Chemotactic signals involve an interaction between CCR2 and FROUNT, a clathrin heavy-chain repeat homology protein that forms clusters at the cell front and facilitates the formation of F-actin-rich protrusions (lamellipodia) required for cell polarisation prior to

chemotaxis (Terashima *et al.*, 2005). Low-level activation of CCR2 is crucial for the homeostatic migration of monocyte subsets. As mentioned previously (Section 1.2.1), CCR2 is expressed by human and mouse monocytes, particularly by classical and intermediate subsets (Table 1.1) (Geissmann *et al.*, 2003). Activation of the CCR2 receptor is required for classical monocyte egression from the bone marrow during *Listeria monocytogenes* (LM) infection (Kurihara *et al.*, 1997; Serbina and Pamer, 2006). Monocytes from mice lacking CCR2 are retained in the bone marrow, making mice more susceptible to LM (Kurihara *et al.*, 1997; Serbina and Pamer, 2006). CCR2-dependent monocyte recruitment is also essential for host defence against *Mycobacterium tuberculosis*, *Toxoplasma gondii*, and *Cryptococcus neoformans* (Serbina *et al.*, 2008), thus highlighting the importance of CCR2 for efficient clearance against bacterial, protozoal, and fungal pathogens.

In non-classical monocyte subsets, expression of CCR2 is either low or absent, whereas expression of CX<sub>3</sub>CR1 is high (Geissmann *et al.*, 2010). However, despite lacking CCR2, non-classical monocytes are also affected by a deficiency in CCR2 due to their dependence on classical monocytes for replenishment (Yona *et al.*, 2013).

Other studies reported by Chan *et al.* (2001) have shown that CCR2 activation induces a conformational change in VLA-4 ( $\alpha_4\beta_1$ -integrin), increasing its affinity for VCAM-1. This finding suggests that the CCL2/CCR2 axis is important for monocyte transmigration, a hypothesis that seems plausible given that several lines of evidence indicate that CCR2 signalling is important for monocyte transmigration during sterile inflammation such as that seen during the development of atherosclerosis (Gu *et al.*, 1998; Boring *et al.*, 1998; Tacke *et al.*, 2007).

### **1.6.5 Involvement in human monocyte pathologies**

Pre-clinical studies on mouse (Ly6C<sup>high</sup>) classical monocytes (counterparts of human (CD14<sup>++</sup>/CD16<sup>-</sup>) classical monocytes), have suggested that CCR2-dependent monocyte trafficking underlies many monocyte-associated pathologies. Murine models of monocyte-associated conditions such as atherosclerosis, multiple sclerosis, and neuropathic pain have shown that a blockade or suppression of CCR2 reduces the severity of these pathologies through a reduced infiltration of monocytes and their progeny (Boring *et al.*, 1998; Gu *et al.*, 1998; Izikson *et al.*, 2000; Abbadie *et al.*, 2003). Motivated by these studies, pharmaceutical companies have sought to develop a number of antagonists targeting CCR2 (Table 1.4). However, despite much investment, progress has been hampered by a lack of clinical efficacy in humans (Bachelier *et al.*, 2014).

**Table 1.4 CCR2 antagonists in clinical development (2014)**

Drug	Company	Indication	Phase/Status
INCB8696	Incyte	MS, Lupus	No longer reported
INCB3284	Incyte	RA, Diabetes	No longer reported
CCX915	ChemoCentryx	MS	Terminated
CCX140	ChemoCentryx	Diabetic nephropathy	II
MK-0812	Merck	MS, RA	No efficacy
PF-4136309	Pfizer	Pain	No longer reported
BMS-741672	BMS	Diabetic nephropathy	II
JNJ-17166864	Johnson & Johnson	Allergic Rhinitis	No efficacy
MLN 1202	Millennium	RA	No efficacy
		Atherosclerosis, MS	II

MS = multiple sclerosis, RA = rheumatoid arthritis. Phase I = safety testing in normal human volunteers. Phase II = drug efficacy trials in a small patient group. Adapted from Bachelierie *et al.* (2014).

Although the CCL2/CCR2 axis is an important signalling pathway for monocytes, it is fast becoming clear that other  $Ca^{2+}$ -mobilising chemoattractants such as extracellular nucleotides (purinoceptor signalling), are also important for steering monocyte migration. Section 1.7 below moves on to discuss the purinoceptor signalling pathway and its involvement in monocyte signalling and function.

## 1.7 Purinoceptor Signalling

### 1.7.1 General overview

Geoffrey Burnstock first coined the term “purinergic” in 1971 after putting forward the hypothesis that purine nucleotides such as adenosine 5'-triphosphate (ATP) and adenosine 5'-diphosphate (ADP) were potent neurotransmitters involved in non-adrenergic/non-cholinergic (NANC) nerves supplying the gut (Burnstock *et al.*, 1970, Burnstock, 1972). While this proposal was initially met with opposition, it was finally accepted, and now describes a widespread intercellular signalling system by which ATP and related nucleotides and nucleosides participate in short-term signalling in neurotransmission, neuromodulation, and secretion, and long-term signalling in cell differentiation, proliferation and death (Burnstock, 2012).

## 1.7.2 Purinoceptors

The purinoceptor signalling system comprises of a network of at least nineteen purinoceptors subdivided into three distinct families termed P1, P2X, and P2Y.

### 1.7.2.1 P1

The adenosine P1 purinoceptors are a family of class-A GPCRs (Section 1.2). Four P1 purinoceptors ( $A_1$ ,  $A_{2A}$ ,  $A_{2B}$ , and  $A_3$ ) have been cloned and characterised (Fredholm *et al.*, 2001, 2011). Although the preferred endogenous ligand of P1 purinoceptors is the nucleoside, adenosine,  $A_1$  and  $A_3$  are also activated by inosine, a product formed from the deamination of adenosine by the enzyme adenosine deaminase (ADA) (Jin *et al.*, 1997; Fredholm *et al.*, 2001, 2011).

P1 receptors share between 31-46% sequence homology (Pirainen *et al.*, 2011) with greatest homology seen between  $A_{2A}$  and  $A_{2B}$  (46%). Although P1 purinoceptors are monomeric, these can self-associate to form homomers ( $A_1$ - $A_1$ ,  $A_{2A}$ - $A_{2A}$ ), or form heteromers with adenosine purinoceptors ( $A_1$ - $A_{2A}$ ), non-adenosine purinoceptors ( $A_1$ -P2Y<sub>1</sub>,  $A_1$ -P2Y<sub>2</sub>), and non-purinoceptors (dopamine D<sub>1</sub>) (Fredholm *et al.*, 2011).

P1 receptors display distinct coupling to secondary effectors and have the ability to couple to multiple G-proteins (Table 1.5) (Fredholm *et al.*, 2001, 2011). Through these interactions,  $A_1$  and  $A_3$  receptors drive the inhibition of AC and the activation of PLC, while  $A_{2A}$  and  $A_{2B}$  drive the activation of AC and PLC (Fredholm *et al.*, 2001; Burnstock, 2012).

### 1.7.2.2 P2X

The P2X purinoceptors are a family of homo- or heterotrimeric ATP-gated ion channels with permeability to sodium ( $Na^+$ ) ions, potassium ( $K^+$ ) ions, calcium ( $Ca^{2+}$ ) ions, and in exceptional circumstances, chloride ( $Cl^-$ ) ions (Khakh *et al.*, 2001; North, 2002; Egan and Khakh, 2004). Seven subunits are encoded in the human genome (P2X1 - P2X7), and these form functional ion channels as homotrimers (homomultimers) which must bind to three molecules of ATP in order to open (Hattori and Gouaux, 2012). P2X1, P2X2, and P2X4 can also combine with other P2X receptor subunits to form heterotrimers with kinetic properties distinct from homotrimers (Khakh *et al.*, 2001).

Each P2X subunit comprises of two hydrophobic transmembrane-spanning regions (TM1 and TM2) separated by a large extracellular loop (ectodomain) containing ten-conserved cysteine residues (Figure 1.9) (Valera *et al.*, 1994). While TM1 is associated with channel gating, TM2 lines the ion pore in the membrane. The ectodomain allows the formation of disulphide bridges and forms the ATP-binding domain. Each P2X subunit also comprises of an intracellular (cytosolic) amino ( $NH_2$ ) and carboxyl ( $COOH$ ) termini. The  $NH_2$  terminal

contains a consensus site for phosphorylation by PKC, and may be involved in modulating P2X receptor currents (Ennion *et al.*, 2000; Ennion and Evans, 2002). The COOH terminus diverges greatly between P2X subunits but the remaining sequence shares 40–55% pairwise identity (North, 2002).

Following activation, the channel pore opens allowing cations to flow. Receptors such as P2X2, P2X4, and P2X7 may also undergo a second permeability state, allowing the flow of larger cations or dyes (Surprenant *et al.*, 1996; Khakh *et al.*, 1999). The recent determination of the crystal structure of zebrafish P2X4 and the location of its ATP binding sites has led to the suggestion that ATP molecules sequentially activate homotrimers, where a binding of the first ATP molecule induces a conformational change that influences the binding of further ATP molecules (Hattori and Gouaux, 2012; Browne and North, 2013).

Like GPCRs, P2X receptors become desensitised by prolonged agonist exposure, resulting in a closure of the receptor pore. Depending on their sensitivity to desensitisation, P2X receptors are either fast- (P2X1 and P2X3), or slow-desensitising (P2X2, P2X4, P2X5, and P2X7) (Khakh *et al.*, 2001; Jarvis and Khakh, 2009).

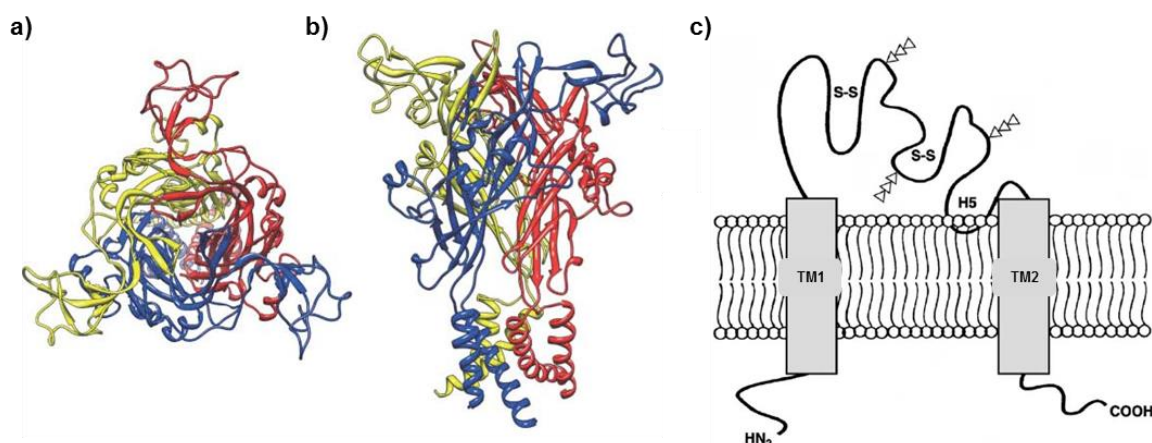


**Figure 1.10 Structure of functional P2X purinoceptors**

P2X receptors are comprised of three subunits. P2X receptor from (a) above, and (b), parallel to the membrane. Homomers exhibit a dolphin-like shape and are arranged around a 3-fold symmetrical axis. (c) P2X transmembrane topology shown, where TM1 and TM2 are separated by an ectodomain containing two disulfide-bonded loops (S–S) and three N-linked glycosyl chains (triangles). Also shown are the intracellular N and C-termini. Adapted from Brake *et al.* (1994) and Browne (2012).

### 1.7.2.3 P2Y

The P2Y receptors are a family of class-A GPCRs (Section 1.3). Eight P2Y receptors (P2Y<sub>1</sub>, P2Y<sub>2</sub>, P2Y<sub>4</sub>, P2Y<sub>6</sub>, P2Y<sub>11</sub>, P2Y<sub>12</sub>, P2Y<sub>13</sub>, and P2Y<sub>14</sub>) are recognised, and a number

of purine and pyrimidine nucleotides activate these (Table 1.5) (Abbracchio *et al.*, 2006). P2Y receptors share 21-48% sequence homology, with greatest similarity observed between P2Y<sub>12</sub> and P2Y<sub>13</sub>. A comparison of the structural and functional features of P2Y receptors has revealed that two distinct groups exist: the first group comprises of P2Y<sub>1</sub>, P2Y<sub>2</sub>, P2Y<sub>4</sub>, P2Y<sub>6</sub>, and P2Y<sub>11</sub>, and the second group comprises of P2Y<sub>12</sub>, P2Y<sub>13</sub>, and P2Y<sub>14</sub> (Abbracchio *et al.*, 2006; Von Kügelgen, 2006). Members of the first group principally signal through G $\alpha_{q/11}$  to activate PLC, whereas members of the second group signal through G $\alpha_{i/o}$  to inhibit AC (Table 1.6) (Abbracchio *et al.*, 2006).

#### 1.7.2.4 Ligands for purinoceptors

Extracellular purine and pyrimidine nucleotides and nucleosides are naturally-occurring molecules that regulate a wide range of cellular processes through purinoceptors (Figure 1.10) (Table 1.5) (Burnstock, 2012). Purinoceptors are also be modulated by nucleotide and nucleoside derivatives (Burnstock, 2012).

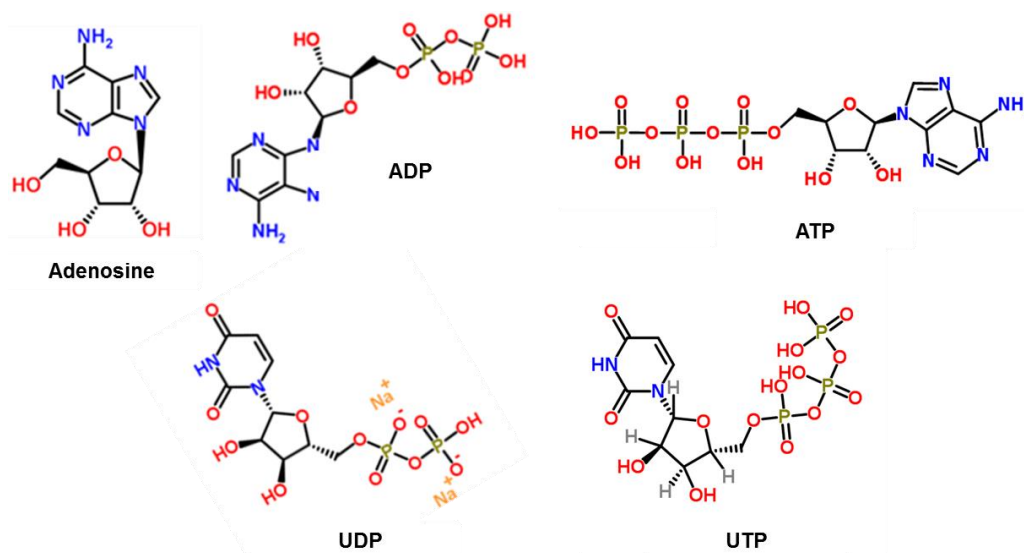


**Figure 1.11 Structures of some naturally-occurring purinoceptor ligands**

Central to all nucleotides and nucleosides is a pentose sugar (ribose) attached to a purine (adenine or uridine) base by its 1'-carbon atom. Attached to the pentose sugar are two or three phosphate groups. Source: <http://www.chemspider.com/> (accessed 23<sup>rd</sup> Dec 2014).

#### 1.7.2.5 Distribution in immune cells and monocytes

In general, all cells possess purinoceptors of some type, with many cells expressing multiple purinoceptors. In immune cells, purinoceptor expression is seen in leukemic cell lines and primary cells of monocyte, macrophage, neutrophil, B- and T-lymphocyte, and dendritic cell origin (Bours *et al.*, 2006). Monocytes express multiple purinoceptors (Table

1.5), with expression levels often dependent on their maturation stage (Muller *et al.*, 1993).

**Table 1.5 Human purinoceptors**

Receptor	Type	Natural ligands	Principle effector	Monocytes?
A <sub>1</sub>	GPCR	Adenosine, Inosine	Gα <sub>i/o</sub> (↓AC)	Yes
A <sub>2A</sub>	GPCR	Adenosine	Gα <sub>s</sub> and Gα <sub>q/11</sub> (↑ AC, ↑PLC)	Yes
A <sub>2B</sub>	GPCR	Adenosine	Gα <sub>s</sub> and Gα <sub>q/11</sub> (↑ AC, ↑PLC)	Yes
A <sub>3</sub>	GPCR	Adenosine, Inosine	Gα <sub>i/o</sub> and Gα <sub>q/11</sub> (↓ AC, ↑ PLC)	Yes
P2X1	LGIC	ATP	Cation influx	Yes
P2X2	LGIC	ATP	Cation influx	Unknown
P2X3	LGIC	ATP	Cation influx	Unknown
P2X4	LGIC	ATP	Cation influx	Yes
P2X5	LGIC	ATP	Cation influx	Unknown
P2X6	LGIC	ATP	Cation influx	Unknown
P2X7	LGIC	ATP	Cation influx	Yes
P2Y <sub>1</sub>	GPCR	ADP, ATP, Ap <sub>4</sub> A	Gα <sub>q/11</sub> and Gα <sub>i/o</sub> (↑ PLC)	Yes
P2Y <sub>2</sub>	GPCR	ATP, UTP	Gα <sub>q/11</sub> , Gα <sub>i/o</sub> , and Gα <sub>12/13</sub> (↓ AC, ↑ PLC, ↑Rho GTPase)	Yes
P2Y <sub>4</sub>	GPCR	UTP	Gα <sub>q/11</sub> and Gα <sub>i/o</sub> (↓ AC, ↑ PLC)	Yes
P2Y <sub>6</sub>	GPCR	UDP, UTP, ADP, ATP	Gα <sub>q/11</sub> (↑PLC)	Yes
P2Y <sub>11</sub>	GPCR	ATP, ADP (UTP?)	Gα <sub>q/11</sub> and Gα <sub>s</sub> (↑ AC, ↑PLC)	Yes
P2Y <sub>12</sub>	GPCR	ADP, ATP	Gα <sub>i/o</sub> (↓ AC)	Yes
P2Y <sub>13</sub>	GPCR	ADP, ATP	Gα <sub>i/o</sub> (↓ AC, ↑ PLC?)	Yes
P2Y <sub>14</sub>	GPCR	UDP, UDP-glucose	Gα <sub>i/o</sub> and Gα <sub>q/11</sub> (↓ AC, ↑ PLC)	Unknown

LGIC = ligand-gated ion channel, Rho GTPase = Rho guanosine triphosphatase (Merrill *et al.*, 1997; Jin *et al.*, 1998; Broussas *et al.*, 1999., Gu *et al.*, 2000; Fredholm *et al.*, 2001; Khakh *et al.*, 2001; Zhang *et al.*, 2002; Thiele *et al.*, 2004; Wang *et al.*, 2004; Kaufmann *et al.*, 2005; Klein *et al.*, 2009; Lazarowski *et al.*, 2011; Burnstock, 2012).

### 1.7.5 ATP release

Cellular events leading to purinoceptor activation often involve a release of extracellular nucleotides such as ATP from intracellular compartments. Following the discovery that non-neuronal cells express functional purinoceptors, elucidating the mechanisms by which cells release ATP has become a major interest for the research community (Bodin and Burnstock, 2001). While early studies proposed that cells leaked ATP only during mechanical stress (Forrester, 1972), it is now apparent that resting and stimulated cells release ATP in a non-lytic manner (Lazarowski *et al.*, 2011). However, under stressful situations such as apoptosis, ATP is released by cells as a “find-me” signal for phagocytes (Elliott *et al.*, 2009). Under these circumstances, the pore-forming P2X7 receptor and connexion/pannexin hemichannels are thought to be the primary modes of ATP release (Bao *et al.*, 2004; Eltzschig *et al.*, 2006; Suadicani *et al.*, 2006). In contrast, the release of constitutive ATP by resting cells may be an important mechanism by which cells determine their “set-points”, or basal activation levels for regulating homeostatic responses such as blood flow, ion transport, and host immunity (Corriden and Insel, 2010). ATP release following the activation of non-purinergic GPCRs is also important for cell homeostasis. For example, neutrophils contain a high concentration of cytosolic ATP (5 mM) and can liberate up to 25  $\mu$ M ATP at the leading edge upon FPR activation in order to activate P2Y<sub>2</sub> and A<sub>3</sub> purinoceptors required for chemotaxis (Chen *et al.*, 2006; Eltzschig *et al.*, 2006; Corriden *et al.*, 2007).

### 1.7.6 Ecto-nucleotidases

The ecto-nucleotidases are a family of extracellular plasma membrane enzymes that rapidly hydrolyse extracellular nucleotides in order to control their availability at purinoceptors (Table 1.6) (Yegutkin, 2008; Zimmermann *et al.*, 2012). Using this approach, ecto-nucleotidases can prevent purinoceptor desensitisation by terminating their activation while facilitating the activation of other purinoceptors by generating ligands (Zimmermann *et al.*, 2012). Although ecto-nucleotidases are the major enzymes involved in this process, a number of other enzymes including the nucleotide-hydrolysing secreted exo-enzymes and the nucleotide-phosphorylating ecto-kinases also regulating nucleotide release and availability (Kukulski *et al.*, 2011).

**Table 1.6 Major ecto-nucleotidase families**

Ecto-nucleotidase	EC number	Main substrate(s)	Specificity
Ecto-nucleoside triphosphate diphosphohydrolase (E-NTPDase)	3.6.1.5	NTP, NDP	Nucleotide-specific
Ecto-5'-nucleotidase (cluster of differentiation 73/CD73/eN)	3.1.3.5	NMP	Nucleotide-specific
Ecto-nucleotide pyrophosphatase/phosphodiesterase (E-NPP)	3.6.1.9/ 3.1.4.1	NTP	Non-specific
Alkaline phosphatase (AP)	3.1.3.1	NTP, NDP, NMP	Non-specific

Adapted from Yegutkin (2008).

### 1.7.7 Involvement in monocyte function

The expression of purinoceptors by monocytes (Table 1.5) suggests that multiple purinoceptor subtypes are involved in regulating physiological responses of monocytes, such as trafficking and function (Burnstock and Boeynaems, 2014).

Evidence for the involvement of P1 receptors is abundant, where studies have shown that individual receptors differentially modulate monocyte function (Haskó *et al.*, 2007; Haskó and Pacher, 2012). Studies in the literature examining the effects of P1 purinoceptors on monocyte adhesion to endothelium have shown that while  $A_{2A}$  receptors promote IL-18-induced monocyte adhesion,  $A_1$  and  $A_3$  receptors attenuate adhesion (Takahashi *et al.*, 2007). However, in general, P1 purinoceptors play a restorative and protective role in monocytes. For example,  $A_{2A}$  and  $A_{2B}$  are known to reduce the production of pro-inflammatory mediators such as TNF $\alpha$ , CCL3, and nitric oxide (Le Vraux *et al.*, 1993; Haskó *et al.*, 1996; Szabo *et al.*, 1998; Haskó *et al.*, 2007). The  $A_3$  receptor is considered the main receptor involved in inhibiting lipopolysaccharide (LPS)-induced TNF $\alpha$  production in monocytic cells (Sajjadi *et al.*, 1996).

Early studies by Cowen *et al.* (1989) were one of the first to suggest an association between P2 purinoceptors and intracellular  $Ca^{2+}$  release from monocytes. This finding was taken further by Altieri *et al.* (1990) who found that nucleotide-evoked  $Ca^{2+}$  release in monocytes regulated the affinity of the integrin complement receptor, macrophage-1 antigen (integrin  $\alpha_M\beta_2$ ). Other groups, including Kaufmann *et al.* (2005) and Elliott *et al.* (2009), have discovered that extracellular nucleotides promote monocyte chemotaxis through P2 purinoceptors, thus indicating that these are likely to influence monocyte trafficking *in vivo* in response to other chemoattractants. A number of other studies

(Grahames *et al.*, 1999; Warny *et al.*, 2001; Cox *et al.*, 2005; Ben Yebdri *et al.*, 2009; Higgins *et al.*, 2014) have also demonstrated that P2 purinoceptors such as P2Y<sub>2</sub>, P2Y<sub>6</sub>, and P2X7, regulate the release of pro-inflammatory mediators such as TNF $\alpha$ , CCL2, and IL-1 $\beta$  from human monocytes and monocytic cells.

### **1.7.8 Involvement in human monocyte pathologies**

It has become increasingly clear that aberrant purinoceptor signalling of monocytes and their progeny is associated with pathologies such as atherosclerosis, thrombosis, diabetes, and neuropathic pain (Fabre *et al.*, 1999; Balasubramanian *et al.*, 2010; Guns *et al.*, 2010; Ulmann *et al.*, 2010). Purinoceptor signalling therefore represents an attractive therapeutic area, with biopharmaceutical companies seeking to develop selective purinoceptor agonists and antagonists, antibodies, ecto-nucleotidase inhibitors, ecto-nucleotidases, and modulators of nucleotide transport (Table 1.7, Table 1.8 and Table 1.9) (Brass *et al.*, 2012; Jacobson *et al.*, 2012; Kaczmarek-Hájek *et al.*, 2012). However, despite continued efforts, few examples of therapeutically useful compounds or approaches exist. While this may reflect the fact that our understanding of purinoceptor signalling is still at an early stage, a second possible explanation for this may be that purinoceptors display a broad expression pattern and are therefore difficult to target. Moreover, purinoceptors are regulated by ecto-nucleotidases and are likely to be co-activated with other purinoceptors and non-purinoceptors. Thus, developing novel therapies targeting purinoceptor signalling in monocyte-associated pathologies remains a challenge for the biopharmaceuticals industry.

**Table 1.7 P1 ligands in clinical development (2012)**

<b>Drug</b>	<b>Action</b>	<b>Company</b>	<b>Indication</b>	<b>Phase/Status</b>
Adenosine	A <sub>1</sub> agonist	Astellas	Tachycardia	Approved
INO-8875	A <sub>1</sub> agonist	Inotek	Glaucoma	I-II
Capadenoson	A <sub>1</sub> agonist	Bayer-Schering	Atrial fibrillation	II
Regadenoson	A <sub>2A</sub> agonist	Dana-Farber Cancer Institute	Sickle cell	I
IB-MECA	A <sub>3</sub> agonist	Can-Fite	RA, psoriasis, dry eye, glaucoma	II/III
CI-IB-MECA	A <sub>3</sub> agonist	Can-Fite	Carcinoma, hepatitis C	II
Caffeine	AR antagonist	Univ. of Texas	Sleep apnea, cancer pain, PD	II/III
Theophylline	AR antagonist	-	Asthma, COPD	Approved
Istradefylline	A <sub>2A</sub> antagonist	Kyowa Hakko	PD	III
KW-6356	A <sub>2A</sub> antagonist	Kyowa Hakko	PD	III
Preladenant	A <sub>2A</sub> antagonist	Schering	PD	III
Tozadenant	A <sub>2A</sub> antagonist	Biotie	PD	IIB
ST-1535	A <sub>2A</sub> antagonist	Sigma-Tau	PD	I
V81444	A <sub>2A</sub> antagonist	Vernalis	PD	I
DT1133	A <sub>2A</sub> antagonist	Domain	PD	Pre-clinical
CVT-6883	A <sub>2B</sub> antagonist	Gilead	Inflammation	I

AR = adenosine receptor, RA = rheumatoid arthritis, PD = Parkinson's Disease, COPD = Chronic Obstructive Pulmonary Disease. Phase I = safety testing in normal human volunteers. Phase II = drug efficacy trials in a small patient group. Phase III = drug efficacy trials in a large patient group (Jacobson *et al.*, 2012).

**Table 1.8 P2X ligands in clinical development (2012)**

<b>Drug</b>	<b>Action</b>	<b>Company</b>	<b>Indication</b>	<b>Phase/Status</b>
AF-219	P2X3 antagonist	Afferent	Chronic cough, pain,	II
CE-224535	P2X7 antagonist	Pfizer	RA	Terminated
EVT-401	P2X7 antagonist	Evotec	Inflammation	II
AZD9056	P2X7 antagonist	AstraZeneca	RA	Terminated
GSK1482160	P2X7 antagonist	GlaxoSmithKline	Pain	Terminated

RA = rheumatoid arthritis. Phase II = drug efficacy trials in a small patient group (Kaczmarek-Hájek *et al.*, 2012).

**Table 1.9 P2Y ligands in clinical development (2012)**

<b>Drug</b>	<b>Action</b>	<b>Company</b>	<b>Indication</b>	<b>Phase/Status</b>
Diquafosol	P2Y <sub>2</sub> agonist	Santen	Dry eye disease	Approved
Suramin	P2Y <sub>2</sub> antagonist	Bayer	Anti- helminthic/protozoal	Approved
Clopidogrel	P2Y <sub>12</sub> antagonist	BMS/Sanofi	ACS, atherosclerosis	Approved
Prasugrel	P2Y <sub>12</sub> antagonist	Lilly/Daiichi Sankyo	ACS, angioplasty	Approved
Ticagrelor	P2Y <sub>12</sub> antagonist	AstraZeneca	ACS	Approved
Cangrelor	P2Y <sub>12</sub> antagonist	The Medicines Co.	Coronary artery bypass	III
Elinogrel	P2Y <sub>12</sub> antagonist	Portola/Novartis	ACS	II

ACS = acute coronary syndrome. Phase II = drug efficacy trials in a small patient group. Phase III = drug efficacy trials in a larger patient group (Jacobson *et al.*, 2012).

## 1.8 Aims and project outline

It is apparent from the literature presented in this chapter that monocytes play pivotal roles in health and disease. The CCL2/CCR2 axis is an important signalling pathway involved in orchestrating monocyte function and is associated with a growing number of monocyte-associated pathologies. However, despite research into this area being plentiful, biopharmaceutical companies have struggled to translate the effects of CCR2 antagonists seen in murine models, into efficacious therapies for humans. The lack of progress made in this area may result from a lot of useful information surrounding the CCL2/CCR2 axis being missing. For example, the contributions of other CCR2 ligands, chemokine receptors, and other chemotactic pathways that steer monocyte function are still to be determined. Recently, the chemotactic effects of extracellular nucleotides have been described, which result in an increased infiltration of monocytes and their progeny during immune responses and monocyte-associated pathologies (Kaufmann *et al.*, 2005; Elliott *et al.*, 2009; Guns *et al.*, 2010; Riegel *et al.*, 2011; Tsuda *et al.*, 2013; Stachon *et al.*, 2014). It is possible, therefore, that the capacity of cells to traffic in response to the CCL2/CCR2 axis is influenced by extracellular nucleotides, arising from crosstalk between these signalling pathways. While many studies have shown that purinoceptor activation evokes CCL2 release from monocytic cells and monocyte progeny (Cox *et al.*, 2005; Stokes and Surprenant, 2007; Morioka *et al.*, 2013; Garcia *et al.*, 2014; Higgins *et al.*, 2014; Shieh *et al.*, 2014), the exact mechanisms by which these pathways crosstalk, is still an open question. Thus, in order to address this gap in knowledge, this thesis principally investigated the requirement of purinoceptor signalling for CCL2/CCR2-mediated monocyte signalling and function using human monocytic THP-1 cells and peripheral blood mononuclear cells (PBMCs) as *in vitro* models, the latter being a primary source of monocytes.

Chapter 3 investigated the expression of mRNA transcripts for monocyte/myeloid cell markers, CC chemokines, CC chemokine receptors, and potential purinoceptors involved in modulating CCL2/CCR2 signalling in THP-1 cells and human monocytes.

Chapter 4 looked at the mechanisms involved in CCL2/CCR2-mediated signalling and function of monocytes using THP-1 cells and PBMCs as *in vitro* models. The research presented here looks specifically at the involvement of individual signalling components on CCL2/CCR2 activation as measured by intracellular Ca<sup>2+</sup> release, cell migration, and adhesion to vascular endothelium.

Chapter 5 examined the requirement of extracellular nucleotides and purinoceptors for efficient CCL2/CCR2-mediated monocyte signalling and function using THP-1 cells and human PBMCs as models. Similarly, to the previous chapter, great importance was given

to CCL2/CCR2 activation as measured by intracellular  $\text{Ca}^{2+}$  release, cell migration, and adhesion to vascular endothelium.

The data generated from these experiments led to my project focussing on the  $\text{P2Y}_6$  purinoceptor. Chapter 6 investigated the requirement of  $\text{P2Y}_6$  for CCL2/CCR2-mediated monocyte signalling and function, using the THP-1 cell line and human PBMCs as models. As with Chapter 4, the research presented here gives importance to CCL2/CCR2 activation as measured by intracellular  $\text{Ca}^{2+}$  release, cell migration, and adhesion to vascular endothelium. The research presented in this chapter also looks at the involvement of the CCL2/CCR2 axis in extracellular nucleotide release from THP-1 cells.

# Chapter 2: Materials and Methods

## 2.1 Materials and reagents

All general salts and reagents were purchased from Sigma-Aldrich or Thermo Scientific unless otherwise stated. All buffers were prepared in deionised water unless otherwise stated.

Tables below provide a complete list of ligands, antagonists, and cell signalling modulators.

**Table 2.1 Chemoattractants and extracellular nucleotides**

Ligand	Purity	Supplier	Vehicle	Final concentration
CCL2	98%	LT	DI	1-500 ng/ml
CCL5	95%	LT	DI	1-50 ng/ml
fMLP	≥97%	SA	DMSO	0.1-10 µM
ATP	≥99%	SA	DI	1-100 µM
ADP	≥95%	SA	DI	1-100 µM
AMP	≥99%	SA	DI	1-100 µM
Adenosine	≥99%	SA	DI	100 µM
UTP	≥96%	SA	DI	1-100 µM
UDP	>98%	Abcam	DI	1-100 µM
UMP	≥99%	SA	DI	100 µM
Uridine	≥99%	SA	DI	100 µM
UDP-glucose	>98%	Abcam	DI	30 µM
β-NAD	≥99%	SA	DI	1 mM
BzATP	>95%	Tocris	DI	50 µM
α,β-MeATP	>98%	Tocris	DI	10-100 µM

DI = deionised water, DMSO = dimethyl sulfoxide, LT = Life Technologies, SA = Sigma-Aldrich

**Table 2.2 Purinoceptor agonists**

Compound	Function	Supplier	Vehicle	Final concentration
MRS-2365	P2Y <sub>1</sub> agonist	Tocris	DI	100 nM

DI = deionised water

**Table 2.3 Chemokine receptor and purinoceptor antagonists**

Compound	Main target receptor	Supplier	Vehicle	Final concentration
BMS-CCR2-22	CCR2	Tocris	DMSO	30 pM-100 nM
CGS-15943	P1	Tocris	DMSO	2.5 µM
Suramin	P2	Tocris	DI	100 µM
PPADS	P2	Tocris	DI	100 µM
Ro-0437626	P2X1	Tocris	DMSO	10-100 µM
5-BDBD	P2X4	Tocris	DMSO	1-5 µM
A-438079	P2X7	Abcam	DMSO	1-10 µM
MRS-2179	P2Y <sub>1</sub>	Abcam	DI	10 µM
MRS-2578	P2Y <sub>6</sub>	Tocris	DMSO	10nM - 10 µM
NF3-40	P2Y <sub>11</sub>	Tocris	DMSO	10 µM
AR-C-66096	P2Y <sub>12</sub>	Tocris	DI	1 µM
MRS-2211	P2Y <sub>13</sub>	Abcam	DI	10 µM

DI = deionised water, DMSO = dimethyl sulfoxide

**Table 2.4 Nucleotide/nucleoside metabolising enzymes**

Enzyme	EC number	Function	Supplier	Vehicle	Final concentration
Apyrase - high NTPase/high NDPase	3.1.6.5	Ecto-nucleotidase	SA	DI	0.01-4 units/ml
Apyrase - high NTPase/low NDPase	3.1.6.5	Ecto-nucleotidase	SA	DI	0.1-4 units/ml
Adenosine deaminase	3.5.4.4	Deaminates adenosine	SA	DI	2 units/ml

DI = deionised water, SA = Sigma-Aldrich

**Table 2.5 Inhibitors and modulators**

Compound/Tool	Function	Supplier	Vehicle	Final concentration
ARL-67156	Ecto-nucleotidase inhibitor	Tocris	DI	100 µM
POM-1	Ecto-nucleotidase inhibitor	Santa-Cruz Biotech	DI	1-100 µM
<i>Bordetella pertussis</i> toxin	Gα <sub>i</sub> inhibitor	Tocris	Distilled water	100 ng/ml
Gallein	Gβγ inhibitor	Tocris	DMSO	10-100 µM
Xestospongine-C	IP <sub>3</sub> R	Abcam	DMSO	5 µM
Dantrolene	RyR	Tocris	DMSO	20 µM
LY-294002	PI3K inhibitor	Tocris	DMSO	5-50 µM
U-73122	PLC inhibitor	Tocris	DMSO	0.25-5 µM
R-59022	DAGK inhibitor	Tocris	DMSO	10-30 µM
RHC-80267	DAGL inhibitor	Abcam	DMSO	1-50 µM
GF-109203X	PKC inhibitor	Tocris	DMSO	1 µM
Thapsigargin	SERCA inhibitor	Tocris	DMSO	300 nM-5 µM
Gly-Phe-β-naphthylamide (GPN)	Cathepsin-C substrate	Santa-Cruz Biotech	DMSO	0.2 mM
SKF-96365	SOCE inhibitor	Tocris	DI	100 µM
BAPTA-AM	Ca <sup>2+</sup> chelator	Tocris	DMSO	100 µM

Abbreviations: DI-deionised water, DMSO-dimethyl sulfoxide

## 2.2 Cell culture

### 2.2.1 Description of cell lines and passage

#### 2.2.1.1 THP-1 cells

THP-1 cells are a human cell line isolated from a patient with acute monocytic leukaemia (Tsuchiya *et al.*, 1980). Cells were obtained from the European Collection of Cell Cultures (ECACC) and cultured in Roswell Park Memorial Institute (RPMI)-1640 medium containing 0.3 g/L L-Glutamine. This was supplemented with 10% (v/v) heat-inactivated foetal calf serum (FCS; PAA Laboratories) and 1% (v/v) penicillin-streptomycin solution containing 50 units/ml of penicillin and 50 µg/ml of streptomycin (Life Technologies).

P2Y<sub>6</sub> knockdown (P2Y<sub>6</sub>-KD) THP-1 cells were prepared by infecting THP-1 cells with lentiviral pLKO.1-puro shRNA constructs targeting the human P2Y<sub>6</sub> receptor. THP-1 cells with non-target control vectors were also prepared. Cells were selected for stable expression and cultured in THP-1 cell culture medium supplemented with puromycin at a final concentration of 1 µg/ml (InvivoGen).

THP-1 cells were cultured in suspension, in vented T75 flasks (Nunc) at 37°C in a humidified 5% CO<sub>2</sub> incubator (Nuair). Routine cell passage was performed by counting cells using a haemocytometer (Sigma-Aldrich) and then diluting cells to the required density using fresh media warmed to 37°C. Cells were maintained below 7x10<sup>5</sup> cells/ml to prevent cells from differentiating to THP-1-macrophages. To promote consistent results in experiments, cells were used at densities between 2x10<sup>5</sup>-4x10<sup>5</sup> cells/ml.

For cryopreservation, 1x10<sup>6</sup> cells were resuspended into 1 ml THP-1 cell culture medium supplemented with 10% (v/v) glycerol. Cells were added to cryovials (Nunc) and stored in a Mr Frosty™ freezing container (Thermo Scientific) for storage at -80 °C overnight before indefinite storage in liquid nitrogen (-196 °C). To thaw, cells were removed from liquid nitrogen and swirled gently in a beaker of warm water before adding 5-10 ml of THP-1 culture medium to dilute the cryopreservant. Cells were centrifuged at 805 x g for 7 minutes at room temperature to allow sedimentation and removal of the supernatant. The cell pellet was finally resuspended in 5 ml of THP-1 culture medium and transferred to a vented T25 flask for incubation at 37°C in a humidified 5% CO<sub>2</sub> incubator.

### **2.2.1.2 1321N1 cells**

Human 1321N1 cells are an astrocytoma cell line isolated as a sub-clone from the 1181N1 line, a line isolated from the parent line U-118 MG (Pontén and Macintyre, 1968). These cells are not known to respond to classical purinoceptor ligands (Communi *et al.*, 1996). 1321N1 cells were kindly donated by Professor Jens George Leipziger (Aarhus University) and were cultured in Dulbecco's Modified Eagle Medium containing L-Glutamine (0.6 g/L) (DMEM) supplemented with 10% (v/v) heat inactivated FCS and 1% (v/v) penicillin-streptomycin solution containing 50 units/ml of penicillin and 50 µg/ml of streptomycin.

Human 1321N1 cells stably expressing the P2Y<sub>6</sub> receptor were also a kind gift from Professor Jens George Leipziger. Cells were transfected as described by Communi *et al.*, (1996) with recombinant pcDNA3 plasmid encoding human P2Y<sub>6</sub> and were selected with 1321N1 cell culture medium as described above supplemented with 400 mg/ml G418 (InvivoGen). Cells stably expressing the P2Y<sub>6</sub> receptor were maintained in this medium.

Human 1321N1 cells are adherent and were cultured in vented T75 flasks at 37°C in a humidified 5% CO<sub>2</sub> incubator. When cells had reached 70-80% confluency, cell monolayers were rinsed with 5 ml Dulbecco's Phosphate Buffered Saline (dPBS). Adherent cells were removed by adding 3 ml TrypLE Express solution (Life Technologies) to the flask and incubating for 5 minutes at 37°C. Following gentle agitation to dislodge adherent cells, the enzymatic reaction was terminated by addition of 10 ml 1321N1 cell culture medium. Cells were centrifuged at 805 x *g* for 7 minutes at room temperature and the supernatant was discarded. The cell pellet was resuspended in 10 ml of 1321N1 culture medium and used or re-seeded into fresh T75 flasks for culture.

Cryopreservation of cells was performed as described for THP-1 cells (Section 2.2.1.2), substituting THP-1 cell culture medium for 1321N1 culture medium supplemented with 10% (v/v) DMSO.

### **2.2.1.3 HUVEC cells**

Human umbilical cord endothelial cells (HUVECs) are primary endothelial cells harvested from human umbilical vein using a technique first described by Jaffe *et al.*, (1973). HUVEC cells form a useful tool for investigating the role of the endothelium cell wall in leukocyte adhesion. Early passage (1-2) cells from a population of pooled donors ( $5 \times 10^5$  cells) were purchased from Caltag Medsystems and cultured in Endothelium Cell Growth Medium (ECGM; PromoCell).

HUVEC cells are adherent and were cultured in vented T75 flasks at 37°C in a humidified 5% CO<sub>2</sub> incubator. When cells had reached 60-80% confluency, cell monolayers were rinsed with 5 ml dPBS. Adherent cells were removed by adding 3 ml TrypLE Express solution to the flask and incubating for 2-3 minutes at room temperature. Following gentle agitation to dislodge adherent cells, the enzymatic reaction was terminated by addition of 10 ml of ECGM. Cells were centrifuged at 220 x *g* for 5 minutes at room temperature and the supernatant was discarded. The cell pellet was resuspended in 10 ml of ECGM and counted for use in experiments.

Cryopreservation of cells was performed by resuspending  $5 \times 10^5$  cells in 1 ml of ECGM supplemented with 10% (v/v) DMSO. Cells were added to cryovials as described for THP-1 cells and stored in a Mr. Frosty™ freezing container at -80 °C prior to indefinite storage in liquid nitrogen (-196 °C). To thaw, cells were removed from liquid nitrogen and swirled gently in a beaker of warm water. Thawed cells were added to two vented T75 flasks, each containing 15 ml of warmed ECGM. Flasks were incubated at 37°C in a humidified 5% CO<sub>2</sub> incubator for 24 hours before replacing the media and returning the flasks to the incubator. The ECGM was replaced every 48 hours until flasks were confluent. Cells were not used beyond 1-2 passages (15 population doublings).

#### **2.2.1.4 HEK293T cells**

HEK293 cells are created by transforming normal human embryonic kidney cells with adenovirus-type 5 DNA (Graham *et al.*, 1977). HEK293T are HEK293 cells transfected with a gene encoding the SV40 large T-antigen and a neomycin resistance gene (DuBridg *et al.*, 1987). These cells are capable of replicating vectors containing the SV40 origin of replication. Cells were obtained from ECACC and cultured in DMEM containing L-Glutamine (0.6 g/L) supplemented 10% (v/v) heat-inactivated FCS and 1% (v/v) penicillin-streptomycin solution containing 50 units/ml of penicillin and 50 µg/ml of streptomycin.

HEK293T cells are adherent and were cultured in vented T75 flasks at 37°C in a humidified 5% CO<sub>2</sub> incubator. HEK293T cells were passaged and cryopreserved in a similar manner to 1321N1 cells (Section 2.2.1.2), replacing 1321N1 culture medium for HEK293T culture medium.

### **2.3 Primary Cell Isolation**

#### **2.3.1 Collection of human peripheral blood and isolation of PBMCs**

Human peripheral blood was collected from healthy volunteers and was approved by the University of East Anglia (UEA) Faculty of Medicine and Health Sciences Research Ethics Committee under the ethical proposal “Inflammation and Cardiovascular Disease” submitted by Dr Samuel J. Fountain. Samples were collected and treated in accordance to guidelines provided under the Human Tissue Act (2004).

Blood from was collected in 4% (w/v) sodium citrate solution. For each 10 ml blood collected, 1 ml of anti-coagulant was used. Accuspin tubes (Sigma-Aldrich) were prepared by adding 13 ml of Histopaque-1077 density gradient media to each tube and centrifuging at 800 x g for 1 minute at room temperature. The collected blood was diluted with an equal volume of dPBS and poured into Accuspin tubes before centrifuging at 1000 x g for 10 minutes at room temperature. Following centrifugation, the opaque interface containing mononuclear cells was carefully pipetted transferred into a fresh centrifuge tube. The cells were washed with an equal volume of dPBS and then sedimented at 250 x g for 10 minutes at room temperature. Following removal of the supernatant, cells were washed twice with dPBS. The resultant PBMC pellet was resuspended in 2-5 ml of the appropriate physiological buffer before counting the number of PBMCs using a haemocytometer.

### **2.3.2 Isolation of monocytes and monocyte-depleted PBMCs**

PBMCs were resuspended in 5 ml salt-buffered solution (SBS) (containing 130 mM sodium chloride, 5 mM potassium chloride, 1.2 mM magnesium chloride, 1.5 mM calcium chloride, 8 mM D-(+)-Glucose and 10 mM hydroxyethyl piperazineethanesulfonic acid (HEPES); pH 7.2). Cells were added to wells of a sterile 24-well plate (Nunc) and incubated at 37°C in a humidified 5% CO<sub>2</sub> incubator for 2 hours. Following incubation, unadhered cells were removed and transferred to fresh wells of a sterile 24-well plate, and reincubated for a further 2 hours. Adhered monocytes were washed twice with dPBS and then treated with TRI reagent for RNA extraction. Monocyte-depleted PBMC fractions were sedimented at 805 x g for 5 minutes at room temperature. The supernatant was discarded, and cells were lysed with TRI reagent for RNA extraction.

## **2.4 Reverse transcription-polymerase chain reaction (RT-PCR)**

### **2.4.1 Total RNA extraction**

RT-PCR was employed to investigate gene expression in human THP-1 cells, peripheral blood monocytes, monocyte-depleted PBMCs, brain RNA, and retina RNA (paramacular). Cellular samples and THP-1 cells ( $1 \times 10^6$  cells) were centrifuged at 805 x g for 7 minutes at room temperature to allow sedimentation and disposal of the supernatant. Cellular disruption was achieved by addition of 1 ml TRI reagent; a single-step RNA isolation reagent modified from Chomczynski and Sacchi (1987). Following addition, cells were vortexed for 1 minute to allow cellular disruption before transferring to a 1.5 ml nuclease-free microcentrifuge tube (Eppendorf). To facilitate visualisation of the cell pellet and to increase the recovery of nucleic acids, 200 µg/ml glycogen (Fermentas) was added and briefly vortexed. In addition, 100 µl of 1-bromo-3-chloropropane (BCP) (for each ml of TRI reagent) was added to this to allow separation of the homogenate into aqueous and organic phases. Samples were briefly vortexed and allowed to stand at room temperature for 15 minutes before centrifuging at 20,000 x g for 15 minutes at 4°C. Centrifugation resulted in 3 phases being established: a lower red organic phase, a cloudy interphase containing denatured proteins and genomic DNA, and an upper aqueous clear phase containing RNA. The upper aqueous phase was transferred to a fresh 1.5 ml microcentrifuge tube. To this, an equal volume of ice-cold isopropanol was added and samples were briefly vortexed and incubated on ice for 15 minutes. Precipitation of the RNA from the aqueous phase was achieved by sedimentation of the sample at 20,000 x g for 20 minutes at 4°C. The supernatant was discarded, leaving a visible RNA pellet that was washed in 1 ml ice-cold 75% (v/v) ethanol. The sample was centrifuged at 20,000 x g for 5 minutes at 4°C, before removing the ethanol and air-drying the pellet for 5-10

minutes at room temperature. Rehydration of the RNA was achieved by addition of 10 µl of nuclease-free water followed by heating at 55°C for 5 minutes.

#### **2.4.2 Total RNA quantification**

The RNA concentration in each sample was determined using a BioPhotometer Plus UV/Vis photometer (Eppendorf). Samples were prepared by diluting 1 in 50 with nuclease-free water in a UVette (Eppendorf). The absorbance was read at A260 (nm) and A280 (nm), with the former being the absorbance at which nucleotides are maximally absorbed. The concentration of RNA in a sample was quantified using the Lambert-Beer law:

$$A = \epsilon C l$$

Where, A is the absorbance at A260 (nm),  $\epsilon$  the molar extinction coefficient for RNA (0.025 (µg/ml) cm<sup>-1</sup>), C the concentration of RNA, and l the path length of the spectrophotometer cuvette. The absorbance at A280 (nm) was read in order to identify the A260/A280 ratio that was used to assess the purity of RNA in the sample where values of 2.0 signified a sample of RNA free of contaminating DNA and proteins.

#### **2.4.3 First strand complementary DNA synthesis**

RNA isolated as described in Section 2.4.1 was reverse transcribed into complementary DNA (cDNA). Human brain RNA (Ambion) at a concentration of 1 mg/ml served as a positive control for gene expression. Reactions for isolated RNA samples were prepared in duplicate, with one reaction containing reverse transcriptase (RT) to produce cDNA from the target RNA sequence, and a second reaction omitting RT (no RT) which was used to confirm that any PCR amplicon was derived from the synthesised cDNA and not genomic DNA. Reactions without RT were not prepared for human brain RNA. For each reaction, 1 µg of total RNA was added to a thin-walled 0.2 ml nuclease-free microcentrifuge tube (Thermo Scientific) containing 1 µl (100 pmol) of 100 µM Oligo (dT)<sub>18</sub> (deoxythymidylic 18-mer oligonucleotide) primer (Fermentas), and 1 µl (0.05 mM) of 10 mM dNTP (deoxyribonucleotide triphosphate) mix (Fermentas). Reactions were made up to a volume of 14.5 µl with nuclease-free water and mixed by flicking the tube before briefly centrifuging. Reactions were incubated at 65°C for 5 minutes to allow the RNA to denature followed by incubation on ice to allow the primer to anneal to the RNA. Reactions for the transcription of RNA to cDNA were prepared by adding 4 µl of 5x RT buffer (Fermentas) to each sample. To limit any degradation of RNA, 0.5 µl (0.5 U) of Ribolock RNase inhibitor (Fermentas) was also added to samples. Reverse transcriptase (1 µl; 200U) was added to RT samples to enable transcription of RNA, and 1 µl of

nuclease-free water (Thermo Scientific) was added to “no RT” samples. All samples were gently flicked before briefly centrifuging. To allow transcription to occur, reactions were incubated at 50°C for 30 minutes followed by inactivation of the enzyme at 85°C for 5 minutes. Complementary DNA samples were stored at -20°C until required.

#### 2.4.4 Primer design and preparation

Primer sequences were designed using the National Centre for Biotechnology Information (NCBI) primer designing tool. Primers were designed to meet the following criteria:

- 1) Located on the coding DNA sequence (CDS) of the gene of interest.
- 2) Limited cross homology with other genes.
- 3) Targets all variants of selected gene.
- 4) Optimal length of 18-22 base pairs (bp).
- 5) A theoretical melting temperature ( $T_m$ ) of 60°C.
- 6) A GC rich 3' end to promote binding.
- 7) Product size above or equal to 200 bp where possible.

All primers were supplied lyophilised from Sigma-Aldrich. Primers were reconstituted to 100 µM in nuclease-free water and kept at -20°C for long-term storage. From these, 10 µM working stocks were prepared in nuclease-free water and stored at -20°C until use.

**Table 2.6 Primer sequences for *ACTB* (actin, beta) and monocyte markers**

Gene	Accession	Sequence	Direction	Size (bp)
<i>ACTB</i>	NM_001101.3	CACAGAGCCTCGCCTTTGCC	Sense (5'-3')	282
		CGATGCCGTGCTCGATGGGG	Antisense (3'-5')	
<i>CD14</i>	NM_000591	AAGCCACAGGACTTGCACTT	Sense (5'-3')	445
		GCGAACGACAGATTGAGGGA	Antisense (3'-5')	
<i>CD16</i>	NM_000569	TAGTTTCAGCTGGCATGCGG	Sense (5'-3')	247
		GTGGAGAGGTTTGTCTGGCA	Antisense (3'-5')	
<i>CD33</i>	NM_001772	ATCCTCATCCCTGGCACTCT	Sense (5'-3')	216
		TCCAGCGAACTTCACCTGAC	Antisense (3'-5')	
<i>CD93</i>	NM_012072	TGACCTGTGCCTCTCGAAAC	Sense (5'-3')	515
		CATGGTGCAAGAGACCCCAT	Antisense (3'-5')	

**Table 2.7 Primer sequences for CC chemokines and receptors**

<b>Gene</b>	<b>Accession</b>	<b>Sequence</b>	<b>Direction</b>	<b>Size (bp)</b>
<i>CCL2</i>	NM_002982.3	GATGCAATCAATGCCCCAGTC	Sense (5'-3')	219
		CTTCGGAGTTTGGGTTTGCT	Antisense (3'-5')	
<i>CCL3</i>	NM_002983.2	CTGCAACCAGTTCTCTGCATC	Sense (5'-3')	209
		CGCTGACATATTTCTGGACCC	Antisense (3'-5')	
<i>CCL4</i>	NM_002984.2	CTGTCCTGTCTCTCCTCATGC	Sense (5'-3')	209
		AGCACAGACTTGCTTGCTTC	Antisense (3'-5')	
<i>CCL5</i>	NM_002985.2	GCATCTGCCTCCCCATATTCC	Sense (5'-3')	201
		AGAGTTGATGTACTCCCGAACC	Antisense (3'-5')	
<i>CCR1</i>	NM_001295.2	GCCTACGAGAGTGGAAGCTG	Sense (5'-3')	358
		TTCCGGAACCTCTCACCAAC	Antisense (3'-5')	
<i>CCR2A</i>	NM_00112304 1.2	GGACCAAGCCACGCAGGTGAC	Sense (5'-3')	160
		TCCTGGACCTCCACACACTGG	Antisense (3'-5')	
<i>CCR2B</i>	NM_00112339 6.1	GGCATAGGGCAGTGAGAGTC	Sense (5'-3')	267
		GCTTGGTGATGTGCTTTTCGG	Antisense (3'-5')	
<i>CCR3</i>	NM_001837.3	TTGTCCATGCTGTGTTTGCC	Sense (5'-3')	323
		AAAAATGAGCCGGATGGCCT	Antisense (3'-5')	
<i>CCR4</i>	NM_005508.4	ATGATCTTTGCCGTGGTGGT	Sense (5'-3')	336
		ATGATCCATGGTGGACTGCG	Antisense (3'-5')	
<i>CCR5</i>	NM_000579.3	ACAGGGCTGTGAGGCTTATC	Sense (5'-3')	277
		CATTTGCAGAAGCGTTTGGC	Antisense (3'-5')	
<i>CCR6</i>	NM_004367.5	CAGCGATGTCTGTGAACCCA	Sense (5'-3')	263
		AATTTGCAGCCGTCACAAGC	Antisense (3'-5')	
<i>CCR7</i>	NM_001838.3	CAAGTCCTGGGTCTTCGGTG	Sense (5'-3')	497
		CCAGGACCACCCCATTGTAG	Antisense (3'-5')	
<i>CCR8</i>	NM_005201.3	GCCGTGTATGCCCTAAAGGT	Sense (5'-3')	432
		GGCATAAGTCAGCTGTTGGC	Antisense (3'-5')	
<i>CCR9</i>	NM_006641.3	GGCAATTGCTGACCTCCTCT	Sense (5'-3')	413
		CGAAGGGAAGGAAGAACCCC	Antisense (3'-5')	
<i>CCR10</i>	NM_016602.2	TTGCTACAAGGCCGATGTCC	Sense (5'-3')	285
		TGGAAGGAGGCCGAGTAGAG	Antisense (3'-5')	
<i>CCRL2</i>	NM_003965.4	TCTTCCTTCTGATGTGGGCG	Sense (5'-3')	272
		TTCCCTCGATGTGCCTTGTG	Antisense (3'-5')	

**Table 2.8 Primer sequences for P1 purinoceptors**

Gene	Accession	Sequence	Direction	Size (bp)
<i>ADORA</i>	NM_000674	GTGCGAGTTTCGAGAAGGTCA	Sense (5'-3')	374
		GGATGCGGAAGGCATAGACA	Antisense (3'-5')	
<i>ADORA2A</i>	NM_000675	CTACCGTATCCGCGAGTTCC	Sense (5'-3')	295
		GCTAAGGAGCTCCACGTCTG	Antisense (3'-5')	
<i>ADORA2B</i>	NM_000676.2	CAGAACCCTGGGATGGAACC	Sense (5'-3')	277
		CAGCACAGGGCAAAAATCCC	Antisense (3'-5')	
<i>ADORA3</i>	NM_001081976	CTGGTGCCGAGGCTATTTCC	Sense (5'-3')	302
		CCTTGCGGACAACCTTTGGGA	Antisense (3'-5')	

**Table 2.9 Primer sequences for P2X purinoceptors**

Gene	Accession	Sequence	Direction	Size (bp)
<i>P2RX1</i>	NM_002558.2	GCTTTCCACGCTTCAAGGTC	Sense (5'-3')	341
		GAGGTGACGGTAGTTGGTCC	Antisense (3'-5')	
<i>P2RX2</i>	NM_170682.2	GCACAGACGGGTACCTGAAG	Sense (5'-3')	200
		GGAGTACTTGGGGTTGCACT	Antisense (3'-5')	
<i>P2RX3</i>	NM_002559	TGTATCAGACAGCCAGTGCG	Sense (5'-3')	564
		CGGATGCCAAAAGCCTTCAG	Antisense (3'-5')	
<i>P2RX4</i>	NM_001256796	AGCAACGGAGTCTCAACAGG	Sense (5'-3')	311
		TGGAAACTGTGTCCTGCGTT	Antisense (3'-5')	
<i>P2RX5</i>	NM_002561.3	GCAATGTGATGGACGTCAAGG	Sense (5'-3')	263
		GTACCCGGAGGAGACAGACT	Antisense (3'-5')	
<i>P2RX6</i>	NM_005446.3	GACTTCGTGAAGCCACCTCA	Sense (5'-3')	405
		TTGTGGTTCATAGCGGCAGT	Antisense (3'-5')	
<i>P2RX7</i>	NM_002562.5	CGGTTGTGTCCCAGATATCC	Sense (5'-3')	414
		AATGCCCATATTCCGCCCT	Antisense (3'-5')	

**Table 2.10 Primer sequences for P2Y purinoceptors**

Gene	Accession	Sequence	Direction	Size (bp)
<i>P2RY1</i>	NM_002563	GTTCAATTTGGCTCTGGCCG	Sense (5'-3')	326
		TTTTGTTTTTGC GGACCCCG	Antisense (3'-5')	
<i>P2RY2</i>	NM_002564.2	CCGCACCCTCTACTACTCCT	Sense (5'-3')	243
		TCAGTTCTGTCGGATCTGCG	Antisense (3'-5')	
<i>P2RY4</i>	NM_002565	CCCCAACCCTATGGCTCTTC	Sense (5'-3')	427
		TGGTCAAACCTTTCAGGCCG	Antisense (3'-5')	
<i>P2RY6</i>	NM_176798	GCTCTCACTGTCATCGGCTT	Sense (5'-3')	391
		TCTGCCATTTGGCTGTGAGT	Antisense (3'-5')	
<i>P2RY11</i>	NM_002566	CATGGCAGCCAACGTCTCG	Sense (5'-3')	622
		CAGGCTATACGCTCTGTAGGC	Antisense (3'-5')	
<i>P2RY12</i>	NM_022788	ACTGGGAACAGGACCACTGA	Sense (5'-3')	698
		CAGAATTGGGGCACTTCAGC	Antisense (3'-5')	
<i>P2RY13</i>	NM_176894	TTCCCAGCCCTCTACACAGT	Sense (5'-3')	461
		GGCCCCTTTAAGGAAGCACA	Antisense (3'-5')	
<i>P2RY14</i>	NM_001081455	CGGAAGTGGCACAAAGCATC	Sense (5'-3')	370
		CCCTAAACGGCTGGCATAGA	Antisense (3'-5')	

#### 2.4.5 Polymerase chain reaction (PCR)

Prepared cDNA samples were used as a template for amplification in PCR using primers detailed in Section 2.4.4. Retinal cDNA kindly gifted by Dr Julie Sanderson (School of Pharmacy, UEA), was also tested. Primers were prepared as described (Section 2.4.4) and included  $\beta$ -actin (Table 2.6); a housekeeping gene that served as a positive control for PCR reactions. Reactions for each primer were prepared in duplicate in thin-walled 0.2 ml nuclease-free microcentrifuge tubes. To each reaction, 1  $\mu$ l of cDNA (either RT or no RT), 1  $\mu$ l (200 nM) of forward primer, 1  $\mu$ l (200 nM) of reverse primer, and 25  $\mu$ l of ReadyMix™ Taq PCR Reaction Mix were added. Reactions were made up to a final volume of 50  $\mu$ l with nuclease-free water and mixed by flicking the tube before briefly centrifuging to allow sedimentation. To allow selective amplification, samples were thermally cycled, allowing an initial denaturation of the DNA helix at 94°C for 1 minute, followed by 35 cycles of denaturation at 94°C for 30 seconds, an annealing of the primers to the DNA template at 55°C for 30 seconds and finally, an extension of the cDNA strand by addition of dNTPs at 72°C for 1 minute. A final extension at 72°C for 5 minutes was

performed to ensure that any remaining single-stranded DNA was fully extended. Samples amplified at this stage were stored at -20°C until further use.

#### **2.4.6 Agarose gel electrophoresis**

Agarose gel electrophoresis is an analytical procedure that utilises an electromotive force to separate DNA molecules based on size and charge. Agarose gel (Melford Laboratories) was prepared as a 2% (w/v) solution in 1x Tris-acetate-EDTA buffer (TAE; Thermo Scientific) and heated in a microwave until clear. To this, 4 µl of ethidium bromide solution was added such that the final concentration was 0.4 µg/ml. This is an intercalating dye that allows visualisation of DNA under ultra-violet (UV) light. The gel was poured into a cast and allowed to set at room temperature for 30 minutes, before being transferred to an electrophoresis chamber containing 1x TAE. Samples were prepared by mixing 10 µl of PCR reactions with 5 µl gel loading dye (New England Biolabs), and adding to wells of the gel. A 100 base-pair (bp) DNA ladder (New England Biolabs) was used as a reference molecular weight marker and was prepared by mixing 4 µl of marker with 10 µl gel loading dye (New England Biolabs). To allow separation of DNA, electrophoresis was performed at 95V (volts) for 45 minutes. Gel visualisation was performed under UV light using a ChemiDoc™ XRS visualiser (Bio-Rad).

### **2.5 Generation of P2Y<sub>6</sub>-knockdown THP-1 cells**

Gene silencing strategies were employed to generate P2Y<sub>6</sub>-knockdown THP-1 cells. The method of choice was the delivery of short-hairpin ribonucleic acid (shRNA) sequences carried by the lentiviral pLKO.1 puro (puromycin-resistant) vector (Moffat *et al.*, 2006; Figure 2.1) as this method enables the generation of long-term stable knockdown lines. The pLKO.1 vector was used together with the second-generation psPAX2 and pMD2.G plasmids. The psPAX2 plasmid encodes for the HIV-1 proteins Gag (structural) and Pol (polymerase) and the accessory proteins, Tat and Rev that are involved in driving the activation of viral transcription and the subsequent migration of genomic RNA from the nucleus (Zufferey *et al.*, 1997). In comparison, the pMD2.G helper/envelope plasmid encodes for glycoproteins of vesicular stomatitis virus (VSV-G) that stabilise the viral particles and allow the vector to be pantropic by binding to ubiquitous phospholipid regions of the plasma membrane (Burns *et al.*, 1993).

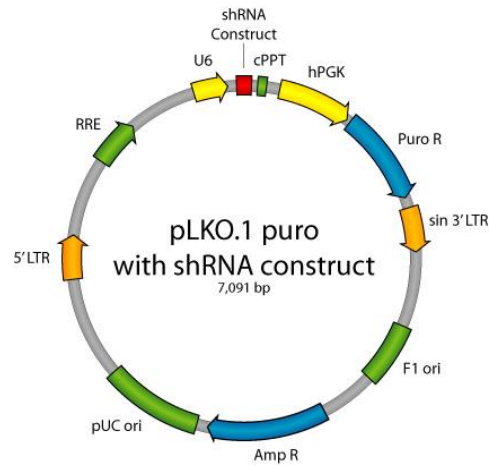


**Figure 2.1 pLKO.1 puro shRNA vector**

Map of the lentiviral pLKO.1-puro vector. The pLKO.1 puro vector is 7032 bp long and includes a U6 promoter that drives RNA polymerase transcription for the generation of shRNA transcripts. Then pLKO.1 puro vector shown here includes a 60 bp shRNA sequence cloned using *AgeI* and *EcoRI* restriction sites. Image source: <http://www.addgene.org/tools/protocols/plko/#A> (accessed 7<sup>th</sup> Jan 2014)

### 2.5.1 Preparation of plasmid DNA for transfection

Bacterial glycerol stocks for pLKO.1 puro vectors carrying shRNA sequences targeting *P2RY6* were selected from the RNA interference (RNAi) consortium (TRC) and purchased from the MISSION™ shRNA library (Sigma-Aldrich).

**Table 2.11 shRNA sequences for *P2RY6***

TRC Number	Clone ID	shRNA sequence
14073	NM_176797.1-	CCGGGCAGCCTTCATATTTGCCATTCTCGAG
	1249s1c1	AATGGCAAATATGAAGGCTGCTTTTT
14075	NM_176797.1-	CCGGCCACTATATGCCCTATGGCATCTCGAG
	806s1c1	ATGCCATAGGGCATATAGTGTTTTT

Bacterial stocks for psPAX2 and pMD2.G were purchased from Addgene. Vectors and plasmids were streaked onto Luria Bertani agar plates (LB; containing 35 g of LB agar in 1 L of distilled water and sterilised by autoclaving) supplemented with 100 µg/ml ampicillin. Plates were incubated overnight at 37°C. A single colony from each plate was transferred to 10 ml of LB broth (containing 20 g of LB broth in 1 L of distilled water and sterilised by autoclaving), supplemented with 100 µg/ml ampicillin. Colonies were allowed to shake at 200 revolutions per minute (rpm) overnight in a 37°C shaking incubator (New Brunswick

Scientific). The following morning, colonies were centrifuged at 652 x *g* for 20 minutes at 4°C and the supernatant was disposed. Plasmid DNA was extracted using an E.Z.N.A Plasmid Mini Kit II (Omega Bio-Tek) as per manufacturer instructions. Quantification of DNA in samples was achieved as described in Section 2.4.2, using the Lambert-Beer law and a molar extinction coefficient of (0.020 (µg/ml) cm<sup>-1</sup>) for DNA. The purity of the sample was assessed using the A<sub>260</sub>/A<sub>280</sub> ratio, which is typically 1.8 for DNA. To check for plasmid DNA quality and recombination, agarose gel electrophoresis as described in section 2.4.6 was performed using a 0.8% (w/v) agarose gel prepared with 0.4 µg/ml ethidium bromide. Gel visualisation was performed under ultraviolet (UV) light to verify DNA forms (Figure 2.2).

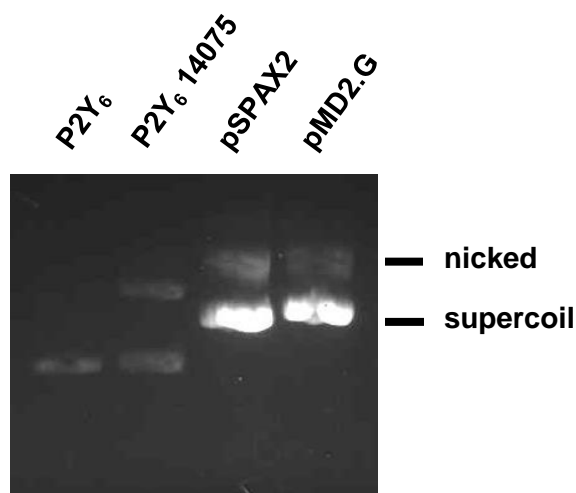


**Figure 2.2 Detection of plasmid DNA**

Plasmid DNA run on a 0.8% (w/v) gel with 0.4 µg/ml ethidium bromide and visualised under UV light. Gel shows nicked and supercoiled DNA forms for pLKO.1 puro *P2RY6* shRNA sequences (clones 14073 and 14075). Also shown are DNA forms for psPAX2 and pMD2.G plasmids.

### 2.5.2 Lentivirus production in HEK293T

Lentivirus production was performed in HEK293T cells (Section 2.2.1.4). For each pLKO.1 puro shRNA plasmid to be transfected, 7.5x10<sup>5</sup> HEK293T cells were required. Cells were counted and harvested by centrifuging at 805 x *g* for 7 minutes at room temperature. The supernatant was discarded and the remaining cell pellet was resuspended in 4.5 ml HEK293T cell culture medium without penicillin-streptomycin solution, and added to a sterile 5 cm cell culture dish (Thermo Scientific). The cells were allowed to adhere overnight at 37°C in a humidified 5% CO<sub>2</sub> incubator. On the following day, 200 µl of serum-free OPTIMEM media (Life Technologies) was added to two sterile

1.5 ml micro-centrifuge tubes designated mix 1 and mix 2. To mix 2, 20 µl of lipofectamine-2000 transfection reagent (Life Technologies) was added. To mix 1, the following concentrations of plasmid DNA and lentivirus vectors were added: 1 µg pLKO.1 *P2RY6* DNA, 0.75 µg psPAX2 packaging DNA, and 0.25 µg pMD2.G envelope DNA. Both mixes were allowed to incubate at room temperature for 30 minutes before adding mix 2 to mix 1. The transfection mixture was added drop-wise to HEK293T cells and incubated at 37°C in a humidified 5% CO<sub>2</sub> incubator for 12-15 hours. Following incubation, the transfection reagent was removed and replaced with 4.5 ml of HEK293T medium containing 1% penicillin-streptomycin solution before re-incubating cells at 37°C in a humidified 5% CO<sub>2</sub> incubator for 24 hours. On the subsequent day, the media (virus) was harvested and transferred to a 15 ml centrifuge tube (Corning) for storage at 4°C. A further 4.5 ml of HEK293T medium was added to the dish before cells were once again incubated for 24 hours at 37°C in a humidified 5% CO<sub>2</sub> incubator. Following incubation, the media (virus) was re-harvested and the HEK293T cells were disposed. The harvested virus was sterile-filtered through a 0.45 µm filter disc and aliquoted into 1.5 ml micro-centrifuge tubes for long-term storage at -80°C.

### 2.5.3 Generation of P2Y<sub>6</sub>-KD cells using lentiviral transduction particles

Lentiviral particles incorporating *P2RY6* pLKO.1-puro shRNA sequences were purchased from the MISSION™ shRNA library. These are listed in Table 2.19.

**Table 2.12 Lentivirus *P2RY6* shRNA sequences**

TRC Number	Clone ID	shRNA sequence
14075	NM_176797.1- 806s1c1	CCGGCCACTATATGCCCTATGGCATCTCGA GATGCCATAGGGCATATAGTGGTTTTT
14076	NM_176797.1- 377s1c1	CCGGCATCTGTGTCATTACCCAGATCTCGA GATCTGGGTAATGACACAGATGTTTTT
14077	NM_176797.1- 1142s1c1	CCGGCCTCTTCTACTTCACCCAGAACTCGA GTTCTGGGTGAAGTAGAAGAGTTTTT
357968	NM_176797.1- 1244s21c1	CCGGCCTGGGCAGCCTTCATATTTGCTCGA GCAAATATGAAGGCTGCCAGTTTTTG
358038	NM_176797.1- 547s21c1	CCGGTGGTCCGCTTCTTCTATGCTCGA GCATAGAAGAGGAAGCGGACCATTTTTG

Using the reported transducing units (TU) of each virus, the volume of lentiviral particles required to achieve a multiplicity of infection of 10 (MOI 10) was calculated for a THP-1

cell number of  $5 \times 10^4$  cells. This volume of lentivirus was used to transduce THP-1 cells as described in Section 2.5.5.

#### **2.5.4 Puromycin kill curve**

A puromycin kill curve was constructed to determine the concentration of puromycin required to kill THP-1 cells. Puromycin (InvivoGen) was tested in duplicate at final concentrations of 0, 1, 5, and 10  $\mu\text{g/ml}$  over a 10-day period. For each test well,  $5 \times 10^4$  cells were required. On day 0, cells were counted and harvested by centrifuging at  $805 \times g$  for 7 minutes at room temperature. The supernatant was discarded and cells were resuspended in THP-1 culture medium (Section 2.2.1.1) such that the final cell density was  $5 \times 10^4$  cells/ml. To each well of a sterile 24-well tissue culture plate, 1 ml of THP-1 cells were added. Puromycin or sterile water was next added to wells and plates were incubated at  $37^\circ\text{C}$  in a humidified 5%  $\text{CO}_2$  incubator. Cell viability was tested on day 0, 2, 4, 6, 8, and 10, using Thiazolyl Blue Tetrazolium Bromide (MTT), a colorimetric reagent measuring mitochondrial function through the ability of cells to convert MTT into formazan crystals (Mosmann, 1983). For this, 1 ml of cells from each treatment were transferred to 1.5 ml microcentrifuge tubes and centrifuged at  $2000 \times g$  for 3 minutes at room temperature. The supernatant was discarded, and cells were washed thrice with 1 ml of THP-1 cell culture medium. After the 3<sup>rd</sup> wash, cells were resuspended in 1 ml THP-1 cell culture medium. Media alone samples (1 ml THP-1 culture medium) were prepared at this stage. Following the addition of 100  $\mu\text{l}$  of 10 mg/ml MTT solution (prepared in distilled water), tubes were incubated at  $37^\circ\text{C}$  in a humidified 5%  $\text{CO}_2$  incubator for 2 hours. All tubes were then centrifuged at  $2000 \times g$  for 3 minutes at room temperature before discarding the supernatant. DMSO (0.5 ml) was added to each tube and incubated for 15 minutes at  $37^\circ\text{C}$ . Sample absorbance was determined by transferring 200  $\mu\text{l}$  of each sample to a UVette and reading the absorbance at A595 (nm) using a BioPhotometer Plus UV/Vis photometer. Cell viability was quantified by taking the absorbance of media alone samples and subtracting this from individual samples. Based on this data, the optimal puromycin regime for killing THP-1 cells was 1  $\mu\text{g/ml}$  for 5 days.

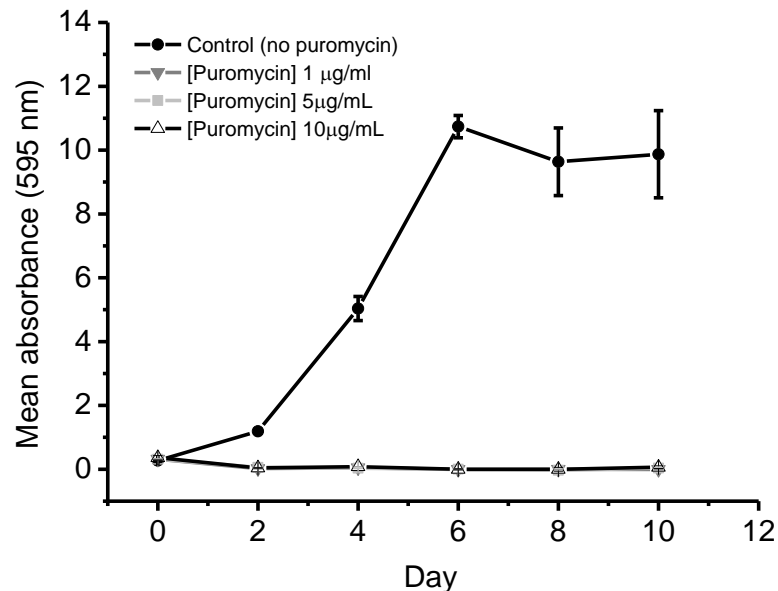


**Figure 2.3 THP-1 cell puromycin kill curve**

THP-1 cells were incubated with 0 (vehicle), 1, 5 or 10 µg/ml puromycin and monitored for cell viability over 10 days using the MTT assay. Results expressed as mean absorbance at A595 (nm) ± SEM for n=2 replicates.

### 2.5.5 THP-1 cell transduction and puromycin selection

For each prepared virus, pLKO.1-puro non-target shRNA transduction particles and control cells (no virus),  $5 \times 10^4$  THP-1 cells were required. Cells were centrifuged at 805 x g for 7 minutes at room temperature before disposing the supernatant. Fresh THP-1 cell culture medium was added to yield a cell density of  $5 \times 10^4$  cells/ml, and 1 ml of this was added to each well of a sterile 24-well tissue culture plate. The following treatments were added: control well (no treatment), scrambled well (5 µl of non-target shRNA transduction particles), *P2RY6* wells (100 µl of virus generated as per Section 2.5.2, or volumes of MISSION™ transduction particles giving MOI 10 as per Section 2.5.3). To each well, 1 µl of 8 mg/ml of hexadimethrine bromide was added to promote transduction. Plates were incubated at 37°C in a humidified 5% CO<sub>2</sub> incubator for 72 hours. To select for cells stably incorporating the viral genome, THP-1 cells were treated for 5 days with 1 µg/ml puromycin (Section 2.5.4). After 5 days, cells were removed from wells and centrifuged at 805 x g for 7 minutes at room temperature. The supernatant was disposed, and cells were washed once with 5 ml of THP-1 cell culture medium before transferring cells to vented T25 flasks containing 5 ml of fresh THP-1 cell culture medium supplemented with 1 µg/ml puromycin.

### 2.5.6 Quantitative real-time PCR (qRT-PCR)

qRT-PCR was performed to test the level of gene expression in *P2RY6*-knockdown and scrambled THP-1 cells. This technique uses the rate of amplification of specific target sequences in a sample to estimate the level of gene expression in the original cDNA template (Higuchi *et al.*, 1992). qRT-PCR was performed using the fluorescent dye SYBR Green (SG;  $\lambda_{Ex} = 494\text{nm}$ ,  $\lambda_{Em} = 521\text{nm}$ ) which preferentially binds to double-stranded DNA (Dragan *et al.*, 2012). cDNA for all cell lines were prepared as in Section 2.4. Samples were diluted to 10 ng using nuclease-free water in thin-walled 0.2 ml nuclease-free microcentrifuge tubes. Samples were then added in triplicate (10  $\mu\text{l}$ ) for each gene tested, to wells of a 96-well MicroAmp® fast optical plate (Applied Biosystems). All cDNA samples were also tested in triplicate for  $\beta$ -actin. Negative control wells were prepared for each gene tested by adding 10  $\mu\text{l}$  of nuclease free-water to separate wells. A reaction mix was then prepared for each gene tested (primers as Section 2.4.4), combining the following for each well in a total volume of 15  $\mu\text{l}$ : 12.5  $\mu\text{l}$  of SG PCR master mix (Applied Biosystems), 0.5  $\mu\text{l}$  forward primer, 0.5  $\mu\text{l}$  reverse primer, and 1.5  $\mu\text{l}$  nuclease-free water. Following addition of 15  $\mu\text{l}$  of the reaction mix to wells, the plate was sealed with an optical adhesive cover (Applied Biosystems) and centrifuged briefly at 400 x *g*. Plates were loaded onto a 7500 fast real-time PCR machine (Applied Biosystems) and run for 20 seconds at 50°C, 10 minutes at 95°C, followed by 40 cycles of 15 seconds at 95°C and 1 min at 60°C and a dissociation step to assess for primer dimers and target specificity. Using the associated 7500 software, the threshold cycle ( $C_t$ ) value was obtained for each set of samples. This is the cycle number required for fluorescence to give a signal over background at the point at which amplification is linear. Values were corrected against  $\beta$ -actin and analysed using the  $\Delta\Delta C_t$  method to calculate the relative quantification (RQ) values ( $2^{-\Delta\Delta C_t}$ ) which measures the fold-change in gene expression relative to control cells. A significant shift in gene expression was given by an RQ value of 0.5.

## 2.6 Calcium mobilisation

Detection of intracellular  $\text{Ca}^{2+}$  signals were undertaken using fluorescent  $\text{Ca}^{2+}$  indicators that altered in their fluorescence when bound to free  $\text{Ca}^{2+}$ . The fluorescent dyes used were Fluo-4 AM and Fura-2 AM (Life Technologies) (Figure 2.4a and c). Fluo-4 AM was used with THP-1 cells and PBMCs, and Fura-2 AM with 1321N1 astrocytoma cells.

The membrane impermeable carboxylate groups of both indicators are esterified into an acetoxymethyl (AM) ester that renders the dyes lipophilic making them cell permeant, non-fluorescent, and insensitive to ions. Once inside the cell, the AM moiety is hydrolysed by esterases resulting in the release of an ion-sensitive and impermeable fluorescent indicator that remains trapped inside the cell (Tsien, 1981).

The  $\text{Ca}^{2+}$  indicator Fluo-4 AM is a di-fluoro analogue of Fluo-3, a  $\text{Ca}^{2+}$  indicator developed from the  $\text{Ca}^{2+}$  chelator, BAPTA (Gee *et al.*, 2000) (Figure 2.4a). As a single-emission wavelength dye excited by visible light, Fluo-4 AM exhibits a fluorescence spectra of  $\lambda_{\text{ex}} = 494\text{nm}$  and  $\lambda_{\text{em}} = 515\text{nm}$ , and increases over 100-fold in fluorescence when bound to  $\text{Ca}^{2+}$  at  $\lambda_{\text{ex}} = 488\text{nm}$  (Gee *et al.*, 2000) (Figure 2.4b). At  $22^\circ\text{C}$ , Fluo-4 AM exhibits a  $K_d$  for  $\text{Ca}^{2+}$  of  $345\text{ nM}$ , and is capable of detecting  $\text{Ca}^{2+}$  concentrations between  $100\text{ nM}$ - $1\text{ }\mu\text{M}$  (Gee *et al.*, 2000).

The  $\text{Ca}^{2+}$  indicator dye Fura-2 AM is a dual excitation/single emission ratiometric dye which obtains its  $\text{Ca}^{2+}$ -binding abilities from the presence a tetracarboxylic acid moiety derived from the  $\text{Ca}^{2+}$  chelator, EGTA (ethylene glycol tetraacetic acid) (Grynkiewicz *et al.*, 1985) (Figure 2.4c). Excited by UV-light, the excitation spectra of Fura-2 AM shifts in peak fluorescence from  $\lambda_{\text{ex}} = 362\text{nm}$  in  $\text{Ca}^{2+}$ -free states, to  $\lambda_{\text{ex}} = 335\text{nm}$  in  $\text{Ca}^{2+}$ -bound states, thus displaying a 2-fold increase in fluorescence (Grynkiewicz *et al.*, 1985). Under both states, the emission spectra remains fixed at  $\lambda_{\text{em}} = 510\text{nm}$ . The  $K_d$  value of Fura-2 AM for  $\text{Ca}^{2+}$  shifts from  $135\text{ nM}$  at  $20^\circ\text{C}$  in the absence of magnesium ions ( $\text{Mg}^{2+}$ ), to  $224\text{ nM}$  at  $37^\circ\text{C}$  in the presence of  $1\text{ mM Mg}^{2+}$  (Grynkiewicz *et al.*, 1985).

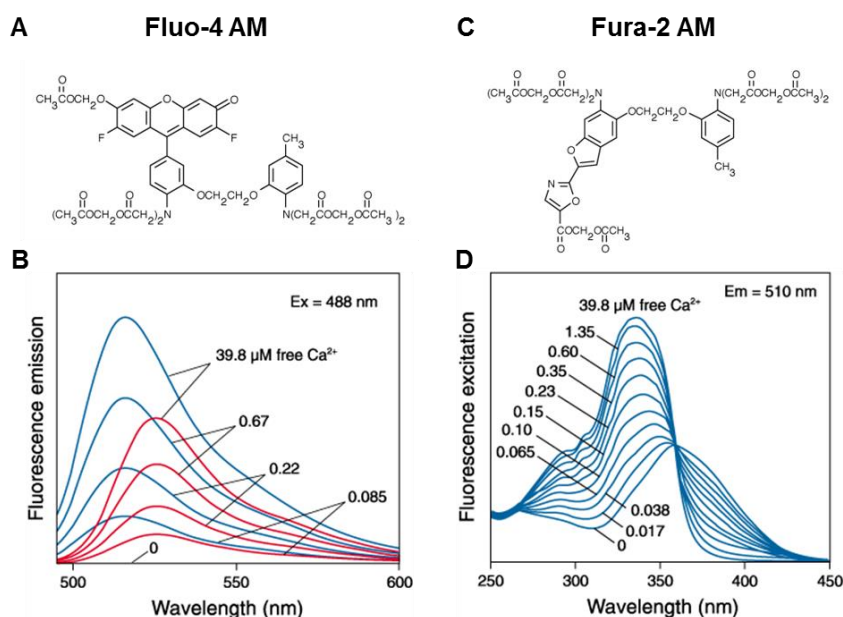


**Figure 2.4 Structure and fluorescence spectra of Fluo-4 AM and Fura-2 AM**

Structure of (A) Fluo-4 AM and (C) Fluo-3 AM. Fluorescence emission spectra of (C) Fluo-4 AM (blue lines) and Fluo-3 AM (red lines), and (D) Fura-2 AM. Fluorescence emission intensity plotted against wavelength (nm) for increasing concentrations of free  $\text{Ca}^{2+}$  at  $\lambda_{\text{ex}} = 488\text{ nm}$  (Fluo-4 AM), and  $\lambda_{\text{em}} = 510\text{ nm}$  (Fura-2 AM). Image source: Johnson (2010).

### **2.6.1 Intracellular Ca<sup>2+</sup> measurements (with extracellular Ca<sup>2+</sup>)**

Cells were counted and harvested as paired replicates. For each replicate,  $2 \times 10^6$  THP-1 cells or  $30 \times 10^6$  PBMCs were required. For PTx studies, THP-1 cells were seeded in vented T75 flasks and incubated with PTx for 4 hours at 37°C in a humidified 5% CO<sub>2</sub> incubator. For all other studies, cells were harvested and centrifuged at 805 x g for 7 minutes at room temperature before discarding the supernatant. The resultant cell pellet was resuspended in Ca<sup>2+</sup> loading buffer (130 mM sodium chloride, 5 mM potassium chloride, 1.2 mM magnesium chloride, 1.5 mM calcium chloride, 8 mM D-(+)-Glucose, 10 mM hydroxyethyl piperazineethanesulfonic acid (HEPES) and 0.01% (w/v) pluronic acid; pH 7.2), such that the final cell density was  $1 \times 10^6$  cells/ml. To this, fluo-4 AM was added such that the final concentration was 2 μM for THP-1 cells and 4 μM for PBMCs. Cells were incubated in the dark for 1 hour at 37°C followed by 30 minutes at room temperature. For each replicate, 2 ml of cells were transferred to a microcentrifuge tube and centrifuged at 805 x g for 3 minutes at room temperature. The supernatant was discarded and cells were resuspended in 2 ml SBS (Section 2.3.2) and transferred to a quartz cuvette (10 mm light path) containing a magnetic stirrer to continuously agitate the cells. Fluorescence signals were detected with an F-2000 spectrofluorometer (Hitachi) set to record measurements at 1 second intervals at  $\lambda_{\text{ex}} = 494$  nm and  $\lambda_{\text{em}} = 516$  nm. Signals were allowed to equilibrate for 5 minutes before measurements. A baseline measurement of 3 minutes was taken before the addition of cell treatments. Cells were pre-incubated with the relevant vehicle or treatment for 10-30 minutes before the addition of ligands. Maximum fluorescent signals (F<sub>max</sub>) were generated by the addition of 40 μM Digitonin (5 mg/ml stock prepared in deionised water heated to 95°C for 5 minutes). Calcium responses were quantified by expressing responses as a percentage of F<sub>max</sub>.

### **2.6.2 Intracellular Ca<sup>2+</sup> measurements (without extracellular Ca<sup>2+</sup>)**

THP-1 cells were counted, harvested, centrifuged, and loaded with 2 μM fluo-4 AM as described above (Section 2.6.2). Following centrifugation of 2 ml cells in microcentrifuge tubes as also described above, cells were resuspended in 2 ml SBS from which calcium chloride was removed and replaced with the calcium chelator, ethylene glycol tetraacetic acid (EGTA) (130 mM sodium chloride, 5 mM potassium chloride, 1.2 mM magnesium chloride, 1 mM EGTA), 8 mM D-(+)-Glucose and 10 mM hydroxyethyl piperazineethanesulfonic acid (HEPES); pH 7.2). Measurements were performed as described above however; 1.5 mM CaCl<sub>2</sub> was added to cells just prior to addition of 40 μM Digitonin to raise extracellular levels of Ca<sup>2+</sup> (“add-back” response).

### 2.6.3 Intracellular Ca<sup>2+</sup> measurements on Fura-2 AM-loaded 1321N1 cells

Human astrocytoma 1321N1 cells were diluted with 1321N1 cell culture media to  $2 \times 10^5$  cells/ml and added to wells (200  $\mu$ l) of a sterile black 96-well, clear-bottomed plate (Corning) such that each well contained  $4 \times 10^4$  cells. Outer wells were not used and instead contained 300  $\mu$ l of 1321N1 cell culture medium. Plates were incubated at 37°C in a humidified 5% CO<sub>2</sub> incubator overnight to allow cells to form a confluent monolayer. On the following day, the media was carefully aspirated and replaced with 200  $\mu$ l of 2  $\mu$ M Fura-2 AM prepared in calcium loading buffer, prior to incubating plates in the dark for 1 hour at 37°C. After loading, the wells were washed once with 200  $\mu$ l SBS buffer (Section 2.3.2) before the addition of 200  $\mu$ l SBS to wells for nucleotide studies, or 180  $\mu$ l SBS for MRS-2578 studies. For nucleotide studies with P2Y<sub>6</sub>-stable cells, half-log, 9-point concentration curves were prepared in triplicate in SBS at 5x the final concentration. Experiments with parental 1321N1 cells involved adding nucleotides at final concentrations of 10  $\mu$ M and 100  $\mu$ M. Antagonist studies with MRS-2578 involved preparing full-log 8-point concentration curves of MRS-2578 in 10% DMSO at 10x the required final concentration. Cells were incubated with MRS-2578 or vehicle for 30 minutes. For all experiments, nucleotides were added by a FlexStation microplate reader (Molecular Devices) set to deliver 50  $\mu$ l from 96-well u-bottomed plates (Thermo Scientific). Measurements were taken at  $\lambda_{em} = 510$  nm,  $\lambda_{ex} = 340$  nm and  $\lambda_{ex} = 380$  nm. Fluorescence at  $\lambda_{ex} = 340$  nm and  $\lambda_{ex} = 380$  nm were used to calculate the change in intracellular calcium (F-ratio) following subtraction of the baseline response.

## 2.7 Transwell chemotaxis assay

Chemotaxis assays were performed in sterile 24-well tissue culture plates using Transwell inserts (Corning) with “track etched” polyethylene terephthalate (PET) membranes with 3  $\mu$ m pores. For each transwell,  $1 \times 10^6$  THP-1 cells or PBMCs were required. For studies with PTx or BAPTA-AM, harvested cells were seeded in vented T75 flasks and pre-incubated with PTx (4 hours), BAPTA-AM (30 minutes) or vehicle. Harvested cells were centrifuged at 805 x *g* for 7 minutes at room temperature to allow sedimentation of cells and disposal of the supernatant. The resultant cell pellet was washed twice in chemotaxis medium (RPMI 1640 media containing 0.3 g/L L-Glutamine and 1% (v/v) penicillin-streptomycin solution containing 50 units/ml of penicillin and 50  $\mu$ g/ml of streptomycin). After washing, the cell pellet was resuspended in fresh chemotaxis medium such that the cell yield was  $1 \times 10^6$  cells per 100  $\mu$ l. Chemotaxis medium or chemoattractants (prepared in chemotaxis medium) (500  $\mu$ l), were added to wells of the culture plate, and transwell inserts were placed into these (Figure 2.5). Cells (100  $\mu$ l) were added to inserts, followed by the immediate addition of treatments. Plates were then incubated at 37°C in a humidified 5% CO<sub>2</sub> incubator for 2 hours. Following incubation, cells were aspirated and

inserts were washed twice in ice-cold dPBS. After washing, inserts were placed in ice-cold methanol for 10 minutes to fix the cells. The methanol was aspirated and inserts were finally stained for 10 minutes with 0.5% (w/v) crystal violet solution (in 25% (v/v) methanol). After staining, cells in the inner membrane of inserts were removed using cotton swabs. Inserts were finally washed twice in deionised water and allowed to dry for 24 hours. The migration of cells was assessed by taking images of cells attached to the outer membrane of inserts using a CKX41 microscope set at 20x objective and ImageJ software. Cellular migration was expressed as a chemotactic ratio and calculated by dividing the number of cells that migrated towards treatment over the number of cells that migrated towards vehicle.

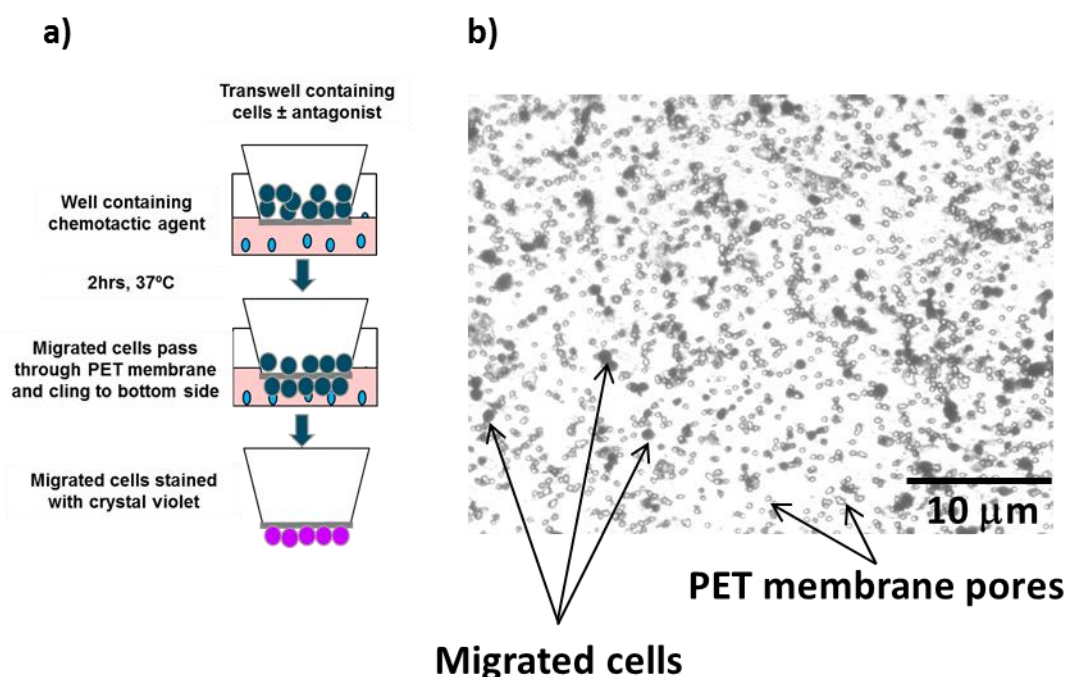


**Figure 2.5 Cell chemotaxis**

Transwell inserts are placed into wells of a culture plate containing chemotactic agents. Cells (THP-1 or PBMCs) are added to inserts prior to addition of compounds. Cells are allowed to migrate for 2 hours at 37°C before removing and washing inserts. Migrated cells are fixed with methanol prior to staining with crystal violet solution. Transwell membrane pores and migrated cells attached to the outer membrane shown

## 2.8 HUVEC adhesion assay

HUVEC adhesion assays were developed using the non-fluorescent membrane-permeable probe Calcein AM (Santa Cruz Biotechnology) using a method first described by Akeson and Woods (1993). Like other fluorescent probes, the carboxylate groups of

Calcein AM are esterified into an AM ester that renders the dye lipophilic and cell permeant. Upon entering cells, the AM group is cleaved by esterases to yield the membrane-impermeable dye, Calcein ( $\lambda_{em} = 496$  nm,  $\lambda_{ex} = 516$  nm). This method serves as a useful tool for detecting the adherence of THP-1 cells to HUVEC monolayers (Akeson and Woods, 1993).

Experiments were performed in sterile 96-well black clear-bottomed tissue culture plates. HUVECs were centrifuged at  $220 \times g$  for 5 minutes at room temperature before discarding the supernatant. Cells were counted and diluted in Endothelium Cell Growth Medium to obtain a cell yield of  $1 \times 10^5$  cells/ml. For each treatment, 4-6 replicates were required, adding 200  $\mu$ l of cells such that each well contained  $1 \times 10^4$  cells. Plates were incubated at 37°C in a humidified 5% CO<sub>2</sub> for 48 hours to allow cells to form a confluent monolayer. On the day of experimentation, cells were washed once with 200  $\mu$ l SBS and treated with either vehicle or TNF $\alpha$  (10 ng/ml final concentration, Life Technologies) for 5 hours in a 37°C humidified 5% CO<sub>2</sub> incubator. During this incubation, THP-1 cells were counted and harvested, removing  $2 \times 10^5$  cells for test wells. Cells were centrifuged at  $805 \times g$  for 7 minutes at room temperature and following disposal of the supernatant, were suspended to  $1 \times 10^6$  cells/ml in calcium loading buffer (Section 2.6.1) containing calcein AM (final concentration of 5  $\mu$ M). Cells were incubated in the dark for 1 hour at 37°C to allow loading of the dye. Following loading, THP-1 cells were centrifuged at  $805 \times g$  for 7 minutes at room temperature, and the supernatant was discarded. Cells were resuspended in SBS buffer to yield  $1 \times 10^6$  cells/ml and transferred to 1.5 ml microcentrifuge tubes. Following the addition of treatments, cells were incubated at 37°C in a humidified 5% CO<sub>2</sub> incubator for 45 minutes. After incubation, cells were centrifuged at  $805 \times g$  for 3 minutes and washed once with SBS before resuspending with SBS to yield  $1 \times 10^6$  cells/ml. At this stage, HUVEC plates were removed from the incubator and aspirated before washing once with 200  $\mu$ l SBS. To each well of HUVEC cells, 200  $\mu$ l of THP-1 cells were added, and plates were incubated at 37°C in a humidified 5% CO<sub>2</sub> incubator for 1 hour. Following incubation, wells were aspirated and washed twice with 200  $\mu$ l SBS buffer before adding 200  $\mu$ l of SBS to each well. The fluorescence was measured using a FlexStation microplate reader set to  $\lambda_{em} = 496$  nm and  $\lambda_{ex} = 516$  nm. Fluorescence values from vehicle wells were subtracted from all treatments. Unless otherwise stated, THP-1 cell adhesion was represented as a percentage of cells treated with CCL2 alone (% control).

## 2.9 ATP/ $\beta$ -hexosaminidase release studies

### 2.9.1 Extracellular nucleotide detection by ion-pair reverse-phase HPLC

For ATP release studies,  $2 \times 10^6$  THP-1 cells were harvested for each time-point tested. Cells were centrifuged at  $805 \times g$  for 7 minutes at room temperature, and the supernatant was discarded. SBS was added to this such that the cell yield was  $1 \times 10^6$  cells/ml. THP-1 cells ( $2 \times 10^6$ ) were next added to a quartz cuvette containing a magnetic stirrer, and cells were allowed to equilibrate for 10 minutes at room temperature. To this, vehicle or CCL2 (50 ng/ml) were added. Sampling was performed at 0, 1, or 2 minutes post-challenge, transferring 200  $\mu$ l of cells to a 1.5 ml microcentrifuge tube and immediately centrifuging at  $4^\circ\text{C}$ ,  $20,000 \times g$  for 1 minute. Clarified samples (150  $\mu$ l) were transferred to a 300  $\mu$ l microsampling vial (Chromacol). For nucleotide detection, 35  $\mu$ l of sample was injected through a 3  $\mu$ m particle size SUPERCOSIL LC-18-T column (Sigma-Aldrich) equilibrated with 10 column volumes of buffer B (organic phase - consisting of 39 mM dipotassium phosphate, 26 mM monopotassium phosphate and 25% (v/v) methanol, pH 6.0), and 30 column volumes of buffer A (mobile phase - consisting of 39 mM dipotassium phosphate, 26 mM monopotassium phosphate and 4 mM tetrabutylammonium hydrogen sulphate; pH 6.0). Buffers were injected at a flow rate of 1 ml per minute. Clarified samples were injected after two blank injections with SBS. Sample retention times were compared with nucleotide standards (Table 2.13 and Appendix Figures A1 and A2). Nucleotide and nucleoside levels were quantified by taking peak height values given by LC-Solutions Software (Shimadzu). The total run time for each sample was 51 minutes and included an 11 minute wash to rinse the column.

**Table 2.13 Nucleotide retention times**

Nucleotide	Approximate retention time (minutes)
ATP	29
ADP	20
AMP	9
Adenosine	13.5
UTP	19
UDP	6.5
UMP	3.5
Uridine	4.5

### 2.9.2 ATP detection by luciferase-luciferin

ATP levels in THP-1 supernatants were also quantified using an ATP Bioluminescence Assay kit HS II (Roche). THP-1 cells ( $4 \times 10^6$ ) were harvested and centrifuged at  $805 \times g$  for 7 minutes at room temperature prior to discarding the supernatant. The cell pellet was resuspended in SBS such that the cell yield was  $1 \times 10^6$  cells/ml. Cells ( $2 \times 10^6$ ) were added to a quartz cuvette containing a magnetic stirrer and were allowed to equilibrate for 10 minutes at room temperature. Cells were challenged with vehicle or CCL2 (50 ng/ml), and sampled every 2 minutes by removing 60  $\mu$ l of cells to a 1.5 ml homopolymer microcentrifuge tube (Axygen) and immediately centrifuging at  $4^\circ\text{C}$ ,  $20,000 \times g$  for 1 minute. Clarified samples were mixed 1:1 with room temperature luciferase reagent and measured for luminescence using a Modulus Luminometer (Turner BioSystems) set to a 7 second integration time. Figure 2.5 shows a log-log plot of ATP concentration against bioluminescence from which sample concentrations were estimated.

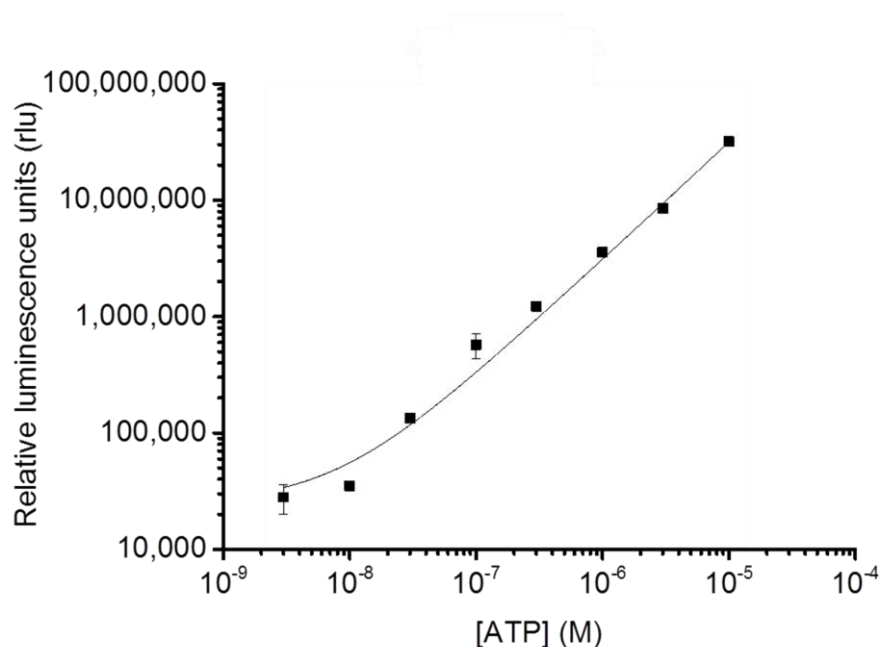


Figure 2.6 Log-log plot of standard curve data for ATP

### 2.10 $\beta$ -hexosaminidase release

For  $\beta$ -hexosaminidase release experiments, THP-1 cells were counted and harvested, removing  $4 \times 10^4$  cells for each well, with each treatment tested in duplicate. Cells were centrifuged at  $805 \times g$  for 7 minutes at room temperature before removing the supernatant and washing cells once with SBS (Section 2.3.2). Following washing, cells were resuspended in SBS such that the cell yield was  $2.1 \times 10^6$  cells/ml. Experiments were performed in sterile clear flat-bottomed 96-well tissue culture plates (Corning). To each well, 190  $\mu$ l of THP-1 cells were added, followed by 10  $\mu$ l of treatments. Triton X-100 at a final concentration of 1% (v/v) was used as a positive control in each experiment. Plates

were then incubated for 20 minutes at 37°C in a humidified 5% CO<sub>2</sub> incubator. Following incubation, plates were centrifuged at 300 x g for 5 minutes at room temperature before transferring 25 µl from each well to wells of a fresh 96-well tissue culture plate. To wells, 25 µl of 4 mM 4-Nitrophenyl N-acetyl-β-D-glucosaminide (pNAG) prepared fresh in citrate buffer (0.05 M citric acid, 0.05 M sodium citrate, pH 4.5) was added. Plates were incubated for 1 hour at 37°C to allow any released β-hexosaminidase to cleave pNAG to yield 4-nitrophenol (Borooah *et al.*, 1961). Reactions were quenched with 50 µl 0.1 M sodium bicarbonate buffer (0.1M sodium carbonate, 0.1M sodium bicarbonate) and absorbance values were read at A405 (nm) on a FlexStation microplate reader. Absorbance values for treatment wells were background subtracted with values from vehicle-alone wells, and normalised to signals generated by 1% (v/v) Triton X-100.

## **2.11 Nucleotide hydrolysis studies**

### **2.11.1 Apyrase studies**

SBS buffer (Section 2.3.2) was added to a quartz cuvette containing a magnetic stirrer. To this, ATP, ADP, UTP or UDP prepared in SBS were added such that the final concentration of each nucleotide was 100 µM. The spontaneous hydrolysis of each nucleotide was initially tested by adding vehicle (de-ionised water) to the cuvette and sampling (150 µl) at 0 and 30 minutes. For apyrase studies, apyrase (high NTPase/high NDPase) was added to the cuvette such that the final concentration was 2 units/ml. At 30 minutes post-apyrase, 150 µl of sample was transferred to a 300 µl microsampling vial and assessed for nucleotide levels using reverse-phase ion-pair HPLC as described in Section 2.9.1. Nucleotide and nucleoside levels were quantified by taking peak height values given by LC-Solutions Software (Shimadzu).

### **2.11.2 THP-1 cell studies**

THP-1 cells were counted and harvested to yield 2x10<sup>6</sup> cells for each test replicate. Cells were centrifuged at 805 x g for 7 minutes at room temperature and the supernatant was disposed. SBS buffer was added to this such that the cell yield was 1.11x10<sup>6</sup> cells/ml. THP-1 cells (2x10<sup>6</sup> cells) were then transferred to a quartz cuvette and agitated using a magnetic stirrer. To this, 200 µl of nucleotide was added such that the final concentration was 100 µM. Sampling was performed at 0 and 30 minutes, removing 200 µl of sample to a 1.5 ml microcentrifuge tube and immediately centrifuging at 20,000 x g, 4°C for 1 minute. Clarified samples (150 µl) were transferred to a 300 µl microsampling vial and assessed for nucleotide levels as described above in Section 2.11.1.

## **2.12 THP-1 cell viability assays**

### **2.12.1 Trypan blue exclusion assay**

THP-1 cell viability was tested after exposing cells to compounds for 2.5 hours as this represented the maximum exposure of BAPTA-AM in chemotaxis studies. Cells were counted and harvested, removing  $3 \times 10^6$  cells for each compound tested. Harvested cells were centrifuged at  $805 \times g$  for 7 minutes at room temperature and the supernatant was disposed. SBS buffer (Section 2.3.2) was then added such that the cell yield was  $1 \times 10^6/100 \mu\text{l}$  SBS. To each well of a sterile 96-well clear flat-bottomed plate,  $100 \mu\text{l}$  of cells, compounds (in triplicate), or vehicle (in triplicate) were added. Following addition, the plate was incubated for 2.5 hours in a  $37^\circ\text{C}$  humidified 5%  $\text{CO}_2$  incubator. After 2.5 hours the plate was removed from the incubator and  $50 \mu\text{l}$  of cells were removed and diluted with  $450 \mu\text{l}$  SBS buffer (1 in 10 dilution). This was diluted further by mixing  $20 \mu\text{l}$  of sample with  $80 \mu\text{l}$  of 0.4% (w/v) Trypan Blue solution. Viable cells displaying a clear cytoplasm were counted using a haemocytometer. Cell viability was represented as a percentage of viable cells treated with vehicle.

### **2.12.2 Lactate dehydrogenase (LDH) assay**

THP-1 cell viability was also tested using a LDH kit (Cayman Chemicals) which works on the principle that the cytosolic enzyme, LDH, is released into cell supernatants by necrotic cells. LDH detection is performed indirectly via a two-step enzymatic reaction that yields formazan; a coloured dye detectable at  $A_{490-520\text{nm}}$ . Cell viability was tested following a 2.5 hour compound incubation as this represented the maximum exposure of BAPTA-AM in chemotaxis studies. All compounds were tested in singlicate under acellular and cellular conditions. Cells were counted and harvested, removing  $1 \times 10^5$  cells for each treatment well. Harvested cells were centrifuged at  $805 \times g$  for 7 minutes at room temperature, and the supernatant was discarded. SBS buffer (Section 2.3.2) was added to this such that the cell yield was  $1 \times 10^5$  cells/ $120 \mu\text{l}$  SBS. Cells or SBS buffer ( $120 \mu\text{l}$ ) were then added to alternate wells of a sterile 96-well clear flat-bottomed plate. Compounds or vehicle (1% DMSO or water) were next added in singlicate to cellular and acellular wells. Digitonin ( $40 \mu\text{M}$ ) and Triton X-100 (0.1% (v/v)) were also added to cellular and acellular wells as positive controls. Following the addition of treatments, the plate was incubated at  $37^\circ\text{C}$  in a humidified 5%  $\text{CO}_2$  incubator for 2.5 hours. At the end of this period, the plate was centrifuged at  $400 \times g$  for 5 minutes at room temperature. Clarified samples ( $100 \mu\text{l}$ ) were transferred to a fresh 96-well clear flat-bottomed plate, performing the remainder of the assay as per manufacturer's instructions, and reading the absorbance at  $A_{490}$  (nm) on a FlexStation microplate reader. The absorbance values for

acellular controls were subtracted from treatments, which were represented as a percentage of absorbance given by 0.1% (v/v) Triton X-100 (% control).

## 2.13 Statistical analysis

All data were analysed using Origin Pro 9.0 software (Origin Lab Corporation, USA) or Excel (Microsoft Corporation, USA). Data is represented as mean±SEM (standard error of the mean), with n given as the number of experiments or the number of replicates. Statistical comparisons between paired data were performed by means of Students paired t-tests, while experiments involving more than two treatment groups were compared by a one-way ANOVA with Bonferroni's multiple comparison. Statistical significance at the 5% ( $p < 0.05$ ) and 1% levels ( $p < 0.01$ ) has been indicated by the asterisks \* and \*\* respectively. Concentration-response curves were fitted with the Hill equation,

$$\text{Min} + ((\text{Max} - \text{Min}) * x^s / (\text{EC}_{50}^s + x^s))$$

where, Min and Max are the minimum and maximal values of the response, x is the concentration, s the slope, and the  $\text{EC}_{50}$  (or  $\text{IC}_{50}$ ) value is the concentration of ligand or antagonist corresponding to a half-maximal response. The  $\text{EC}_{20}$  and  $\text{EC}_{10}$  values of ligands were also generated using the Hill equation. Decay rates ( $\tau$  (tau), second) for  $\text{Ca}^{2+}$  transients were estimated by fitting a first order exponential model (with offset) using the following formula:

$$y_0 + \text{Ampl} * \text{Exp}^{-x/t_1}$$

Where  $y_0$  is the y-axis offset, Ampl is the amplitude, Exp is the exponential, x is the x-axis value, and  $t_1$  is the decay constant.

# Chapter 3: Comparison of mRNA expression of monocyte markers, CC chemokines, CC chemokine receptors and purinoceptors in THP-1 cells and human monocytes

---

## 3.1 Introduction

Monocytes are a heterogeneous population of immune effector cells that originate from common monocyte/macrophage and dendritic cell precursors located in the bone marrow (Akashi *et al.*, 2000). Once formed, mature classical monocytes egress from the bone marrow in a CCR2-dependent manner and enter the blood stream (Serbina and Pamer, 2006; Tsou *et al.*, 2007; Shi *et al.*, 2011). Here they participate in a wide range of protective activities that include the clearance of pathogens/cell debris, patrolling of blood vessels, and acting as precursors for other mononuclear phagocytes (Van Furth *et al.*, 1972; Serbina *et al.*, 2008; Cros *et al.*, 2010; Lauvau *et al.*, 2014).

Monocyte fates are pre-determined by their expression of PRRs and scavenging receptors, which affect their ability to detect chemical cues in their local microenvironment. While monocytes were initially characterised by their cellular density and size (Van Furth *et al.*, 1972), later technical advancements led to monocytes being classified by their expression of CD14, CD16, and the chemokine receptors CX<sub>3</sub>CR1 and CCR2 (Passlick *et al.*, 1989; Weber *et al.*, 2000; Geissmann *et al.*, 2003; Ziegler-Heitbrock 2007; Yona and Jung, 2009). Based on this evidence, human monocyte subsets have been divided into classical (CD14<sup>++</sup>/CD16<sup>-</sup>), intermediate (CD14<sup>++</sup>/CD16<sup>+</sup>), and non-classical (CD14<sup>+</sup>/CD16<sup>++</sup>) monocytes.

Although freshly isolated human monocytes represent a useful tool for studying monocyte function *ex vivo*, the use of these cells remains technically challenging due to the low availability of human samples, low cell yields, limited cell survival, and high degree of variability due to their heterogeneous nature. The human monocytic THP-1 cell line is a well-established *in vitro* model for investigating monocyte function (Qin, 2012). Isolated from a young male patient with acute monocytic leukaemia (Tsuchiya *et al.*, 1980), THP-1 cells represent a homogeneous cell population that share a similar cell morphology and molecular marker expression as human monocytes (Auwerx, 1991).

Although THP-1 cells are a useful tool for assessing broad-range monocyte functions, the full experimental capabilities of this cell line are not fully understood. For example, it is not

known whether THP-1 cells and human monocytes display a similar pattern of expression of CC chemokines, CC chemokine receptors, or purinoceptors.

## 3.2 Aims

To determine whether THP-1 cells represented a suitable model for investigating monocyte signalling and function, RT-PCR was employed to compare the expression of mRNA transcripts for monocyte and myeloid genes between THP-1 cells and human peripheral blood monocytes. To address the principle objectives of this thesis, it was also necessary to examine and compare the expression of mRNA for CC chemokines, CC chemokine receptors, and purinoceptors between THP-1 cells and monocytes. To confirm specificity and functionality, all primers were also tested using commercial human brain RNA.

## 3.3 Results

### 3.3.1 RT-PCR analysis of monocyte and myeloid markers

Initial studies examined and compared the expression of  $\beta$ -actin and monocyte/myeloid markers in THP-1 cells and human monocytes. The markers tested were CD14, CD16, and the less well-known markers, cluster of differentiation 33 (CD33/Siglec-33), and cluster of differentiation 93 (CD93/C1qRP) (Nepomuceno *et al.*, 1997; Lock *et al.*, 2004). To address this aim, the specificity and functionality of all primers were first tested in human brain. Following the validation of primers, the expression of mRNA transcripts for these markers in THP-1 cells and human monocytes, were examined. Table 3.1 and Figure 3.1 give a summary of the results obtained for this study.

**Table 3.1 Detection of mRNA for  $\beta$ -actin (*ACTB*) and monocyte/myeloid markers in human brain, THP-1 cells, and human monocytes**

Gene	Human brain	THP-1 cells	Human monocytes
<i>ACTB</i>	+	+	+
<i>CD14</i>	+	+	+
<i>CD16</i>	(+)	-	+
<i>CD33</i>	+	+	(+)
<i>CD93</i>	+	+	+

A + sign indicates that the gene is detected, a (+) sign indicates that the gene is detected but is represented by a faint band, and a – sign indicates that the gene is not detected.

As can be seen from Table 3.1 and Figure 3.1a, mRNA transcripts for  $\beta$ -actin and all of the cell markers were detected in human brain. These results, while supporting the use of these primers for further studies, also suggest that mRNA for these markers are naturally present in human brain. Table 3.1 and Figures 3.1b and 3.1c also show the detection of these genes in THP-1 cells and human monocytes. As shown, THP-1 cells were found to express mRNA for all the markers tested, apart from CD16. Although this indicates that THP-1 cells lack CD16 similar to classical ( $CD14^{++}/CD16^{-}$ ) monocytes, it is also possible that levels of CD16 mRNA in THP-1 cells fell below the limits of detection. In comparison, human monocytes were found to express mRNA transcripts for  $\beta$ -actin and all of the cell markers tested, including CD14 and CD16 (Table 3.1 and Figure 3.1c). While this suggests that RT-PCR may be unable to discriminate between  $CD16^{-}$  and  $CD16^{+}$  monocyte populations, it is also possible that the sample tested represents a monocyte population comprising of all three subsets. Interestingly, although THP-1 cells and human monocytes showed differential mRNA expression for CD16, mRNA transcripts for CD33 and CD93 were detected in both cell types, suggesting that both are of myeloid origin.

Taken together, these results suggest that THP-1 cells express several monocyte/myeloid cell markers but lack *CD16* similar to classical ( $CD14^{++}/CD16^{-}$ ) monocytes. Furthermore, human monocytes express a similar pattern of cell markers, but also express *CD16*. This indicates that the monocyte sample employed by this study may represent a heterogeneous monocyte population.

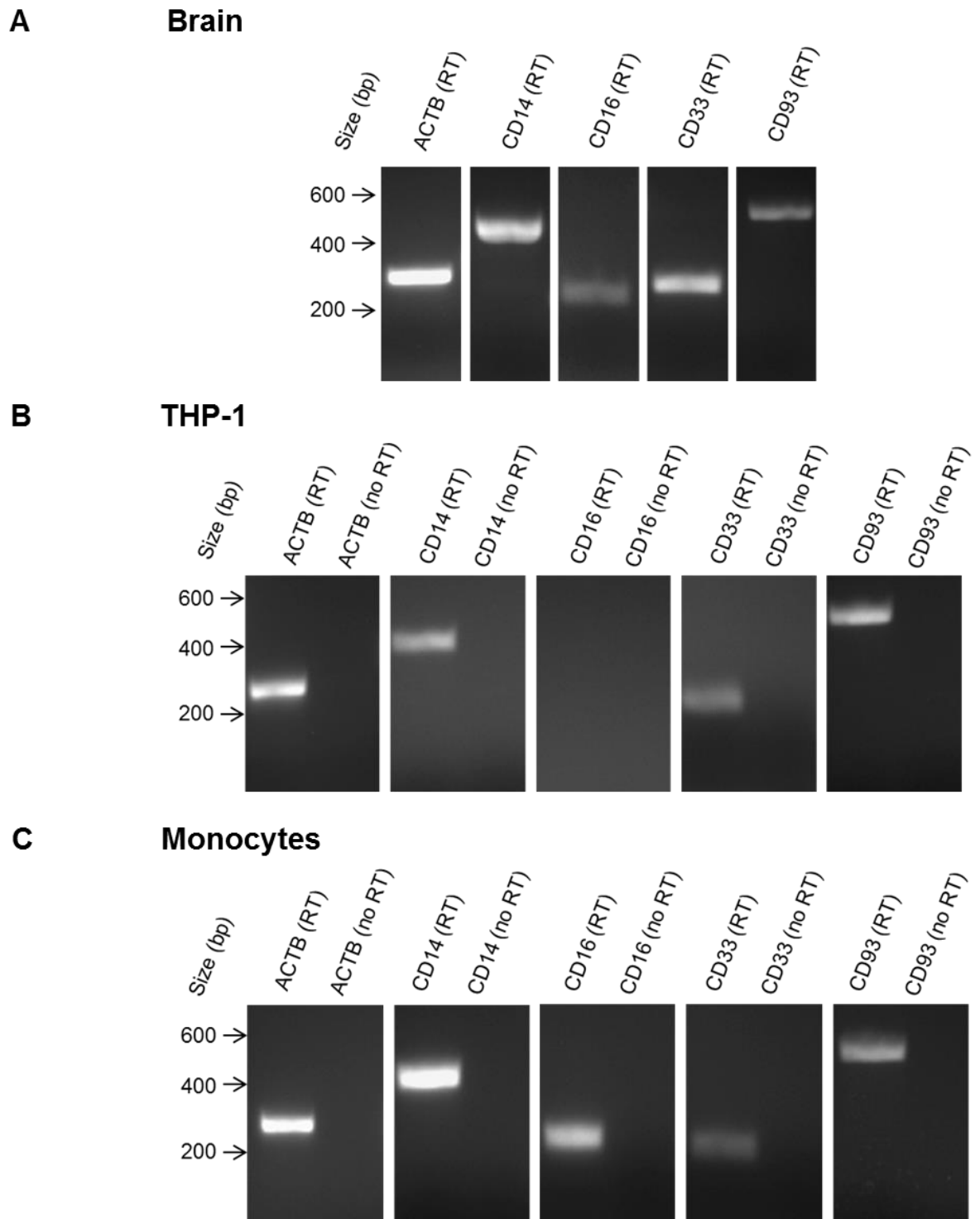


**Figure 3.1 Detection of mRNA for  $\beta$ -actin (*ACTB*) and monocyte/myeloid markers in human brain, THP-1 cells, and human monocytes**

Detection of housekeeping gene *ACTB* and cell markers in (A) human brain, (B) THP-1 cells, and (C) human monocytes using RT-PCR and agarose gel electrophoresis. Expression was detected at 282 bp (*ACTB*), 445 bp (*CD14*), 247 bp (*CD16*), 216 bp (*CD33*) and 515 bp (*CD93*). RT and no RT constitute first strand cDNA synthesis reactions with and without reverse transcriptase, respectively.

### 3.3.2 RT-PCR analysis of CC chemokines

Despite the fact that over 25 human CC chemokines have been identified to date (Zweemer *et al.*, 2014), only a small handful of studies have examined the expression of CC chemokines in resting THP-1 cells and human monocytes (Colotta *et al.*, 1992; Lu *et al.*, 2004; Stubbs *et al.*, 2010). Although further research is required in this area, in recent years there has been an increased interest in understanding how chemokine expression is modulated within inflammatory disease (Bruegel *et al.*, 2006; Schildberger *et al.*, 2013). While it is understandable that this is crucial for determining the involvement of chemokines in disease, knowing whether CC chemokines are expressed by resting cells is important since it allows a greater understanding of the homeostatic roles played by these peptides.

Hence, the next aim of this chapter was to compare the expression of mRNA for a number of CC chemokines, between THP-1 cells and human monocytes. As described previously, commercial human brain RNA was employed to test primer specificity and functionality. Table 3.2 and Figure 3.2 display a summary of the results of this study.

**Table 3.2 Detection of mRNA for CC chemokines in human brain, THP-1 cells, and human monocytes**

Gene	Human brain	THP-1 cells	Human monocytes
<i>CCL2</i>	+	+	+
<i>CCL3</i>	+	+	+
<i>CCL4</i>	(+)	(+)	+
<i>CCL5</i>	(+)	+	+

A + sign indicates that the gene is detected, a (+) sign indicates that the gene is detected but is represented by a faint band, and a – sign indicates that the gene is not detected.

As shown in Table 3.2 and Figure 3.2, mRNA transcripts for all four CC chemokines tested were detected in human brain, producing a PCR amplicon of the predicted size. As also shown, mRNA for all four CC chemokines, including *CCL2*, were also detected in THP-1 cells and human monocytes, suggesting that both cell types constitutively expressed genes encoding for these chemokines.

Taken together, these results suggest that THP-1 cells and human peripheral blood monocytes display an overlapping expression pattern among genes encoding for *CCL2*, *CCL3*, *CCL4*, and *CCL5*.

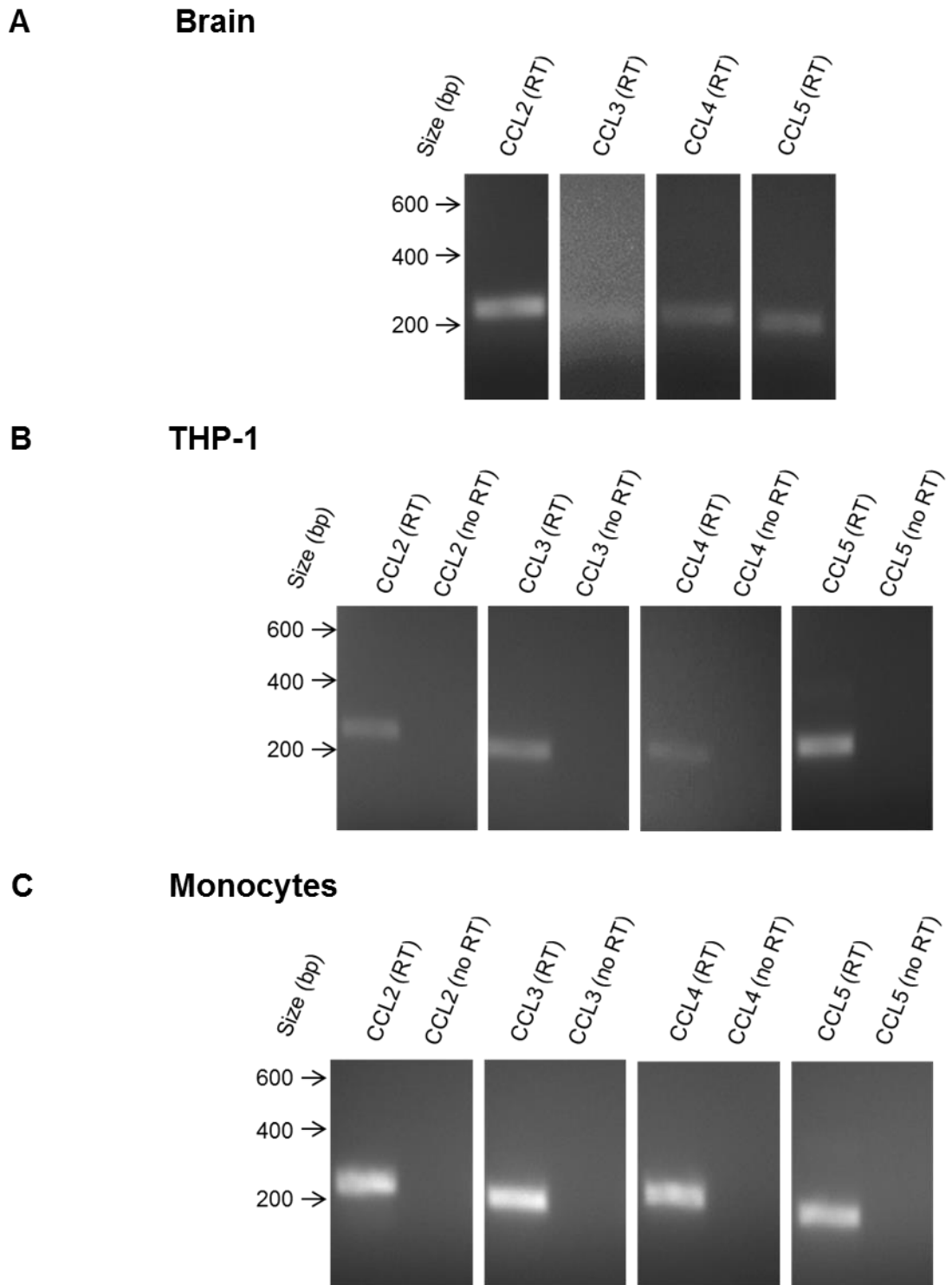


**Figure 3.2 Detection of mRNA for CC chemokines in human brain, THP-1 cells, and human monocytes**

Detection of CC chemokines in (A) human brain, (B) THP-1 cells, and (C) human monocytes using RT-PCR and agarose gel electrophoresis. Primers were designed to amplify all splice variants of the selected gene. Expression was detected at 219 bp (*CCL2*), 209 bp (*CCL3*), 209 bp (*CCL4*) and 201 bp (*CCL5*). RT and no RT constitute first strand cDNA synthesis reactions with and without reverse transcriptase, respectively.

### 3.3.3 RT-PCR analysis of CC chemokine receptors

To date, ten CC chemokine receptors have been cloned and characterised, and are consecutively encoded by the genes *CCR1* to *CCR10* (Bachelierie *et al.*, 2014). Although a number of groups (Neote *et al.*, 1993; Yamagami *et al.*, 1994; Combadiere *et al.*, 1996; Weber *et al.*, 2000; Gouwy *et al.*, 2014) have reported the expression of several CC chemokine receptors in THP-1 cells and human monocytes, a full and complete assessment has been lacking. Thus, in order to address this gap in knowledge, the next study investigated the expression of mRNA transcripts for CC chemokine receptors in THP-1 cells and human peripheral blood monocytes. To address this aim, the specificity and functionality of all CC chemokine primers were first tested in human brain. *CCR3* primers were further tested in human monocyte-depleted PBMCs. Following their validation, primers were used to test for the expression of mRNA transcripts for CC chemokine receptors in THP-1 cells and human monocytes. All primers, except those for *CCR2* were designed to amplify all splice variants of the selected gene. *CCR2* primers were designed to individually target *CCR2A* and *CCR2B* (Charo *et al.*, 1994). The current study also examined the expression of mRNA for *CCRL2* (chemokine (C-C motif) receptor-like 2), a receptor initially identified as *CCR11* (Fan *et al.*, 1998), but now remains unclassified (Bachelierie *et al.*, 2014). The results of this study are summarised in Table 3.3 and shown in Figure 3.3 (human brain and monocyte-depleted PBMCs), Figure 3.4 (THP-1 cells), and Figure 3.5 (human monocytes).

As shown in Table 3.3 (and Figure 3.3), mRNA for all CC chemokine receptors except *CCR3* were detected in human brain. To rule out the possibility of poor primer design or specificity, *CCR3* primers were also tested in monocyte-depleted PBMCs as these are known to be a source of *CCR3*-expressing T-helper 2 (Th2) lymphocytes (Gerber *et al.*, 1997). As shown in Figure 3.3, *CCR3* mRNA was detected in this sample. While this suggests that *CCR3* is likely to be expressed at the mRNA level by some cell types in PBMCs, a lack of expression in human brain is interesting and may indicate that *CCR3* is not expressed by human brain, or that levels of *CCR3* mRNA in brain fall below the limits of detection.

Table 3.3, Figure 3.4, and Figure 3.5 show the expression of mRNA for CC chemokine receptors in THP-1 cells and human monocytes. As shown, THP-1 cells were found to express mRNA transcripts for all CC chemokine receptors except *CCR3* while human monocytes were found to express mRNA transcripts for all receptors, including *CCR3*. It is also interesting that both cell types express mRNA for *CCR2A* and *CCR2B*. As shown by Figure 3.4, in THP-1 cells *CCR10* primers produced a second PCR amplicon of ~500 base pairs in addition to an amplicon for the *CCR10* receptor. A similar PCR amplicon was also observed in human monocytes (Figure 3.5), but not in brain (Figure 3.3). An

analysis of these primers using a basic local alignment search tool (BLAST) was unable to identify this product.

Taken together, the results presented here suggest that with the exception of the CCR3 receptor, THP-1 cells and human monocytes exhibit an overlapping expression pattern of genes encoding for CC chemokine receptors. Furthermore, these results suggest that both cell types express genes encoding for CCR2A and CCR2B.

**Table 3.3 Detection of mRNA for CC chemokine receptors in human brain, THP-1 cells, and human monocytes**

<b>Gene</b>	<b>Human brain</b>	<b>THP-1 cells</b>	<b>Human monocytes</b>
<i>CCR1</i>	+	+	+
<i>CCR2A</i>	(+)	(+)	(+)
<i>CCR2B</i>	+	+	+
<i>CCR3</i>	-	-	+
<i>CCR4</i>	(+)	+	+
<i>CCR5</i>	+	+	+
<i>CCR6</i>	+	+	+
<i>CCR7</i>	+	(+)	+
<i>CCR8</i>	+	(+)	(+)
<i>CCR9</i>	(+)	+	+
<i>CCR10</i>	(+)	(+)	(+)
<i>CCRL2</i>	+	+	+

A + sign indicates that the gene is detected, a (+) sign indicates that the gene is detected but is represented by a faint band, and a – sign indicates that the gene is not detected.

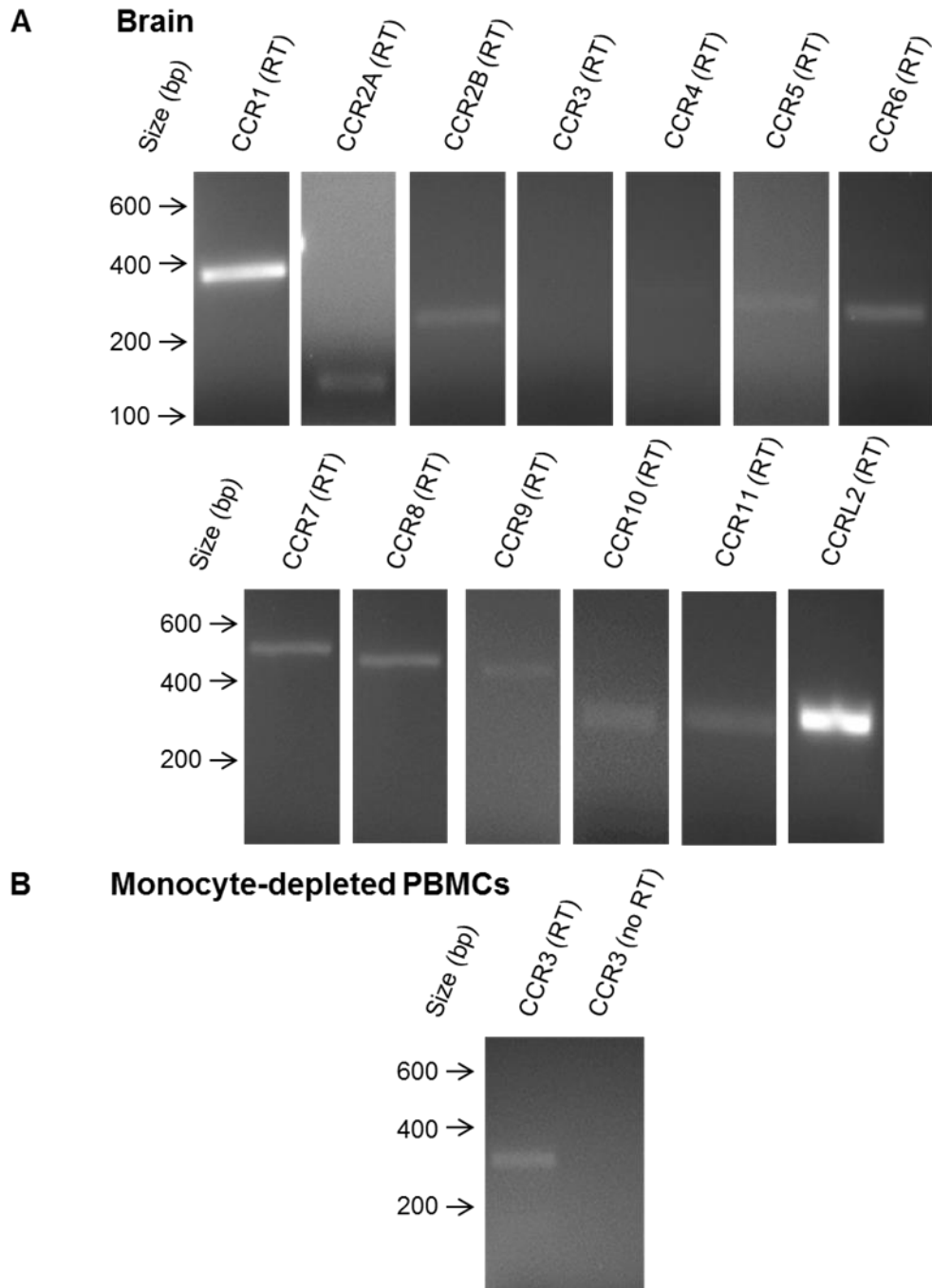


**Figure 3.3 Detection of mRNA for CC chemokine receptors in human brain and human monocyte-depleted PBMCs**

Detection of CC chemokine receptors in (A) human brain and (B) monocyte-depleted PBMCs using RT-PCR and agarose gel electrophoresis. Primers amplify all splice variants of the selected gene. Expression was detected at 358 bp (*CCR1*), 160 bp (*CCR2A*), 267 bp (*CCR2B*), 323 bp (*CCR3*), 336 bp (*CCR4*), 277 bp (*CCR5*), 263 bp (*CCR6*), 497 bp (*CCR7*), 432 bp (*CCR8*), 413 bp (*CCR9*), 285 bp (*CCR10*) and 272 bp (*CCRL2*). RT and no RT constitute first strand cDNA synthesis reactions with and without reverse transcriptase, respectively.

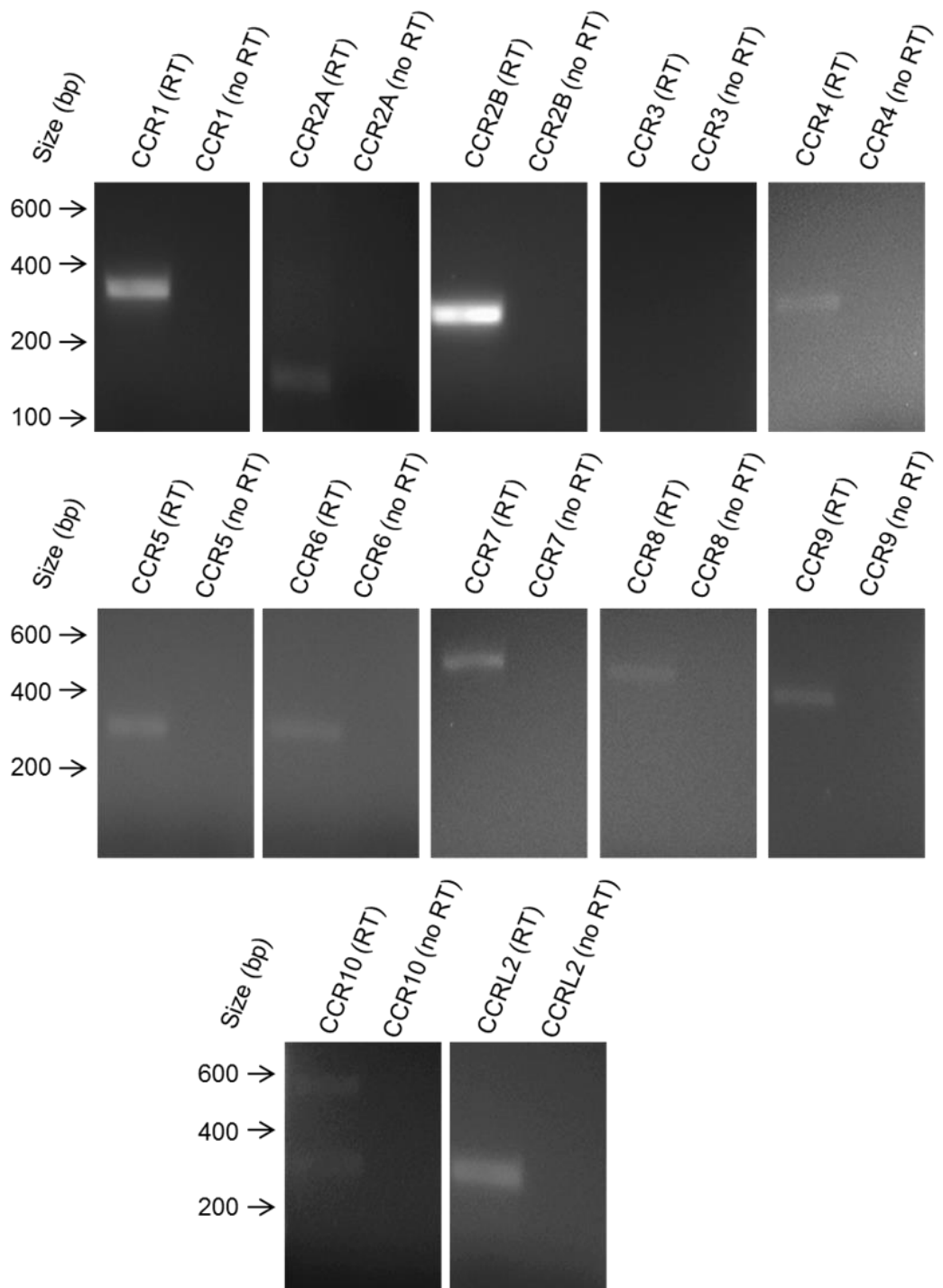


**Figure 3.4 Detection of mRNA for CC chemokine receptors in THP-1 cells**

Detection of CC chemokine receptors in THP-1 cells using RT-PCR and agarose gel electrophoresis. Primers amplify all splice variants of the selected gene. Expression was detected at 358 bp (*CCR1*), 160 bp (*CCR2A*), 267 bp (*CCR2B*), 323 bp (*CCR3*), 336 bp (*CCR4*), 277 bp (*CCR5*), 263 bp (*CCR6*), 497 bp (*CCR7*), 432 bp (*CCR8*), 413 bp (*CCR9*), 285 bp (*CCR10*) and 272 bp (*CCRL2*). RT and no RT constitute first strand cDNA synthesis reactions with and without reverse transcriptase, respectively.

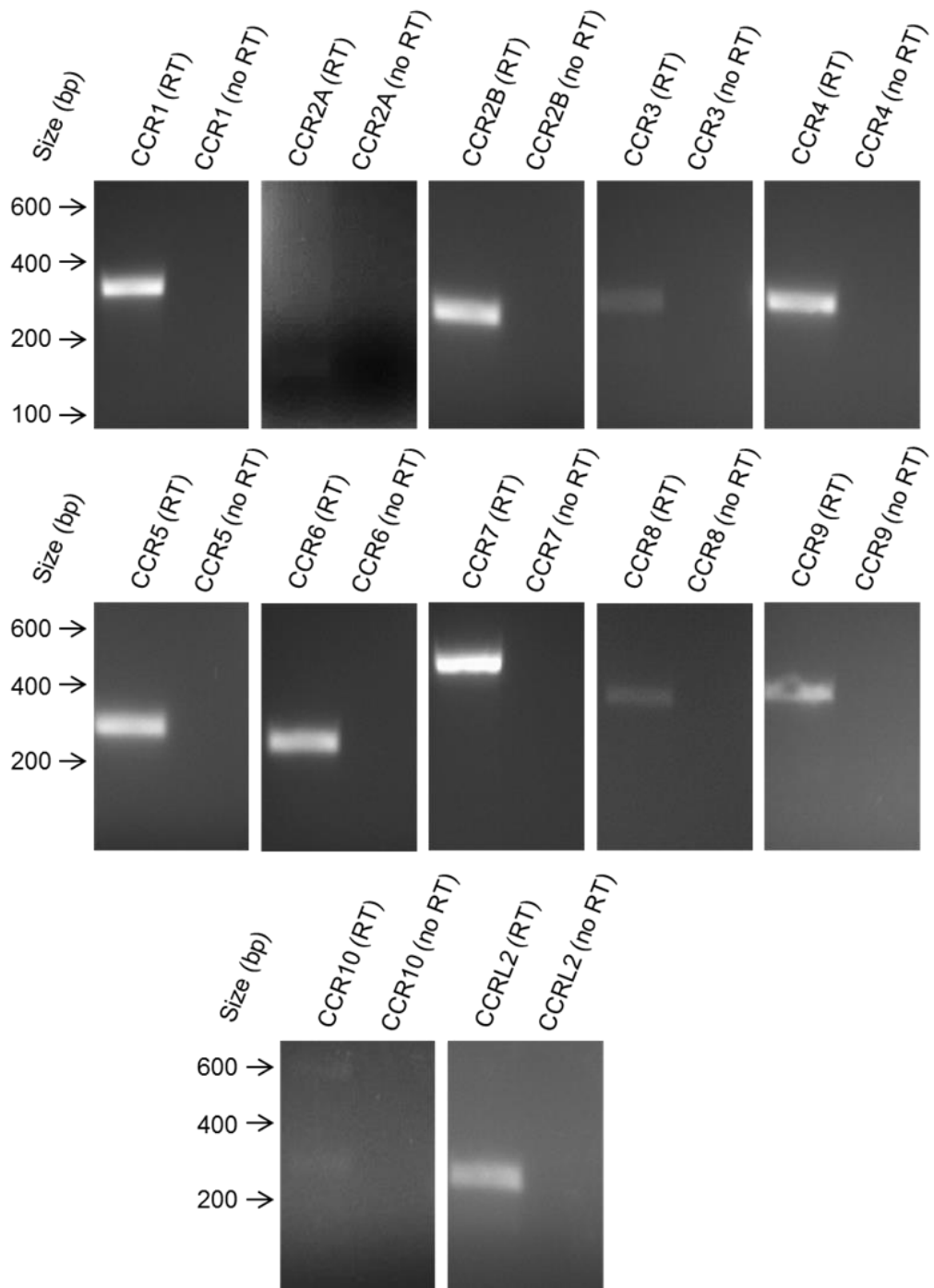


**Figure 3.5 Detection of mRNA for CC chemokine receptors in human monocytes**

Detection of CC chemokine receptors in monocytes using RT-PCR and agarose gel electrophoresis. Primers amplify all splice variants of the selected gene. Expression was detected at 358 bp (*CCR1*), 160 bp (*CCR2A*), 267 bp (*CCR2B*), 323 bp (*CCR3*), 336 bp (*CCR4*), 277 bp (*CCR5*), 263 bp (*CCR6*), 497 bp (*CCR7*), 432 bp (*CCR8*), 413 bp (*CCR9*), 285 bp (*CCR10*) and 272 bp (*CCRL2*). RT and no RT constitute reactions with and without reverse transcriptase.

### 3.3.4 RT-PCR analysis of P1 purinoceptors

The next aim was to investigate the gene expression of purinoceptors in THP-1 cells and human monocytes. The purpose of this study was firstly to identify the purinoceptors expressed by THP-1 cells and human monocytes, and secondly, to compare the expression patterns between both cell types. To simplify this aim, the findings of this study have been divided into sections for P1, P2X, and P2Y receptors. The current section focuses on P1 purinoceptors.

The human P1 purinoceptors are  $A_1$ ,  $A_{2A}$ ,  $A_{2B}$ , and  $A_3$ , and are encoded by the genes *ADORA1*, *ADORA2A*, *ADORA2B*, and *ADORA3*, respectively (Fredholm *et al.*, 2001; Fredholm *et al.*, 2011). Studies in literature indicate that the expression pattern of P1 purinoceptors in monocytes and THP-1 cells differ. While monocytes are known to express genes for all four P1 purinoceptors (Merrill *et al.*, 1997; Broussas *et al.*, 1999; Thiele *et al.*, 2004), THP-1 cells have only been examined for their expression of  $A_{2A}$  and  $A_{2B}$  (Munro *et al.*, 1998; Khoa *et al.*, 2001; Bshesh *et al.*, 2002). The expression of other P1 purinoceptors ( $A_1$  and  $A_3$ ) in THP-1 cells is therefore, uncertain. This study therefore set out to confirm the findings of published studies and compare the expression of mRNA for P1 purinoceptors between THP-1 cells and human monocytes. As with previous studies, an initial assessment of the selectivity and functionality of primers was performed using human brain RNA. The results of this study are presented in Table 3.4 and Figure 3.6.

**Table 3.4 Detection of mRNA for P1 purinoceptors in human brain, THP-1 cells, and human monocytes**

Gene	Human brain	THP-1 cells	Human monocytes
<i>ADORA1</i>	+	+	(+)
<i>ADORA2A</i>	+	(+)	+
<i>ADORA2B</i>	+	+	+
<i>ADORA3</i>	(+)	+	(+)

A + sign indicates that the gene is detected, a (+) sign indicates that the gene is detected but is represented by a faint band, and a – sign indicates that the gene is not detected.

As summarised in Table 3.4, mRNA for all P1 receptors were detected in human brain, THP-1 cells, and human monocytes. Although a detection of mRNA transcripts for  $A_{2A}$  and  $A_{2B}$  in THP-1 cells is consistent with previous studies (Munro *et al.*, 1998; Khoa *et al.*, 2001; Bshesh *et al.*, 2002), it is interesting that mRNA for  $A_1$  and  $A_3$  were also detected in these cells, which may represent a novel finding. As can also be seen (Table 3.4 and

Figure 3.6), human monocytes were also found to express mRNA transcripts for all P1 purinoceptors, a finding which agrees with prior work (Merrill *et al.*, 1997; Broussas *et al.*, 1999; Thiele *et al.*, 2004).

Taken together, the results of this study suggest that both cell types exhibit an overlapping expression profile among genes encoding for P1 purinoceptors.

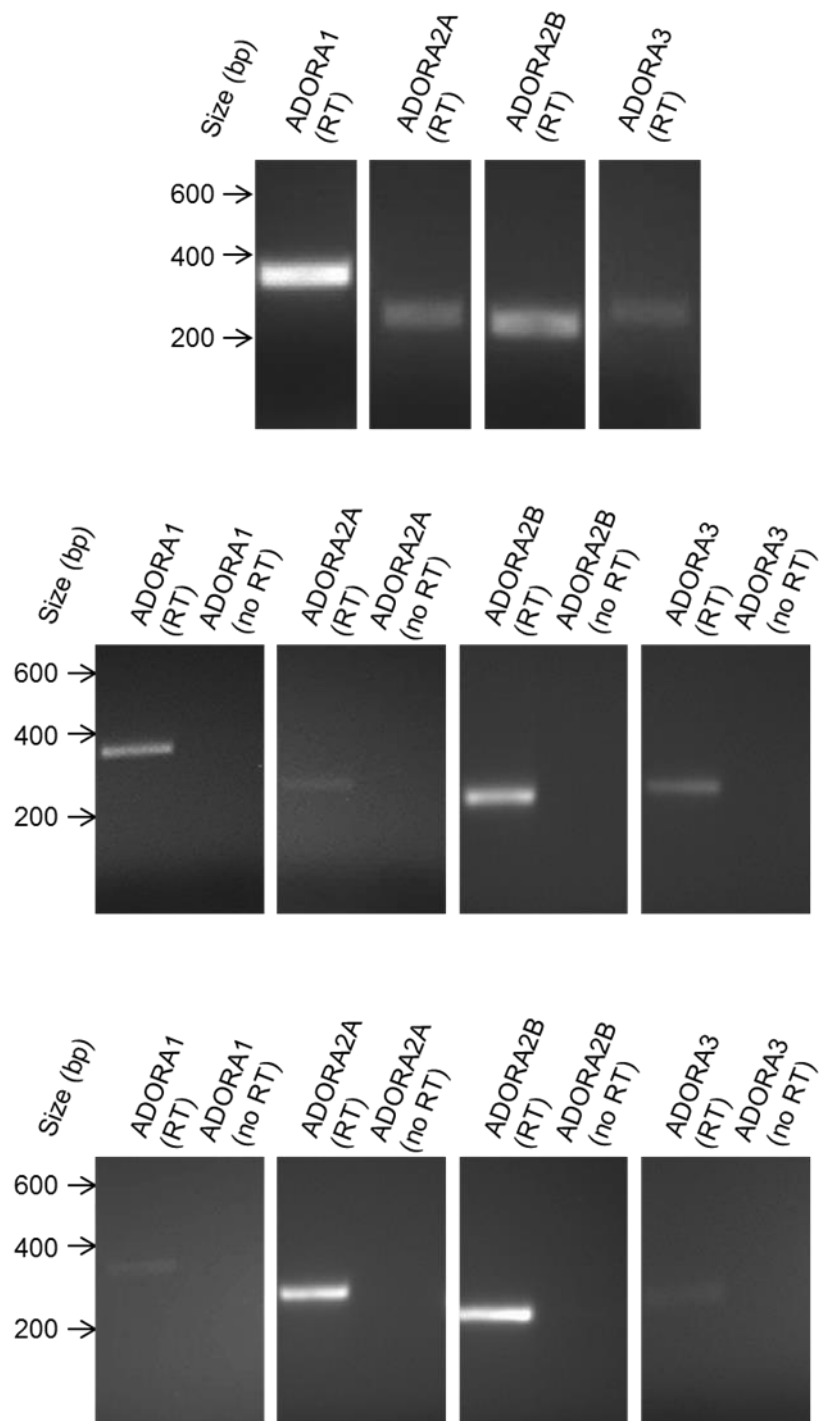


**Figure 3.6 Detection of mRNA for P1 purinoceptors in human brain, THP-1 cells, and human monocytes**

Detection of P1 (ADORA) purinoceptors in (A) human brain, (B) THP-1 cells and (C), human monocytes using RT-PCR and agarose gel electrophoresis. Primers amplify all splice variants of the selected gene. Expression was detected at 374 bp (*ADORA1*), 295 bp (*ADORA2A*), 277 bp (*ADORA2B*) and 302 bp (*ADORA3*). RT and no RT constitute first strand cDNA synthesis reactions with and without reverse transcriptase, respectively.

### 3.3.5 RT-PCR analysis of P2X purinoceptors

To date, seven mammalian P2X receptors have been cloned and characterised, and are encoded by the genes *P2RX1* through to *P2RX7* (Khakh *et al.*, 2001). Although P2X1, P2X4, and P2X7 are known to be expressed in human monocytes and THP-1 cells (Humphreys and Dubyak, 1998; Gu *et al.*, 2000; Into *et al.*, 2002; Wang *et al.*, 2004; Kaufmann *et al.*, 2005; Li and Fountain, 2011), much uncertainty still exists about the expression of other P2X receptors in these cells. This study therefore sought to investigate the expression of genes encoding for P2X receptors in THP-1 cells and human monocytes at the mRNA level. As with previous studies in this chapter, primer specificity and functionality was first tested using human brain RNA. As will be discussed later, primers for *P2RX2* and *P2RX3* were also tested on human retina.

The results of this study are presented in Table 3.5, Figure 3.7 (brain and retina), Figure 3.8 (THP-1 cells), and Figure 3.9 (monocytes).

**Table 3.5 Detection of mRNA for P2X purinoceptors in human brain, THP-1 cells, and human monocytes**

Gene	Human brain	THP-1 cells	Human monocytes
<i>P2RX1</i>	+	+	+
<i>P2RX2</i>	-	-	-
<i>P2RX3</i>	-	-	-
<i>P2RX4</i>	+	+	+
<i>P2RX5</i>	+	+	+
<i>P2RX6</i>	(+)	+	-
<i>P2RX7</i>	+	+	+

A + sign indicates that the gene is detected, a (+) sign indicates that the gene is detected but is represented by a faint band, and a – sign indicates that the gene is not detected.

As shown in the Table 3.5 and Figure 3.7, mRNA transcripts for all P2X receptors except P2X2 and P2X3 were detected in human brain. To rule out the possibility of poor primer design or specificity, primers for these receptors were also tested in human retina (paramacular) samples isolated as described by Niyadurupola *et al.*, (2011). As shown (Figure 3.7), mRNA for P2X2 and P2X3 were detected in this sample, therefore confirming the specificity and functionality of these primers. Table 3.5 also summarises the expression of P2X receptors in THP-1 cells and human monocytes. THP-1 cells (Figure 3.8) were found to express mRNA for all P2X receptors except P2X2 and P2X3, therefore exhibiting a similar pattern of expression as human brain. In THP-1 cells (Figure 3.8), it

was also seen that *P2RX6* primers produced a second PCR amplicon of a lower molecular weight in addition to a PCR amplicon for *P2RX6*. A similar PCR amplicon was also detected in human brain (Figure 3.7). Although an analysis of these primers using BLAST was unable to identify this product, it may be that this is a second variant of *P2RX6*. As also shown (Table 3.5 and Figure 3.9), mRNA for all P2X receptors, except P2X2, P2X3, and P2X6, were detected in human monocytes. These results suggest that with the exception of mRNA for P2X6, human monocytes and THP-1 cells exhibit an overlapping expression pattern among genes encoding for P2X receptors. In human monocytes (Figure 3.9), it can also be seen that primers for P2X4, P2X5, and P2X7 all produced secondary PCR amplicons in addition to a PCR amplicon of the predicted size. Although a BLAST analysis was unable to confirm the identity of these amplicons, these may refer to other splice variants of these genes. Interestingly, these additional PCR amplicons were not detected in human brain or THP-1 cells.

Taken together, the results of this study suggest that with the exception of mRNA for P2X6, THP-1 cells and human monocytes exhibit an overlapping expression pattern among genes encoding for P2X receptors. Furthermore, the results of this study indicate a number of novel findings with respect to the expression of P2X receptors in both cell types.

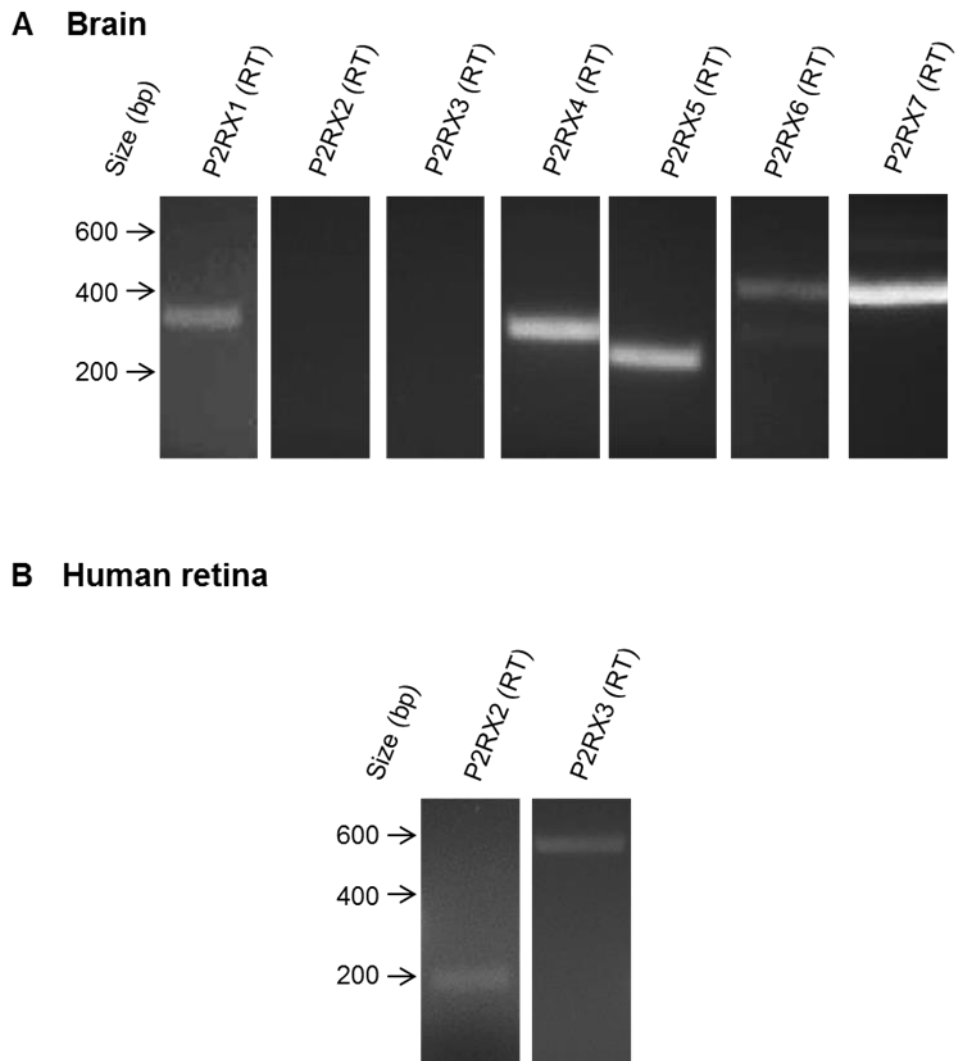


**Figure 3.7 Detection of mRNA transcripts for P2X purinoceptors in human brain and retina**

Detection of P2X purinoceptors in (A) human brain and (B) human retina (paramacular region), using RT-PCR and agarose gel electrophoresis. Primers amplify all splice variants of the selected gene. Expression was detected at 341 bp (*P2RX1*), 200 bp (*P2RX2*), 564 bp (*P2RX3*), 311 bp (*P2RX4*), 263 bp (*P2RX5*), 405 bp (*P2RX6*), and 414 bp (*P2RX7*). RT and no RT constitute first strand cDNA synthesis reactions with and without reverse transcriptase, respectively.

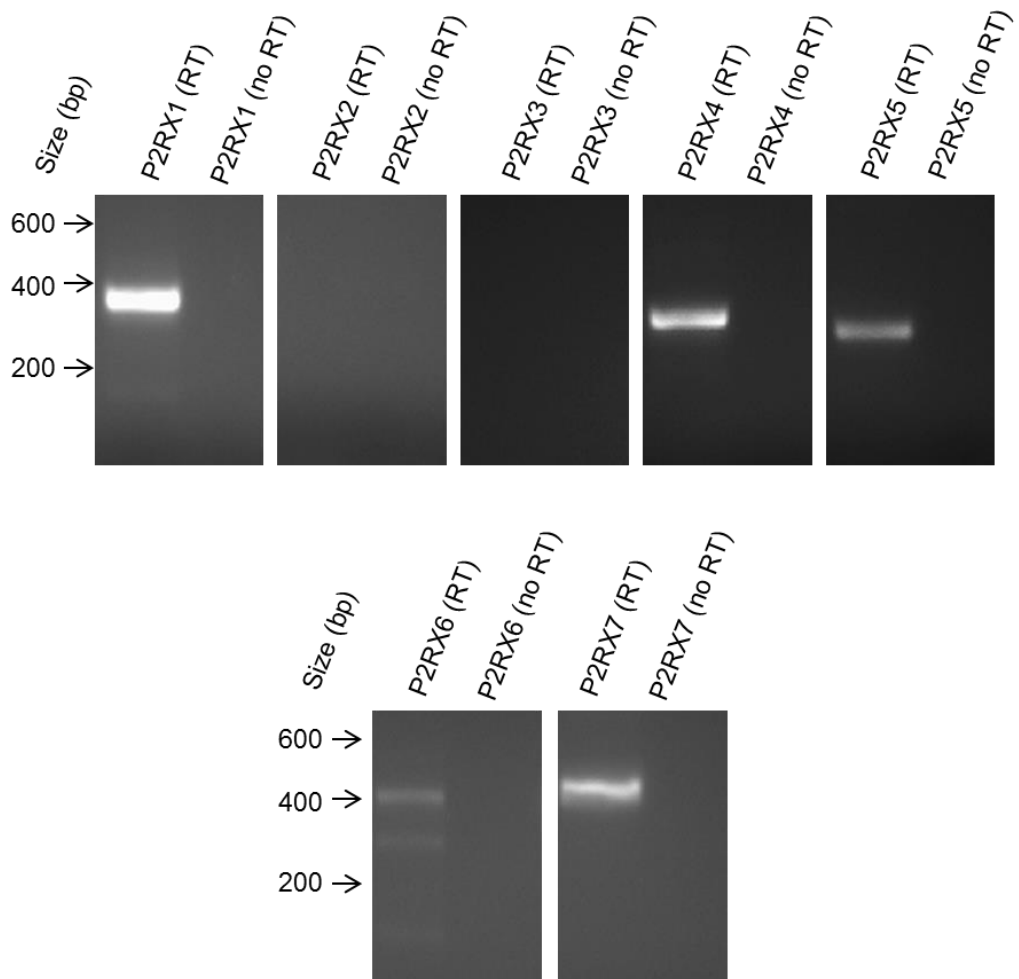


**Figure 3.8 Detection of mRNA transcripts for P2X purinoceptors in THP-1 cells**

Detection of P2X purinoceptors in THP-1 cells using RT-PCR and agarose gel electrophoresis. Primers amplify all splice variants of the selected gene. Expression was detected at 341 bp (*P2RX1*), 200 bp (*P2RX2*), 564 bp (*P2RX3*), 311 bp (*P2RX4*), 263 bp (*P2RX5*), 405 bp (*P2RX6*), and 414 bp (*P2RX7*). RT and no RT constitute first strand cDNA synthesis reactions with and without reverse transcriptase, respectively.

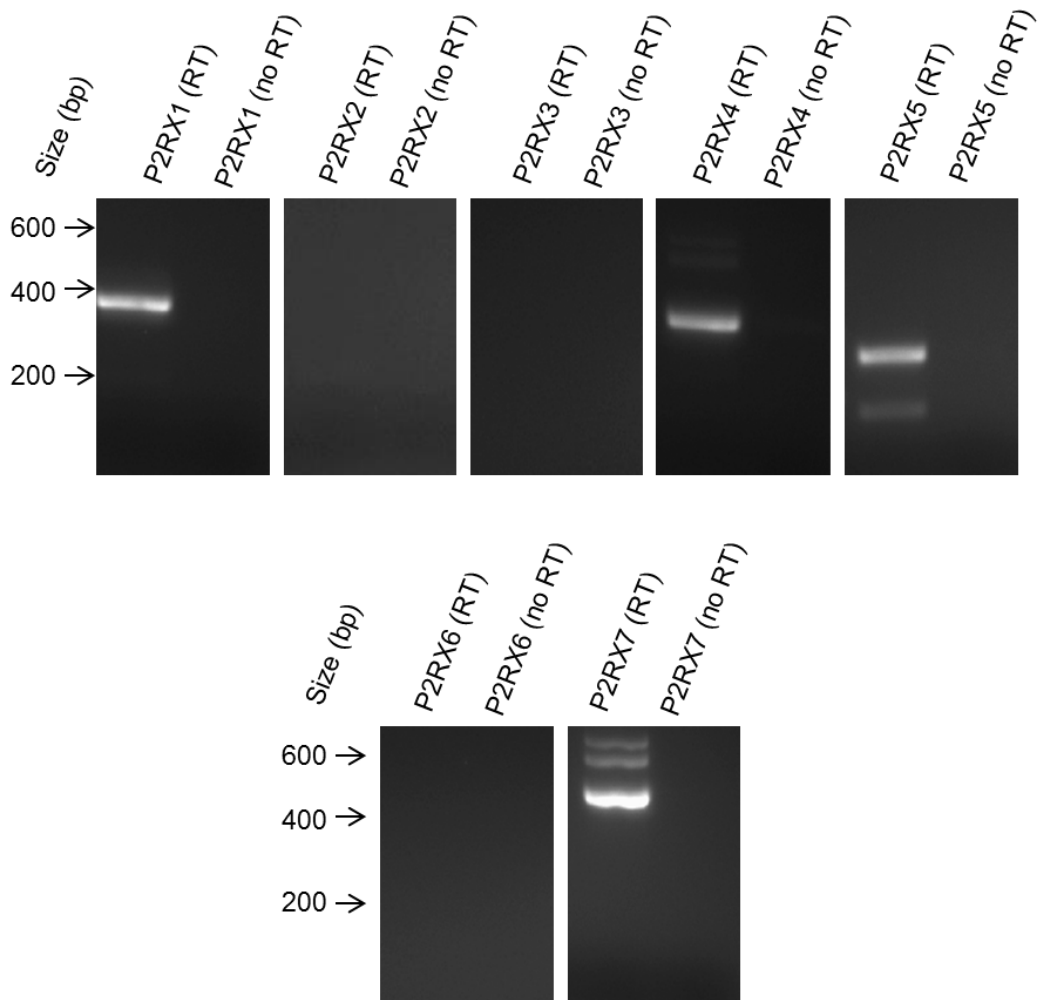


**Figure 3.9 Detection of mRNA for P2X purinoceptors in human monocytes**

Detection of P2X purinoceptors in human monocytes using RT-PCR and agarose gel electrophoresis. Primers amplify all splice variants of the selected gene. Expression was detected at 341 bp (*P2RX1*), 200 bp (*P2RX2*), 564 bp (*P2RX3*), 311 bp (*P2RX4*), 263 bp (*P2RX5*), 405 bp (*P2RX6*), and 414 bp (*P2RX7*). RT and no RT constitute first strand cDNA synthesis reactions with and without reverse transcriptase, respectively.

### 3.3.6 RT-PCR analysis of P2Y purinoceptors

To date, eight mammalian P2Y receptors have been cloned and characterised, and are encoded by the genes *P2RY1*, *P2RY2*, *P2RY4*, *P2RY6*, *P2RY11*, *P2RY12*, *P2RY13*, and *P2RY14*. The missing gene numbers represent either non-mammalian receptors or other GPCRs that exhibit a similar sequence homology to P2Y receptors, but cannot be activated by extracellular nucleotides (Abbracchio *et al.*, 2006).

A considerable amount of literature has been published on the expression of P2Y receptors in human monocytes and THP-1 cells. These studies have shown that human monocytes express P2Y<sub>1-13</sub>, (Jin *et al.*, 1998; Zhang *et al.*, 2002; Wang *et al.*, 2004; Kaufmann *et al.*, 2005; Klein *et al.*, 2009), and THP-1 cells express P2Y<sub>1</sub>, P2Y<sub>2</sub>, P2Y<sub>6</sub>, and P2Y<sub>11</sub> (Clifford *et al.*, 1997; Moore *et al.*, 2001; Ben Yebdri *et al.*, 2009). However, while this suggests that both cell types differ in their expression of P2Y purinoceptors, the results reported by these studies are not consistent. Moreover, the expression of P2Y<sub>14</sub> in these cells is unknown. Thus, the aim of this study was to determine the gene expression of all P2Y purinoceptors in THP-1 cells and human monocytes. As mentioned previously, all primer pairs were tested for specificity and functionality in human brain. The results of this study are presented in Table 3.6, Figure 3.10 (brain and THP-1 cells) and Figure 3.11 (monocytes).

**Table 3.6 Detection of mRNA for P2Y purinoceptors in human brain, THP-1 cells, and human monocytes**

Gene	Human brain	THP-1 cells	Human monocytes
<i>P2RY1</i>	+	+	+
<i>P2RY2</i>	+	+	+
<i>P2RY4</i>	+	+	+
<i>P2RY6</i>	+	+	+
<i>P2RY11</i>	(+)	(+)	+
<i>P2RY12</i>	+	(+)	+
<i>P2RY13</i>	+	(+)	+
<i>P2RY14</i>	+	+	+

A + sign indicates that the gene is detected, a (+) sign indicates that the gene is detected but is represented by a faint band, and a – sign indicates that the gene is not detected.

As summarised in the Table 3.6 and Figure 3.10, mRNA transcripts for all P2Y receptors, including P2Y<sub>14</sub> were detected in human brain. As also shown (Table 3.6, Figure 3.10 and

Figure 3.11), mRNA for all P2Y receptors were also detected in THP-1 cells and human monocytes. These results suggest that THP-1 cells and human monocytes express all P2Y receptors, but also exhibit an overlapping expression pattern among genes encoding for these receptors. In THP-1 cells (Figure 3.10), it was also seen that primers for *P2RY6* also produced a second PCR amplicon of a lower molecular weight in addition to an amplicon of the predicted size. Interestingly, a second PCR amplicon was not seen in human brain or monocytes. Although a BLAST analysis was unable to identify this product, it is possible that this amplicon is a splice variant of *P2RY6*.

In summary, the results of this study have demonstrated for the first time that THP-1 cells and human monocytes exhibit an overlapping expression pattern among genes encoding for P2Y receptors. Moreover, both cell types also express mRNA for the human P2Y<sub>14</sub> receptor, which is also a novel finding.

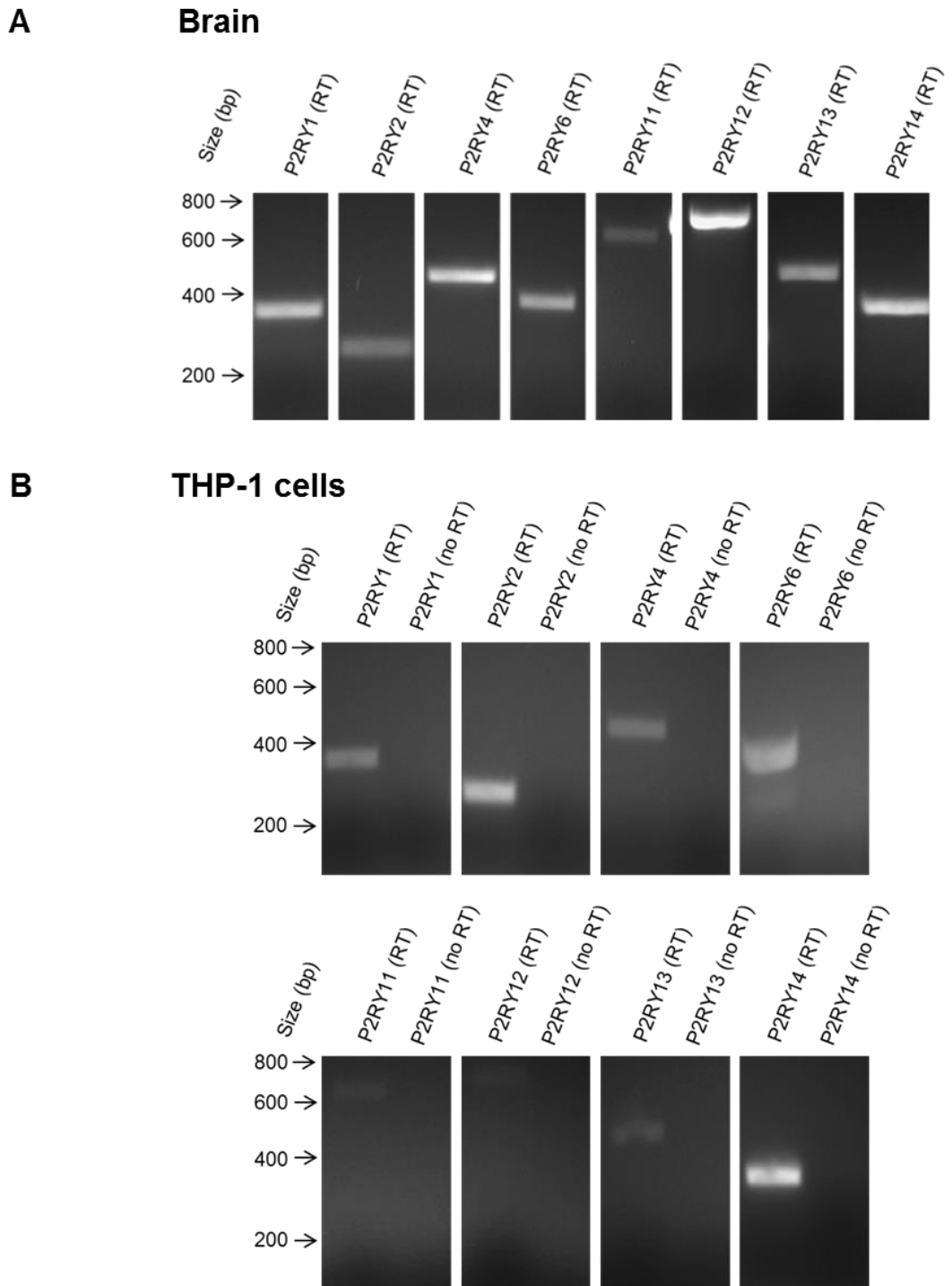


**Figure 3.10 Detection of mRNA for P2Y purinoceptors in human brain and THP-1 cells**

Detection of P2Y purinoceptors in (A) human brain, and (B) THP-1 cells using RT-PCR and agarose gel electrophoresis. Primers amplify all splice variants of the selected gene. Expression was detected at 326 bp (*P2RY1*), 243 bp (*P2RY2*), 427 bp (*P2RY4*), 391 bp (*P2RY6*), 622 bp (*P2RY11*), 698 bp (*P2RY12*), 461 bp (*P2RY13*), and 371 bp (*P2RY14*). RT and no RT constitute first strand cDNA synthesis reactions with and without reverse transcriptase, respectively.

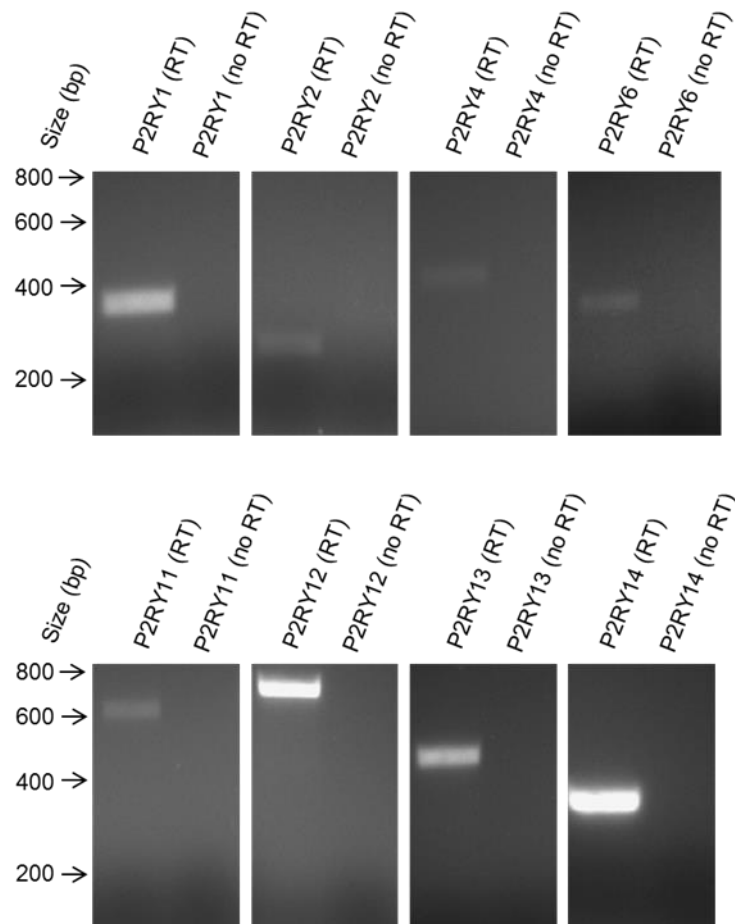


**Figure 3.11 Detection of mRNA for P2Y purinoceptors in human monocytes**

Detection of P2Y purinoceptors in human monocytes using RT-PCR and agarose gel electrophoresis. Primers amplify all splice variants of the selected gene. Expression was detected at 326 bp (*P2RY1*), 243 bp (*P2RY2*), 427 bp (*P2RY4*), 391 bp (*P2RY6*), 622 bp (*P2RY11*), 698 bp (*P2RY12*), 461 bp (*P2RY13*), and 371 bp (*P2RY14*). RT and no RT constitute first strand cDNA synthesis reactions with and without reverse transcriptase, respectively.

### 3.4 Summary

The principle aim of this chapter was to compare the gene expression of monocyte/myeloid cell markers, CC chemokines, CC chemokine receptors and purinoceptors between monocytic THP-1 cells and human peripheral blood monocytes. The purpose of these studies was also to examine the suitability of THP-1 cells as a model for investigating the role of the CCL2/CCR2 axis in monocytes and its modulation by extracellular nucleotides. The individual aims of this chapter were addressed by employing non-quantitative RT-PCR to detect mRNA transcripts. While mRNA for CD14, CD33, and CD93 were detected in both cell types, mRNA for CD16 was not detected in THP-1 cells, but was found in heterogeneous monocytes. Although these results suggested that THP-1 cells and human monocytes displayed an overlapping expression pattern for most monocyte/myeloid markers, they also indicated that THP-1 cells lacked mRNA for CD16, similar to classical (CD14<sup>++</sup>/CD16<sup>-</sup>) monocytes. The results of CC chemokines studies suggested that both cell types expressed mRNA for CCL2, CCL3, CCL4, and CCL5. Interestingly, investigations into CC chemokine receptors suggested that mRNA for CCR3 could be detected in human monocytes, but not in THP-1 cells. However, mRNA for all other CC chemokine receptors was detected in both cell types. Both cell types also displayed slightly different purinoceptor expression patterns. While THP-1 cells and human monocytes displayed an overlapping expression pattern for P1 and P2Y purinoceptors, a slightly different expression pattern for P2X receptors was observed. Interestingly, mRNA for P2X6 was not detected in heterogeneous monocytes, but was found in THP-1 cells. Despite this difference, mRNA for all other P2X receptors (except P2X2 and P2X3), were detected in both cell types.

In summary, the results of this study have provided evidence for the expression of genes encoding for monocyte/myeloid cell markers, CC chemokines, CC chemokine receptors and purinoceptors in THP-1 cells and human monocytes. This finding suggests that monocytic THP-1 cells represents a suitable alternative to human peripheral blood monocytes for studying CC chemokine and purinoceptor biology.

The next chapter in this thesis (Chapter 4) therefore used THP-1 cells (and human PBMCs) as *in vitro* models to investigate the mechanisms involved in CCL2/CCR2-mediated signalling and function of monocytes. As described previously in Chapter 1, the research presented in the next chapter looked specifically at the involvement of individual signalling components in CCL2/CCR2 activation as measured by intracellular Ca<sup>2+</sup> release, cell migration, and adhesion to vascular endothelium.

# Chapter 4: Mechanisms involved in CCL2/CCR2-mediated monocyte signalling and function

---

## 4.1 Introduction

The CCR2 receptor is a 7TM GPCR comprising of two almost identical splice variants (CCR2A and CCR2B) that differ only in an alternatively spliced carboxyl terminus (Section 1.6, Chapter 1) (Charo *et al.*, 1994; Yamagami *et al.*, 1994). CCR2 is activated by the CC chemokines CCL2, CCL7, CCL8, CCL11, and CCL13, of which all, except CCL11, represent members of the monocyte-chemoattractant protein (MCP) family (Bachelierie *et al.*, 2014). The preferred ligand of CCR2 is CCL2 (monocyte-chemoattractant protein-1) which activates CCR2 to initiate an important signalling pathway in immune cells referred to as the CCL2/CCR2 axis (Van Coillie *et al.*, 1999; Bachelierie *et al.*, 2014).

The CCL2/CCR2 axis plays a number of important developmental and immuno-regulatory roles in many types of immune cells including monocytes, T-lymphocytes, natural killer cells, and dendritic cells (Loetscher *et al.*, 1996; Sozzani *et al.*, 1997; Polentarutti *et al.*, 1997). Considered essential for monocyte trafficking (Yoshimura *et al.*, 1989), the CCL2/CCR2 axis determines the ability of different monocyte subsets to migrate under homeostatic and inflammatory conditions (Weber *et al.*, 2000; Geissmann *et al.*, 2003). Studies on mouse classical (Ly6C<sup>high</sup>) monocytes (counterparts of human classical (CD14<sup>++</sup>/CD16<sup>-</sup>) monocytes), suggest that the CCL2/CCR2 axis is important, if not crucial, for monocyte egression from the bone marrow during host defence (Kurihara *et al.*, 1997; Serbina and Pamer, 2006; Tsou *et al.*, 2007; Shi *et al.*, 2011).

Although the CCL2/CCR2 axis is considered a very important signalling pathway, pre-clinical studies on mouse (Ly6C<sup>high</sup>) monocytes have suggested that CCR2-dependent monocyte trafficking underlies many monocyte-associated pathologies including cancer, multiple sclerosis, allergic rhinitis, and atherosclerosis (Boring *et al.*, 1998; Gu *et al.*, 1998; Izikson *et al.*, 2000; Abbadie *et al.*, 2003; Brühl *et al.*, 2004). For example, Boring *et al.* (1998) and Gu *et al.* (1998) have shown that mice deficient in CCR2 display a reduced formation of atherosclerotic plaques. Later studies by Tacke *et al.* (2007) have shown that CCR2-dependent mouse (Ly6C<sup>high</sup>) monocyte migration towards arterial walls is associated with atherosclerotic plaque formation. Taken together, these studies have emphasised the pleiotropic role played by the CCL2/CCR2 axis that is both beneficial and deleterious for organismal homeostasis.

However, while these studies indicate that the CCL2/CCR2 axis is important for monocyte trafficking under homeostatic and inflammatory conditions, the exact mechanisms by which the CCL2/CCR2 axis couples to monocyte signalling and function are not entirely clear. However, despite there being a lot of useful information missing, prior work by others has suggested that CCR2 activation involves  $G_{\alpha_{i/o}}$ -type G-proteins coupled to an inhibition of adenylate cyclase and an activation of PLC and PI3K (Bizzarri *et al.*, 1995; Myers *et al.*, 1995; Turner *et al.*, 1998). Furthermore, studies by others (Wei *et al.*, 2009) have suggested that the intracellular second messenger  $Ca^{2+}$  is also important for cell migration. However, although  $Ca^{2+}$  is thought to be required for CCL2/CCR2-mediated monocyte chemotaxis (Olszak *et al.*, 2000; Gouwy *et al.*, 2008), the mechanisms by which this important ion directs cellular movement are also unclear.

## 4.2 Aims

THP-1 cells and human PBMCs were employed as *in vitro* models to elucidate the signalling mechanisms involved in CCL2/CCR2-mediated monocyte signalling and function. To address this aim, the involvement of signal transduction components thought to be downstream of the CCL2/CCR2 axis were investigated using a number of biological and pharmacological tools (Figure 4.1). The involvement of individual signalling components was assessed indirectly by intracellular  $Ca^{2+}$  release, cellular migration, and THP-1 cell adhesion to vascular endothelial cells.

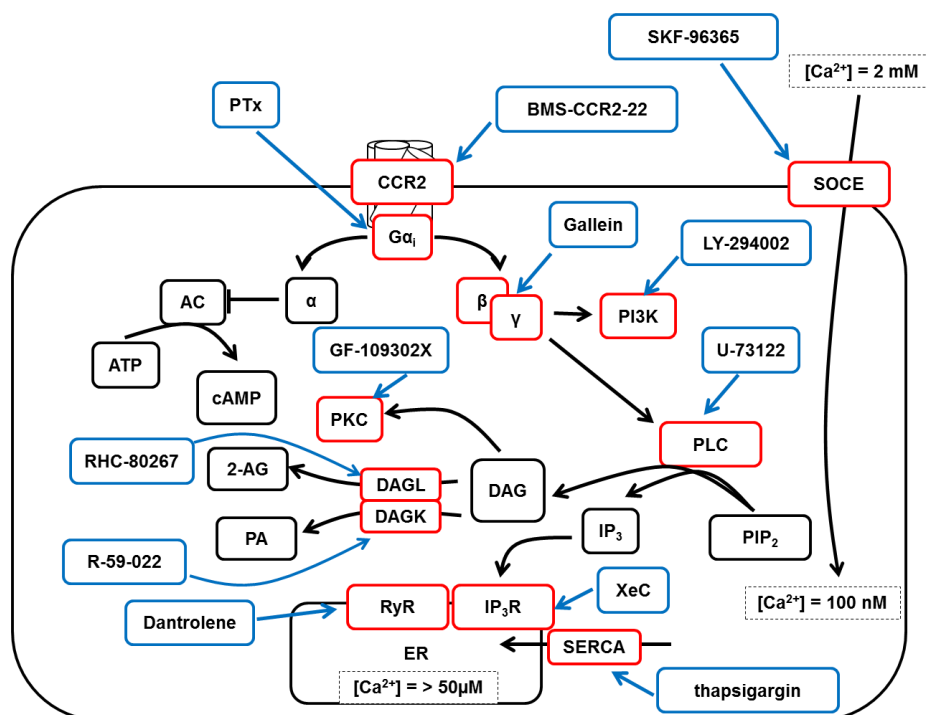


**Figure 4.1** Signalling pathways investigated in this chapter

Areas of investigation shown in (red) alongside antagonists and inhibitors used (blue).

## 4.3 Results

### 4.3.1 CCL2-evoked $\text{Ca}^{2+}$ responses in THP-1 cells and human PBMCs

The mobilisation of intracellular  $\text{Ca}^{2+}$  upon receptor activation is considered an integral component of cellular signalling and activation (Berridge *et al.*, 2000). Thus, the initial aim of this chapter was to determine whether CCL2 would evoke intracellular  $\text{Ca}^{2+}$  release from THP-1 cells and human PBMCs. Initial studies set out to test the effects of a range of CCL2 concentrations (1-100 ng/ml) on THP-1 cells and the effects of a single concentration of CCL2 (50 ng/ml) on human PBMCs.

As can be seen (Figure 4.2c), CCL2 evoked a concentration-dependent increase in intracellular  $\text{Ca}^{2+}$  from THP-1 cells. Maximal  $\text{Ca}^{2+}$  %Fmax responses were observed between 50 and 100 ng/ml of CCL2 and were  $15 \pm 2\%$  (n=3) and  $18 \pm 2\%$  (n=3), respectively. Since 50 ng/ml CCL2 (Figure 4.2a) evoked a maximal response, this concentration was used in the majority of studies within this thesis. Based on this data, the estimated  $\text{EC}_{50}$ ,  $\text{EC}_{20}$  and  $\text{EC}_{10}$  concentrations for CCL2 were  $15 \pm 3$  ng/ml (n=3),  $6 \pm 2$  ng/ml (n=3), and  $4 \pm 1$  ng/ml (n=3), respectively. The  $\text{EC}_{50}$  in nM for CCL2 was 1.9 nM. As shown (Figure 4.2b), human PBMCs were also challenged with 50 ng/ml CCL2 and demonstrated a transient intracellular  $\text{Ca}^{2+}$  response which was approximately 3-fold less than THP-1 cells ( $5 \pm 1\%$ , n=3).

The results of this study indicated that CCL2 evokes intracellular  $\text{Ca}^{2+}$  responses in THP-1 cells. These data also suggest that CCL2 evokes similar intracellular  $\text{Ca}^{2+}$  responses from human CCR2-expressing monocytes.

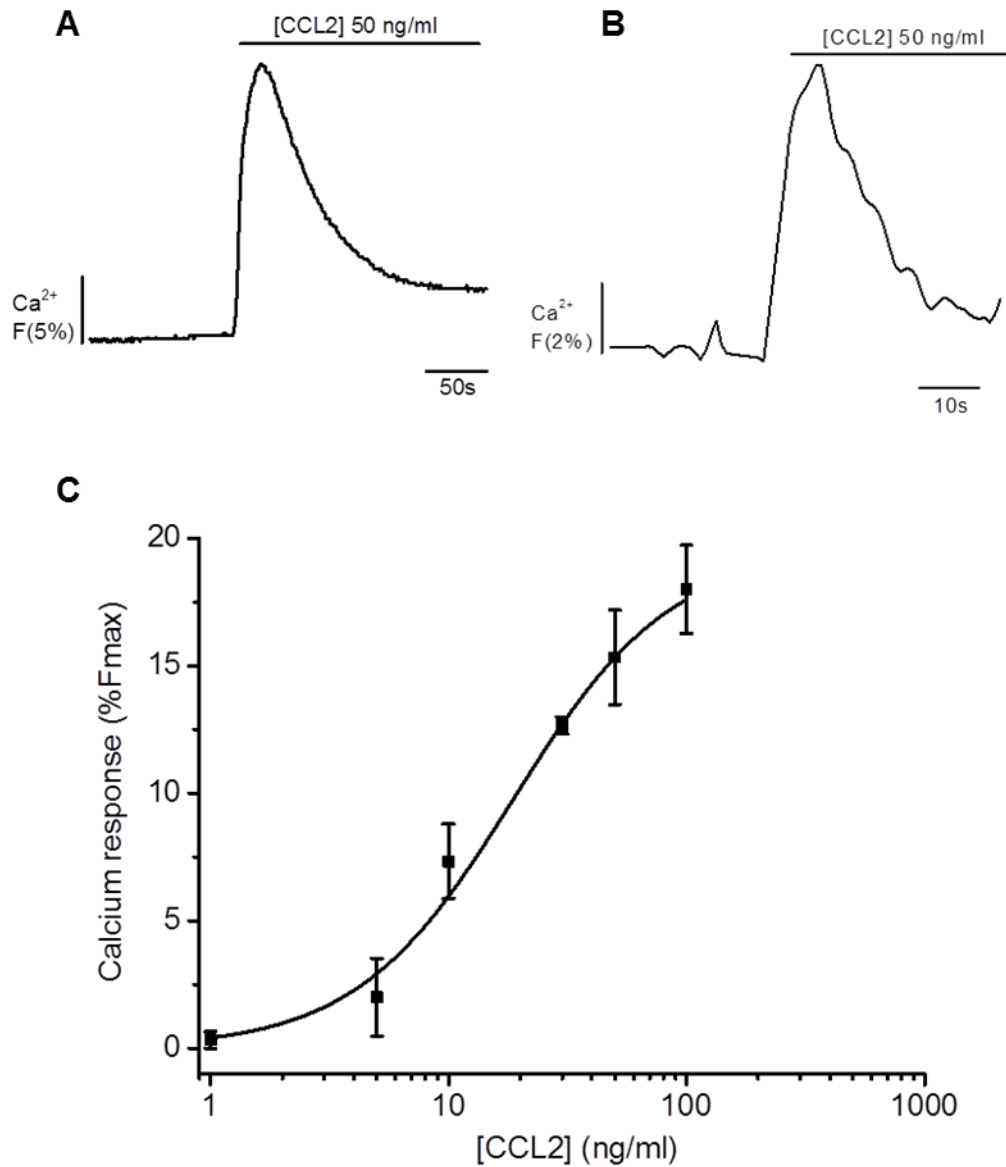


**Figure 4.2 CCL2-evoked Ca<sup>2+</sup> responses in THP-1 cells and PBMCs**

Representative Ca<sup>2+</sup> transients to 50 ng/ml CCL2 challenge in (A) THP-1 cells and (B), human PBMCs. (C) Concentration-response curve showing normalised THP-1 cell intracellular Ca<sup>2+</sup> responses to CCL2 (1-100 ng/ml). Responses normalised to Ca<sup>2+</sup> signals elicited by 40  $\mu$ M digitonin (%Fmax). Data represents mean  $\pm$  SEM from n=3 replicates.

### **4.3.2 Effect of Ca<sup>2+</sup> removal on CCL2-mediated THP-1 cell signalling and function**

In the classical scheme of GPCR activation, PLC drives the formation IP<sub>3</sub> which in return, acts as second messenger for the release of intracellular Ca<sup>2+</sup> from IP<sub>3</sub>R-expressing internal stores such as the ER (Berridge, 1993). Following a rise in intracellular Ca<sup>2+</sup> concentrations ([Ca<sup>2+</sup>]<sub>i</sub>), a number of OFF mechanisms such as SERCA pumps strive to return [Ca<sup>2+</sup>]<sub>i</sub> to basal levels (Parekh and Putney, 2005).

#### **4.3.2.1 Effect Ca<sup>2+</sup> removal on CCL2-evoked Ca<sup>2+</sup> responses in THP-1 cells**

The previous studies in this chapter (Section 4.3.1) suggest that CCL2 evokes intracellular Ca<sup>2+</sup> responses from THP-1 cells and human PBMCs. These data further indicate that CCL2 is likely to participate in activating downstream pathways involved in increasing [Ca<sup>2+</sup>]<sub>i</sub>, either by promoting a release from internal stores, or by allowing Ca<sup>2+</sup> influx. The next studies therefore investigated the requirement of Ca<sup>2+</sup> for monocyte signalling and function by examining the effects of removing extracellular Ca<sup>2+</sup> on THP-1 cell intracellular Ca<sup>2+</sup> responses evoked by 50 ng/ml CCL2.

As shown (Figure 4.3), in conditions where extracellular Ca<sup>2+</sup> (1.5 mM) was present, CCL2 evoked an expected intracellular Ca<sup>2+</sup> response, where the %Fmax value for CCL2 was 20 ± 1% (n=5). In contrast, in conditions where extracellular Ca<sup>2+</sup> (1.5 mM) was removed and replaced with the Ca<sup>2+</sup>-chelator EGTA (1 mM), the %Fmax value for CCL2 dropped to 11 ± 0.4% (n=5), indicating a 48 ± 2% (n=5, p<0.01) reduction. The decay rates for CCL2 transients in with Ca<sup>2+</sup> (98 ± 12 seconds, n=5) and without Ca<sup>2+</sup> conditions (115 ± 14 seconds, n=5) were compared but were not significantly different (n=5, p=0.49).

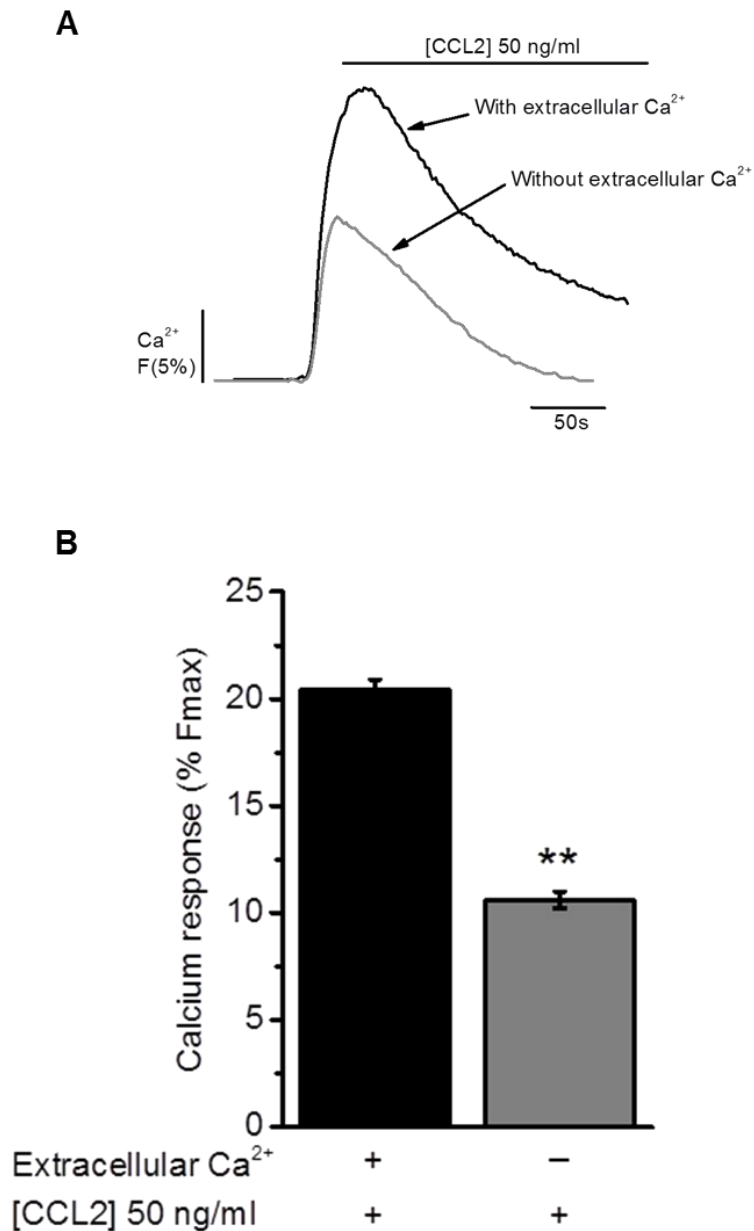


**Figure 4.3 Effect of extracellular Ca<sup>2+</sup> removal on CCL2-evoked Ca<sup>2+</sup> responses in THP-1 cells**

(A) Representative Ca<sup>2+</sup> transients to CCL2 (50 ng/ml) in THP-1 cells in the presence and absence of extracellular Ca<sup>2+</sup>. (B) Bar chart showing normalised intracellular Ca<sup>2+</sup> responses to CCL2 (50 ng/ml) in THP-1 cells in the presence and absence of extracellular Ca<sup>2+</sup>. Responses normalised to Ca<sup>2+</sup> signals elicited by 40µM digitonin (%Fmax). Data represents mean ± SEM from n=3 replicates. Asterisks indicate significant changes towards control (\*\*p<0.01, Students t-test).

#### 4.3.2.2 Effect of BAPTA-AM on CCL2-mediated THP-1 cell chemotaxis

To investigate the requirement for  $\text{Ca}^{2+}$  in CCL2-evoked intracellular  $\text{Ca}^{2+}$  responses further, studies employed the pharmacological tool BAPTA-AM. As a high-affinity  $\text{Ca}^{2+}$ -chelating agent, BAPTA-AM has a  $K_d$  value of 0.11  $\mu\text{M}$  (Tsien, 1980). Because of its ability of being able to sequester  $\text{Ca}^{2+}$ , BAPTA-AM could only be used to investigate the requirement of  $\text{Ca}^{2+}$  for THP-1 cell chemotaxis towards CCL2 (50 ng/ml).

As shown (Figure 4.4), THP-1 cells demonstrated a significantly higher chemotactic index ( $n=4$ ,  $p<0.01$ ) towards CCL2 ( $6 \pm 1$ ,  $n=4$ ) than towards vehicle ( $1 \pm 0.5$ ,  $n=4$ ), which indicated that CCL2 was chemotactic. As also shown, BAPTA-AM treatment abolished THP-1 cell chemotaxis towards CCL2, where the chemotactic index for BAPTA-AM-treated cells was  $0 \pm 0$  ( $n=4$ ,  $p<0.01$ ) and suggested that  $\text{Ca}^{2+}$  was essential not only for monocyte chemotaxis towards CCL2, but also for chemokinesis. While it is possible that this result could also be attributed to a loss in THP-1 cell viability, trypan blue and LDH studies (Appendix Figure A3 and A5), showed no significant loss in cell viability after a 2.5 hour exposure of THP-1 cells with BAPTA-AM.

Taken together, the results of this study indicate that intracellular and extracellular sources of  $\text{Ca}^{2+}$  contribute to efficient CCL2-mediated THP-1 cell signalling and function. The effects of BAPTA-AM further suggest that  $\text{Ca}^{2+}$  is essential for cellular migration in general. In an *in vivo* setting, this would suggest that CCR2-expressing monocytes would also require  $\text{Ca}^{2+}$  for efficient CCL2-mediated signalling and function.

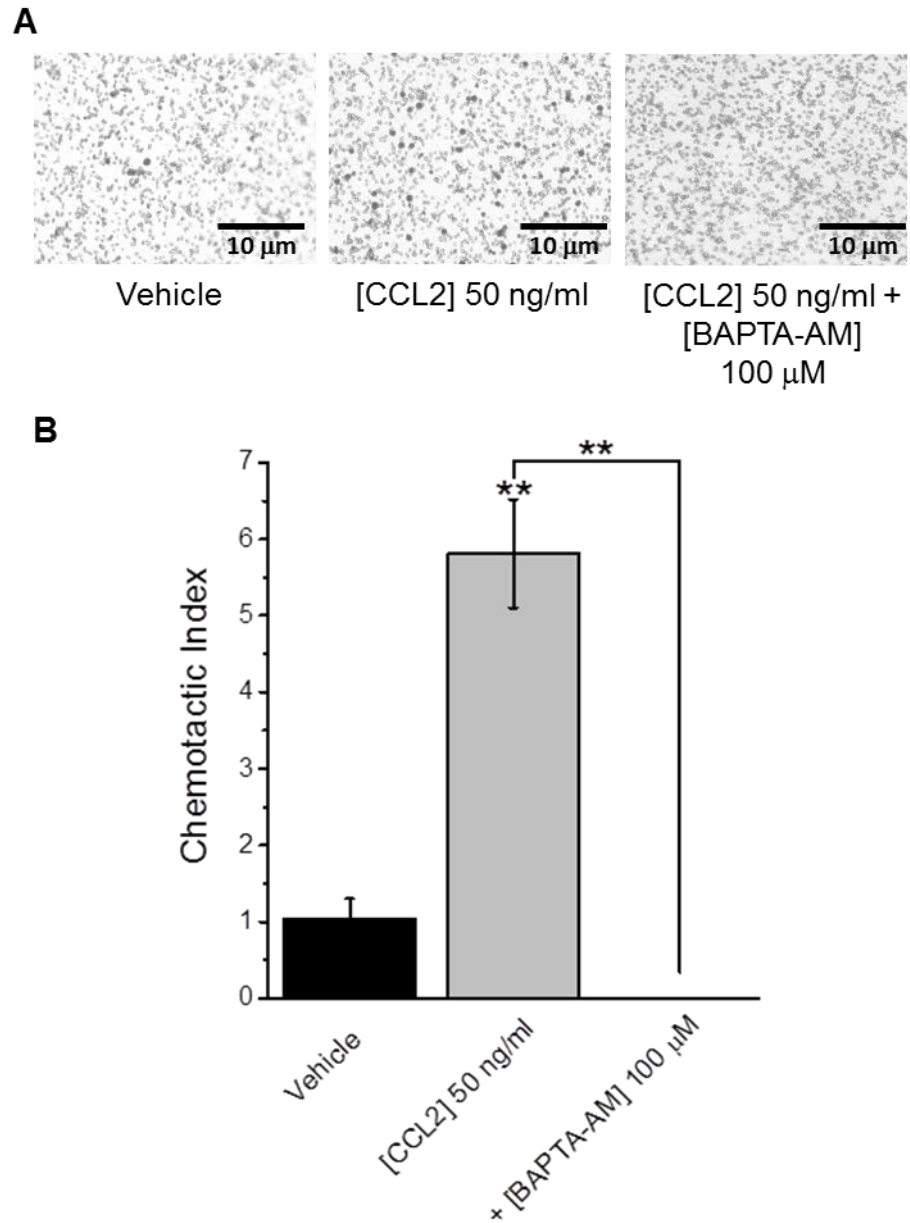


**Figure 4.4 Effect of BAPTA-AM on CCL2-mediated THP-1 cell chemotaxis**

(A) Representative images showing the effect of BAPTA-AM (100 μM, 30 minutes) on THP-1 cell chemotaxis towards CCL2 (50 ng/ml, lower chamber, 2 hrs). Scale bar represents 10 μm. (B) Bar chart showing normalised THP-1 cell chemotaxis towards vehicle (water) or CCL2 (50 ng/ml, lower chamber, 2hrs) with or without BAPTA-AM (100 μM; 30 minutes). Chemotactic index is a ratio of the number of cells that migrated towards CCL2 over the number of cells that migrated towards vehicle. Data represents mean ± SEM from n=4 transwells. Asterisks indicate significant changes towards vehicle (\*\*p<0.01, One-way ANOVA with Bonferroni's multiple comparison).

### 4.3.3 Effect of CCR2 antagonism on CCL2-mediated THP-1 cell signalling and function

Experiments designed to elucidate the signalling mechanisms involved in CCL2-mediated monocyte signalling and function were next performed with monocytic THP-1 cells.

As described previously (Section 1.6, Chapter 1), CCL2 is the preferred ligand of the CCR2 receptor and forms the CCL2/CCR2 axis, a pathway considered important for monocyte trafficking and function (Van Coillie *et al.*, 1999; Bachelierie *et al.*, 2014). The next studies therefore sought to confirm the association between CCL2 and CCR2 and understand the requirement of CCR2 for monocyte signalling and function. To address this aim, studies employed BMS-CCR2-22, a pan-CCR2 antagonist reported to be highly selective for CCR2 over other CC chemokine receptors. Studies by Cherney *et al.* (2008), have demonstrated that the IC<sub>50</sub> values for BMS-CCR2-22 against CCL2-mediated Ca<sup>2+</sup> mobilisation and chemotaxis of human PBMCs are 18 nM and 1 nM, respectively.

#### 4.3.3.1 Effect of BMS-CCR2-22 on CCL2- and CCL5-evoked Ca<sup>2+</sup> responses in THP-1 cells

Using THP-1 cells as a model, experiments examined the effects of BMS-CCR2-22 (30 pM – 100 nM) on intracellular Ca<sup>2+</sup> responses evoked by 50 ng/ml CCL2. As shown (Figure 4.5), BMS-CCR2-22 produced a concentration-dependent inhibition of CCL2-evoked intracellular Ca<sup>2+</sup> responses. Furthermore, it was seen that BMS-CCR2-22 abolished CCL2-evoked Ca<sup>2+</sup> responses at 100 nM (n=3, p<0.01), where the %Fmax values for CCL2 in untreated and BMS-CCR2-22-treated cells were 20 ± 1% (n=3) and 0 ± 0% (n=3), respectively. This result suggests that CCR2 is essential for Ca<sup>2+</sup> responses evoked by CCL2. The IC<sub>50</sub> concentration of BMS-CCR2-22 was also estimated (IC<sub>50</sub> = 2.9 ± 0.3 nM, n=3), and indicated quite interestingly, that BMS-CCR2-22 was more potent against CCL2-evoked Ca<sup>2+</sup> responses in THP-1 cells than for similar responses in PBMCs (Cherney *et al.*, 2008).

To address whether BMS-CCR2-22 also affected the decay of Ca<sup>2+</sup> responses, the  $\tau$  values were analysed and compared. Due to a lack of decay, the  $\tau$  values for 30 nM and 100 nM BMS-CCR2-22 could not be determined. The  $\tau$  values of Ca<sup>2+</sup> transients for all other BMS-CCR2-22 concentrations were analysed, but were not significantly different from vehicle. For example, in paired experiments with 10 nM BMS-CCR2-22, the  $\tau$  values of transients in untreated and BMS-CCR2-22-treated cells were 111 ± 8 seconds (n=3) and 114 ± 10 seconds (n=3), respectively (n=3, p>0.05).

It was also necessary to understand the selectivity of BMS-CCR2-22. Although considered selective for CCR2, BMS-CCR2-22 is reported to inhibit CCR3 binding by 37%

at 10  $\mu\text{M}$  (Cherney *et al.*, 2008). While this suggests that the effects of BMS-CCR2-22 in the current experiments are attributable to a blockade of CCR3, mRNA transcripts for CCR3 were not detected in THP-1 cells (Chapter 3). Although these data supported the use of BMS-CCR2-22, an additional experiment was performed to examine the effects of BMS-CCR2-22 (30 and 100 nM) on  $\text{Ca}^{2+}$  responses evoked by 50 ng/ml CCL5 in THP-1 cells. CCL5 was selected due to its reported activation of CCR1, CCR3, and CCR5 (Bachelierie *et al.*, 2014).

As shown (Figure 4.6), the %Fmax values for CCL5 in untreated cells varied between paired experiments testing the effects of 30 and 100 nM BMS-CCR2-22. Despite this, it was seen that CCL5-evoked intracellular  $\text{Ca}^{2+}$  responses were not significantly attenuated by 30 nM BMS-CCR2-22, where the %Fmax values for CCL5 in untreated ( $7 \pm 0.3\%$ ,  $n=3$ ) and BMS-CCR2-22-treated cells ( $8 \pm 0\%$ ,  $n=3$ ) were not significantly different ( $n=3$ ,  $p>0.05$ ). However, as Figure 4.6 shows, 100 nM BMS-CCR2-22 significantly impaired CCL5-evoked  $\text{Ca}^{2+}$  responses by  $20 \pm 5\%$  ( $n=4$ ,  $p<0.05$ ), where the %Fmax values for CCL5 in untreated and BMS-CCR2-22-treated THP-1 cells were  $12 \pm 1\%$  ( $n=4$ ) and  $10 \pm 1\%$  ( $n=4$ ), respectively. These data indicate that higher concentrations of BMS-CCR2-22 impair CCL5-evoked intracellular  $\text{Ca}^{2+}$  responses.

A comparison of the decay rates for both sets of treatments did not reveal any significant differences. For example in experiments with 100 nM BMS-CCR2-22, the  $\tau$  values for CCL5 in untreated ( $178 \pm 8$  seconds,  $n=4$ ) and BMS-CCR2-22-treated cells ( $180 \pm 16$  seconds,  $n=4$ ), were not significantly different ( $n=4$ ,  $p>0.05$ ). This data suggests that BMS-CCR2-22 does not influence the decay of CCL5  $\text{Ca}^{2+}$  responses in THP-1 cells.

Taken together, these results suggest that BMS-CCR2-22 attenuates CCL5-evoked intracellular  $\text{Ca}^{2+}$  responses via a mechanism that is unlikely to involve CCR3.

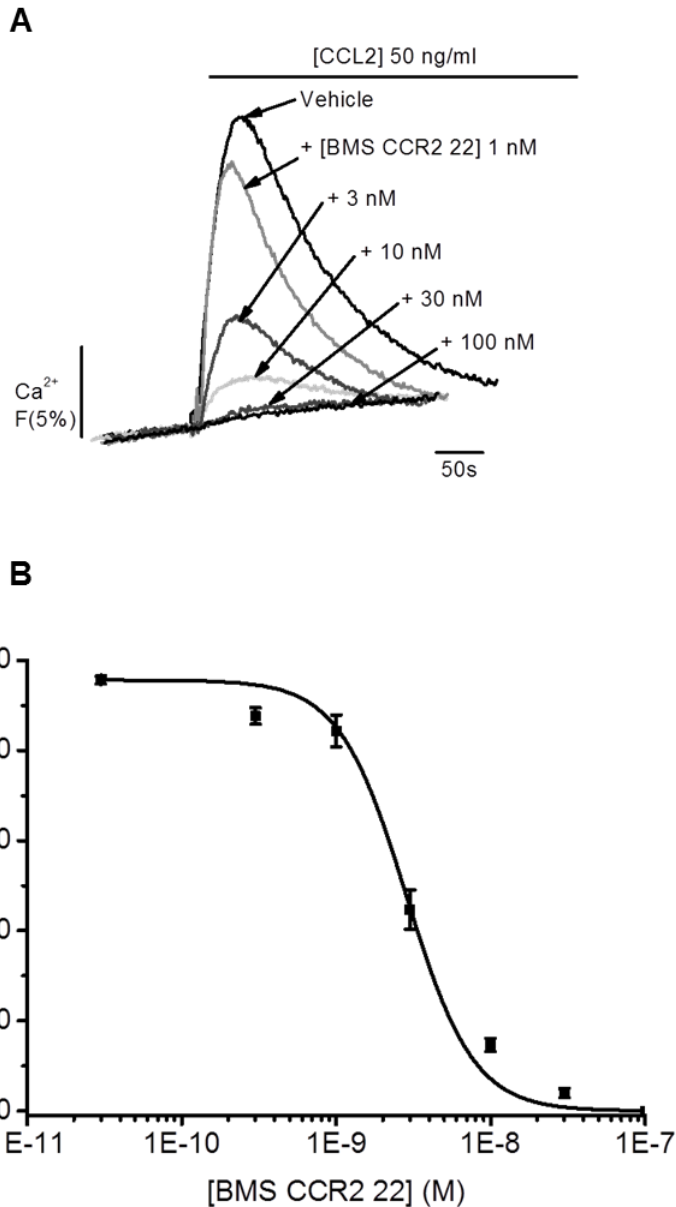


**Figure 4.5 Effect of BMS-CCR2-22 on CCL2-evoked Ca<sup>2+</sup> responses in THP-1 cells**

(A) Representative Ca<sup>2+</sup> transients to CCL2 (50 ng/ml) in THP-1 cells pre-treated with vehicle (DMSO) or BMS-CCR2-22 (1-100 nM) for 15 minutes. (B) Normalised concentration-response curve showing the effect of BMS CCR2 22 (30 pM–100 nM, 15 minutes) on intracellular Ca<sup>2+</sup> responses to CCL2 (50 ng/ml) in THP-1 cells. Responses given as a percentage of CCL2 %F<sub>max</sub> in the absence of BMS-CCR2-22. Responses normalised to Ca<sup>2+</sup> signals elicited by 40 μM digitonin (%F<sub>max</sub>). Data represents mean ± SEM from n=3 replicates.

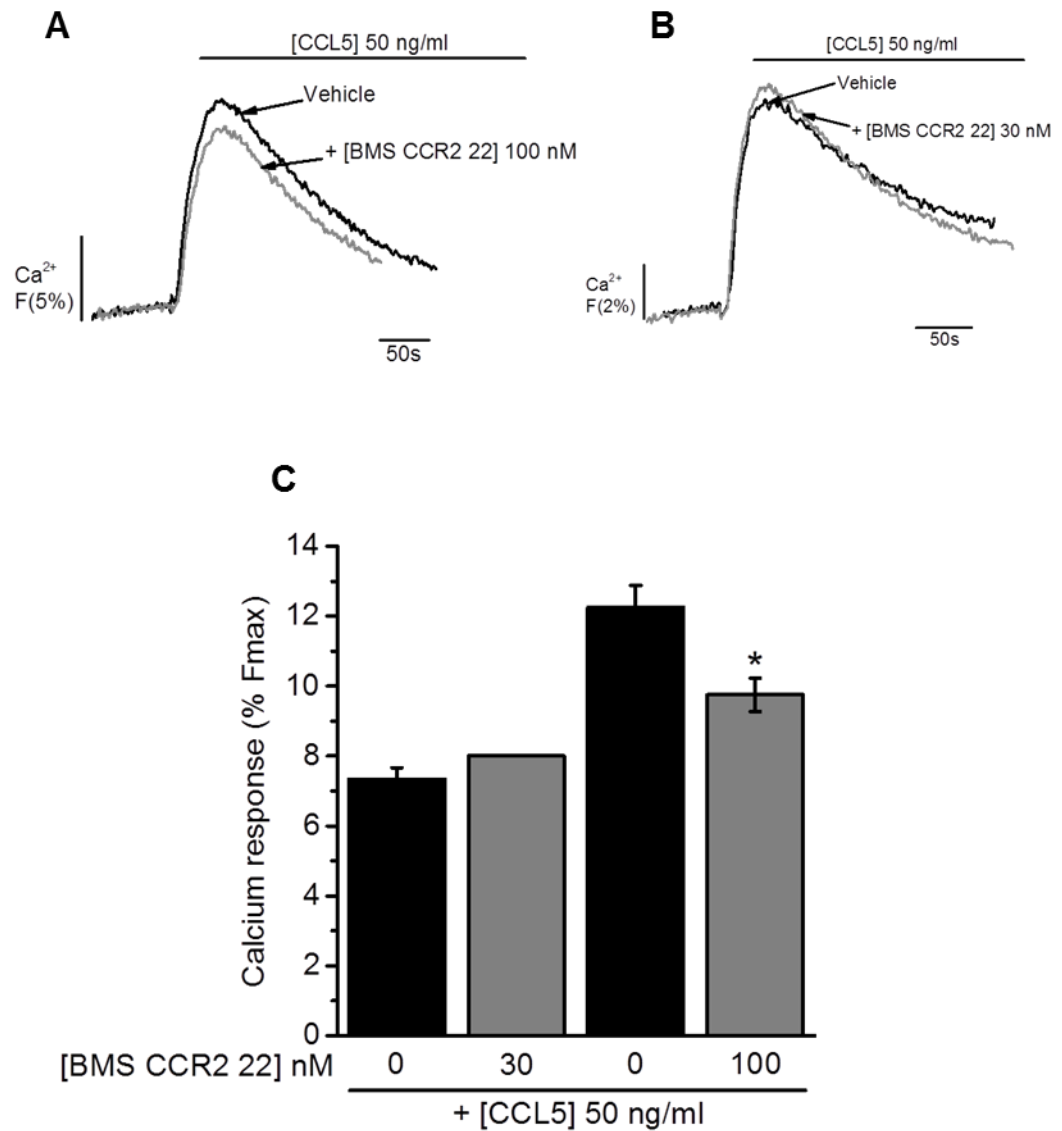


**Figure 4.6 Effect of BMS-CCR2-22 on CCL5-evoked Ca<sup>2+</sup> responses in THP-1 cells**

Representative Ca<sup>2+</sup> transients to CCL5 (50 ng/ml) in THP-1 cells pre-treated with vehicle (DMSO) or (A) 100 nM or (B) 30 nM BMS-CCR2-22 for 15 minutes. (C) Bar chart showing normalised intracellular Ca<sup>2+</sup> responses to CCL5 (50 ng/ml) in THP-1 cells pre-treated with vehicle (DMSO) or BMS-CCR2-22 (30-100 nM) for 15 minutes. Responses normalised to Ca<sup>2+</sup> signals elicited by 40 μM digitonin (% Fmax). Data represents mean ± SEM from n=3 (30 nM BMS-CCR2-22), or n=4 (100 nM BMS-CCR2-22) replicates. Asterisks indicate significant changes towards vehicle (\*p<0.05, Students t-test).

#### 4.3.3.2 Effect of BMS-CCR2-22 on CCL2-mediated THP-1 cell chemotaxis and adhesion

BMS-CCR2-22 was also employed to investigate the role of the CCR2 receptor in CCL2-mediated monocyte trafficking and adhesion. Experiments first examined the effects of BMS-CCR2-22 (100 nM) on THP-1 cell chemotaxis towards 50 ng/ml CCL2.

As can be seen (Figure 4.7), the chemotactic indexes of THP-1 cells towards vehicle or CCL2 were  $1 \pm 0.2$  (n=4) and  $14 \pm 4$  (n=4) respectively, and indicated a significant (n=4,  $p < 0.01$ ) increase in cell migration towards CCL2. As also shown (Figure 4.7), a significant inhibition of THP-1 cell chemotaxis was observed with 100 nM BMS-CCR2-22 ( $91 \pm 3\%$ , n=4,  $p < 0.05$ ), where the chemotactic index for BMS-CCR2-22-treated THP-1 cells was  $1.5 \pm 1$  (n=4) and thus similar to vehicle-treated cells. While it is possible that this effect reflects a loss in THP-1 cell viability, trypan blue and LDH studies (Appendix Figure A3 and A5) showed no significant loss in cell viability after a 2.5 hour exposure of THP-1 cells with BMS-CCR2-22. These data therefore suggest that monocyte trafficking towards CCL2 requires CCR2 activation.

The adhesion of monocytes and their subsequent diapedesis into the vascular endothelium is an important process in monocyte-driven responses during infection and inflammation, and during the development of inflammatory disease (Beekhuizen and van Furth, 1993; Woollard and Geissmann, 2010). Hence, it is important to understand the mechanisms involved in driving this process. To address this aim, the requirement of CCR2 for THP-1 cell adhesion to quiescent and TNF $\alpha$ -treated HUVEC monolayers was investigated. An experimental model was set-up where CCL2 primed THP-1 cells were incubated with 100 nM BMS-CCR2-22 for 45 minutes and then allowed to adhere to vehicle or TNF $\alpha$ -treated (10 ng/ml) HUVEC cell monolayers. The results of these experiments are shown in Figure 4.8a (quiescent) and Figure 4.8b (TNF $\alpha$ -treated).

As shown (Figure 4.8a), in quiescent HUVEC experiments, vehicle-treated THP-1 cells exhibited a % adhesion of  $31 \pm 9\%$  (n=20,  $p < 0.01$ ). This result is interesting since it suggests that THP-1 cells adhere to HUVEC monolayers under basal conditions. In contrast, a significant increase in % adhesion ( $100 \pm 18\%$ , n=20,  $p < 0.01$ ) was seen when THP-1 cells were primed with CCL2, and suggests that CCL2 priming promotes adhesion. Interestingly, treatment of CCL2-primed THP-1 cells with 100 nM BMS-CCR2-22 significantly disrupted CCL2-dependent adhesion by  $68 \pm 12\%$  (n=5,  $p < 0.01$ ), bringing down the % adhesion ( $32 \pm 13\%$ , n=20) to levels almost identical to vehicle-treated cells.

In experiments with TNF $\alpha$ -treated HUVEC monolayers (Figure 4.8b), the % adhesion of vehicle-treated THP-1 cells was  $28 \pm 12\%$  (n=8). As also shown, priming of THP-1 cells with CCL2 significantly increased the % adhesion to  $100 \pm 26\%$  (n=8,  $p < 0.05$ ). This

suggests that CCL2-priming also enhances the adhesion of THP-1 cells to TNF $\alpha$ -treated HUVECs. However, it was observed that treatment with 100 nM BMS-CCR2-22 abolished adhesion, where the % adhesion of cells was  $0 \pm 0\%$  (n=8, p<0.01). This result is interesting, and indicates that primary monocyte adhesion to the vascular endothelium during inflammation is entirely CCR2-dependent.

Taken together with the results of Ca<sup>2+</sup> studies, these data suggest that CCR2 is likely to be critical for CCL2/CCR2-mediated monocyte signalling and function.

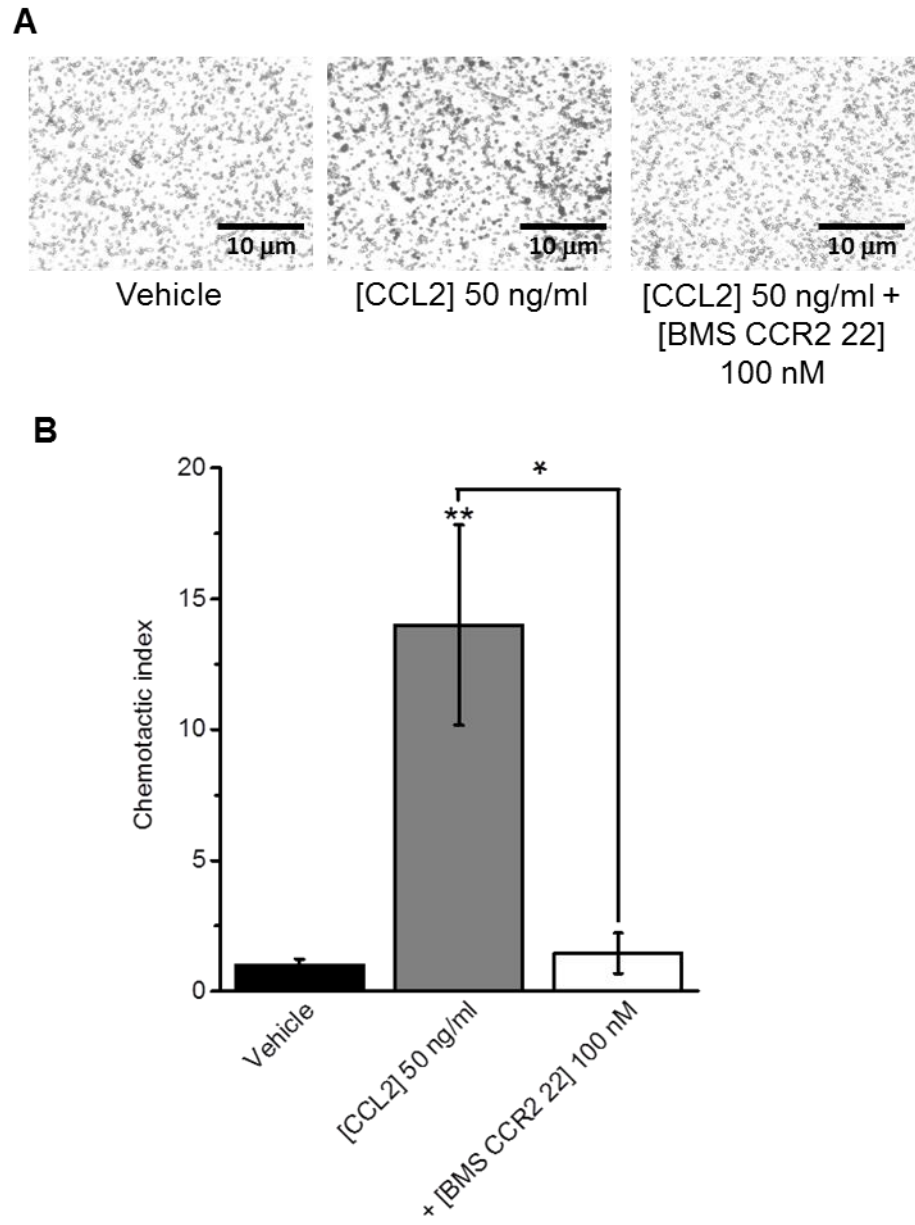


**Figure 4.7 Effect of BMS-CCR2-22 on CCL2-mediated THP-1 cell chemotaxis**

(A) Representative images showing the effect of BMS-CCR2-22 (100 nM) on THP-1 cell chemotaxis towards CCL2 (50 ng/ml, lower chamber, 2hrs). Scale bar represents 10 µm.

(B) Bar chart showing normalised THP-1 cell chemotaxis towards vehicle (water) or CCL2 (50 ng/ml, lower chamber, 2hrs) in the presence of BMS-CCR2-22 (100 nM). Chemotactic index is a ratio of the number of cells that migrated towards CCL2 over the number of cells that migrated towards vehicle. Data represents mean  $\pm$  SEM from n=4 transwells. Asterisks indicate significant changes towards vehicle (\*p<0.05, \*\*p<0.01, One-way ANOVA with Bonferroni's multiple comparison).

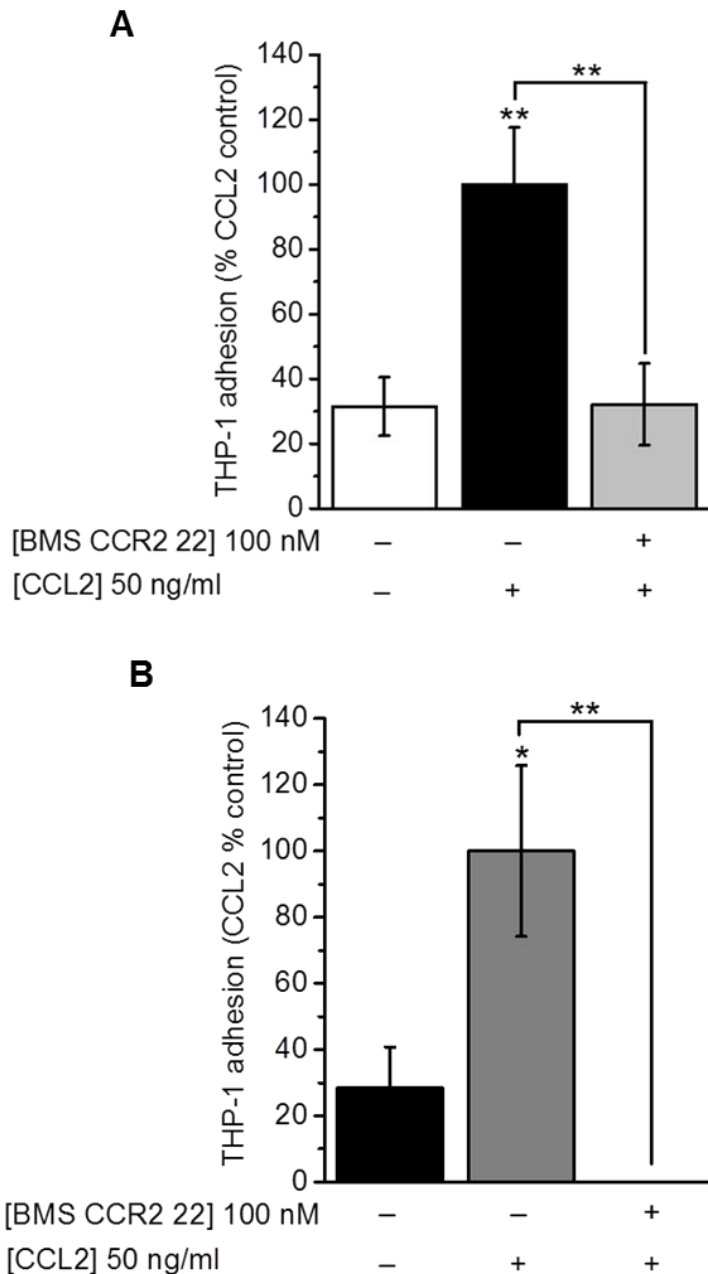


**Figure 4.8 Effect of BMS-CCR2-22 on CCL2-mediated THP-1 cell adhesion to quiescent and TNF $\alpha$ -treated HUVEC monolayers**

Bar chart shows normalised adhesion of vehicle-treated or CCL2-primed (50 ng/ml) THP-1 cells to (A) quiescent and (B) TNF $\alpha$ -treated (10 ng/ml, 5 hours) HUVEC monolayers following treatment with vehicle (DMSO) or BMS-CCR2-22 (100 nM, 45 minutes). Normalised adhesion represents a percentage of mean adhesion of CCL2-primed THP-1 cells in the absence of BMS-CCR2-22. Data represents mean  $\pm$  SEM from a total of n=20 replicates from n=4 experiments (quiescent), or a total of n=8 replicates from n=2 experiments (TNF $\alpha$ -treated). Asterisks indicate significant changes towards vehicle (\*p<0.05, \*\*p<0.01, respectively, One-way ANOVA with Bonferroni's multiple comparison).

#### 4.3.4 Effect of $G\alpha_{i/o}$ inhibition on CCL2/CCR2-mediated THP-1 cell signalling and function

The CCR2 receptor has been shown to activate  $G\alpha_{i/o}$ -type G-proteins in a number of studies (Bizzarri *et al.*, 1995; Myers *et al.*, 1995; Turner *et al.*, 1998). A key study is that of Bizzarri *et al.* (1995), which showed that CCL2-evoked  $Ca^{2+}$  responses in human monocytes were almost abolished by *Bordetella Pertussis* (PTx). This is a bacterial toxin that ribosylates ADP of the  $G\alpha_{i/o}$  subunit thereby preventing the exchange of guanine diphosphate (GDP) for guanine triphosphate (GTP), rendering the  $\alpha$  subunit unable to dissociate from the  $\beta\gamma$  dimer (Katada and Ui, 1982). Although PTx has been used extensively to show that CCR2 couples to  $G\alpha_{i/o}$ , no prior studies have employed PTx to demonstrate an association between  $G\alpha_{i/o}$ , CCL2-evoked  $Ca^{2+}$  mobilisation, and monocyte migration.

##### 4.3.4.1 Effect of PTx on CCL2-, ATP- and ADP-evoked $Ca^{2+}$ responses in THP-1 cells

Using THP-1 cells as a model, studies examined the effects of PTx (100 ng/ml) on intracellular  $Ca^{2+}$  responses evoked by CCL2 (50 ng/ml), ATP (30  $\mu$ M), and ADP (30  $\mu$ M). ATP and ADP were selected as both are known to also activate PTx-insensitive  $G\alpha_{q/11}$ -type G-proteins (Burnstock, 2012).

As shown (Figure 4.9), PTx almost completely abolished CCL2-evoked intracellular  $Ca^{2+}$  responses in THP-1 cells, demonstrating a % inhibition of  $96 \pm 1\%$  ( $n=7$ ,  $p<0.01$ ). In paired experiments, the %Fmax values for CCL2 in untreated and PTx-treated cells were  $24 \pm 1\%$  ( $n=7$ ) and  $1 \pm 0.2\%$  ( $n=7$ ), respectively. Due to a lack of decay of  $Ca^{2+}$  transients in treated cells, the  $\tau$  values were not possible to determine and compare with untreated cells. As can also be seen (Figure 4.9), intracellular  $Ca^{2+}$  responses evoked by ATP and ADP were not significantly affected by PTx. In experiments with ATP, the %Fmax values for ATP in untreated and PTx-treated cells were  $38 \pm 1\%$  ( $n=11$ ) and  $36 \pm 2\%$  ( $n=11$ ), respectively ( $n=11$ ,  $p>0.05$ ). In comparison, the %Fmax responses for ADP in untreated and PTx-treated THP-1 cells were  $26 \pm 3\%$  ( $n=7$ ) and  $25 \pm 1\%$  ( $n=7$ ) respectively. A further analysis of the decay rates ( $\tau$ , sec) indicated no significant differences in  $\tau$  between untreated and PTx-treated cells for either ATP ( $n=11$ ,  $p>0.05$ ) or ADP ( $n=7$ ,  $p>0.05$ ). While the  $\tau$  values for ATP in untreated and PTx-treated cells were  $98 \pm 5$  seconds ( $n=11$ ) and  $107 \pm 14$  seconds ( $n=11$ ) respectively, for ADP these were  $288 \pm 27$  seconds ( $n=7$ ) and  $424 \pm 80$  seconds ( $n=7$ ), respectively. These results suggest that PTx does not affect the decay of ATP and ADP  $Ca^{2+}$  transients.

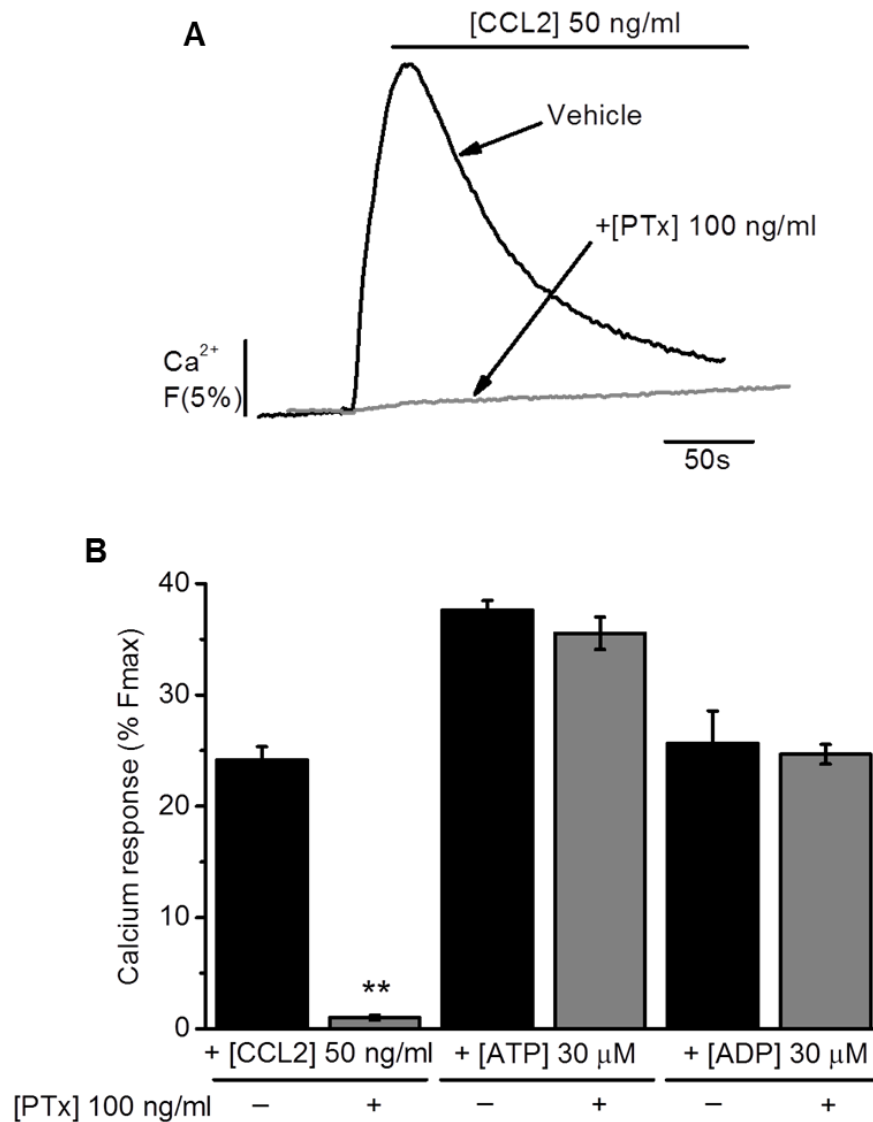


**Figure 4.9 Effect of PTx on CCL2, ATP, and ADP-evoked Ca<sup>2+</sup> responses in THP-1 cells**

(A) Representative Ca<sup>2+</sup> transients to CCL2 (50 ng/ml) in THP-1 cells pre-treated with vehicle (water) or PTx (100 ng/ml) for 4 hours. (B) Bar chart showing normalised intracellular Ca<sup>2+</sup> responses to CCL2 (50 ng/ml), ATP (30 µM), or ADP (30 µM) in THP-1 cells treated with vehicle (water) or PTx (100 ng/ml) for 4 hours. Responses normalised to Ca<sup>2+</sup> signals elicited by 40 µM digitonin (%Fmax). Data represents mean ± SEM from n=7 (CCL2), n=11 (ATP) and n=3 (ADP) replicates. Asterisks indicate significant changes towards control (\*\*p<0.01, Students t-test).

#### 4.3.4.2 Effect of PTx on CCL2-mediated THP-1 cell chemotaxis

To examine the requirement of  $G\alpha_{i/o}$  for monocyte function, the effects of PTx (100 ng/ml) on THP-1 cell migration towards CCL2 were next investigated. As shown (Figure 4.10), untreated THP-1 cells migrated readily towards CCL2, where the chemotactic indexes for vehicle and CCL2-challenged cells were  $1 \pm 0.1$  (n=4) and  $10 \pm 1$  (n=4), respectively (n=4,  $p < 0.01$ ). Interestingly, a significant inhibition of THP-1 cell chemotaxis was observed with PTx ( $86 \pm 3\%$ , n=4,  $p < 0.01$ ), where the chemotactic index for these cells was  $1.5 \pm 0.5$  (n=4) and therefore similar to vehicle-treated cells (Figure 4.10). These results suggest that CCR2-dependent monocyte chemotaxis is likely to involve  $G\alpha_{i/o}$ -type G-proteins.

Taken together, these results suggest that THP-1 cell signalling and function are almost completely abolished by the  $G\alpha_{i/o}$  inhibitor, PTx. These data contribute to the existing knowledge that CCR2 signalling involves an activation  $G\alpha_{i/o}$ -type G-proteins in monocytes. Interestingly, these data also suggest that ATP and ADP evoke intracellular  $Ca^{2+}$  responses in THP-1 cells are PTx-insensitive and are unlikely to be mediated through the activation of  $G\alpha_{i/o}$ -type G-proteins.

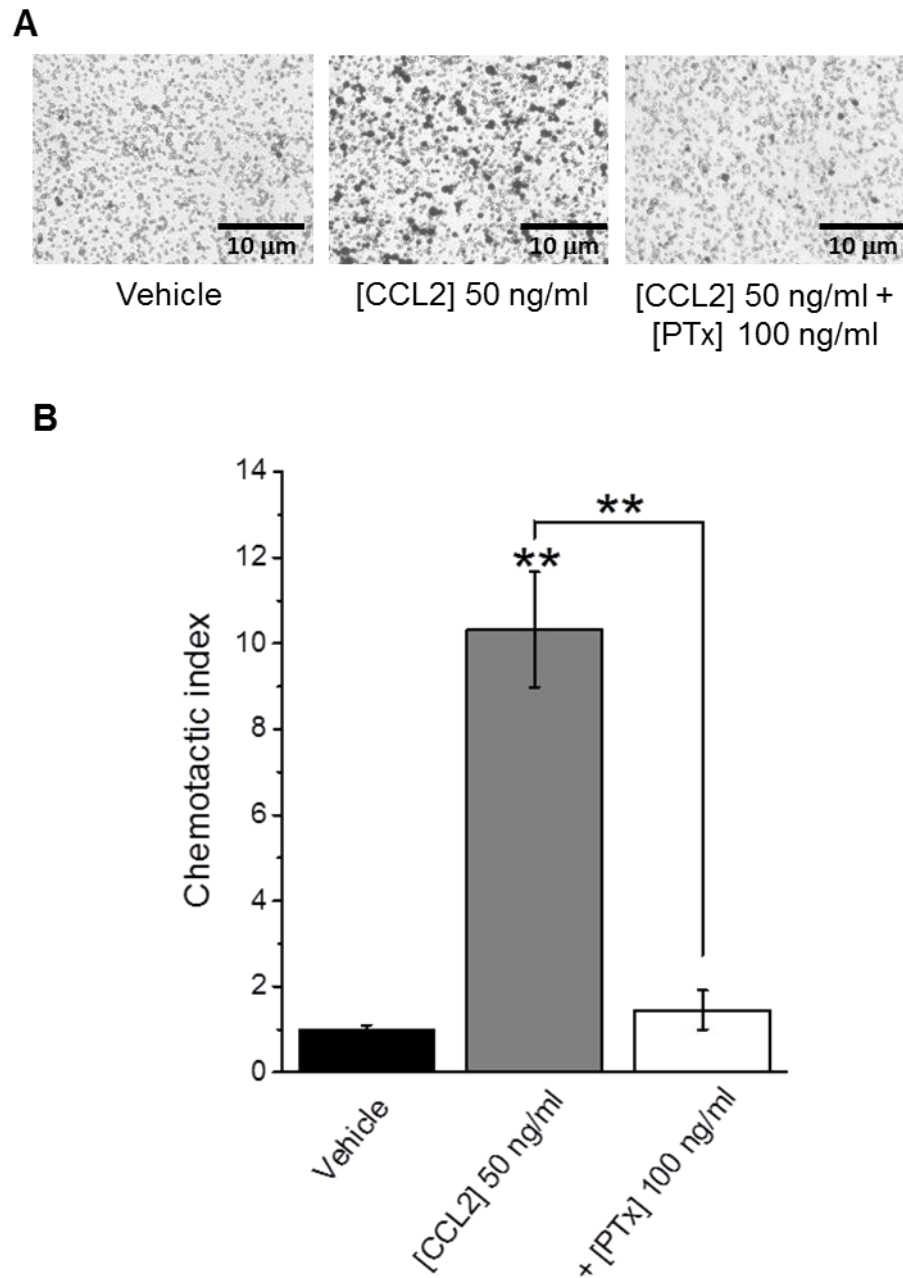


**Figure 4.10 Effect of PTx on CCL2-mediated THP-1 cell chemotaxis**

(A) Representative images showing the effect of PTx (100 ng/ml) on THP-1 cell chemotaxis towards CCL2 (50 ng/ml, lower chamber, 2 hours). Scale bar represents 10  $\mu$ m. (B) Bar chart showing normalised THP-1 cell chemotaxis towards vehicle (water) or CCL2 (50 ng/ml, lower chamber, 2 hours), with or without PTx (100 ng/ml) pre-treatment. Chemotactic index is a ratio of the number of cells that migrated towards CCL2 over the number of cells that migrated towards vehicle. Data represents mean  $\pm$  SEM from  $n=4$  transwells. Asterisks indicate significant changes towards vehicle (\*\* $p<0.01$ , One-way ANOVA with Bonferroni's multiple comparison).

#### 4.3.5 Effect of G $\beta\gamma$ inhibition on CCL2-mediated THP-1 cell chemotaxis

In the classical GPCR signalling paradigm, G $\alpha_{i/o}$ -type receptors activate PLC through their G $\beta\gamma$  dimers (Kadamur and Ross, 2013). It is possible, therefore, that CCR2 activation in monocytes involves an activation of effectors by G $\beta\gamma$ . Using THP-1 cells as a model, studies examined this hypothesis by employing gallein, a  $\beta\gamma$ -dimer inhibitor reported to bind reversibly with a high-affinity ( $K_d = 400$  nM) to the protein-protein interaction “hot spot” on the G $\beta\gamma$  subunit, rendering it inactive (Bonacci *et al.*, 2006).

Initial experiments examined the effects of gallein (100  $\mu$ M) on CCL2-evoked intracellular Ca<sup>2+</sup> responses in THP-1 cells. As shown (Figure 4.11), gallein quenched the fluorescent signal through interference with fluo-4 AM. To overcome this effect, a lower concentration of gallein (10  $\mu$ M) was tested, but was also seen to quench the fluorescent signal. Further Ca<sup>2+</sup> experiments with gallein were therefore not undertaken. On this basis, the next experiments focused on testing the effects of gallein (50  $\mu$ M) on THP-1 cell chemotaxis towards CCL2 (50 ng/ml).

As shown (Figure 4.27), THP-1 cells demonstrated a significantly higher ( $n=4$ ,  $p<0.01$ ) chemotactic index towards CCL2 ( $14 \pm 2$ ,  $n=4$ ), than towards vehicle ( $1 \pm 0.5$ ,  $n=4$ ). As also shown, gallein produced a significant inhibition of THP-1 cell migration towards CCL2 ( $65 \pm 2\%$ ,  $n=4$ ,  $p<0.01$ ), where the chemotactic indexes for vehicle and gallein-treated cells were  $14 \pm 2$  ( $n=4$ ) and  $5 \pm 0.2$  ( $n=4$ ), respectively. Although a possible explanation for this result may be that gallein affected cell viability, trypan blue and LDH studies (Appendix Figure A3 and A5) showed no significant loss after a 2.5 hour exposure of THP-1 cells with gallein. These data therefore suggest an association between  $\beta\gamma$  dimers and monocyte chemotaxis towards CCL2.

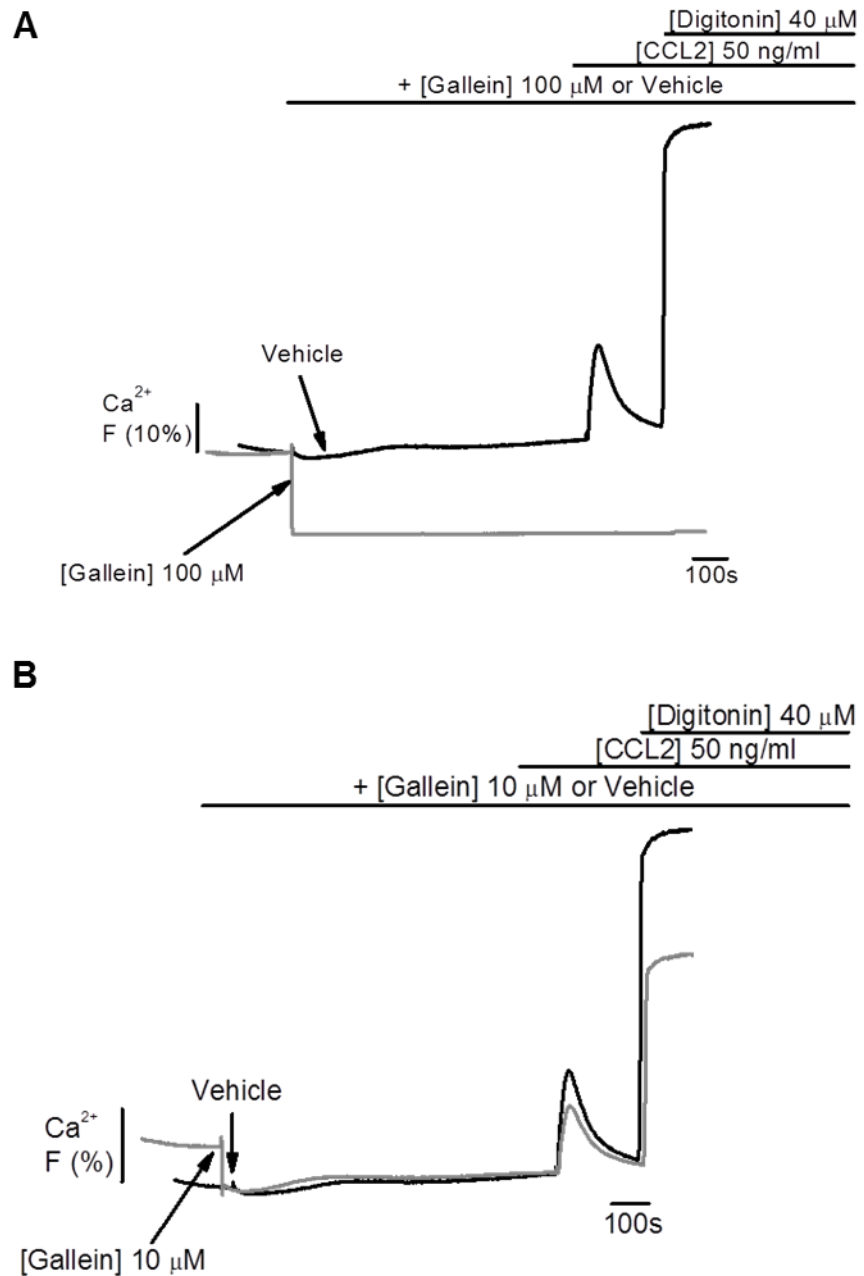


**Figure 4.11 Effect of gallein on fluo 4-AM Ca<sup>2+</sup> signal detection**

Representative traces showing effect of (A) 100  $\mu\text{M}$  and (B) 10  $\mu\text{M}$  gallein on Ca<sup>2+</sup> responses in THP-1 cells. Traces show pre-treatment of THP-1 cells for 15 minutes with gallein (10-100  $\mu\text{M}$ ) or vehicle (DMSO) prior to challenge with CCL2 (50 ng/ml) and application of 40  $\mu\text{M}$  digitonin to achieve %Fmax.

#### 4.3.6 Effect of PI3K inhibition on CCL2/CCR2-mediated THP-1 cell signalling and function

Classical GPCR signalling via the G $\beta\gamma$  subunit involves the activation of phospholipase C (PLC) (Smrcka, 2008). In recent years however, it has become apparent that the  $\beta\gamma$  dimer of G $\alpha_{i/o}$ -type G-proteins, also activates other downstream effectors such as PI3K (Krugmann *et al.*, 1999; Brock *et al.*, 2003).

The studies performed in this chapter suggest a requirement of G $\beta\gamma$  for CCL2/CCR2-mediated monocyte chemotaxis. Based on these results, it was hypothesised that CCR2 activation of G $\beta\gamma$  might lead to an activation of PI3K. To address this hypothesis, studies examined the effects of PI3K inhibition on CCL2/CCR2-mediated THP-1 cell Ca<sup>2+</sup> responses and chemotaxis. Studies employed LY-294002, a PI3K inhibitor reported to inhibit bovine brain PI3K activity with an IC<sub>50</sub> of 1.4  $\mu$ M (Vlahos *et al.*, 1994).

##### 4.3.6.1 Effect of LY-294002 on CCL2-evoked Ca<sup>2+</sup> responses in THP-1 cells

Initial experiments tested the effects of LY-294002 (5-50  $\mu$ M) on intracellular Ca<sup>2+</sup> responses evoked by 50 ng/ml CCL2. As shown (Figure 4.12a), application of LY-294002 to cells caused a small dip in baseline Ca<sup>2+</sup> (< 1%Fmax). A similar dip was also seen upon addition of 50  $\mu$ M LY-294002, but not upon addition of vehicle. This effect is difficult to explain, but suggests a modulation of Ca<sup>2+</sup> homeostasis by LY-294002 possibly through an inhibition of PI3K. As also shown (Figure 4.12b and c), LY-294002 attenuated CCL2-evoked intracellular Ca<sup>2+</sup> responses, producing a bell-shaped effect where the greatest inhibition was seen with 25  $\mu$ M LY-294002. However, with 5  $\mu$ M LY-294002 CCL2 Ca<sup>2+</sup> responses were not significantly affected, where the %Fmax values for CCL2 in untreated and LY-294002-treated cells were 22  $\pm$  3% (n=3) and 24  $\pm$  2% (n=3), respectively. In comparison, 25  $\mu$ M and 50  $\mu$ M LY-294002 attenuated CCL2-evoked intracellular Ca<sup>2+</sup> responses by 22  $\pm$  2% (n=3, p<0.05) and 12  $\pm$  2% (n=3, p<0.05), respectively. At 25  $\mu$ M, the %Fmax values for CCL2 in untreated and LY-294002-treated THP-1 cells were 27  $\pm$  1% (n=3) and 20  $\pm$  1% (n=3), respectively. For 50  $\mu$ M LY-294002, these values were 23  $\pm$  1 (n=3) and 20  $\pm$  1% (n=3), respectively, and suggested that 50  $\mu$ M LY-294002 impaired responses less than 25  $\mu$ M LY-294002.

A comparison of the  $\tau$  values suggested no significant differences between untreated and LY-294002-treated cells for any of the LY-294002 concentrations tested (n=3, p>0.05). For 5  $\mu$ M LY-294002, the  $\tau$  values for CCL2 in untreated and LY-294002-treated cells were 43  $\pm$  3 seconds (n=3) and 44  $\pm$  3 seconds (n=3), respectively, while for 25  $\mu$ M LY-294002 these were 62  $\pm$  2 seconds (n=3) and 75  $\pm$  6 seconds (n=3), respectively. Finally for 50  $\mu$ M LY-294002, the  $\tau$  values for CCL2 in untreated and LY-294002-treated cells were 49  $\pm$  5 seconds (n=3) and 57  $\pm$  8 seconds (n=3), respectively. These results

suggest that PI3K inhibition does not influence the decay of CCL2 Ca<sup>2+</sup> transients in THP-1 cells.

#### **4.3.6.2 Effect of LY-294002 on CCL2-mediated THP-1 cell chemotaxis**

To understand the requirement of PI3K for CCL2/CCR2-mediated monocyte chemotaxis, studies tested the effects of LY-294002 (25 µM) on THP-1 cell chemotaxis towards CCL2. As shown (Figure 4.27), THP-1 cells demonstrated a significantly higher (n=4, p<0.01) chemotactic index towards CCL2 ( $14 \pm 2$ , n=4) than towards vehicle ( $1 \pm 0.5$ , n=4). Interestingly, treatment with LY-294002 caused a significant inhibition of THP-1 cell chemotaxis towards CCL2 ( $53 \pm 4$  %, n=4, p<0.05), where the chemotactic index for LY-294002-treated cells was  $7 \pm 1$  (n=4). This result suggested a requirement of PI3K for THP-1 cell, and possibly, monocyte chemotaxis towards CCL2. This finding is supported by trypan blue and LDH cell viability studies (Appendix Figure A3 and A5), which showed no significant loss in THP-1 cell viability after 2.5 hours exposure with 25µM LY-294002.

Taken together, these results suggest that PI3K is required for efficient CCL2/CCR2-mediated monocyte signalling and function.

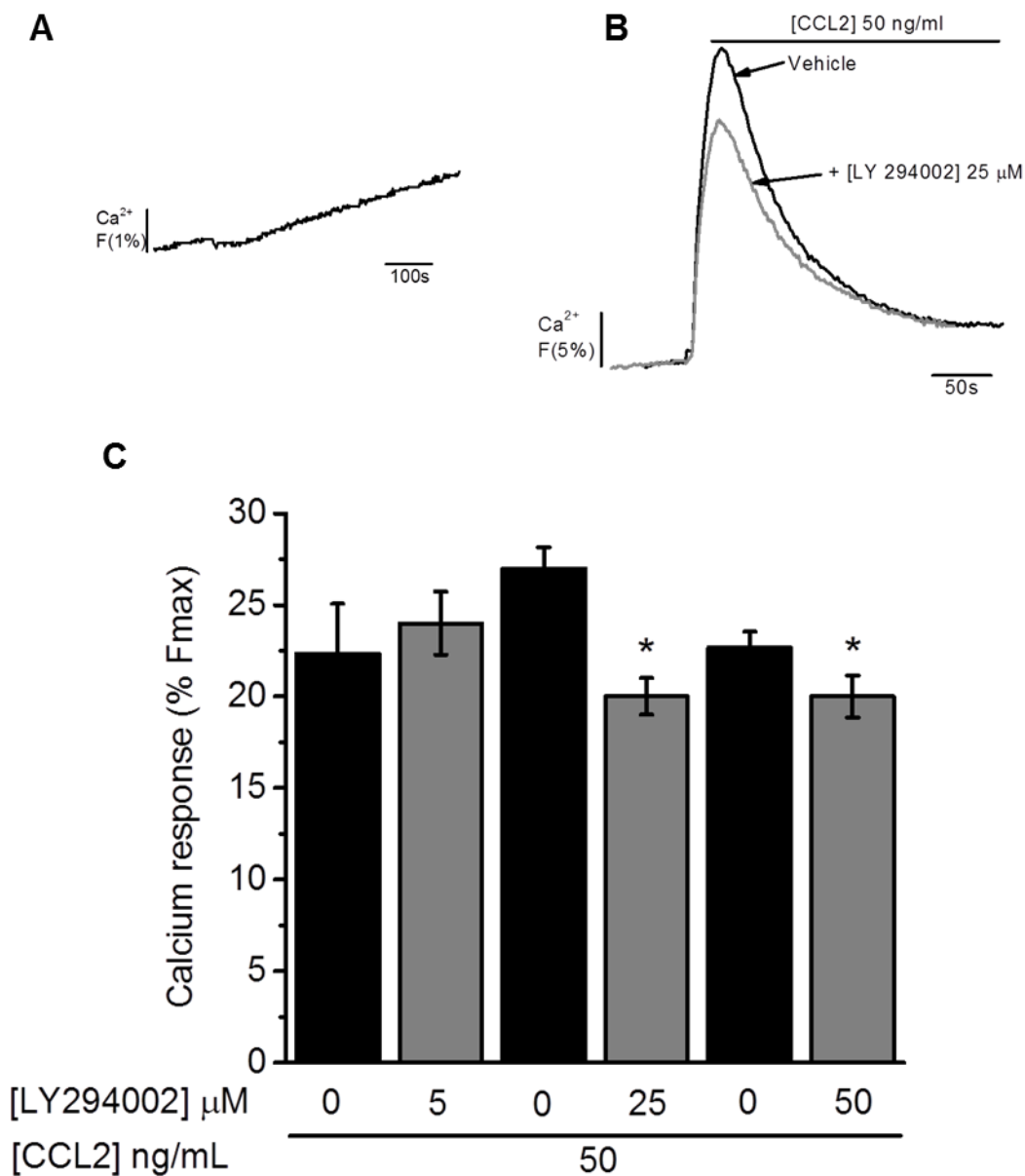


**Figure 4.12 Effect of LY-294002 on CCL2-evoked Ca<sup>2+</sup> responses in THP-1 cells**

(A) Representative trace showing the effect of 25 μM LY-294002 on baseline Ca<sup>2+</sup>. (B) Representative Ca<sup>2+</sup> transients to CCL2 (50 ng/ml) in THP-1 cells pre-treated with vehicle (DMSO) or LY-294002 (25 μM) for 15 minutes. (C) Bar chart showing normalised intracellular Ca<sup>2+</sup> responses to CCL2 (50 ng/ml) in THP-1 cells pre-treated with vehicle (DMSO) or LY-294002 (5-50 μM) for 15 minutes. Responses normalised to Ca<sup>2+</sup> signals elicited by 40 μM digitonin (%Fmax). Data represents mean ± SEM from n=3 replicates. Asterisks indicate significant changes towards vehicle (\*p<0.05, Student's t-test).

#### 4.3.7 Effect of PLC inhibition on CCL2/CCR2-mediated THP-1 cell signalling and function

One of the main effectors of G $\beta\gamma$  dimers of G $\alpha_{i/o}$ -type G-proteins are the PLC enzymes, a family of soluble enzymes that hydrolyse PIP<sub>2</sub> to yield DAG and IP<sub>3</sub> (Yang *et al.*, 2013) (Chapter 1). Although the activation of PLC isoenzymes (PLC $\beta$ , PLC $\epsilon$  and PLC $\eta$ ) by the G $\beta\gamma$  dimer has been widely accepted (Boyer *et al.*, 1992; Smrcka *et al.*, 1993; Hains *et al.*, 2006), studies showing an association between PLC activation and CCR2 are limited, and have only been performed in COS-7 cells, (simian fibroblast) (Kuang *et al.*, 1996). Moreover, in monocytes, a requirement of PLC for CCL2-mediated monocyte trafficking has not yet been shown.

To address this gap in knowledge, studies examined the requirement of PLC for CCL2/CCR2-mediated monocyte signalling and function, employing THP-1 cells as an *in vitro* model. Studies also employed the pan-PLC inhibitor, U-73122 which has a reported IC<sub>50</sub> of 1-5  $\mu$ M against PLC-dependent platelet activation (Bleasdale *et al.*, 1990).

##### 4.3.7.1 Effect of U-73122 on CCL2-evoked Ca<sup>2+</sup> responses in THP-1 cells

The effects of U-73122 (0.25-5  $\mu$ M) on intracellular Ca<sup>2+</sup> responses evoked by CCL2 (50 ng/ml) in THP-1 cells were examined in the presence and absence of extracellular Ca<sup>2+</sup>. The purpose of Ca<sup>2+</sup>-free experiments was to investigate the requirement of PLC specifically for store-operated intracellular Ca<sup>2+</sup> release.

As shown (Figure 4.13a), application of U-73122 to cells in the presence of extracellular Ca<sup>2+</sup> caused a small dip in baseline Ca<sup>2+</sup>, where the %Fmax responses for dips given by 0.25  $\mu$ M and 5  $\mu$ M U-73122 were  $-2.7 \pm 0.3\%$  (n=3) and  $-4 \pm 0.4\%$  (n=3), respectively. A similar effect was not observed with vehicle or in the absence of extracellular Ca<sup>2+</sup>, suggesting that this effect was attributed to a modulation of Ca<sup>2+</sup> homeostasis by U-73122 connected to its inhibition of PLC. As also shown (Figure 4.13b and c), U-73122 caused a concentration-dependent inhibition of CCL2-evoked intracellular Ca<sup>2+</sup> responses, where the % inhibition values for 0.25  $\mu$ M and 5  $\mu$ M U-73122 were  $68 \pm 7\%$  (n=3, p<0.05) and  $100 \pm 0\%$  (n=4, p<0.01), respectively. For 0.25  $\mu$ M, the %Fmax values for CCL2 in untreated and U73122-treated THP-1 cells were  $26 \pm 1\%$  (n=3) and  $8 \pm 2\%$  (n=3), respectively. In comparison, for experiments with 5  $\mu$ M U-73122, the %Fmax values for CCL2 in untreated and U-73122-treated THP-1 cells were  $22 \pm 1\%$  (n=4) and  $0 \pm 0\%$  (n=4), respectively. These data suggest that PLC activation is required for CCL2/CCR2-mediated THP-1 cell signalling.

A comparison of the decay kinetics for vehicle and 0.25  $\mu$ M U-73122-treated cells was also made, but did not reveal any significant shifts (n=3, p>0.05) between the  $\tau$  values for

untreated ( $66 \pm 2$  seconds,  $n=3$ ) and U-73122-treated THP-1 cells ( $68 \pm 7$  seconds,  $n=3$ ). This data suggests that PLC inhibition does not affect the decay of CCL2  $\text{Ca}^{2+}$  transients.

Experiments performed in SBS from which extracellular  $\text{Ca}^{2+}$  (1.5 mM  $\text{CaCl}_2$ ) was replaced with the calcium chelator EGTA (1 mM) (Chapter 2, Section 2.6.2), showed that 5  $\mu\text{M}$  U-73122 abolished CCL2-evoked intracellular  $\text{Ca}^{2+}$  responses ( $100 \pm 0\%$ ,  $n=3$ ,  $p<0.05$ ) (Figure 4.13d and e), where the %Fmax responses for CCL2 in untreated and U-73122-treated cells were  $10 \pm 2\%$  ( $n=3$ ) and  $0 \pm 0\%$  ( $n=3$ ), respectively. Due to no  $\text{Ca}^{2+}$  response in the presence of U-73122, the decay rates ( $\tau$ , sec) could not be determined.

#### **4.3.7.2 Effect of U-73122 on CCL2-mediated THP-1 cell chemotaxis**

Studies next sought to investigate the requirement of PLC for monocyte chemotaxis towards CCL2, using THP-1 cells as an in vitro model. As shown (Figure 4.27), U-73122 treatment (5  $\mu\text{M}$ ) significantly impaired THP-1 cell chemotaxis towards CCL2 by  $76 \pm 10\%$  ( $n=4$ ,  $p<0.01$ ), where the chemotactic indexes for untreated and U-73122-treated cells were  $14 \pm 2$  ( $n=4$ ) and  $3 \pm 1$  ( $n=4$ ), respectively. Although these data supported a possible role for PLC in CCL2/CCR2-mediated monocyte chemotaxis, some caution may need to be applied in interpreting these results since LDH release studies showed that THP-1 cells exposed for 2.5 hours with 5  $\mu\text{M}$  U-73122 released LDH at % control levels (% of Triton-X) above the 20% threshold (36%,  $n=1$ ) (Appendix Figure A3). Cell toxicity however, was not observed in trypan blue assays ( $n=3$ ,  $p>0.05$ ) (Appendix Figure A5), where the % viable cells for untreated and treated wells were  $100 \pm 15\%$  ( $n=3$ ) and  $82 \pm 6\%$  ( $n=3$ ), respectively. Given that data obtained in LDH assays reflected a 2.5 hour exposure rather than a 2 hour exposure, and are only  $n=1$ , firm conclusions about the effect of U-73122 on THP-1 cell viability in chemotaxis and intracellular  $\text{Ca}^{2+}$  experiments may not be drawn.

Taken together, these results suggest that PLC is required for efficient CCL2/CCR2-mediated monocyte signalling and function.

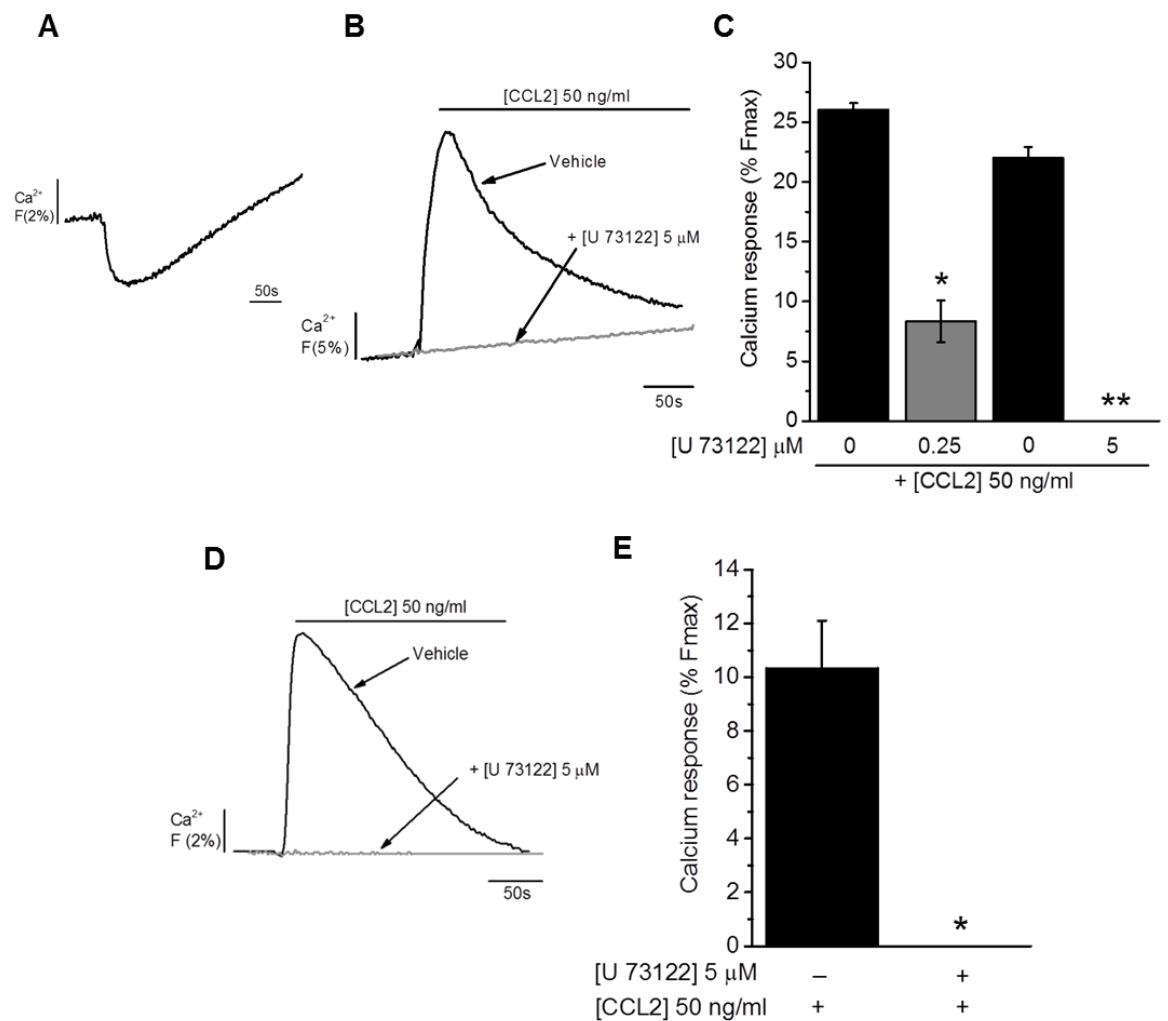


**Figure 4.13 Effect of U-73122 on CCL2-evoked  $\text{Ca}^{2+}$  responses in THP-1 cells**

(A) Representative trace showing the effect of 5  $\mu\text{M}$  U-73122 on baseline  $\text{Ca}^{2+}$ . (B) Representative  $\text{Ca}^{2+}$  transients and (C) normalised bar chart showing intracellular  $\text{Ca}^{2+}$  responses to CCL2 (50 ng/ml) in THP-1 cells pre-treated with vehicle (DMSO) or U-73122 (0.25-5  $\mu\text{M}$ ) for 15 minutes. Experiments performed in the presence of extracellular  $\text{Ca}^{2+}$  (1.5 mM  $\text{CaCl}_2$ ) where data represents mean  $\pm$  SEM from  $n=3$  (0.25  $\mu\text{M}$ ) or  $n=4$  (5  $\mu\text{M}$ ) replicates. (D) Representative  $\text{Ca}^{2+}$  transients and (E) normalised bar chart showing intracellular  $\text{Ca}^{2+}$  responses to CCL2 (50 ng/ml) in THP-1 cells pre-treated with vehicle (DMSO) or U-73122 (5  $\mu\text{M}$ ) for 15 minutes. Experiments performed in the absence of extracellular  $\text{Ca}^{2+}$ , where data represents mean  $\pm$  SEM from  $n=3$  replicates. Responses normalised to  $\text{Ca}^{2+}$  signals elicited by 40  $\mu\text{M}$  digitonin (% Fmax). Asterisks indicate significant changes towards vehicle (\*\* $p<0.01$ , \* $p<0.05$ , Students t-test).

#### 4.3.8 Effect of IP<sub>3</sub>R inhibition on CCL2/CCR2-mediated THP-1 cell signalling and function

The release of Ca<sup>2+</sup> from the ER into the cellular cytoplasm is a major pathway for the supply of intracellular Ca<sup>2+</sup> (Clapham, 2007). The inositol 1,4,5-trisphosphate receptors (IP<sub>3</sub>Rs), ryanodine receptors (RyRs), and Ca<sup>2+</sup> are the primary inducers of Ca<sup>2+</sup> release from the ER and/or Golgi apparatus (GA) (Chandra *et al.*, 1991; Pinton *et al.*, 1998). Of these, IP<sub>3</sub>Rs constitute the major mechanism by which GPCRs induce intracellular Ca<sup>2+</sup> release (Chapter 1) (Clapham, 2007; Vetter, 2012).

The IP<sub>3</sub>Rs are intracellular Ca<sup>2+</sup> channels encoded by three different genes which give rise to IP<sub>3</sub>R1 (splice variants S1, S2 and S3), IP<sub>3</sub>R2, and IP<sub>3</sub>R3 (Patel *et al.*, 1999). Although structurally similar, all IP<sub>3</sub>Rs possess differential binding affinities to IP<sub>3</sub> courtesy of structural differences in the N-terminal region that acts as a suppressor of IP<sub>3</sub> binding (Iwai *et al.*, 2007). Although IP<sub>3</sub>Rs can be modulated by over 50 different proteins including protein kinase A (PKA) and protein kinase C (PKC) (Berridge *et al.*, 2003; Parys and De Smedt, 2012), the primary activators of these receptors are the essential co-agonists IP<sub>3</sub> and Ca<sup>2+</sup> (Finch *et al.*, 1991; Dupont and Goldbeter, 1993).

The evidence presented has suggested that CCL2/CCR2 activation is associated with a release of intracellular Ca<sup>2+</sup> via an activation of PLC. It is possible, therefore, that intracellular Ca<sup>2+</sup> released via PLC involves an activation of IP<sub>3</sub>Rs located on ER and GA. To address this hypothesis and assess the requirement of IP<sub>3</sub>Rs for efficient CCL2/CCR2-mediated monocyte signalling and function, THP-1 cells were employed as an *in vitro* model along with the pan-IP<sub>3</sub>R inhibitor Xestospongine-C (XeC). As a macrocyclic bis-1-oxaquinolizidine isolated from the Australian sponge, *Xestospongia*, XeC has a reported IC<sub>50</sub> against IP<sub>3</sub>R of 358 nM (Gafni *et al.*, 1997)

##### 4.3.8.1 Effect of XeC on CCL2-evoked Ca<sup>2+</sup> responses in THP-1 cells

Experiments examined the effects of XeC (5 µM) on 50 ng/ml CCL2-evoked intracellular Ca<sup>2+</sup> responses in THP-1 cells. As shown (Figure 4.14a and b), XeC caused a significant inhibition of CCL2-evoked intracellular Ca<sup>2+</sup> responses (30 ± 3%, n=3, p<0.05), where the %Fmax values for CCL2 in untreated and XeC-treated cells were 22 ± 1 % (n=3) and 15 ± 1% (n=3), respectively. These data were interesting because they suggested that IP<sub>3</sub>R are required for CCL2 Ca<sup>2+</sup> responses in monocytes.

An analysis of the decay rates of Ca<sup>2+</sup> transients showed that XeC significantly increased the τ value for CCL2 in treated cells by 43 ± 8% (n=3, p<0.05), where τ for CCL2 shifted from 69 ± 10 seconds (n=3) for untreated cells to 98 ± 15 seconds (n=3) for XeC-treated

cells (Figure 4.14c). These data suggested that IP<sub>3</sub>R inhibition slowed the decay of CCL2 Ca<sup>2+</sup> transients.

To examine the requirement for IP<sub>3</sub>R in CCL2/CCR2 signalling further, experiments were designed to test the effects of XeC in the absence of extracellular Ca<sup>2+</sup>. However, pilot experiments suggested that THP-1 cells were unable to retain a signal to fluo-4 AM over 30 minutes as was required for XeC (data not shown).

#### **4.3.8.2 Effect of XeC on CCL2-mediated THP-1 cell chemotaxis**

To understand the requirement of IP<sub>3</sub>R for CCL2/CCR2-mediated monocyte chemotaxis, studies examined the effects of XeC (5 µM) on THP-1 cell chemotaxis towards 50 ng/ml CCL2. As shown (Figure 4.15), THP-1 cells displayed a significantly higher (n=4, p<0.01) chemotactic index towards CCL2 (6 ± 0.7, n=4) than towards vehicle (1 ± 0.3, n=4). Interestingly, treatment with XeC significantly attenuated THP-1 cell chemotaxis towards CCL2 by 73 ± 10% (n=4, p<0.01), where the chemotactic indexes for untreated and XeC-treated cells were 6 ± 1 (n=4) and 1.4 ± 0.4 (n=4) respectively. Although it may be that these results are biased due to XeC-mediated cytotoxicity, trypan blue and LDH studies were not able to provide any evidence of this (Appendix Figure A3 and A5). This result suggests that XeC attenuates CCL2-mediated THP-1 cell chemotaxis through an inhibition of IP<sub>3</sub>Rs.

The results of this study suggested that XeC significantly inhibited the magnitude and decay of CCL2-evoked intracellular Ca<sup>2+</sup> responses in THP-1 cells. Moreover, it was seen that XeC treatment also attenuated THP-1 cell chemotaxis towards CCL2. Taken together, these results suggest that IP<sub>3</sub>Rs are required for CCL2/CCR2-mediated monocyte signalling and function.

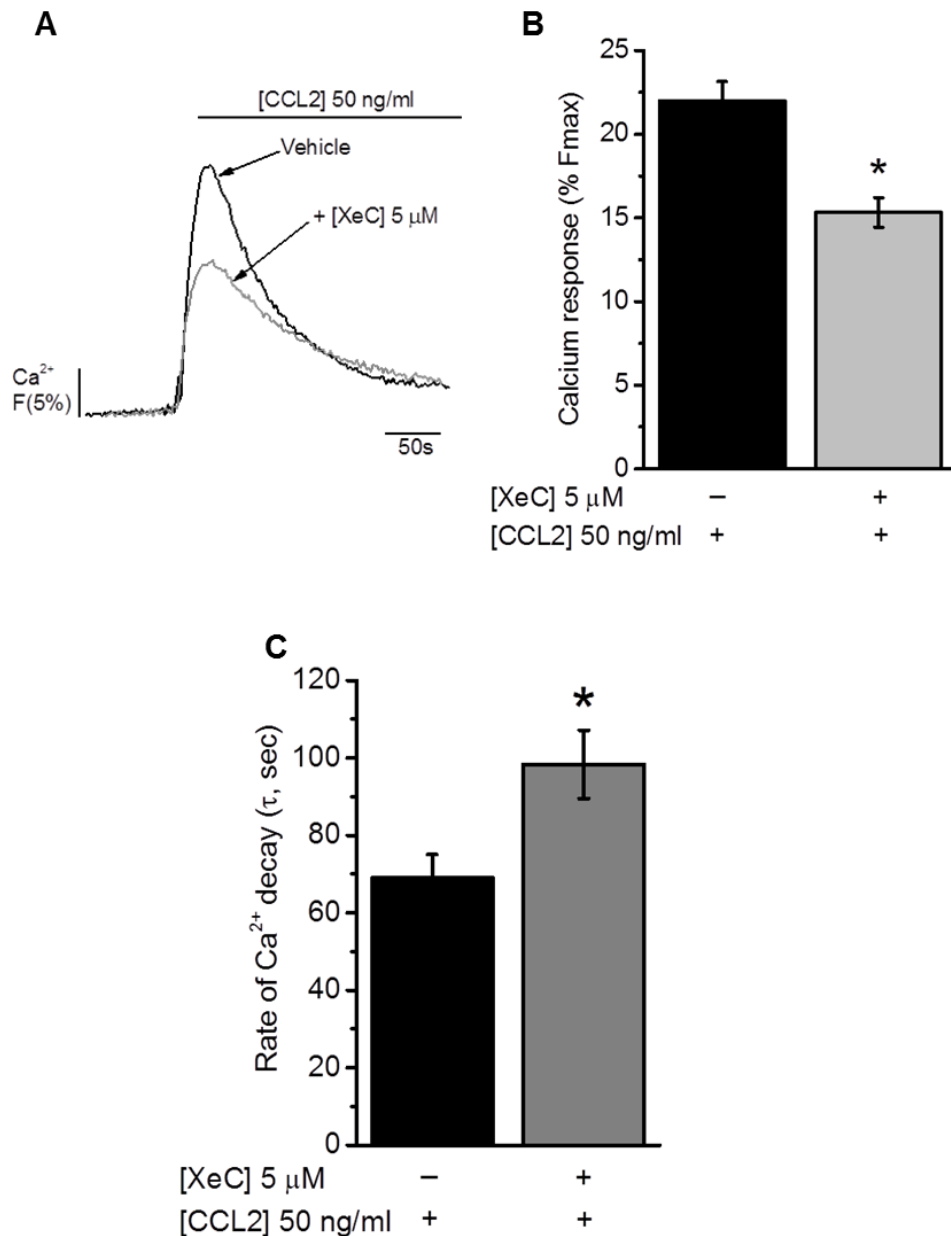


**Figure 4.14 Effect of XeC on CCL2-evoked Ca<sup>2+</sup> responses in THP-1 cells**

(A) Representative Ca<sup>2+</sup> transients to CCL2 (50 ng/ml) in THP-1 cells pre-treated with vehicle (DMSO) or XeC (5  $\mu$ M) for 30 minutes. (B) Bar chart showing normalised intracellular Ca<sup>2+</sup> responses to CCL2 (50 ng/ml) in THP-1 cells pre-treated with vehicle (DMSO) or XeC (5  $\mu$ M), for 30 minutes. (C) Bar chart showing decay rates ( $\tau$ , sec) for CCL2 (50 ng/ml) Ca<sup>2+</sup> transients in THP-1 cells pre-treated with vehicle (DMSO) or XeC (5  $\mu$ M), for 30 minutes. Responses normalised to Ca<sup>2+</sup> signals elicited by 40  $\mu$ M digitonin (% Fmax). Data represents mean  $\pm$  SEM from n=3 replicates. Asterisks indicate significant changes towards vehicle (\*p<0.05, Students t-test).

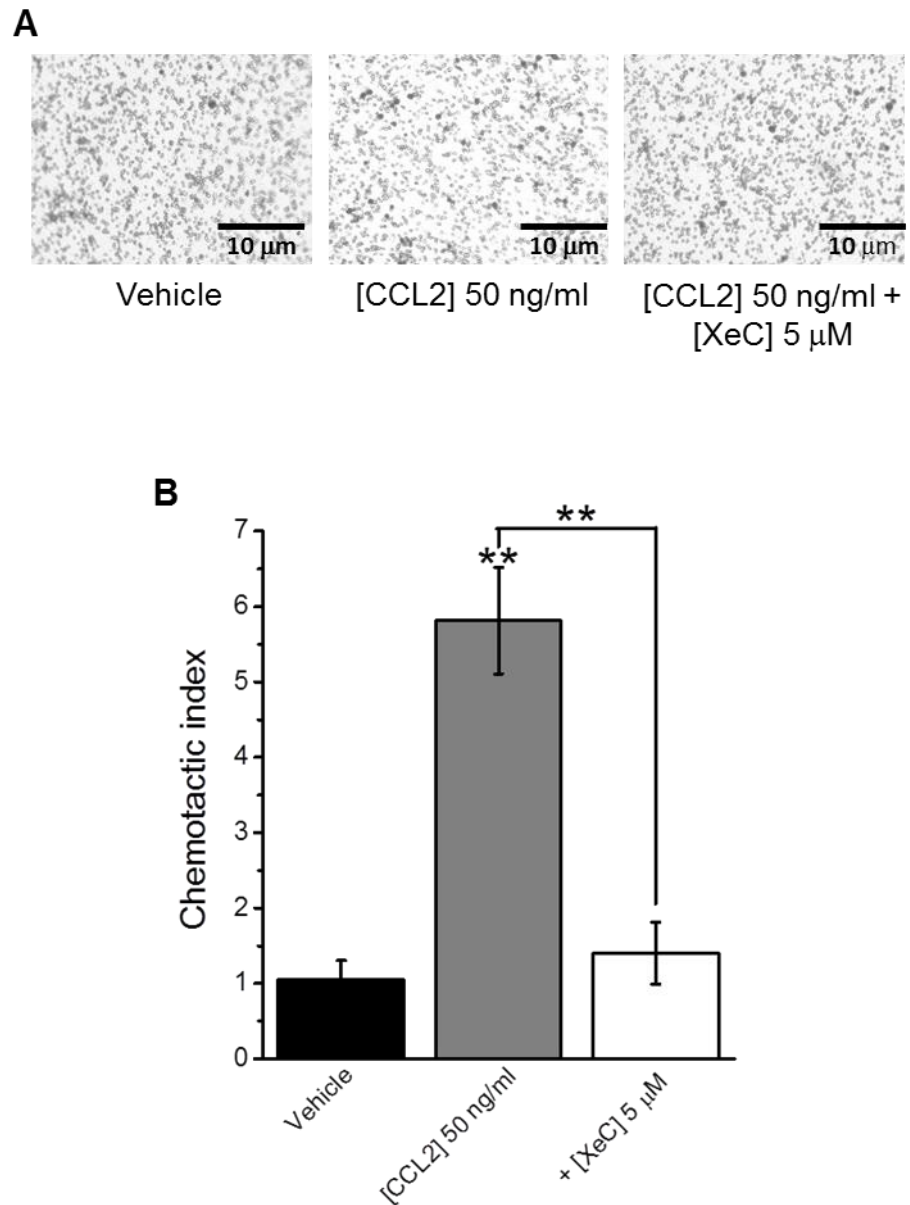


**Figure 4.15 Effect of XeC on CCL2-mediated THP-1 cell chemotaxis**

(A) Representative images showing the effect of XeC (5 μ M; 30 minutes) on CCL2-mediated THP-1 chemotaxis (50 ng/ml, lower chamber, 2 hours). Scale bar represents 10 μm. (B) Bar chart showing normalised THP-1 cell chemotaxis towards vehicle (water) or CCL2 (50 ng/ml, lower chamber, 2 hours) following 30 minute pre-treatment of cells with vehicle (DMSO), or XeC (5 μM). Chemotactic index is a ratio of the number of cells that migrated towards CCL2 over the number of cells that migrated towards vehicle. Data represents mean ± SEM from n=4 transwells. Asterisks indicate significant changes towards vehicle (\*\*p<0.01, One-way ANOVA with Bonferroni's multiple comparison).

#### **4.3.9 Effect of RyR inhibition on CCL2/CCR2-mediated THP-1 cell signalling and function**

The ryanodine receptors (RyR) are a family of large (>2.2 MDa) homotetrameric Ca<sup>2+</sup> ion channels located within the ER membrane (Van Petegem, 2012). Identified by their activation by the plant alkaloid ryanodine, the RyR family comprises of three isoforms in humans (RyR1, RyR2 and RyR3), with each receptor displaying differential expression patterns in cells and tissues (Lanner *et al.*, 2010). Although RyR activity can be modulated by a number of mechanisms including Protein kinase A and L-type Ca<sup>2+</sup> channels (Lanner *et al.*, 2010; Van Petegem, 2012), the principle agonist is Ca<sup>2+</sup>, which activates RyRs by a mechanism known as Ca<sup>2+</sup>-induced-Ca<sup>2+</sup>-release (CICR) (Berridge *et al.*, 2000).

The data presented in this chapter suggests that IP<sub>3</sub>R activation is required for efficient CCL2/CCR2-mediated monocyte signalling and function. This suggests that RyRs might also be involved. To examine this hypothesis, studies used THP-1 cells as an *in vitro* model to investigate the effects of the RyR inhibitor dantrolene, on CCL2/CCR2-mediated intracellular Ca<sup>2+</sup> responses and chemotaxis. As a RyR inhibitor, dantrolene is reported to primarily target RyR1 but also has an affinity for RyR3 (Zhao *et al.*, 2001). Used therapeutically as a postsynaptic muscle relaxant, the therapeutic concentration of dantrolene is reported to be 10 µM (Flewellen *et al.*, 1983).

##### **4.3.9.1 Effect of dantrolene on CCL2-evoked Ca<sup>2+</sup> responses in THP-1 cells**

To examine the requirement of RyR, studies investigated the effects of dantrolene (20 µM) on intracellular Ca<sup>2+</sup> responses evoked by 50 and 10 ng/ml CCL2.

As shown below in Table 4.1, no significant effects of dantrolene were observed on either 50 ng/ml (n=3, p>0.05), or 10 ng/ml CCL2 (n=3, p>0.05). The τ values of 50 ng/ml and 10 ng/ml CCL2 Ca<sup>2+</sup> transients in untreated and dantrolene-treated cells were also not significantly different (n=3, p>0.05). For 50 ng/ml CCL2, the τ values for untreated and dantrolene-treated cells were 57 ± 2 seconds (n=3) and 58 ± 1 seconds (n=3), while for 10 ng/ml CCL2 these were 98 ± 7 seconds (n=3), and 99 ± 18 seconds (n=3). These results suggest that the magnitude and decay of CCL2 Ca<sup>2+</sup> transients are not significantly affected by dantrolene. Therefore, RyRs are unlikely to be involved in CCL2-mediated Ca<sup>2+</sup> responses.

**Table 4.1 Effect of dantrolene on CCL2-evoked Ca<sup>2+</sup> responses in THP-1 cells**

Ligand	Ca <sup>2+</sup> response (%Fmax)	
	Vehicle	20 µM Dantrolene
CCL2 50 ng/ml	23 ± 0%	23 ± 0.5
CCL2 10 ng/ml	5 ± 0.3%	5 ± 0.9%

Intracellular Ca<sup>2+</sup> responses to CCL2 in THP-1 cells pre-treated with vehicle (DMSO) or dantrolene for 15 minutes. Responses normalised to maximum Ca<sup>2+</sup> signals elicited by 40 µM digitonin (%Fmax). Data represents mean ± SEM from n=3 replicates.

#### 4.3.9.2 Effect of dantrolene on CCL2-mediated THP-1 cell chemotaxis

To investigate whether RyRs contributed to monocyte trafficking, transwell experiments were designed to test the effects of dantrolene (20 µM) on THP-1 cell chemotaxis towards CCL2. As shown (Figure 4.27), THP-1 cells demonstrated a significantly higher (n=4, p<0.01) chemotactic index towards CCL2 (14 ± 2, n=4), than towards vehicle (1 ± 0.5, n=4). As can also be seen, dantrolene significantly attenuated THP-1 cell chemotaxis towards CCL2 by 40 ± 4% (n=4, p=<0.05), where the chemotactic indexes shifted from 14 ± 2 (n=4) for untreated cells to 8 ± 1 (n=4) for dantrolene-treated cells. This data suggests that RyRs are required for CCL2/CCR2-mediated monocyte trafficking.

These results showed that CCL2/CCR2-mediated THP-1 chemotaxis, but not intracellular Ca<sup>2+</sup> release, was attenuated by 20 µM dantrolene. Based on these data, RyRs are unlikely to play a role in CCL2/CCR2-mediated monocyte signalling but may play a role in their function.

#### 4.3.10 Effect of SERCA inhibition on CCL2/CCR2-mediated THP-1 cell signalling and function

The sarco(endo)plasmic reticulum ATPase (SERCA) pump is a high-affinity 110-kDA transmembrane Ca<sup>2+</sup> transporter located in the ER membrane. In addition to a role in regulating [Ca<sup>2+</sup>]<sub>i</sub> levels in the cytoplasm, SERCA is also crucial for replenishing ER stores following a depletion caused by agonist activation or leakage (Chapter 1).

The next aim of this chapter was to investigate the requirement of SERCA activation for CCL2/CCR2-mediated monocyte signalling and function. The evidence presented in this chapter has indicated a requirement of the ER for efficient CCL2/CCR2-mediated signalling and function. It was therefore hypothesised that SERCA pumps located on the membrane of the ER would replenish the ER following CCL2-mediated depletion.

Studies therefore sought to examine this hypothesis using THP-1 cells as a model and the pan-SERCA inhibitor thapsigargin; a sesquiterpene lactone derived from the plant *Thapsia garganica* L. (Linnaeus) (Thastrup *et al.*, 1990). Mechanistically, thapsigargin binds to the transmembrane domain of SERCA while it is in a low  $\text{Ca}^{2+}$ -affinity state (Wuytack *et al.*, 2002). The  $\text{IC}_{50}$  of thapsigargin varies depending on the test model used as well as the conformational state of the receptor, and although it is reported to be between 5-50 nM, it can also be as high at 4  $\mu\text{M}$  (Sagara and Inesi, 1991; Treiman *et al.*, 1998).

#### 4.3.10.1 Effect of thapsigargin on CCL2-evoked $\text{Ca}^{2+}$ responses in THP-1 cells

Initial experiments investigated the effects of thapsigargin (300 nM and 5  $\mu\text{M}$ ) on 50 ng/ml CCL2-evoked intracellular  $\text{Ca}^{2+}$  responses in THP-1 cells. As shown (Figure 4.16a), thapsigargin produced an intracellular  $\text{Ca}^{2+}$  response, where the %Fmax values for 300 nM and 5  $\mu\text{M}$  thapsigargin were  $46 \pm 1\%$  (n=3) and  $36 \pm 3\%$  (n=3), respectively. This effect suggests that SERCA impairment leads to a spontaneous leakage of  $\text{Ca}^{2+}$  from the ER. As also shown (Figure 4.16b and c), 300 nM and 5  $\mu\text{M}$  thapsigargin attenuated CCL2-evoked intracellular  $\text{Ca}^{2+}$  responses with % inhibition values of  $73 \pm 5\%$  (n=3,  $p < 0.05$ ) and  $82 \pm 2\%$  (n=3,  $p < 0.05$ ), respectively. For experiments with 300 nM thapsigargin, the %Fmax values for CCL2 in untreated and thapsigargin-treated cells were  $28 \pm 3\%$  (n=3) and  $5 \pm 0\%$  (n=3), respectively. In comparison, in experiments with 5  $\mu\text{M}$  thapsigargin, the %Fmax values for CCL2 in untreated and thapsigargin-treated cells were  $19 \pm 2\%$  (n=3) and  $5 \pm 1\%$  (n=3), respectively. These results suggested that SERCA inhibition suppressed the magnitude of CCL2-evoked intracellular  $\text{Ca}^{2+}$  responses. Although it was also useful to determine whether SERCA impairment affected the response decay, the lack of decay of  $\text{Ca}^{2+}$  transients in treated cells prevented the  $\tau$  values from being determined.

In further experiments performed in the absence of extracellular  $\text{Ca}^{2+}$  where 1.5 mM  $\text{CaCl}_2$  was omitted from SBS and replaced with 1 mM of the  $\text{Ca}^{2+}$  chelator EGTA, it was seen that both concentrations (300 nM and 5  $\mu\text{M}$ ) of thapsigargin abolished CCL2-evoked intracellular  $\text{Ca}^{2+}$  responses, giving % inhibition values of  $100 \pm 0\%$  (n=3,  $p < 0.05$ ) and  $100 \pm 0\%$  (n=3,  $p < 0.01$ ), respectively (Figure 4.17). For experiments with 300 nM thapsigargin, the %Fmax values for CCL2 in untreated and thapsigargin-treated cells were  $7 \pm 1\%$  (n=3) and  $0 \pm 0\%$  (n=3), respectively, whereas for 5  $\mu\text{M}$  experiments they were  $12 \pm 0.3\%$  (n=3) and  $0 \pm 0$  (n=3), respectively. These data support evidence from experiments in the presence of extracellular  $\text{Ca}^{2+}$ , and suggest that SERCA activation is essential for intracellular  $\text{Ca}^{2+}$  release in the absence of extracellular  $\text{Ca}^{2+}$ .

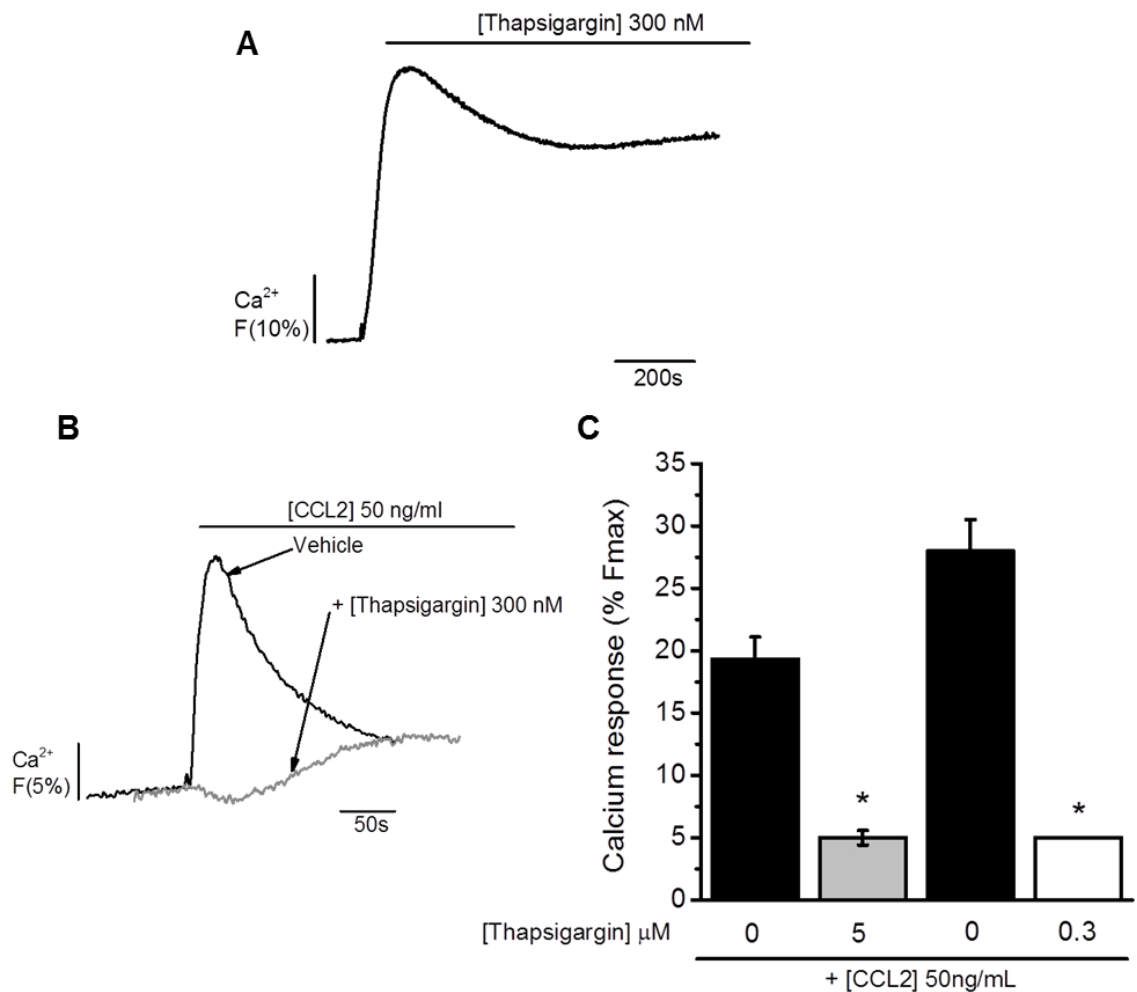


**Figure 4.16 Effect of thapsigargin on CCL2-evoked Ca<sup>2+</sup> responses in THP-1 cells**

(A) Representative trace showing the effect of thapsigargin (300 nM) on baseline Ca<sup>2+</sup>. (B) Representative Ca<sup>2+</sup> transients to CCL2 (50 ng/ml) in THP-1 cells pre-treated with vehicle (DMSO) or thapsigargin (300 nM) for 15 minutes. (C) Bar chart showing normalised intracellular Ca<sup>2+</sup> responses to CCL2 (50 ng/ml) in THP-1 cells pre-treated with vehicle (DMSO) or thapsigargin (5 μM or 300 nM), for 15 minutes. Responses normalised to Ca<sup>2+</sup> signals elicited by 40 μM digitonin (% Fmax). Data represents mean ± SEM from n=3 replicates. Asterisks indicate significant changes towards vehicle (\*p<0.05, Students t-test).

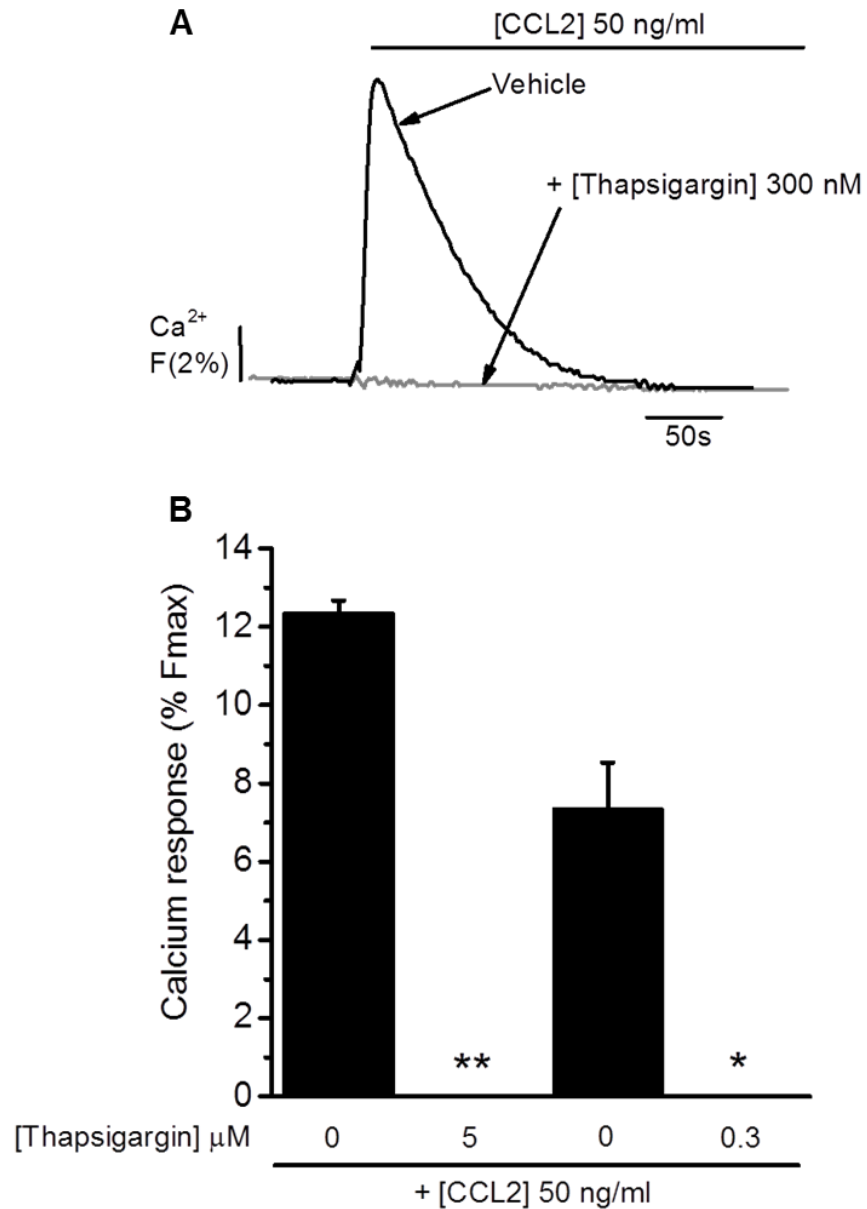


**Figure 4.17 Effect of thapsigargin on CCL2-evoked Ca<sup>2+</sup> responses in THP-1 cells in the absence of extracellular Ca<sup>2+</sup>**

(A) Representative Ca<sup>2+</sup> transients to CCL2 (50 ng/ml) in THP-1 cells pre-treated with vehicle (DMSO) or thapsigargin (300 nM) for 15 minutes. (B) Bar chart showing normalised intracellular Ca<sup>2+</sup> responses to CCL2 (50 ng/ml) in THP-1 cells pre-treated with vehicle (DMSO) or thapsigargin (5 μM or 300 nM), for 15 minutes. Responses normalised to Ca<sup>2+</sup> signals elicited by 40 μM digitonin (% Fmax). Data represents mean ± SEM from n=3 replicates. Asterisks indicate significant changes towards vehicle (\*p<0.05, \*\*p<0.01 Students t-test).

#### 4.3.10.2 Effect of thapsigargin on CCL2-mediated THP-1 cell chemotaxis

It was next important to investigate the requirement of SERCA for monocyte function. Using THP-1 cells as a model, studies tested the effects of thapsigargin (5  $\mu$ M) on cellular chemotaxis towards 50 ng/ml CCL2. As shown (Figure 4.18), THP-1 cells demonstrated a significantly higher ( $n=4$ ,  $p<0.01$ ) chemotactic index towards CCL2 ( $11 \pm 1$ ,  $n=4$ ) than towards vehicle ( $1 \pm 0.2$ ,  $n=4$ ). As also shown, treatment of cells with thapsigargin attenuated CCL2-mediated chemotaxis by  $48 \pm 10\%$  ( $n=4$ ,  $p<0.01$ ), where the chemotactic indexes for untreated and thapsigargin-treated cells were  $11 \pm 3$  ( $n=3$ ) and  $6 \pm 1$  ( $n=3$ ), respectively. Although these results were positive and suggested a requirement for SERCA in monocyte function, data from LDH cell viability studies suggested that THP-1 cells released LDH (21% of Triton-X,  $n=1$ ) after 2.5 hours exposure. However, this result is only an  $n=1$  and was not supported by the results of trypan blue studies which showed that the % of viable cells in vehicle-treated ( $100 \pm 15\%$ ,  $n=3$ ) and 5  $\mu$ M thapsigargin-treated wells ( $88 \pm 7\%$ ,  $n=3$ ) were not significantly different ( $n=3$ ,  $p>0.05$ ) (Appendix Figure A3 and A5). Thus, further studies are required to confirm this finding.

In summary, these results suggest that SERCA activity is required for efficient CCL2/CCR2-mediated monocyte signalling and function.

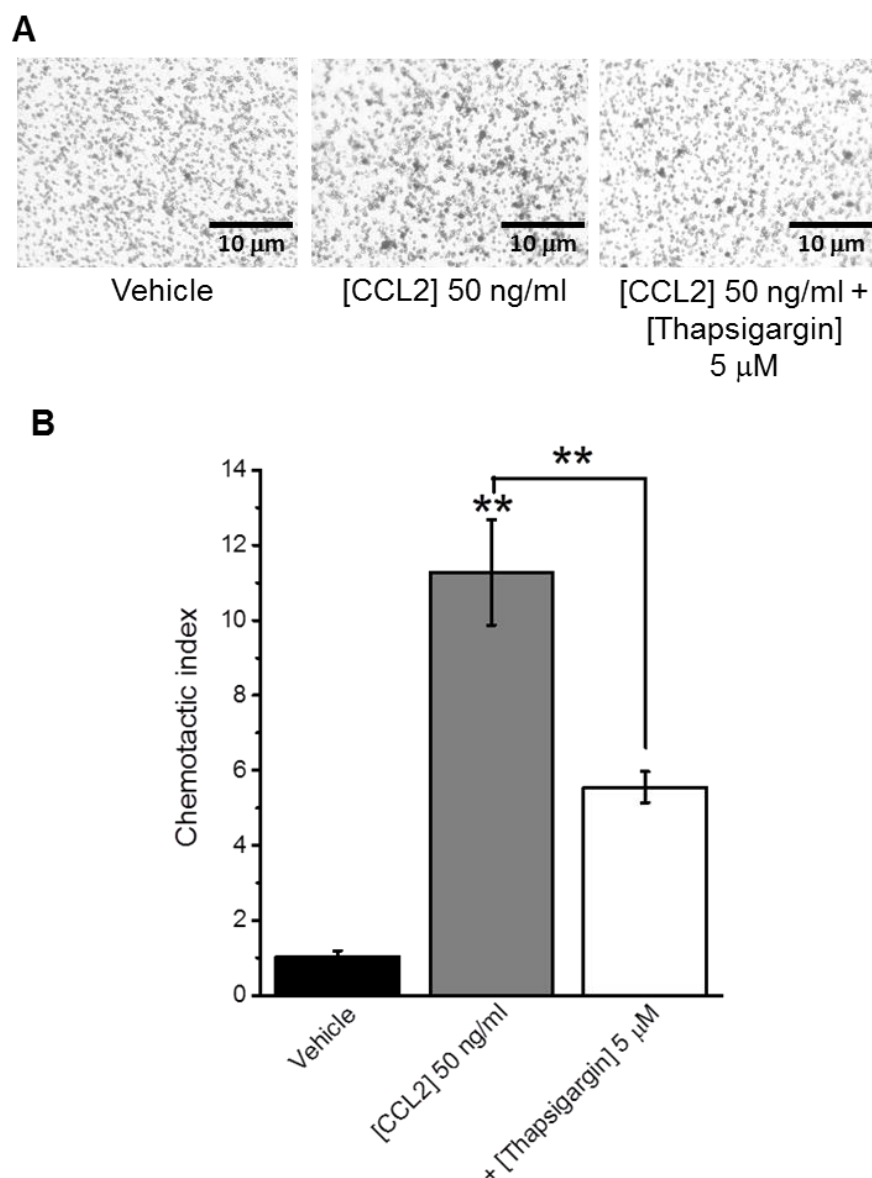


**Figure 4.18 Effect of thapsigargin on CCL2-mediated THP-1 cell chemotaxis**

(A) Representative images showing the effect of thapsigargin (5 µM) on THP-1 cell chemotaxis towards CCL2 (50 ng/ml). Scale bar represents 10 µm. (B) Bar chart showing normalised THP-1 cell chemotaxis towards vehicle (water) or CCL2 (50 ng/ml, lower chamber, 2 hours), in the presence of vehicle (DMSO) or thapsigargin (5 µM). Chemotactic index is a ratio of the number of cells that migrated towards CCL2 over the number of cells that migrated towards vehicle. Data represents mean ± SEM from n=4 transwells. Asterisks indicate significant changes towards vehicle (\*\*p<0.01, One-way ANOVA with Bonferroni's multiple comparison).

#### **4.3.11 Effect of SOCE inhibition on CCL2/CCR2-associated THP-1 cell signalling and function**

Classical GPCR activation involving PLC drives the release of intracellular  $\text{Ca}^{2+}$  from internal stores such as the ER. A release of  $\text{Ca}^{2+}$  from the ER results in the activation of SERCA, an ATPase pump involved in replenishing the ER. However, this mechanism can only prove effective if  $[\text{Ca}^{2+}]_i$  within the cytoplasm is sufficient. As such, mechanisms such as plasma membrane store-operated  $\text{Ca}^{2+}$  channels (SOCCs) open following internal store depletion in a bid to maintain cellular homeostasis (Parekh and Putney, 2005) (Section 1.4.2.1, Chapter 1).

A number of SOCCs participating in store-operated  $\text{Ca}^{2+}$  entry (SOCE) have been identified of which  $\text{Ca}^{2+}$ -release activated  $\text{Ca}^{2+}$  channels (CRAC) are the most well-characterised (Parekh and Putney, 2005; Feske, 2010). CRAC regulation is undertaken by stromal interaction molecule 1 (STIM1), a protein which acts both as a  $\text{Ca}^{2+}$  sensor within the ER membrane and as an activator of CRAC channels (Roos *et al.*, 2005; Liou *et al.*, 2005). A second protein, Orai1 (CRACM1) forms the channel-forming subunit of CRAC which couples to STIM1 upon ER  $\text{Ca}^{2+}$  depletion (Prakriya *et al.*, 2006; Feske *et al.*, 2006).

Hence, it is important to understand the requirement of SOCE for CCL2/CCR2-mediated monocyte signalling and function. Studies therefore examined this hypothesis using THP-1 cells and the pharmacological tool SKF-96365, an SOCE inhibitor with a reported  $\text{IC}_{50}$  of 10  $\mu\text{M}$  against  $I_{\text{CRAC}}$  (CRAC-channel current) (Merritt *et al.*, 1990).

##### **4.3.11.1 Effect of SKF-96365 on CCL2-evoked $\text{Ca}^{2+}$ responses in THP-1 cells**

Studies tested the effects of SKF-96365 (100  $\mu\text{M}$ ) on CCL2-evoked intracellular  $\text{Ca}^{2+}$  responses in THP-1 cells. Prior to experimentation, the presence of SOCE was verified in the absence of extracellular  $\text{Ca}^{2+}$  by challenging THP-1 cells with 50 ng/ml CCL2 followed by the addition of  $\text{CaCl}_2$  (1.5 mM) to produce an “add-back” response characteristic of SOCE (Figure 4.19a).

In experiments assessing the requirement of SOCE in the presence of extracellular  $\text{Ca}^{2+}$  (Figure 4.19b and c), it was seen that treatment of THP-1 cells with SKF-96365 almost abolished CCL2-evoked intracellular  $\text{Ca}^{2+}$  responses ( $99 \pm 1\%$ ,  $n=3$ ,  $p<0.01$ ), where the %Fmax values for untreated and SKF-96365-treated cells were  $24 \pm 2\%$  ( $n=3$ ) and  $0.3 \pm 0.3\%$  ( $n=3$ ), respectively. These data suggested that CCL2/CCR2-mediated  $\text{Ca}^{2+}$  responses were almost entirely dependent on SOCE. Although it was possible that these results were due to a reduction in cell viability, trypan blue and LDH assays were unable to provide any evidence of this (Appendix Figures A1 and A2). This suggested that the

effects of SKF-96365 were caused by an inhibition of other  $\text{Ca}^{2+}$  channels. Further experiments with SKF-96365 were not undertaken as it was discovered that prior work by others provided evidence of off-target effects of SKF-96365 (Merritt *et al.*, 1990; Mason *et al.*, 1993; Singh *et al.*, 2010). Consequently, firm conclusions about the involvement of SOCE for efficient CCL2/CCR2 signalling in THP-1 cells may not be drawn.

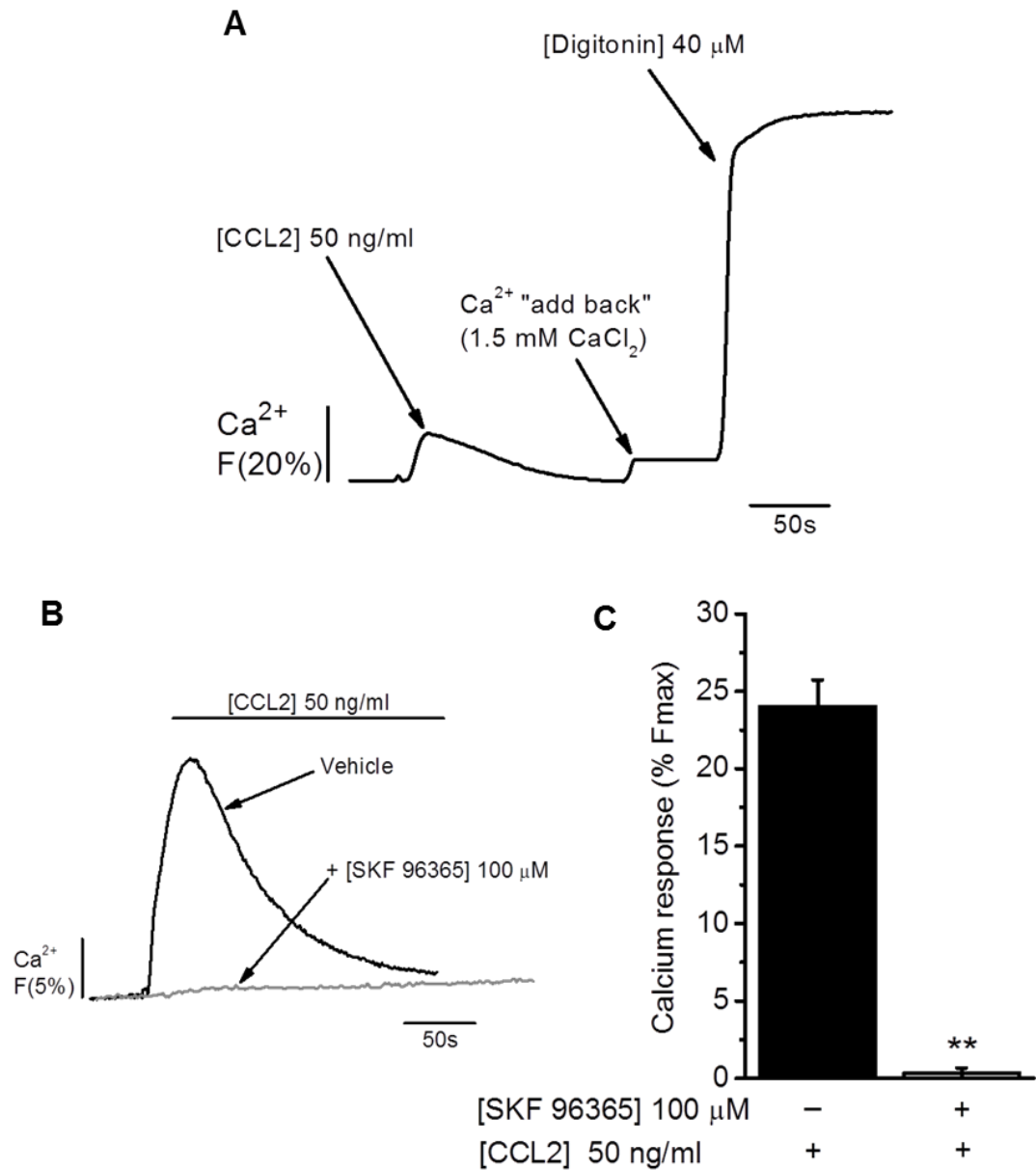


**Figure 4.19 Effect of SKF-96365 on CCL2-evoked Ca<sup>2+</sup> responses in THP-1 cells**

(A) Representative trace showing Ca<sup>2+</sup> "add-back" response upon addition of 1.5 mM CaCl<sub>2</sub> after CCL2 (50 ng/ml) challenge. (B) Representative Ca<sup>2+</sup> transients to CCL2 (50 ng/ml) in THP-1 cells pre-treated with vehicle (water) or SKF-96365 (100  $\mu$ M) for 15 minutes. (C) Bar chart showing normalised intracellular Ca<sup>2+</sup> responses to CCL2 (50 ng/ml) in THP-1 cells pre-treated with vehicle (water) or SKF-96365 (100  $\mu$ M) for 15 minutes. Responses normalised to Ca<sup>2+</sup> signals elicited by 40  $\mu$ M digitonin (% Fmax). Data represents mean  $\pm$  SEM from n=3 replicates. Asterisks indicate significant changes towards vehicle (\*\*p<0.01, Students t-test).

#### **4.3.12 Effect of inhibiting DAG metabolism on CCL2/CCR2-mediated THP-1 cell signalling and function**

Diacylglycerols (DAG) are multifunctional lipids that serve as signalling molecules and precursors for other signalling lipids (Baldanzi, 2014). DAG typically exerts its function as a signalling molecule by binding to the diacylglycerol-binding C<sub>1</sub> domain of target proteins such as Munc13s, protein kinase D (PKD), Ras guanyl nucleotide-releasing proteins (RasGRP), and chimaerins. However, the prototypical target of DAG is protein kinase C (PKC) (Baldanzi, 2014).

As mentioned previously (Section 1.3.4.2.1, Chapter 1), PLC isoenzymes generate DAG and IP<sub>3</sub> from the hydrolysis of PIP<sub>2</sub> (Yang *et al.*, 2013). It is possible, therefore, that DAG, like IP<sub>3</sub>, is also important for CCL2/CCR2-mediated monocyte signalling and function. To examine this hypothesis, studies employed inhibitors of diacylglycerol lipase (DAGL) and diacylglycerol kinase (DAGK) as these enzymes are involved in DAG metabolism. Studies investigated the requirement of these enzymes for CCL2/CCR2-mediated monocyte signalling and function using THP-1 cells as a model.

##### **4.3.12.1 Effect of RHC-80267 on CCL2-evoked Ca<sup>2+</sup> responses in THP-1 cells**

The DAGLs are a family of enzymes comprising of two isoenzymes, DAGL $\alpha$  and DAGL $\beta$  (Bisogno *et al.*, 2003). Both isoenzymes hydrolyse DAG at the sn-1 fatty acid position to yield 2-arachidonolyglycerol (2-AG), an endocannabinoid receptor ligand important for neuronal and brain development and function (Harkany *et al.*, 2007). Within the endocannabinoid system, 2-AG signalling is regulated primarily by monoacylglycerol lipase (MAGL), an enzyme that hydrolyses 2-AG to yield arachidonic acid (AA), a precursor for the synthesis of pro-inflammatory thromboxanes and prostaglandins (Smith *et al.*, 1991).

The requirement for DAGL was investigated using RHC-80267, a dual DAGL $\alpha$ / $\beta$  inhibitor reported to inhibit DAGL in canine and guinea pig platelets (IC<sub>50</sub> = 4  $\mu$ M) (Sutherland and Amin, 1982; Canonico *et al.*, 1985).

In experiments assessing the effects of RHC-80267 (1-50  $\mu$ M) on CCL2-evoked intracellular Ca<sup>2+</sup> responses in THP-1 cells, it was seen that RHC-80267 caused a concentration-dependent inhibition (Figure 4.20). While 1  $\mu$ M RHC-80267 produced no significant effects (n=3, p>0.05), it was seen that 50  $\mu$ M RHC-80267 attenuated CCL2-evoked intracellular Ca<sup>2+</sup> responses by 18  $\pm$  4% (n=5, p<0.01). In conditions where 50  $\mu$ M RHC-80267 was used, the %Fmax values for CCL2 in untreated and RHC-80267-treated THP-1 cells were 20  $\pm$  1% (n=5) and 17  $\pm$  1% (n=5), respectively. In comparison, in experiments with 1  $\mu$ M RHC-80267, the %Fmax values for CCL2 in untreated and

RHC80267-treated cells were  $25 \pm 2\%$  ( $n=3$ ) and  $23 \pm 2\%$  ( $n=3$ ), respectively. A further analysis of the decay rates showed that  $\tau$  for CCL2  $\text{Ca}^{2+}$  transients in untreated ( $77 \pm 1$  seconds,  $n=3$ ) and  $1\mu\text{M}$ -RHC-80267-treated cells ( $76 \pm 5$  seconds,  $n=3$ ) remained largely unchanged ( $n=3$ ,  $p>0.05$ ) (Figure 4.20c). However, it was seen that  $50\mu\text{M}$  RHC-80267 increased  $\tau$  by  $15 \pm 5\%$  ( $n=5$ ,  $p<0.05$ ), where the  $\tau$  values for CCL2 in untreated and RHC-80267-treated cells were  $60 \pm 5$  seconds ( $n=5$ ) and  $69 \pm 6$  seconds ( $n=5$ ), respectively. These data suggested that RHC-80267, through an impairment of DAGL activity, slowed the decay of CCL2  $\text{Ca}^{2+}$  transients.

To understand the requirement of  $\text{Ca}^{2+}$  for DAGL impairment, similar experiments were performed in the absence of extracellular  $\text{Ca}^{2+}$  with  $50\mu\text{M}$  RHC-80267, where  $1.5\text{mM}$   $\text{CaCl}_2$  was omitted from SBS and replaced with  $1\text{mM}$  of the  $\text{Ca}^{2+}$  chelator EGTA. As shown (Figure 4.21), CCL2-evoked intracellular  $\text{Ca}^{2+}$  responses were not significantly affected by RHC-80267 ( $n=4$ ,  $p>0.05$ ), where the %Fmax values for untreated and RHC-80267-treated cells were  $10 \pm 0.3\%$  ( $n=4$ ) and  $9 \pm 1\%$  ( $n=4$ ), respectively. These data suggest that the attenuation of DAGL by RHC-80267 is calcium-dependent. The  $\text{Ca}^{2+}$  decay rates ( $\tau$ , sec) were also analysed and compared for both treatments, but suggested that  $\tau$  for untreated ( $69 \pm 7$  seconds,  $n=4$ ) and RHC-80267-treated cells ( $64 \pm 5$  seconds,  $n=4$ ), were not significantly different ( $n=4$ ,  $p>0.05$ ).

#### **4.3.12.2 Effect of RHC-80267 on CCL2-mediated THP-1 cell chemotaxis**

In an effort to examine the requirement of DAGL for monocyte function, studies next investigated the effects of RHC-80267 ( $50\mu\text{M}$ ) on THP-1 cell chemotaxis towards CCL2 ( $50\text{ng/ml}$ ). As shown (Figure 4.27), a significantly higher chemotactic index was observed towards CCL2 ( $14 \pm 2$ ,  $n=4$ ) than towards vehicle ( $1 \pm 0.5$ ,  $n=4$ ,  $p<0.01$ ). As also shown treatment of THP-1 cells with RHC-80267 impaired chemotaxis by  $49 \pm 4\%$  ( $n=4$ ,  $p<0.01$ ), where the chemotactic indexes for untreated and RHC-80267-treated cells decreased from  $14 \pm 2$  ( $n=4$ ) to  $7.2 \pm 0.6$  ( $n=4$ ), respectively. These results were interesting and indicated a requirement of DAGL for monocyte function. However, in LDH studies, it was observed that THP-1 cells exposed to RHC-80267 for 2.5 hours released LDH at levels close to the 20% threshold ( $18\%$  of Triton-X,  $n=1$ ) (Appendix Figure A3), suggesting that the effects of RHC-80267 on THP-1 cell signalling and function could also be caused by cytotoxicity. Although this is a possibility, trypan blue assays were unable to support the results of LDH studies (Appendix Figure A5). While this study may have indicated that further cell viability tests are required, it nevertheless suggested that DAGL is required for monocyte function.

Taken together, these results suggest that DAGL activity is required for efficient CCL2/CCR2-mediated monocyte signalling and function.

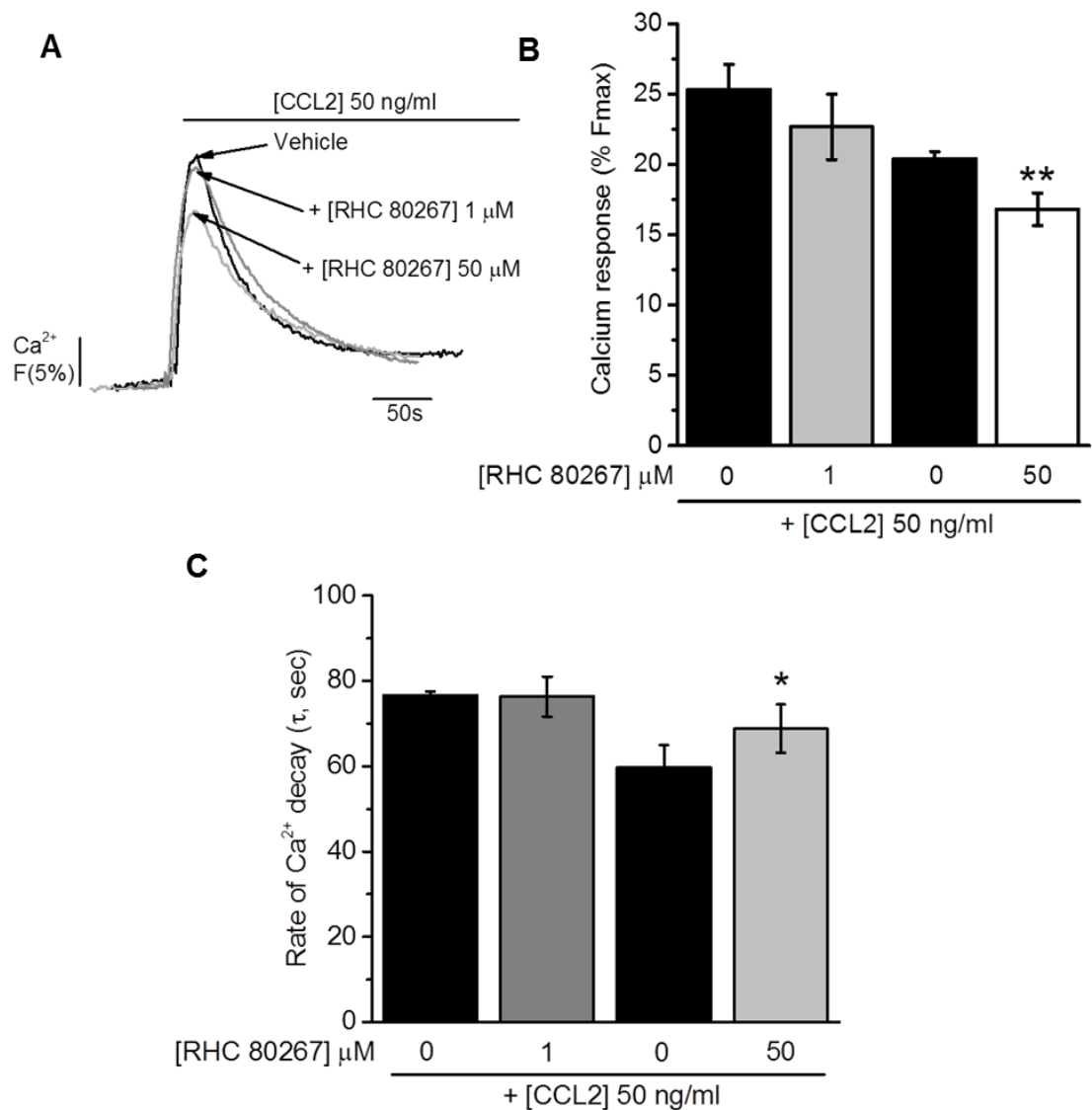


**Figure 4.20 Effect of RHC-80267 on CCL2-evoked Ca<sup>2+</sup> responses in THP-1 cells**

(A) Representative Ca<sup>2+</sup> transients and (B) bar chart showing normalised intracellular Ca<sup>2+</sup> responses to CCL2 (50 ng/ml) in THP-1 cells pre-treated with vehicle (DMSO) or RHC-80267 (1 - 50  $\mu$ M) for 15 minutes. Responses normalised to Ca<sup>2+</sup> signals elicited by 40  $\mu$ M digitonin (%Fmax). (C) Bar chart showing Ca<sup>2+</sup> decay rates ( $\tau$ , sec) for Ca<sup>2+</sup> transients to CCL2 (50 ng/ml) in THP-1 cells pre-treated with vehicle (DMSO) or RHC-80267 (1-50  $\mu$ M) for 15 minutes. Data represents mean  $\pm$  SEM from n=3 (1  $\mu$ M) or n=5 (50  $\mu$ M) replicates. Asterisks indicate significant changes towards vehicle (\*\*p<0.01, \*p<0.05, Students t-test).

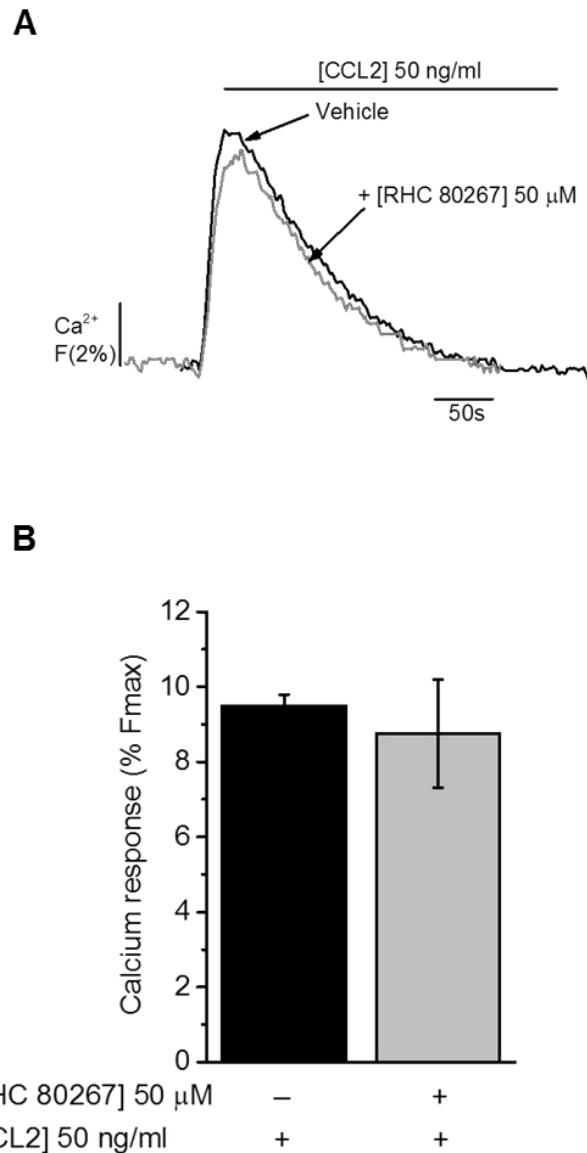


**Figure 4.21 Effect of RHC-80267 on CCL2-evoked  $\text{Ca}^{2+}$  responses in THP-1 cells in the absence of extracellular  $\text{Ca}^{2+}$**

(A) Representative  $\text{Ca}^{2+}$  transients to CCL2 (50 ng/ml) in THP-1 cells pre-treated with vehicle (DMSO) or RHC-80267 (50  $\mu$ M) for 15 minutes. (B) Bar chart showing normalised intracellular  $\text{Ca}^{2+}$  responses to CCL2 (50 ng/ml) in THP-1 cells pre-treated with vehicle (DMSO) or RHC-80267 (50  $\mu$ M) for 15 minutes. Responses normalised to  $\text{Ca}^{2+}$  signals elicited by 40  $\mu$ M digitonin (% Fmax). Data represents mean  $\pm$  SEM from n=4 replicates.

#### 4.3.12.3 Effect of R-59-022 on CCL2-evoked Ca<sup>2+</sup> responses in THP-1 cells

The enzyme diacylglycerol kinase (DAGK) is responsible for phosphorylating DAG. Although this metabolic pathway is considered a quantitatively minor pathway, it has been proposed to be the primary route for maintaining levels of “signalling” DAG (Baldanzi, 2014). In mammals, ten DAGKs have been cloned and characterised, and are classified into five distinct families (I ( $\alpha$ ,  $\beta$ ,  $\gamma$ ), II ( $\delta$ ,  $\eta$ ,  $\kappa$ ), III ( $\epsilon$ ), IV ( $\zeta$ ,  $\iota$ ), and V ( $\theta$ )), based primarily on differences in their structural motifs (Merida *et al.*, 2008). All DGKs phosphorylate DAG to yield phosphatidic acid (PA), which is mainly generated as a means of regulating DAG levels. However, PA is also accepted as a signalling molecule, and is known to activate a number signalling proteins including, atypical PKC, chimaerins, and PLC (Limatola *et al.*, 1994; Litosch, 2002; Caloca *et al.*, 2003). PA-specific phosphatases (PAPS) and other enzymes responsible for dephosphorylating PA to DAG (Brindley *et al.*, 2009; Baldanzi, 2014) also interchangeably regulate PA levels.

Experiments examining the involvement of DAGK in CCL2/CCR2-mediated monocyte signalling and function were performed in THP-1 cells. The pharmacological tool R-59-022 was also employed as this is an inhibitor of several mammalian DAGKs including type I DGK $\alpha$ , type III DGK $\epsilon$ , and type V DGK $\theta$  (Jiang *et al.*, 2000). R-59-022 exhibits an IC<sub>50</sub> of 2.8  $\mu$ M against human DAGK (De Chaffoy De Courcelles *et al.*, 1985).

Initial experiments tested the effects of R-59-022 (10-30  $\mu$ M) on CCL2-evoked intracellular Ca<sup>2+</sup> responses in THP-1 cells. As shown (Figure 4.22), application of 30  $\mu$ M R-59-022 to cells produced a small increase in baseline Ca<sup>2+</sup>. While rises caused by 10  $\mu$ M R-59-022 could not be quantified, the %Fmax for 30  $\mu$ M R-59-022 was 5  $\pm$  1% (n=3). This observation is interesting, and although difficult to explain, reflects the possibility that DAGK inhibition alters Ca<sup>2+</sup> homeostasis. As also shown (Figure 4.22), R-59-022 produced a concentration-dependent inhibition of CCL2-evoked Ca<sup>2+</sup> responses, where it was observed that 10  $\mu$ M and 30  $\mu$ M R-59-022 attenuated CCL2 Ca<sup>2+</sup> responses by 38  $\pm$  7% (n=3, p<0.05) and 81  $\pm$  2% (n=3, p<0.05), respectively. In paired experiments with 10  $\mu$ M R-59-022, the %Fmax values for CCL2 in untreated and R-59-022-treated cells were 24  $\pm$  1% (n=3) and 15  $\pm$  1% (n=3), whereas in experiments with 30  $\mu$ M R-59-022 these values were 24  $\pm$  2% (n=3) and 5  $\pm$  1% (n=3), respectively.

To enable a greater understanding of the effects of DAGK inhibition, the decay rates for all treatments were analysed and compared. As shown (Figure 4.22d), 10  $\mu$ M R-59-022 significantly slowed the decay of CCL2 Ca<sup>2+</sup> transients (n=3, p<0.05), where the  $\tau$  values for CCL2 in untreated and R-59-022-treated cells were 77  $\pm$  2 seconds (n=3) and 108  $\pm$  5 seconds (n=3), respectively. Interestingly, a significant effect was not observed with 30

$\mu\text{M}$  R-59-022 for which the  $\tau$  values for CCL2 in untreated and R-59-022-treated cells were  $32 \pm 10$  seconds ( $n=3$ ) and  $59 \pm 7$  seconds ( $n=3$ ), respectively ( $n=3$ ,  $p>0.05$ ).

In an effort to understand the requirement of  $\text{Ca}^{2+}$  for DAGK inhibition, studies examined the effects of  $30 \mu\text{M}$  R-59-022 on CCL2-evoked intracellular  $\text{Ca}^{2+}$  responses in the absence of extracellular  $\text{Ca}^{2+}$  (for method see Chapter 2, Section 2.6.2) (Figure 4.23). Although not shown, R-59-022 addition to cells increased baseline  $\text{Ca}^{2+}$  by  $4 \pm 1\%F_{\text{max}}$  ( $n=3$ ). This effect suggested that R-59-022 affected  $\text{Ca}^{2+}$  mobilisation by releasing  $\text{Ca}^{2+}$  from internal stores. As also shown (Figure 4.23), R-59-022 attenuated CCL2-evoked intracellular  $\text{Ca}^{2+}$  responses by  $58 \pm 9\%$  ( $n=3$ ,  $p<0.01$ ), where the  $\%F_{\text{max}}$  values for CCL2 in untreated and R-59-022-treated cells were  $10 \pm 1\%$  ( $n=3$ ) and  $4 \pm 1\%$  ( $n=3$ ), respectively. The  $\%$  inhibition seen under these conditions was less than that observed in the presence of intracellular  $\text{Ca}^{2+}$  (Figure 4.22), and suggested that the effects of R-59-022 were partially dependent on extracellular  $\text{Ca}^{2+}$ . The decay rates for CCL2  $\text{Ca}^{2+}$  transients in untreated ( $83 \pm 16$  seconds,  $n=3$ ) and treated cells ( $102 \pm 21$  seconds,  $n=3$ ) suggested that R-59-022 did not significantly affect the decay of  $\text{Ca}^{2+}$  transients in the absence of extracellular  $\text{Ca}^{2+}$  ( $n=3$ ,  $p>0.05$ ).

#### **4.3.12.4 Effect of R-59-022 on UDP-evoked $\text{Ca}^{2+}$ responses in THP-1 cells**

Given the universal role of DAG in PLC-mediated signalling, a brief study was undertaken to investigate whether DAGK activity would also be required for THP-1 cell  $\text{Ca}^{2+}$  responses evoked by the  $\text{P2Y}_6/\text{P2Y}_{14}$  ligand, UDP. As shown (Figure 4.24), R-59-022 ( $30 \mu\text{M}$ ) treatment significantly inhibited UDP-evoked intracellular  $\text{Ca}^{2+}$  responses by  $70 \pm 4\%$  ( $n=3$ ,  $p<0.01$ ), where the  $\%F_{\text{max}}$  values for UDP in untreated and R-59-022-treated cells were  $25 \pm 1\%$  ( $n=3$ ) and  $7 \pm 1\%$  ( $n=3$ ), respectively. Interestingly, the level of inhibition of UDP responses by R-59-022 was comparable to CCL2, and suggested that DAGK contributed equally to UDP and CCL2 signalling. Due to the sustained UDP  $\text{Ca}^{2+}$  responses in R-59-022-treated cells, the  $\tau$  values of these could not be determined.

#### **4.3.12.5 Effect of R-59-022 on CCL2-mediated THP-1 cell chemotaxis**

In an effort to assess the requirement of DAGK activity for CCL2/CCR2-mediated monocyte function, studies tested the effects of R-59-022 ( $30 \mu\text{M}$ ) on THP-1 cell chemotaxis towards  $50 \text{ ng/ml}$  CCL2. As shown (Figure 4.27), R-59-022 significantly inhibited THP-1 cell chemotaxis towards CCL2 by  $82 \pm 3$  ( $n=4$ ,  $p<0.01$ ), where the chemotactic indexes for untreated and R-59-022-treated cells were  $14 \pm 2$  ( $n=4$ ) and  $2.6 \pm 0.4$  ( $n=4$ ), respectively. Although these data strongly suggested a requirement of DAGK for CCL2/CCR2-mediated monocyte chemotaxis, LDH cell viability studies showed that THP-1 cells exposed for 2.5 hours to  $30 \mu\text{M}$  R-59-022, released LDH at levels above the 20% threshold ( $31\%$  of Triton-X-100,  $n=1$ ) (Appendix Figure A3). However, in trypan blue

studies (Appendix Figure A5), the % viable cells in vehicle ( $100 \pm 15\%$ ,  $n=3$ ) and R-59-022-treated wells ( $81 \pm 7\%$ ,  $n=3$ ) were not significantly different ( $n=3$ ,  $p>0.05$ ). It may be the case therefore that further cell viability tests are required.

Taken together, these data suggest a requirement of DAGK for CCL2/CCR2-mediated and UDP-associated monocyte signalling (and function).

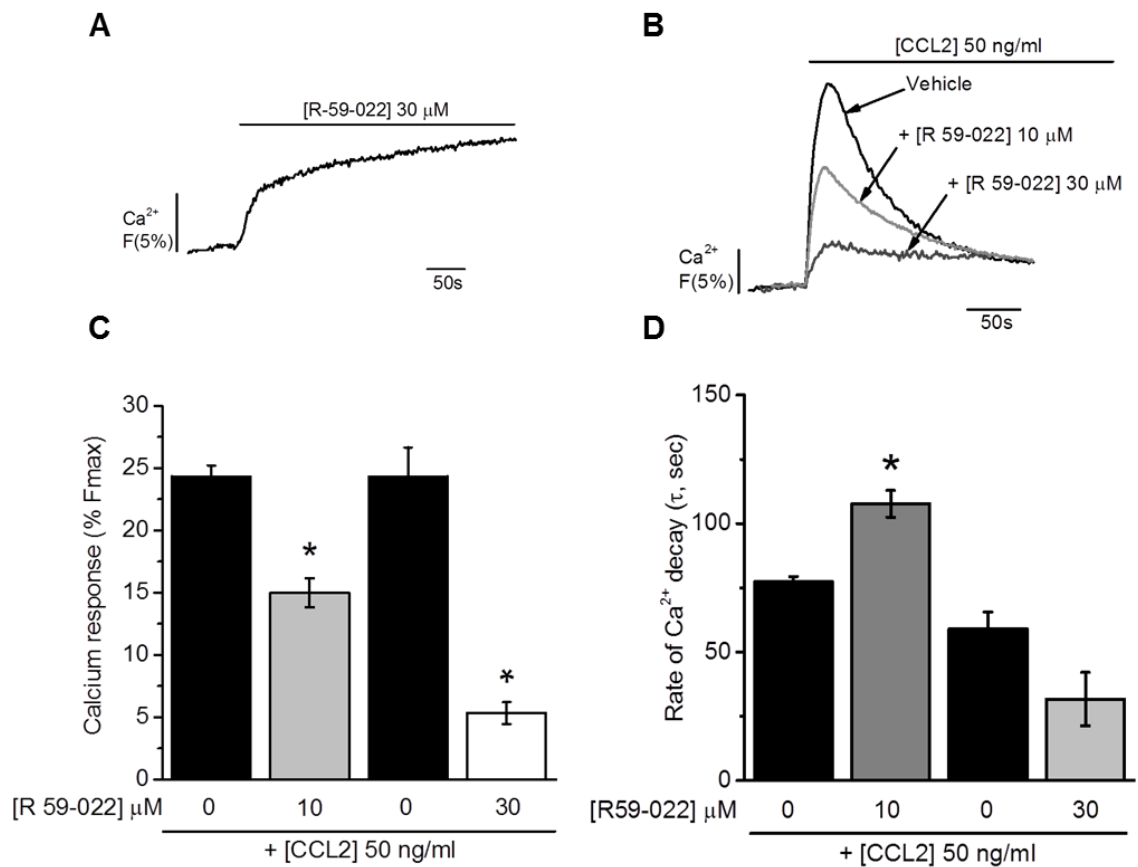


**Figure 4.22 Effect of R-59-022 on CCL2-evoked Ca<sup>2+</sup> responses in THP-1 cells**

(A) Representative trace showing the effect of 30 μM R-59-022 on baseline Ca<sup>2+</sup>. (B) Representative Ca<sup>2+</sup> transients to CCL2 (50 ng/ml) in THP-1 cells pre-treated with vehicle (DMSO) or R-59-022 (10 - 30 μM), for 15 minutes. (C) Bar chart showing normalised intracellular Ca<sup>2+</sup> responses to CCL2 (50 ng/ml) in THP-1 cells pre-treated with vehicle (DMSO) or R-59-022 (10 - 30 μM), for 15 minutes. Responses normalised to Ca<sup>2+</sup> signals elicited by 40 μM digitonin (% Fmax). (D) Bar chart showing CCL2 (50 ng/ml) Ca<sup>2+</sup> decay rates (τ, sec) for THP-1 cells pre-treated with vehicle (DMSO) or R-59-022 (10 - 30 μM) for 15 minutes. Data represents mean ± SEM from n=3 replicates. Asterisks indicate significant changes towards vehicle (\*p<0.05, Students t-test).

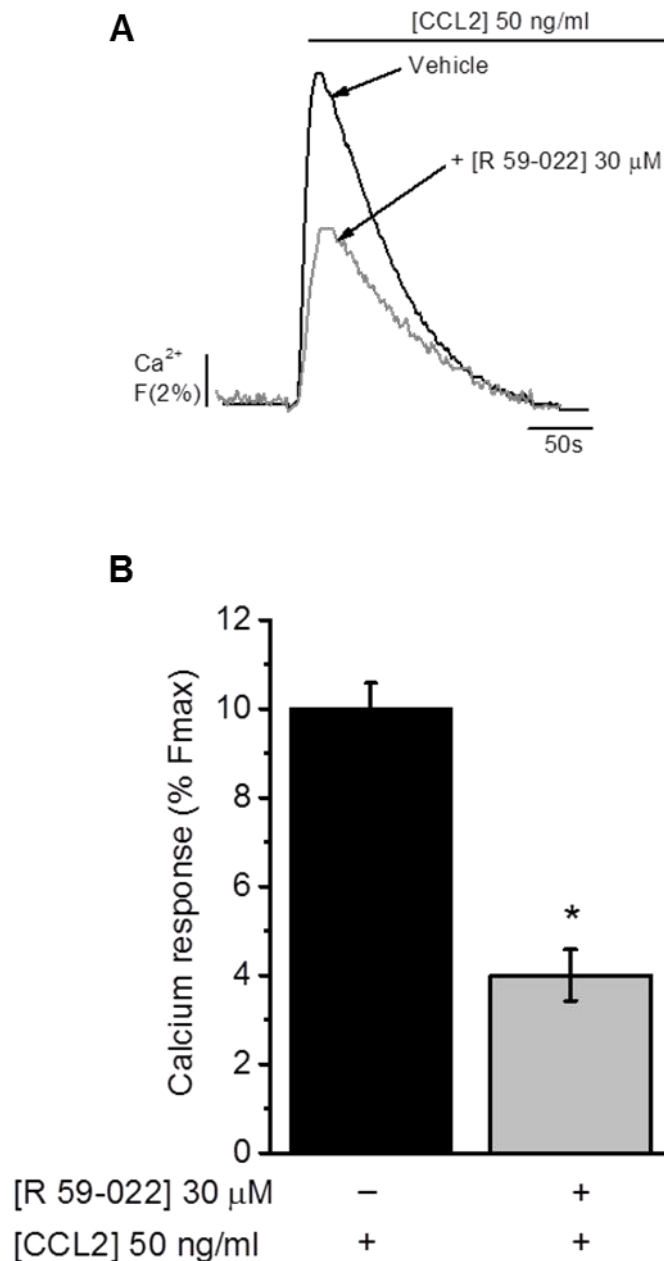


**Figure 4.23 Effect of R-59-022 on CCL2-evoked  $\text{Ca}^{2+}$  responses in THP-1 cells in the absence of extracellular  $\text{Ca}^{2+}$**

(A) Representative  $\text{Ca}^{2+}$  transients to CCL2 (50 ng/ml) in THP-1 cells pre-treated with vehicle (DMSO) or R-59-022 (30  $\mu$ M) for 15 minutes. (B) Bar chart showing normalised intracellular  $\text{Ca}^{2+}$  responses to CCL2 (50 ng/ml) in THP-1 cells pre-treated with vehicle (DMSO) or R-59-022 (30  $\mu$ M), for 15 minutes. Responses normalised to  $\text{Ca}^{2+}$  signals elicited by 40  $\mu$ M digitonin (% Fmax). Data represents mean  $\pm$  SEM from n=3 replicates. Asterisks indicate significant changes towards vehicle (\* $p$ <0.05, Students t-test).

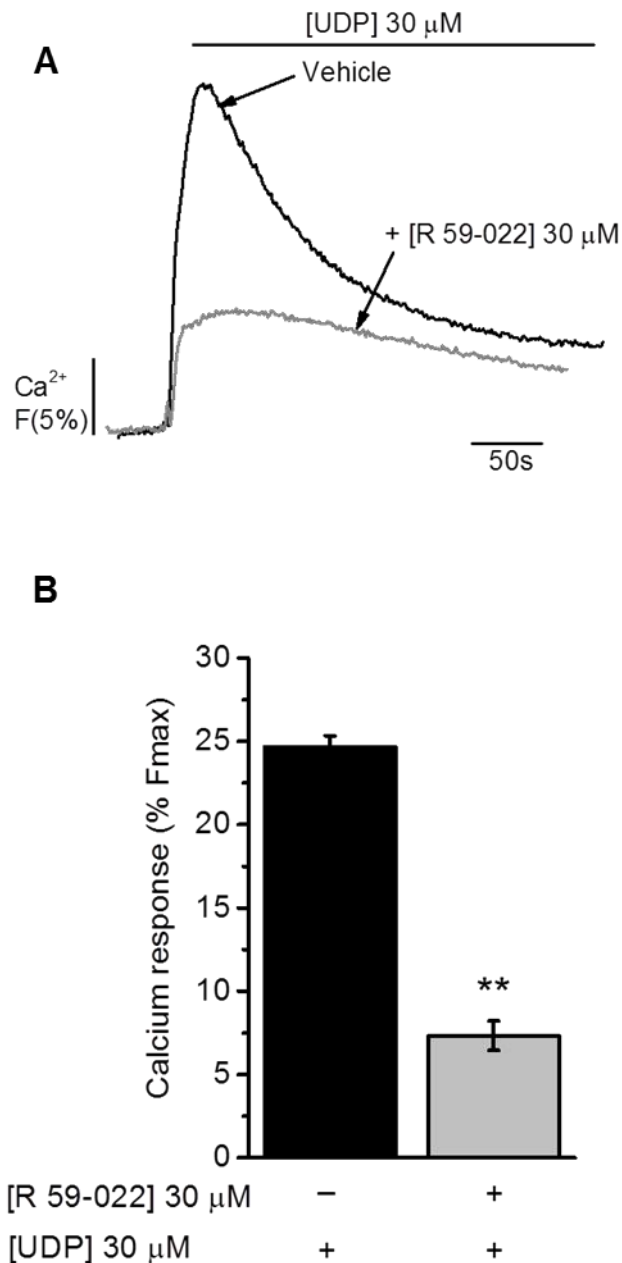


**Figure 4.24 Effect of R-59-022 on UDP-evoked  $\text{Ca}^{2+}$  responses in THP-1 cells**

(A) Representative  $\text{Ca}^{2+}$  transients to UDP (30  $\mu\text{M}$ ) in THP-1 cells pre-treated with vehicle (DMSO) or R-59-022 (30  $\mu\text{M}$ ) for 15 minutes. (B) Bar chart showing normalised intracellular  $\text{Ca}^{2+}$  responses to UDP (30  $\mu\text{M}$ ) in THP-1 cells pre-treated with vehicle (DMSO) or R-59-022 (30  $\mu\text{M}$ ) for 15 minutes. Responses normalised to  $\text{Ca}^{2+}$  signals elicited by 40  $\mu\text{M}$  digitonin (% Fmax). Data represents mean  $\pm$  SEM from n=3 replicates. Asterisks indicate significant changes towards vehicle (\*\* $p < 0.01$ , Students t-test).

#### 4.3.13 Effect of PKC inhibition on CCL2/CCR2-mediated THP-1 cell signalling and function

Protein kinase C (PKC) enzymes drive the phosphorylation of downstream signalling proteins. Comprised of 10 members encoded by 9 genes, the PKC family is split into three families of isoenzymes that are grouped according to their sensitivities to specific cofactors. The conventional/classical cPKCs ( $\alpha$ ,  $\beta$ I,  $\beta$ II,  $\gamma$ ) are activated by DAG, phorbol esters, and (IP<sub>3</sub>)-mediated Ca<sup>2+</sup>, the novel nPKCs ( $\delta$ ,  $\epsilon$ ,  $\eta$ ,  $\theta$ ) are activated by DAG, phorbol esters but not by Ca<sup>2+</sup>, and the atypical aPKCs ( $\zeta$ ,  $\lambda$ ) are activated by anionic phospholipids and protein-protein complexes (Suzuki *et al.*, 2001; Yang and Kazanietz, 2003). PKC isoenzymes are involved in regulating cellular events including, T-cell recognition, cell polarity, migration, and cell cycle progression (Ng *et al.*, 1999; Martin *et al.*, 2005; Hayashi and Altman, 2007).

Given that PKC isoenzymes are important modulators of a wide variety of cellular processes, it was important to understand the requirement of PKC isoenzymes for CCL2/CCR2-mediated monocyte signalling and function. To address this aim, studies investigate the effects of PKC inhibition on CCL2/CCR2-mediated THP-1 cell intracellular Ca<sup>2+</sup> responses and chemotaxis. Studies also employed GF-109203X, a pan-PKC inhibitor reported to inhibit isoenzymes from all three classes, but with a mild preference for cPKCs and nPKCs. The IC<sub>50</sub> values for GF-109203X range from 8.4 nM for PKC $\alpha$  to 5.8  $\mu$ M for PKC $\zeta$  (Toullec *et al.*, 1991; Martiny-Baron *et al.*, 1993; Gschwendt *et al.*, 1996; Anastassiadis *et al.*, 2011).

##### 4.3.13.1 Effect of GF-109203X on CCL2-evoked Ca<sup>2+</sup> responses in THP-1 cells

In experiments investigating the effects of GF-109203X (1  $\mu$ M) on (20-50 ng/ml) CCL2-evoked intracellular Ca<sup>2+</sup> responses, it was seen that responses evoked by 50 ng/ml CCL2 were not significantly affected by GF-109203X (Figure 4.25), where the %Fmax values for CCL2 in untreated and GF-109203X-untreated cells were 25  $\pm$  2% (n=4) and 27  $\pm$  1% (n=4), respectively. However, it was interesting to observe that Ca<sup>2+</sup> responses evoked by 20 ng/ml CCL2 were significantly attenuated by GF-109203X (26  $\pm$  3%, n=3, p<0.05), where %Fmax values for untreated and GF-109203X-treated cells were 10  $\pm$  0.3 (n=3), and 8  $\pm$  0.3 (n=3), respectively.

To further understand the effects of PKC inhibition, the decay rates for all treatments were analysed and compared. As shown (Figure 4.25c), the  $\tau$  values for 20 ng/ml CCL2 (91  $\pm$  3 seconds, n=3) were higher than 50 ng/ml CCL2 (40  $\pm$  2 seconds, n=3). These differences were interesting, but most likely due to variability between experiments. As also shown, GF-109203X reduced the decay rate of Ca<sup>2+</sup> responses evoked by CCL2 20 ng/ml by 53  $\pm$  8% (n=3, p<0.05), where the  $\tau$  values for CCL2 transients in untreated and

treated cells were  $91 \pm 3$  seconds ( $n=3$ ) and  $42 \pm 4$  seconds ( $n=3$ ) respectively. A smaller reduction in  $\tau$  was also observed for  $\text{Ca}^{2+}$  transients to 50 ng/ml CCL2 ( $16 \pm 3$  %,  $n=3$ ,  $p<0.05$ ), where the  $\tau$  values for CCL2 in untreated and treated cells were  $40 \pm 2$  seconds ( $n=3$ ) and  $34 \pm 0.3$  seconds ( $n=3$ ), respectively. These data suggested that GF-109203X, through a possible inhibition of PKC, promoted a faster decay of CCL2  $\text{Ca}^{2+}$  transients. This is interesting because it suggests that GF-109203X affects the decay, but not the magnitude of CCL2  $\text{Ca}^{2+}$  transients.

To understand whether these effects were  $\text{Ca}^{2+}$ -dependent, a study was next undertaken to test the effects of 1  $\mu\text{M}$  GF-109203X on CCL2  $\text{Ca}^{2+}$  responses in the absence of extracellular  $\text{Ca}^{2+}$ . As shown (Figure 4.26), CCL2 intracellular  $\text{Ca}^{2+}$  responses evoked by 50 and 20 ng/ml CCL2 were not significantly affected by GF-109203X ( $n=3$ ,  $p>0.05$ ). The %Fmax values for 50 ng/ml CCL2 in untreated and GF-109203X-treated cells were  $9 \pm 1$  % ( $n=3$ ) and  $7 \pm 1$  % ( $n=3$ ), respectively, and for 20 ng/ml CCL2 they were  $8 \pm 1$  % ( $n=3$ ) and  $9 \pm 2$  % ( $n=3$ ), respectively. Interestingly, the decay rates for these treatments suggested that GF-109203X promoted a faster decay of CCL2 20 ng/ml and 50 ng/ml transients, increasing these by  $63 \pm 3$  % ( $n=3$ ,  $p<0.01$ ) and  $52 \pm 6$  % ( $n=4$ ,  $p<0.01$ ), respectively. For 20 ng/ml CCL2, the  $\tau$  values for CCL2 in untreated and GF-109-203X-treated cells were  $98 \pm 9$  seconds ( $n=3$ ) and  $37 \pm 3$  seconds ( $n=3$ ), respectively, whereas for 50 ng/ml CCL2, they were  $80 \pm 6$  seconds ( $n=4$ ) and  $37 \pm 1$  ( $n=4$ ), respectively. Similar to experiments in the presence of extracellular  $\text{Ca}^{2+}$ , these data suggested that PKC inhibition promoted a more rapid decay of  $\text{Ca}^{2+}$  transients

#### **4.3.13.2 Effect of GF-109203X on CCL2-mediated THP-1 cell chemotaxis**

In an effort to examine the requirement of PKC activity for CCL2/CCR2-mediated monocyte function, studies investigated the effects of GF-109203X (1  $\mu\text{M}$ ) on THP-1 cell chemotaxis towards 50 ng/ml CCL2. As shown (Figure 4.27), THP-1 cell chemotaxis towards CCL2 was not significantly affected by GF-109203X, where the chemotactic indexes for untreated and GF-109203X-treated cells were  $14 \pm 2$  ( $n=4$ ) and  $13 \pm 2$  ( $n=4$ ), respectively ( $n=4$ ,  $p>0.05$ ). These data suggest that PKC is not required for CCL2/CCR2-mediated monocyte chemotaxis.

Taken together, these data suggest that the PKC inhibitor GF-109203X modulates the magnitude and decay of CCL2-evoked intracellular  $\text{Ca}^{2+}$  responses. Furthermore, the data provided by chemotaxis studies suggests that PKC is not required for monocyte trafficking towards CCL2.

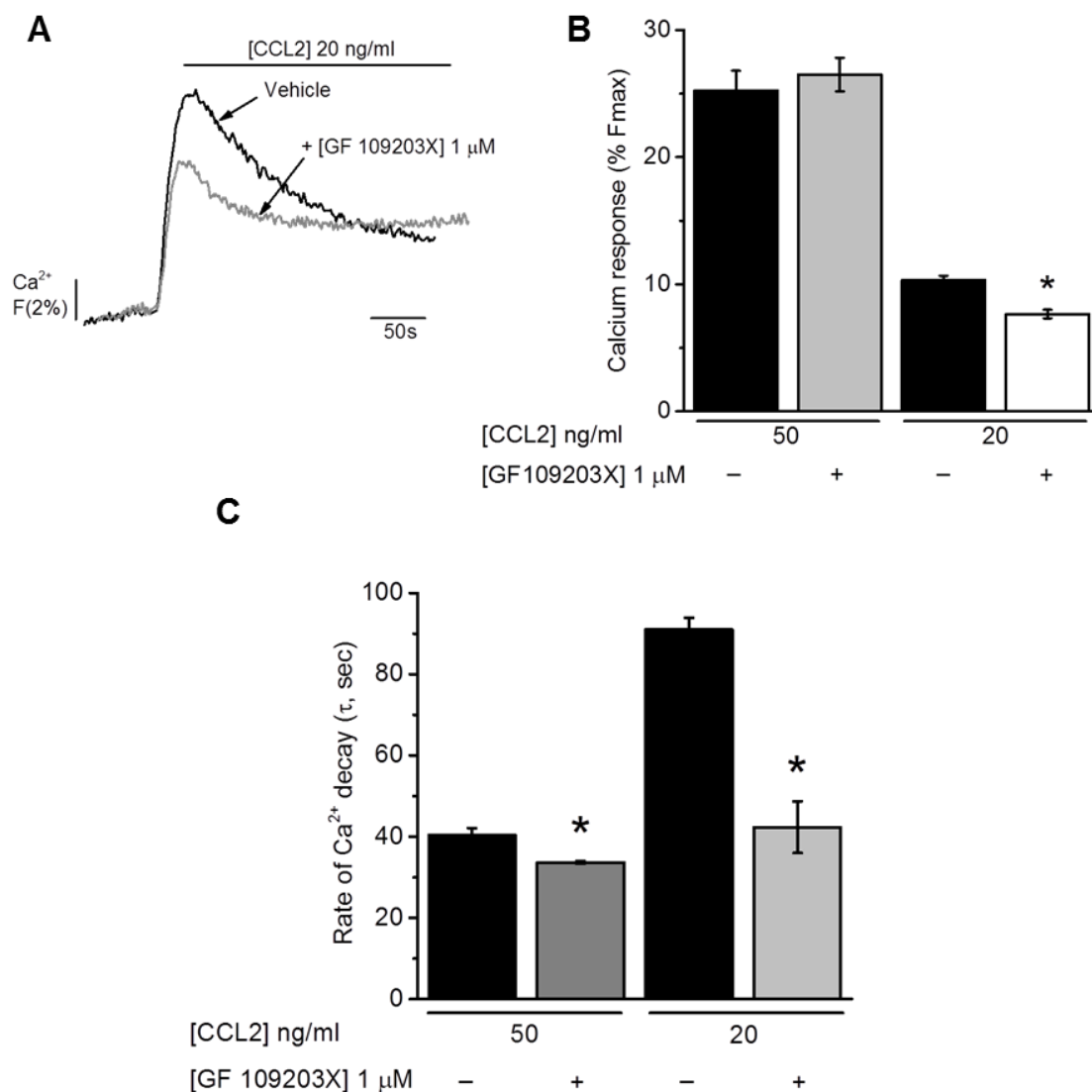


**Figure 4.25 Effect of GF-109203X on CCL2-evoked Ca<sup>2+</sup> responses in THP-1 cells**

(A) Representative Ca<sup>2+</sup> transients to CCL2 (20 ng/ml) in THP-1 cells pre-treated with vehicle (DMSO) or GF-109203X (1  $\mu$ M) for 15 minutes. (B) Bar chart showing normalised intracellular Ca<sup>2+</sup> responses to CCL2 (50 and 20 ng/ml) in THP-1 cells pre-treated with vehicle (DMSO) or GF-109203X (1  $\mu$ M), for 15 minutes. (C) Bar chart showing Ca<sup>2+</sup> decay rates ( $\tau$ , sec) for Ca<sup>2+</sup> transients to CCL2 (50 and 20 ng/ml) in THP-1 cells pre-treated with vehicle (DMSO) or GF-109203X (1  $\mu$ M), for 15 minutes. Responses normalised to Ca<sup>2+</sup> signals elicited by 40  $\mu$ M digitonin (% Fmax). Data represents mean  $\pm$  SEM from n=3 replicates. Asterisks indicate significant changes towards vehicle (\*p<0.05, Students t-test).

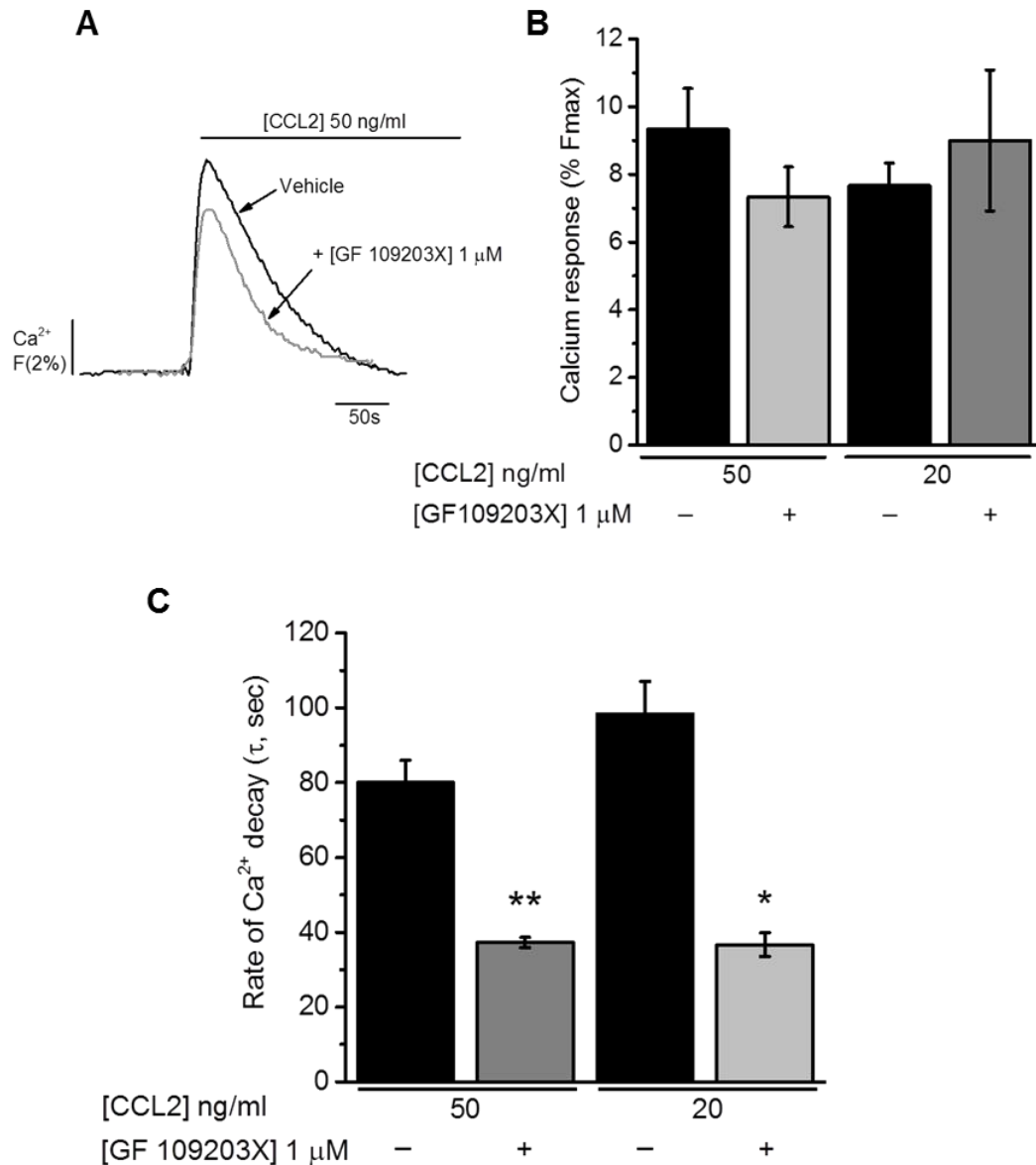


**Figure 4.26 Effect of GF-109203X on CCL2-evoked Ca<sup>2+</sup> responses in THP-1 cells in the absence of extracellular Ca<sup>2+</sup>**

(A) Representative Ca<sup>2+</sup> transients to CCL2 (50 ng/ml) in THP-1 cells pre-treated with vehicle (DMSO) or GF-109203X (1  $\mu$ M) for 15 minutes. (B) Bar chart showing normalised intracellular Ca<sup>2+</sup> responses to CCL2 (50 and 20 ng/ml) in THP-1 cells pre-treated with vehicle (DMSO) or GF-109203X (1  $\mu$ M), for 15 minutes. (C) Bar chart showing Ca<sup>2+</sup> decay rates ( $\tau$ , sec) for Ca<sup>2+</sup> transients to CCL2 (50 and 20 ng/ml) in THP-1 cells pre-treated with vehicle (DMSO) or GF-109203X (1  $\mu$ M), for 15 minutes. Responses normalised to Ca<sup>2+</sup> signals elicited by 40  $\mu$ M digitonin (% Fmax). Data represents mean  $\pm$  SEM from n=4 (CCL2 50 ng/ml) and n=3 (CCL2 20 ng/ml) replicates. Asterisks indicate significant changes towards vehicle (\*p<0.05, \*\*p<0.01, Students t-test).

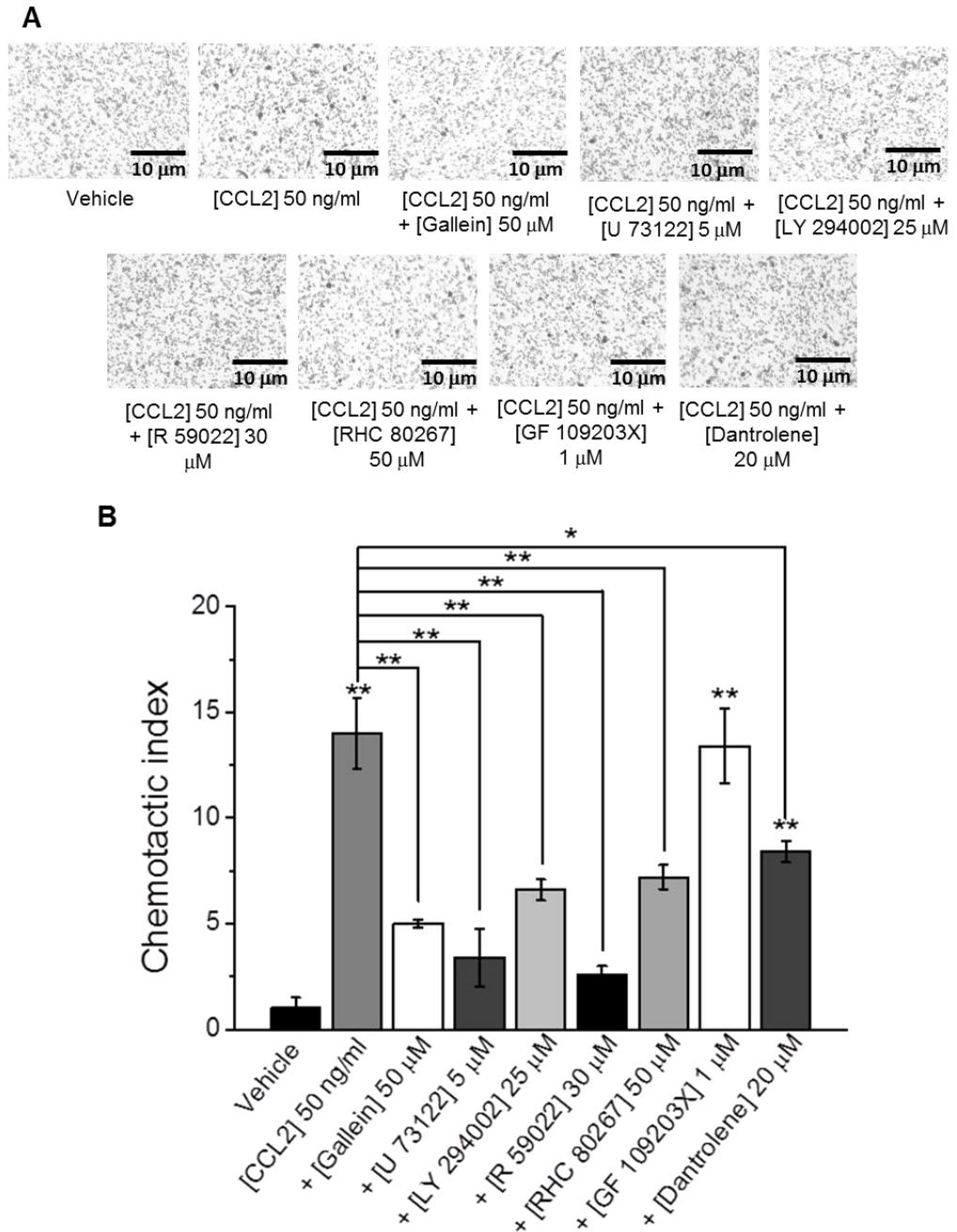


**Figure 4.27 Effect of signalling inhibitors on CCL2-mediated THP-1 cell chemotaxis**

(A) Representative images showing the effect of gallein ( $G\beta\gamma$ ), U-73122 (PLC), LY-294002 (PI3K), R-59-022 (DAGK), RHC-80267 (DAGL), GF-109203X (PKC), and dantrolene (RyR) on THP-1 cell chemotaxis towards CCL2 (50 ng/ml, lower chamber, 2 hours). Scale bar represents 10  $\mu$ m. (B) Bar chart showing normalised THP-1 cell chemotaxis towards vehicle (water) or CCL2 (50 ng/ml, lower chamber, 2 hours) in the presence of vehicle (DMSO) or inhibitors at concentrations shown. Chemotactic index is a ratio of the number of cells that migrated towards CCL2 over the number of cells that migrated towards vehicle. Data represents mean  $\pm$  SEM from  $n=4$  transwells. Asterisks indicate significant changes towards vehicle (\*\* $p < 0.01$ , One-way ANOVA with Bonferroni's multiple comparison).

## 4.4 Summary

This chapter employed monocytic THP-1 cells and human PBMCs as *in vitro* models in order to elucidate the basic signalling mechanisms involved in CCL2/CCR2-mediated monocyte signalling and function as measured by intracellular  $\text{Ca}^{2+}$  mobilisation, cell migration, and adhesion to vascular endothelium. Using a combination of methodology, a number of important findings were made. Initial observations suggested a role of CCL2 in intracellular  $\text{Ca}^{2+}$  release and cell migration. The inhibitory effects of BAPTA-AM and other studies in the absence of extracellular  $\text{Ca}^{2+}$  suggested that  $\text{Ca}^{2+}$  was required for efficient CCL2 signalling. Further studies with BMS-CCR2-22 indicated that CCL2-mediated monocyte intracellular  $\text{Ca}^{2+}$  release, migration and adhesion to vascular endothelium required CCR2 activation. The impairment of CCL2-mediated intracellular  $\text{Ca}^{2+}$  release and migration by PTx strongly suggested that CCR2 coupled to  $\text{G}\alpha_{i/o}$ -type G-proteins. Although intracellular  $\text{Ca}^{2+}$  experiments using gallein could not be performed, the inhibitory effects of this on THP-1 cell chemotaxis suggested that  $\text{G}\beta\gamma$  activation was required for monocyte chemotaxis towards CCL2. Further experiments with LY-294002 and U-73122 pointed towards an involvement of PI3K and PLC in CCL2/CCR2-mediated monocyte signalling and function. Studies with XeC supported PLC studies further by suggesting that  $\text{IP}_3$ -mediated  $\text{Ca}^{2+}$  release from internal stores was required for CCL2/CCR2-mediated monocyte intracellular  $\text{Ca}^{2+}$  release and chemotaxis. Experiments using the inhibitor dantrolene however, suggested that RyR activation was required for efficient CCL2/CCR2-mediated monocyte function, but not signalling. The results of thapsigargin studies indicated an involvement of SERCA while also indirectly confirming an involvement of the ER for efficient CCL2/CCR2-mediated monocyte signalling and function. An involvement of SOCE was tested using the SOCE inhibitor SKF 96365, but the results of these studies pointed towards a possible “off-target” effect of this compound. In other studies investigating a requirement of DAG, experiments with DAGL (RHC-80267) and DAGK (R-59-022) inhibitors suggested a requirement of these enzymes for efficient CCL2/CCR2-mediated monocyte signalling and function. Interestingly, the inhibitory effect of GF-109203X on low concentrations of CCL2 indicated that PKC was needed for CCL2/CCR2 monocyte signalling, but not function. Interestingly, GF-109203X studies also suggested that PKC regulated the decay of CCL2  $\text{Ca}^{2+}$  transients.

Taken together, these findings suggest that CCL2/CCR2-mediated monocyte signalling and function involves an activation of a number of signal transduction components. These findings highlight the importance of understanding the influence of other chemotactic pathways on CCL2/CCR2-mediated monocyte signalling and function. Chapter 5 therefore addressed this gap in knowledge by examining the requirement of extracellular nucleotides and purinoceptors for efficient CCL2/CCR2-mediated monocyte signalling and

function using THP-1 cells and human PBMCs as models. Similarly, to the previous chapter, great importance was given to CCL2/CCR2 activation as measured by intracellular  $\text{Ca}^{2+}$  release, cell migration, and adhesion to vascular endothelium.

# Chapter 5: Modulation of CCL2/CCR2-mediated monocyte signalling and function by extracellular nucleotides

---

## 5.1 Introduction

Purinoreceptor signalling describes a widespread intercellular system by which purine and pyrimidine nucleotides and nucleosides participate in short-term and long-term signalling in many cellular processes such as neurotransmission, secretion, cell differentiation, proliferation and death (Burnstock, 2012). The term “purinergic” signalling was initially proposed by Burnstock (1971), following studies identifying the role of ATP and ADP in non-adrenergic, non-cholinergic (NANC) transmission in the gut (Burnstock *et al.*, 1970). The purinoreceptor signalling system has since expanded from its humble beginnings and now forms an extensive network comprising of nineteen purinoreceptors subdivided into three distinct families termed P1, P2X and P2Y (Section 1.7.2, Chapter 1) (Khakh *et al.*, 2001; Abbracchio *et al.*, 2006; Fredholm *et al.*, 2011).

As discussed in Chapter 1, multiple purinoreceptors are expressed by monocytes (Chapter 1, Table 1.5), suggesting that purinoreceptors regulate monocyte signalling and function. Early studies by Fischer *et al.* (1976) first postulated a role for P1 purinoreceptors in monocyte maturation by showing that adenosine catabolism by ADA prevented their maturation to macrophages. However, it is now known that P1 receptors differentially modulate monocyte signalling and function (Haskó *et al.*, 2007; Haskó and Pacher, 2012). For example, studies by Takahashi *et al.* (2007) have shown that while  $A_{2A}$  receptors promote IL-18-induced monocyte adhesion to the vascular endothelium, other subtypes such as  $A_1$  and  $A_3$  prevent adhesion. However, in general, P1 receptors play a restorative and protective role in monocytes where their activation is known to decrease the production of pro-inflammatory mediators such as TNF $\alpha$ , CCL3, and nitric oxide (Le Vraux *et al.*, 1993; Haskó *et al.*, 1996; Szabo *et al.*, 1998).

P2 receptors are also thought to coordinate monocyte signalling and function. For example, studies by Kaufmann *et al.* (2005), Elliott *et al.* (2009) and Kronlage *et al.* (2010) have shown that apoptotic, damaged, or infected cells release extracellular nucleotides into their environments as “host tissue damage” signals in a bid to recruit monocyte and macrophages required for their clearance. Other groups (Grahames *et al.*, 1999; Warny *et al.*, 2001; Cox *et al.*, 2005; Ben Yebdri *et al.*, 2009; Higgins *et al.*, 2014) have also shown through their experiments that P2 receptors such as P2Y<sub>2</sub>, P2Y<sub>6</sub>, and P2X7

regulate the release of the pro-inflammatory mediators TNF $\alpha$ , CCL2, and IL-1 $\beta$  from human monocytes and monocytic cells.

Although the studies described above suggest that purinoceptor signalling is important for monocyte signalling and function, it is fast becoming clear that aberrant purinoceptor signalling is associated with the onset and progression of an increasing number of monocyte-associated pathologies. For example, studies by Buchheiser *et al.* (2011) have shown that CD73, the enzyme responsible for hydrolysing nucleoside monophosphates (Chapter 1, Table 1.6), protects against monocyte recruitment in atherogenesis. Other studies (Seye *et al.*, 2003), have shown that P2Y<sub>2</sub> activation promotes monocyte adhesion during atherogenesis by inducing the expression of VCAM-1 on arterial smooth muscle cells.

Hence, there seems a strong association between purinoceptor signalling and monocyte-associated pathologies. Although purinoceptor signalling represents an attractive therapeutic area, the development of novel therapies targeting purinoceptor signalling remains at an early stage. With the obvious exception of anti-thrombotic P2Y<sub>12</sub> antagonists that prevent the formation of platelet-monocyte aggregates (Wijeyeratne and Heptinstall, 2011), progress in this area has been relatively slow (Jacobson *et al.*, 2012). Considering that other chemoattractants such as chemokines also steer monocyte function, the challenges faced within purinoceptor drug discovery may be due to an incomplete understanding of the interactions of purinoceptor pathways with other established chemotactic pathways.

## 5.2 Aims

THP-1 cells and human PBMCs were used as *in vitro* models to investigate the signalling interactions between purinoceptor and CCL2/CCR2 signalling pathways in monocytes. Studies were performed with a view to investigating the modulation of CCL2/CCR2-mediated monocyte signalling and function by P1 and P2 purinoceptors as measured by intracellular Ca<sup>2+</sup> release, monocyte migration, and adhesion to vascular endothelial cells. Biological and pharmacological tools were employed in order to address each of the smaller objectives in this chapter.

## 5.3 Results

### 5.3.1 Chemotactic effects of extracellular nucleotides on THP-1 cells

Recent evidence suggests that apoptotic cells release extracellular nucleotides into their microenvironment in order to recruit mononuclear phagocytes (Elliott *et al.*, 2009). It is possible, therefore, that extracellular nucleotides coordinate with chemokines to influence the signalling and function of receptor-expressing monocytes. To enable an examination of this hypothesis, a brief study was undertaken to investigate whether extracellular nucleotides were chemotactic for monocytes. To address this hypothesis, studies assessed THP-1 cell chemotaxis towards 1  $\mu$ M ATP, ADP, UTP, and UDP.

As shown (Figure 5.1), the chemotactic index for THP-1 cells towards vehicle was  $1 \pm 0.2$  (n=4). A significant increase in chemotaxis was observed in cells exposed to ATP ( $4 \pm 1$ , n=4,  $p < 0.05$ ) and UTP ( $6 \pm 1$ , n=4,  $p < 0.01$ ), which suggested that both nucleotides are chemotactic. Although THP-1 cells migrated readily towards ADP ( $3 \pm 0.1$ , n=4) and UDP ( $3 \pm 0.4$ , n=4), the chemotactic indexes for these were not significantly different from vehicle (n=4,  $p > 0.05$ ). This data suggested that while ATP and UTP were chemotactic for THP-1 cells, ADP and UDP were not. It is possible, however, that higher concentrations of ADP and UDP are required to evoke a chemotactic response.

Taken together, these data suggest that the extracellular nucleotides ATP and UTP are chemotactic for THP-1 cells. It is possible, therefore, that monocytes expressing CCR2 and specific purinoceptors are responsive to CCL2 as well as ATP and UTP and that this influences their signalling and function.

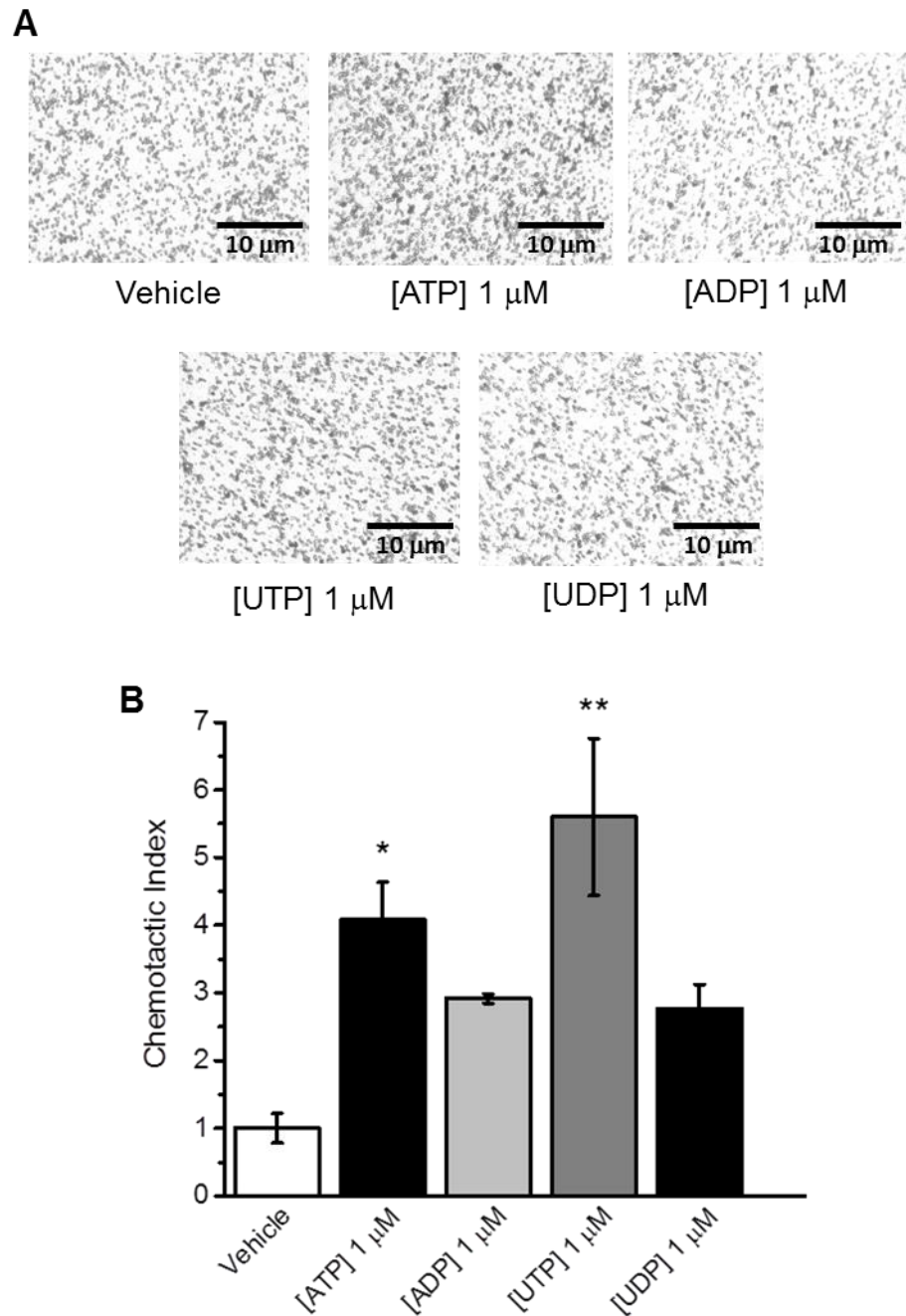


**Figure 5.1 THP-1 cell migration towards extracellular nucleotides**

(A) Representative images showing THP-1 cell chemotaxis towards vehicle (water), ATP, ADP, UTP or UDP (1  $\mu$ M, lower chamber, 2 hours). Scale bar represents 10  $\mu$ m. (B) Bar chart showing normalised THP-1 cell chemotaxis towards vehicle (water), ATP, ADP, UTP or UDP (1  $\mu$ M, lower chamber, 2hrs). Chemotactic index is a ratio of the number of cells that migrated towards extracellular nucleotides over the number of cells that migrated towards vehicle. Data represents mean  $\pm$  SEM from n=4 transwells. Asterisks indicate significant changes towards vehicle (\*\* $p$ <0.01, \* $p$ <0.05, One-way ANOVA with Bonferroni's multiple comparison).

### 5.3.2 Effect of ecto-nucleotidases on CCL2/CCR2-mediated THP-1 cell and PBMC signalling and function

The ecto-nucleotidases are a family of extracellular enzymes that hydrolyse extracellular nucleotides in order to modulate their release and availability at purinoceptors (Chapter 1, Section 1.7.6) (Zimmermann *et al.*, 2012). The ecto-nucleoside triphosphate diphosphohydrolases (E-NTPDases) are the major ecto-nucleotidase family involved in hydrolysing nucleoside triphosphates (NTP) and diphosphates (NDP) to nucleoside monophosphates (NMP) (Robson *et al.*, 2006). To date, eight E-NTPDase isoenzymes (NTPDase1-8) encoded by the genes *ENTPD1-8* have been identified (Robson *et al.*, 2006; Zimmermann *et al.*, 2012). While NTPDase1, NTPDase2, NTPDase3, and NTPDase8 are type II plasma membrane proteins, NTPDase4, NTPDase5, NTPDase6, and NTPDase7 are cytosolic and do not hydrolyse nucleotides (Robson *et al.*, 2006).

The results presented in Figure 5.1 suggest that in an *in vivo* environment, the capacity of monocytes to traffic in response to CCL2 is likely to be influenced by extracellular nucleotides. However, these data also suggest that extracellular nucleotides are far less chemotactic for monocytes than CCL2 (Chapter 4) and may therefore play a much smaller role than CCL2 as chemoattractants. While this is possible, it may be that both pathways direct monocyte signalling and function downstream of receptor activation through signalling crosstalk. To examine the validity of this hypothesis, studies assessed the requirement of extracellular nucleotides for CCL2/CCR2-mediated monocyte signalling and function using THP-1 cells and human PBMCs as models. Studies also employed apyrase, an NTPDase1 isolated from potato (*S. tuberosum*) and described by the manufacturers (Sigma-Aldrich, UK) as a mixture of two ATP/ADP specific isoenzymes: one with a high ratio of ATPase to ADPase activity (10:1), and one with a low ratio of ATPase to ADPase activity (1:1) (Kettlun *et al.*, 1982).

#### 5.3.2.1 Investigating the selectivity of apyrase

Prior to conducting experiments, it was first important to perform studies to confirm that apyrase was selective for ATP and ADP. To address this goal, salt-buffered solution (SBS) was spiked with 100  $\mu$ M of ATP, ADP, UTP, or UDP, and vehicle or apyrase (2 U/ml), and sampled at 0 and 30 minutes. Levels of NTPs, NDPs, and nucleosides (peak height) were detected in samples using ion-pair reverse-phase HPLC.

As shown (Table 5.1 and Appendix Figures A6-A9), when incubated with vehicle, the peak heights (a measure of nucleotide quantity) of all four nucleotides between 0 and 30 minutes were not significantly different ( $n=3$ ,  $p>0.05$ ). This result suggested that nucleotide levels in SBS remained stable over this period. As also shown, apyrase treatment caused a drop in the peak heights of all four nucleotides, where experiments

showed that levels of ATP, ADP, and UDP were significantly less in apyrase-treated samples than in vehicle-treated 0 minute and 30 minute samples ( $n=3$ ,  $p<0.01$ ). Although apyrase also decreased levels of UTP, a significant reduction was only observed between vehicle-treated 30 minute samples and apyrase-treated samples ( $n=3$ ,  $p<0.05$ ). In experiments involving ATP or ADP (Appendix Figures A6 and A7), a drop in nucleotide levels was accompanied by a significant increase in adenosine ( $n=3$ ,  $p<0.01$ , compared to vehicle-treated 0 and 30 minutes). Similarly, a reduction in UTP and UDP by apyrase (Table 5.1), resulted in an increase in UMP and uridine ( $n=3$ ,  $p<0.01$ , compared to vehicle-treated 0 and 30 minutes) (Appendix Figures A8 and A9).

Taken together, these data suggest that apyrase hydrolyses purine and pyrimidine NTPs and NDPs. These data also suggest that apyrase exhibits CD73-like activity.

**Table 5.1 Hydrolysis of nucleotides by apyrase**

<b>Nucleotide/ Nucleoside</b>	<b>Peak height (Absorbance 254 nm)</b>		
<b>100 <math>\mu</math>M ATP</b>	<b>Vehicle 0 minutes</b>	<b>Vehicle 30 minutes</b>	<b>Apyrase 30 minutes</b>
ATP	38150 $\pm$ 4007	37325 $\pm$ 4423	471 $\pm$ 471**
ADP	6445 $\pm$ 2604	5800 $\pm$ 1948	581 $\pm$ 47
AMP	390 $\pm$ 194	383 $\pm$ 151	1068 $\pm$ 1019
Adenosine	319 $\pm$ 319	556 $\pm$ 284	65077 $\pm$ 17289**
<b>100 <math>\mu</math>M ADP</b>	<b>Vehicle 0 minutes</b>	<b>Vehicle 30 minutes</b>	<b>Apyrase 30 minutes</b>
ATP	1751 $\pm$ 137	1299 $\pm$ 443	0 $\pm$ 0
ADP	32677 $\pm$ 1635	32558 $\pm$ 1754	517 $\pm$ 64**
AMP	2743 $\pm$ 201	1875 $\pm$ 292	853 $\pm$ 230
Adenosine	620 $\pm$ 312	1734 $\pm$ 220	64701 $\pm$ 6518**
<b>100 <math>\mu</math>M UTP</b>	<b>Vehicle 0 minutes</b>	<b>Vehicle 30 minutes</b>	<b>Apyrase 30 minutes</b>
UTP	23045 $\pm$ 4521	23689 $\pm$ 4307	3156 $\pm$ 95* (vehicle 30 minutes)
UDP	5062 $\pm$ 989	4508 $\pm$ 674	10 $\pm$ 10
UMP	687 $\pm$ 66	646 $\pm$ 47	36189 $\pm$ 9890**
Uridine	49 $\pm$ 26	32 $\pm$ 32	30479 $\pm$ 4862**
<b>100 <math>\mu</math>M UDP</b>	<b>Vehicle 0 minutes</b>	<b>Vehicle 30 minutes</b>	<b>Apyrase 30 minutes</b>
UTP	1489 $\pm$ 605	1671 $\pm$ 675	1326 $\pm$ 482
UDP	39213 $\pm$ 3256	37527 $\pm$ 2846	0 $\pm$ 0**
UMP	2248 $\pm$ 73	2173 $\pm$ 60	40600 $\pm$ 5145**
Uridine	87 $\pm$ 44	213 $\pm$ 50	30432 $\pm$ 132**

Peak height (absorbance at  $A_{254nm}$ ) for extracellular nucleotides (100  $\mu$ M) at 0 and 30 minutes in the presence of vehicle (SBS) and after 30 minutes incubation with apyrase (2 U/ml). Data represents mean  $\pm$  SEM from n=3 replicates. Asterisks indicate significant changes towards vehicle-treated samples at 0 and 30 minutes unless otherwise stated (\*\*p<0.01, \*p<0.05, One-way ANOVA with Bonferroni's multiple comparison).

### 5.3.2.2 Effect of apyrase on CCL2-evoked Ca<sup>2+</sup> responses in THP-1 cells and human PBMCs

To determine the requirement of extracellular nucleotides for CCL2/CCR2-mediated monocyte signalling, studies examined the effects of apyrase (2 U/ml) on CCL2-evoked intracellular Ca<sup>2+</sup> responses in THP-1 cells and human PBMCs. Initial experiments tested the effects of apyrase on THP-1 intracellular Ca<sup>2+</sup> responses evoked by a range of concentrations of CCL2 (1-500 ng/ml).

As shown (Figure 5.2a), addition of apyrase to THP-1 cells caused a small dip in the baseline Ca<sup>2+</sup> response ( $-3\% \pm 0.3\%F_{max}$ ,  $n=3$ ). A similar effect was not seen with vehicle, which indicated the possibility that Ca<sup>2+</sup> homeostasis was being modulated by apyrase through its ability to scavenge nucleotides. As also shown (Figure 5.2b and c), apyrase attenuated intracellular Ca<sup>2+</sup> responses evoked by all concentrations of CCL2, causing a rightward parallel shift in the CCL2 concentration-response curve which could only be surmounted by increasing the concentration of CCL2. The EC<sub>50</sub> values for CCL2 in untreated and apyrase-treated THP-1 cells were  $15 \pm 3$  ng/ml ( $n=3$ ) and  $65 \pm 8$  ng/ml ( $n=3$ ), respectively, and indicated that apyrase reduced the potency of CCL2 by 4-fold. For a single concentration of 50 ng/ml CCL2, the %F<sub>max</sub> values of untreated ( $15 \pm 2\%$ ,  $n=3$ ) and apyrase-treated ( $6 \pm 0.3\%$ ,  $n=3$ ) cells indicated a % inhibition of  $59 \pm 5\%$  ( $n=3$ ,  $p<0.01$ ).

To determine whether apyrase treatment also affected the decay of CCL2 Ca<sup>2+</sup> transients, the  $\tau$  values for treatments were analysed and compared. Figure 5.2d shows the decay rates ( $\tau$ , sec) for Ca<sup>2+</sup> transients to CCL2 100, 50, and 30 ng/ml in untreated and apyrase-treated THP-1 cells. Although apyrase treatment reduced the  $\tau$  values for all three CCL2 concentrations, a significant reduction ( $80 \pm 1\%$ ,  $n=3$ ,  $p<0.01$ ) was only observed for 30 ng/ml CCL2, where the  $\tau$  values for untreated and apyrase-treated cells were  $123 \pm 6$  seconds ( $n=3$ ) and  $25 \pm 1$  seconds ( $n=3$ ), respectively. Although apyrase also caused a reduction in  $\tau$  for 100 ng/ml CCL2, the values for untreated ( $82 \pm 16$  seconds,  $n=3$ ) and apyrase-treated ( $39 \pm 1$  seconds,  $n=3$ ) cells were not significantly different ( $n=3$ ,  $p>0.05$ ). Similarly, the  $\tau$  values for 50 ng/ml CCL2 in untreated ( $74 \pm 14$  seconds,  $n=3$ ) and apyrase-treated ( $35 \pm 1$  seconds,  $n=3$ ) cells were also not significantly different ( $n=3$ ,  $p>0.05$ ). Although a significant reduction in  $\tau$  was not seen with higher concentrations of CCL2, these data suggest that apyrase promotes a more rapid decay of CCL2 Ca<sup>2+</sup> transients.

It is widely accepted that E-NTPDases require Ca<sup>2+</sup> or Mg<sup>2+</sup> for activity (Kukulski *et al.*, 2005). Thus, it was hypothesised that the effects of apyrase would be partially dependent on Ca<sup>2+</sup>. To examine this hypothesis, the effects of apyrase (2 U/ml) on CCL2 (50 ng/ml)-

evoked intracellular  $\text{Ca}^{2+}$  responses were assessed in the absence of extracellular  $\text{Ca}^{2+}$  by resuspending cells in an SBS buffer from which  $\text{Ca}^{2+}$  was omitted (1.5 mM  $\text{CaCl}_2$ ) and replaced with the  $\text{Ca}^{2+}$  chelator, EGTA (1 mM) (see Chapter 2, Section 2.6.2 for details). As shown (Figure 5.3a), apyrase again produced a small dip in the baseline  $\text{Ca}^{2+}$  response. Although this effect of apyrase was similar to previous experiments, the %Fmax values were <1% and therefore, not possible to quantify. As also shown (Figure 5.3b and c), apyrase attenuated CCL2-evoked intracellular  $\text{Ca}^{2+}$  responses by  $85 \pm 7\%$  ( $n=3$ ,  $p<0.05$ ), where the %Fmax values for untreated and apyrase-treated cells were  $10 \pm 2\%$  ( $n=3$ ) and  $1 \pm 1\%$  ( $n=3$ ), respectively. This result is interesting because it suggests that CCL2-evoked  $\text{Ca}^{2+}$  responses are more susceptible to apyrase in the absence of extracellular  $\text{Ca}^{2+}$  than in the presence of extracellular  $\text{Ca}^{2+}$ , where 50 ng/ml CCL2 responses were attenuated by  $59 \pm 5\%$  ( $n=3$ ,  $p<0.01$ ). What is also interesting about these data is that they suggest that  $\text{Mg}^{2+}$  (1.2 mM) in the experimental buffer may have compensated for the lack of  $\text{Ca}^{2+}$ . From the data in Figure 5.3, it can also be seen that THP-1 cells exhibited an apyrase-resistant component of  $\sim 15\%$ Fmax, which may indicate a bona-fide activation of CCR2 by CCL2. Due to the low CCL2  $\text{Ca}^{2+}$  responses in apyrase-treated cells, the decay rates for treatments could not be determined.

The effects of apyrase (2 U/ml) were next examined on CCL2 (50 ng/ml)-evoked intracellular  $\text{Ca}^{2+}$  responses in human PBMCs. As shown (Figure 5.4), apyrase attenuated CCL2-evoked  $\text{Ca}^{2+}$  responses by  $47 \pm 3\%$  ( $n=3$ ,  $p<0.01$ ), where the %Fmax values for untreated and apyrase-treated PBMCs were  $6 \pm 0.3\%$  ( $n=3$ ) and  $3 \pm 0.3\%$  ( $n=3$ ), respectively. These data support THP-1 cell data but also suggest that apyrase attenuates CCL2-evoked  $\text{Ca}^{2+}$  responses in a mixed cell population likely to contain CCR2-expressing monocytes. The heterogeneous nature of PBMCs may also explain why apyrase attenuated CCL2-evoked  $\text{Ca}^{2+}$  responses less in PBMCs than in THP-1 cells. A further analysis of the decay rates for all treatments showed that the  $\tau$  values for untreated ( $59 \pm 29$  seconds,  $n=3$ ) and apyrase-treated cells ( $39 \pm 12$  seconds,  $n=3$ ) were not significantly different ( $n=3$ ,  $p>0.05$ ). This data suggests that apyrase does not influence the decay of CCL2  $\text{Ca}^{2+}$  transients in PBMCs.

Taken together, these results suggest that extracellular nucleotides are likely to be required for efficient CCL2/CCR2-mediated monocyte signalling.

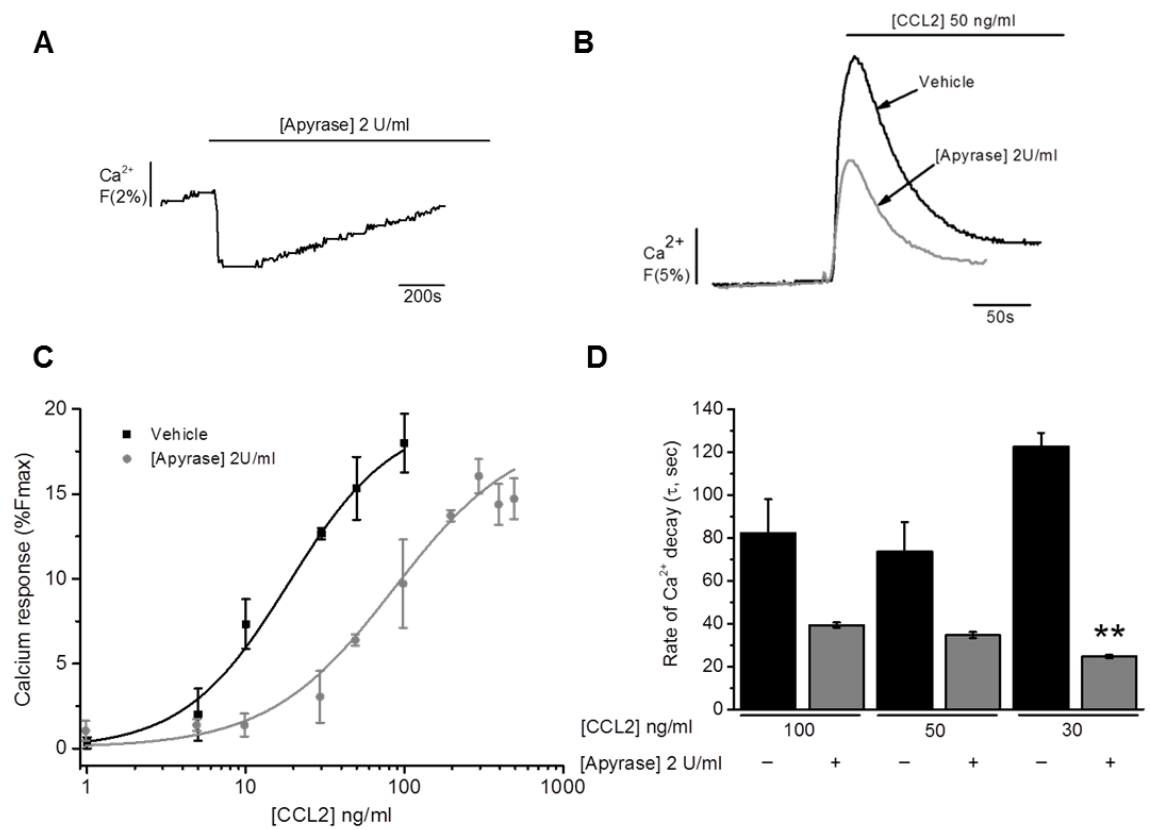


**Figure 5.2 Effect of apyrase on CCL2-evoked  $\text{Ca}^{2+}$  responses in THP-1 cells**

(A) Representative trace showing the effect of apyrase (2U /ml) on baseline  $\text{Ca}^{2+}$ . (B) Representative  $\text{Ca}^{2+}$  transients and (C) normalised concentration-response curve showing intracellular  $\text{Ca}^{2+}$  responses to CCL2 (1-500 ng/ml) in THP-1 cells pre-treated with vehicle (water) or apyrase (2 U/ml), for 10 minutes. Responses normalised to  $\text{Ca}^{2+}$  signals elicited by 40  $\mu\text{M}$  digitonin (% Fmax). (D) Bar chart showing  $\text{Ca}^{2+}$  decay rates ( $\tau$ , sec) for  $\text{Ca}^{2+}$  transients to CCL2 (30-100 ng/ml) in THP-1 cells pre-treated with vehicle (water) or apyrase (2 U/ml), for 10 minutes. Data represents mean  $\pm$  SEM from n=3 replicates. Asterisks indicate significant changes towards vehicle (\*\*p<0.01, Students t-test).

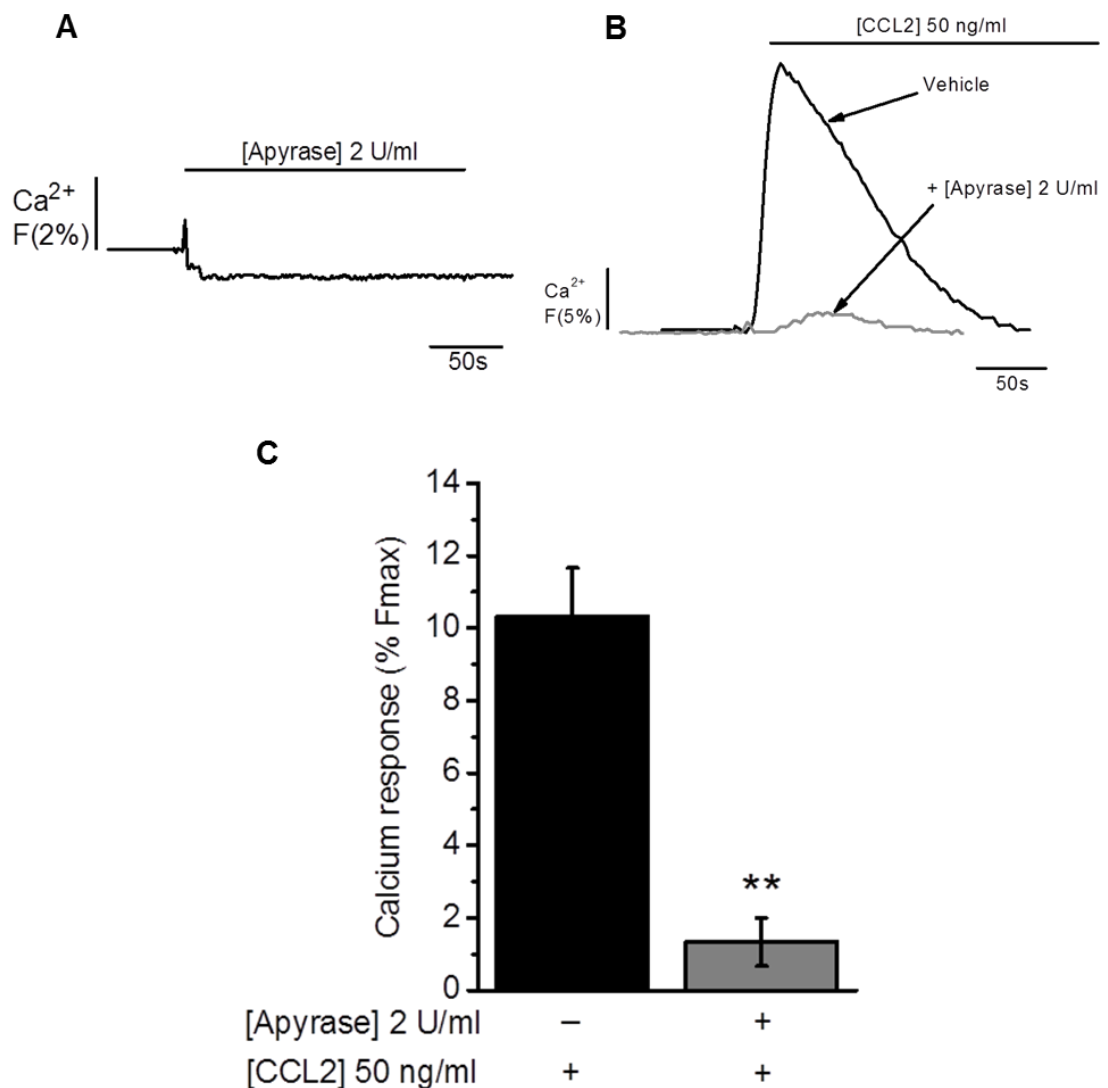


**Figure 5.3** Effect of apyrase on CCL2-evoked Ca<sup>2+</sup> responses in THP-1 cells in the absence of extracellular Ca<sup>2+</sup>

(A) Representative trace showing the effect of apyrase (2U /ml) on baseline Ca<sup>2+</sup>. (B) Representative Ca<sup>2+</sup> transients to CCL2 (50 ng/ml) in THP-1 cells pre-treated with vehicle (water) or apyrase (2 U/ml), for 10 minutes. (C) Bar chart showing normalised intracellular Ca<sup>2+</sup> responses to CCL2 (50 ng/ml) in THP-1 cells pre-treated with vehicle (water) or apyrase (2 U/ml), for 10 minutes. Responses normalised to Ca<sup>2+</sup> signals elicited by 40 µM digitonin (% Fmax). Data represents mean ± SEM from n=3 replicates. Asterisks indicate significant changes towards vehicle (\*\*p<0.01, Students t-test).

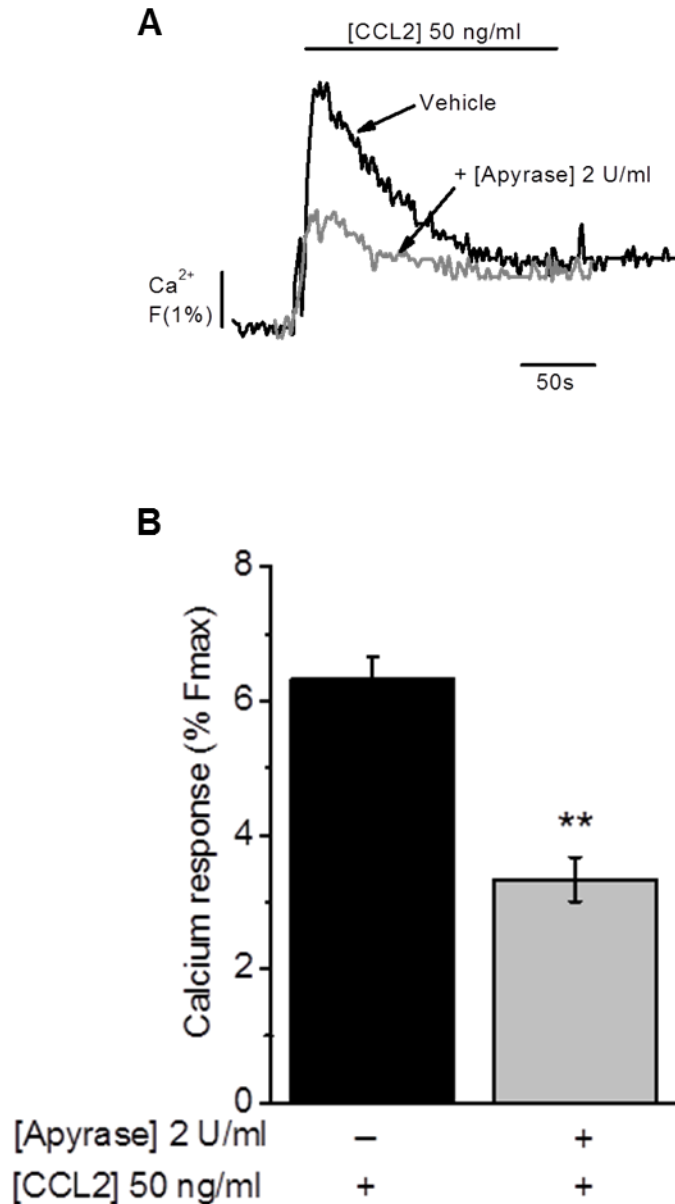


**Figure 5.4 Effect of apyrase on CCL2-evoked  $\text{Ca}^{2+}$  responses in human PBMCs**

(A) Representative  $\text{Ca}^{2+}$  transients to CCL2 (50 ng/ml) in PBMCs pre-treated with vehicle (water) or apyrase (2 U/ml), for 10 minutes. (B) Bar chart showing normalised intracellular  $\text{Ca}^{2+}$  responses to CCL2 (50 ng/ml) in PBMCs pre-treated with vehicle (water) or apyrase (2 U/ml), for 10 minutes. Responses normalised to  $\text{Ca}^{2+}$  signals elicited by 40  $\mu\text{M}$  digitonin (% Fmax). Data represents mean  $\pm$  SEM from n=3 replicates. Asterisks indicate significant changes towards vehicle (\*\* $p < 0.01$ , Students t-test).

### 5.3.2.3 Effect of apyrase on CCL2-mediated THP-1 cell chemotaxis and adhesion

To examine the requirement of extracellular nucleotides for CCL2/CCR2-mediated monocyte function, THP-1 cells and PBMCs were employed as models to test the effects of apyrase (2 U/ml) on cellular chemotaxis towards CCL2 (50 ng/ml). As shown (Figures 5.5 and 5.6), apyrase attenuated THP-1 cell chemotaxis, but enhanced PBMC chemotaxis. In THP-1 cell experiments (Figure 5.5), a significantly higher chemotactic index was observed towards CCL2 ( $7 \pm 2$ ,  $n=5$ ) than towards vehicle ( $1 \pm 0.2$ ,  $n=5$ ,  $p<0.01$ ). Interestingly, the chemotactic indexes for untreated ( $7 \pm 2$ ,  $n=5$ ) and apyrase-treated cells ( $2 \pm 0.4$ ,  $n=5$ ) reflected an inhibition of  $71 \pm 11\%$  ( $n=5$ ,  $p<0.05$ ), and suggested that apyrase almost abolished CCL2-dependent chemotaxis. In experiments with human PBMCs (Figure 5.6), although a one-way ANOVA analysis suggested that the chemotactic index of cells exposed to CCL2 ( $17 \pm 2$ ,  $n=12$ ) was significantly higher than cells migrating towards vehicle ( $1 \pm 0.2$ ,  $n=12$ ,  $p<0.01$ ), a Bonferroni's means comparison suggested that these populations were not significantly different ( $n=12$ ,  $p>0.05$ ). Despite this, it was seen that apyrase enhanced PBMC migration towards CCL2 by  $3.7 \pm 1$ -fold ( $n=12$ ,  $p<0.01$ ), where the chemotactic indexes for untreated and apyrase-treated PBMCs were  $17 \pm 2$  ( $n=12$ ) and  $62 \pm 11$  ( $n=12$ ), respectively. These data are difficult to explain, but it might be that apyrase has a chemotactic effect on mixed cell populations.

Studies by Grünwald and Ridley (2010) have shown that the ecto-nucleotidase, CD73 represses THP-1 cell adhesion to HUVECs by generating adenosine. In HPLC studies (Section 5.3.2.1), incubation of ATP and ADP with apyrase produced adenosine, suggesting that apyrase exhibits CD73-like activity. This suggests that in an *in vitro* or *in vivo* environment, apyrase would prevent monocyte adhesion to the vascular endothelium. Thus, in an effort to examine this hypothesis, studies tested the effects of apyrase (2 U/ml) on the adhesion of CCL2-primed THP-1 cells to quiescent HUVEC monolayers.

As shown (Figure 5.7), apyrase treatment caused a  $5.9 \pm 1$ -fold ( $n=16$ ,  $p<0.01$ ) increase in the adhesion of vehicle-treated THP-1 cells, where the %CCL2 control values for untreated (vehicle alone) and apyrase/vehicle-treated cells were  $19 \pm 7\%$  ( $n=16$ ) and  $111 \pm 25\%$  ( $n=16$ ), respectively. The %CCL2 control values for CCL2-primed untreated and apyrase-treated cells were  $100 \pm 13\%$  ( $n=16$ ,  $p<0.05$ ) and  $118 \pm 26\%$  ( $n=16$ ,  $p<0.01$ ), respectively. These data suggested that CCL2-priming and/or apyrase treatment promoted THP-1 cell adhesion.

Taken together, these data suggest that apyrase differentially modulates CCL2/CCR2-mediated THP-1 cell and PBMC function. The effects of apyrase in these models would need to be considered when performing *in vivo* studies.

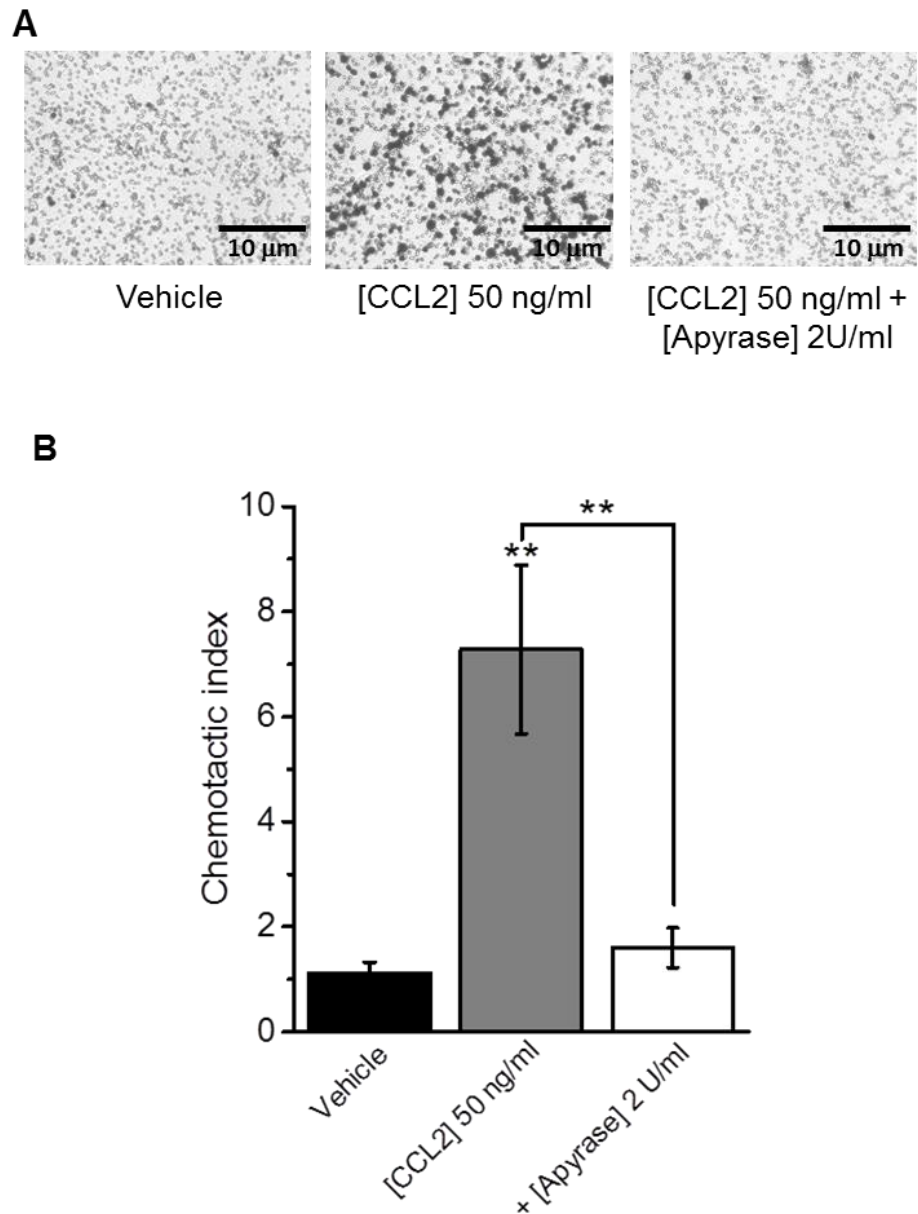


**Figure 5.5 Effect of apyrase on CCL2-mediated THP-1 cell chemotaxis**

(A) Representative images showing the effect of apyrase (2 U/ml) on THP-1 cell chemotaxis towards CCL2 (50 ng/ml, lower chamber, 2hrs). Scale bar represents 10 µm.

(B) Bar chart showing normalised THP-1 cell chemotaxis towards vehicle (water) or CCL2 (50 ng/ml, lower chamber, 2hrs), in the presence of apyrase (2U/ml). Chemotactic index is a ratio of the number of cells that migrated towards CCL2 over the number of cells that migrated towards vehicle. Data represents mean  $\pm$  SEM from n=4 transwells. Asterisks indicate significant changes towards vehicle (\*\*p<0.01, One-way ANOVA with Bonferroni's multiple comparison).

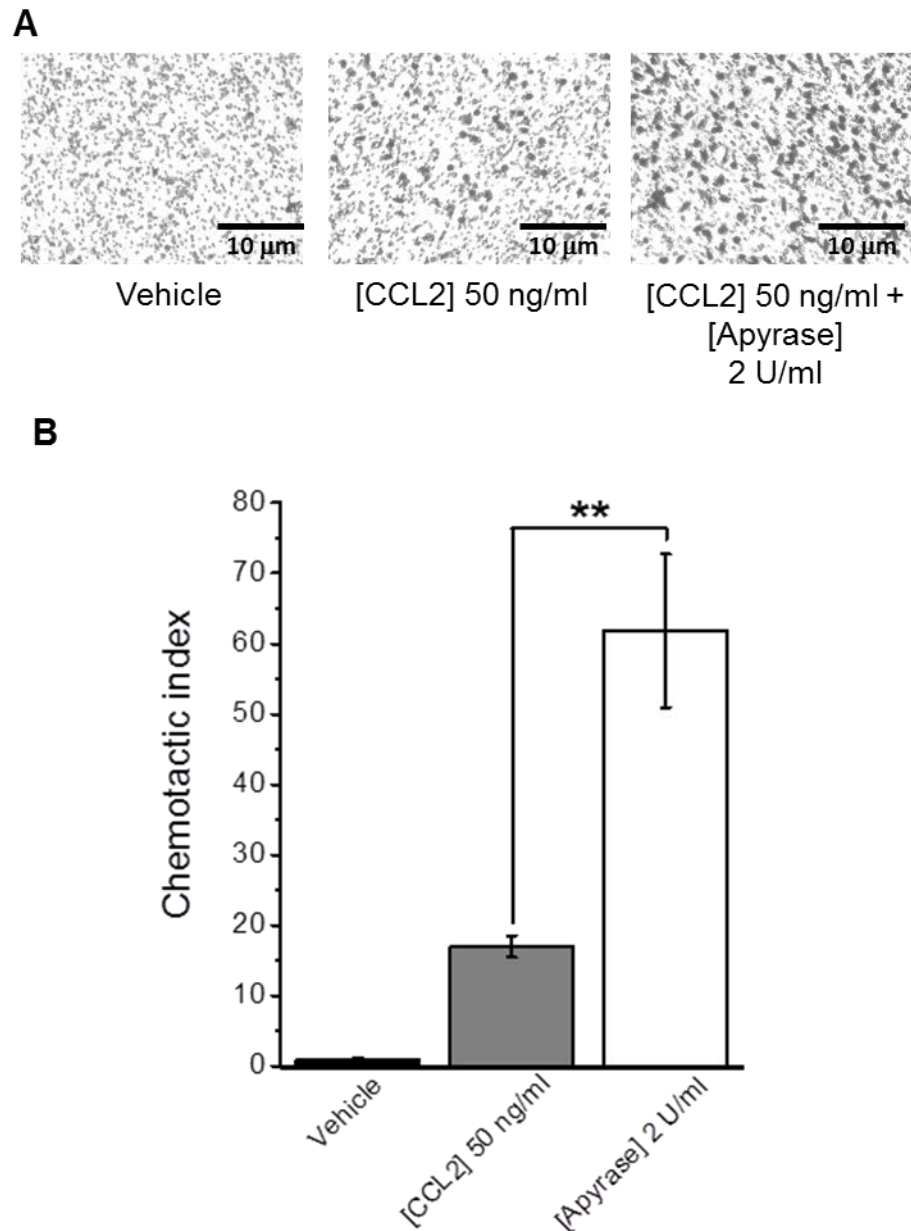


**Figure 5.6 Effect of apyrase on CCL2-mediated human PBMC chemotaxis**

(A) Representative images showing the effect of apyrase (2 U/ml) on PBMC chemotaxis towards CCL2 (50 ng/ml, lower chamber, 2hrs). Scale bar represents 10  $\mu\text{m}$ . (B) Bar chart showing normalised PBMC chemotaxis towards vehicle (water) or CCL2 (50 ng/ml, lower chamber, 2hrs), in the presence of apyrase (2U/ml). Chemotactic index is a ratio of the number of cells that migrated towards CCL2 over the number of cells that migrated towards vehicle. Data represents mean  $\pm$  SEM from a total of n=12 transwells from n=3 donors. Asterisks indicate significant changes towards vehicle (\*\*p<0.01, One-way ANOVA with Bonferroni's multiple comparison).

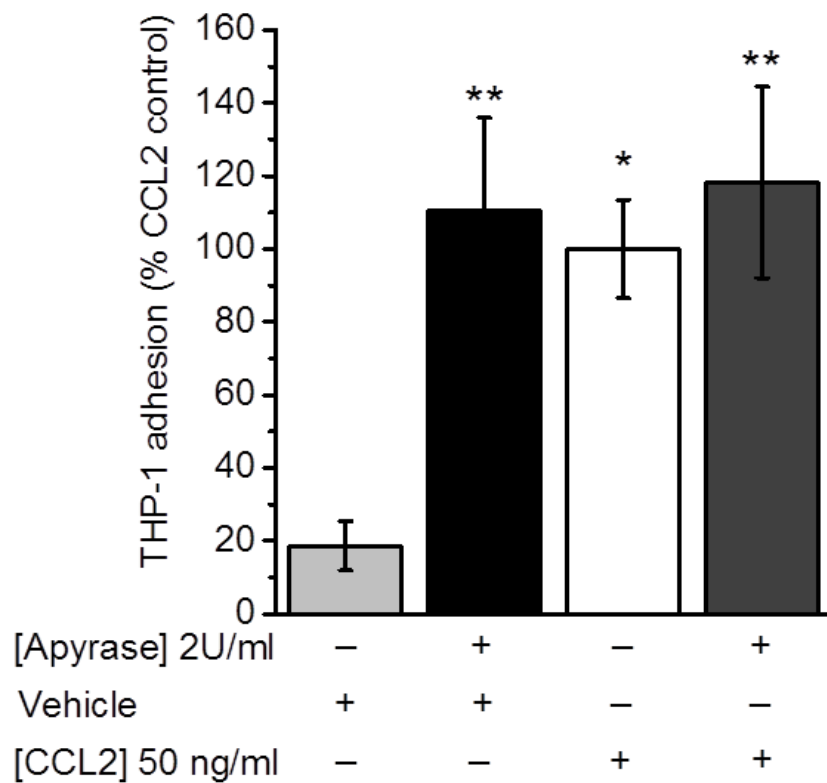


**Figure 5.7 Effect of apyrase on THP-1 cell adhesion to quiescent HUVEC monolayers**

Bar chart showing normalised adhesion of vehicle or CCL2-primed (50 ng/ml) THP-1 cells to quiescent HUVEC monolayers following treatment with vehicle (water) or apyrase (2 U/ml, 45 minutes). Normalised adhesion represented as a percentage of mean adhesion of CCL2-primed THP-1 cells in the absence of apyrase. Data represents mean  $\pm$  SEM from a total of n=16 replicates from n=4 experiments. Asterisks indicate significant changes towards vehicle (\*p<0.05, \*\*p<0.01, One-way ANOVA with Bonferroni's multiple comparison).

#### 5.3.2.4 Effect of apyrase isoenzymes on CCL2-evoked Ca<sup>2+</sup> responses in THP-1 cells

The data presented has shown that apyrase hydrolyses NTPs, NDPs, and NMPs. As mentioned previously, the manufacturers claim that this apyrase consists of two isoenzymes, one with a high ratio (10:1) of ATPase to ADPase activity, and one with a low ratio (1:1) of ATPase to ADPase activity. Thus, for the purpose of this study, these isoenzymes were renamed “high NTPase/low NDPase” and “high NTPase/high NDPase”, respectively. The apyrase employed for the studies in thesis will be described in the current study as a “high NTPase/high NDPase” apyrase.

To examine the specific requirement of NTPs and NDPs for CCL2/CCR2-mediated monocyte signalling, studies employed a “high NTPase/high NDPase” apyrase (0-4 U/ml), and a second NTP-preferring “high NTPase/low NDPase” apyrase (0-4 U/ml). Studies tested the effects of these on THP-1 cell intracellular Ca<sup>2+</sup> responses evoked by 50 ng/ml CCL2.

As shown in Figure 5.8a, a small dip in the baseline Ca<sup>2+</sup> response was seen upon application of the “high NTPase/high NDPase” apyrase to cells (%Fmax 3 ± 0%, n=3), but not upon application of the “high NTPase/low NDPase”. This data suggests that baseline Ca<sup>2+</sup> responses may be more dependent on NDPs than NTPs. As also shown, a greater inhibition of CCL2-evoked intracellular Ca<sup>2+</sup> responses was observed with the “high NTPase/high NDPase” apyrase than with the “high NTPase/low NDPase” apyrase. At the highest concentration tested (4 U/ml), the “high NTPase/high NDPase” and “high NTPase/low NDPase” apyrases attenuated CCL2-evoked Ca<sup>2+</sup> responses by 79 ± 5% (n=3, p<0.05) and 44 ± 5% (n=3, p<0.01), respectively. Although these data suggested that the “high NTPase/high NDPase” apyrase attenuated CCL2 Ca<sup>2+</sup> responses almost 2-fold more than the “high NTPase/low NDPase” apyrase, a significant difference between these data sets was not found (n=3, p>0.05). However, at 0.25 U/ml, the “high NTPase/high NDPase” apyrase attenuated CCL2 Ca<sup>2+</sup> responses (36 ± 4%, n=3, p<0.05) significantly more (n=3, p<0.05) than the “high NTPase/low NDPase” apyrase (7 ± 7%, n=3, p>0.05). In paired experiments with 0.25 U/ml of the “high NTPase/high NDPase” apyrase, the %Fmax values for CCL2 in untreated and apyrase-treated cells were 18 ± 1% (n=3) and 10 ± 1% (n=3) respectively. For 0.25 U/ml of the “high NTPase/low NDPase” apyrase, these were 16 ± 2% (n=3) and 13 ± 3% (n=3), respectively. A significantly higher inhibition with the “high NTPase/high NDPase” over the “high NTPase/low NDPase”, was also observed at 0.1 U/ml, where the % inhibition values were 28 ± 4% (n=3, p<0.05) and 5 ± 3% (n=3, p>0.05), respectively. In these paired experiments, for the “high NTPase/high NDPase” apyrase, the %Fmax values for CCL2 in untreated and apyrase-treated cells were 18 ± 1% (n=3) and 12 ± 2% (n=3) respectively, while for the “high NTPase/low NDPase” apyrase, these were 16 ± 2% (n=3) and 14 ± 3%

(n=3), respectively. In general, these data suggested that at lower concentrations, the “high NTPase/high NDPase” apyrase attenuated CCL2 Ca<sup>2+</sup> responses far better than the “high NTPase/low NDPase” apyrase. Interestingly, these data also showed that a 10-fold higher concentration (0.1 U/ml) of the “high NTPase/low NDPase” apyrase was required than the “high NTPase/high NDPase” apyrase to redeem 100% of the control CCL2 Ca<sup>2+</sup> response.

To assess whether these isoenzymes differentially affected the decay of CCL2 Ca<sup>2+</sup> transients, the decay rates ( $\tau$ , sec) for all treatments were analysed and compared where possible. A significant difference in  $\tau$  between the apyrases was not observed for any of the concentrations examined (4, 2, 1, 0.5, 0.25, 0.1 U/ml) (n=3, p<0.05). For example, at 0.25 U/ml, the  $\tau$  values for the “high NTPase/high NDPase” apyrase (46 ± 4 seconds, n=3) and “high NTPase/low NDPase” apyrase (69 ± 8 seconds, n=3) were not significantly different (n=3, p>0.05).

Taken together, these data suggest that CCL2-evoked intracellular Ca<sup>2+</sup> responses in THP-1 cells are more sensitive to inhibition by “high NTPase/high NDPase” apyrase. This suggests that NDPs contribute to CCL2/CCR2-mediated monocyte signalling more than NTPs.

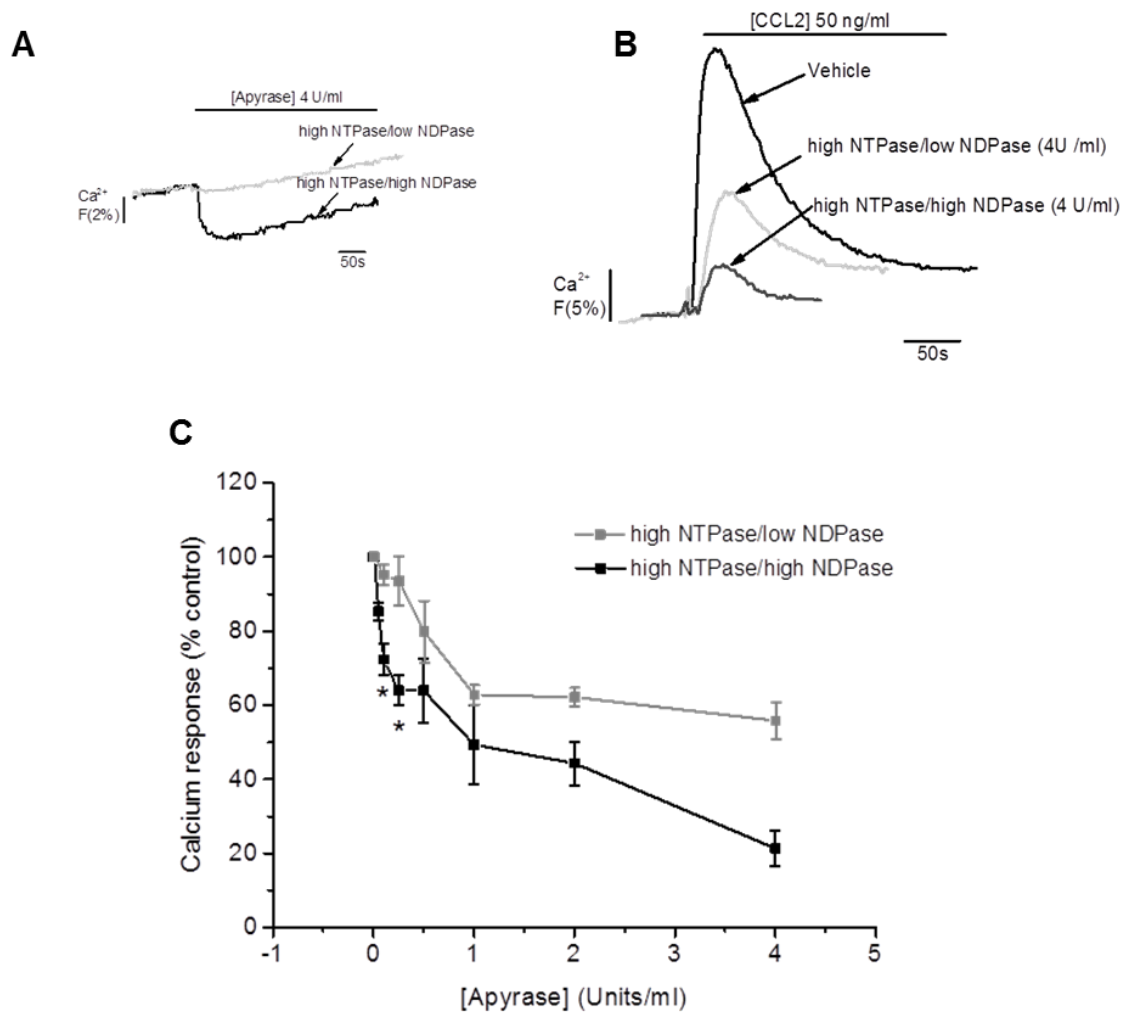


**Figure 5.8 Effect of apyrase isoenzymes on CCL2-evoked Ca<sup>2+</sup> responses in THP-1 cells**

(A) Representative trace showing the effect of two different apyrases on baseline Ca<sup>2+</sup>. (B) Representative Ca<sup>2+</sup> transients to CCL2 (50 ng/ml) in THP-1 cells pre-treated with vehicle (water) or apyrases with varying NDPase activity (0-4 U/ml) for 10 minutes. (C) Concentration-response graph showing % CCL2 control values for normalised intracellular Ca<sup>2+</sup> responses to CCL2 (50 ng/ml) in THP-1 cells pre-treated with vehicle (water) or apyrases with varying NDPase activity (0-4 U/ml) for 10 minutes. Responses given as a percentage of normalised intracellular Ca<sup>2+</sup> responses to CCL2 (50 ng/ml) in the absence of apyrase. Responses normalised to Ca<sup>2+</sup> signals elicited by 40 μM digitonin (%Fmax). Data represents mean ± SEM from n=3 replicates (\*p<0.05, Students t-test).

### 5.3.3 Effect of ADA on CCL2-evoked Ca<sup>2+</sup> responses in THP-1 cells

The HPLC results presented in this chapter suggest that apyrase exhibits CD73-like activity and produces adenosine from ATP and ADP. It is possible, therefore, that the effects of apyrase on THP-1 cells and PBMCs reflect an activation of P1 purinoceptors by adenosine. In an effort to examine this hypothesis, studies employed adenosine deaminase (ADA, EC 3.5.4.4), an enzyme responsible for irreversibly deaminating adenosine to inosine (Yegutkin, 2008). In humans, two isoenzymes of ADA have been identified, ADA1 (ADA) and ADA2 which can exist either as intracellular cytosolic enzymes, or as ecto-ADAs (Wiginton *et al.*, 1986; Zavialov and Engström, 2005).

To address the aim of this study, experiments tested the effects of ADA on intracellular Ca<sup>2+</sup> responses evoked by 50, 20, and 10 ng/ml CCL2. As shown in Table 5.2, Ca<sup>2+</sup> responses evoked by all three CCL2 concentrations were not significantly affected by ADA (n=3, p>0.05). For example, in experiments with CCL2 20 ng/ml, the %Fmax values for CCL2 in untreated and ADA-treated cells were 22 ± 1% (n=4) and 18 ± 2% (n=4), respectively.

The decay rates ( $\tau$ , sec) for Ca<sup>2+</sup> transients were also compared for all treatments but were not found to be significantly different (n=4, p>0.05, data not shown). For example, for 20 ng/ml CCL2, the  $\tau$  values for untreated and apyrase-treated cells were 79 ± 2 seconds (n=4) and 77 ± 2 seconds (n=4), respectively.

Taken together, these data suggest that CCL2/CCR2-mediated monocyte signalling is unlikely to involve adenosine.

**Table 5.2 Effect of ADA on CCL2-evoked Ca<sup>2+</sup> responses in THP-1 cells**

[CCL2] ng/ml	Ca <sup>2+</sup> response (%Fmax)	
	Vehicle	ADA 2U/ml
50	29 ± 1	27 ± 1
20	22 ± 1	18 ± 2
10	16 ± 1	14 ± 1

Intracellular Ca<sup>2+</sup> responses to CCL2 (50, 20 and 10 ng/ml) in THP-1 cells pre-treated with vehicle (water) or ADA (2 U/ml), for 15 minutes. Responses normalised to Ca<sup>2+</sup> signals elicited by 40 µM digitonin (% Fmax). Data represents mean ± SEM from n=3 (CCL2 50 and 10 ng/ml) and n=4 (CCL2 20 ng/ml) replicates.

### **5.3.4 Effect of endogenous ecto-nucleotidases on CCL2/CCR2-mediated THP-1 cell signalling**

The ecto-nucleotidases are a family of extracellular plasma membrane enzymes that rapidly hydrolyse extracellular nucleotides in order to control their availability at purinoceptors (Zimmermann *et al.*, 2012). Although the E-NTPDases serve as the major ecto-nucleotidase family involved in hydrolysing NTPs and NDPs, the ecto-nucleotide pyrophosphatase/phosphodiesterases (E-NPPs) and alkaline phosphatases (APs) also contribute to NTP and NDP hydrolysis (Zimmermann *et al.*, 2012).

Given their ubiquitous expression in essentially every tissue and cell (Robson *et al.*, 2006; Kukulski *et al.*, 2011), ecto-nucleotidases are likely to be constantly involved in regulating extracellular nucleotide availability. The evidence presented in this chapter has suggested that extracellular nucleotides are required for CCL2/CCR2-mediated monocyte signalling and function. It is possible, therefore, that by regulating the availability of extracellular nucleotides, endogenous ecto-nucleotidases also regulate CCL2/CCR2 signalling. To examine this hypothesis, the next studies tested for the presence of endogenous ecto-nucleotidases in monocytic THP-1 cells, and following confirmation of their presence, investigated the effects of ecto-nucleotidases inhibitors on CCL2-evoked intracellular Ca<sup>2+</sup> responses.

#### **5.3.4.1 Endogenous ecto-nucleotidases in THP-1 cells**

Experiments testing for the presence of endogenously active ecto-nucleotidases involved spiking THP-1 cells or SBS with 100  $\mu$ M ATP, and incubating for 30 minutes at room temperature. Levels of ATP in supernatants (as measured by peak height) were tested using HPLC and compared with 0 minute samples.

As shown (Table 5.3 and Appendix Figure A10), incubation of ATP with THP-1 cells significantly reduced the peak height of ATP by  $11 \pm 2\%$  ( $n=4$ ,  $p<0.05$ ). A reduction in the levels of ATP in THP-1 cell supernatants was accompanied by a  $1.9 \pm 0.05$ -fold ( $n=4$ ,  $p<0.01$ ) and  $13 \pm 0.2$ -fold ( $n=4$ ,  $p<0.01$ ) increase in ADP and AMP, respectively. Interestingly, the peak heights of ATP, ADP and AMP were unchanged in experiments involving SBS ( $n=4$ ,  $p>0.05$ ) (Table 5.3 and Appendix Figure A10). These data suggested that a reduction in ATP levels in the presence of THP-1 cells occurred as a direct result of hydrolysis by endogenous ecto-nucleotidases.

Taken together, these data suggest that endogenous ecto-nucleotidases in THP-1 cells are capable of hydrolysing extracellular nucleotides.

**Table 5.3 Effect of THP-1 cells and SBS on nucleotide and nucleoside levels**

Peak height (Absorbance 254 nm)		
THP-1 cells	0 minutes	30 minutes
ATP	50211 ± 1086 (100 µM ATP)	44688 ± 479*
ADP	2732 ± 215	5052 ± 133**
AMP	75 ± 44	950 ± 11**
Adenosine	67 ± 67	154 ± 60

Peak height (Absorbance 254 nm)		
SBS	0 minutes	30 minutes
ATP	44983 ± 522 (100 µM ATP)	45128 ± 178
ADP	2989 ± 790	2630 ± 814
AMP	29 ± 29	0 ± 0

Peak heights for extracellular nucleotides and nucleosides following incubation of ATP (100 µM) for 0 or 30 minutes with THP-1 cells or SBS. Data represents mean ± SEM from n=4 experiments. Asterisks indicate significant changes towards 0 minutes (\*\*p<0.01, \*p<0.05, Students t-test).

#### 5.3.4.2 Effect of ecto-nucleotidase inhibitors on CCL2-evoked Ca<sup>2+</sup> responses in THP-1 cells

Based on the above data, it was hypothesised that inhibiting endogenous ecto-nucleotidases would modulate CCL2/CCR2-mediated monocyte signalling. To examine the validity of this hypothesis, studies tested the effects of the E-NTPDase-preferring ecto-nucleotidase inhibitors ARL-67156 and POM-1 on CCL2-evoked intracellular Ca<sup>2+</sup> responses in THP-1 cells.

##### 5.3.4.2.1 ARL-67156

Initial experiments employed ARL-67156, a structural analogue of ATP reported to weakly inhibit NTPDase1, NTPDase3, and E-NPP1 with K<sub>i</sub> values of 11, 18, and 12 µM, respectively (Lévesque *et al.*, 2007). To address the above aim, the effects of 100 µM ARL-67156 on intracellular Ca<sup>2+</sup> responses evoked by 50, 20 and 10 ng/ml CCL2, were examined. As shown (Figure 5.9), treatment of THP-1 cells with ARL-67156 potentiated Ca<sup>2+</sup> responses evoked by 20 ng/ml CCL2 by 1.2 ± 0.05-fold (n=9, p<0.05), where the %F<sub>max</sub> values for CCL2 shifted from 15 ± 2% (n=9) for untreated cells to 17 ± 1% (n=9) for ARL-67156-treated cells. These data suggested that an inhibition of ecto-nucleotidases potentiated CCL2/CCR2-mediated monocyte signalling. Interestingly, Ca<sup>2+</sup>

responses evoked by 50 ng/ml CCL2 (n=4, p>0.05) and 10 ng/ml CCL2 (n=9, p>0.05) were not potentiated by ARL-67156. The %Fmax values for 50 ng/ml CCL2 in untreated and ARL-67156-treated cells were 25 ± 4% (n=4) and 25 ± 4% (n=4), respectively, while for 10 ng/ml CCL2 these were 20 ± 1% (n=9) and 22 ± 1% (n=9), respectively. A possible explanation for these results may be that the effects of ARL-67156 on these concentrations were difficult to detect as 10 ng/ml and 50 ng/ml CCL2 are the near-minimum and maximum concentrations on the CCL2 concentration-response curve (Chapter 4, Figure 4.1). When analysing the decay rates for all treatments, no significant differences between the  $\tau$  values for CCL2 in untreated and treated were observed (n=4-9, p>0.05). For example, in paired experiments with 20 ng/ml CCL2, the  $\tau$  values for untreated and ARL-67156-treated cells were 102 ± 5 seconds (n=9) and 97 ± 7 seconds (n=9), respectively (n=9, p>0.05).

Members of the E-NTPDase family of ecto-nucleotidases are known to depend on millimolar concentrations of Ca<sup>2+</sup> (or Mg<sup>2+</sup>) for activity (Kukulski *et al.*, 2005). It is possible, therefore, that the effects of ARL-67156 on CCL2-evoked intracellular Ca<sup>2+</sup> responses involve an inhibition of Ca<sup>2+</sup> or Mg<sup>2+</sup>-dependent E-NTPDases. To investigate the validity of this hypothesis, it was necessary to test the effects of ARL-67156 (100  $\mu$ M) on THP-1 cell intracellular Ca<sup>2+</sup> responses to 50, 20, and 10 ng/ml CCL2 in the absence of at least one of these ions, Ca<sup>2+</sup>.

As shown (Figure 5.10a and b), no significant differences between the %Fmax values for untreated and ARL-67156-treated cells were observed for any of the CCL2 concentrations tested (n=3-4, p>0.05). For example, in experiments with 50 ng/ml CCL2, the %Fmax values for untreated (7 ± 1%, n=3) and ARL-67156-treated cells (5 ± 1%, n=3) were not significantly different (n=3, p>0.05). These data are interesting as they suggest that the effects of ARL-67156 are Ca<sup>2+</sup>-dependent. Furthermore, the results of this study, together with apyrase studies, indicate that Ca<sup>2+</sup>-independent and -dependent E-NTPDases are likely to be involved in modulating CCL2-evoked intracellular Ca<sup>2+</sup> responses in monocytes.

To assess the effects of ARL-67156 on the decay of CCL2 Ca<sup>2+</sup> responses, the  $\tau$  values for all treatments were compared. As shown (Figure 5.10c), ARL-67156 significantly reduced  $\tau$  for Ca<sup>2+</sup> transients to 20 ng/ml CCL2 by 11 ± 3% (n=4, p<0.05), where the  $\tau$  values for CCL2 in untreated and ARL-67156-treated cells were 267 ± 51 seconds (n=4), and 246 ± 50 seconds (n=4), respectively. Although these data suggested that ARL-67156 promoted a faster decay of CCL2 Ca<sup>2+</sup> transients, the opposite effect was seen on transients evoked by 10 ng/ml CCL2 where ARL-67156 increased  $\tau$  by 10 ± 7-fold (n=3, p<0.05). In these experiments, the  $\tau$  values for CCL2 in untreated and ARL-67156-treated

THP-1 cells were  $3094 \pm 2655$  seconds (n=3) and  $8184 \pm 3683$  seconds (n=3), respectively. Collectively, these data suggested that ARL-67156 differentially affected the decay of CCL2  $\text{Ca}^{2+}$  transients.

Taken together, these data suggest that  $\text{Ca}^{2+}$ -dependent endogenous ecto-nucleotidases contribute to modulating CCL2/CCR2-mediated  $\text{Ca}^{2+}$  responses.

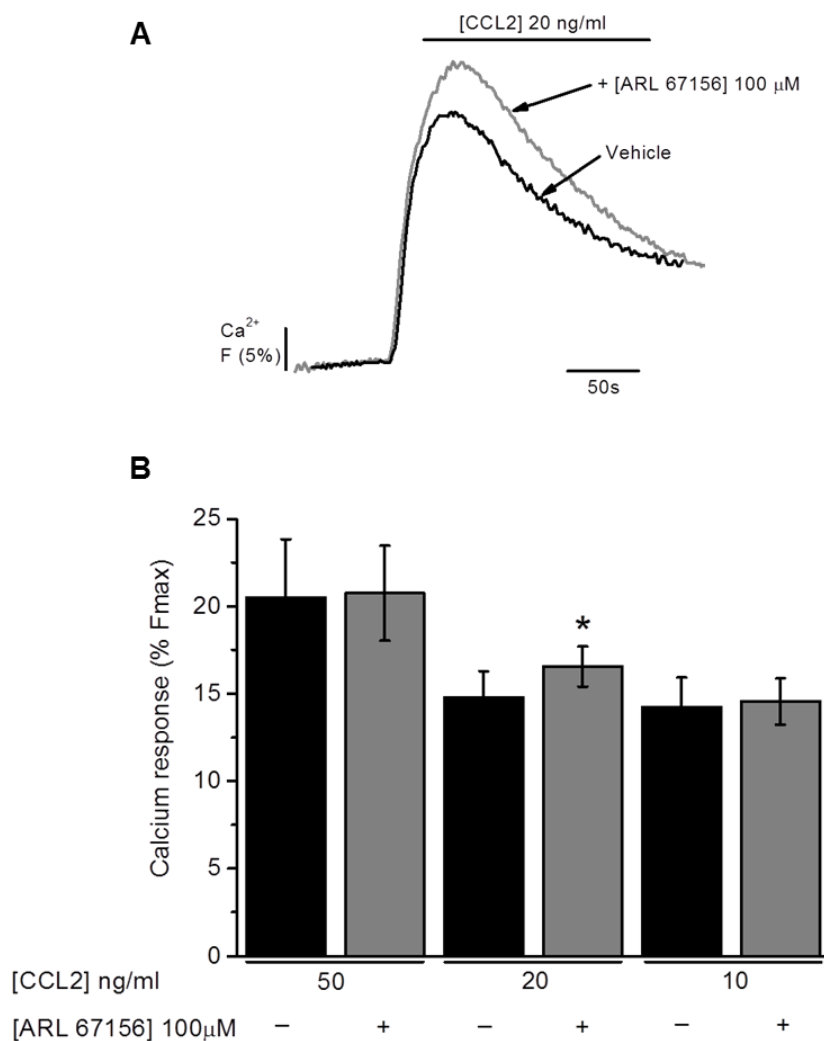


**Figure 5.9 Effect of ARL-67156 on CCL2-evoked  $\text{Ca}^{2+}$  responses in THP-1 cells**

(A) Representative  $\text{Ca}^{2+}$  transients to CCL2 (20 ng/ml) in THP-1 cells pre-treated with vehicle (water) or ARL-67156 (100  $\mu\text{M}$ ) for 15 minutes. (B) Bar chart showing normalised intracellular  $\text{Ca}^{2+}$  responses to CCL2 (50, 20 and 10 ng/ml) in THP-1 cells pre-treated with vehicle (water) or ARL-67156 (100  $\mu\text{M}$ ) for 15 minutes. Responses normalised to  $\text{Ca}^{2+}$  signals elicited by 40  $\mu\text{M}$  digitonin (% Fmax). Data represents mean  $\pm$  SEM from  $n=4$  (CCL2 50 ng/ml) or  $n=9$  (CCL2 20 and 10 ng/ml) replicates. Asterisks indicate significant changes towards vehicle (\* $p<0.05$ , Students t-test).

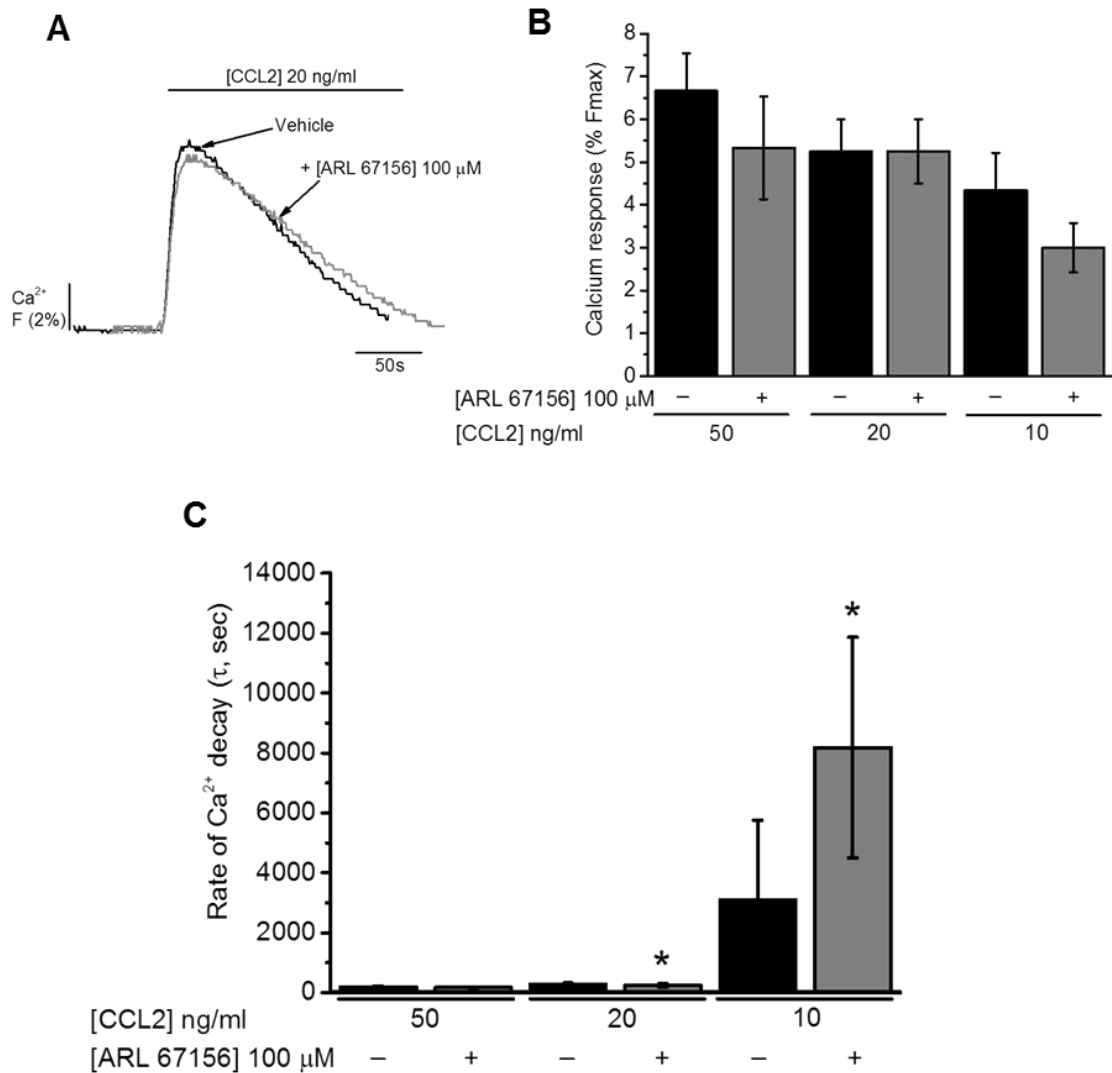


**Figure 5.10 Effect of ARL-67156 on CCL2-evoked Ca<sup>2+</sup> responses in THP-1 cells in the absence of extracellular Ca<sup>2+</sup>**

(A) Representative Ca<sup>2+</sup> transients and (B) bar chart showing normalised intracellular Ca<sup>2+</sup> responses to CCL2 (50, 20 and 10 ng/ml) in THP-1 cells pre-treated with vehicle (water) or ARL-67156 (100  $\mu$ M), for 15 minutes. Responses normalised to Ca<sup>2+</sup> signals elicited by 40  $\mu$ M digitonin (% Fmax). (C) Bar chart showing Ca<sup>2+</sup> decay rates ( $\tau$ , sec) for Ca<sup>2+</sup> transients to CCL2 (50, 20 and 10 ng/ml) in THP-1 cells pre-treated with vehicle (water) or ARL-67156 (100  $\mu$ M), for 15 minutes. Data represents mean  $\pm$  SEM from n=3 (CCL2 50 and 10 ng/ml) or n=4 (20 ng/ml) replicates. Asterisks indicate significant changes towards vehicle (\*p<0.05, Students t-test).

#### 5.3.4.2.2 POM-1

The polyoxymetalate compound POM-1 is an anionic complex comprised of transition metal ions bridged together by oxygen atoms. As an ecto-nucleotidase inhibitor, POM-1 inhibits NTPDase1, NTPDase2 and NTPDase3 with  $K_i$  values of 2.58, 28.8, and 3.26  $\mu\text{M}$ , respectively (Müller *et al.*, 2006). This data suggests that POM-1 is 4-times more potent than ARL-67156 at inhibiting NTPDase1.

In an effort to provide further support for the results of ARL-67156 studies, it was necessary to test the effects of POM-1 (1 and 100  $\mu\text{M}$ ) on THP-1 cell intracellular  $\text{Ca}^{2+}$  responses evoked by 50, 20, and 10 ng/ml CCL2. As shown (Figure 5.11a), POM-1 caused a transient dip ( $-5 \pm 2\%F_{\text{max}}$ ,  $n=3$ ), in the baseline  $\text{Ca}^{2+}$  response. Although this result was interesting and similar to the effect of apyrase on baseline  $\text{Ca}^{2+}$ , it suggested that nucleotide accumulation by POM-1 suppressed baseline  $\text{Ca}^{2+}$ .

As also shown (Figure 5.11), 100  $\mu\text{M}$  POM-1 abolished intracellular  $\text{Ca}^{2+}$  responses evoked by 50 ng/ml ( $100 \pm 0\%$  inhibition,  $n=3$ ,  $p<0.01$ ) and 20 ng/ml CCL2 ( $100 \pm 0\%$ ,  $n=3$ ,  $p<0.01$ ), and almost abolished responses to 10 ng/ml CCL2 ( $96 \pm 4\%$ ,  $n=3$ ,  $p<0.01$ ). In these experiments, the  $\%F_{\text{max}}$  values for 50 ng/ml CCL2 in untreated and POM-1-treated cells were  $23 \pm 1\%$  ( $n=3$ ) and  $0 \pm 0\%$  ( $n=3$ ), respectively. For 20 ng/ml CCL2 these were  $10 \pm 2\%$  ( $n=3$ ) and  $0 \pm 0\%$  ( $n=3$ ), respectively, and for 10 ng/ml CCL2 these were ( $10 \pm 3\%$ ,  $n=3$ ) and ( $0.3 \pm 0.3\%$ ,  $n=3$ ), respectively. From Figure 5.11, it can also be seen that intracellular  $\text{Ca}^{2+}$  responses evoked by 50, 20, or 10 ng/ml CCL2 were not significantly affected by 1  $\mu\text{M}$  POM-1 ( $n=3$ ,  $p>0.05$ ). For example, the  $\%F_{\text{max}}$  values for 50 ng/ml CCL2 in untreated and POM-1-treated cells were  $23 \pm 1\%$  ( $n=3$ ) and  $21 \pm 0.3\%$  ( $n=3$ ), respectively. These data indicate that 100  $\mu\text{M}$  POM-1 attenuates CCL2/CCR2-mediated monocyte signalling.

The decay rates for CCL2  $\text{Ca}^{2+}$  transients for THP-1 cells treated with vehicle or 1  $\mu\text{M}$  POM-1 were also compared, but were not significantly different ( $n=3$ ,  $p>0.05$ , data not shown). For example, the  $\tau$  values for 50 ng/ml CCL2  $\text{Ca}^{2+}$  transients from untreated and treated cells were  $65 \pm 3$  seconds ( $n=3$ ) and  $64 \pm 2$  seconds ( $n=3$ ), respectively ( $n=3$ ,  $p>0.05$ ). Together, these data suggest that POM-1 (1  $\mu\text{M}$ ) does not affect the decay of CCL2  $\text{Ca}^{2+}$  transients.

While these data indicated that effects of 100  $\mu\text{M}$  POM-1 in experiments might be due to cytotoxicity, cell viability studies were unable to demonstrate a significant reduction in THP-1 cell viability following a 2.5-hour exposure (Appendix Figure A3 and A4). It was seen that LDH release with POM-1 fell below the 20% threshold (6% of Triton-X-100,  $n=1$ ), while trypan blue studies indicated that the % viable cells in vehicle ( $100 \pm 12\%$ ,

n=3) and POM-1 treatments ( $58 \pm 9\%$ , n=3), were not significantly different (n=3, p=0.1). Thus, the effects of POM-1 were unlikely to be attributed to cytotoxicity.

In an effort to understand the mechanism of POM-1 further, the effects of POM-1 (100  $\mu\text{M}$ ) on intracellular  $\text{Ca}^{2+}$  responses evoked by ATP, ADP, UTP and UDP (30  $\mu\text{M}$ ), were examined. As shown (Table 5.4 and Appendix Figures A11 and A12), treatment of THP-1 cells with POM-1 abolished intracellular  $\text{Ca}^{2+}$  responses evoked by the NDPs, ADP and UDP by  $100 \pm 0\%$  (n=3, p<0.05 for both). However, it was interesting to observe that POM-1 only attenuated  $\text{Ca}^{2+}$  responses evoked by the NTPs, ATP and UTP by  $16 \pm 3\%$  (n=3, p<0.05) and  $17 \pm 2\%$  (n=3, p<0.05), respectively. These data suggested that POM-1 preferentially abolished  $\text{Ca}^{2+}$  responses evoked by NDPs. Where possible, the decay rates ( $\tau$ , sec) for  $\text{Ca}^{2+}$  transients were also compared, but were not found to be significantly different (n=3, p>0.05). For example, in ATP experiments, the  $\tau$  values for untreated ( $85 \pm 1$  seconds, n=3) and POM-1-treated cells ( $86 \pm 1$  seconds, n=3) were not significantly different (n=3, p>0.05).

Taken together, these data suggest that POM-1 exhibits an off-target effect that is preferential for NDPs. This finding is interesting because it suggests that POM-1 targets CCL2- and NDP-evoked intracellular  $\text{Ca}^{2+}$  responses through a similar mechanism.

**Table 5.4 Effect of POM-1 on extracellular nucleotide-evoked  $\text{Ca}^{2+}$  responses in THP-1 cells**

Nucleotide	$\text{Ca}^{2+}$ response (%Fmax)	
	Vehicle	POM-1 100 $\mu\text{M}$
ATP	$38 \pm 1$	$32 \pm 0.3^*$
ADP	$26 \pm 3$	$0 \pm 0^*$
UTP	$44 \pm 0.3$	$36 \pm 1^*$
UDP	$18 \pm 2$	$0 \pm 0^{**}$

Intracellular  $\text{Ca}^{2+}$  responses to nucleotides (30  $\mu\text{M}$ ) in THP-1 cells pre-treated with vehicle (water) or POM-1 (100  $\mu\text{M}$ ) for 15 minutes. Responses normalised to  $\text{Ca}^{2+}$  signals elicited by 40  $\mu\text{M}$  digitonin (%Fmax). Data represents mean  $\pm$  SEM from n=3 replicates. Asterisks indicate significant changes towards vehicle (\*\*p<0.01, \*p<0.05, Students t-test).

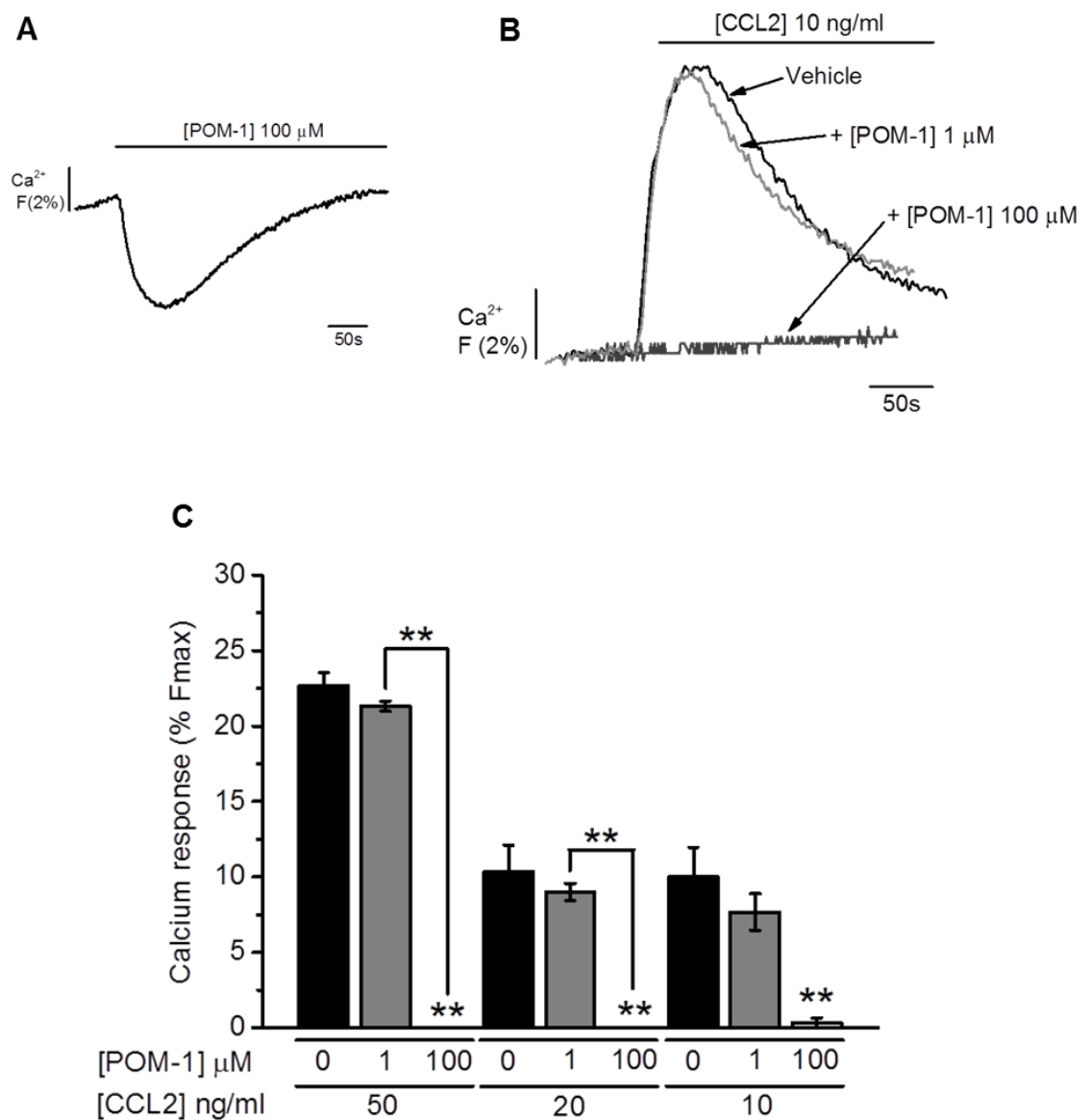


**Figure 5.11 Effect of POM-1 on CCL2-evoked intracellular Ca<sup>2+</sup> responses in THP-1 cells**

(A) Representative trace showing the effect of POM-1 (100  $\mu$ M) on baseline Ca<sup>2+</sup>. (B) Representative Ca<sup>2+</sup> transients to CCL2 (10 ng/ml) in THP-1 cells pre-treated with vehicle (water) or POM-1 (1 or 100  $\mu$ M) for 15 minutes. (C) Bar chart showing normalised intracellular Ca<sup>2+</sup> responses to CCL2 (50, 20 and 10 ng/ml) in THP-1 cells pre-treated with vehicle (water) or POM-1 (1 or 100  $\mu$ M) for 15 minutes. Responses normalised to Ca<sup>2+</sup> signals elicited by 40  $\mu$ M digitonin (%Fmax). Data represents mean  $\pm$  SEM from n=3 replicates. Asterisks indicate significant changes towards vehicle (\*\*p<0.01, One-way ANOVA with Bonferroni's multiple comparison).

### 5.3.5 Effect of P1 receptor antagonism on CCL2-evoked Ca<sup>2+</sup> responses in THP-1 cells

Although studies with ADA were unable to support an involvement of adenosine in CCL2/CCR2-mediated THP-1 cell signalling (Section 5.3.3), the expression mRNA for P1 purinoceptors in THP-1 cells and human monocytes (Chapter 3, Section 3.3.4) suggests that P1 purinoceptors may still be involved. The next studies therefore examined the involvement of P1 purinoceptors using CGS-15943, a triazoloquinazoline derivative reported to antagonise all human P1 purinoceptors with a preference for A<sub>1</sub> (K<sub>i</sub> = 3.5 nM) and A<sub>2A</sub> (K<sub>i</sub> = 1.2 nM), over A<sub>2B</sub> (K<sub>i</sub> = 32.4 nM) and A<sub>3</sub> (K<sub>i</sub> = 35 nM) (Williams *et al.*, 1987; Ongini *et al.*, 1999).

Initial studies examined the effects of CGS-15943 (2.5 µM) on THP-1 cell intracellular Ca<sup>2+</sup> responses evoked by CCL2 (50, 20 and 10 ng/ml). As shown (Figure 5.12), treatment of cells with CGS-15943 potentiated Ca<sup>2+</sup> responses evoked by 10 ng/ml CCL2 by 1.3 ± 0.1-fold (n=4, p<0.05), where the %Fmax values for CCL2 in untreated and CGS-15943-treated cells increased from 13 ± 0.4% (n=4) to 16 ± 0.4% (n=4), respectively. Interestingly, Ca<sup>2+</sup> responses evoked by 50 and 20 ng/ml CCL2 were not significantly affected by CGS-15943 (n=4, p>0.05). For example, the %Fmax values for 20 ng/ml in untreated and CGS-15943-treated cells were 19 ± 1% (n=4) and 19 ± 2% (n=4), respectively (n=4, p>0.05). Although these data appeared to support a role for P1 receptors at low concentrations (10 ng/ml) of CCL2, a comparison of the Ca<sup>2+</sup> decay rates suggested that CGS-15943 did not significantly affect the decay of CCL2 Ca<sup>2+</sup> transients (n=4, p>0.05 for all). For example, the τ values for 10 ng/ml CCL2 in untreated and CGS-15943-treated cells were 185 ± 82 seconds (n=4) and 122 ± 23 seconds (n=4), respectively (n=4, p>0.05).

Given the possible involvement of P1 purinoceptors, it was important to ascertain whether CGS-15943 would be able to overcome the inhibitory effects of apyrase on CCL2-evoked intracellular Ca<sup>2+</sup> responses. Thus, the effects of CGS-15943 (2.5 µM) on 10 ng/ml CCL2-evoked Ca<sup>2+</sup> responses in apyrase-treated THP-1 cells, were examined. As shown (Figure 5.13), no significant shift in the CCL2 %Fmax response was seen in apyrase-treated cells co-incubated with CGS-15943 (n=3, p>0.05), where the %Fmax values for CCL2 in apyrase-treated and apyrase/CGS-15943-treated cells were 3 ± 0% (n=3) and 3 ± 0.3% (n=3), respectively. Although these data are negative, it is possible that the effects of apyrase masked the effects of CGS-15943. A further comparison of the decay rates (τ, sec) of CCL2 Ca<sup>2+</sup> transients indicated no significant differences between treatments (n=3, p>0.05). In these experiments, the τ values for CCL2 in apyrase-treated and apyrase/CGS-15943-treated cells were 74 ± 20 seconds (n=3) and 42 ± 5 seconds (n=3),

respectively. This data suggests that CGS-15943 does not affect the decay of CCL2  $\text{Ca}^{2+}$  transients.

Although these data showed that CGS-15943 modulated low-level CCL2/CCR2-mediated THP-1 cell signalling, additional studies were unable to confirm these findings. Taken together, these data suggest that further studies may be required to address the involvement of P1 purinoceptors in regulating CCL2/CCR2-signalling in monocytes.

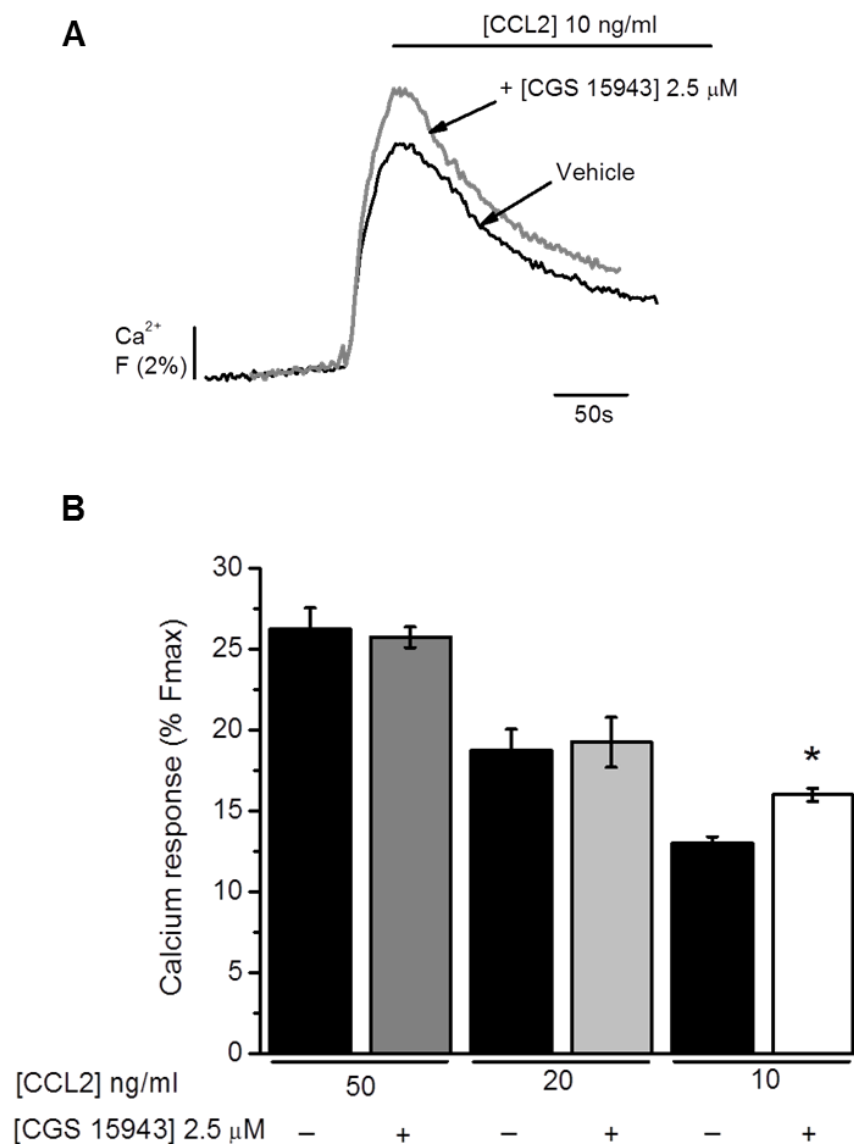


**Figure 5.12 Effect of CGS-15943 on CCL2-evoked  $\text{Ca}^{2+}$  responses in THP-1 cells**

(A) Representative  $\text{Ca}^{2+}$  transients to CCL2 (10 ng/ml) in THP-1 cells pre-treated with vehicle (DMSO) or CGS-15943 (2.5  $\mu\text{M}$ ) for 15 minutes. (B) Bar chart showing normalised intracellular  $\text{Ca}^{2+}$  responses to CCL2 (50, 20 and 10 ng/ml) in THP-1 cells pre-treated with vehicle (DMSO) or CGS-15943 (2.5  $\mu\text{M}$ ) for 15 minutes. Responses normalised to  $\text{Ca}^{2+}$  signals elicited by 40  $\mu\text{M}$  digitonin (% Fmax). Data represents mean  $\pm$  SEM from  $n=4$  replicates. Asterisks indicate significant changes towards vehicle ( $*p<0.05$ , Students t-test).

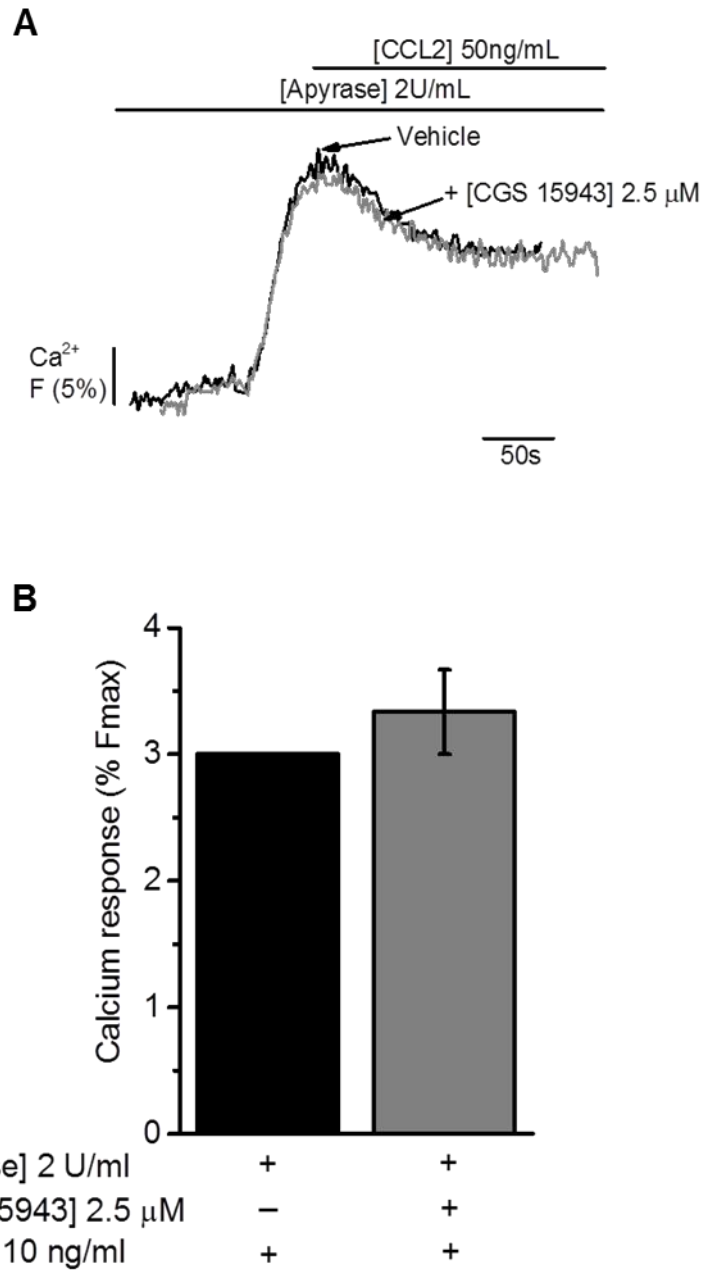


**Figure 5.13 Effect of CGS-15943 on CCL2-evoked  $\text{Ca}^{2+}$  responses in apyrase-treated THP-1 cells**

(A) Representative  $\text{Ca}^{2+}$  transients to CCL2 (10 ng/ml) in apyrase-treated THP-1 cells pre-treated with vehicle (DMSO) or CGS-15943 (2.5  $\mu\text{M}$ ) for 15 minutes. (B) Bar chart showing normalised intracellular  $\text{Ca}^{2+}$  responses to CCL2 (10 ng/ml) in apyrase-treated THP-1 cells pre-treated with vehicle (DMSO) or CSG-15943 (2.5  $\mu\text{M}$ ) for 15 minutes. Responses normalised to  $\text{Ca}^{2+}$  signals elicited by 40  $\mu\text{M}$  digitonin (% Fmax). Data represents mean  $\pm$  SEM from n=3 paired replicates.

### 5.3.6 Effect of P2 receptor antagonists on CCL2/CCR2-mediated THP-1 cell signalling and function

The results of apyrase studies suggest that scavenging extracellular nucleotides attenuates THP-1 cell signalling and function. It is possible, therefore, that P2 purinoceptors are required for CCL2/CCR2-mediated monocyte signalling and function. To address this hypothesis, experiments were conducted to examine the effects of the P2 purinoceptor antagonists, suramin and PPADS on CCL2/CCR2-mediated THP-1 cell signalling and function.

#### 5.3.6.1 Suramin

The polysulfonate compound suramin is a non-competitive and reversible P2 antagonist and G $\alpha$  G-protein inhibitor that displays an IC<sub>50</sub> at homomeric human P2X receptors of 1-10  $\mu$ M (P2X1, P2X2, P2X3, P2X5), >100  $\mu$ M (P2X6), and  $\geq$ 300  $\mu$ M (P2X4, P2X7) (Dunn and Blakeley, 1988, Khakh *et al.*, 2001). At P2Y receptors, suramin exhibits K<sub>B</sub> values of 0.8-3  $\mu$ M (P2Y<sub>1</sub>, P2Y<sub>11</sub> and P2Y<sub>12</sub>) and 50  $\mu$ M (P2Y<sub>2</sub>), while also inhibiting P2Y<sub>6</sub> by 27% and P2Y<sub>13</sub> by 80% at 100  $\mu$ M and 10  $\mu$ M, respectively (Von K $\ddot{u}$ gelgen, 2008).

To address the aims of this study, experiments were designed to test the effects of suramin (100  $\mu$ M) on CCL2 (50 ng/ml)-evoked intracellular Ca<sup>2+</sup> responses in THP-1 cells. As shown (Figure 5.14), treatment of cells with suramin abolished CCL2-evoked Ca<sup>2+</sup> responses (100  $\pm$  0%, n=4, p<0.01), where the %Fmax values for CCL2 in untreated and suramin-treated cells were 27  $\pm$  4% (n=4) and 0  $\pm$  0% (n=4), respectively. These results were unexpected and suggested that P2 purinoceptors antagonised by suramin were required for CCL2/CCR2-mediated monocyte signalling. However, while this seemed possible, it was discovered that prior work by Yu *et al.* (2006) showed that suramin bound to CCL2, thus preventing its engagement with CCR2. A second possible explanation for these results may be that suramin reduced cell viability. However, trypan blue studies were unable to support this theory (Appendix Figure A4), where the % viable cells for THP-1 cells exposed to vehicle (water) and 100 $\mu$ M suramin were 100  $\pm$  12% (n=3) and 82  $\pm$  8% (n=3), respectively. Also in LDH studies (Appendix Figure A3), levels of LDH fell below the 20% threshold (14% of Triton-X-100, n=1).

Based on the evidence provided by Yu *et al.* (2006), further experiments with suramin were not performed.

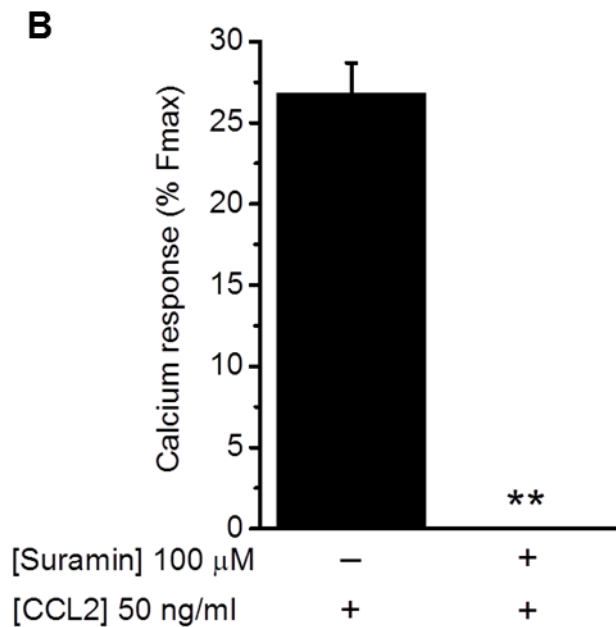
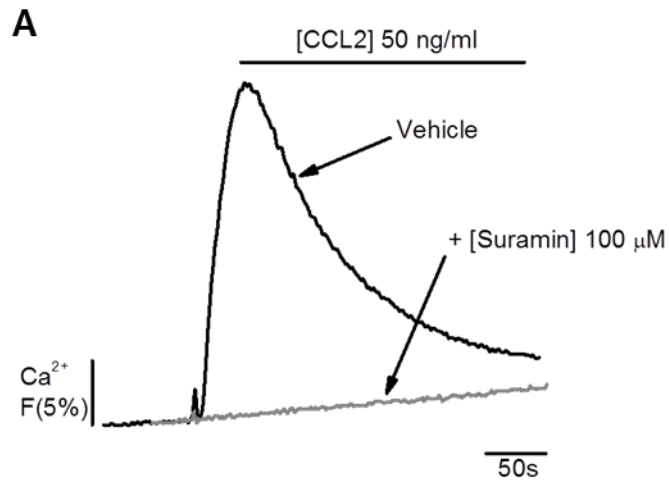


**Figure 5.14 Effect of suramin on CCL2-evoked  $\text{Ca}^{2+}$  responses in THP-1 cells**

(A) Representative  $\text{Ca}^{2+}$  transients to CCL2 (50 ng/ml) in THP-1 cells pre-treated with vehicle (water) or suramin (100  $\mu$ M) for 15 minutes. (B) Bar chart showing normalised intracellular  $\text{Ca}^{2+}$  responses to CCL2 (50 ng/ml) in THP-1 cells pre-treated with vehicle (water) or suramin (100  $\mu$ M) for 15 minutes. Responses normalised to  $\text{Ca}^{2+}$  signals elicited by 40  $\mu$ M digitonin (%Fmax). Data represents mean  $\pm$  SEM from n=4 replicates. Asterisks indicate significant changes towards vehicle (\*\*p<0.01, Students t-test).

### 5.3.6.2 PPADS

The P2 purinoceptor antagonist PPADS (Lambrecht *et al.*, 1992) is a non-competitive antagonist at human P2X and P2Y receptors. At P2X receptors, PPADS exhibits IC<sub>50</sub> values of 1-3 µM (P2X1, P2X2, P2X3), 100-300 µM (P2X4), 200-600 nM (P2X5), and 10-45 µM (P2X7) (Khakh *et al.*, 2001; Coddou *et al.*, 2011). At P2Y receptors, PPADS exhibits a K<sub>B</sub> of 4-12 µM at P2Y<sub>1</sub>, and at 10 µM-100 µM inhibits P2Y<sub>13</sub> by 50%, P2Y<sub>4</sub> by 30%, and P2Y<sub>6</sub> by 69% (von Kügelgen, 2008).

The effects of PPADS (100 µM) on CCL2 (50 ng/ml)-evoked intracellular Ca<sup>2+</sup> responses in THP-1 cells were next tested. As shown (Figure 5.15a), 100 µM PPADS quenched the fluo-4 AM signal, therefore preventing the use of this concentration. In experiments using 10 µM PPADS (Figure 5.15b and c), no significant inhibition of CCL2-evoked Ca<sup>2+</sup> responses were observed (n=3, p>0.05), where the %Fmax values for CCL2 in untreated and PPADS-treated cells were 26 ± 3% (n=3) and 22 ± 5% (n=3), respectively. These data showed that at 10 µM, PPADS did not modulate CCL2-evoked intracellular Ca<sup>2+</sup> responses. This result was interesting because it suggested that P2 purinoceptors antagonised by 10 µM PPADS were not required for CCL2/CCR2-mediated monocyte signalling. An analysis of the decay rates (τ, sec) for untreated (86 ± 6 seconds, n=3) and treated cells (75 ± 4 seconds, n=3) suggested that PPADS did not affect the decay of CCL2 Ca<sup>2+</sup> transients (n=3, p>0.05).

The effects of 100 µM and 1 mM PPADS on THP-1 cell chemotaxis towards CCL2 were next tested to understand the involvement of PPADS-sensitive purinoceptors in CCL2/CCR2-mediated monocyte functions. As shown (Figure 5.16), THP-1 cells demonstrated a significantly higher (n=4, p<0.01) chemotactic index towards CCL2 (14 ± 4, n=4) than towards vehicle (1 ± 0.2, n=4). As also shown, 100 µM and 1 mM PPADS attenuated THP-1 cell chemotaxis towards CCL2 by 78 ± 6% (n=4, p<0.05) and 85 ± 4% (n=4, p<0.05), respectively, where the chemotactic indexes for these treatments were 3 ± 1 (n=4) and 2 ± 1 (n=4), respectively. Although it is possible that these effects may have been attributed to cytotoxicity, 100 µM PPADS exposure for 2.5 hours demonstrated no significant loss in THP-1 cell viability in trypan blue assays where the %viable cells for cells treated with vehicle and PPADS were 100 ± 12% (n=3) and 71 ± 9% (n=3), respectively (n=3, p>0.05). The LDH release (% Triton-X 100) of cells exposed to 100 µM PPADS (4%, n=1) also fell below the 20% threshold (Appendix Figures A3 and A4).

Taken together, these data suggest that PPADS-sensitive P2 purinoceptors are likely to be involved in modulating CCL2/CCR2-mediated monocyte function.

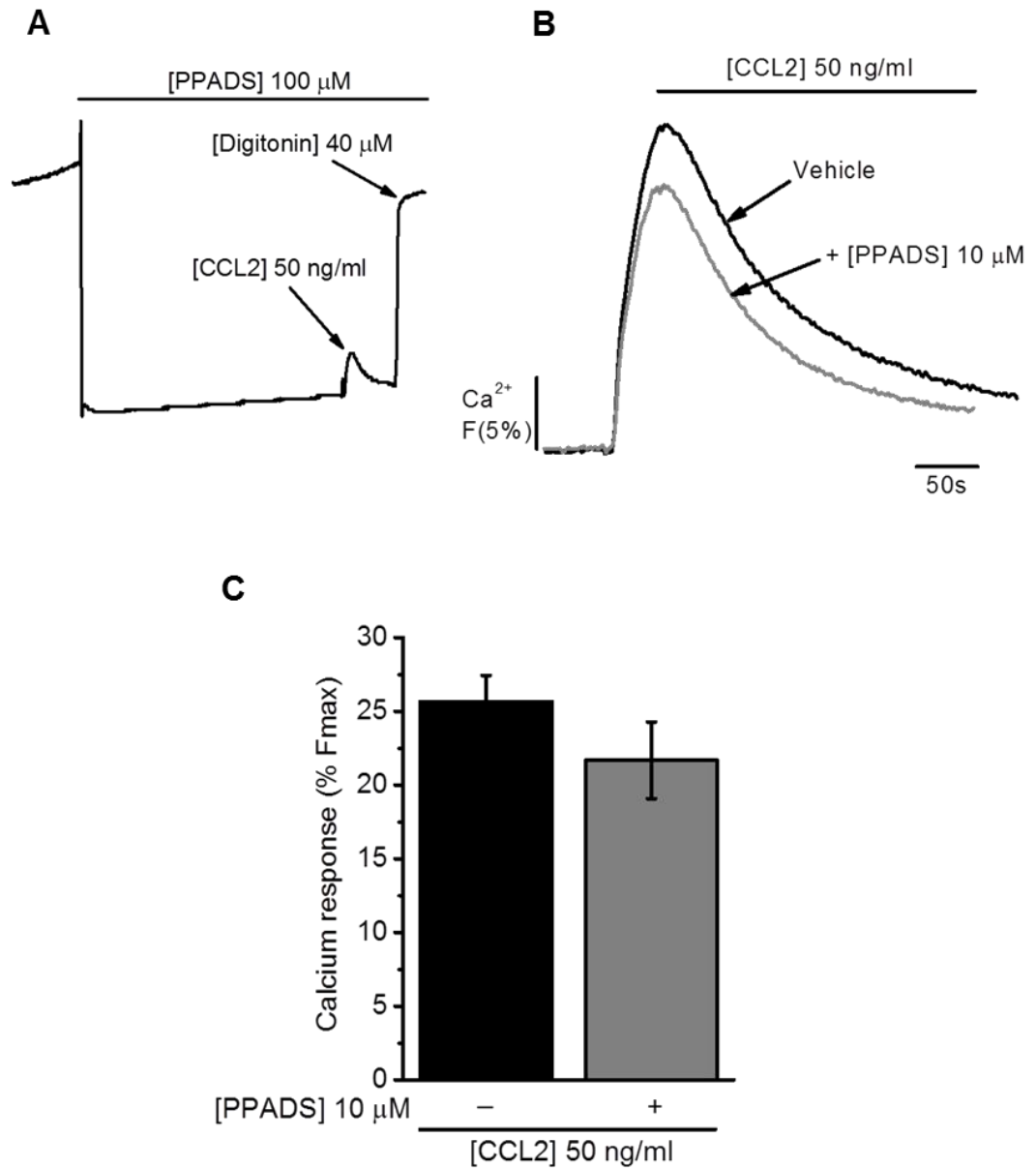


**Figure 5.15 Effect of PPADS on CCL2-evoked Ca<sup>2+</sup> responses in THP-1 cells**

(A) Representative trace showing the effect of PPADS on Ca<sup>2+</sup> signals. (B) Representative Ca<sup>2+</sup> transients to CCL2 (50 ng/ml) in THP-1 cells pre-treated with vehicle (water) or PPADS (100  $\mu$ M) for 15 minutes. (C) Bar chart showing normalised intracellular Ca<sup>2+</sup> responses to CCL2 (50 ng/ml) in THP-1 cells pre-treated with vehicle (water) or PPADS (100  $\mu$ M) for 15 minutes. Responses normalised to Ca<sup>2+</sup> signals elicited by 40  $\mu$ M digitonin (%Fmax). Data represents mean  $\pm$  SEM from n=3 replicates.

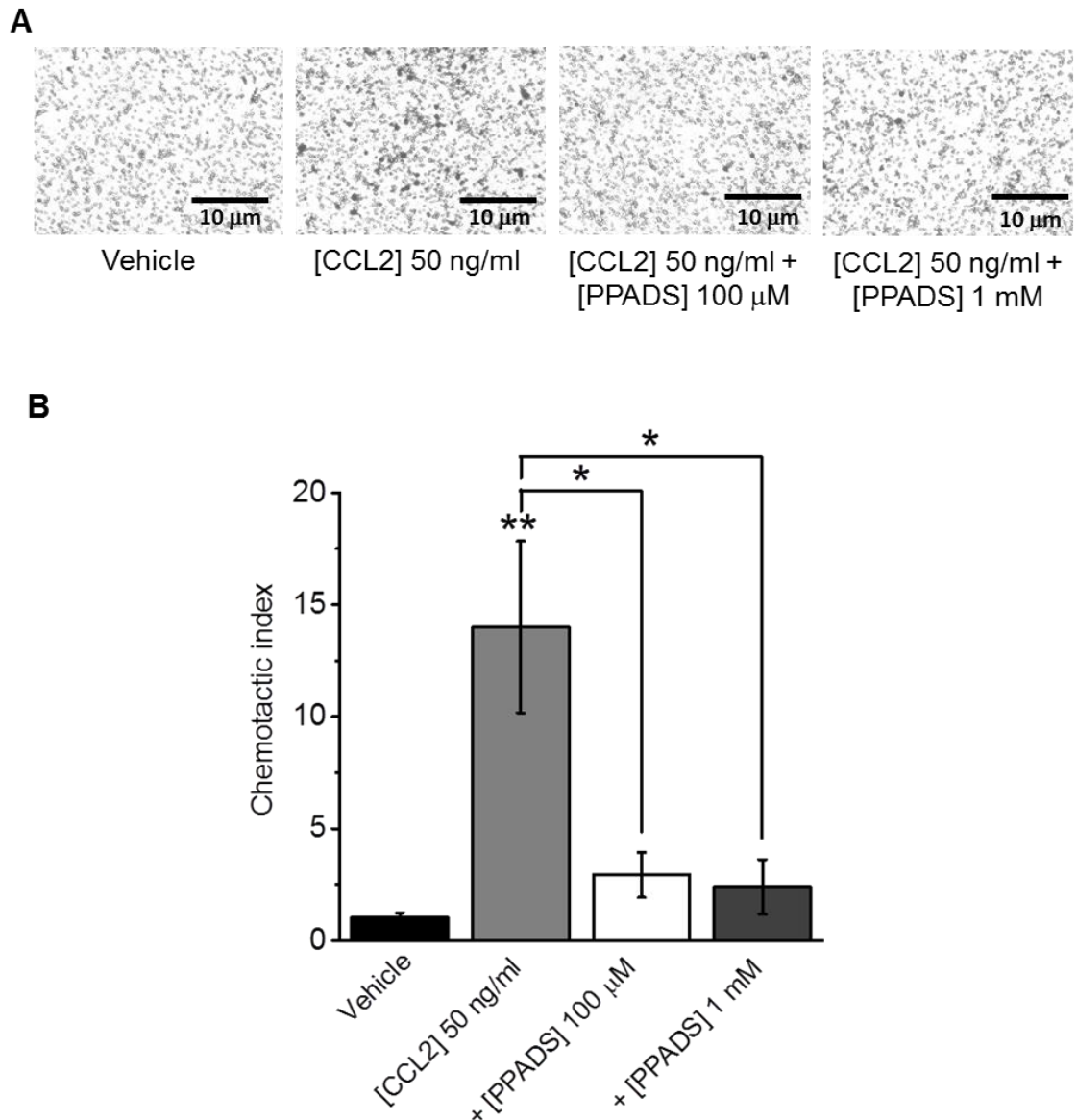


**Figure 5.16 Effect of PPADS on CCL2-mediated THP-1 chemotaxis**

(A) Representative images showing the effect of PPADS (10 and 100  $\mu$ M) on THP-1 cell chemotaxis towards CCL2 (50 ng/ml, lower chamber, 2hrs). Scale bar represents 10  $\mu$ m. (B) Bar chart showing normalised THP-1 cell chemotaxis towards vehicle (water) or CCL2 (50 ng/ml, lower chamber, 2hrs), in the presence of PPADS (10 and 100  $\mu$ M). Chemotactic index is a ratio of the number of cells that migrated towards CCL2 over the number of cells that migrated towards vehicle. Data represents mean  $\pm$  SEM from  $n=4$  transwells. Asterisks indicate significant changes towards vehicle (\*\* $p<0.01$ , \* $p<0.05$ , One-way ANOVA with Bonferroni's multiple comparison).

### 5.3.6.3 Effect of P2X receptor antagonists on CCL2/CCR2-mediated THP-1 cell signalling and function

The next studies sought to examine the requirement of individual P2X purinoceptors. The evidence presented in Chapter 3 has suggested that THP-1 cells and human monocytes exhibit a similar pattern of mRNA expression for P2X1, P2X4, P2X5, and P2X7. It is possible, therefore, that these PPADS-sensitive purinoceptors are required for CCL2/CCR2-mediated monocyte signalling and function. Thus, in order to examine these receptors, the effects of P2X antagonists on CCL2/CCR2-mediated THP-1 cell intracellular  $\text{Ca}^{2+}$  responses and chemotaxis were examined. Due to no selective antagonists available, the requirement of P2X5 could not be examined.

#### 5.3.6.3.1 P2X1

The human P2X1 receptor is encoded by the *P2RX1* gene and is located on the short arm of chromosome 17 (17p13.3). The P2X1 subunit shares 40-50% pair-wise identity with other P2X receptors (Valera *et al.*, 1994). P2X1 subunits are able to combine with subunits from other P2X receptors (P2X1/2, P2X1/4, and P2X1/5) to form heterotrimers (Torres *et al.*, 1998, 1999; Nicke *et al.*, 2005). As a rapidly desensitising receptor, P2X1 undergoes rapid internalisation (<1 second) upon ATP exposure (North, 2002). Of all human P2X receptors, P2X1 has the highest affinity for ATP ( $\text{EC}_{50} = <1 \mu\text{M}$ ) (Evans *et al.*, 1995).

Investigations for P2X1 employed Ro-0437626, a benzimidazole-2-carboxamide derivative exhibiting 30-fold selectivity at P2X1 over P2X2 and P2X3, and shown to attenuate  $\alpha,\beta$ -Methylene-ATP ( $\alpha,\beta$ -meATP)  $\text{Ca}^{2+}$  release in P2X1-transfected Chinese hamster ovary (CHO) cells ( $\text{IC}_{50} = 3 \mu\text{M}$ ) (Jaime-Figueroa *et al.*, 2005). Studies examined the effects of Ro-0437626 (10 and/or 100  $\mu\text{M}$ ) on  $\text{Ca}^{2+}$  responses evoked by 50 ng/ml CCL2 and 100  $\mu\text{M}$   $\alpha,\beta$ -meATP in the presence and/or absence of extracellular  $\text{Ca}^{2+}$  (Chapter 2, Section 2.6.2 for methodology). Experiments in the absence of extracellular  $\text{Ca}^{2+}$  were to confirm that the effects of Ro-0437626 were attributed a blockade of  $\text{Ca}^{2+}$  influx. The stable ATP analogue  $\alpha,\beta$ -meATP is reported to be selective for P2X1 and P2X3 ( $\text{EC}_{50} <1 \mu\text{M}$ ) over P2X6 ( $\text{EC}_{50} >100 \mu\text{M}$ ) and P2X2, P2X4, P2X5, and P2X7 ( $\text{EC}_{50} >300 \mu\text{M}$ ) (Valera *et al.*, 1994; Jarvis and Khakh, 2009).

**Table 5.5 Effect of Ro-0437626 on CCL2- and  $\alpha,\beta$ -meATP-evoked  $\text{Ca}^{2+}$  responses in THP-1 cells**

Condition	Ligand	$\text{Ca}^{2+}$ response (%Fmax)			
		Vehicle	10 $\mu\text{M}$ Ro-0437626	Vehicle	100 $\mu\text{M}$ Ro-0437626
With $\text{Ca}^{2+}$	CCL2	24 $\pm$ 0.3	23 $\pm$ 1	24 $\pm$ 2	16 $\pm$ 1*
Without $\text{Ca}^{2+}$	CCL2	NT	NT	10 $\pm$ 1	10 $\pm$ 0.3
With $\text{Ca}^{2+}$	$\alpha,\beta$ -meATP	NT	NT	3 $\pm$ 0.4	3 $\pm$ 0.3

Intracellular  $\text{Ca}^{2+}$  responses to CCL2 (50 ng/ml) and  $\alpha,\beta$ -MeATP (100  $\mu\text{M}$ ) in THP-1 cells pre-treated with vehicle (DMSO) or Ro-0437626 (10 or 100  $\mu\text{M}$ ), for 15 minutes in the presence and/or absence of extracellular  $\text{Ca}^{2+}$ . Without  $\text{Ca}^{2+}$  conditions in the presence of 1 mM EGTA. Responses normalised to  $\text{Ca}^{2+}$  signals elicited by 40  $\mu\text{M}$  digitonin (%Fmax). NT = not tested. Data represents mean  $\pm$  SEM from n=3 replicates. Asterisks indicate significant changes towards vehicle (\* $p$ <0.05, Students t-test).

As shown above in Table 5.6 (and Appendix Figure A13), in the presence of extracellular  $\text{Ca}^{2+}$ , higher concentrations of Ro-0437626 (100  $\mu\text{M}$ ) attenuated CCL2-evoked  $\text{Ca}^{2+}$  responses by 32  $\pm$  2% (n=3,  $p$ <0.05). An analysis of the decay rates showed that the  $\tau$  values for CCL2 in untreated and Ro-0437626-treated cells were 69  $\pm$  2 seconds (n=3) and 70  $\pm$  2 (n=3), respectively and not significantly different (n=3,  $p$ >0.05). For 10  $\mu\text{M}$  Ro-0437626, the decay rates for untreated (67  $\pm$  3 seconds, n=3) and Ro-0437626-treated cells (67  $\pm$  3 seconds, n=3) were also not significantly different (n=3,  $p$ >0.05). Although these data suggested an effect attributable to P2X1 antagonism, it was seen in experiments that application of 100  $\mu\text{M}$  Ro-0437626 to THP-1 cells produced an erratic baseline response following by a sustained increase of  $\sim$  5% Fmax (Appendix Figure A13). A similar result was also observed in the absence of extracellular  $\text{Ca}^{2+}$  and might be attributed to a release of  $\text{Ca}^{2+}$  from internal stores.

In an attempt to rule out cytotoxicity, THP-1 cells were incubated with 100  $\mu\text{M}$  Ro-0437626 for 2.5 hours and tested in trypan blue and LDH assays. The results of trypan blue studies indicated no significant differences in %viable cells between vehicle (100%  $\pm$  15%, n=3) and Ro-0437626-treated cells (95  $\pm$  7%, n=3,  $p$ >0.05). Moreover, LDH release (% Triton X-100) for Ro-0437626 fell below the 20% threshold (15%, n=1) (Appendix Figure A3 and A5).

From the data in Table 5.6 (and Appendix Figure A13), it is also apparent that CCL2-evoked  $\text{Ca}^{2+}$  responses in the absence of extracellular  $\text{Ca}^{2+}$  were not significantly affected by 100  $\mu\text{M}$  Ro-0437626 (n=3,  $p$ >0.05). This suggests that Ro-0437626 attenuates CCL2

Ca<sup>2+</sup> responses by reducing Ca<sup>2+</sup> influx. The decay rates of CCL2 Ca<sup>2+</sup> transients in untreated (80 ± 6 seconds, n=3) and Ro-0437626-treated cells (81 ± 7 seconds, n=3) suggests that Ro-0437626 does not affect the decay of CCL2 Ca<sup>2+</sup> transients (n=3, p>0.05). The data in Table 5.6 (and Appendix Figure A14) also show that α,β-meATP-evoked Ca<sup>2+</sup> responses were not significantly affected by 100 μM Ro-0437626 (n=3, p>0.05). Although this result indicates that THP-1 cells might not express protein for P2X1 receptors, a rapid desensitisation of P2X1 is also possible. Although a comparison of the decay rates for α,β-meATP between untreated (321 ± 120 seconds, n=3) and treated cells (112 ± 15 seconds, n=3) suggested that Ro-0437626 promoted a faster decay, these data were not significantly different (n=3, p=0.2).

To assess the requirement of P2X1 for monocyte function, studies investigated the effects of Ro-0437626 (100 μM) on THP-1 cell chemotaxis towards CCL2 (50 ng/ml). As shown (Figure 5.17), THP-1 cells demonstrated a significantly higher (n=4, p<0.01) chemotactic index towards CCL2 (11 ± 1, n=4) than towards vehicle (1 ± 0.2, n=4). Although the chemotactic index for Ro-0437626-treated cells (8 ± 3, n=4) indicated that Ro-0437626 attenuated migration by 25 ± 23% (n=4), these data were not significant (n=4, p>0.05). In general, therefore, these data suggest that THP-1 cell chemotaxis towards CCL2 is unaffected by Ro-0437626.

These data suggest that Ro-0437626 attenuates CCL2-mediated Ca<sup>2+</sup> influx via a mechanism independent of P2X1. Furthermore, these effects do not appear to couple to THP-cell trafficking. Taken together, these data suggest that P2X1 activation is not required for CCL2/CCR2-mediated monocyte signalling and function.

#### **5.3.6.3.2 P2X4**

The human P2X4 receptor is encoded by the *P2RX4* gene located on the long arm of chromosome 12 (12q24.32) and shares 47-55% pair-wise identity with other P2X receptors (Garcia-Guzman *et al.*, 1997a). P2X4 subunits form heterotrimers with P2X1 (P2X1/4), P2X6 (P2X4/6) and P2X7 (P2X4/7) (Lê *et al.*, 1998; Nicke *et al.*, 2005; Guo *et al.*, 2007). Unlike P2X1, the P2X4 receptor is slow desensitising (>20 seconds), and has a lower affinity towards ATP (EC<sub>50</sub> = 3-10 μM) (Khakh *et al.*, 2001; Jarvis and Khakh, 2009). Nucleotide derivatives such as α,β-meATP are also ligands at P2X4, which, as receptors, can also be allosterically modulated by zinc ions (Zn<sup>2+</sup>) and the antiparasitic drug, ivermectin (Coddou *et al.*, 2011).

Studies for P2X4 employed 5-BDBD, a benzofurodiazepine derivative shown to inhibit ATP-evoked Ca<sup>2+</sup> responses in human P2X4-expressing CHO cells (IC<sub>50</sub> = 0.5 μM) (Fischer *et al.*, 2004). Studies tested the effects of 5-BDBD (1-5 μM) on Ca<sup>2+</sup> responses evoked by 50 ng/ml CCL2 in the presence and absence of extracellular Ca<sup>2+</sup>. The

selectivity of 5-BDBD for P2X4 could not be tested as no selective ligands for P2X4 were available.

**Table 5.6 Effect of 5-BDBD on CCL2-evoked Ca<sup>2+</sup> responses in THP-1 cells**

Condition	Ligand	Vehicle	Ca <sup>2+</sup> response (%Fmax)		
			1 $\mu$ M 5-BDBD	Vehicle	5 $\mu$ M 5-BDBD
With Ca <sup>2+</sup>	CCL2	24 $\pm$ 2	22 $\pm$ 1	17 $\pm$ 0.3	14 $\pm$ 0.3*
Without Ca <sup>2+</sup>	CCL2	NT	NT	10 $\pm$ 0.3	9 $\pm$ 1

Intracellular Ca<sup>2+</sup> responses to CCL2 (50 ng/ml) in THP-1 cells pre-treated with vehicle (DMSO) or 5-BDBD (1 or 5  $\mu$ M) for 15 minutes. Without Ca<sup>2+</sup> conditions in the presence of 1 mM EGTA. Responses normalised to Ca<sup>2+</sup> signals elicited by 40  $\mu$ M digitonin (% Fmax). NT = not tested. Data represents mean  $\pm$  SEM from n=3 (with Ca<sup>2+</sup>) and n=4 (without Ca<sup>2+</sup>) replicates. Asterisks indicate significant changes towards vehicle (\*p<0.05, Students t-test).

As shown in Table 5.6 above (and Appendix Figure A15), in the presence of intracellular Ca<sup>2+</sup>, 5  $\mu$ M 5-BDBD significantly inhibited CCL2-evoked intracellular Ca<sup>2+</sup> responses (17  $\pm$  3%, n=3, p<0.05). In addition, the decay rates revealed a slower (1.2  $\pm$  0.03-fold, n=3, p<0.01) decay of CCL2 Ca<sup>2+</sup> transients in cells treated with 5  $\mu$ M 5-BDBD, where the  $\tau$  values for untreated and 5-BDBD-treated cells were 66  $\pm$  4 seconds (n=3) and 76  $\pm$  4 seconds (n=3), respectively. Although cells treated with 1  $\mu$ M 5-BDBD were also slowed by 1.2  $\pm$  0.05-fold (n=3), the  $\tau$  values for CCL2 in untreated (46  $\pm$  2 seconds, n=3) and 5-BDBD-treated cells (53  $\pm$  1 seconds, n=3) were not significantly different (n=3, p>0.05). These data suggest that 5  $\mu$ M 5-BDBD attenuates CCL2 Ca<sup>2+</sup> responses, and slows their decay. This hypothesis was further supported by cell viability studies which showed no significant difference in the %viable cells between vehicle (100%  $\pm$  15%, n=3) and 5-BDBD-treated cells (93  $\pm$  11%, n=3, p>0.05). Moreover, LDH release (% Triton X-100) for 5-BDBD fell below 20% (4%, n=1) (Appendix Figure A3 and A5). However, although these data ruled out cytotoxicity, addition of 5  $\mu$ M 5-BDBD to THP-1 cells in Ca<sup>2+</sup> experiments resulted in a small increase in baseline Ca<sup>2+</sup> (Appendix Figure A15). This was difficult to quantify but was also observed in the absence of extracellular Ca<sup>2+</sup> (below) and suggested that 5-BDBD modulated intracellular Ca<sup>2+</sup> by a mechanism independent of Ca<sup>2+</sup> influx.

In experiments in the absence of extracellular Ca<sup>2+</sup> (Table 5.6), CCL2-evoked Ca<sup>2+</sup> responses were not significantly affected by 5  $\mu$ M 5-BDBD (n=4, p>0.05). The  $\tau$  values for untreated (87  $\pm$  7 seconds, n=4) and 5-BDBD-treated cells (82  $\pm$  9 seconds, n=4) were

also not significantly different ( $n=4$ ,  $p>0.05$ ). These data suggest that 5-BDBD does not modulate the decay of CCL2  $Ca^{2+}$  transients in the absence of extracellular  $Ca^{2+}$ .

It was also important to examine the requirement of P2X4 for CCL2/CCR2-mediated monocyte function. Studies on THP-1 cells showed that although THP-1 cell chemotaxis towards CCL2 was reduced by  $38 \pm 10\%$  ( $n=4$ ), the chemotactic indexes for untreated ( $11 \pm 1$ ,  $n=4$ ) and 5-BDBD-treated cells ( $1 \pm 0.2$ ,  $n=4$ ) were not significantly different ( $n=4$ ,  $p = 0.2$ ) (Figure 5.17). Although these data were interesting, they were unable to confirm a requirement of P2X4 for CCL2/CCR2-mediated monocyte chemotaxis.

Although intracellular  $Ca^{2+}$  experiments suggested a potential requirement of P2X4 for CCL2/CCR2-mediated monocyte signalling, secondary observations indicated off-target effects of 5-BDBD. Taken together, these data suggest that P2X4 is not required for CCL2/CCR2-mediated monocyte signalling and function.

#### **5.3.6.3.3 P2X7**

The human P2X7 receptor is encoded by the *P2RX7* gene located on the long arm of chromosome 12 (12q24.32), and shares the least pair-wise identity (41 to 50%) with other P2X receptors (Rassendren *et al.*, 1997; North, 2002). The P2X7 protein is the longest of the P2X receptors due to a longer C-terminus, which is required for determining its kinetics, desensitisation, and pore-forming properties (Surprenant *et al.*, 1996). As mentioned previously, P2X7 subunits are able to form heterotrimers with P2X4 subunits (P2X4/7) (Guo *et al.*, 2007). The P2X7 receptor is slow desensitising (>20 seconds), but is also the least sensitive purinoceptor to ATP ( $EC_{50} >100 \mu M$ ) (Khakh *et al.*, 2001; North, 2002; Jarvis and Khakh, 2009). Due to this characteristic, P2X7 activation is restricted, and occurs only in response to prolonged agonist exposure, or ATP release caused by cell damage or inflammation (Ferrari *et al.*, 1997; Di Virgilio, 2007). For this reason, P2X7 is considered an important therapeutic target (Bartlett *et al.*, 2014). The gating properties of P2X7 also differ from other P2X receptors where a prolonged agonist exposure produces a biphasic response that coincides with an increase in pore dilation allowing the flow of larger molecules such as the nucleic dye, YO-PRO-1 (Surprenant *et al.*, 1996).

Studies for P2X7 employed A-438079, a disubstituted tetrazolymethylpyridine characterised as a reversible and competitive blocker of human P2X7. A-438079 has a reported  $IC_{50}$  of  $\sim 123$  nM for BzATP-evoked  $Ca^{2+}$  release in P2X7-transfected 1321N1 cells (Nelson *et al.*, 2006). The current studies first examined the effects of A-438079 (1  $\mu M$  and 10  $\mu M$ ) on  $Ca^{2+}$  responses evoked by 50 ng/ml CCL2 and 50  $\mu M$  of the ribose derivative, 3'-O-(4-benzoyl)benzoyl adenosine 5'-triphosphate (BzATP) in the presence and/or absence of extracellular  $Ca^{2+}$ . BzATP exhibits a greater potency towards P2X7 ( $EC_{50} \sim 5 \mu M$ ) than any other nucleotide, but also activates other P2 receptors including

P2Y<sub>11</sub> and P2Y<sub>13</sub> with similar or greater potency (Bianchi *et al.*, 1999; Donnelly-Roberts *et al.*, 2009; Jarvis and Khakh, 2009).

**Table 5.7 Effect of A-438079 on CCL2 and BzATP-evoked Ca<sup>2+</sup> responses in THP-1 cells**

Condition	Ligand	Vehicle	Ca <sup>2+</sup> response (%Fmax)		
			1 $\mu$ M A-438079	Vehicle	10 $\mu$ M A-438079
With Ca <sup>2+</sup>	CCL2	24 $\pm$ 2	22 $\pm$ 1	17 $\pm$ 0.3	14 $\pm$ 0.3*
Without Ca <sup>2+</sup>	CCL2	NT	NT	10 $\pm$ 0.3	9 $\pm$ 1
With Ca <sup>2+</sup>	BzATP	NT	NT	31 $\pm$ 1	32 $\pm$ 0.3

Intracellular Ca<sup>2+</sup> responses to CCL2 (50 ng/ml) and BzATP (50  $\mu$ M) in THP-1 cells pre-treated with vehicle DMSO) or A-438079 (1 or 10  $\mu$ M), for 15 minutes. Without Ca<sup>2+</sup> conditions in the presence of 1 mM EGTA. Responses normalised to Ca<sup>2+</sup> signals elicited by 40  $\mu$ M digitonin (%Fmax). NT = not tested. Data represents mean  $\pm$  SEM from n=3 experiments. Asterisks indicate significant changes towards paired vehicle (\*p<0.05, Students t-test).

As shown above in Table 5.7, experiments in the presence of extracellular Ca<sup>2+</sup> showed that 10  $\mu$ M A-438079 significantly attenuated CCL2-evoked Ca<sup>2+</sup> responses by 10  $\pm$  3% (n=3, p<0.05). In support of these data, cell viability studies (Appendix Figure A3 and A5) showed no reduction in cell viability with 10  $\mu$ M A-438079 (2.5-hour exposure). Interestingly, the decay rates of Ca<sup>2+</sup> transients suggested that 10  $\mu$ M A-438079 also promoted a 8  $\pm$  1% (n=3, p<0.05) faster decay of CCL2 Ca<sup>2+</sup> transients, where the  $\tau$  values for CCL2 in untreated and A-438079-treated cells were 92  $\pm$  3 seconds (n=3) and 85  $\pm$  4 seconds (n=3), respectively. These data suggest that P2X7 antagonism promotes a more rapid decay of CCL2 Ca<sup>2+</sup> transients. It was also interesting to observed that in experiments performed in the absence of extracellular Ca<sup>2+</sup>, CCL2-evoked Ca<sup>2+</sup> responses were not significantly affected by 10  $\mu$ M A-438079 (n=3, p>0.05). This suggested that the effects of A-438079 on CCL2-evoked Ca<sup>2+</sup> responses were attributed to a blockade of Ca<sup>2+</sup> influx (Table 5.7). These data were supported by data showing that A-438079 did not significantly affect the  $\tau$  values for CCL2 in untreated (57  $\pm$  7 seconds, n=3) and A-438079-treated cells (45  $\pm$  3 seconds, n=3, p>0.05).

In additional experiments examining the selectivity of A-438079, it was seen that Ca<sup>2+</sup> responses evoked by BzATP were not significantly affected by 10  $\mu$ M A-438079 (Table 5.8 and Appendix Figure A16). While a possible explanation for this result may be that

BzATP also activates other P2 receptors, a second explanation may be that P2X7 receptors are not expressed by THP-1 cells at the post-translational level.

To determine the requirement of P2X7 receptors for CCL2/CCR2-mediated monocyte trafficking, the effects of A-438079 (10  $\mu$ M) on THP-1 cells trafficking towards CCL2 were tested. As shown (Figure 5.17), CCL2 chemotaxis towards CCL2 was not significantly affected by A-438079 ( $n=4$ ,  $p<0.05$ ), where the chemotactic indexes for untreated and A-438079-treated cells were  $11 \pm 3$  ( $n=4$ ) and  $12 \pm 4$  ( $n=4$ ), respectively. In general, therefore, these data suggest that P2X7 is not required for CCL2/CCR2-associated monocyte trafficking.

These data suggest that A-438079 impairs CCL2-evoked intracellular  $Ca^{2+}$  responses in THP-1 cells in the presence of extracellular  $Ca^{2+}$ . However, the results of BzATP  $Ca^{2+}$  studies do not support a functional presence of P2X7 in THP-1 cells. Taken together, the findings of this study indicate that P2X7 receptor activation is not required for CCL2/CCR2-mediated monocyte signalling and function.

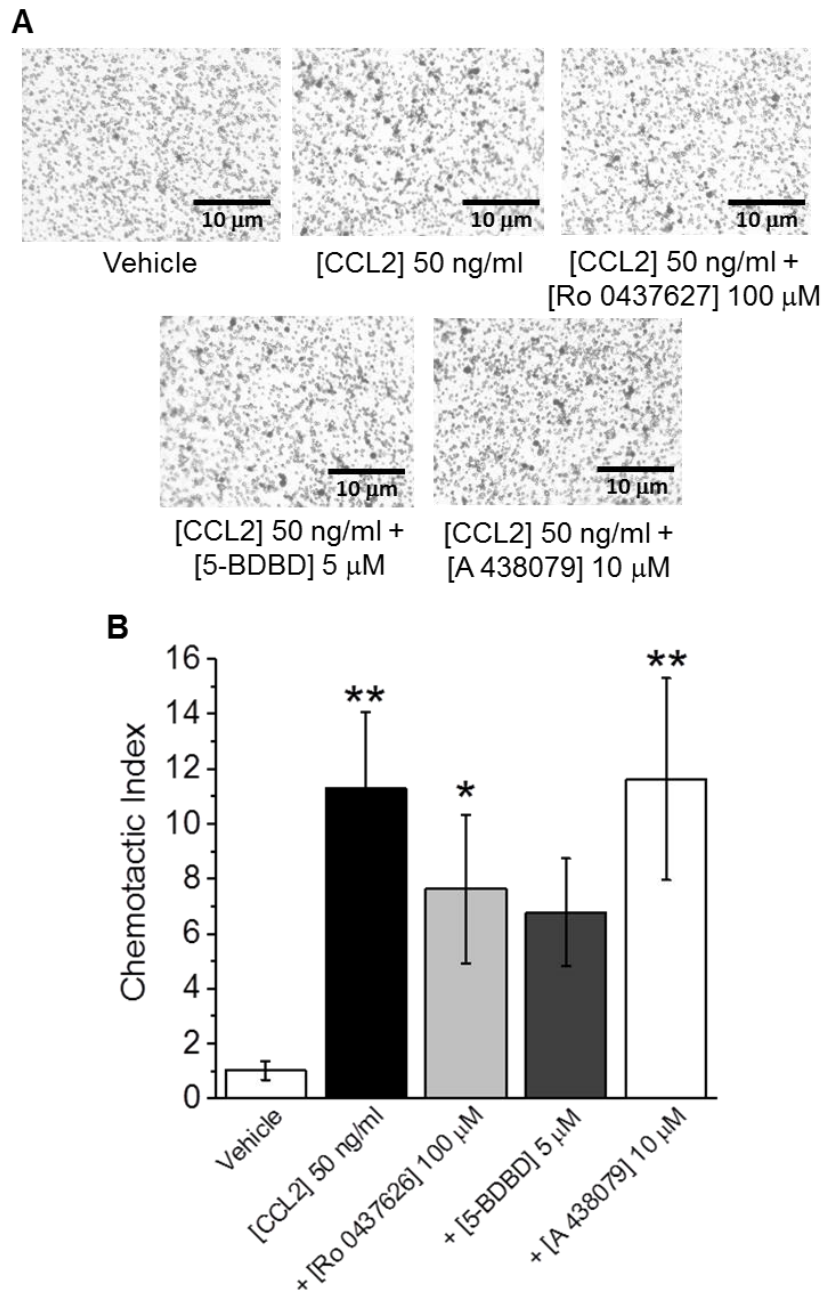


**Figure 5.17 Effect of P2X antagonists on CCL2-mediated THP-1 cell chemotaxis**

(A) Representative images showing the effect of P2X antagonists Ro-0437626 (P2X1), 5-BDBD (P2X4) and A-438079 (P2X7) on THP-1 cell chemotaxis towards vehicle CCL2 (50 ng/ml, lower chamber, 2hrs). Scale bar represents 10 μm. (B) Bar chart showing normalised THP-1 cell chemotaxis towards vehicle (water) or CCL2 (50 ng/ml, lower chamber, 2hrs), in the presence of P2X antagonists (concentrations as shown). Chemotactic index is a ratio of the number of cells that migrated towards CCL2 over the number of cells that migrated towards vehicle. Data represents mean ± SEM from n=4 transwells. Asterisks indicate significant changes towards vehicle (\*\*p<0.01, \*p<0.05, One-way ANOVA with Bonferroni's multiple comparison).

#### 5.3.6.4 Effect of P2Y receptor antagonism on CCL2/CCR2-mediated THP-1 cell signalling and function

The next principle aim of this chapter was to examine the requirement of individual P2Y receptors. The evidence presented in Chapter 3 has suggested that THP-1 cells and human monocytes express mRNA for all P2Y receptors (P2Y<sub>1</sub>-P2Y<sub>14</sub>). Of these receptors, P2Y<sub>1</sub>, P2Y<sub>4</sub>, P2Y<sub>6</sub>, and P2Y<sub>13</sub> are PPADS-sensitive (von Kügelgen, 2008). It is possible, therefore that these and other P2Y receptors are required for CCL2/CCR2-mediated monocyte signalling and function. In an effort to examine the requirement of these receptors, the effects of P2Y antagonists on CCL2/CCR2-mediated THP-1 cell intracellular Ca<sup>2+</sup> responses and chemotaxis were examined. Due to no selective antagonists available for P2Y<sub>2</sub>, P2Y<sub>4</sub>, and P2Y<sub>14</sub>, it was not possible to examine the role of these receptors. A requirement of P2Y<sub>6</sub> has been addressed in Chapter 6.

##### 5.3.6.4.1 P2Y<sub>1</sub>

The human P2Y<sub>1</sub> receptor is encoded by the *P2YR1* gene located on the long arm of chromosome 3 (3q25.2) and shares 24-46% pair-wise identity with other P2Y receptors (Ayyanathan *et al.*, 1996; Janssens *et al.*, 1996; Abbracchio *et al.*, 2006). P2Y<sub>1</sub> is coupled to a PTx-insensitive G<sub>αq/11</sub>-type G-protein involved in PLC activation (Waldo and Harden, 2004). Although the preferred endogenous ligand of P2Y<sub>1</sub> is ADP (EC<sub>50</sub> ~ 250 nM), ATP is also a ligand (EC<sub>50</sub> >1 μM) but may also act as an antagonist at low concentrations (Schachter and Harden, 1997; Léon *et al.*, 1997). Studies in platelets and endothelial cells have shown that P2Y<sub>1</sub> is rapidly desensitised by ADP, an effect prevented by NTPDase1 (Enjyoji *et al.*, 1999; Zimmermann *et al.*, 2012).

Studies involving P2Y<sub>1</sub> employed the competitive P2Y<sub>1</sub> antagonist MRS-2179, which, at 100 nM, almost abolishes P2Y<sub>1</sub>-mediated IP<sub>3</sub> formation in P2Y<sub>1</sub>-transfected 1321N1 astrocytoma cells (Boyer *et al.*, 1998). MRS-2179 exhibits a K<sub>i</sub> of 84 nM for P2Y<sub>1</sub> and lacks an effect at P2Y<sub>12</sub> and P2Y<sub>13</sub> (Waldo *et al.*, 2002). The current studies tested the effects of MRS-2179 (10 μM) on Ca<sup>2+</sup> responses evoked by 50 ng/ml CCL2 and 3 μM ADP. Additional studies examined the effects of apyrase (2 U/ml) on Ca<sup>2+</sup> responses evoked by the P2Y<sub>1</sub> agonist, MRS-2365 ((N)-methanocarpa-2-methylthio-ADP), which is selective for human P2Y<sub>1</sub> (EC<sub>50</sub> = 1.2 nM) over P2Y<sub>12</sub> (inactive) and P2Y<sub>13</sub> (EC<sub>50</sub> = >1 μM) (Chhratriwala *et al.*, 2004).

As shown below in Table 5.8, CCL2 and ADP-evoked Ca<sup>2+</sup> responses were not significantly affected by MRS-2179 (n=3, p>0.05 for both experiments). A comparison of the decay rates (τ sec) also showed no differences between treatments. The τ values for CCL2 in untreated and MRS-2179-treated cells were 115 ± 10 seconds (n=3) and 119 ± 12 seconds (n=3), respectively (n=3, p>0.05), while for ADP they were 14137 ± 12335

seconds (n=3) and  $5455 \pm 4660$  seconds (n=3), respectively (n=3,  $p > 0.05$ ). These data were interesting because they suggested that MRS-2179 did not influence the magnitude or the decay of CCL2 and ADP  $Ca^{2+}$  transients. A possible explanation for a lack of effect of MRS-2179 on ADP  $Ca^{2+}$  responses may be that  $P2Y_1$  is not expressed by THP-1 cells at the post-translational level. However, other possible reasons include an activation of other ADP-sensitive receptors by ADP, or a desensitisation of  $P2Y_1$ .

**Table 5.8 Effect of MRS-2179 on CCL2- and ADP-evoked  $Ca^{2+}$  responses in THP-1 cells**

<b><math>Ca^{2+}</math> response (%Fmax)</b>		
<b>Ligand</b>	<b>Vehicle</b>	<b>10 <math>\mu</math>M MRS-2179</b>
CCL2	$24 \pm 0.3$	$26 \pm 0.3$
ADP	$9 \pm 1$	$10 \pm 1$

Intracellular  $Ca^{2+}$  responses to CCL2 (50 ng/ml) and ADP (3  $\mu$ M) in THP-1 cells pre-treated with vehicle (water) or MRS 2179 (10  $\mu$ M) for 15 minutes. Responses normalised to  $Ca^{2+}$  signals elicited by 40  $\mu$ M digitonin (% Fmax). Data represents mean  $\pm$  SEM from n=3 replicates.

In experiments designed to unmask  $P2Y_1$ -mediated  $Ca^{2+}$  responses, it was seen that apyrase potentiated  $Ca^{2+}$  responses evoked by the  $P2Y_1$  agonist MRS-2365 by  $2.5 \pm 1$ -fold (n=3,  $p < 0.05$ ) (Table 5.9 and Appendix Figure A17). These data suggest that apyrase potentiates  $P2Y_1$  signalling by limiting receptor desensitisation. Due to the sustained  $Ca^{2+}$  responses seen with MRS-2365, the decay rates for  $Ca^{2+}$  transients could not be determined. While these data were interesting because they supported the presence of functional  $P2Y_1$  receptors in THP-1 cells, they also indicated that  $P2Y_1$  might only play a small role in  $Ca^{2+}$  mobilisation in these cells.

**Table 5.9 Effect of apyrase on MRS-2365-evoked  $Ca^{2+}$  responses in THP-1 cells**

<b><math>Ca^{2+}</math> response (%Fmax)</b>		
<b>Ligand</b>	<b>Vehicle</b>	<b>Apyrase 2 U/ml</b>
MRS-2365	$2.7 \pm 1$	$5.3 \pm 1^*$

Intracellular  $Ca^{2+}$  responses to MRS-2365 (100 nM) in THP-1 cells pre-treated with vehicle (water) or apyrase (2 U/ml) for 10 minutes. Responses normalised to  $Ca^{2+}$  signals elicited by 40  $\mu$ M digitonin (%Fmax). Data represents mean  $\pm$  SEM from n=3 replicates. Asterisks indicate significant changes towards vehicle ( $*p < 0.05$ , Students t-test).

To examine the requirement of P2Y<sub>1</sub> for CCL2/CCR2-mediated monocyte chemotaxis, experiments tested the effects of MRS-2179 (10 μM) on THP-1 cell chemotaxis towards CCL2 (50 ng/ml). As shown (Figure 5.18), THP-1 cells demonstrated a significantly higher (n=4, p<0.01) chemotactic index towards CCL2 (13 ± 1, n=4) than towards vehicle (1 ± 0.1, n=4). As also shown, the chemotactic index of MRS-2179-treated cells (12 ± 2, n=4) was not significantly different from untreated cells (n=4, p>0.05). These data suggest that MRS-2179 does not influence THP-1 cell chemotaxis towards CCL2.

Taken together, these data suggest that P2Y<sub>1</sub> activation is not required for CCL2/CCR2-mediated monocyte signalling and function.

#### **5.3.6.4.2 P2Y<sub>11</sub>**

The human P2Y<sub>11</sub> receptor is encoded by the *P2YR11* gene located on the short arm of chromosome 19 (19p13.2), and is the only P2Y receptor containing an intron (1.9Kb) in its coding sequence (Communi *et al.*, 1997, 1999). The P2Y<sub>11</sub> receptor shares 21-34% pairwise identity with other P2Y receptors (Abbracchio *et al.*, 2006). Signalling through P2Y<sub>11</sub> involves PTx-insensitive Gα<sub>q/11</sub> and Gα<sub>s</sub>-type G-proteins which activate PLC and to a lower extent, adenylate cyclase (Communi *et al.*, 1997, 1999; Qi *et al.*, 2001). The preferred ligand for P2Y<sub>11</sub> is ATP (EC<sub>50</sub> >8 μM), but ADP is also a weak agonist (EC<sub>50</sub> >100 μM) (Communi *et al.*, 1997, 1999; Qi *et al.*, 2001). The role of UTP as a ligand is uncertain, where studies by White *et al.* (2003) suggest that UTP evokes Ca<sup>2+</sup> in the absence of IP<sub>3</sub> formation, while more recent studies (Morrow *et al.*, 2014) indicate that UTP is ineffective at releasing Ca<sup>2+</sup>.

To examine the requirement of P2Y<sub>11</sub>, studies employed the competitive P2Y<sub>11</sub> antagonist NF-340 (IC<sub>50</sub> = 20-400 nM), a tetrasulfonic-acid suramin analogue shown to inhibit ATPγS-evoked Ca<sup>2+</sup> release from human P2Y<sub>11</sub>-transfected 1321N1 astrocytoma cells by 93% (Meis *et al.*, 2010). The current studies therefore examined the effects of NF-340 (10 μM) on THP-1 cell Ca<sup>2+</sup> responses evoked by CCL2 (50 ng/ml), ATP (3-30 μM), and the P2Y<sub>11</sub> ligand, β-nicotinamide adenine dinucleotide hydrate (β-NAD). Studies reported by Moreschi *et al.* (2006) have shown that 1 mM β-NAD releases intracellular Ca<sup>2+</sup> and promotes the formation of IP<sub>3</sub>, cAMP, and cyclic ADP-ribose from human granulocytes and human P2Y<sub>11</sub>-transfected 1321N1 astrocytoma cells.

**Table 5.10 Effect of NF-340 on CCL2, ATP and  $\beta$ -NAD-evoked  $\text{Ca}^{2+}$  responses in THP-1 cells**

Ligand	$\text{Ca}^{2+}$ response (%Fmax)	
	Vehicle	10 $\mu\text{M}$ NF-340
CCL2	30 $\pm$ 0.3	31 $\pm$ 0.3
ATP 3 $\mu\text{M}$	39 $\pm$ 1	39 $\pm$ 1
ATP 30 $\mu\text{M}$	45 $\pm$ 1	43 $\pm$ 1**
$\beta$ -NAD+	4 $\pm$ 0	5 $\pm$ 1

Intracellular  $\text{Ca}^{2+}$  responses to CCL2 (50 ng/ml), ATP (3-30  $\mu\text{M}$ ), and  $\beta$ -NAD (1 mM) in THP-1 cells pre-treated with vehicle (DMSO) or NF-340 (10  $\mu\text{M}$ ) for 15 minutes. Responses normalised to  $\text{Ca}^{2+}$  signals elicited by 40  $\mu\text{M}$  digitonin (%Fmax). Data represents mean  $\pm$  SEM from n=3 replicates. Asterisks indicate significant changes towards vehicle (\*\*p<0.01, Students t-test).

As shown in Table 5.10 above, CCL2  $\text{Ca}^{2+}$  responses were not significantly affected by NF-340 (n=3, p>0.05). A comparison of the  $\tau$  values of  $\text{Ca}^{2+}$  transients for treatments also showed no significant differences (n=3, p>0.05) between untreated (61  $\pm$  2 seconds, n=3), and NF-340-treated cells (60  $\pm$  2 seconds, n=3). Collectively, these data suggested that NF-340 did not affect the magnitude or the decay of CCL2  $\text{Ca}^{2+}$  transients in THP-1 cells.

In a bid to confirm the functional presence of P2Y<sub>11</sub>, studies next examined the effects of NF-340 on ATP and  $\beta$ -NAD-evoked  $\text{Ca}^{2+}$  responses in THP-1 cells. As shown by Table 5.10 (and Appendix Figure A18),  $\text{Ca}^{2+}$  responses evoked by 3  $\mu\text{M}$  ATP were not significantly affected by NF-340 (n=3, p>0.05). However, it was seen that NF-340 attenuated  $\text{Ca}^{2+}$  responses evoked by 30  $\mu\text{M}$  ATP by 4  $\pm$  0.3% (n=3, p<0.05). These data suggest that NF-340 attenuates  $\text{Ca}^{2+}$  responses evoked by 30  $\mu\text{M}$  ATP, but not 3  $\mu\text{M}$  ATP. This is interesting because it ties in with the knowledge that the potency of ATP at human P2Y<sub>11</sub> is EC<sub>50</sub> = >8  $\mu\text{M}$  (Communi *et al.*, 1997, 1999; Qi *et al.*, 2001). A comparison of the decay rates for treatments showed that the  $\tau$  values for 3  $\mu\text{M}$  or 30  $\mu\text{M}$  ATP were not significantly affected by NF-340 (n=3, p>0.05, data not shown). For example, the  $\tau$  values for 30  $\mu\text{M}$  ATP in untreated and treated cells were 106  $\pm$  7 seconds (n=3) and 111  $\pm$  3 seconds (n=3), respectively (n=3, p>0.05).

In additional experiments (Table 5.10 and Appendix Figure A18), it was seen that  $\beta$ -NAD  $\text{Ca}^{2+}$  responses were not significantly affected by NF-340 (n=3, p>0.05). This is interesting and suggests that NF-340 is unable to modulate  $\text{Ca}^{2+}$  responses evoked by a

more selective P2Y<sub>11</sub> ligand. The sustained responses of  $\beta$ -NAD prevented the decay rates of Ca<sup>2+</sup> transients from being analysed.

As with previous experiments, the effects of NF-340 (10  $\mu$ M) on THP-1 cell chemotaxis towards CCL2 (50 ng/ml) were investigated. As shown (Figure 5.18), THP-1 cell chemotaxis towards CCL2 was not significantly affected by NF-340 (n=4, p>0.05), although the chemotactic indexes of untreated (13  $\pm$  1, n=4) and NF-340-treated cells (7  $\pm$  2, n=4) suggested that trafficking was attenuated by 40  $\pm$  21% (n=4). These data hinted at the possibility that NF-340 attenuated THP-1 cell chemotaxis towards CCL2, but also suggested that further work was needed.

In summary, these results indicate that P2Y<sub>11</sub> is not required for CCL2/CCR2-mediated monocyte signalling and function.

#### **5.3.6.4.3 P2Y<sub>12</sub>**

The human P2Y<sub>12</sub> receptor is encoded by the *P2YR12* gene located on the long arm of chromosome 3 (3q24-q25) (Zhang *et al.*, 2001; Bodor *et al.*, 2003). In general, P2Y<sub>12</sub> shares 22-48 % pair-wise identity with other P2Y receptors (Abbracchio *et al.*, 2006). The preferred ligand is ADP which has a reported K<sub>i</sub> of 5.9-6.3 in P2Y<sub>12</sub>-transfected CHO cells and human platelets (Hollopeter *et al.*, 2001; Savi *et al.*, 2001). P2Y<sub>12</sub> is also activated by ATP which is much weaker (K<sub>i</sub> = 5.2-6.1) (Savi *et al.*, 2001). Unlike most other P2Y purinoceptors, P2Y<sub>12</sub> signals via PTx-sensitive G $\alpha_{i/o}$ -type G-proteins coupled to the inhibition of adenylate cyclase (Hollopeter *et al.*, 2001; Jantzen *et al.*, 2001). Activation of PI3K by the G $\beta\gamma$  dimer of P2Y<sub>12</sub> is considered important for the completion ADP-mediated platelet aggregation (Reséndiz *et al.*, 2003). For this reason, P2Y<sub>12</sub> is considered an important therapeutic target (Wijeyeratne and Heptinstall, 2011). The role of P2Y<sub>12</sub> in Ca<sup>2+</sup> mobilisation however, is less clear.

To examine the requirement of P2Y<sub>12</sub>, studies employed the P2Y<sub>12</sub> antagonist, AR-C-66096, a difluoromethylene ATP analogue shown to impair ADP-mediated human platelet aggregation with an IC<sub>50</sub> of 11 nM (Humphries *et al.*, 1994). The current studies investigated the effects of AR-C-66096 (1  $\mu$ M) on THP-1 cell Ca<sup>2+</sup> responses evoked by CCL2 (50 ng/ml) and ADP (30  $\mu$ M).

**Table 5.11 Effect of AR-C-66096 on CCL2 and ADP-evoked Ca<sup>2+</sup> responses in THP-1 cells**

Ligand	Ca <sup>2+</sup> response (%Fmax)	
	Vehicle	1 μM AR-C-66066
CCL2	23 ± 3	25 ± 1
ADP	32 ± 2	33 ± 1

Intracellular Ca<sup>2+</sup> responses to CCL2 (50 ng/ml) and ADP (30 μM) in THP-1 cells pre-treated with vehicle (water) or AR-C-66096 (1 μM) for 15 minutes. Responses normalised to Ca<sup>2+</sup> signals elicited by 40 μM digitonin (% Fmax). Data represents mean ± SEM from n=3 replicates.

As shown by Table 5.11 above, CCL2 Ca<sup>2+</sup> responses were not significantly affected by AR-C-66096 (n=3, p>0.05). These data suggest that CCL2/CCR2-mediated intracellular Ca<sup>2+</sup> responses in THP-1 cells are unlikely to require P2Y<sub>12</sub>. A comparison of the decay rates for untreated (90 ± 1 seconds, n=3) and AR-C-66096-treated cells (93 ± 3 seconds, n=3) were also not significantly different (n=3, p>0.05), suggesting that AR-C-66096 did not affect the decay of CCL2 Ca<sup>2+</sup> transients. As also shown, similar experiments with ADP showed that Ca<sup>2+</sup> responses were also not significantly affected by AR-C-66096 (n=3, p>0.05). The τ values for ADP in untreated (197 ± 16 seconds, n=3) and AR-C-66096-treated cells (210 ± 4 seconds, n=3) were also not significantly different (n=3, p>0.05). Collectively, these results suggested that neither the magnitude nor the decay of CCL2 and ADP Ca<sup>2+</sup> transients were affected by AR-C-66096. A possible reason for these results might be that P2Y<sub>12</sub> receptors may not couple to intracellular Ca<sup>2+</sup> release in THP-1 cells and monocytes.

The requirement of the P2Y<sub>12</sub> receptor for CCL2/CCR2-mediated monocyte function was examined by testing the effects of AR-C-66096 on THP-1 cell chemotaxis towards CCL2 (50 ng/ml). As shown (Figure 5.18), although the chemotactic indexes between untreated (13 ± 1, n=4) and AR-C-66096-treated THP-1 cells (10 ± 2, n=4) suggested that AR-C-66096 attenuated chemotaxis by 17 ± 19% (n=4), these data were not statistically significant (n=4, p>0.05). In general, therefore, these data suggest that AR-C-66096 does not modulate THP-1 cell migration towards CCL2.

Taken together, these data do not support a requirement of P2Y<sub>12</sub> receptors for efficient CCL2/CCR2-mediated monocyte signalling and function. Furthermore, these data support the hypothesis that P2Y<sub>12</sub> does not couple to intracellular Ca<sup>2+</sup> signalling.

#### 5.3.6.4.4 P2Y<sub>13</sub>

The next studies in this chapter examined the requirement of the human P2Y<sub>13</sub> receptor for CCL2/CCR2-mediated monocyte signalling and function. The P2Y<sub>13</sub> receptor is encoded by the *P2YR13* gene located on the long arm of chromosome 3 (3q24) (Communi *et al.*, 2001; Zhang *et al.*, 2002). Structurally, P2Y<sub>13</sub> is most similar to P2Y<sub>12</sub> and P2Y<sub>14</sub>, and in general, shares 21-48 % pair-wise identity with other P2Y receptors (Abbracchio *et al.*, 2006). Although the preferred ligand for P2Y<sub>13</sub> is ADP (pIC<sub>50</sub> = 6.5), ATP is also a ligand (pIC<sub>50</sub> = 5.4) (Marteau *et al.*, 2003). P2Y<sub>13</sub> drives adenylate cyclase inhibition through a PTx-sensitive Gα<sub>i/o</sub>-type G-protein (Communi *et al.*, 2001). Studies by Marteau *et al.* (2003) suggest that high concentrations of ADP enable P2Y<sub>13</sub> to dually couple to PTx-insensitive Gα<sub>s</sub>-type G-proteins. Communi *et al.* (2001) and Marteau *et al.* (2003) have additionally shown that P2Y<sub>13</sub> activation leads to an accumulation of IP<sub>3</sub>, thereby suggesting a possible involvement in Ca<sup>2+</sup> release. Further support for this hypothesis has come from studies using dual P2Y<sub>12</sub>/P2Y<sub>13</sub> antagonists and the P2Y<sub>13</sub> antagonist, MRS-2211 (Bianco *et al.*, 2005; Ceruti *et al.*, 2008; Carrasquero *et al.*, 2009).

To examine the requirement of P2Y<sub>13</sub>, studies employed the competitive P2Y<sub>13</sub> antagonist, MRS-2211. Described as a 2-chloro-5-nitro analogue of PPADS, MRS-2211 exhibits an pIC<sub>50</sub> of 5.97 against ADP-mediated IP<sub>3</sub> formation in human P2Y<sub>13</sub>-1321N1 astrocytoma cells (Kim *et al.*, 2005). The current studies first examined the effects of MRS-2211 (10 μM) on THP-1 cell Ca<sup>2+</sup> responses evoked by CCL2 (50 ng/ml) and ADP (3 μM).

**Table 5.12 Effect of MRS-2211 on CCL2- and ADP-evoked Ca<sup>2+</sup> responses in THP-1 cells**

Ligand	Ca <sup>2+</sup> response (%Fmax)	
	Vehicle	10 μM MRS-2211
CCL2	23 ± 3	25 ± 1
ADP	9 ± 1	4 ± 1**

Intracellular Ca<sup>2+</sup> responses to CCL2 (50 ng/ml) and ADP (3 μM) in THP-1 cells pre-treated with vehicle (water) or MRS 2211 (10 μM) for 15 minutes. Responses normalised to Ca<sup>2+</sup> signals elicited by 40 μM digitonin (%Fmax). Data represents mean ± SEM from n=3 experiments. Asterisks indicate significant changes towards vehicle (\*\*p<0.01, Students t-test).

As shown in Appendix Figure A19a, MRS-2211 caused a mild quenching of the fluorescent signal, dropping the %Fmax signal by ~ -3%. As also shown by Table 5.12 above and Appendix Figure A19, CCL2 Ca<sup>2+</sup> responses were not significantly affected by

MRS-2211 (n=3, p>0.05). These data suggest that P2Y<sub>13</sub> is not required for CCL2-Ca<sup>2+</sup> responses. A comparison of the decay rates for CCL2 Ca<sup>2+</sup> transients in untreated (78 ± 4 seconds, n=3) and MRS-2211-treated cells (78 ± 3 seconds, n=3), showed that these were also not significantly affected by MRS-2211 (n=3, p>0.05). While CCL2 Ca<sup>2+</sup> responses appeared not to be affected by MRS-2211, it was interesting to observe that MRS-2211 significantly attenuated ADP-evoked Ca<sup>2+</sup> responses by 51 ± 3% (n=3, p<0.01) (Table 5.12 and Appendix Figure A19). These data suggest that Ca<sup>2+</sup> responses evoked by ADP are MRS-2211-sensitive. Due to a lack of decay of ADP Ca<sup>2+</sup> transients in MRS-2211-treated cells, the  $\tau$  values could not be determined.

To rule out cytotoxicity, cell viability studies tested the effects of 10  $\mu$ M MRS-2211 on THP-1 cell viability over 2.5 hours. Trypan blue studies indicated that the %viable cells for untreated (100 ± 12%, n=3) and MRS-2211-treated cells (115 ± 9%, n=3) were not significantly different (Appendix Figure A4). Likewise, LDH release for 10  $\mu$ M MRS-2211 fell below the 20% toxic threshold (5% of Triton-X-100, n=1) (Appendix Figure A3). In general, therefore, it seems that THP-1 cells exposed to MRS-2211 for 2.5 hours remain viable.

In chemotaxis experiments with THP-1 cells, it was seen that although 10  $\mu$ M MRS-2211 reduced migration by 27 ± 24% (n=4), the chemotactic indexes for untreated (13 ± 1, n=4) and MRS-2211-treated cells (9 ± 2, n=4) were not significantly different (n=4, p>0.05). These data were therefore in agreement with CCL2 Ca<sup>2+</sup> studies but also suggested that MRS-2211 was unable to significantly modulate CCL2/CCR2-mediated THP-1 cell migration.

Taken together, these data suggest that CCL2/CCR2-mediated monocyte signalling and function does not require an activation of P2Y<sub>13</sub>.

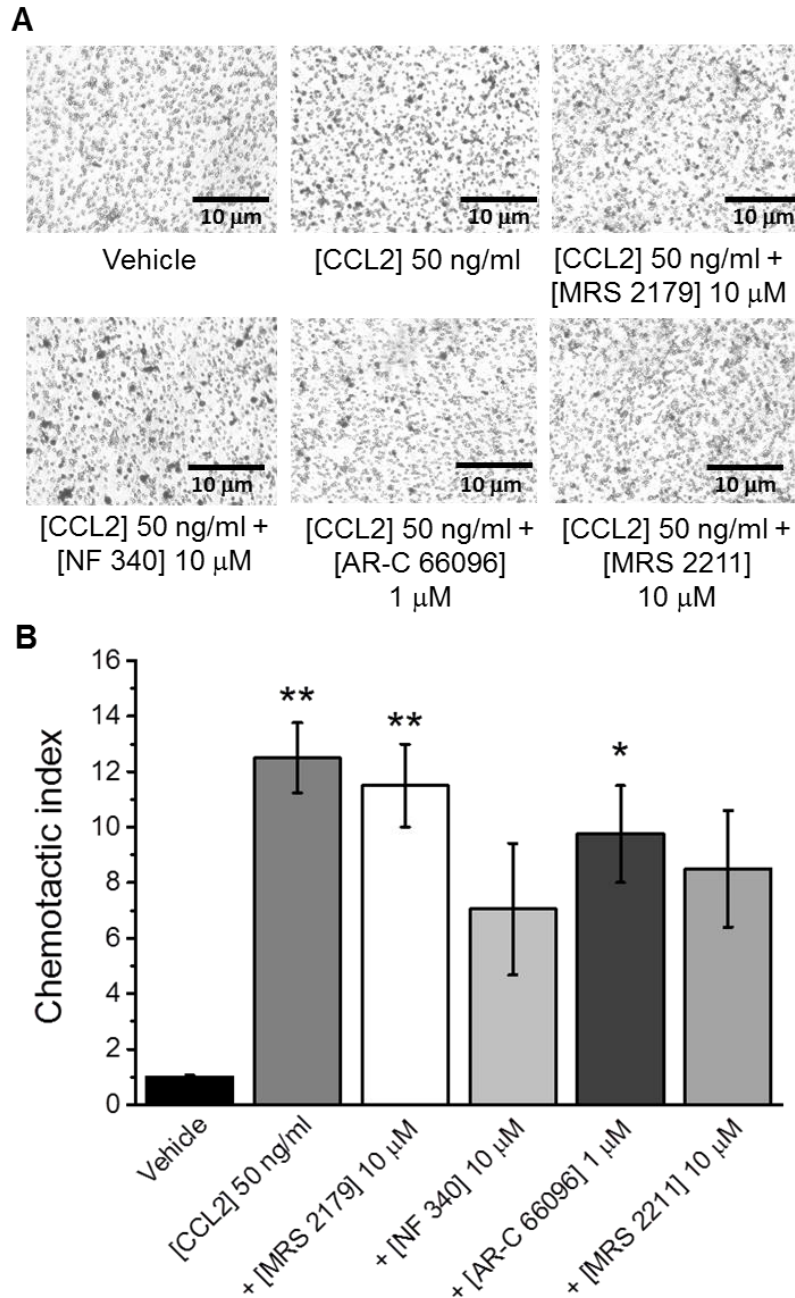


**Figure 5.18 Effect of P2Y antagonists on CCL2-mediated THP-1 chemotaxis**

(A) Representative images showing the effect of P2Y antagonists for P2Y<sub>1</sub> (MRS-2179), P2Y<sub>11</sub> (NF-340), P2Y<sub>12</sub> (AR-C-66096), or P2Y<sub>13</sub> (MRS-2211) on THP-1 cell chemotaxis towards CCL2 (50 ng/ml, lower chamber, 2hrs). Scale bar represents 10 µm. (B) Bar chart showing normalised THP-1 cell chemotaxis towards vehicle (water) or CCL2 (50 ng/ml, lower chamber, 2hrs), in the presence of P2Y antagonists (concentrations as shown). Chemotactic index is a ratio of the number of cells that migrated towards CCL2 over the number of cells that migrated towards vehicle. Data represents mean ± SEM from n=4 transwells. Asterisks indicate significant changes towards vehicle (\*p<0.05, \*\*p<0.01, One-way ANOVA with Bonferroni's multiple comparison).

## 5.4 Summary

This chapter employed monocytic THP-1 cells and human PBMCs as *in vitro* models to investigate the requirement of extracellular nucleotides for CCL2/CCR2-mediated monocyte signalling and function. A number of methodology and pharmacological tools were employed to assess nucleotide hydrolysis, Ca<sup>2+</sup> mobilisation, cell migration, and cell adhesion to vascular endothelium. Using these tools, several important findings were made. Initial observations suggested that extracellular nucleotides were chemotactic. Further experiments with apyrase indicated that extracellular nucleotides were required for CCL2/CCR2-mediated monocyte intracellular Ca<sup>2+</sup> release and cell migration. However, an enhancement of human PBMC chemotaxis by apyrase conflicted with these findings, but also suggested that these differences might reflect the heterogeneous nature of these cells. Additional studies with different apyrases pointed towards a greater requirement of NDPs than NTPs. In THP-1 cells, a potentiation of CCL2 Ca<sup>2+</sup> responses was seen with ARL-67156, and suggested that extracellular nucleotides were required for CCL2/CCR2 signalling. In further investigations assessing the requirement of individual purinoceptors, it was seen that while studies with ADA were unable to identify a role for adenosine, studies with CGS-15943 indicated a requirement of P1 receptors at low CCL2 concentrations. While suramin could not be used due to its ability to bind to CCL2, THP-1 cell chemotaxis experiments with the P2 antagonist PPADS indicated that P2X<sub>1</sub>, P2X<sub>4</sub>, P2X<sub>5</sub>, P2X<sub>7</sub>, P2Y<sub>1</sub>, P2Y<sub>4</sub>, P2Y<sub>6</sub>, and P2Y<sub>13</sub> were candidate purinoceptors for modulating CCL2/CCR2-mediated monocyte chemotaxis. Further THP-1 cell experiments with the P2X antagonists Ro-0436726, 5-BDBD, and A-438079 and the P2Y antagonists MRS-2179, NF-340, AR-C-66096 and MRS-2211, were unable to show that P2X<sub>1</sub>, P2X<sub>4</sub>, P2X<sub>7</sub>, P2Y<sub>1</sub>, P2Y<sub>11</sub>, P2Y<sub>12</sub> or P2Y<sub>13</sub> receptors modulated CCL2/CCR2-mediated monocyte signalling and function.

Taken together, the findings of this study suggest that extracellular nucleotides are required for efficient CCL2/CCR2-mediated monocyte signalling and function. The findings of this study also indicate that P1, P2X<sub>1</sub>, P2X<sub>4</sub>, P2X<sub>7</sub>, P2Y<sub>1</sub>, P2Y<sub>11</sub>, P2Y<sub>12</sub> and P2Y<sub>13</sub> purinoceptors are unlikely to be involved in modulating CCL2/CCR2-mediated monocyte signalling and function. It is possible, therefore, that other purinoceptors are required. Although a number of purinoceptors such as P2X<sub>5</sub>, P2Y<sub>2</sub>, P2Y<sub>4</sub>, P2Y<sub>6</sub> and P2Y<sub>14</sub> still remain candidates, commercially available antagonists are only available for P2Y<sub>6</sub>. The focus of the next chapter (Chapter 6) was therefore to investigate the requirement of P2Y<sub>6</sub> for CCL2/CCR2-mediated monocyte signalling and function using THP-1 cells and human PBMCs as *in vitro* models. The research presented in this chapter gives importance to CCL2/CCR2 activation as measured by intracellular Ca<sup>2+</sup> release, cell migration, and cell adhesion to vascular endothelium.

# Chapter 6: Investigating the requirement of the P2Y<sub>6</sub> receptor for CCL2/CCR2-mediated monocyte signalling and function

---

## 6.1 Introduction

The P2Y<sub>6</sub> purinoceptor was first cloned and characterised by Chang and colleagues from rat aortic smooth muscle cells in 1995 (Chang *et al.*, 1995). The human P2Y<sub>6</sub> receptor was later cloned from human placenta and human T-cells by Communi *et al.* (1996) and Southey *et al.* (1996), respectively. It is now known that P2Y<sub>6</sub> has 328 amino acids and is encoded by the *P2RY6* gene located on the long arm of chromosome 11 (11q13.5) which lies adjacent to the *P2RY2* gene for P2Y<sub>2</sub> (11q13.5-q14.1) (Communi *et al.*, 1996; Pidlaon *et al.*, 1997; Somers *et al.*, 1997). The human P2Y<sub>6</sub> receptor is 23-46% homologous to other human P2Y receptors and shares most pair-wise identity with P2Y<sub>1</sub> (46%), P2Y<sub>2</sub> (41%) and P2Y<sub>4</sub> (43%) (Communi *et al.*, 1996; Abbracchio *et al.*, 2006). RT-PCR studies on human osteoblastic MG-63 cells have identified three isoforms (1, 2, and 3) of the human *P2RY6* gene (Maier *et al.*, 1997). Isoform 1 is encoded by seven splice variants (1, 2, 3, 5, 6, 7, and 8) that differ only in their 5' UTR (untranslated region). Isoform 2, which is encoded by splice variant 9, has a longer N-terminus compared to other variants and contains a 5' UTR and 5' coding region that differs from splice variant 1. Finally, isoform 3 appears to be a pseudogene that has a coding region containing an extra base that causes a frame shift resulting in a truncation of the translated protein thereby rendering it non-functional (Maier *et al.*, 1997).

The human P2Y<sub>6</sub> receptor is involved in the activation of PLC through a PTx-insensitive G $\alpha_{q/11}$ -type G-protein (Communi *et al.*, 1996). Other studies (Nishida *et al.*, 2008) suggest that P2Y<sub>6</sub> can also couple to G $\alpha_{12/13}$ -type G-proteins in rat cardiomyocytes, where activation increases the expression of TGF- $\beta$  (transforming growth factor- $\beta$ ), periostin, connective tissue growth factor, and ACE (angiotensin-converting enzyme).

The preferred natural ligand of the human P2Y<sub>6</sub> receptor is UDP, which exhibits an EC<sub>50</sub> in P2Y<sub>6</sub>-transfected 1321N1 astrocytoma cells of 300 nM and 11 nM for IP<sub>3</sub> formation and intracellular Ca<sup>2+</sup> release, respectively (Communi *et al.*, 1996; Cox *et al.*, 2005). Other natural ligands are UTP (EC<sub>50</sub> 6  $\mu$ M), ADP (EC<sub>50</sub> 30  $\mu$ M), and ATP (EC<sub>50</sub> >3 mM) (Communi *et al.*, 1996). As a slow-desensitising receptor, P2Y<sub>6</sub> exhibits a slow and sustained response upon activation. Robaye *et al.* (1996) first noticed this characteristic in studies looking at IP<sub>3</sub> formation in human P2Y<sub>6</sub>-transfected 1321N1 cells challenged

with UDP or ADP. In their studies, the authors noted that IP<sub>3</sub> levels peaked after 15-30 minutes post-challenge and remained sustained for over 60 minutes. Brinson and Harden (2001) later discovered that the possession of a single threonine in the carboxyl-terminal domain and the lack of the serine residues Ser-333 and Ser-334 were responsible for the slow desensitisation of P2Y<sub>6</sub>. Truncation of these residues in P2Y<sub>4</sub>-transfected 1321N1 cells prevented UTP-mediated phosphorylation, desensitisation, and internalisation of P2Y<sub>4</sub> receptors.

Transcripts of the human P2Y<sub>6</sub> receptor have been found in a variety of tissues including heart, placenta, brain, spleen, and thymus (Communi *et al.*, 1996; Moore *et al.*, 2001; Wihlborg *et al.*, 2006). Transcripts for P2Y<sub>6</sub> are also detected in a variety of cells including epithelial cells, endothelial cells, and leukocytes (Communi *et al.*, 1996; Wong *et al.*, 2009; Riegel *et al.*, 2011). In leukocytes, P2Y<sub>6</sub> expression is evident in neutrophils, monocytes, macrophages, dendritic cells, and T lymphocytes (Jin *et al.*, 1998; Berchtold *et al.*, 1999; Moore *et al.*, 2001; Wang *et al.*, 2004).

Physiological and pharmacological studies on the P2Y<sub>6</sub> receptor in both human and animal models have identified a number of possible roles. For example, studies in human omental and cerebral arteries (Malmsjö *et al.*, 2003) and separate P2Y<sub>6</sub>-knockout (KO) mice (Bar *et al.*, 2008) have shown that P2Y<sub>6</sub> is capable of eliciting arterial smooth muscle contraction. Other authors including Wihlborg *et al.* (2006), Wong *et al.* (2008), and Bernier *et al.* (2013) have also reported an involvement of P2Y<sub>6</sub> in ion channel regulation. For example, activation of P2Y<sub>6</sub> in LPS-treated (lipopolysaccharide) microglia reduces P2X<sub>4</sub> Ca<sup>2+</sup> entry and impairs ATP-dependent migration (Bernier *et al.*, 2013).

More recently, attention has focussed on the role of P2Y<sub>6</sub> in regulating innate immunity and inflammation. Somers *et al.* (1997) first speculated a role by showing a UDP-mediated upregulation of P2Y<sub>6</sub> expression and intracellular Ca<sup>2+</sup> release in activated T-cells, but not in resting T-cells. Since these early observations, other groups (Warny *et al.*, 2001; Cox *et al.*, 2005) have demonstrated P2Y<sub>6</sub>-dependent release of pro-inflammatory cytokines such as TNF- $\alpha$  and IL-8 from monocytic THP-1 cells and U937 cells. An enhanced expression and release of CCL2 and CCL3 from microglia and astrocytes following P2Y<sub>6</sub> activation has also been reported (Kim *et al.*, 2011; Morioka *et al.*, 2013). Of greater interest however, are studies placing a direct link between P2Y<sub>6</sub> and inflammation. For example, Viera *et al.* (2011) have associated P2Y<sub>6</sub> activation with cytokine release from epithelial cells in airway inflammation. Other studies also link P2Y<sub>6</sub> with vascular inflammation and atherosclerosis. Riegel *et al.* (2011) have shown that chemokine expression, adhesion molecule expression, and vascular leakage in LPS-induced inflammation, is impaired in P2Y<sub>6</sub>-deficient mice, or, in wild-type mice treated with the P2Y<sub>6</sub> antagonist MRS-2578. Similarly, Guns *et al.* (2010) observed an increase in

P2Y<sub>6</sub> expression in aortic segments from atherosclerotic mice, an effect attributed to an increased infiltration of macrophages into aortic segments. More recently, Stachon *et al.* (2014) have reported a correlation between P2Y<sub>6</sub> and leukocyte adhesion to the vessel wall. In their studies the authors reported seeing a greater expression of P2Y<sub>6</sub> in atherosclerotic aortas from apolipoprotein E-deficient/P2Y<sub>6</sub><sup>+/+</sup> mice than from mice exhibiting an apolipoprotein E-deficient/P2Y<sub>6</sub><sup>-/-</sup> phenotype, the latter of which also exhibited smaller atherosclerotic lesions than their apolipoprotein E-deficient/P2Y<sub>6</sub><sup>+/+</sup> counterparts.

Together, these studies provide important insights into the P2Y<sub>6</sub> receptor and its proposed involvement in innate immunity and inflammation. Based on the evidence provided by these studies, it seems plausible that P2Y<sub>6</sub> may engage in crosstalk with chemokine pathways involved in steering monocyte function.

## 6.2 Aims

The aim of this chapter was to investigate the requirement of the human P2Y<sub>6</sub> receptor for CCL2/CCR2-mediated monocyte signalling and function using monocytic THP-1 cells and human PBMCs as *in vitro* models. CCL2/CCR2-mediated signalling and function were indirectly measured by intracellular Ca<sup>2+</sup> release, cell migration, and adhesion to endothelial cells. Studies employed pharmacological and molecular tools for this purpose. The research presented in this chapter also looks at the involvement of the CCL2/CCR2 axis in extracellular nucleotide release from THP-1 cells.

## 6.3 Results

### 6.3.1 Effect of P2Y<sub>6</sub> antagonism on CCL2/CCR2-mediated THP-1 cell and human PBMC signalling and function

The initial aim of this chapter was to examine the requirement of the P2Y<sub>6</sub> receptor for CCL2/CCR2-mediated monocyte signalling and function. To address this aim, studies employed MRS-2578, a non-competitive and insurmountable P2Y<sub>6</sub> antagonist exhibiting an IC<sub>50</sub> of 37 ± 16 nM against UDP-mediated IP<sub>3</sub> formation in human P2Y<sub>6</sub>-transfected 1321N1 astrocytoma cells (Mamedova *et al.*, 2004). MRS-2578 (10 µM) has been shown to demonstrate little or no antagonist activity against other P2Y receptors (P2Y<sub>1</sub>, P2Y<sub>2</sub>, P2Y<sub>4</sub> and P2Y<sub>11</sub>) (Mamedova *et al.*, 2004).

#### 6.3.1.1 Effect of MRS-2578 on CCL2-evoked Ca<sup>2+</sup> responses in THP-1 cells

To investigate the requirement of P2Y<sub>6</sub> for CCL2/CCR2-mediated monocyte signalling, studies first examined the effects of a range of MRS-2578 concentrations (10 nM – 10 µM) on intracellular Ca<sup>2+</sup> responses evoked by CCL2 (50 ng/ml) in THP-1 cells. As shown in

Figure 6.1a, following the addition of 1  $\mu\text{M}$  MRS-2578 to cells, a small and sustained rise in the baseline  $\text{Ca}^{2+}$  response was seen ( $4.3 \pm 1\%F_{\text{max}}$ ,  $n=3$ ). A similar increase was also seen upon addition of 100 nM, 300 nM, and 10  $\mu\text{M}$  MRS-2578, but not upon addition of vehicle. This effect is difficult to explain, but suggests a modulation of  $\text{Ca}^{2+}$  homeostasis by MRS-2578 that might be related to its antagonism of  $\text{P2Y}_6$ . As also shown (Figure 6.1b and c), MRS-2578 produced a concentration-dependent inhibition of CCL2-evoked intracellular  $\text{Ca}^{2+}$  responses. Under these conditions, the estimated  $\text{IC}_{50}$  for MRS-2578 was  $418 \pm 68$  nM ( $n=3$ ). At the higher concentrations of MRS-2578 tested, 1 and 10  $\mu\text{M}$ , CCL2-evoked intracellular  $\text{Ca}^{2+}$  responses were impaired by  $73 \pm 7\%$  ( $n=3$ ,  $p<0.01$ ) and  $79 \pm 1\%$  ( $n=3$ ,  $p<0.01$ ), respectively. In paired experiments with 1  $\mu\text{M}$  MRS-2578, the  $\%F_{\text{max}}$  values for CCL2 in untreated and MRS-2578-treated cells were  $25 \pm 1\%$  ( $n=3$ ), and  $7 \pm 2\%$  ( $n=3$ ), respectively. Similarly, for experiments with 10  $\mu\text{M}$  MRS-2578, the  $\%F_{\text{max}}$  values for untreated and MRS-2578-treated cells were  $25 \pm 1\%$  ( $n=3$ ) and  $5 \pm 0.3\%$  ( $n=3$ ), respectively. Together, these data show a significant reduction of CCL2-evoked intracellular  $\text{Ca}^{2+}$  responses by MRS-2578.

The decay rates of  $\text{Ca}^{2+}$  transients for all treatments were also compared, but were not significantly different ( $p<0.05$ ). For example, in paired experiments with 1  $\mu\text{M}$  MRS-2578, the  $\tau$  values for CCL2 in untreated and treated cells were  $90 \pm 11$  seconds ( $n=3$ ) and  $80 \pm 14$  seconds ( $n=3$ ), respectively ( $n=3$ ,  $p>0.05$ ).

To rule out the possibility of cytotoxicity, THP-1 cells were exposed to MRS-2578 (1 and 10  $\mu\text{M}$ ) for 2.5 hours prior to viability testing in trypan blue and LDH assays (Appendix Figures A3 and A5). The results of trypan blue assays suggested a possible cytotoxic effect with 10  $\mu\text{M}$ , but not 1  $\mu\text{M}$ -MRS 2578. The  $\%$  viable cells for vehicle, 10  $\mu\text{M}$  and 1  $\mu\text{M}$  MRS-2578 were  $100 \pm 15\%$  ( $n=3$ ),  $49 \pm 4\%$  ( $n=3$ ), and  $85 \pm 4\%$  ( $n=3$ ,  $p>0.05$ ), respectively. While a significant difference between vehicle and 10  $\mu\text{M}$  MRS-2578 was not evident using a paired t-test ( $n=3$ ,  $p>0.05$ ), a one-way ANOVA with Bonferroni's multiple comparison suggested that 10  $\mu\text{M}$  MRS-2578 reduced cell viability ( $n=3$ ,  $p<0.01$ ). THP-1 cells treated with 1  $\mu\text{M}$  MRS-2578 however, did not cause a reduction in cell viability with either statistical test ( $n=3$ ,  $p>0.05$ ). In the LDH assay, the  $\%$  control values ( $\%$  of Triton-X) for 1  $\mu\text{M}$  (13%,  $n=1$ ) and 10  $\mu\text{M}$  MRS-2578 (14%,  $n=1$ ) fell below the 20% toxic threshold. Since these experiments were performed at 2.5 hours and in the case of LDH were only an  $n=1$  replicate, firm conclusions about the effect of MRS-2578 on THP-1 cell viability in intracellular  $\text{Ca}^{2+}$  experiments may not be drawn.

To understand the requirement of  $\text{P2Y}_6$  further, the effects of 1  $\mu\text{M}$  MRS-2578 were examined in the absence of extracellular  $\text{Ca}^{2+}$  (see Chapter 2, Section 2.6.2 for methodology). As shown (Figure 6.2a), 1  $\mu\text{M}$  MRS-2578 produced a small elevation in baseline  $\text{Ca}^{2+}$ . The response was less than that seen in experiments with extracellular

Ca<sup>2+</sup> and thus, was difficult to quantify. As also shown (Figure 6.2b and c), MRS-2578 significantly impaired CCL2-evoked intracellular Ca<sup>2+</sup> responses by 42 ± 2% (n=3, p<0.05), where the %Fmax values for CCL2 in untreated and MRS-2578-treated cells were 9 ± 1% (n=3) and 5 ± 1% (n=3), respectively. These data indicate that MRS-2578 impairs CCL2-evoked intracellular Ca<sup>2+</sup> responses in the absence of extracellular Ca<sup>2+</sup>. This is interesting because it suggests that MRS-2578 impairs GPCR-mediated intracellular Ca<sup>2+</sup> release. What is also interesting about these data is that the % inhibition of CCL2-evoked intracellular Ca<sup>2+</sup> responses under these conditions is almost 2-fold less than that seen in the presence of intracellular Ca<sup>2+</sup> (73 ± 7%, n=3, p<0.01). This suggests that the level of inhibition by MRS-2578 depends almost equally on GPCR-mediated intracellular Ca<sup>2+</sup> release and Ca<sup>2+</sup> influx.

The decay rates for both treatments were also interesting as they suggested that MRS-2578 promoted a 32 ± 1% (n=3, p<0.01) faster decay of Ca<sup>2+</sup> transients in the absence of extracellular Ca<sup>2+</sup> (Figure 6.2d). The τ values for untreated and MRS-2578-treated THP-1 cells were 146 ± 5 seconds (n=3) and 99 ± 3 seconds (n=3), respectively. Since a similar effect is not evident with MRS-2578 in the presence of extracellular Ca<sup>2+</sup>, it seems possible that the effects seen here support an impairment of GPCR-mediated intracellular Ca<sup>2+</sup> release by MRS-2578.

Together, these data suggest that the P2Y<sub>6</sub> antagonist MRS-2578 attenuates CCL2-evoked intracellular Ca<sup>2+</sup> responses in THP-1 cells. These data suggest a possible requirement of P2Y<sub>6</sub> for CCL2/CCR2-mediated intracellular Ca<sup>2+</sup> signalling in monocytes.

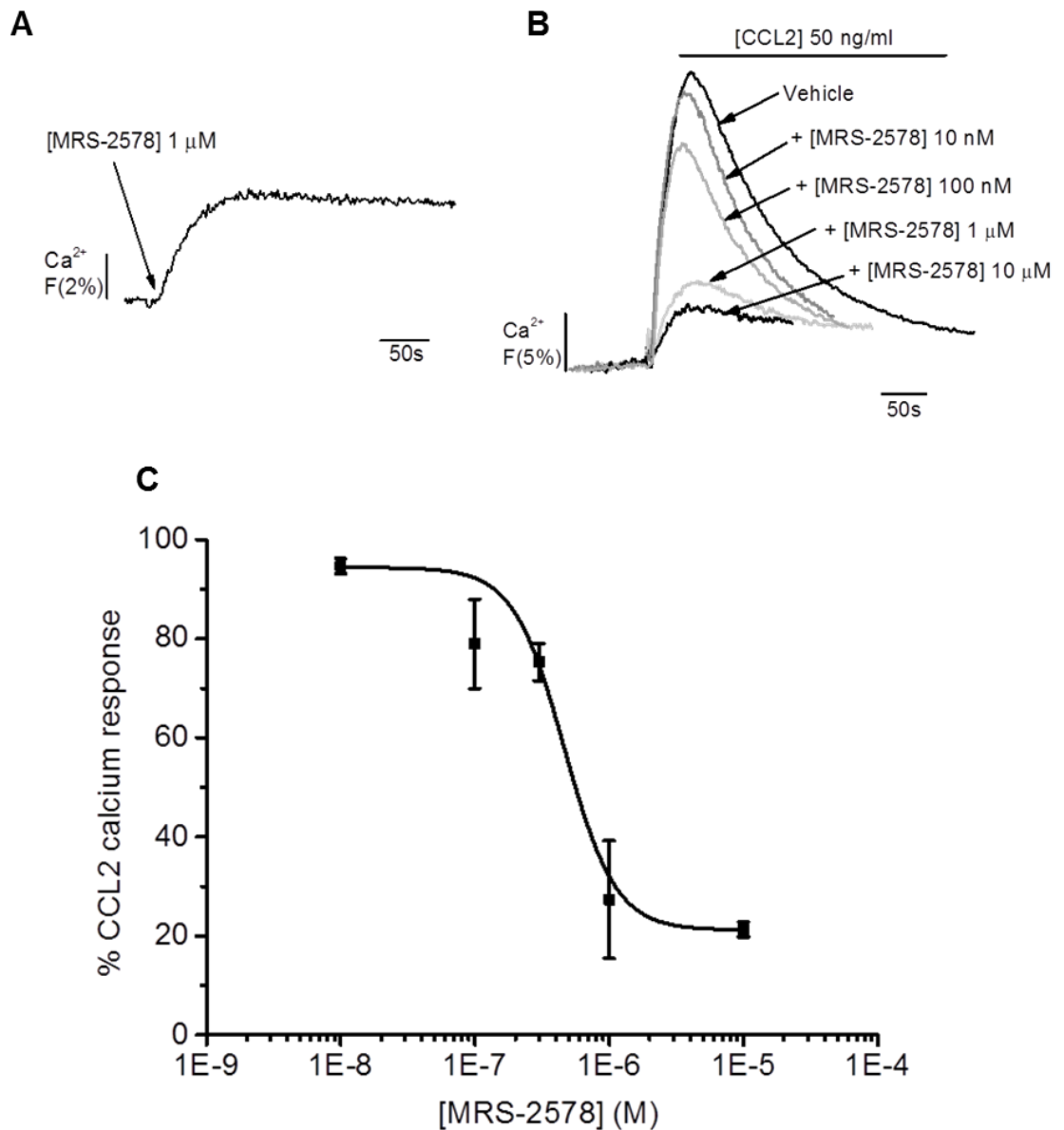


**Figure 6.1 Effect of MRS-2578 on CCL2-evoked Ca<sup>2+</sup> responses in THP-1 cells**

(A) Representative trace showing the effect of 1  $\mu$ M MRS-2578 on baseline intracellular Ca<sup>2+</sup>. (B) Representative Ca<sup>2+</sup> transients to CCL2 (50 ng/ml) in THP-1 cells pre-treated with vehicle (DMSO) or MRS-2578 (10 nM-10  $\mu$ M) for 15 minutes. Responses normalised to Ca<sup>2+</sup> signals elicited by 40  $\mu$ M digitonin (%Fmax). (C) Normalised concentration-response curve showing the effect of MRS-2578 (10 nM-10  $\mu$ M, 15 minutes), on intracellular Ca<sup>2+</sup> responses to 50 ng/ml CCL2. Responses given as a percentage of CCL2 %Fmax in the absence of MRS-2578. Data represents mean  $\pm$  SEM from n=3 replicates.

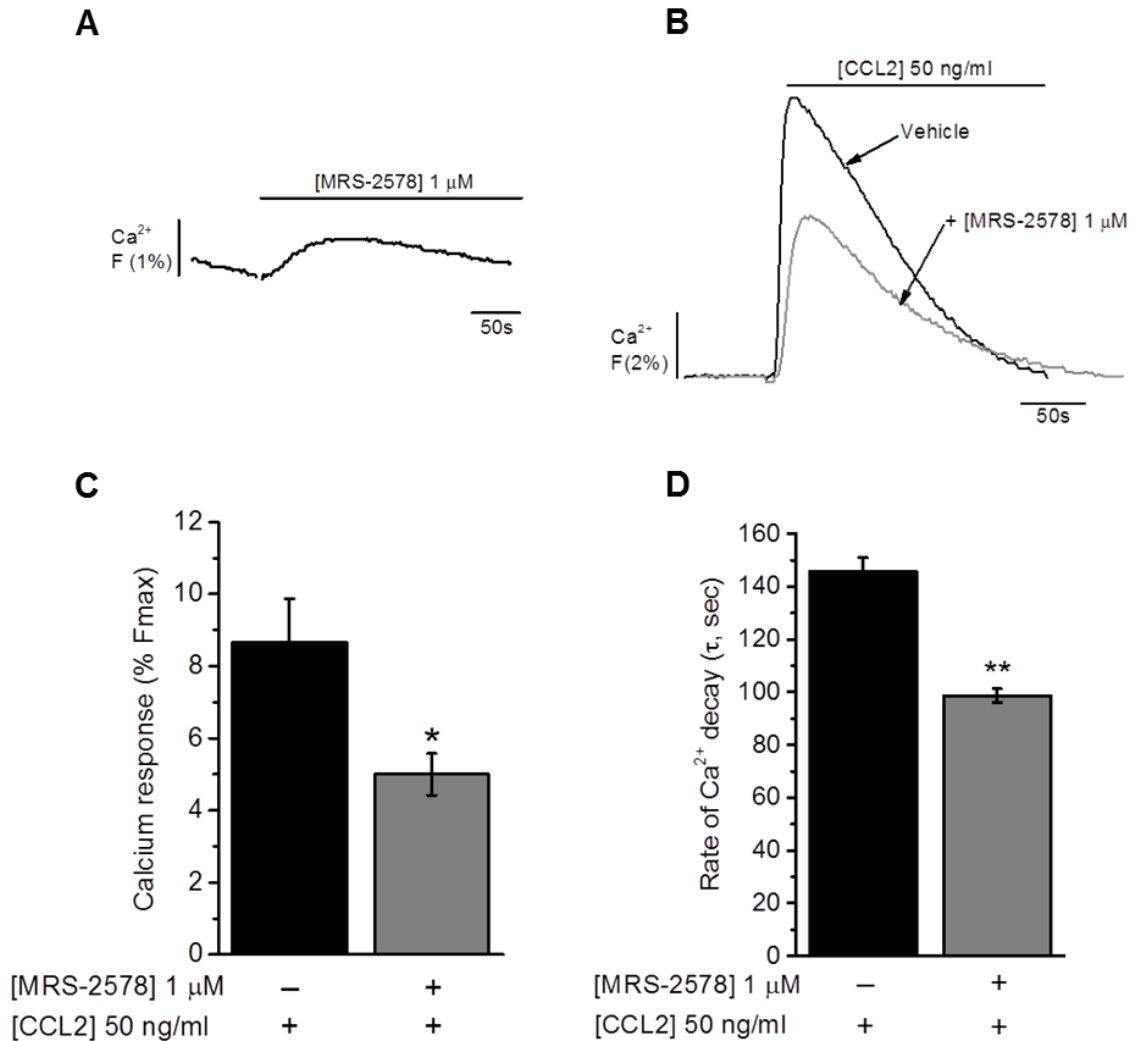


**Figure 6.2 Effect of MRS-2578 on CCL2-evoked Ca<sup>2+</sup> responses in THP-1 cells in the absence of extracellular Ca<sup>2+</sup>**

(A) Representative trace showing the effect of 1 μM MRS-2578 on baseline intracellular Ca<sup>2+</sup>. (B) Representative Ca<sup>2+</sup> transients to CCL2 (50 ng/ml) in THP-1 cells pre-treated with vehicle (DMSO) or MRS-2578 (1 μM) for 15 minutes. (C) Bar chart showing normalised intracellular Ca<sup>2+</sup> responses to CCL2 (50 ng/ml) in THP-1 cells pre-treated with vehicle (DMSO) or MRS-2578 (1 μM) for 15 minutes. Responses normalised to Ca<sup>2+</sup> signals elicited by 40 μM digitonin (% Fmax). (D) Bar chart showing Ca<sup>2+</sup> decay rates (τ, sec) for Ca<sup>2+</sup> transients to CCL2 (50 ng/ml) in THP-1 cells pre-treated with vehicle (DMSO) or MRS-2578 (1 μM) for 15 minutes. Data represents mean ± SEM from n=3 replicates. Asterisks indicate significant changes towards vehicle (\*p<0.05, \*\*p<0.01, Students t-test).

### 6.3.1.2 Effect of MRS-2578 on CCL2-evoked Ca<sup>2+</sup> responses in human PBMCs

The next experiments sought to examine the effects of 1  $\mu$ M MRS-2578 on (50 ng/ml) CCL2-evoked intracellular Ca<sup>2+</sup> responses in human PBMCs. The rationale behind these studies was to understand the requirement of P2Y<sub>6</sub> for CCL2/CCR2-mediated signalling in monocytes using primary human cells comprising of a mixed cell population. As shown (Figure 6.3a), a small increase in the baseline Ca<sup>2+</sup> response was observed upon addition of 1  $\mu$ M MRS-2578. Although this effect was difficult to quantify, it mirrored the effects of MRS-2578 on baseline Ca<sup>2+</sup> in THP-1 cells. As also shown (Figure 6.3b and c), MRS-2578 attenuated CCL2-evoked intracellular Ca<sup>2+</sup> responses in PBMCs by  $34 \pm 9\%$  ( $n=3$ ,  $p<0.05$ ), where the %Fmax values for untreated and MRS2578-treated cells were  $5 \pm 1\%$  ( $n=3$ ) and  $3 \pm 1\%$  ( $n=3$ ), respectively. Interestingly, the % inhibition in PBMCs with MRS-2578 was ~2-fold less than that observed in THP-1 cells ( $73 \pm 7\%$ ,  $n=3$ ,  $p<0.01$ ). This result may reflect the fact that PBMCs are heterogeneous and comprise of several cell types in addition to monocytes. Although the magnitude of responses were affected by MRS-2578, a comparison of the decay rates for treatments did not reveal a significant difference ( $n=3$ ,  $p>0.05$ ) between untreated ( $36 \pm 8$  seconds,  $n=3$ ) and MRS-2578-treated cells ( $46 \pm 5$  seconds,  $n=3$ ). This data suggests that MRS-2578 does not influence the decay of CCL2 Ca<sup>2+</sup> transients in PBMCs.

These results suggest that MRS-2578 impairs CCL2-evoked intracellular Ca<sup>2+</sup> responses in human PBMCs, of which a subset are monocytes. Taken together, these data suggest that P2Y<sub>6</sub> is required for CCL2/CCR2-mediated signalling in human PBMCs.

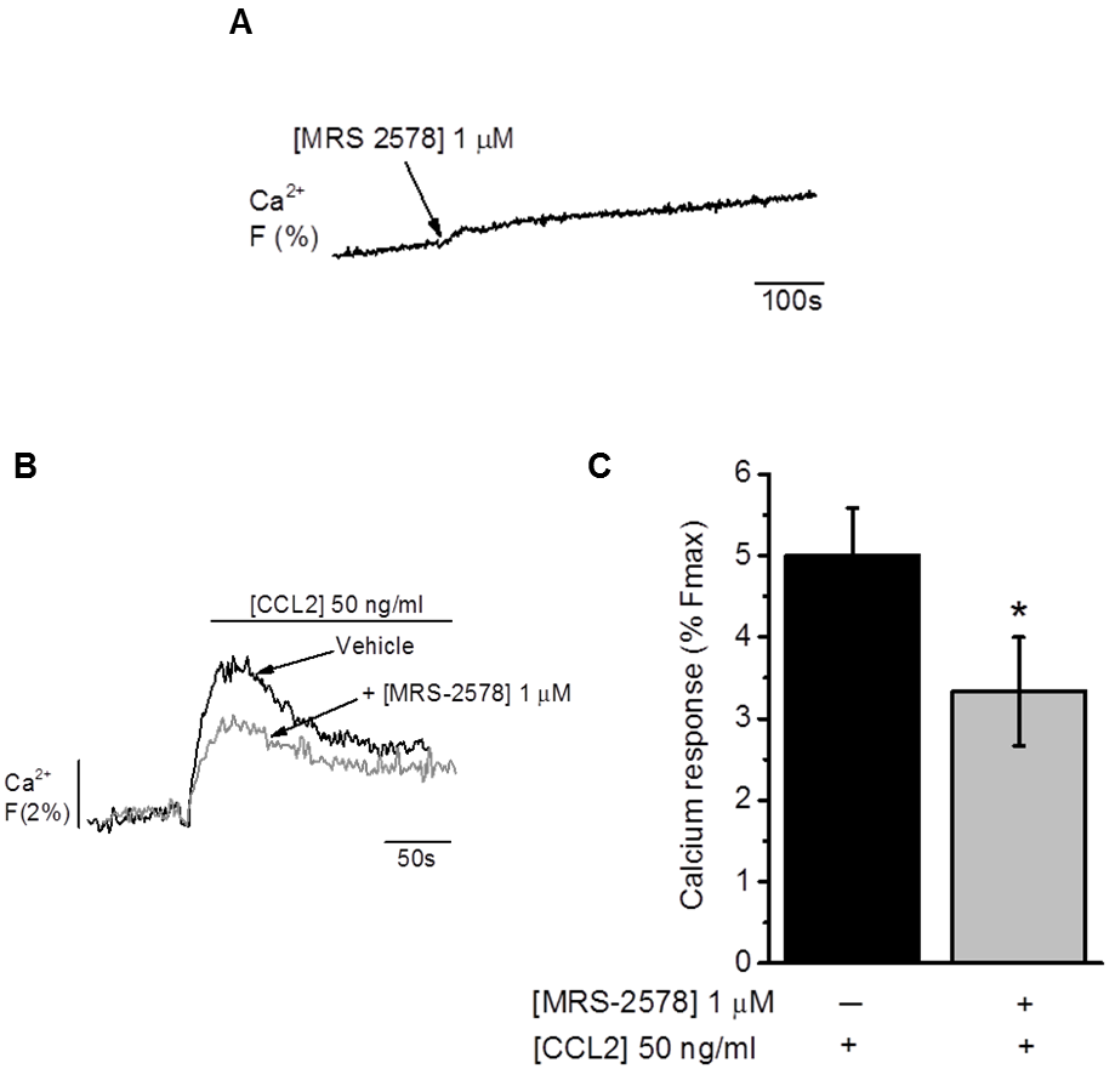


**Figure 6.3 Effect of MRS-2578 on CCL2-evoked Ca<sup>2+</sup> responses in human PBMCs**

(A) Representative trace showing the effect of 1  $\mu$ M MRS-2578 on baseline intracellular Ca<sup>2+</sup>. (B) Representative Ca<sup>2+</sup> transients to CCL2 (50 ng/ml) in PBMCs pre-treated with vehicle (DMSO) or MRS-2578 (1  $\mu$ M) for 15 minutes. (C) Bar chart showing normalised intracellular Ca<sup>2+</sup> responses to CCL2 (50 ng/ml) in PBMCs pre-treated with vehicle (DMSO) or MRS-2578 (1  $\mu$ M) for 15 minutes. Responses normalised to Ca<sup>2+</sup> signals elicited by 40  $\mu$ M digitonin (%Fmax). Data represents mean  $\pm$  SEM from n=3 replicates. Asterisks indicate significant changes towards vehicle (\*p<0.05, Students t-test).

### 6.3.1.3 Effect of dual P2Y<sub>6</sub>/CCR2 antagonism on CCL2-evoked Ca<sup>2+</sup> responses in THP-1 cells

Previous studies conducted by Mamedova *et al.* (2004) have shown that 1  $\mu$ M MRS-2578 abolishes agonist-induced P2Y<sub>6</sub> activation. In THP-1 cell experiments presented earlier in this chapter (Section 6.3.1.2), it was seen that 1  $\mu$ M MRS-2578 impaired CCL2-evoked Ca<sup>2+</sup> responses by  $73 \pm 7\%$  ( $n=3$ ,  $p<0.01$ ). Hence, it could conceivably be hypothesised that 73% of the CCL2-evoked intracellular Ca<sup>2+</sup> response is attributable to P2Y<sub>6</sub>, and 27% to bona-fide CCR2. Thus, it was important to test the effects of dual P2Y<sub>6</sub>/CCR2 antagonism on CCL2-evoked intracellular Ca<sup>2+</sup> responses in THP-1 cells. To this end, cells were pre-treated with either vehicle, 1  $\mu$ M MRS-2578, or 1  $\mu$ M MRS-2578 plus 100 nM of the CCR2 antagonist, BMS-CCR2-22 prior to CCL2 (50 ng/ml) challenge.

A small increase in baseline Ca<sup>2+</sup> was observed following the addition of 1  $\mu$ M MRS-2578 to THP-1 cells. This was also seen in experiments where MRS-2578 and BMS-CCR2-22 were co-applied (Figure 6.4a). As also shown (Figure 6.4b and c), 1  $\mu$ M MRS-2578 inhibited CCL2-evoked intracellular Ca<sup>2+</sup> responses to a similar degree as seen previously ( $64 \pm 6\%$ ,  $n=3$ ,  $p<0.01$ ), where the %Fmax values for CCL2 in untreated and MRS-2578-treated cells were  $25 \pm 1\%$  ( $n=3$ ) and  $9 \pm 2\%$  ( $n=3$ ), respectively. The residual CCL2 Ca<sup>2+</sup> response was abolished ( $100 \pm 0\%$  inhibition,  $n=3$ ,  $p<0.01$ ), by pre-treatment of cells with 1  $\mu$ M MRS-2578 and 100 nM BMS-CCR2-22, where the %Fmax value for CCL2 was  $0 \pm 0\%$  ( $n=3$ ). This result suggests that 36% of the CCL2-evoked intracellular Ca<sup>2+</sup> response in THP-1 cells is attributable to bona-fide CCR2 activation.

An examination of the decay rates ( $\tau$ , sec) for untreated ( $89 \pm 1$  seconds,  $n=3$ ) and 1  $\mu$ M MRS-2578-treated THP-1 cells ( $108 \pm 12$  seconds,  $n=3$ ) showed that these were not significantly different ( $n=3$ ,  $p>0.05$ ), therefore supporting previous results (Section 6.3.1.2). As Ca<sup>2+</sup> transients for CCL2 were abolished by a co-application of 1  $\mu$ M MRS-2578 and 100 nM BMS-CCR2-22, the  $\tau$  values for these transients could not be analysed.

Taken together, these data suggest that CCL2-evoked intracellular Ca<sup>2+</sup> responses in monocytes involve an activation of CCR2 and P2Y<sub>6</sub>.

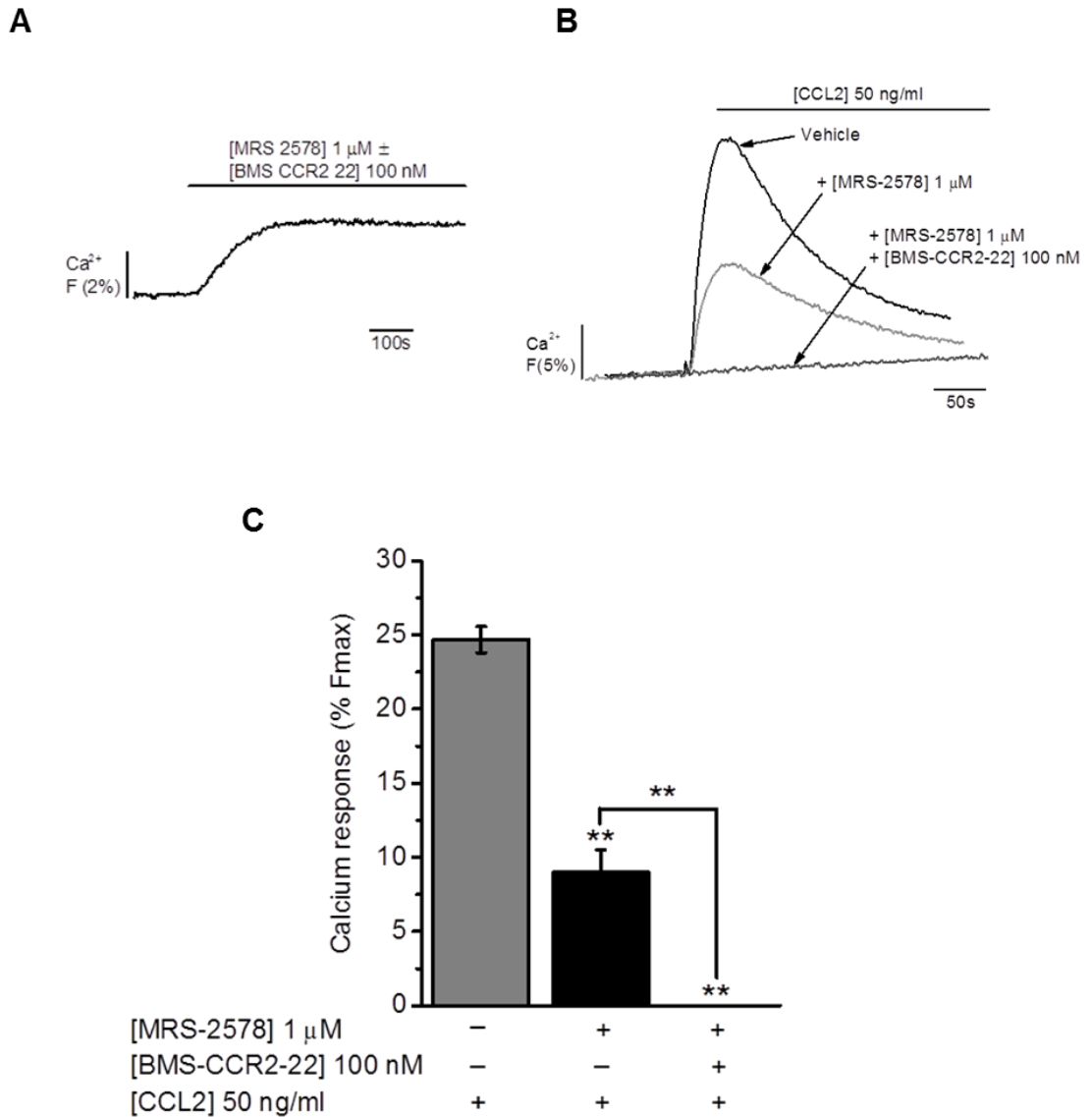


**Figure 6.4 Effect of MRS-2578 and BMS-CCR2-22 on CCL2-evoked Ca<sup>2+</sup> responses in THP-1 cells**

(A) Representative trace showing the effect of 1  $\mu$ M MRS-2578 on baseline intracellular Ca<sup>2+</sup>. (B) Representative Ca<sup>2+</sup> transients to CCL2 (50 ng/ml) in THP-1 cells pre-treated with vehicle (DMSO), MRS-2578 (1  $\mu$ M), or MRS-2578 (1  $\mu$ M) plus BMS-CCR2-22 (100 nM) for 15 minutes. (C) Bar chart showing normalised intracellular Ca<sup>2+</sup> responses to CCL2 (50 ng/ml) in THP-1 cells pre-treated with vehicle (DMSO), MRS-2578 (1  $\mu$ M), or MRS-2578 (1  $\mu$ M) plus BMS-CCR2-22 (100 nM) for 15 minutes. Responses normalised to Ca<sup>2+</sup> signals elicited by 40  $\mu$ M digitonin (% Fmax). Data represents mean  $\pm$  SEM from n=3 replicates. Asterisks indicate significant changes towards vehicle (\*\*p<0.01, One-way ANOVA with Bonferroni's multiple comparison).

#### 6.3.1.4 Effect of MRS-2578 on CCL2-mediated THP-1 cell and PBMC chemotaxis

To determine the requirement of P2Y<sub>6</sub> for CCL2/CCR2-mediated monocyte function, studies examined the effects of MRS-2578 on THP-1 cell/PBMC migration towards CCL2, and THP-1 cell adhesion to quiescent and TNF $\alpha$ -treated HUVEC monolayers.

The effects of 1  $\mu$ M MRS-2578 on THP-1 cell migration towards CCL2 (50 ng/ml) were first tested. As shown in Figure 6.5, the chemotactic indexes of THP-1 cells towards vehicle ( $1 \pm 1$ , n=4) and CCL2 ( $7 \pm 2$ , n=4) indicated a significant increase in cell migration towards CCL2 (n=4, p<0.01). As also shown, 1  $\mu$ M MRS-2578 significantly attenuated THP-1 cell chemotaxis towards CCL2 by  $82 \pm 2\%$  (n=4, p<0.01), where the chemotactic index for MRS-2578-treated cells was  $1 \pm 0.2$  (n=4) and therefore similar to vehicle. In general, therefore, these results suggest a significant impairment of THP-1 cell chemotaxis towards CCL2 by MRS-2578. While it is possible that this effect could be attributed to MRS-2578 cytotoxicity, trypan blue and LDH studies (Appendix Figures A3 and A5) showed no significant loss in cell viability after a 2.5 hour exposure of THP-1 cells with 1  $\mu$ M MRS-2578.

A similar experiment with 1  $\mu$ M MRS-2578 was conducted in human PBMCs. As shown (Figure 6.6), THP-1 cells demonstrated a significantly (n=12, p<0.01) higher chemotactic index towards CCL2 ( $25 \pm 4$ , n=12) than towards vehicle ( $1 \pm 0.5$ , n=12). From this data it is also noticeable that PBMCs displayed a higher chemotactic index towards CCL2 than THP-1 cells. This is interesting and may reflect less chemokinesis by PBMCs. As also shown, treatment of cells with MRS-2578 significantly attenuated PBMC chemotaxis towards CCL2 by  $82 \pm 5\%$  (n=12, p<0.01), where a chemotactic index of  $6 \pm 2$  (n=12) was seen. Interestingly, the % inhibition observed in PBMCs was similar to that of THP-1 cells, and may reflect the level of P2Y<sub>6</sub> involvement in CCL2/CCR2-mediated migration.

In summary, these data suggests that MRS-2578 significantly impairs THP-1 cell and human PBMC migration towards CCL2. This suggests that P2Y<sub>6</sub> is required for CCL2/CCR2-mediated monocyte chemotaxis.

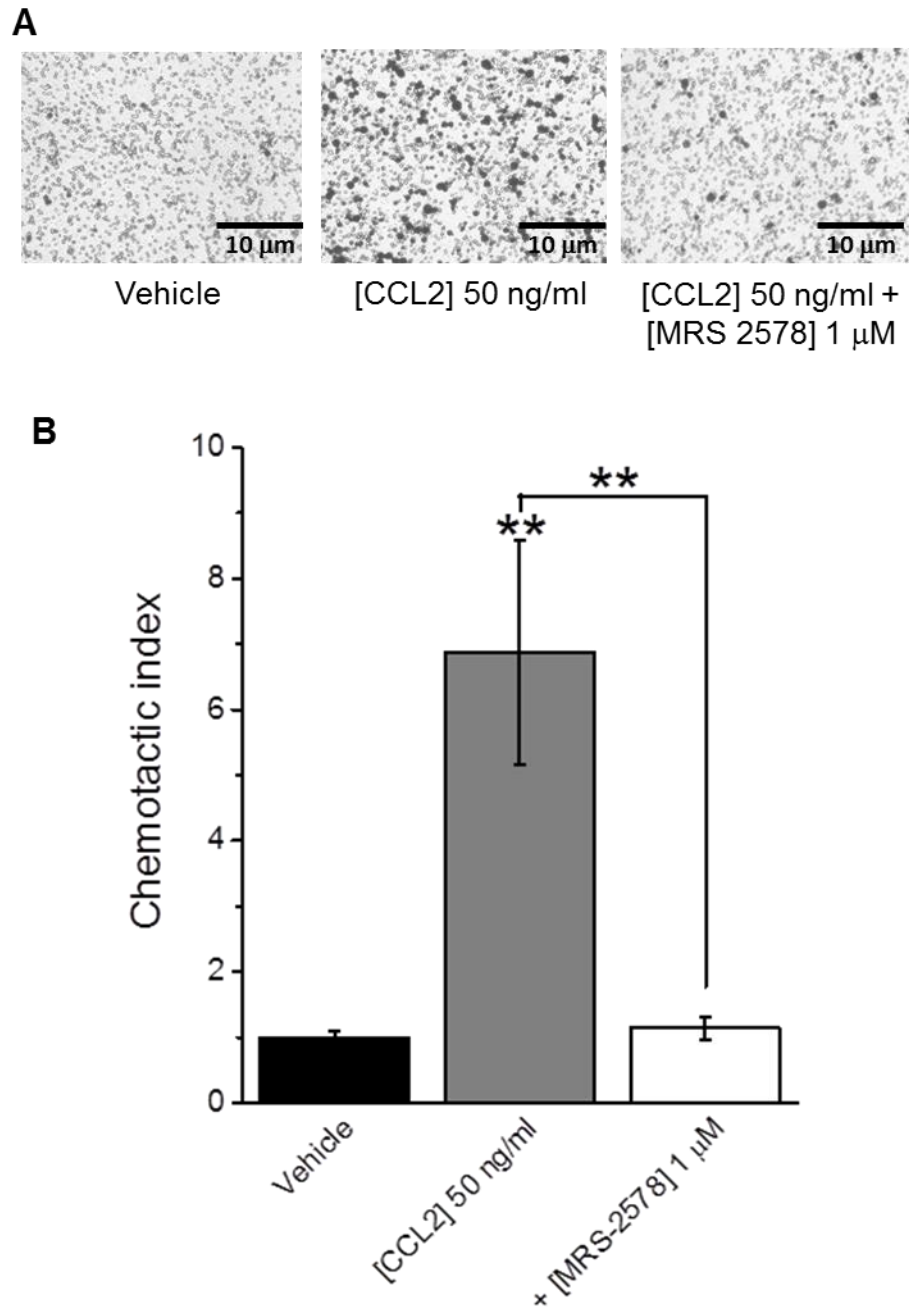


**Figure 6.5 Effect of MRS-2578 on CCL2-mediated THP-1 cell chemotaxis**

(A) Representative images showing the effect of MRS-2578 (1 μM) on THP-1 cell chemotaxis towards CCL2 (50 ng/ml, lower chamber, 2hrs). Scale bar represents 10 μm. (B) Bar chart showing normalised THP-1 cell chemotaxis towards vehicle (water) or CCL2 (50 ng/ml, lower chamber, 2hrs) with or without MRS-2578 (1 μM). Chemotactic index is a ratio of the number of cells that migrated towards CCL2 over the number of cells that migrated towards vehicle. Data represents mean ± SEM from n=4 transwells. Asterisks indicate significant changes towards vehicle (\*\*p<0.01, One-way ANOVA with Bonferroni's multiple comparison).

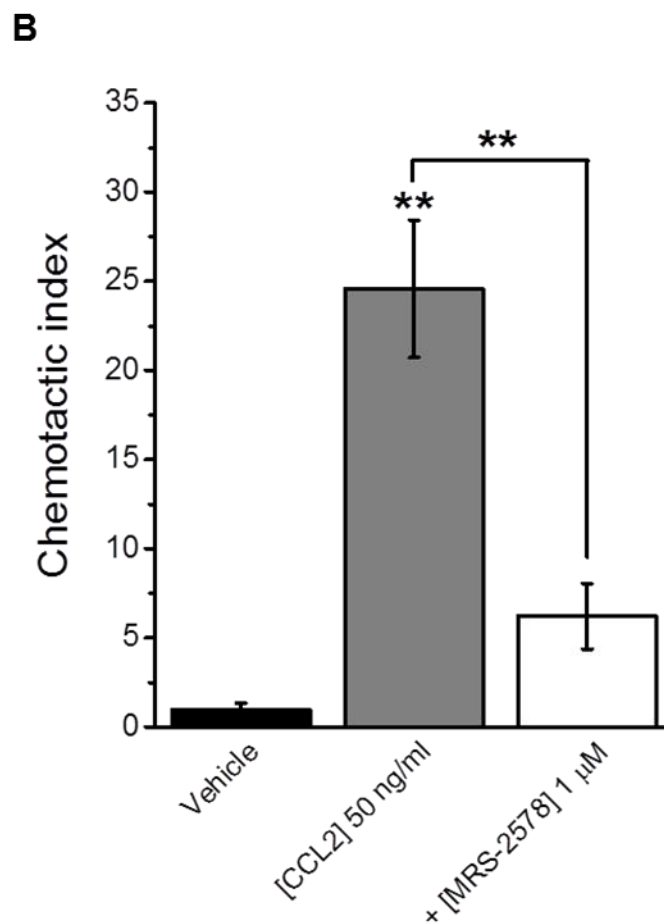
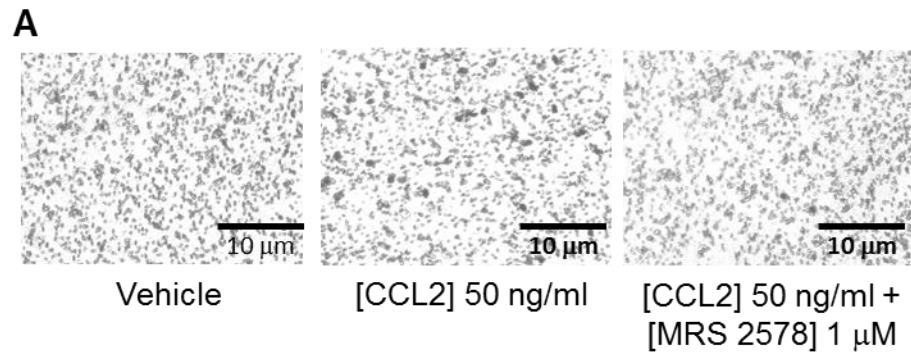


**Figure 6.6 Effect of MRS-2578 on CCL2-mediated human PBMC chemotaxis**

(A) Representative images showing the effect of MRS-2578 (1 μM) on PBMC chemotaxis towards CCL2 (50 ng/ml, lower chamber, 2hrs). Scale bar represents 10 μm. (B) Bar chart showing normalised PBMC chemotaxis towards vehicle (water) or CCL2 (50 ng/ml, lower chamber, 2hrs), with or without MRS-2578 (1 μM). Chemotactic index is a ratio of the number of cells that migrated towards CCL2 over the number of cells that migrated towards vehicle. Data represents mean ± SEM from a total of n=12 transwells from n=3 donors. Asterisks indicate significant changes towards vehicle (\*\*p<0.01, One-way ANOVA with Bonferroni's multiple comparison).

### 6.3.1.5 Effect of MRS-2578 on CCL2-mediated THP-1 cell adhesion

Several studies thus far have linked P2Y<sub>6</sub> with vascular inflammation (Bar *et al.*, 2008; Guns *et al.*, 2010; Riegel *et al.*, 2011; Stachon *et al.*, 2014). One of these studies by Riegel *et al.* (2011), demonstrated a selective induction of P2RY6 expression in human microvascular endothelial cells following treatment with TNF $\alpha$ . In follow-on experiments in a mouse model of endotoxemia, the authors noticed that knockout of P2Y<sub>6</sub> reduced cytokine and adhesion molecule expression, and reduced LPS-dependent vascular leakage. Other studies by Guns *et al.* (2010) and Stachon *et al.* (2014) discovered a correlation between P2RY6 expression and an increased infiltration of macrophages and other leukocytes towards vessel walls in aortic segments from atherosclerotic mice. As described previously in this thesis, a number of studies have also suggested a similar involvement of CCR2 in vascular inflammation (Boring *et al.*, 1998; Gu *et al.*, 1998; Weber *et al.*, 1999). It is possible, therefore, that monocyte adhesion to the vascular endothelium involves crosstalk between P2Y<sub>6</sub> and CCR2.

To examine the above hypothesis, studies employed MRS-2578 to investigate the requirement of P2Y<sub>6</sub> for adhesion of CCL2-primed THP-1 cells to quiescent and TNF $\alpha$ -treated HUVEC monolayers. For experiments, CCL2-primed THP-1 cells were incubated with 1  $\mu$ M MRS-2578 for 45 minutes and then allowed to adhere to vehicle or TNF $\alpha$ -treated (10 ng/ml) HUVEC cell monolayers.

In quiescent HUVEC experiments (Figure 6.7a), vehicle-treated THP-1 cells exhibited a % adhesion of  $31 \pm 10\%$  (n=12). This result is interesting since it suggests that THP-1 cells adhere to HUVECs in the absence of stimulus. A significant increase in % adhesion ( $100 \pm 11\%$ , n=12, p<0.01) was seen with CCL2-primed THP-1 cells and suggested that CCL2 priming facilitated adhesion. As also shown (Figure 6.7a), treatment of CCL2-primed THP-1 cells with MRS-2578 significantly attenuated adhesion by  $70 \pm 9\%$  (n=12, p<0.01), bringing the % adhesion down a level comparable to vehicle-treated cells ( $30 \pm 9\%$ , n=12).

A similar effect with 1  $\mu$ M MRS-2578 was observed in experiments with TNF $\alpha$ -treated HUVEC monolayers (Figure 6.7b). The % adhesion of vehicle-treated THP-1 cells was  $28 \pm 12\%$  (n=12) and therefore similar to adhesion of these cells to quiescent HUVECs. As also shown, CCL2-priming significantly increased the % adhesion of THP-1 cells to TNF $\alpha$ -treated HUVEC monolayers by  $100 \pm 26\%$  (n=12, p<0.05), therefore supporting quiescent HUVEC experiments. As also shown (Figure 6.7b), treatment of CCL2-primed THP-1 cells with 1  $\mu$ M MRS-2578 attenuated adhesion by  $78 \pm 15\%$  (n=12, p<0.05), with cells displaying a % adhesion comparable to vehicle-treated cells ( $22 \pm 15\%$ , n=12).

Taken together, these data indicate that MRS-2578 significantly impairs adhesion of CCL2-primed THP-1 cells to quiescent and TNF $\alpha$ -treated HUVEC monolayers. Based on this evidence, a requirement of P2Y<sub>6</sub> for CCL2/CCR2-mediated monocyte adhesion to the vascular endothelium seems plausible.

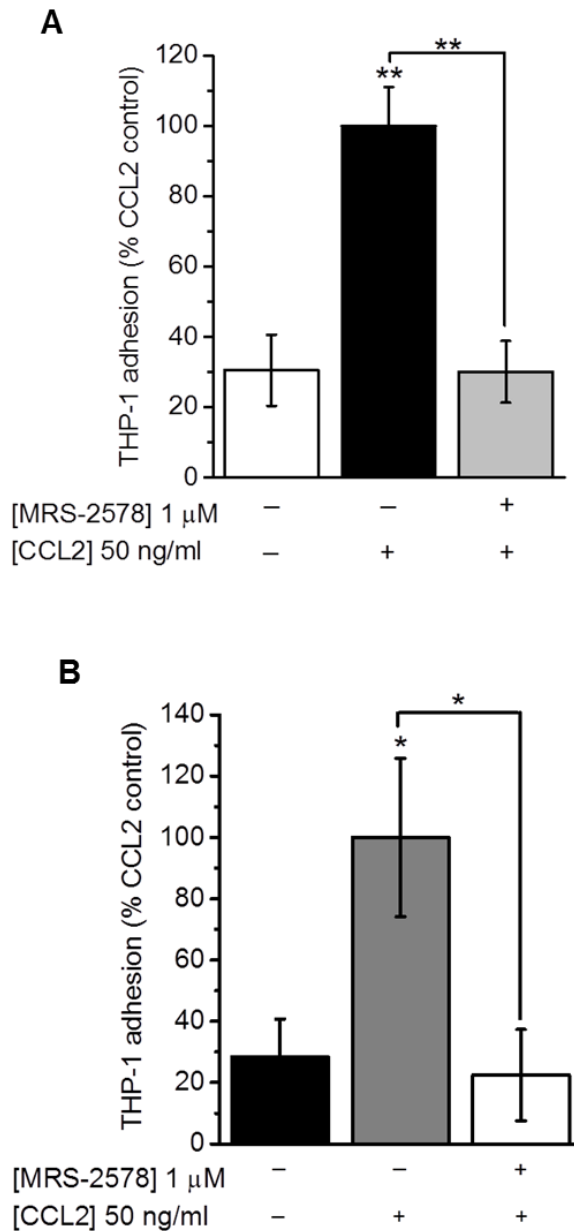


**Figure 6.7 Effect of MRS-2578 on CCL2-mediated THP-1 cell adhesion to quiescent and TNF $\alpha$ -treated HUVEC monolayers**

Bar chart showing normalised adhesion of vehicle or CCL2-primed (50 ng/ml) THP-1 cells to (A) quiescent and (B) TNF $\alpha$ -treated (10 ng/ml, 5 hours) HUVEC monolayers after treatment with vehicle (DMSO) or MRS-2578 (1  $\mu$ M, 45 minutes). Normalised adhesion represented as a percentage of mean adhesion of CCL2-primed THP-1 cells in the absence of MRS-2578. Data represents mean  $\pm$  SEM from a total of n=12 replicates from n=3 experiments. Asterisks indicate significant changes towards vehicle (\*p<0.05, \*\*p<0.01, One-way ANOVA with Bonferroni's multiple comparison).

### 6.3.2 Characterisation of P2Y<sub>6</sub>-stable and parental 1321N1 astrocytoma cells

#### 6.3.2.1 Extracellular nucleotide-evoked Ca<sup>2+</sup> responses in P2Y<sub>6</sub>-stable 1321N1 cells

The human P2Y<sub>6</sub> receptor has been shown in human P2Y<sub>6</sub>-transfected 1321N1 astrocytoma cells to be activated by UDP, UTP, ADP and ATP with EC<sub>50</sub> values of 300 nM, 6 μM, 30 μM, and >3 mM, respectively (Communi *et al.*, 1996). It is possible therefore, that one or more of these ligands are involved in activating P2Y<sub>6</sub> upon activation of CCR2. Thus, in an effort to examine this hypothesis, the human P2Y<sub>6</sub> receptor was pharmacologically characterised by examining intracellular Ca<sup>2+</sup> responses evoked by ATP, ADP, UTP, and UDP in human P2Y<sub>6</sub>-stable and parental 1321N1 cells (gift from Professor Jens George Leipziger).

**Table 6.1 Nucleotide Ca<sup>2+</sup> responses in P2Y<sub>6</sub>-stable 1321N1 cells**

Ligand	EC <sub>50</sub>	F-Ratio at highest concentration	Concentration at which minimum response detected and F-Ratio
ATP	>100μM	0.3 ± 0.1 (100 μM)	300 nM (0.01 ± 0.01)
ADP	3.4 ± 0.2 μM	0.9 ± 0.06 (100 μM).	300 nM (0.004 ± 0.002)
UTP	887 ± 113 nM	1 ± 0.1 (100 μM)	10 nM (0.0004 ± 0.0004)
UDP	23 ± 2.6 nM	0.7 ± 0.06 (10 μM)	10 nM (0.14 ± 0.04)

EC<sub>50</sub> values represent mean ± SEM from n=3 estimations. F-Ratio is a change in intracellular Ca<sup>2+</sup> following subtraction of the baseline response. F-ratio represents mean ± SEM from a total of n=9 replicates from n=3 experiments.

As shown above in Table 6.1 (and Appendix Figures A20 and A21), all of the nucleotides tested (ATP, ADP, UTP, and UDP) evoked concentration-dependent increases in intracellular Ca<sup>2+</sup> in P2Y<sub>6</sub>-stable 1321N1 cells. Of the ligands tested, the weakest ligand was ATP with an EC<sub>50</sub> of >100μM, and the most potent ligand was UDP with an estimated EC<sub>50</sub> of 23 ± 2.6 nM (n=3).

Together, these data suggest an order of potency of UDP > UTP > ADP > ATP that is consistent with the order of potency proposed by Communi *et al.* (1996). The EC<sub>50</sub> values estimated in the current study suggest a greater potency of these ligands in driving intracellular Ca<sup>2+</sup> release than IP<sub>3</sub> formation.

#### 6.3.2.2 Extracellular nucleotide-evoked Ca<sup>2+</sup> responses in parental 1321N1 cells

Studies reported by Communi *et al.* (1996) and Cox *et al.* (2005) have demonstrated that parental 1321N1 cells and pcDNA3-transfected 1321N1 cells do not respond to classical extracellular nucleotides. If correct, then it is reasonable to suggest that ATP, ADP, UTP,

and UDP are ligands of the human P2Y<sub>6</sub> purinoceptor. Thus, to confirm the findings of Communi *et al.* (1996) and Cox *et al.* (2005), ATP-, ADP-, UTP-, and UDP-evoked intracellular Ca<sup>2+</sup> responses in parental 1321N1 cells were tested.

**Table 6.2 Nucleotide Ca<sup>2+</sup> responses in parental 1321N1 cells**

Ligand	Ca <sup>2+</sup> response	
	F-Ratio at 100 µM	F-Ratio at 10 µM
Vehicle	0.13 ± 0.02	
ATP	0.15 ± 0.01	0.14 ± 0.01
ADP	0.17 ± 0.01	0.16 ± 0.009
UTP	0.15 ± 0.01	0.15 ± 0.01
UDP	0.18 ± 0.01	0.15 ± 0.009

The F-Ratio is a change in intracellular calcium following subtraction of the baseline response. Data represents mean ± SEM from a total of n=9 replicates from n=3 experiments.

As shown above in Table 6.2 (and Appendix Figure A22), no significant changes in the F-Ratio were observed with any of the nucleotides tested when compared with vehicle (n=9, p>0.05 for all treatments). These results suggest that parental 1321N1 cells do not respond to the extracellular nucleotides ATP, ADP, UTP, or UDP. It can therefore be assumed that intracellular Ca<sup>2+</sup> responses evoked by these ligands in P2Y<sub>6</sub>-1321N1 cells, involves a selective activation of the human P2Y<sub>6</sub> purinoceptor.

### 6.3.2.3 Effect of MRS-2578 on ADP and UDP-evoked Ca<sup>2+</sup> responses in P2Y<sub>6</sub>-stable 1321N1 cells

The P2Y<sub>6</sub>-stable 1321N1 cells were next employed to examine the effects of MRS-2578 on ADP- and UDP-evoked intracellular Ca<sup>2+</sup> responses. The aim of this study was to understand the effects of P2Y<sub>6</sub> antagonism on P2Y<sub>6</sub>-specific Ca<sup>2+</sup> responses. To address this aim, cells were pre-treated with MRS-2578 (0.1 pM – 1 µM) prior to challenge with EC<sub>50</sub> concentrations of ADP (3.4 µM) or UDP (23 nM).

As shown in Figure 6.8 and Figure 6.9, MRS-2578 produced a concentration-dependent inhibition of ADP- and UDP-evoked intracellular Ca<sup>2+</sup> responses. In experiments involving ADP, the % control values in cells treated with vehicle or 1 µM MRS-2578 were 100 ± 5% (n=9) and 70 ± 6% (n=9), respectively and although not statistically significant (n=9, p=0.7), suggested an inhibition of 29 ± 6% (n=9). A possible explanation for the variability of this data may be the poor solubility of MRS-2578. In experiments with UDP, the %

control values for untreated and MRS-2578-treated cells were  $100 \pm 4\%$  (n=9) and  $62 \pm 6\%$  (n=9), respectively and were indicative of a  $36 \pm 6\%$  inhibition (n=9,  $p < 0.05$ ). UDP  $\text{Ca}^{2+}$  responses were also significantly attenuated by 1 pM ( $23 \pm 5\%$ , n=9,  $p < 0.05$ ), 10 pM ( $24 \pm 4\%$ , n=9,  $p < 0.05$ ), 10 nM ( $22 \pm 6\%$ , n=9,  $p < 0.01$ ) and 100 nM MRS-2578 ( $35 \pm 4\%$ , n=9,  $p < 0.01$ ).

An examination of the decay rates of  $\text{Ca}^{2+}$  transients showed that 1  $\mu\text{M}$  MRS-2578 facilitated a  $14 \pm 6\%$  (n=9,  $p < 0.05$ ) faster decay of ADP  $\text{Ca}^{2+}$  transients, where the  $\tau$  values of untreated and MRS-2578-treated cells were  $33 \pm 2$  seconds (n=9) and  $28 \pm 1$  seconds (n=9), respectively (Figure 6.8c). UDP  $\text{Ca}^{2+}$  transients for untreated ( $40 \pm 2$  seconds, n=9) and 1  $\mu\text{M}$  MRS-2578-treated cells ( $40 \pm 2$  seconds, n=9) were not significantly different (n=9,  $p > 0.05$ ).

Taken together, these data suggest that MRS-2578 attenuates UDP-evoked  $\text{Ca}^{2+}$  responses in  $\text{P2Y}_6$ -stable 1321N1 cells. This may reflect a preferential activation of  $\text{P2Y}_6$  by UDP.

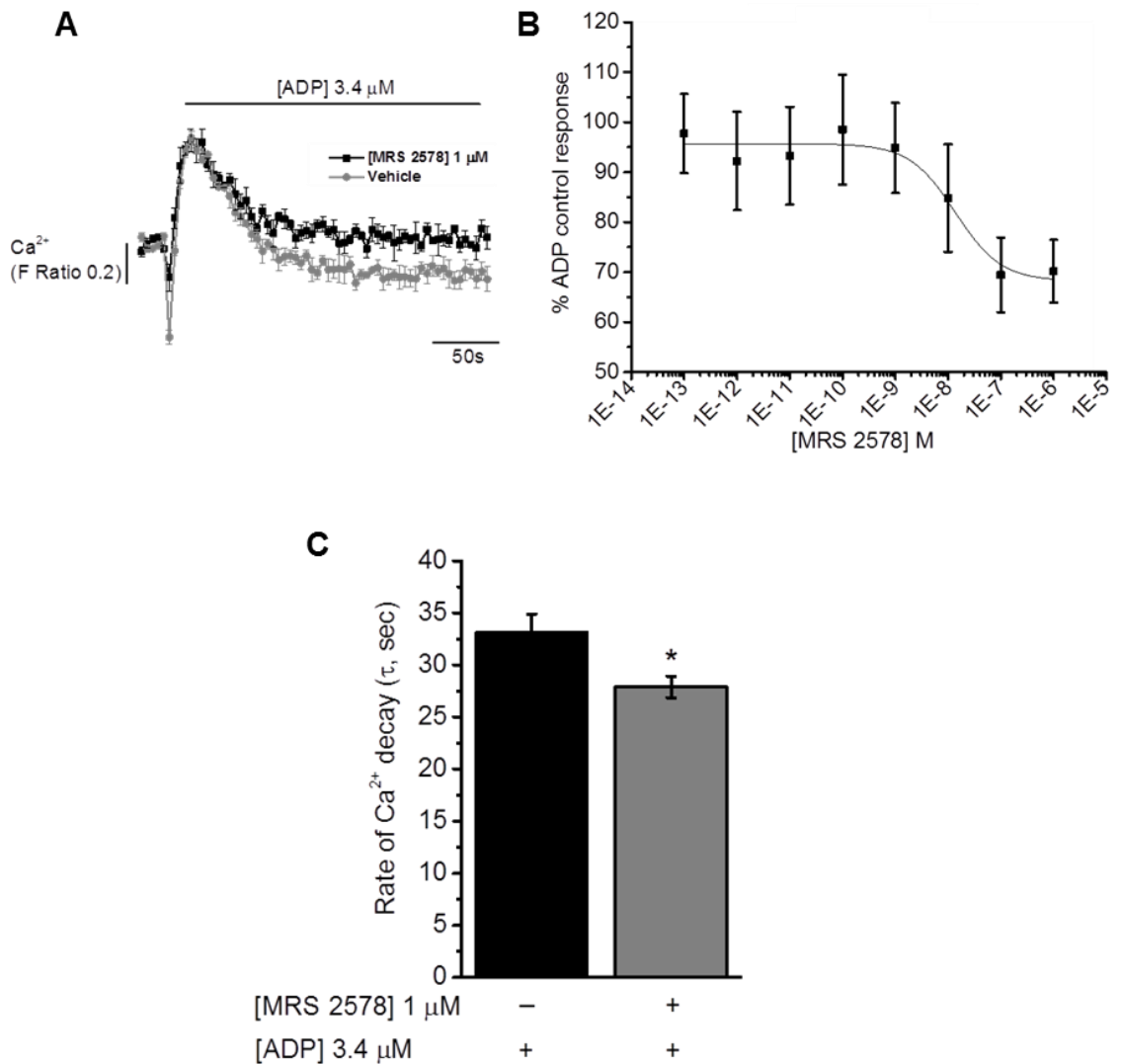


**Figure 6.8 Effect of MRS-2578 on ADP-evoked Ca<sup>2+</sup> responses in P2Y<sub>6</sub>-stable 1321N1 cells**

(A) Representative Ca<sup>2+</sup> transients to ADP (3.4  $\mu$ M) in P2Y<sub>6</sub>-transfected 1321N1 cells pre-treated with vehicle (DMSO) or MRS-2578 (1  $\mu$ M), for 30 minutes. (B) Concentration-response curve showing the effect of MRS-2578 (0.1 pM – 1  $\mu$ M, 30 minutes) on normalised intracellular Ca<sup>2+</sup> responses to ADP (3.4  $\mu$ M) in P2Y<sub>6</sub>-transfected 1321N1 cells. Responses given as a percentage of normalised peak Ca<sup>2+</sup> responses to ADP in the absence of MRS-2578. (C) Bar chart showing Ca<sup>2+</sup> decay rates ( $\tau$ , sec) for Ca<sup>2+</sup> transients to ADP (3.4  $\mu$ M) in P2Y<sub>6</sub>-transfected 1321N1 cells pre-treated with vehicle (DMSO) or MRS-2578 (1  $\mu$ M) for 30 minutes. Data represents mean  $\pm$  SEM from a total of n=9 replicates from n=3 experiments. Asterisks indicate significant changes towards vehicle (\*p<0.05, Students t-test).

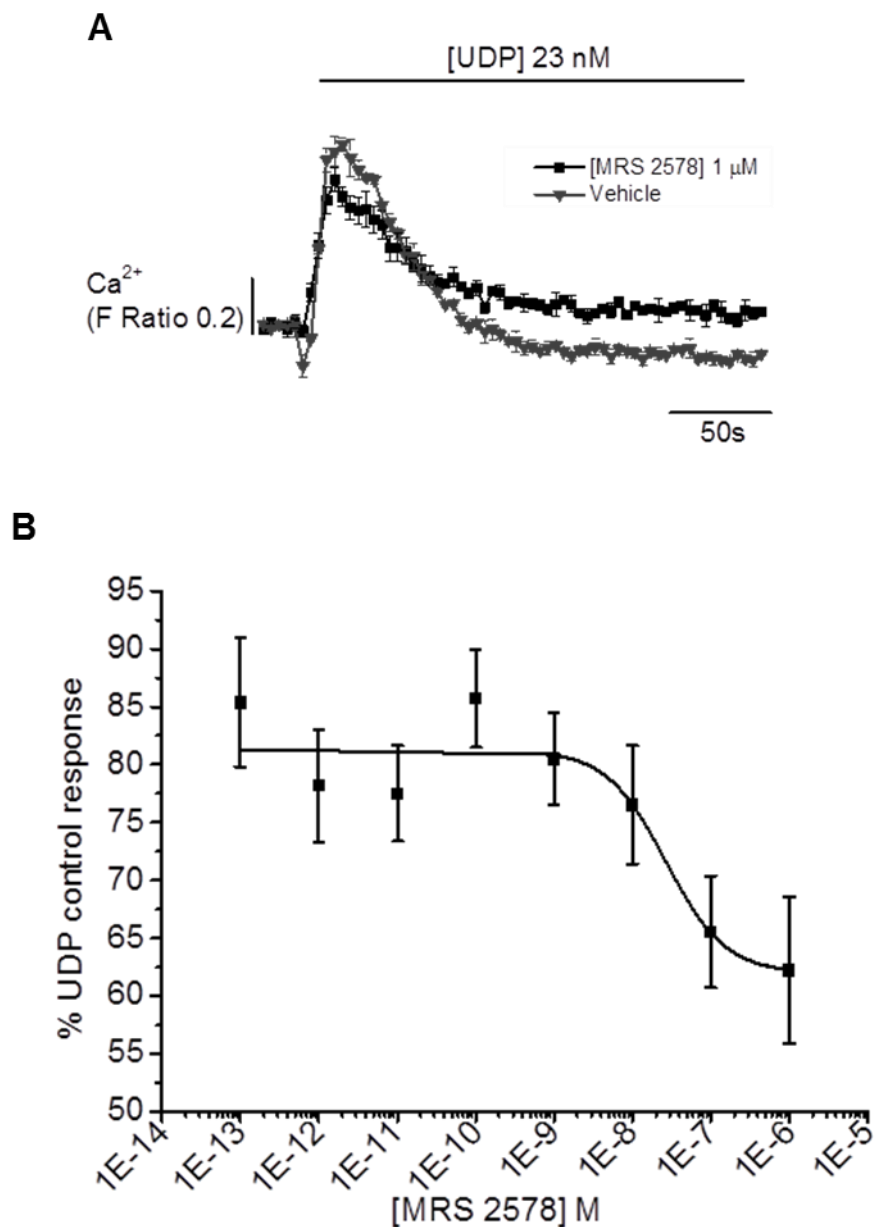


**Figure 6.9 Effect of MRS-2578 on UDP-evoked Ca<sup>2+</sup> responses in P2Y<sub>6</sub>-stable 1321N1 cells**

(A) Representative Ca<sup>2+</sup> transients to UDP (23 nM) in P2Y<sub>6</sub>-transfected 1321N1 cells pre-treated with vehicle (DMSO) or MRS-2578 (1 μM), for 30 minutes. (B) Concentration-response curve showing the effect of MRS-2578 (0.1 pM – 1 μM, 30 minutes) on normalised intracellular Ca<sup>2+</sup> responses to UDP (23 nM) in P2Y<sub>6</sub>-transfected 1321N1 cells. Responses given as a percentage of normalised peak Ca<sup>2+</sup> responses to UDP in the absence of MRS-2578. Data represents mean ± SEM from a total of n=9 replicates from n=3 experiments.

### 6.3.3 Effect of P2Y<sub>6</sub> antagonism on extracellular nucleotide-evoked Ca<sup>2+</sup> responses in THP-1 cells

The results presented in this chapter suggest a requirement of P2Y<sub>6</sub> for efficient CCL2/CCR2-mediated monocyte signalling and function. These data also suggest that ATP, ADP, UTP, and UDP activate P2Y<sub>6</sub>. It is possible, therefore, that one or more of these ligands participate in P2Y<sub>6</sub> activation after CCR2 is activated. It may also be that MRS-2578 blocks P2Y<sub>6</sub> activation by these ligands. The next studies therefore tested the effects of 1 μM MRS-2578 on intracellular Ca<sup>2+</sup> responses evoked by 1 μM ATP, ADP, UTP, and UDP-evoked in monocytic THP-1 cells.

**Table 6.3 Effect of MRS-2578 on extracellular nucleotide-evoked Ca<sup>2+</sup> responses in THP-1 cells**

Ligand	Ca <sup>2+</sup> response (%Fmax)	
	Vehicle	1 μM MRS-2578
ATP	29 ± 1	20 ± 0.3**
ADP	6 ± 0.3	3 ± 0.3*
UTP	38 ± 1	26 ± 2**
UDP	6 ± 0.3	5 ± 0.3*

Intracellular Ca<sup>2+</sup> responses to ATP, ADP, UTP, and UDP (all 1 μM) in THP-1 cells pre-treated with vehicle (DMSO) or MRS-2578 (1 μM) for 15 minutes. Responses normalised to Ca<sup>2+</sup> signals elicited by 40 μM digitonin (%Fmax). Data represents mean ± SEM from n=3 replicates. Asterisks indicate significant changes towards vehicle (\*p<0.05, \*\*p<0.01, Students t-test).

As shown in Table 6.3 (and Appendix Figures A23 and A24), MRS-2578 significantly inhibited intracellular Ca<sup>2+</sup> responses evoked by all four extracellular nucleotides. The % inhibition values for ATP (31 ± 1%, n=3, p<0.01), ADP (41 ± 5%, n=3, p<0.05), UTP (32 ± 5%, n=3, p<0.01) and UDP (26 ± 5%, n=3, p<0.05) suggested that intracellular Ca<sup>2+</sup> responses evoked by ATP and ADP were more sensitive than UTP or UDP to attenuation by MRS-2578. Interestingly, the τ values for ADP and UDP Ca<sup>2+</sup> transients were not possible to determine, and may have indicated a preferential activation of P2Y<sub>6</sub>, which is a slow-desensitising receptor (Robaye *et al.*, 1996). In experiments involving ATP, the decay rates for Ca<sup>2+</sup> transients for untreated (129 ± 4 seconds, n=3) and MRS-2578-treated cells (156 ± 5 seconds, n=3) were not significantly different (n=3, p=0.06), but indicated that MRS-2578 slowed the decay of ATP Ca<sup>2+</sup> transients by 1.2 ± 0.1 fold (n=3). In experiments involving UTP however, MRS-2578 increased the decay of Ca<sup>2+</sup> transients

by  $1.3 \pm 0.1$ -fold ( $n=3$ ,  $p<0.05$ ), where the  $\tau$  values for ADP in untreated and MRS-2578-treated cells were  $108 \pm 3$  seconds ( $n=3$ ) and  $142 \pm 8$  seconds ( $n=3$ ), respectively. These data are interesting because they suggest that MRS-2578 preferentially slows the decay of NTP-evoked  $\text{Ca}^{2+}$  transients.

Taken together, these data suggest that MRS-2578 attenuates intracellular  $\text{Ca}^{2+}$  responses evoked by 1  $\mu\text{M}$  ATP, ADP, UTP and UDP with a rank order of ADP>UTP>ATP>UDP. This finding suggests that ADP is likely to play a bigger role than other extracellular nucleotides in engaging with  $\text{P2Y}_6$  upon CCR2 activation in monocytes.

#### **6.3.4 The functional presence of $\text{P2Y}_{14}$ in THP-1 cells**

The human  $\text{P2Y}_{14}$  receptor was first cloned by Nomura et al. (1994) from human myeloid KG-1 cells and is encoded by the *P2YR14* gene located on the long arm of chromosome 3 (3q24-q25.1).  $\text{P2Y}_{14}$  shares most pair-wise identity with  $\text{P2Y}_{12}$  and  $\text{P2Y}_{13}$  (47%) (Nomura et al., 1994; Chambers, 2000; Abbracchio et al., 2006). Although  $\text{P2Y}_{14}$  signalling is primarily through PTx-sensitive  $\text{G}\alpha_{i/o}$ -type G-proteins coupled to adenylate cyclase inhibition, PLC activation has also been reported, and is likely to involve a dual coupling of  $\text{P2Y}_{14}$  to  $\text{G}\alpha_{i/o}$  and  $\text{G}\alpha_{q/11}$  (Chambers, 2000; Skelton et al., 2003; Müller et al., 2005).

The human  $\text{P2Y}_{14}$  purinoceptor is activated by several UDP-sugars, including UDP-glucose, UDP-*N*-acetyl glucosamine, and UDP-glucuronic acid (Fricks et al., 2009). In humans, the preferred ligands of  $\text{P2Y}_{14}$  are UDP and UDP-galactose (Fricks et al., 2009; Carter et al., 2009). Although studies by Fricks et al. (2009) initially suggested that UDP blocked  $\text{P2Y}_{14}$ , the same group later reported that UDP acted as an agonist of  $\text{P2Y}_{14}$  ( $\text{EC}_{50}$  29-74 nM), and that earlier experiments were inaccurate as they were performed using test models expressing low levels of  $\text{P2Y}_{14}$  and non-cognate  $\text{G}\alpha_{15/16}$  G-proteins (Carter et al., 2009).

The experiments presented in this chapter have shown that 1  $\mu\text{M}$  MRS-2578 attenuates UDP-evoked  $\text{Ca}^{2+}$  responses in THP-1 cells by  $26 \pm 5\%$  ( $n=3$ ,  $p<0.05$ ) (Section 6.3.3). This result suggests that 74% of the UDP response is resistant to MRS-2578. Since UDP is also a ligand of  $\text{P2Y}_{14}$ , it is possible that the MRS-2578-resistant component is attributed to  $\text{P2Y}_{14}$ . An experiment to assess this hypothesis would have ideally involved the use of a  $\text{P2Y}_{14}$ -selective antagonist, but due to none being commercially available, this experiment could not be performed. Instead, the current study sought to provide functional evidence for  $\text{P2Y}_{14}$  in THP-1 cells by testing  $\text{Ca}^{2+}$  responses to 30  $\mu\text{M}$  UDP-glucose, a  $\text{P2Y}_{14}$  ligand exhibiting an  $\text{EC}_{50}$  of 72-323 nM in cAMP inhibition assays in human  $\text{P2Y}_{14}$ -transfected HEK 293, CHO and rat C6-glioma cells (Carter et al., 2009).

As shown (Figure 6.10), UDP-glucose caused a transient intracellular  $\text{Ca}^{2+}$  response in THP-1 cells, where the %Fmax responses for cells challenged with vehicle or UDP-glucose (30  $\mu\text{M}$ ) were  $0.7 \pm 0.3\%$  (n=3) and  $4.7 \pm 0.3\%$  (n=3), respectively (n=3,  $p < 0.05$ ). These data suggest that functional  $\text{P2Y}_{14}$  purinoceptors are expressed in THP-1 cells. Furthermore, since no studies in literature have tested the effects of UDP-glucose or other UDP sugars on  $\text{P2Y}_6$  activation, these data also indicate that UDP-glucose-evoked intracellular  $\text{Ca}^{2+}$  responses in THP-1 cells do not involve  $\text{P2Y}_6$ .

Taken together and in combination with the previous results presented in Section 6.3.3, these data suggest that UDP-evoked intracellular  $\text{Ca}^{2+}$  responses in THP-1 cells and monocytes involve the UDP-sensitive receptors,  $\text{P2Y}_6$  and  $\text{P2Y}_{14}$ .

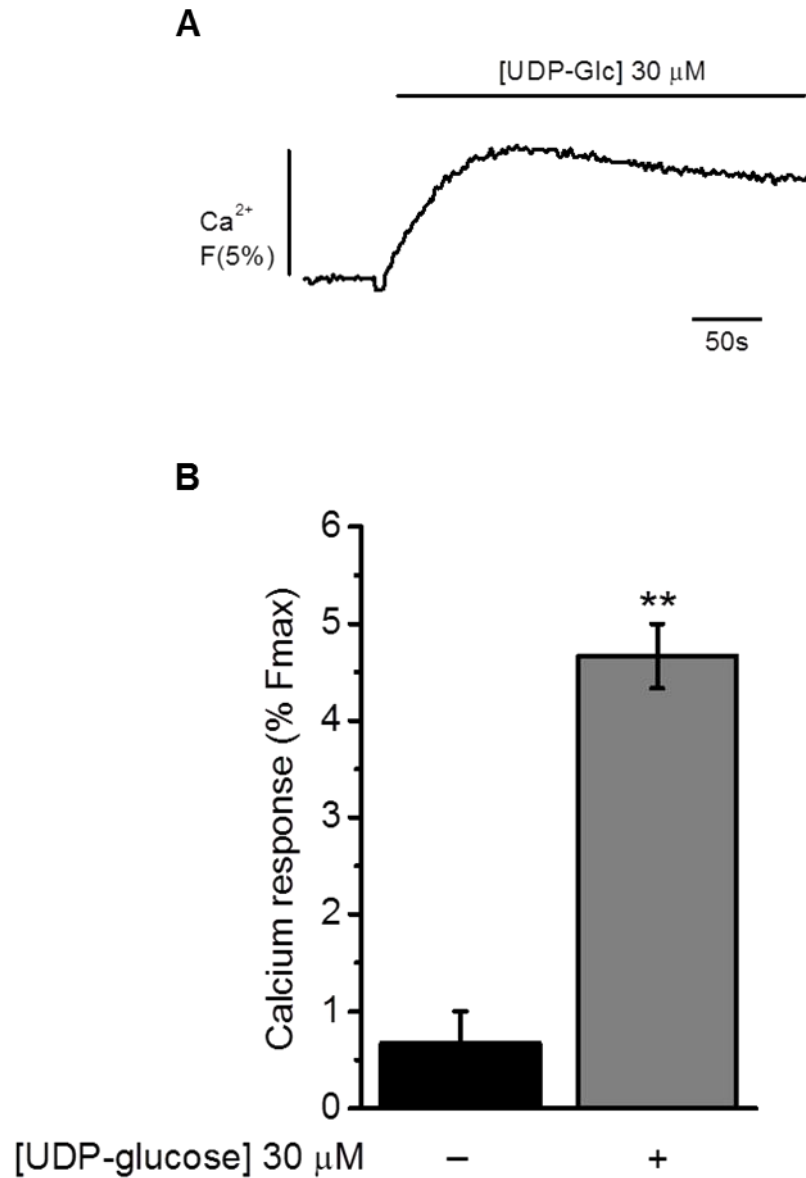


**Figure 6.10 UDP-glucose-evoked  $\text{Ca}^{2+}$  responses in THP-1 cells**

(A) Representative  $\text{Ca}^{2+}$  transient in THP-1 cells to UDP-glucose (30  $\mu\text{M}$ ). (B) Bar chart showing normalised intracellular  $\text{Ca}^{2+}$  responses to vehicle (water) or UDP-glucose (30  $\mu\text{M}$ ) in THP-1 cells. Responses normalised to  $\text{Ca}^{2+}$  signals elicited by 40  $\mu\text{M}$  digitonin (% Fmax). Data represents mean  $\pm$  SEM from  $n=3$  replicates. Asterisks indicate significant changes towards vehicle (\*\* $p<0.01$ , Students t-test).

### 6.3.5 Investigating CCR2 and P2Y<sub>6</sub> crosstalk in THP-1 cells

The evidence presented thus far suggests that CCL2/CCR2-mediated monocyte signalling and function involves crosstalk between CCR2 and P2Y<sub>6</sub>. Indeed, crosstalk of purinoceptors with other signalling pathways is not a novel phenomenon and was first seen by Ralevic and Burnstock (1990) in studies which identified ATP as a synergistic co-transmitter with noradrenaline in sympathetic nerves. Other groups have since identified crosstalk between purinoceptors and a number of other signalling pathways, including those driven by N-formyl-Met-Leu-Phe (fMLP) (Chen *et al.*, 2006), thromboxanes (Oestreich *et al.*, 2013), and cysteinyl leukotrienes (Mellor *et al.*, 2001).

Crosstalk between different GPCR pathways can also result in an amplification of intracellular Ca<sup>2+</sup> responses through the activation of different G-proteins (Gerwins and Fredholm, 1992; Werry *et al.*, 2003). Purinoceptors have also been reported to engage in crosstalk with other GPCRs via common isoforms of PLC. For example, Roach *et al.* (2008) discovered that Ca<sup>2+</sup> responses in RAW264-7 macrophage cells and mouse bone marrow-derived macrophages involved synergism between UDP and complement 5a through the activation of PLCβ3.

#### 6.3.5.1 Effect of CCL2/UDP co-application on Ca<sup>2+</sup> responses in THP-1 cells

Given the possibility that monocyte signalling and function involves crosstalk between CCR2 and P2Y<sub>6</sub>, it is possible that the ligands of these receptors, CCL2 and UDP, act synergistically. To examine this hypothesis, intracellular Ca<sup>2+</sup> responses in THP-1 cells were tested following challenge with either CCL2 alone (50 ng/ml), UDP alone (30 μM), or a combination of both (CCL2/UDP).

As shown (Figure 6.11), the %Fmax responses for THP-1 cells challenged with CCL2 (25 ± 1%, n=4) and UDP (11 ± 2%, n=4) were significantly different (n=4, p<0.01). In THP-1 cells challenged with CCL2/UDP, a %Fmax of 30 ± 1% (n=4) was seen and gave a significantly higher response than UDP alone (n=4, p<0.05) (Figure 6.11). The %Fmax response for CCL2/UDP was not significantly higher than cells challenged with CCL2 alone (n=4, p=0.055), but suggested a 1.4 ± 0.2 fold (n=4) increase. Although not statistically significant, this result suggests that further experiments may show that a co-application of CCL2 and UDP amplifies CCL2-evoked intracellular Ca<sup>2+</sup> responses in THP-1 cells. A further analysis of the decay rates showed that the τ values for CCL2 (114 ± 6 seconds, n=4) and UDP (291 ± 73 seconds, n=4) were significantly different (n=4, p<0.05), with UDP Ca<sup>2+</sup> transients exhibiting a slower decay, possibly from P2Y<sub>6</sub> activation (Figure 6.11c). In comparison, cells challenged with CCL2/UDP exhibited a τ value of 94 ± 8 seconds (n=4), which indicated a significantly faster decay than UDP alone

(n=4, p<0.05), but no faster or slower than CCL2 (n=4, p>0.05). This result suggests that the rate of decay of Ca<sup>2+</sup> transients for CCL2 and CCL2/UDP are similar.

Taken together, these data suggest that a co-application of CCL2 and UDP to THP-1 cells does not amplify CCL2 intracellular Ca<sup>2+</sup> responses. However, as data hinted at a possible amplification, it may be that further studies are required to confirm this.

#### **6.3.5.2 Effect of BMS-CCR2-22 on UDP-evoked Ca<sup>2+</sup> responses in THP-1 cells**

To examine further for crosstalk between CCR2 and P2Y<sub>6</sub>, the next studies investigated the effects of the CCR2 antagonist, BMS-CCR2-22 (100 nM) on UDP (30 μM)-evoked intracellular Ca<sup>2+</sup> responses in THP-1 cells. As shown (Figure 6.12), UDP-evoked Ca<sup>2+</sup> responses were not significantly affected by BMS-CCR2-22, where the %Fmax responses for UDP in untreated (11 ± 0.3, n=3) and BMS-CCR2-22-treated cells (12 ± 0.3, n=3) were not statistically different (n=3, p>0.05). A further comparison of the decay rates for UDP Ca<sup>2+</sup> transients in untreated (235 ± 46 seconds, n=3) and BMS-CCR2-22-treated cells (218 ± 48 seconds, n=3) also revealed no significant differences between the two treatments (n=3, p>0.05).

Taken together, these data suggest that BMS-CCR2-22 does not impair UDP-evoked intracellular Ca<sup>2+</sup> responses in monocytes. This suggests that crosstalk between CCR2 and P2Y<sub>6</sub> may be unidirectional.

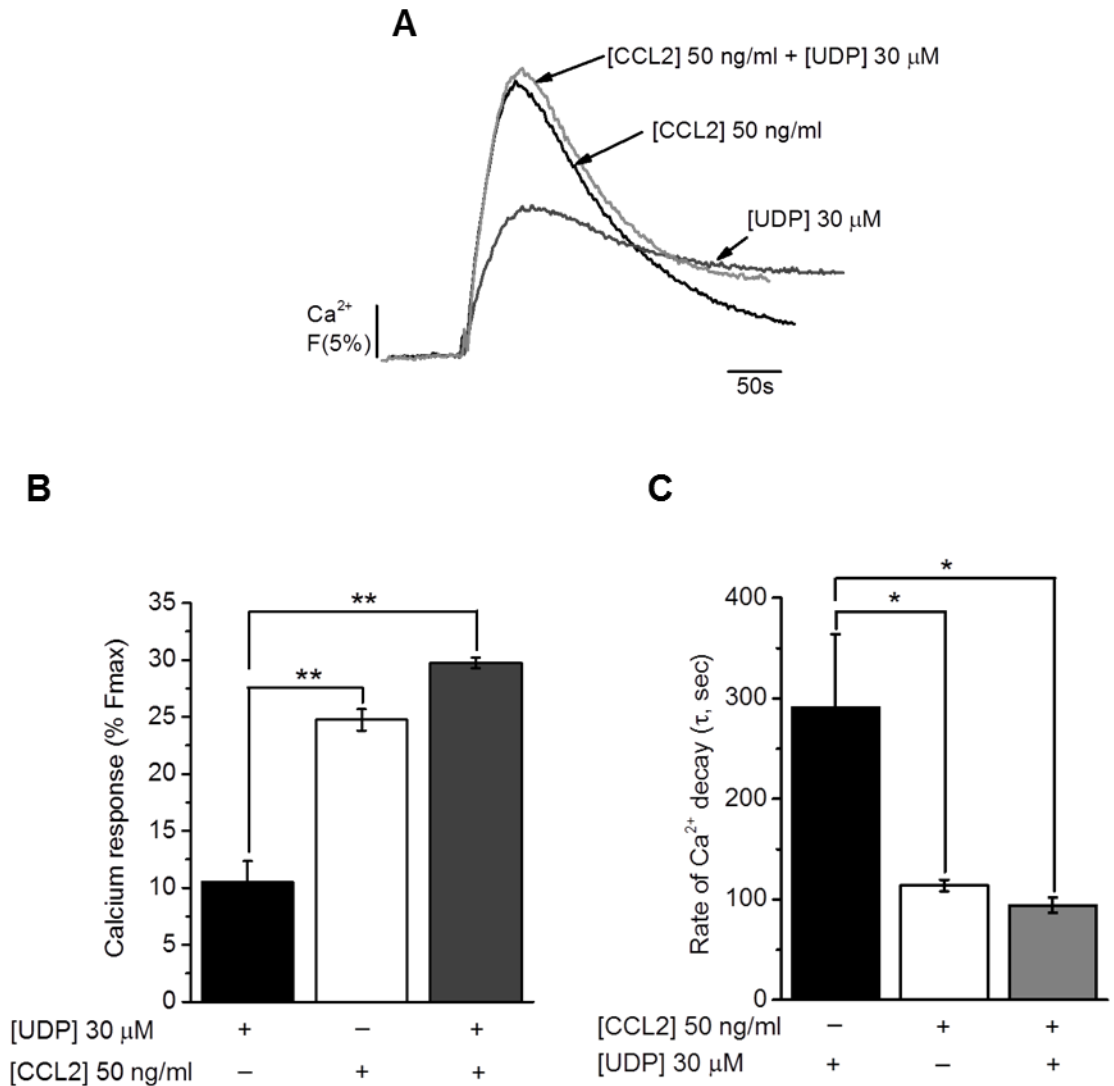


**Figure 6.11 Effect of CCL2/UDP co-application on Ca<sup>2+</sup> responses in THP-1 cells**

(A) Representative Ca<sup>2+</sup> transients to CCL2 (50 ng/ml), UDP (30  $\mu$ M) and CCL2/UDP (50 ng/ml + 30  $\mu$ M). (B) Bar chart showing normalised intracellular Ca<sup>2+</sup> responses to CCL2 (50 ng/ml), UDP (30  $\mu$ M) and CCL2/UDP (50 ng/ml + 30  $\mu$ M) in THP-1 cells. (C) Bar chart showing decay rates ( $\tau$ , sec) for Ca<sup>2+</sup> transients to CCL2 (50 ng/ml), UDP (30  $\mu$ M) and CCL2/UDP (50 ng/ml + 30  $\mu$ M) in THP-1 cells. Responses normalised to Ca<sup>2+</sup> signals elicited by 40  $\mu$ M digitonin (%Fmax). Data represents mean  $\pm$  SEM from n=3 replicates (\*p<0.05, \*\*p<0.01, One-way ANOVA with Bonferroni's multiple comparison).

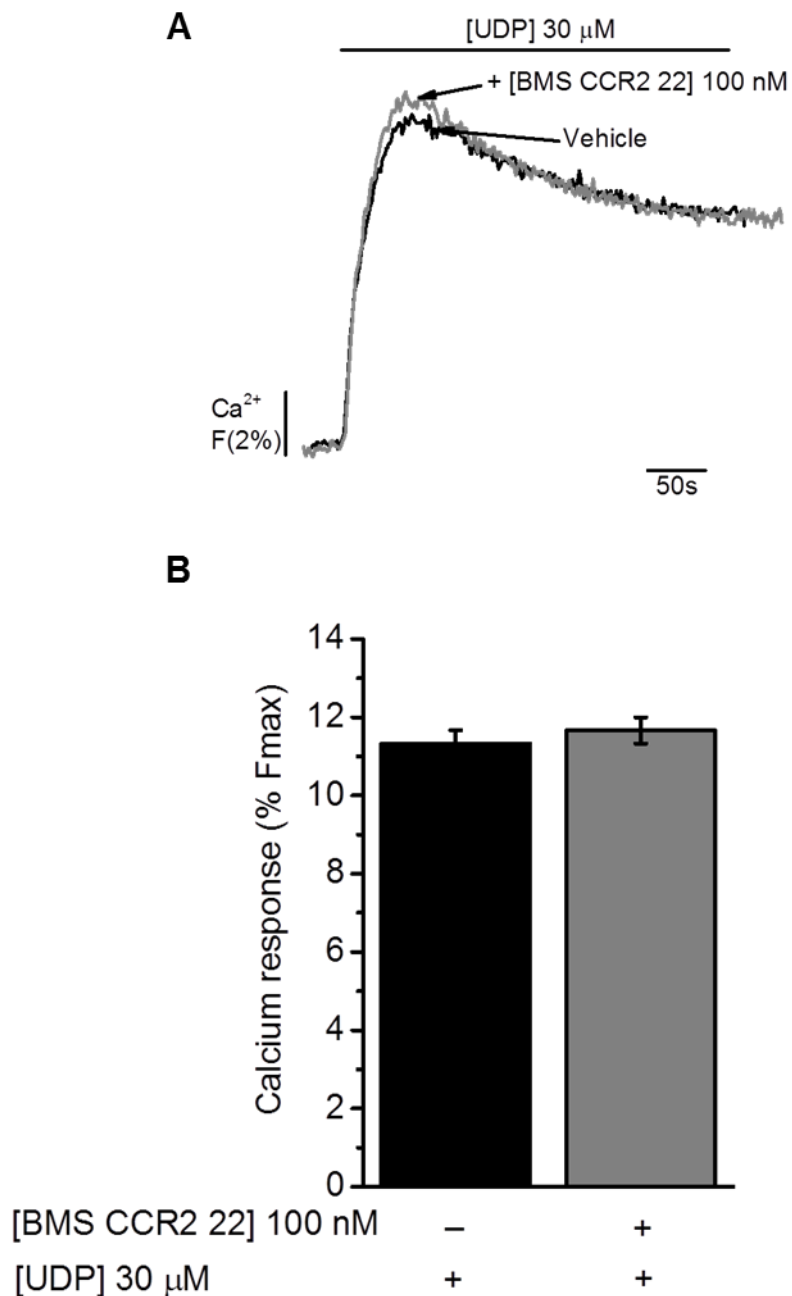


**Figure 6.12 Effect of BMS-CCR2-22 on UDP-evoked  $\text{Ca}^{2+}$  responses in THP-1 cells**

(A) Representative  $\text{Ca}^{2+}$  transients to UDP (30  $\mu\text{M}$ ) in THP-1 cells pre-treated with BMS-CCR2-22 (100 nM) for 15 minutes. (B) Bar chart showing normalised intracellular  $\text{Ca}^{2+}$  responses to UDP (30  $\mu\text{M}$ ) in THP-1 cells pre-treated with BMS-CCR2-22 (100 nM) for 15 minutes. Responses normalised to  $\text{Ca}^{2+}$  signals elicited by 40  $\mu\text{M}$  digitonin (%Fmax). Data represents mean  $\pm$  SEM from n=3 replicates.

### 6.3.6 Investigating crosstalk between P2Y<sub>6</sub> and FPRs in THP-1 cells

The chemoattractant N-formyl-Methionyl-Leucyl-Phenylamine (fMLP) is a product derived from degraded bacterial or mitochondrial peptides (Showell *et al.*, 1976). It is now considered a potent chemoattractant and lysoenzyme inducer for a variety of leukocytes, and in particular, for neutrophils (Carp, 1982). fMLP signalling occurs through PTx-sensitive G $\alpha_{i/o}$ -coupled formyl peptide receptors (FPR), a group of PRRs comprising of three family members (FPR1, FPR2 and FPR3) in humans that are expressed by cells of both non-myeloid (e.g. platelets, endothelial cells) and myeloid origin (monocytes, neutrophils) (Ye *et al.*, 2009). In monocytes, FPR activation induces intracellular Ca<sup>2+</sup> release, cytokine and superoxide anion release, and also chemotaxis (Yasaka *et al.*, 1982; Ohura *et al.*, 1987; Godfrey *et al.*, 1988; Gouwy *et al.*, 2009).

The evidence presented in this chapter has suggested that P2Y<sub>6</sub> is required for monocyte signalling and function mediated by the chemotactic peptide, CCL2. However, while these data suggest a novel association between P2Y<sub>6</sub> and CCR2, the requirement of P2Y<sub>6</sub> for monocyte signalling and function may also extend to other chemotactic peptides. To examine the validity of this hypothesis, the effects of apyrase and MRS-2578 on fMLP-mediated THP-1 cell intracellular Ca<sup>2+</sup> responses and chemotaxis were examined,

#### 6.3.6.1 Effect of apyrase and MRS-2578 on fMLP-evoked Ca<sup>2+</sup> responses in THP-1 cells

Initial studies examined the ability of fMLP to evoke intracellular Ca<sup>2+</sup> responses in THP-1 cells. Cells were therefore challenged with 0.01, 0.1, 1 and 10  $\mu$ M fMLP. As shown (Figure 6.13a), fMLP elicited a concentration-dependent intracellular Ca<sup>2+</sup> response. Using the results from this study, a median concentration of 1  $\mu$ M fMLP was used in further assays.

In further experiments, it was seen that apyrase (2 U/ml) significantly attenuated fMLP-evoked intracellular Ca<sup>2+</sup> responses in THP-1 cells by  $61 \pm 6\%$  ( $n=3$ ,  $p<0.05$ ), where it was seen that the %Fmax responses for fMLP in untreated and apyrase-treated cells were  $3 \pm 0.3\%$  ( $n=3$ ) and  $1 \pm 0\%$  ( $n=3$ ), respectively (Figure 6.13). This result was unexpected, and suggests that extracellular nucleotide scavenging impairs fMLP-FPR monocyte signalling. Due to a lack of decay of CCL2 Ca<sup>2+</sup> transients in apyrase-treated cells, the  $\tau$  values could not be determined.

In experiments investigating the requirement of P2Y<sub>6</sub> for fMLP-FPR signalling, it was seen that THP-1 cell intracellular Ca<sup>2+</sup> responses to fMLP were insensitive to 1  $\mu$ M MRS-2578 ( $n=3$ ,  $p>0.05$ ), where no change in the % Fmax values for fMLP in untreated ( $2 \pm 0$ ,  $n=3$ ), and MRS-2578-treated cells ( $2 \pm 0$ ,  $n=3$ ) was seen (Figure 6.14). The decay rates for

fMLP  $\text{Ca}^{2+}$  transients for untreated ( $78 \pm 25$  seconds,  $n=3$ ) and MRS-2578-treated cells ( $42 \pm 3$  seconds,  $n=3$ ) were compared, and although the data suggested that MRS-2578 promoted a faster decay of  $\text{Ca}^{2+}$  transients, these data were not significantly different ( $n=3$ ,  $p=0.2$ ).

These data have shown that fMLP-evoked intracellular  $\text{Ca}^{2+}$  responses in THP-1 cells are sensitive to inhibition by apyrase, but not by MRS-2578. Taken together, these data suggest a requirement of extracellular nucleotides for fMLP-FPR-associated signalling, but exclude a role for  $\text{P2Y}_6$ .

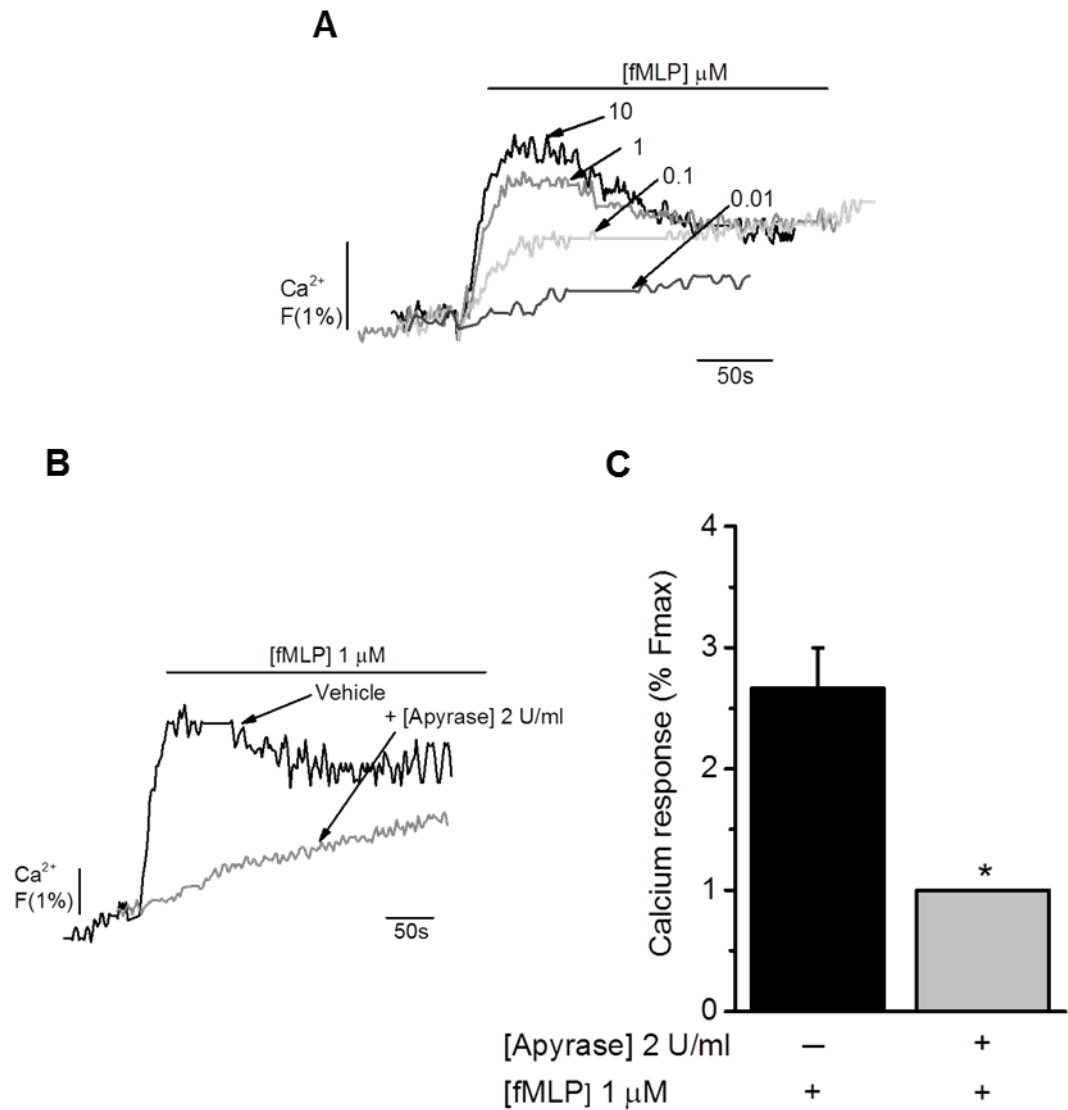


**Figure 6.13 Effect of apyrase on fMLP-evoked  $\text{Ca}^{2+}$  responses in THP-1 cells**

(A) Representative  $\text{Ca}^{2+}$  transients in THP-1 cells following challenge with fMLP (0.01 - 10  $\mu\text{M}$ ). (B) Representative  $\text{Ca}^{2+}$  transients to fMLP (1  $\mu\text{M}$ ) in THP-1 cells pre-treated with apyrase (2 U/ml) for 10 minutes. (C) Bar chart showing normalised intracellular  $\text{Ca}^{2+}$  responses to fMLP (1  $\mu\text{M}$ ) in THP-1 cells pre-treated with apyrase (2 U/ml) for 10 minutes. Responses normalised to  $\text{Ca}^{2+}$  signals elicited by 40  $\mu\text{M}$  digitonin (%Fmax). Data represents mean  $\pm$  SEM from  $n=3$  replicates. Asterisks indicate significant changes towards vehicle (no apyrase) (\* $p<0.05$ , Students t-test).

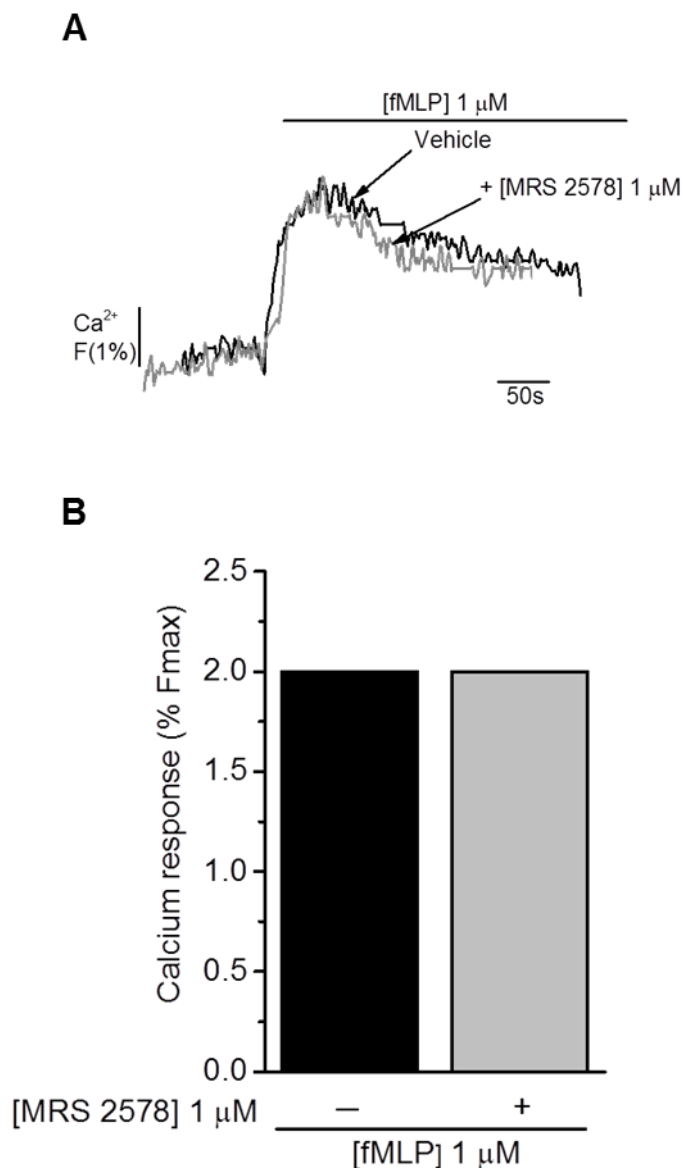


**Figure 6.14 Effect of MRS-2578 on fMLP-evoked  $\text{Ca}^{2+}$  responses in THP-1 cells**

(A) Representative  $\text{Ca}^{2+}$  transients to fMLP ( $1 \mu\text{M}$ ) in THP-1 cells pre-treated with MRS-2578 ( $1 \mu\text{M}$ ) for 15 minutes. (B) Bar chart showing normalised intracellular  $\text{Ca}^{2+}$  responses to fMLP ( $1 \mu\text{M}$ ) in THP-1 cells pre-treated with MRS-2578 ( $1 \mu\text{M}$ ) for 15 minutes. Responses normalised to  $\text{Ca}^{2+}$  signals elicited by  $40 \mu\text{M}$  digitonin (%Fmax). Data represents mean  $\pm$  SEM from  $n=3$  replicates.

### 6.3.6.2 Effect of apyrase and MRS-2578 on fMLP-mediated THP-1 cell chemotaxis

To examine the requirement of extracellular nucleotides and P2Y<sub>6</sub> for fMLP-mediated chemotaxis, experiments next tested the effects of apyrase (2 U/ml) and MRS-2578 (1 μM) on THP-1 cell chemotaxis towards 1 μM fMLP. As shown (Figure 6.15), THP-1 cells demonstrated a significantly higher (n=4, p<0.01) chemotactic index towards fMLP (4.3 ± 0.4, n=4), than towards vehicle (1 ± 0.12, n=4). This result supports the hypothesis that fMLP is a chemoattractant for monocytes. As also shown, apyrase significantly inhibited chemotaxis of THP-1 cells towards fMLP by 77 ± 6% (n=4, p<0.01), where cells displayed a chemotactic index that was comparable to vehicle (1 ± 0.3, n=4). Interestingly, no significant reduction in the chemotactic index for THP-1 cells treated with MRS-2578 was seen, where the chemotactic indexes of untreated (4.3 ± 0.4, n=4) and MRS-2578-treated cells (3.5 ± 0.3, n=4) were not significantly different (n=4, p>0.05).

Taken together, these data suggest a requirement of extracellular nucleotides for fMLP-FPR-associated monocyte signalling and function but do not support a requirement of the P2Y<sub>6</sub> purinoceptor. It is possible, therefore, that fMLP-FPR-associated monocyte signalling and function involves crosstalk between FPRs and other purinoceptors.

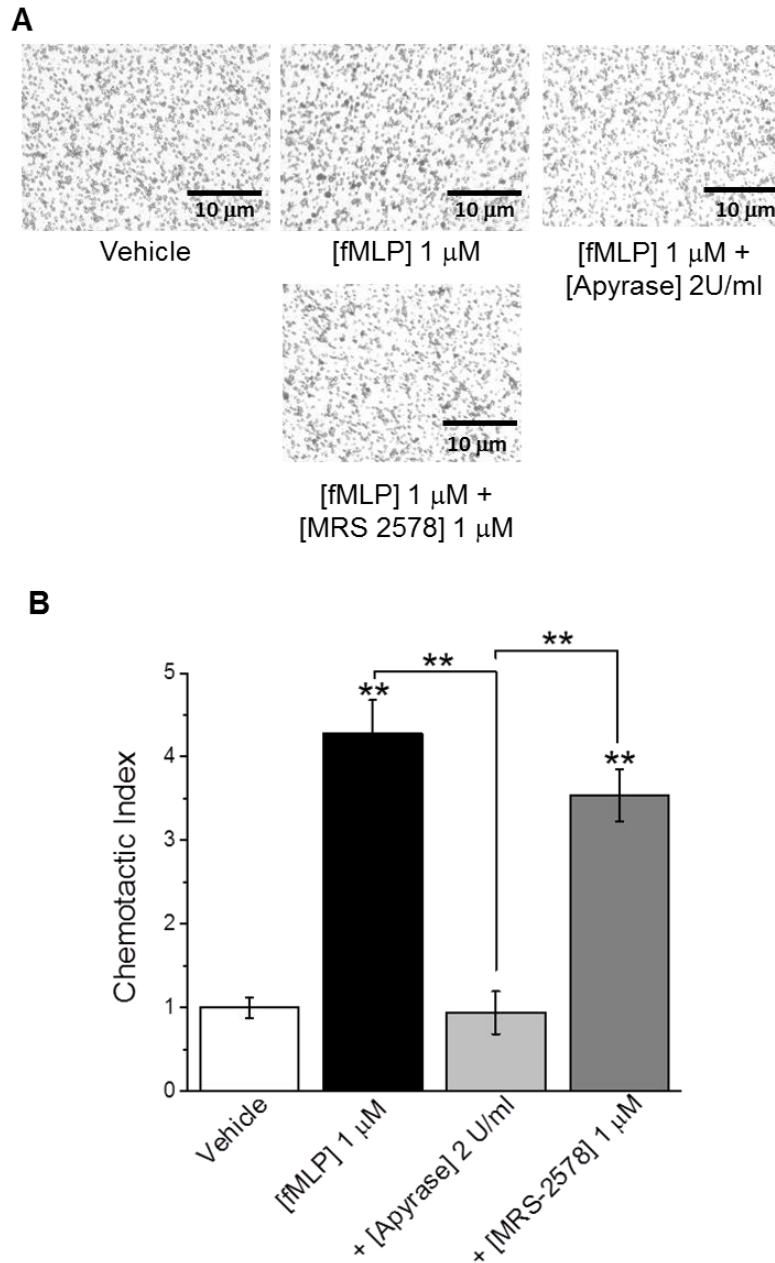


**Figure 6.15 Effect of apyrase and MRS-2578 on fMLP-mediated THP-1 cell chemotaxis**

(A) Representative images showing the effect of apyrase (2 U/ml) and MRS-2578 (1  $\mu$ M) on THP-1 cell chemotaxis towards fMLP (1  $\mu$ M, lower chamber, 2hrs). Scale bar represents 10  $\mu$ m. (B) Bar chart showing normalised THP-1 cell chemotaxis towards vehicle (water) or fMLP (1  $\mu$ M, lower chamber, 2hrs), with or without apyrase (2 U/ml) or MRS-2578 (1  $\mu$ M). Chemotactic index is a ratio of the number of cells that migrated towards fMLP over the number of cells that migrated towards vehicle. Data represents mean  $\pm$  SEM from n=4 transwells. Asterisks indicate significant changes towards vehicle (\*\*p<0.01, One-way ANOVA with Bonferroni's multiple comparison).

### 6.3.7 Effect of P2Y<sub>6</sub> desensitisation on CCL2-evoked Ca<sup>2+</sup> responses in THP-1 cells

The P2Y<sub>6</sub> receptor is a slow-desensitising receptor that displays a slow and sustained response upon agonist activation (Abbracchio *et al.*, 2006). Studies have previously shown that challenging P2Y<sub>6</sub>-transfected 1321N1 cells with UDP or ADP evokes a cellular response (IP<sub>3</sub> formation) that declines after 60 minutes, but remains detectable for up to 3 hours post-challenge (Robaye *et al.*, 1996). Furthermore, P2Y<sub>6</sub> responses can be fully restored at 45 minutes post-first-challenge Robaye *et al.* (1996).

In order to provide further evidence for a requirement of P2Y<sub>6</sub> for CCL2/CCR2-mediated monocyte signalling and function, studies next examined the effects of P2Y<sub>6</sub> desensitisation on CCL2-evoked intracellular Ca<sup>2+</sup> responses in THP-1 cells. However, in order to justify these experiments, it was first important to examine whether the P2Y<sub>6</sub> ligands, ADP and UDP desensitised P2Y<sub>6</sub>-mediated intracellular Ca<sup>2+</sup> responses.

#### 6.3.7.1 Effect of repeat ADP or UDP challenge on Ca<sup>2+</sup> responses in THP-1 cells

To determine whether ADP or UDP desensitised P2Y<sub>6</sub>-mediated intracellular Ca<sup>2+</sup> responses, THP-1 cells were challenged with ADP or UDP (3 μM) twice, once at 0 minutes (1<sup>st</sup> challenge) and another at 10 minutes (2<sup>nd</sup> challenge). A concentration of 3 μM of ADP and UDP was chosen as this is shown to elicit a reasonable intracellular Ca<sup>2+</sup> response in P2Y<sub>6</sub>-stable 1321N1 cells (Section 6.3.2).

As shown (Figure 6.16a and b), the %Fmax responses for 1<sup>st</sup> and 2<sup>nd</sup> ADP challenges were 8 ± 0.3% (n=3) and 5 ± 1% (n=3), respectively, and indicated a reduction of 40 ± 8% (n=3, p<0.05), consistent with a slow desensitisation of P2Y<sub>6</sub>. The Ca<sup>2+</sup> transient decay rates for ADP were also different. Although the τ values for ADP at 0 minutes (1<sup>st</sup>) could not be accurately determined due to the sustained responses, the τ value for ADP at 10 minutes (2<sup>nd</sup>) was 34604 ± 12244 seconds (n=3) and suggested a faster decay due to P2Y<sub>6</sub> desensitisation. As also shown (Figure 6.16c and d), intracellular Ca<sup>2+</sup> responses to 3 μM UDP were attenuated by 68 ± 10 % (n=3, p<0.05), where the %Fmax values for 1<sup>st</sup> and 2<sup>nd</sup> UDP challenges were 9 ± 0.3% (n=3) and 3 ± 1% (n=3), respectively. Due to the sustained intracellular Ca<sup>2+</sup> responses, the decay rates for UDP could not be accurately determined.

Taken together, these data suggest that prior activation of P2Y<sub>6</sub> with ADP or UDP desensitises P2Y<sub>6</sub> to further challenge by ADP or UDP. A greater impairment of UDP Ca<sup>2+</sup> responses may reflect its greater potency at P2Y<sub>6</sub>.

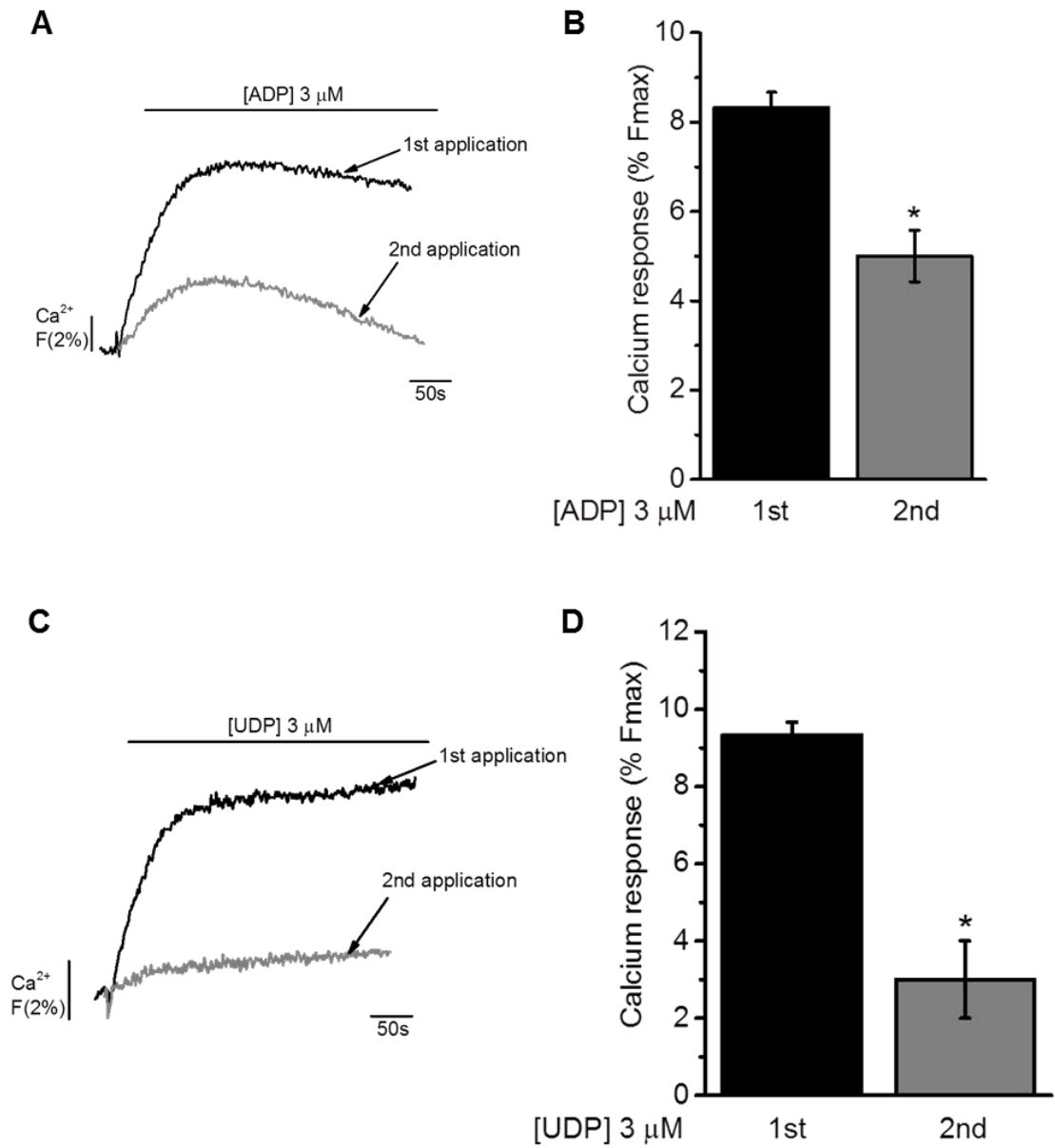


**Figure 6.16 Effect of repeat ADP- or UDP-challenge on Ca<sup>2+</sup> responses in THP-1 cells**

Representative Ca<sup>2+</sup> transients to (A) ADP (3  $\mu$ M) or (C) UDP (3  $\mu$ M) in THP-1 cells at 0 minutes (1<sup>st</sup> challenge), and 10 minutes (2<sup>nd</sup> challenge). Bar chart showing normalised intracellular Ca<sup>2+</sup> responses to (B) ADP (3  $\mu$ M) or (D) UDP (3  $\mu$ M) in THP-1 cells at 0 minutes (1<sup>st</sup> application), and 10 minutes (2<sup>nd</sup> application). Responses normalised to Ca<sup>2+</sup> signals elicited by 40  $\mu$ M digitonin (% Fmax). Data represents mean  $\pm$  SEM from n=3 replicates. Asterisks indicate significant changes towards 1<sup>st</sup> challenge (\*p<0.05, Students t-test)

### 6.3.7.2 Effect of ADP and UDP challenge on CCL2-evoked Ca<sup>2+</sup> responses in THP-1 cells

A similar experimental design was applied to examine the effects of ADP and UDP on CCL2-evoked intracellular Ca<sup>2+</sup> responses. To this end, THP-1 cells were challenged with vehicle, ADP (3 μM) or UDP (3 μM) at 0 minutes, and then challenged with CCL2 (50 ng/ml) 10 minutes later. As shown (Figure 6.17a and b), prior challenge of THP-1 cells with ADP resulted in a 27 ± 5% reduction (n=3, p<0.05) in the CCL2-evoked Ca<sup>2+</sup> response, where the %Fmax responses for CCL2 in cells challenged with vehicle and 3 μM ADP were 26 ± 1% (n=3) and 19 ± 1% (n=3), respectively. This result suggests that prior activation of P2Y<sub>6</sub> by ADP impairs CCL2-evoked intracellular Ca<sup>2+</sup> responses. A comparison of the τ values for CCL2 across treatments was also made, but did not reveal any significant differences (n=3, p>0.05) between vehicle (89 ± 1 seconds, n=3) and ADP-challenged THP-1 cells (94 ± 4 seconds, n=3).

A similar impairment (28 ± 4%, n=5, p<0.01) of CCL2-evoked intracellular Ca<sup>2+</sup> responses was observed in cells challenged with 3 μM UDP (Figure 6.17c and d). As shown, the %Fmax responses for CCL2 in vehicle and UDP-challenged cells were 22 ± 1% (n=5), and 16 ± 0.3% (n=5), respectively. These data supported the results of ADP experiments and suggested a similar impairment of CCL2-evoked intracellular Ca<sup>2+</sup> responses following nucleotide challenge. Interestingly, a significant reduction (14 ± 4%, n=5, p<0.05) in the decay rates between vehicle (79 ± 5 seconds, n=5) and UDP-challenged cells (67 ± 4 seconds, n=5) was observed (Figure 6.17e), indicating a faster decay of CCL2 Ca<sup>2+</sup> transients following UDP challenge.

In summary, these results suggest that prior challenge of THP-1 cells with ADP or UDP attenuates CCL2-evoked intracellular Ca<sup>2+</sup> responses. This indicates that P2Y<sub>6</sub> activation cross-desensitises CCL2/CCR2-mediated signalling in monocytes.

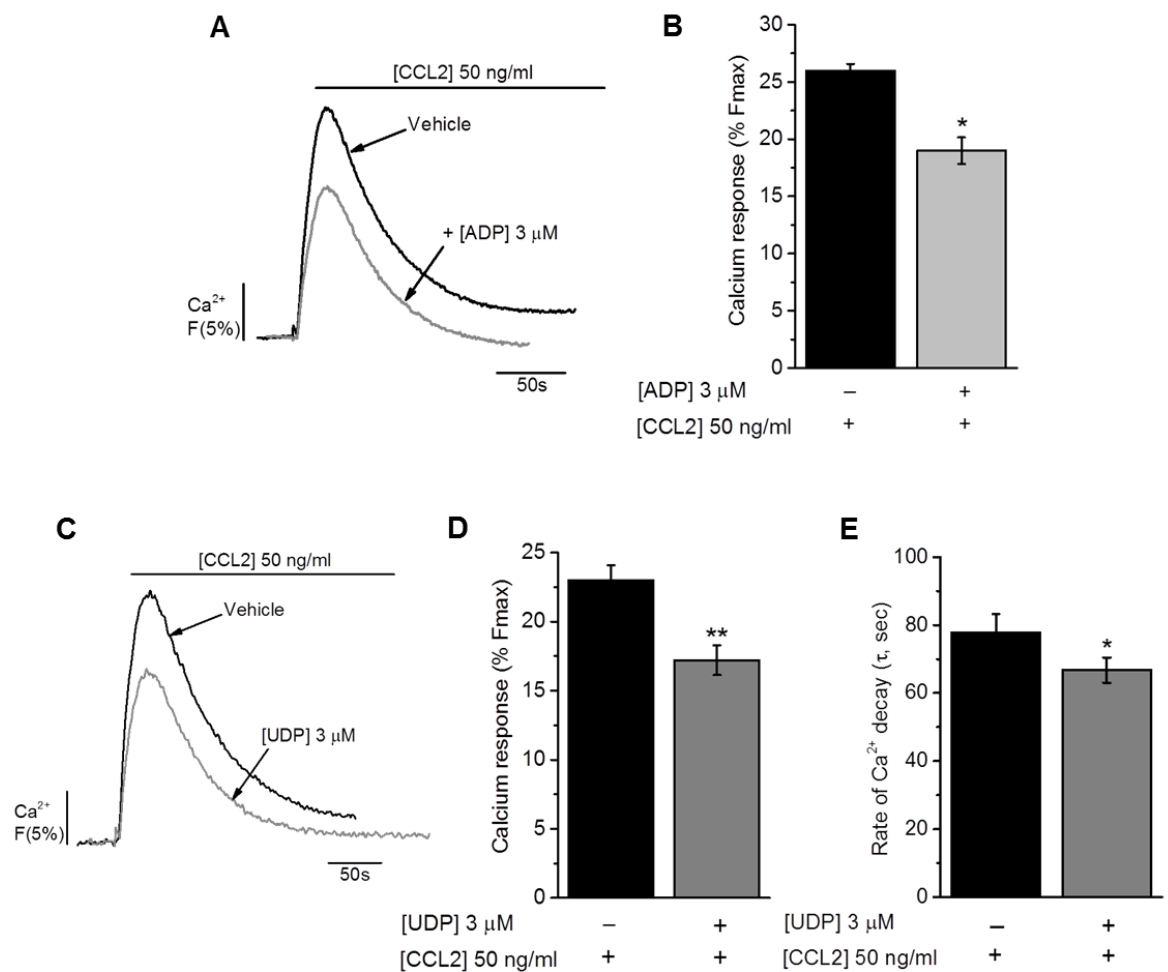


**Figure 6.17 Effect of ADP or UDP challenge on CCL2-evoked Ca<sup>2+</sup> responses in THP-1 cells**

Representative Ca<sup>2+</sup> transients to CCL2 (50 ng/ml) in THP-1 cells pre-treated with vehicle (water) or (A) ADP (3 μM) or (C) UDP (3 μM) for 10 minutes. Bar chart showing normalised intracellular Ca<sup>2+</sup> responses to CCL2 (50 ng/ml) in THP-1 cells pre-treated with vehicle (water) or (B) ADP (3 μM) or (D) UDP (3 μM) for 10 minutes. (E) Bar chart showing Ca<sup>2+</sup> decay rates (τ, sec) for CCL2 Ca<sup>2+</sup> transients in THP-1 cells pre-treated with vehicle (water) or UDP (3 μM) for 10 minutes. Responses normalised to Ca<sup>2+</sup> signals elicited by 40 μM digitonin (%Fmax). Data represents mean ± SEM from n=3 (ADP), or n=5 (UDP) replicates. Asterisks indicate significant changes towards vehicle (\*p<0.05, \*\*p<0.01, Students t-test).

### 6.3.8 Generation and evaluation of *P2RY6*-KD THP-1 cells

To provide further evidence for crosstalk between CCR2 and  $P2Y_6$ , it was important to employ a molecular-based approach to silence the *P2RY6* gene. The methodology employed involved the use of a lentiviral vector (pLKO.1) to deliver a short hairpin RNA (shRNA) sequence for *P2RY6* into THP-1 cells to enable a stable and long-term gene knockdown (Section 2.5, Chapter 2). *P2RY6*-KD lines were generated using two methods, either by generating pLKO.1-puro shRNA-encoding lentivirus in-house, or by purchasing lentiviral particles incorporating pLKO.1-puro *P2RY6*-shRNA sequences. Both studies also involved the use of pLKO.1-puro non-target-shRNA lentiviral particles to generate a “scrambled” THP-1 cell line that acted as a negative control.

#### 6.3.8.1 Generation of *P2RY6*-KD THP-1 cells with in-house *P2RY6*-shRNA lentivirus

##### 6.3.8.1.1 UDP-evoked $Ca^{2+}$ responses

*P2RY6*-KD THP-1 cell lines were generated using in-house lentiviral particles encoding the *P2RY6*-shRNA sequences 14073 and 14075, as identified by the RNA interference (RNAi) consortium (TRC) (Table 2.11, Chapter 2). Sequence 14075 was identified from studies conducted by Ben Yebdri *et al.* (2009).

Following the generation of cell lines, the first approach taken was to triage *P2RY6*-KD THP-1 cells based on the functional efficacies of their shRNA sequences. This was done by comparing UDP (30  $\mu$ M)-evoked intracellular  $Ca^{2+}$  responses between scrambled and *P2RY6*-KD cell lines (14073 and 14075).

**Table 6.4** UDP-evoked  $Ca^{2+}$  responses in scrambled and *P2RY6*-KD cell lines

$Ca^{2+}$ response (% Fmax)			
Scrambled	14073	Scrambled	14075
10 $\pm$ 1	10 $\pm$ 2	10 $\pm$ 1	17 $\pm$ 1**
Decay rate ( $\tau$ , sec)			
Scrambled	14073	Scrambled	14075
242 $\pm$ 24	227 $\pm$ 69 s	109 $\pm$ 18	124 $\pm$ 7

Intracellular  $Ca^{2+}$  responses and decay rates ( $\tau$ , sec) for UDP (30  $\mu$ M) in THP-1 cells transduced with non-target (scrambled) or *P2RY6*-shRNA sequences 14073 and 14075. Responses normalised to  $Ca^{2+}$  signals elicited by 40  $\mu$ M digitonin (%Fmax). Data represents mean  $\pm$  SEM from n=3 (14073) or n=4 (14075) replicates. Asterisks indicate significant changes towards scrambled (\*\*p<0.01, Students t-test).

As shown above in Table 6.4, no significant changes in the %Fmax values for UDP were detected between scrambled and 14073-cells (n=3, p>0.05). The decay rates ( $\tau$ , sec) of scrambled and 14073-cells were also not significantly different (n=3, p>0.05). These data suggest that 14073-cells do not exhibit a functional impairment of P2Y<sub>6</sub>. In similar experiments with 14075 cells, a 1.6 ± 0.3-fold increase in UDP Ca<sup>2+</sup> responses over scrambled cells was seen (n=4, p<0.01). These data were interesting because they suggested that shRNA 14075 enhanced P2Y<sub>6</sub> function. However, it was interesting to observe that the decay rates of UDP Ca<sup>2+</sup> transients for scrambled and 14075 cells were not significantly different (n=4, p>0.05), suggesting that shRNA 14075 did not affect the decay of UDP Ca<sup>2+</sup> transients.

### 6.3.8.1.2 qRT-PCR analysis of *P2RY6* expression

A pilot qRT-PCR (quantitative real-time-polymerase chain reaction) study was next conducted using primers detailed in Chapter 2 to assess for *P2RY6* expression in scrambled and 14075 cells lines. 14073 cells were excluded from this study as these showed no functional P2Y<sub>6</sub> knockdown. Table 6.5 lists the relative quantitation (RQ) and fold-shift values for *P2RY6* in scrambled and 14075 cells. As described previously (Chapter 2), the RQ value represents the fold-change in gene expression relative to scrambled cells.

**Table 6.5 Relative quantitation and fold-shift values for scrambled and *P2RY6*-KD 14075 THP-1 cells**

shRNA	Gene	RQ	Fold-shift
Scrambled	<i>P2YR6</i>	1.0	1.0
14075	<i>P2YR6</i>	1.1	0.9

Data represent n=1 replicate. Relative quantification (RQ) values were normalised to  $\beta$ -actin and then further normalised to scrambled cells according to the 2<sup>- $\Delta\Delta$ Ct</sup> method (Livat and Schmittgen, 2001). An RQ value of 0.5 (2-fold shift) was considered significant.

As shown (Table 6.5), a 0.9 fold-(10%) increase in *P2RY6* expression was seen in 14075 cells (n=1). Although this data is interesting and may explain the increased UDP-evoked Ca<sup>2+</sup> responses seen in these cells (Table 6.4), these data are only an n=1 replicate and below the reliable detection limits of qRT-PCR which is unable to reliably detect less than a 2-fold change (1 PCR cycle) in gene expression (Karlen *et al.*, 2007).

Taken together, these data suggest that the shRNA sequences 14073 and 14075 do not encode for *P2YR6* knockdown in THP-1 cells.

### 6.3.8.2 Generation of *P2RY6*-KD THP-1 cells using MISSION® *P2RY6*-shRNA lentivirus

Due to difficulties with shRNA sequences 14073 and 14075, it was decided that the most convenient and rapid method for generating *P2RY6*-KD THP-1 cells was to use Sigma MISSION® lentivirus particles. To enable generation of *P2RY6*-KD THP-1 cells, five shRNA sequences including 14075, were selected (Table 2.12, Chapter 2). *P2RY6*-KD and scrambled THP-1 lines were generated as described in Section 2.5.5 (Chapter 2). Cell lines were triaged in terms of shRNA functional efficacies as measured by UDP- and CCL2-evoked intracellular Ca<sup>2+</sup> responses.

#### 6.3.8.2.1 UDP-evoked Ca<sup>2+</sup> responses

The functional efficacies of shRNA sequences were examined by comparing (30 µM) UDP-evoked intracellular Ca<sup>2+</sup> responses for all *P2RY6*-KD cell lines with scrambled cells.

**Table 6.6** UDP-evoked Ca<sup>2+</sup> responses in scrambled and *P2RY6*-KD cell lines

Ca <sup>2+</sup> response (% Fmax)					
Scrambled	14075	14076	14077	357968	358038
15 ± 1	17 ± 0.3	10 ± 0.3**	11 ± 1**	9 ± 1**	8 ± 1**
Decay rate (τ, sec)					
Scrambled	14075	14076	14077	357968	358038
88 ± 2	90 ± 6	63 ± 2	161 ± 26*	51 ± 10	85 ± 3

Intracellular Ca<sup>2+</sup> responses and decay rates (τ, sec) for UDP (30 µM) in THP-1 cells transduced with non-target (scrambled) or *P2RY6*-shRNA sequences. Responses normalised to Ca<sup>2+</sup> signals elicited by 40 µM digitonin (%Fmax). Data represents mean ± SEM from n=3 replicates. Asterisks indicate significant changes towards scrambled (\*p<0.05, \*\*p<0.01, One-way ANOVA with Bonferroni's multiple comparison).

As shown above in Table 6.6 (and Appendix Figure A25), a significant impairment of UDP-evoked intracellular Ca<sup>2+</sup> responses was seen with the majority of *P2RY6* shRNA sequences, with the greatest impairment seen in cells transduced with 358038 (50 ± 5%, n=3, p<0.01). UDP %Fmax responses were also attenuated in THP-1 cells transduced with 14076 (37 ± 4%, n=3, p<0.01), 14077 (30 ± 1%, n=3, p<0.01) and 357968 (39 ± 3%, n=3, p<0.01). As also shown by Table 6.6 (and Appendix Figure A25), THP-1 cells transduced with 14075 were not significantly different from scrambled cells (n=3, p>0.05). Interestingly, an assessment of the decay rates for scrambled and *P2RY6*-KD THP-1 cell lines showed that only 14077 cells exhibited a significant 1.8 ± 0.3 fold (n=3, p<0.05)

increase in  $\tau$  over scrambled cells (Table 6.6 and Appendix Figure A25). This result therefore suggested that UDP  $\text{Ca}^{2+}$  transients in cells transduced with 14077 decayed ~2-fold slower than scrambled cells. This data is difficult to explain but suggests a greater effect of this shRNA on  $\text{P2Y}_6$  desensitisation. In contrast, the  $\tau$  values for all other  $\text{P2RY6}$  shRNA sequences were not significantly different from scrambled cells ( $n=3$ ,  $p>0.05$  for all).

Taken together, these data suggest that THP-1 cells transduced with shRNA sequences 14076, 14077, 357968, and 358038, display reduced intracellular  $\text{Ca}^{2+}$  responses to UDP. From these data, it also apparent that 358038 is the best-performing shRNA, while 14075 is the worst-performing shRNA.

### 6.3.8.2.2 CCL2-evoked $\text{Ca}^{2+}$ responses

The results above have suggest that THP-1 cells transduced with the  $\text{P2RY6}$  shRNA sequences 14076, 14077, 357968, and 358038 show reduced  $\text{Ca}^{2+}$  responses to UDP. It is possible, therefore, that these also display a reduced intracellular  $\text{Ca}^{2+}$  response to CCL2. To examine this hypothesis, CCL2-evoked intracellular  $\text{Ca}^{2+}$  responses in scrambled and  $\text{P2RY6-KD}$  THP-1 lines were compared.

**Table 6.7 CCL2-evoked  $\text{Ca}^{2+}$  responses in scrambled and  $\text{P2RY6-KD}$  cell lines**

Ca <sup>2+</sup> response (%Fmax)					
Scrambled	14075	14076	14077	357968	358038
26 ± 0.3	29 ± 1	24 ± 1	24 ± 1	24 ± 1	21 ± 0**
Decay rate ( $\tau$ , sec)					
Scrambled	14075	14076	14077	357968	358038
104 ± 1	91 ± 1**	76 ± 2**	85 ± 1**	84 ± 3**	84 ± 2**

Intracellular  $\text{Ca}^{2+}$  responses and decay rates ( $\tau$ , sec) for CCL2 (50 ng/ml) in THP-1 cells transduced with non-target (scrambled) or  $\text{P2YR6}$ -shRNA sequences. Responses normalised to  $\text{Ca}^{2+}$  signals elicited by 40  $\mu\text{M}$  digitonin (%Fmax). Data represents mean  $\pm$  SEM from  $n=3$  replicates. Asterisks indicate significant changes towards scrambled (\*\* $p<0.01$ , One-way ANOVA with Bonferroni's multiple comparison).

As shown above in Table 6.7 (and Appendix Figure A26), CCL2-evoked intracellular  $\text{Ca}^{2+}$  responses were significantly impaired by  $20 \pm 1\%$  ( $n=3$ ,  $p<0.01$ ) in THP-1 cells transduced with shRNA 358038. In comparison, no significant reduction in CCL2  $\text{Ca}^{2+}$  responses was seen in cells transduced with 14075, 14076, 14077, or 357968 (all  $n=3$ ,  $p>0.05$ ). These results are interesting because the results of UDP  $\text{Ca}^{2+}$  experiments identified that 358038

was the best-performing *P2YR6*-shRNA (Table 6.6). It may be the case therefore, that *P2YR6*-shRNA functional efficacy correlates with CCR2 function.

A further comparison of the decay rates revealed that the CCL2  $\text{Ca}^{2+}$  transients of all *P2RY6*-KD cell lines decayed significantly faster than scrambled cells (Table 6.7 and Appendix Figure A26). The % reduction for 14075 ( $12 \pm 1\%$ ,  $n=3$ ,  $p<0.01$ ), 14076 ( $26 \pm 1\%$ ,  $n=3$ ,  $p<0.01$ ), 14077 ( $18 \pm 1\%$ ,  $n=3$ ,  $p<0.01$ ), 357968 ( $19 \pm 3\%$ ,  $n=3$ ,  $p<0.01$ ) and 358038 ( $19 \pm 1\%$ ,  $n=3$ ,  $p<0.01$ ) suggested that this might be a general characteristic of *P2RY6*-shRNA.

In summary, these results suggest that THP-1 cells transduced with *P2RY6*-shRNA 358038 show an attenuated  $\text{Ca}^{2+}$  response to CCL2. This finding supports the hypothesis that  $\text{P2Y}_6$  is required for CCL2/CCR2-mediated monocyte signalling.

### 6.3.8.2.3 qRT-PCR analysis of *P2RY6* and *CCR2* expression

THP-1 cells transduced with shRNA 358038 (positive) and 14075 (negative) and non-target (scrambled) shRNA were tested for *CCR2* and *P2RY6* expression using qRT-PCR. As previously described, cells were examined for *P2RY6* expression in order to assess for gene knockdown. Cells were also tested for *CCR2* expression, which served as a control. Primers used for qRT-PCR are listed in Table 2.7 and 2.10 (Chapter 2). Table 6.8 shows the relative expression values (RQ) and fold-shifts for *CCR2* and *P2YR6* in scrambled, 358038 and 14075 cells.

**Table 6.8** Relative quantitation and fold-shift values for scrambled and *P2RY6*-KD cells

shRNA	Gene	RQ $\pm$ SEM	Fold-shift in gene expression
Scrambled	<i>CCR2</i>	$1.0 \pm 0$	$1.0 \pm 0$
14075	<i>CCR2</i>	$0.8 \pm 0.1$	$1.3 \pm 0.2$
358038	<i>CCR2</i>	$0.8 \pm 0.1$	$1.3 \pm 0.2$
Scrambled	<i>P2RY6</i>	$1.0 \pm 0$	$1.0 \pm 0$
14075	<i>P2RY6</i>	$1.0 \pm 0.1$	$1.1 \pm 0.1$
358038	<i>P2RY6</i>	$0.5 \pm 0.1$	$2.0 \pm 0.3$

Data represent  $n=3$  replicates. Relative quantification (RQ) values were normalised to  $\beta$ -actin and then further normalised to scrambled cells according to the  $2^{-\Delta\Delta\text{Ct}}$  method (Livat and Schmittgen, 2001). An RQ value of 0.5 (2-fold reduction) or 2.0 (2-fold increase) was considered significant.

As shown (Table 6.8), all three shRNA exhibited a similar RQ value for *CCR2* mRNA. Although the fold-shift values for *CCR2* in 14075 and 358038 cells indicated a  $1.3 \pm 0.2$ -fold reduction ( $n=3$ ), these data were considered unreliable as they were below the reliable detection limit of qRT-PCR (Karlen *et al.*, 2007). As Table 6.8 shows, cells transduced with 358038 exhibited a  $2.0 \pm 0.3$  ( $n=3$ ) fold-reduction in *P2RY6* expression. This result was within the reliable detection limit of qRT-PCR and indicated that these cells were knocked down for *P2RY6*. This result accords with earlier observations, which showed a  $50 \pm 5\%$  ( $n=3$ ,  $p<0.01$ ) attenuation of UDP  $Ca^{2+}$  responses.

Taken together, these data suggest that shRNA 358038 produces a 2-fold knockdown (KD) in *P2RY6* expression in THP-1 cells. These data also suggest that *CCR2* expression is not knocked down.

### 6.3.9 CCL2/CCR2-mediated function of P2Y<sub>6</sub>-KD cells

The next aim of this chapter was to examine the requirement of P2Y<sub>6</sub> for CCL2/CCR2-mediated monocyte function using THP-1 cells transduced with shRNA 358038 ("P2Y<sub>6</sub>-KD" cells).

Experiments first tested the ability of scrambled and P2Y<sub>6</sub>-KD cells to migrate towards CCL2 (50 ng/ml). As shown (Figure 6.18), scrambled cells demonstrated a significantly higher ( $n=4$ ,  $p<0.01$ ) chemotactic index towards CCL2 ( $13 \pm 1$ ,  $n=4$ ) than towards vehicle ( $1 \pm 0.1$ ,  $n=4$ ). Although P2Y<sub>6</sub>-KD cells also demonstrated a significantly higher ( $n=4$ ,  $p<0.01$ ) chemotactic index towards CCL2 ( $5 \pm 1$ ,  $n=4$ ) than towards vehicle ( $1 \pm 0.1$ ,  $n=4$ ), their migration towards CCL2 was  $59 \pm 5\%$  ( $n=4$ ) less than scrambled cells ( $n=4$ ,  $p<0.01$ ). This suggests that P2Y<sub>6</sub>-KD cells have a reduced capacity to chemotax towards CCL2.

To understand the effects of P2Y<sub>6</sub>-KD on other monocyte functions, experiments tested the adhesion of scrambled and P2Y<sub>6</sub>-KD cells to quiescent and TNF- $\alpha$ -treated HUVEC monolayers. Cells were CCL2-primed (50 ng/ml) or vehicle-treated prior to co-incubation with HUVEC monolayers treated with vehicle or TNF $\alpha$  (10 ng/ml). As shown in Figure 6.19a, the adhesion values (% scrambled CCL2 control) of vehicle-treated scrambled and P2Y<sub>6</sub>-KD cells to quiescent HUVECs were  $21 \pm 9\%$  ( $n=12$ ) and  $42 \pm 19\%$  ( $n=12$ ), respectively. However, although these data suggested that P2Y<sub>6</sub>-KD cells adhered to quiescent HUVECs better than scrambled cells, it was observed that the capacity of both cell types to adhere differed slightly following CCL2-priming. While the % scrambled CCL2 control value for scrambled cells ( $100 \pm 19\%$ ,  $n=12$ ,  $p<0.05$ ) indicated a significant  $5 \pm 1$ -fold ( $n=12$ ,  $p<0.05$ ) increase in adhesion, the % scrambled CCL2 control value for P2Y<sub>6</sub>-KD cells ( $109 \pm 27\%$ ,  $n=12$ ) was not significantly different from vehicle-treated cells ( $n=12$ ,  $p=0.1$ ). A possible explanation for these results may be that P2Y<sub>6</sub>-KD cells adhered variably to THP-1 cells to quiescent HUVEC monolayers.

As shown in Figure 6.19b, the adhesion values (% scrambled CCL2 control) of vehicle-treated scrambled and P2Y<sub>6</sub>-KD cells to TNF $\alpha$ -treated HUVECs were 6  $\pm$  6% (n=8) and 12  $\pm$  9% (n=8), respectively. CCL2-priming of scrambled cells resulted in a significant 16  $\pm$  6-fold increase (n=8) in adhesion, where the % scrambled CCL2 control value was 100  $\pm$  37% (n=8, p<0.05). Interestingly, this increase was greater than that seen in quiescent HUVECs experiments, and may indicate an enhancement of CCL2-mediated cellular adhesion by TNF $\alpha$ . However, the most interesting result to emerge from this experiment was the lack of adhesion of CCL2-primed P2Y<sub>6</sub>-KD THP-1 cells, which exhibited a % scrambled CCL2 control value that was comparable to vehicle-treated P2Y<sub>6</sub>-KD cells (14  $\pm$  10%, n=8, p>0.05). These data suggest that P2Y<sub>6</sub>-KD attenuates monocyte adhesion under inflammatory conditions.

Collectively, these data suggest that P2Y<sub>6</sub>-KD attenuates CCL2-mediated THP-1 cell adhesion to TNF $\alpha$ -treated HUVECs. In the wider context, these findings suggest that a blockade of P2Y<sub>6</sub> attenuates CCL2/CCR2-mediated monocyte adhesion to the vascular endothelium under inflammatory conditions.

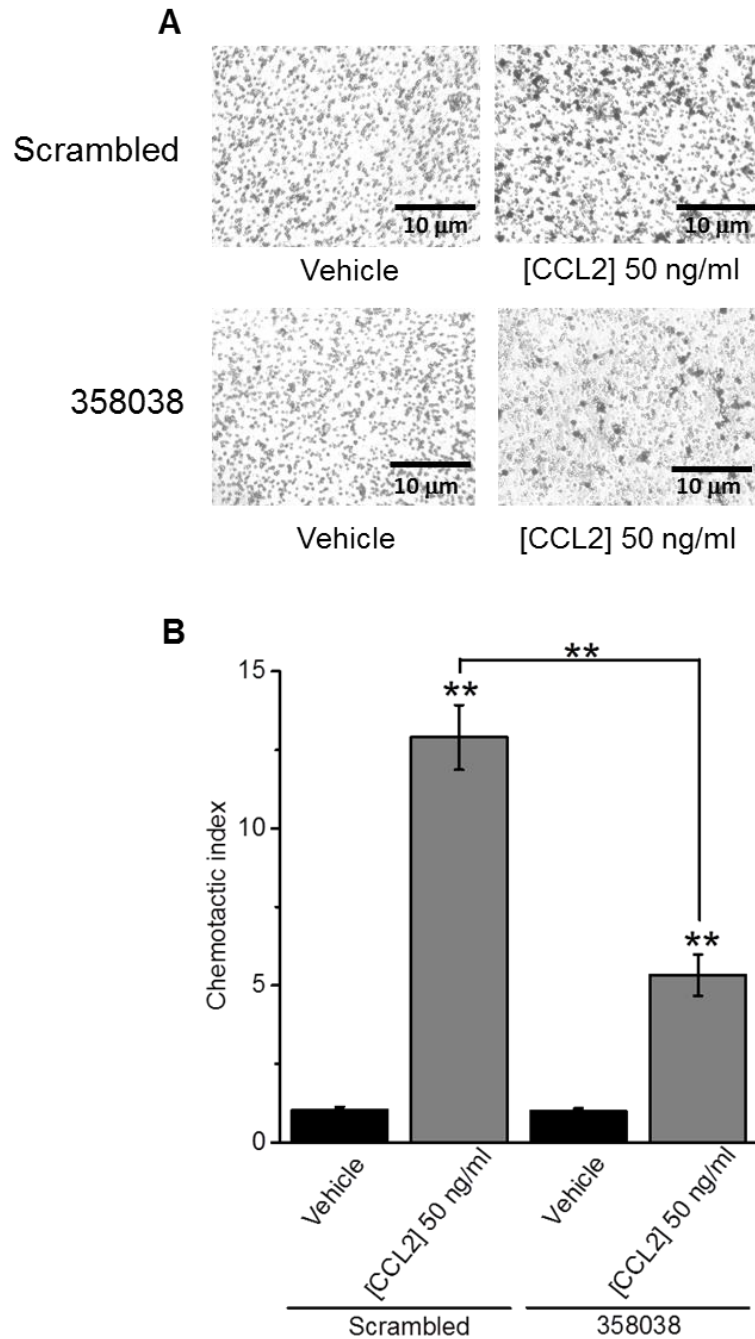


**Figure 6.18 CCL2-mediated scrambled and P2Y<sub>6</sub>-KD cell chemotaxis**

(A) Representative images showing scrambled and P2Y<sub>6</sub>-KD THP-1 cell migration towards vehicle (water) or CCL2 (50 ng/ml, lower chamber, 2hrs). Scale bar represents 10 μm. (B) Bar chart showing normalised scrambled and P2Y<sub>6</sub>-KD THP-1 cell chemotaxis towards vehicle (water) or CCL2 (50 ng/ml, lower chamber, 2hrs). Chemotactic index is a ratio of the number of cells that migrated towards CCL2 over the number of cells that migrated towards vehicle. Data represents mean ± SEM from n=4 transwells. Asterisks indicate significant changes towards paired vehicle (\*\*p<0.01, One-way ANOVA with Bonferroni's multiple comparison).

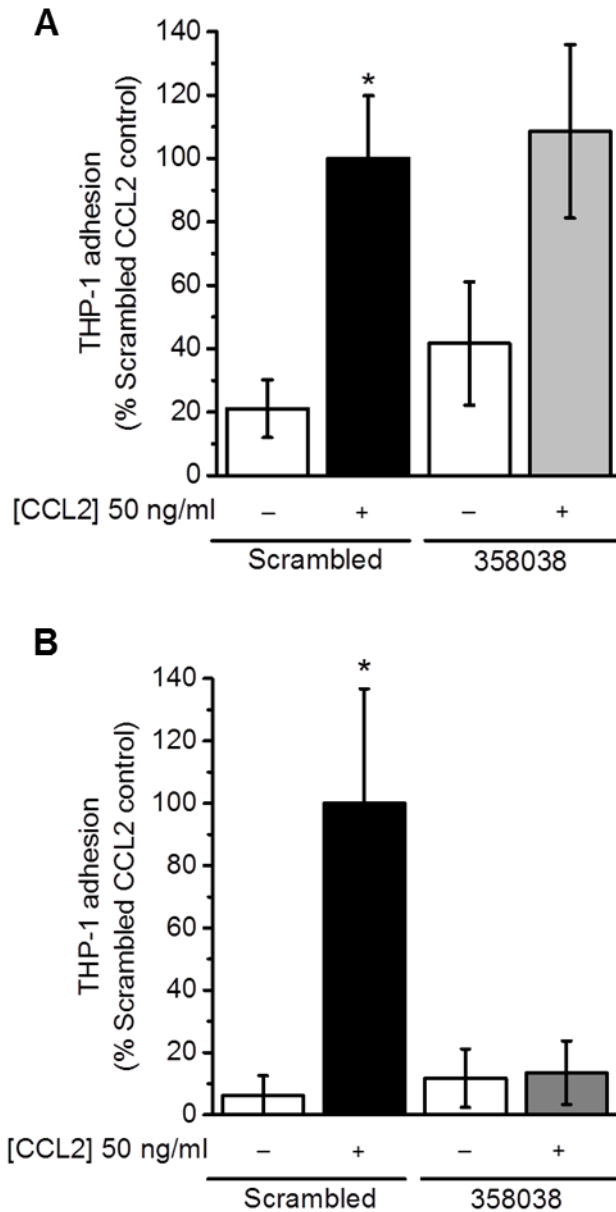


**Figure 6.19 CCL2-mediated adhesion of scrambled and P2Y<sub>6</sub>-KD cells to quiescent and TNF $\alpha$ -treated HUVEC monolayers**

Bar chart showing normalised adhesion (1 hour) of scrambled and P2Y<sub>6</sub>-KD THP-1 cells to (A) quiescent and (B) TNF $\alpha$ -treated (10 ng/ml, 5 hours) HUVEC monolayers following priming of THP-1 cells with CCL2 (50 ng/ml) or vehicle (water) (45 minutes). Normalised adhesion represented as a percentage of mean adhesion of CCL2-primed scrambled THP-1 cells. Data represents mean  $\pm$  SEM from a total of n=12 replicates from n=3 experiments (quiescent HUVECs), or a total of n=8 replicates from n=2 experiments (TNF $\alpha$ -treated). Asterisks indicate significant changes towards vehicle-treated scrambled cells (\*p<0.05, One-way ANOVA with Bonferroni's multiple comparison).

### 6.3.10 CCL2-mediated extracellular nucleotide release in THP-1 cells

#### 6.3.10.1 Detecting CCL2-mediated extracellular nucleotide release

While the evidence from the studies in this thesis suggest that P2Y<sub>6</sub> is required for CCL2/CCR2-mediated monocyte signalling and function, the mechanism(s) by which CCR2 and P2Y<sub>6</sub> crosstalk remains an unresolved question. However, recent studies by Chen *et al.* (2006) and Sumi *et al.* (2010) have given important insights into the possible mechanisms by which purinoceptors and non-purinoceptors crosstalk. For example, Chen *et al.* (2006) have shown that in neutrophils, activation of FPR receptors by fMLP releases ATP and guides neutrophil chemotaxis via a co-activation of P2Y<sub>2</sub> and A<sub>3</sub> purinoceptors. The same group (Sumi *et al.*, 2010) have recently shown that adrenergic  $\alpha_1$  receptors activation on mice aortic rings drives tissue contraction and ATP release, an effect weakened by apyrase or P2Y<sub>2</sub>-knockout. Together, these studies suggest purinoceptor crosstalk with other GPCRs involves a release of ATP. It is possible, therefore, that CCR2 and P2Y<sub>6</sub> also crosstalk through a release of extracellular nucleotides.

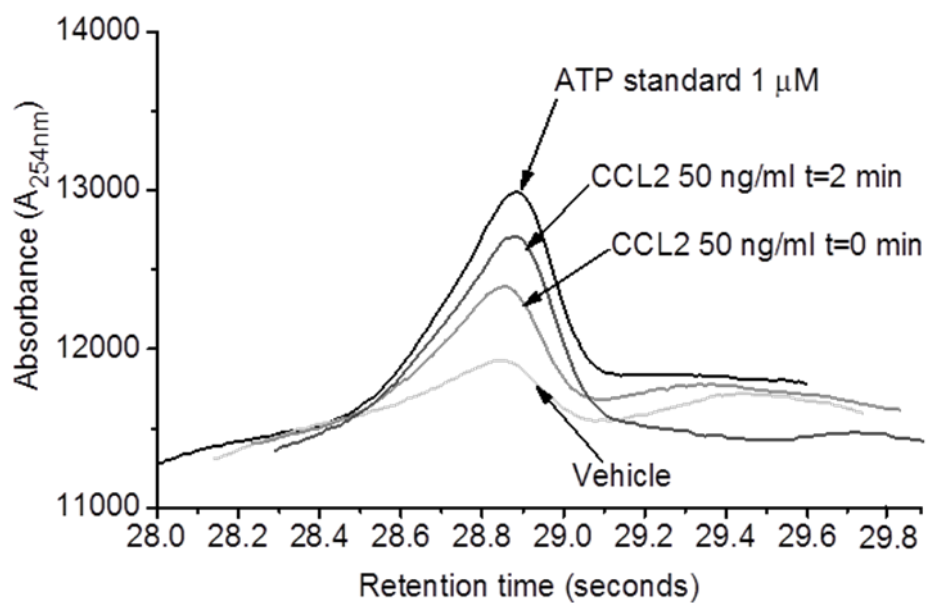
Hence, it was important to investigate this hypothesis. Experiments were therefore performed to investigate if CCL2-challenged THP-1 cells would release P2Y<sub>6</sub> ligands (ATP, ADP, UTP, and UDP) into cell supernatants. THP-1 cells were challenged with vehicle or CCL2 (50 ng/ml) and sampled immediately (0 minutes/t=0 min) and at 2 minutes (t=2 min). Clarified samples were analysed for extracellular nucleotides using ion-pair reverse-phase HPLC, a technique able to detect a minimum nucleotide concentration of 1  $\mu$ M (Section 2.9, Chapter 2).

Interestingly, ATP was the only nucleotide consistently detected within samples (n=5). Other nucleotides (ADP, UTP, and UDP) were also detected, but not consistently in every experiment. Figure 6.20 shows a representative experiment for ATP. As shown, CCL2 challenge produced a time-dependent increase in ATP absorbance (n=5). These data suggest that an activation of the CCL2/CCR2 axis in monocytes evokes a release of ATP. However, since these data were not quantitative, it was not possible to determine whether ATP released by THP-1 cells in response to CCL2 activated P2Y<sub>6</sub>. Therefore, in order to quantify the amount of ATP released by cells, a commercial luciferin-luciferase ATP assay was employed to quantify ATP release over time. In these experiments, THP-1 cells were challenged with vehicle or CCL2 (50 ng/ml) and sampled every two minutes for 14 minutes. The concentration of ATP ([ATP]) in samples was then determined.

As shown (Figure 6.21a), CCL2-challenge resulted in a transient rise in [ATP] in THP-1 cell supernatants. At its highest level at 8 minutes, the [ATP] in cell supernatants was  $1013 \pm 108$  nM (n=7) and was significantly higher than all other time-points (n=7, p<0.01).

The average [ATP] of all other time-points was  $228 \pm 37$  nM (n=36). Figure 6.21b shows the [ATP] at 8 minutes in supernatants from THP-1 cells challenged with vehicle or CCL2. As shown, a significantly higher [ATP] was detected in supernatants from THP-1 cells challenged with CCL2 ( $1013 \pm 108$  nM, n=7) than from cells challenged with vehicle ( $217 \pm 38$  nM, n=7,  $p < 0.01$ ). These data suggest that CCL2 challenge increases the [ATP] in THP-1 cell supernatants by 4.7-fold.

Taken together, these data indicate that CCL2 challenge liberates  $\sim 1$   $\mu$ M ATP from THP-1 cells. Although HPLC experiments were not always able to detect ADP in these experiments, as a metabolic product of ATP, a release of ADP following CCL2 challenge seems plausible.



Treatment	Peak Absorbance (A <sub>254nm</sub> )
1 μM ATP	12994
Vehicle	11983
CCL2 t=0 min	12441
CCL2 t=2 min	12802

**Figure 6.20 Detection of CCL2-mediated ATP release in THP-1 cells by ion-pair reverse-phase HPLC**

Representative experiment showing absorbance (A<sub>254nm</sub>) of ATP liberated from THP-1 cells challenged with vehicle (water) or CCL2 (50 ng/ml). Sampling performed at 0 minutes (t=0 min), or 2 minutes (t=2 min) post-CCL2 challenge, or at 0 minutes post-vehicle challenge. ATP standard (1 μM) serves as a reference.

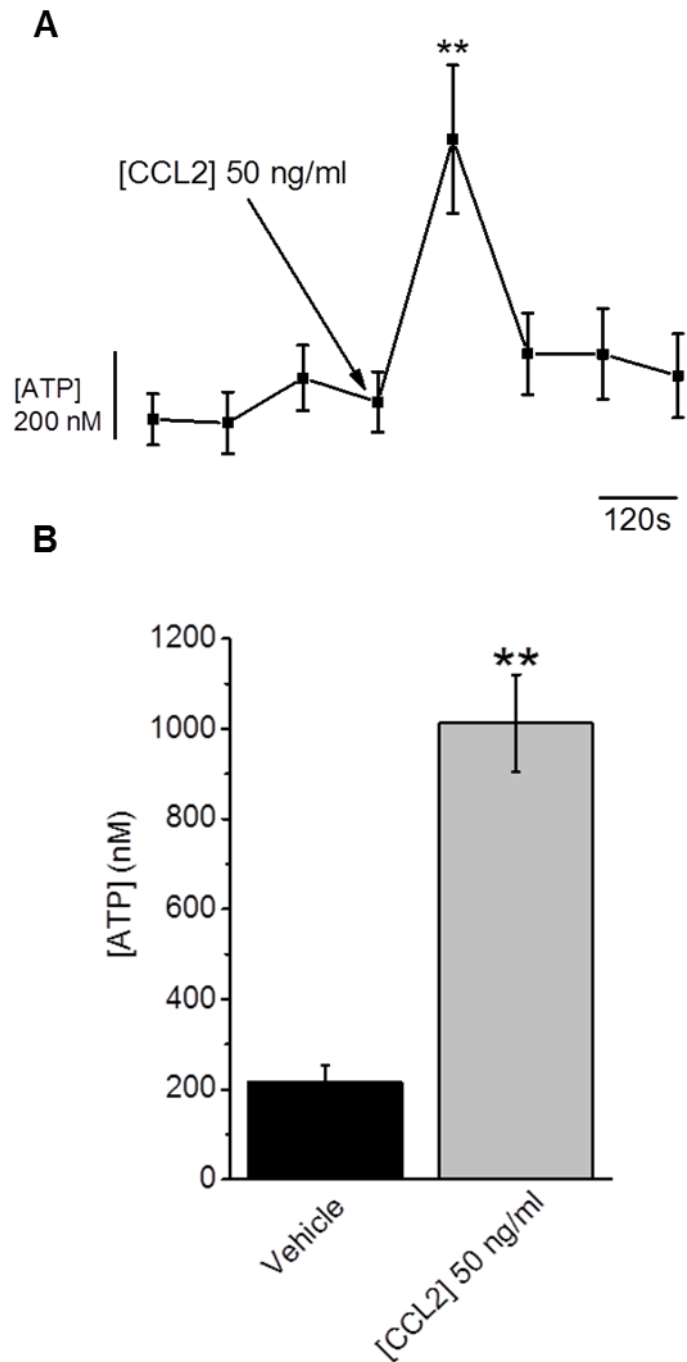


**Figure 6.21 Detection of CCL2-mediated ATP release in THP-1 cells by luciferase-luciferin**

(A) Trace showing amount of ATP in THP-1 cell supernatants following challenge with CCL2 (50 ng/ml) at 6 minutes (shown by arrow). (B) Bar chart showing ATP concentration (nM) at 8 minutes in supernatants from THP-1 cells challenged with vehicle (water) or CCL2 (50 ng/ml). Data represents mean  $\pm$  SEM from  $n=7$  replicates. Asterisks indicate significant changes towards other time-points (A), or vehicle (B) (\*\* $p<0.01$ , One-way ANOVA with Bonferroni's multiple comparison (A), or Student's  $t$ -test (B)).

### 6.3.10.2 Investigating THP-1 cell lysosomes as a source of ATP

The release of ATP from THP-1 cells following CCL2 challenge represents a novel finding but at the same time, raises some important questions about the mechanisms involved in coupling CCR2 activation to ATP release, and the subsequent coupling of P2Y<sub>6</sub> activation to the CCL2/CCR2 axis. In an effort to understand how ATP release occurs, the source of ATP in THP-1 cells was investigated. Given the amount of evidence linking ATP release with lysosomes and secretory vesicles (Chen *et al.*, 2006; Eltzschig *et al.*, 2006; Sivaramakrishnan *et al.*, 2012), it was important to investigate whether CCL2 caused ATP release from lysosomes containing the enzyme  $\beta$ -hexosaminidase. To this end, THP-1 cells were incubated with Triton X-100 (positive control), vehicle (SBS or DMSO), CCL2 (50 or 100 ng/ml), or GPN (0.2 mM) and tested for  $\beta$ -hexosaminidase release as described in Section 2.10 (Chapter 2).

**Table 6.9**  $\beta$ -hexosaminidase in THP-1 cell supernatants

Treatment	$\beta$ -hexosaminidase (% Triton X-100)
Triton X-100 (1%)	100 $\pm$ 7 (p<0.01 versus SBS)
SBS	0.7 $\pm$ 0.3
DMSO (2%)	0.0 $\pm$ 0.3
GPN (0.2 mM)	28 $\pm$ 3 (p<0.01 versus DMSO)
CCL2 50 ng/ml	0.7 $\pm$ 0.3
CCL2 100 ng/ml	0.4 $\pm$ 0.1

Data represents mean  $\pm$  SEM from a total of n=6 replicates from n=3 experiments. Statistical tests performed using one-way ANOVA with Bonferroni's multiple comparison.

As shown in Table 6.9, Triton X-100 caused a significant release of  $\beta$ -hexosaminidase from THP-1 cells over SBS (n=6, p<0.01), therefore supporting the presence of lysosomes in THP-1 cells. A significant increase in  $\beta$ -hexosaminidase was also seen in cells treated with GPN (n=6, p<0.01). This result supported prior work by Sivaramakrishnan *et al.* (2012). Interestingly, no significant increase in  $\beta$ -hexosaminidase release over SBS was seen with either 50 ng/ml CCL2 (n=6, p>0.05) or 100 ng/ml CCL2 (n=6, p>0.05). These data suggest that CCL2 does not evoke  $\beta$ -hexosaminidase release from THP-1 cells.

Taken together, these data suggest that CCL2 does not cause  $\beta$ -hexosaminidase release from THP-1 cells. These results also suggest that ATP release may not be from lysosomes containing  $\beta$ -hexosaminidase.

## 5.4 Summary

This chapter set out to investigate the requirement of the P2Y<sub>6</sub> purinoceptor for CCL2/CCR2-mediated monocyte signalling and function using monocytic THP-1 cells and where possible, human PBMCs as models. A number of methodology combined with molecular and pharmacological tools were employed to examine intracellular Ca<sup>2+</sup> mobilisation, cell migration, adhesion, and ATP release. A number of important findings were made. Initial experiments in THP-1 cells with the P2Y<sub>6</sub> antagonist, MRS-2578 revealed a requirement for P2Y<sub>6</sub> in CCL2/CCR2-mediated Ca<sup>2+</sup> signalling, cellular migration, and adhesion to HUVECs. Additional studies in human PBMCs supported these findings. Further studies in THP-1 cells led to the identification that 64-70% of the CCL2 Ca<sup>2+</sup> response was attributed to P2Y<sub>6</sub>, and the remaining to a bona-fide activation of CCR2. Intracellular Ca<sup>2+</sup> studies in P2Y<sub>6</sub>-stable 1321N1 cells indicated that P2Y<sub>6</sub> could be activated by the extracellular nucleotides ATP, ADP, UTP, and UDP, at concentrations ≤300 nM. The most potent of these ligands, UDP, evoked Ca<sup>2+</sup> responses that were attenuated by MRS-2578, but not abolished. Further data indicated that THP-1 cells expressed functional P2Y<sub>14</sub>, a receptor activated by UDP. Additional studies in THP-1 cells with MRS-2578 supported 1321N1 experiments in that they suggested that ATP, ADP, UTP and UDP activated P2Y<sub>6</sub>. While the results of co-application studies pointed towards a lack of synergy between CCL2 and UDP, they also indicated the need for additional studies. The results of fMLP-FPR studies ruled out a requirement of P2Y<sub>6</sub>, but indicated that other purinoceptors were likely to be involved in regulating FPR signalling. Interestingly, desensitisation studies suggested that CCR2 receptors could be cross-desensitised by P2Y<sub>6</sub>. Further support for these data came from experiments with P2Y<sub>6</sub>-KD cells, which showed that knockdown of *P2RY6* attenuated THP-1 cell Ca<sup>2+</sup> responses to UDP and CCL2, and also reduced cellular chemotaxis and adherence to TNF $\alpha$ -treated HUVEC monolayers. ATP release studies indicated that THP-1 cells challenged with CCL2 released ATP into supernatants. However, additional experiments suggested that this did not involve secretory vesicles containing  $\beta$ -hexosaminidase.

Taken together, these findings suggest that CCL2/CCR2 signalling in monocytes involves crosstalk with the P2Y<sub>6</sub> purinoceptor. Furthermore, activation of P2Y<sub>6</sub> upon CCR2 engagement involves a concomitant release of ATP.

# Chapter 7: Discussion

---

## 7.1 Overview

The CCL2/CCR2 axis is important for orchestrating monocyte function under physiological conditions, but is also associated with a growing number of monocyte-associated pathologies. Although this has led to several CCR2 antagonists being developed, a lack of efficacy of these in clinical trials has meant that none are therapeutically useful. The lack of progress made in this area indicates a need to better understand *in vivo* models, the contributions of other CCR2 ligands, as well as the influence of other chemotactic pathways (such as purinoceptor signalling). Indeed, a considerable amount of evidence has been published on the involvement of purinoceptors in monocyte function and CCL2 release (Cox *et al.*, 2005; Stokes and Surprenant, 2007; Morioka *et al.*, 2013; Garcia *et al.*, 2014; Higgins *et al.*, 2014; Shieh *et al.*, 2014). It is possible, therefore, that monocyte signalling and function involves crosstalk between purinoceptors and CCR2. This hypothesis was therefore investigated in this thesis using human monocytic THP-1 cells and human PBMCs as *in vitro* models. Areas studied in this thesis included:

- (i) The expression of mRNA transcripts for monocyte/myeloid cell markers, CC chemokines, CC chemokine receptors, and purinoceptors in THP-1 cells and human monocytes (Chapter 3).
- (ii) The mechanisms involved in CCL2/CCR2-mediated monocyte signalling and function (Chapter 4).
- (iii) The requirement of extracellular nucleotides and purinoceptors for CCL2/CCR2-mediated monocyte signalling and function (Chapter 5)
- (iv) The requirement of P2Y<sub>6</sub> for CCL2/CCR2-mediated monocyte signalling and function (Chapter 6).
- (v) The involvement of the CCL2/CCR2 axis in extracellular nucleotide release (Chapter 6).

## 7.2 Concluding Remarks

In conclusion, this study has characterised in some depth, the CCL2/CCR2 axis, and its involvement in monocyte signalling and function. This research has supported some of the established pathways involved in CCL2/CCR2 signalling, while indicating the requirement of novel and less well-established pathways (Figure 7.1). Investigating the individual contributions of these complex pathways further may enhance our understanding of monocyte-associated pathologies and drive future research towards novel therapies.

The findings of this study have also suggested a novel requirement of the P2Y<sub>6</sub> purinoceptor for CCL2/CCR2-mediated monocyte signalling and function (Figure 7.1). The data presented has indicated for the first time that ATP released by monocytes upon CCR2 activation under homeostatic and inflammatory conditions is important for deciphering chemical cues in the microenvironment. Although it is likely that other chemotactic signals also influence monocyte function *in vivo*, it is evident from the findings presented here that crosstalk between CCR2 and P2Y<sub>6</sub> is crucial for CCL2/CCR2-mediated monocyte trafficking and adhesion. Thus, the association between CCR2 and P2Y<sub>6</sub> identified by this research will serve as a base for future studies directed towards developing novel therapies targeting monocyte-associated pathologies.

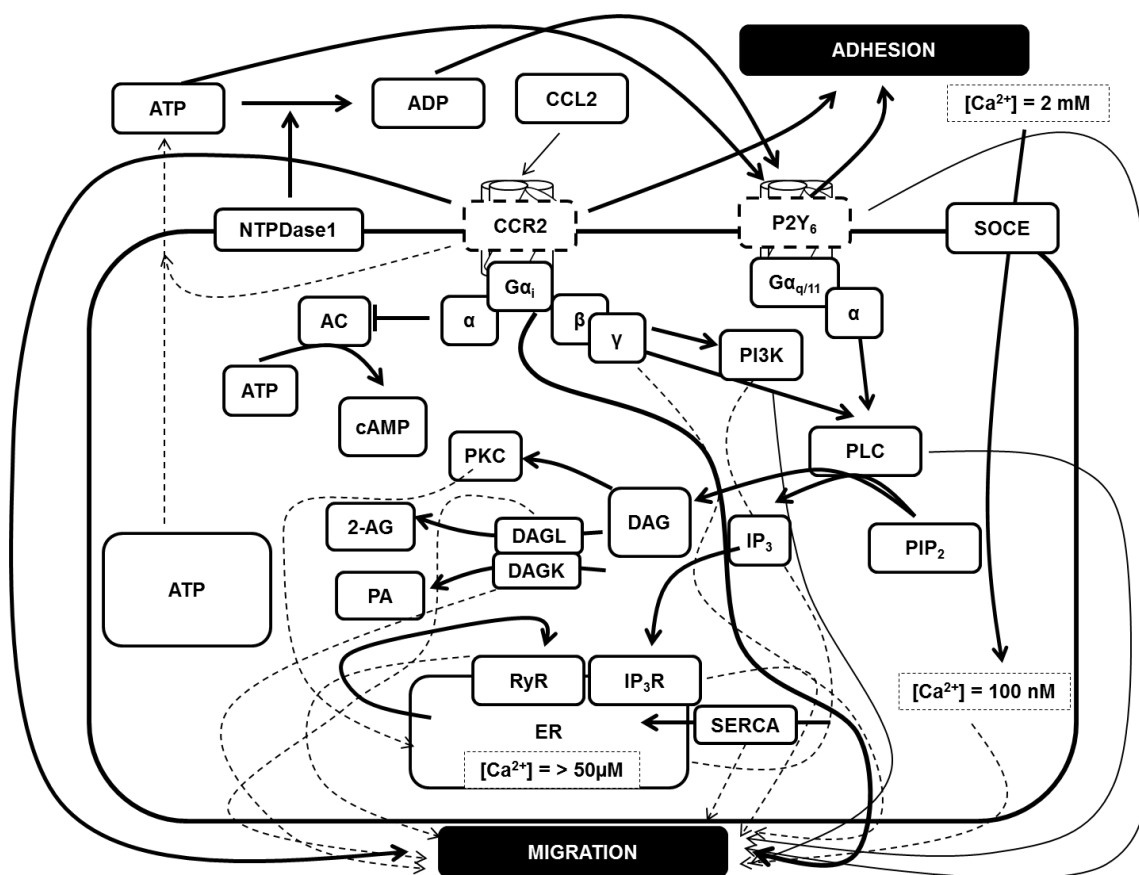


**Figure 7.1 CCR2 and P2Y<sub>6</sub> crosstalk in monocytes**

Diagram showing some of the main signalling pathways proposed by this work. Thick arrows represent established pathways investigated in this thesis, or pathways that are widely known to occur. Thinner arrows represent less-established pathways that have been suggested by this work. Dashed arrows represent novel pathways that have been suggested by this work. Diagram does not show the possible involvement of non-ER Ca<sup>2+</sup> stores. Further studies are required to confirm these findings and to better understand the involvement of these signalling cascades in monocyte signalling and function.

## 7.3 Key Findings

### ***mRNA transcripts for monocyte and myeloid markers are expressed by THP-1 cells and human monocytes***

The monocytic leukaemia cell line THP-1 was employed as an *in vitro* model for this work. However, prior to performing experiments it was important to understand if these cells represented a suitable model for studying monocyte signalling and function. This was done initially by comparing the expression of mRNA for the monocyte and myeloid markers, CD14, CD16, CD33, and CD93, between THP-1 cells and human peripheral blood monocytes.

RT-PCR results suggested that THP-1 cells expressed mRNA for CD14, CD33, and CD93, while monocytes expressed mRNA for CD14, CD16, CD33, and CD93. This finding supports the hypothesis that both cell types are of myeloid origin (Pilling *et al.*, 2009). A second interesting finding from this study was that mRNA for CD16 was not detected in THP-1 cells. Although it is possible that levels may have fallen below the limits of detection by RT-PCR, it could also be that THP-1 cells genuinely lack CD16 which would agree with post-translational studies (Auwerx, 1991; Fleit and Kobasiuk, 1991). In this study, it was found that THP-1 cells expressed mRNA for CD14. This is interesting because other groups suggest that THP-1 cells either express low levels of mRNA or protein for CD14 (Daigneault *et al.*, 2010; Bruckmeier *et al.*, 2012), or only express this upon differentiation to macrophages (Kohro *et al.*, 2004; Aldo *et al.*, 2013). Given that THP-1 cells have a natural tendency to differentiate into macrophages when cultured at high densities (above  $1e^6/ml$ ), expression of CD14 may be density-dependent. However, while this might be why CD14 mRNA was detected in THP-1 cells, this is unlikely because cells were always cultured below  $7e^5/ml$  (Chapter 2).

The results of this study suggested that human monocytes expressed mRNA for CD14 and CD16. This result was expected, and suggests that samples comprised of multiple monocyte subtypes. The expression of mRNA for these markers agrees with the findings of mRNA and post-translational studies performed on human monocyte populations (Passlick *et al.*, 1989; Auwerx, 1991; Geissmann *et al.*, 2003). However, while the results of this study are interesting, it is important to bear in mind that the monocyte isolation methodology employed may not have provided a pure monocyte population, resulting in the detection of CD14 and CD16 on other myeloid cells (Pilling *et al.*, 2009). Further studies with purified monocyte populations are therefore recommended.

The findings of this study, while preliminary, suggest that THP-1 cells and peripheral-blood monocytes express a similar pattern of mRNA transcripts for monocyte and myeloid

markers. These findings may help us to understand the suitability of THP-1 cells as a model for investigating monocyte signalling and function.

### ***mRNA transcripts for CC chemokines and their receptors are expressed by THP-1 cells and human monocytes***

Monocyte-associated inflammatory diseases are often associated with an up-regulated expression of CC chemokines and their receptors (Bruegel *et al.*, 2006; Kaminsky *et al.*, 2008; Selvaraj *et al.*, 2012). Therefore, assessing any alterations in expression would provide an effective biomarker for inflammatory diseases. To understand the suitability of THP-1 cells as a model for investigating CC chemokine signalling, studies compared the expression of mRNA transcripts for CC chemokines and their receptors between THP-1 cells and human monocytes.

RT-PCR results suggested that both cell types expressed mRNA for all of the CC chemokines tested (CCL2, CCL3, CCL4, and CCL5). This finding suggests that these chemokines would serve as useful biomarkers. The results of further mRNA studies suggested that THP-1 cells expressed all CC chemokine receptors, except mRNA for CCR3. In comparison, mRNA transcripts for all CC chemokine receptors including CCR3 were detected in human monocytes. These results agree with prior work showing that THP-1 cells express CCR1, CCR2, CCR5, and CCR9 and human monocytes express CCR1, CCR2, CCR3, CCR5, and CCRL2 (Neote *et al.*, 1993; Yamagami *et al.*, 1994; Combadiere *et al.*, 1996; Weber *et al.*, 2000; Migeotte *et al.*, 2002; Kim *et al.*, 2004; Apostolakis *et al.*, 2010; Schmutz *et al.*, 2010). However, the expression of other receptors is a novel finding. The lack of mRNA for CCR3 in THP-1 cells is also interesting. Although this result differs from the findings of post-translational studies (Martinelli *et al.*, 2001), it may be that levels of mRNA fell below the limits of RT-PCR detection.

A second important finding was that mRNA for CCR2A and CCR2B were detected in THP-1 cells and human monocytes. The expression of mRNA for both variants in THP-1 cells supports post-translational studies by Campwala *et al.* (2014). The detection of mRNA for CCR2A and CCR2B in monocytes is also interesting because CCR2B is known to be more readily expressed on the cell surface and activated than CCR2A (Wong *et al.*, 1997; Sanders *et al.*, 2000). Thus, identifying which of these participate in monocyte function would be interesting. However, in general, the finding that monocytes express mRNA for CCR2 agrees with prior studies (Weber *et al.*, 2000; Tacke *et al.*, 2007). This suggests that monitoring CCR2 mRNA expression would be useful as it would enable a greater understanding of pathologies where monocytes differentiate to macrophages,

which results in a loss of CCR2 expression (Fantuzzi *et al.*, 1999; Kaufmann *et al.*, 2001; Phillips *et al.*, 2005).

The findings of this study suggest that THP-1 cells and human monocytes express a similar pattern of expression of CC chemokines and their receptors. The expression of novel CC chemokine receptors may help enhance our understanding of the role played by these receptors in monocyte function.

### ***mRNA transcripts for purinoceptors are expressed by THP-1 cells and human monocytes***

RT-PCR results suggested that THP-1 cells and human monocytes expressed mRNA for all P1 purinoceptors. While the expression of these in monocytes is consistent with prior reports (Merrill *et al.*, 1997; Broussas *et al.*, 1999; Thiele *et al.*, 2004), only A<sub>2A</sub> and A<sub>2B</sub> receptors have been previously detected in THP-1 cells (Munro *et al.*, 1998; Khoa *et al.*, 2001; Bshesh *et al.*, 2002). The expression of A<sub>1</sub> and A<sub>3</sub> in THP-1 cells therefore represents a novel finding and may enhance our understanding of the involvement of these receptors in monocyte-associated pathologies. Although further studies at the post-translational level are required, the current findings are important because they suggest that THP-1 cells and human monocytes express all P1 purinoceptors.

Studies of P2X purinoceptors suggested that THP-1 cells express mRNA for all P2X receptors except P2X2 and P2X3, while human monocytes express all P2X receptors except P2X2, P2X3, and P2X6. The expression of P2X1, P2X4, and P2X7 in both cell types is consistent with prior reports (Humphreys and Dubyak, 1998; Into *et al.*, 2002; Wang *et al.*, 2004; Kaufmann *et al.*, 2005; Li and Fountain, 2012), but suggests that the expression of P2X5 and P2X6 in THP-1 cells, and P2X5 in human monocytes, represent novel findings. The detection of mRNA for P2X5 in both cell types is interesting but could not be compared with previous studies as the results from these are not in agreement (Lê *et al.*, 1997; Kaufmann *et al.*, 2005). Thus, our own studies at the post-translational level are recommended. Although these results also suggested that THP-1 cells expressed mRNA for P2X6, a functional role of this receptor is unlikely as it is unable to establish functional homotrimers (Barrera *et al.*, 2005). The findings of this study also suggested that both cell types lack mRNA for P2X2 and P2X3 which may reflect the fact that both receptors are mainly found in sensory neurones (Burnstock and Knight, 2004). What is also interesting about P2X2 and P2X3 is that mRNA transcripts for these purinoceptors could not be detected in human brain. While the lack of P2X3 mRNA transcripts in human brain fits well with prior work published by Garcia-Guzman *et al.* (1997b), it is interesting that the lack of P2X2 mRNA in human brain differs from the findings of Lynch *et al.* (1999) whose cloning work on the human P2X2 receptor from the pituitary gland showed that

mRNA transcripts for P2X2 splice variants could be detected in amygdala and brain tissue. It may be the case therefore, that the brain RNA samples used within the current study represent a section of the human brain which poorly expresses P2X2.

RT-PCR results suggested that THP-1 cells and human monocytes expressed mRNA for P2Y purinoceptors. However, while this suggested that both cell types exhibited a similar pattern of expression, these results could not be compared with prior work due to inconsistencies in these earlier studies. For example, quantitative studies on THP-1 cells suggest that these express mRNA for P2Y<sub>2</sub>, but not P2Y<sub>1</sub> or P2Y<sub>4</sub> (Moore *et al.*, 2001), while non-quantitative studies detect P2Y<sub>1</sub>, P2Y<sub>2</sub>, P2Y<sub>6</sub>, and P2Y<sub>11</sub> (Ben Yebdri *et al.*, 2009). Similarly, non-quantitative studies on monocytes (Kaufmann *et al.*, 2005) suggest that they express P2Y<sub>2</sub>, P2Y<sub>11</sub>, and P2Y<sub>13</sub>, while quantitative studies report mRNA for all P2Y purinoceptors except P2Y<sub>14</sub>, which was not tested (Wang *et al.*, 2004). It may be the case, therefore, that these inconsistencies between studies are due to differences in the methodologies and samples used. The results of this study also indicated that both cell types expressed mRNA for P2Y<sub>14</sub>. Although the involvement of P2Y<sub>14</sub> in immune cells is unclear (Burnstock and Boeynaems, 2014), the expression of this receptor in both cell types represents a novel finding.

### ***CCL2-evokes intracellular Ca<sup>2+</sup> release from THP-1 cells and human PBMCs***

The mobilisation of intracellular Ca<sup>2+</sup> upon receptor activation is considered an integral component of cellular signalling and activation (Berridge *et al.*, 2000). From studies in literature, it is clear that CC chemokines such as CCL2 induce Ca<sup>2+</sup> release from intracellular Ca<sup>2+</sup> stores in monocytes, THP-1 cells, and human PBMCs upon receptor activation (Sozzani *et al.*, 1993; Bizzarri *et al.*, 1995; Kim *et al.*, 2004; Cherney *et al.*, 2008).

Intracellular Ca<sup>2+</sup> studies using THP-1 cells and human PBMCs showed that application of CCL2 to cells induced a transient release of Ca<sup>2+</sup>. This finding is considered significant since it supports prior work in THP-1 cells and human PBMCs (Kim *et al.*, 2004; Cherney *et al.*, 2008) and suggests that CCL2 drives intracellular Ca<sup>2+</sup> release in monocytes. Additional studies of THP-1 cells indicated that CCL2 exhibited an EC<sub>50</sub> of 1.9 nM for intracellular Ca<sup>2+</sup> release. This is interesting because it compares well with EC<sub>50</sub> values for CCL2 (0.7–10 nM) previously published through work performed on human monocytes and CCR2-transfected cell lines (Charo *et al.*, 1994; Myers *et al.*, 1995; Combadiere *et al.*, 1995; Sozzani *et al.*, 1995; Wong *et al.*, 1997). However, while the present study suggested an involvement of CCR2 in CCL2-mediated Ca<sup>2+</sup> mobilisation, it was unable to identify which CCR2 variant (CCR2A or CCR2B) was involved in initiating these responses. Identifying which variant is involved in intracellular Ca<sup>2+</sup> release would

therefore be useful to address given that CCR2A and CCR2B are known to differentially regulate Ca<sup>2+</sup> release and chemotaxis of Jurkat T-cells (Sanders *et al.*, 2000).

### ***Removal of extracellular Ca<sup>2+</sup> attenuates CCL2-mediated THP-1 cell signalling and function***

The association between CCL2-evoked intracellular Ca<sup>2+</sup> release and monocyte function is not completely understood. Although previous work by others has suggested that Ca<sup>2+</sup> release is chemotactic for human monocytes (Olszak *et al.*, 2000; Gouwy *et al.*, 2008), the signalling events that couple intracellular Ca<sup>2+</sup> release to monocyte trafficking have not been fully established. Therefore, to address this gap in knowledge, studies examined the requirement of extracellular Ca<sup>2+</sup> for CCL2-mediated THP-1 intracellular Ca<sup>2+</sup> release and chemotaxis.

The results from intracellular Ca<sup>2+</sup> studies suggested that CCL2-evoked intracellular Ca<sup>2+</sup> responses in monocytes were partially dependent on Ca<sup>2+</sup> influx. This finding is interesting, and directly supports prior work by Bizzarri *et al.* (1995) whose studies showed a similar attenuation of CCL2-evoked Ca<sup>2+</sup> responses in single monocytes following a removal of extracellular Ca<sup>2+</sup>. Interestingly, earlier studies by the same group on heterogeneous monocytes (Sozzani *et al.*, 1993), suggested that CCL2-induced Ca<sup>2+</sup> responses were entirely dependent on Ca<sup>2+</sup> influx, therefore contradicting the findings of Bizzarri *et al.* (1995). It is possible, therefore, that the results presented by Sozzani *et al.* (1993) could be attributed to errors in their methodology.

THP-1 cell chemotaxis studies suggested that the Ca<sup>2+</sup> chelator BAPTA-AM abolished CCL2-mediated and CCL2-independent cellular chemotaxis. This finding is important since it suggests that THP-1 cell chemotaxis and chemokinesis are fully dependent on the availability of intracellular Ca<sup>2+</sup>. A lack of cytotoxicity of BAPTA-AM in cell viability studies supported these results. While previous studies have not dealt with the effects of sequestering Ca<sup>2+</sup> on CCL2-mediated monocyte chemotaxis, it is interesting that Moyano Cardaba *et al.* (2012) proposed that THP-1 cell chemotaxis towards the CC chemokine CCL3 occurs independently of intracellular Ca<sup>2+</sup> release. Although this implies that individual chemokines differ in their Ca<sup>2+</sup> requirements for chemotaxis, it is interesting that other groups (Wei *et al.*, 2009; Tsai *et al.*, 2014), have discovered that “calcium flickers” at the leading edge of migrating cells are required for directed cell migration and adhesion. This supports the hypothesis that intracellular Ca<sup>2+</sup> is required for CCL2-mediated and CCL2-independent cellular chemotaxis. Given the importance of these findings, other Ca<sup>2+</sup> chelators (e.g. EGTA) should be used to provide further support of a requirement of Ca<sup>2+</sup> for monocyte chemotaxis.

### **CCR2 antagonism attenuates CCL2-mediated THP-1 cell signalling and function**

Although the association between CCL2 and its cognate receptor CCR2 is well-recognised (Bachelierie *et al.*, 2014), CCL2 is also known to bind to other chemokine receptors including ACKR1, ACKR2, CCR3, and CCR5 (Daugherty *et al.*, 1996; Blanpain *et al.*, 1999; Bachelierie *et al.*, 2014). Thus, CCL2-mediated signalling and function of monocytes may not be entirely driven by CCR2. To investigate this hypothesis, studies employed the CCR2A/CCR2B antagonist BMS-CCR2-22.

The results of intracellular  $\text{Ca}^{2+}$  experiments showed that BMS-CCR2-22 attenuated CCL2-evoked intracellular  $\text{Ca}^{2+}$  responses in a concentration-dependent manner, exhibiting an  $\text{IC}_{50}$  of 2.9 nM. At higher concentrations (100 nM), BMS-CCR2-22 abolished CCL2  $\text{Ca}^{2+}$  signals, suggesting that CCL2-mediated signalling depended entirely on CCR2. This finding supports the expression of mRNA for CCR2 as shown by the work in this thesis, but also stands in agreement with other published studies showing that CCL2 signals primarily through CCR2 (Charo *et al.*, 1994; Yamagami *et al.*, 1994; Myers *et al.*, 1995). In further intracellular  $\text{Ca}^{2+}$  studies, it was interesting to observe that human PBMCs were less sensitive than THP-1 cells to the effects of BMS-CCR2-22. Although this result is difficult to explain, it may be that PBMCs express lower levels of CCR2 at the post-translational level. Although the findings of this study suggested that BMS-CCR2-22 selectively targets CCR2, the results of additional experiments showed that CCL5-evoked  $\text{Ca}^{2+}$  responses were also attenuated by BMS-CCR2-22, suggesting a possible antagonism of receptors activated by this ligand (CCR1, CCR3 and CCR5) (Bachelierie *et al.*, 2014). This seems possible given that Cherney *et al.* (2008) have shown that high concentrations of BMS-CCR2-22 (10  $\mu\text{M}$ ) inhibit CCR3 binding (Cherney *et al.*, 2008). However, while it is possible that the concentrations of BMS-CCR2-22 used in the current study could have also targeted CCR3, it is important to bear in mind that mRNA for CCR3 could not be detected in THP-1 cells. Furthermore, the CCL5 used for these studies was only 95% pure and may have contained contaminants. Thus, further work with CCL5 of a greater purity, or studies with CCR3-transfected cells, are required.

In migration experiments, it was seen that BMS-CCR2-22 abolished THP-1 cell chemotaxis towards CCL2, effectively bringing cell migration down to chemokinesis levels. This result was quite striking, and suggests that monocyte trafficking and signalling in response to CCL2 *in vivo* would be entirely dependent on CCR2. Moreover, these results suggested that constitutive CCL2 signalling does not control chemokinesis. The effects of BMS-CCR2-22 on CCL2-mediated cellular trafficking is in agreement with prior work in PBMCs (Cherney *et al.*, 2008), showing that BMS-CCR2-22 impairs PBMC chemotaxis towards CCL2 more readily than intracellular  $\text{Ca}^{2+}$  responses. This is interesting, and

suggests that in an *in vivo* setting, monocyte trafficking towards excessive CCL2 gradients would be more sensitive to CCR2-blockade than to intracellular  $\text{Ca}^{2+}$  signalling.

The results of studies investigating the requirement of CCR2 for monocyte adhesion showed that BMS-CCR2-22 nearly abolished CCL2-dependent adhesion to quiescent HUVEC monolayers, but completely abolished CCL2-dependent and independent adhesion to TNF $\alpha$ -treated monolayers. These findings support prior work showing that CCR2 is required for monocyte adherence to the vascular endothelium (Shyy *et al.*, 1993; Kuziel *et al.*, 1997; Gerszten *et al.*, 1999), but also suggest that monocyte adhesion under inflammatory conditions is fully-dependent on CCL2/CCR2. This seems plausible given that treatment of HUVEC monolayers with IL-1 $\beta$  or TNF $\alpha$  upregulates CCR2 surface expression and CCL2 release (Weber *et al.*, 1999). This may also help to explain why inflammatory pathologies involving monocyte adhesion and infiltration are significantly attenuated by CCL2/CCR2-blockade (Boring *et al.*, 1998; Gu *et al.*, 1998).

The findings of this study are therefore important as they help us to understand the involvement of the CCL2/CCR2 axis in monocyte signalling and function under physiological and inflammatory conditions. However, a key area for further research is the involvement of adhesion molecules in these interactions and the release of CCL2 by TNF $\alpha$ -treated HUVECs.

### ***Inhibition of G $\alpha_i$ -G-proteins and G $\beta\gamma$ dimers attenuates CCL2/CCR2-mediated THP-1 cell signalling and/or function***

In the literature, it is widely accepted that CCR2 signals through G $\alpha_i$ -type G-proteins coupled to an inhibition of adenylate cyclase (Bachelierie *et al.*, 2014). The current study therefore set out to provide confirmation of this by examining the effects of PTx on CCL2/CCR2-mediated THP-1 cell intracellular  $\text{Ca}^{2+}$  mobilisation and chemotaxis.

The results of  $\text{Ca}^{2+}$  experiments showed that CCL2-evoked  $\text{Ca}^{2+}$  responses were almost abolished by PTx. However, while these results agree with prior work showing that CCL2/CCR2 intracellular  $\text{Ca}^{2+}$  signalling involves an activation of G $\alpha_i$  (Bizzarri *et al.*, 1995; Myers *et al.*, 1995; Kuang *et al.*, 1996), they also indicated that CCL2/CCR2 signalling might not entirely involve G $\alpha_i$ . Interestingly, Bizzarri *et al.* (1995) and Myers *et al.* (1995) were unable to fully abolish CCL2/CCR2  $\text{Ca}^{2+}$  responses with PTx. Although this suggests that other G-proteins might be involved, it may just be that a longer incubation with PTx (> 6-hours) is required to abolish  $\text{Ca}^{2+}$  responses. Interestingly, the results of chemotaxis studies showed that PTx abolished CCL2-dependent migration. Although these results differed from  $\text{Ca}^{2+}$  experiments, they suggested that CCL2-mediated monocyte trafficking *in vivo* would be entirely through G $\alpha_i$ . These findings are consistent with studies by Sozzani *et al.* (1994) which demonstrated a complete block of CCL2-

mediated PBMC chemotaxis by PTx. In general, therefore, it seems that CCL2-mediated monocyte signalling and function primarily involves  $G\alpha_i$ .

In  $Ca^{2+}$  experiments, quenching of the fluorescent signal prevented the use of gallein. Given that gallein has a high affinity (400 nM) for  $G\beta\gamma$  (Bonacci *et al.*, 2006), a possible way to prevent quenching in future studies is to use a lower concentration of gallein. However, in chemotaxis experiments, gallein treatment attenuated CCL2-mediated THP-1 cell chemotaxis. These results support prior work in lymphocytic cells showing that  $G\beta\gamma$  activation drives CCL2-dependent trafficking (Arai *et al.*, 1997). A wider implication of these findings is that  $G\beta\gamma$  inhibitors selectively blocking CCR2 would be able to attenuate excessive monocyte trafficking towards CCL2. Although these findings suggested a very important discovery, an arguable weakness with this study is that gallein was used at a high concentration (100  $\mu$ M). Future studies should therefore re-test gallein at lower concentrations or use molecular approaches such as the overexpression of  $G\alpha$ -transducin to inactivate free  $G\beta\gamma$  dimers (Lustig *et al.*, 1993). While this study may have identified that further work is required, it nevertheless enhanced our understanding of the signalling cascades downstream of CCR2 activation in monocytes.

### ***Inhibition of PI3K attenuates CCL2/CCR2-mediated THP-1 cell signalling and function***

The classical scheme of GPCR signalling implies that  $G\beta\gamma$  dimers regulate PI3-kinase (Krugmann *et al.*, 1999; Brock *et al.*, 2003). It is possible, therefore, that PI3K is required for CCL2/CCR2-mediated monocyte signalling and function. To this end, studies examined the effects of the PI3K inhibitor, LY-294002 (Vlahos *et al.*, 1994) on CCL2-mediated THP-1 cell intracellular  $Ca^{2+}$  responses and chemotaxis.

The results of  $Ca^{2+}$  studies showed that LY-294002 induced a transient dip in the baseline  $Ca^{2+}$  response while also significantly attenuating CCL2-evoked intracellular  $Ca^{2+}$  responses. These results suggest that PI3K participates in  $Ca^{2+}$  homeostasis and CCL2/CCR2 signalling. An involvement of PI3K in  $Ca^{2+}$  homeostasis is supported by prior work showing that PI3K isoenzymes activate L-type  $Ca^{2+}$  channels and PLC, but attenuate CRAC channels (Rameh *et al.*, 1998; Suzuki *et al.*, 2010; Carnevale and Lembo, 2012). It is possible, therefore, that the effects seen here with LY-294002 reflect a modulation of  $Ca^{2+}$  homeostasis by one of these routes. Interestingly, studies reported by Turner *et al.* (1998) have also shown that CCL2/CCR2 signalling in THP-1 cells activates PI3K (p110 $\gamma$  and C2 $\alpha$ ). This suggests that CCL2/CCR2 signalling is coupled to PI3K activation, which could be required for downstream signalling events in monocytes. However, although the findings of the current study are interesting, a particular weakness in these data is that LY-294002 is not exclusively selective for PI3K and can inhibit other targets such as NF $\kappa$ B

and mTOR, which may have influenced the results (Gharbi *et al.*, 2007; Avni *et al.*, 2012). Thus, these findings may need to be interpreted with caution and further supported by other approaches.

In chemotaxis experiments, it was discovered that LY-294002 attenuated CCL2-mediated THP-1 cell chemotaxis, thus suggesting a requirement of PI3K for CCL2/CCR2-mediated monocyte chemotaxis. Although the selectivity of LY-294002 may have been an issue, the present findings support prior THP-1 chemotaxis studies showing a similar result with LY-294002 (Turner *et al.*, 1998). However, other more recent studies (Volpe *et al.*, 2010) suggest that PI3K activation is not essential for THP-1 cell chemotaxis towards CCL2. A wider implication of this is that CCL2-mediated leukocyte trafficking *in vivo*, would not require PI3K activation. While firm evidence for a requirement of PI3K for CCL2-mediated monocyte trafficking may yet be required, it is apparent from the literature that PI3K activation at the leading edge of other cell types such as neutrophils, is essential for cell polarisation and chemotaxis (Wang *et al.*, 2002). Moreover, studies in apoE<sup>-/-</sup> mice have demonstrated that deleting PI3K in macrophages attenuates atherosclerotic plaque formation (Chang *et al.*, 2007). This finding indicates that PI3K activation could be up-regulated in monocytes under inflammatory conditions such as atherosclerosis.

### ***Inhibition of PLC attenuates CCL2/CCR2-mediated THP-1 cell signalling and function***

It is generally accepted that classical GPCR signalling also involves an activation of the PLC isoenzymes PLC $\beta$ , PLC $\epsilon$ , and PLC $\eta$  by the G $\beta\gamma$  dimer (Blank *et al.*, 1992; Boyer *et al.*, 1992; Smrcka *et al.*, 1993). Although it is accepted that CCR2 activation in monocytes leads to an accumulation of IP<sub>3</sub> and a release of Ca<sup>2+</sup>, only studies by Kuang *et al.* (1996), suggest that these events involve PLC. Moreover, in monocytes, a requirement of PLC for CCL2-mediated monocyte trafficking has not yet been shown. Studies therefore sought to address this gap in knowledge using the PLC inhibitor U-73122.

The results of Ca<sup>2+</sup> mobilisation studies showed that U-73122 produced a concentration-dependent inhibition of CCL2-evoked Ca<sup>2+</sup> responses in THP-1 cells, where it was seen that high concentrations of U-73122 abolished responses. This result is interesting because it suggests that PLC is essential for CCL2-mediated monocyte signalling. Although studies by Kuang *et al.* (1996) have shown that CCR2 activation in monkey fibroblast COS-7 cells leads to an activation of PLC $\beta$ 3, no prior studies have reported a similar association in monocytic cells or monocytes. The findings of the present study are therefore both novel and important since they indicate an involvement of PLC in CCL2/CCR2-mediated monocyte signalling. A second important finding from this study was the modulation (dip) in baseline Ca<sup>2+</sup> by U-73122. This result supported the widely-

accepted notion that PLC activation is required for generating IP<sub>3</sub> for Ca<sup>2+</sup> release (Kadamur and Ross, 2013). It may be the case therefore that constitutive PLC activation is necessary for Ca<sup>2+</sup> homeostasis. Moreover, these results also indirectly support the involvement of PI3K in PLC activation (Rameh *et al.*, 1998), since application of LY-294002 to THP-1 cells also resulted in a similar dip in baseline Ca<sup>2+</sup>.

In chemotaxis experiments, it was seen that U-73122 almost abolished CCL2-mediated THP-1 cell chemotaxis. These findings match those observed in Ca<sup>2+</sup> studies and suggest that PLC activation is necessary for CCL2-mediated monocyte signalling and trafficking. It is also encouraging to compare this finding with that of Lee *et al.* (2009) who discovered that CCL2-mediated chemotaxis of human eosinophilic leukaemia EoL-1 cells involved PLC. More recently, Moyano Cardaba *et al.* (2012) have shown that PLC activation is necessary for THP-1 cell chemotaxis towards CCL3. The evidence in literature therefore points towards a requirement of PLC for CC chemokine-mediated monocyte chemotaxis. However, although these findings represent a very important discovery, it is important to bear in mind that further investigations suggested that prolonged U-73122 exposure led to a loss in THP-1 cell viability. While this suggests that U-73122 could have attenuated THP-1 cell migration independent of PLC, it is well-known that all PLC inhibitors are generally cytotoxic (Powis *et al.*, 1982). A second issue which might also have influenced the interpretation of these results is that U-73122, at the concentrations tested, may have inhibited other targets including PTx-sensitive G-proteins and lipid kinases (Horowitz *et al.*, 2005). A further study with a more selective inhibitor, such as edelfosine (Powis *et al.* 1982), or a molecular-based approach is therefore recommended. Although the findings of the present study may need to be interpreted with caution, they nevertheless indicated that PLC activation is required for CCL2/CCR2-mediated monocyte signalling and function, which is a novel finding.

### ***Inhibition of IP<sub>3</sub> and RyR receptors attenuates CCL2/CCR2-mediated THP-1 cell signalling and/or function***

From the literature, it is clear that in the classical paradigm of GPCR signalling, IP<sub>3</sub> is formed from the hydrolysis of PIP<sub>2</sub> by PLC. Furthermore, it is recognised that IP<sub>3</sub> and Ca<sup>2+</sup> are essential co-activators of IP<sub>3</sub>Rs (Clapham, 2007; Vetter, 2012). Thus, in an effort to examine the requirement of IP<sub>3</sub>R for CCL2/CCR2-mediated monocyte signalling and function, studies employed the IP<sub>3</sub>R antagonist Xestospongine-C (XeC).

Analysis of results from THP-1 Ca<sup>2+</sup> mobilisation studies showed that XeC attenuated the magnitude and slowed the decay of CCL2-evoked intracellular Ca<sup>2+</sup> responses. Furthermore, chemotaxis experiments showed that XeC nearly abolished CCL2-dependent THP-1 cell chemotaxis. These results are interesting because they suggest

that CCL2-mediated  $\text{Ca}^{2+}$  responses and monocyte trafficking requires a release of  $\text{Ca}^{2+}$  from the ER and GA. Although, these results conflict with those of Sozzani *et al.* (1993) whose studies reported that monocyte CCL2/CCR2-mediated  $\text{Ca}^{2+}$  responses did not involve intracellular  $\text{Ca}^{2+}$  stores, they are consistent with later findings of the same group (Bizzarri *et al.*, 1995) which showed that intracellular stores and plasma membrane channels equally contributed to CCL2-mediated  $\text{Ca}^{2+}$  responses in monocytes. The results of the present study also indirectly support additional studies showing that CCR2 activation in monocytes leads to an accumulation of  $\text{IP}_3$  (Wong *et al.*, 1997). However, although the findings of this study indicate a very important discovery, they also need to be interpreted with caution because XeC is known to inhibit SERCA at concentrations similar to those used in this study (De Smet *et al.*, 1999). Although more recent studies (Saleem *et al.*, 2014) do not agree with the findings of De Smet *et al.* (1999), they suggest that XeC is a poor inhibitor of  $\text{IP}_3$ R compared to its counterpart, heparin. Thus, performing similar experiments with heparin are recommended.

To determine the involvement of other  $\text{Ca}^{2+}$ -release mechanisms in CCL2/CCR2-mediated monocyte signalling and function, studies investigated the effects of the RyR inhibitor, dantrolene. The results of  $\text{Ca}^{2+}$  and chemotaxis studies suggested that RyR activation was not required for CCL2-mediated intracellular  $\text{Ca}^{2+}$  release, but was required for chemotaxis. The findings of this study are significant and suggest that RyRs participate in CCL2-mediated monocyte chemotaxis. Although further research should be done to confirm these results, it is interesting that the findings of this study support Clark and Petty (2005) whose experiments showed that RyRs localise at the leading-edge of cells where F-actin-rich protrusions and uropods for cell polarity and chemotaxis are formed. Moreover, Matyash *et al.* (2002) have shown that macrophages fail to migrate towards chemotactic agents following RyR disruption. Thus, RyRs may yet be important for monocyte signalling and trafficking.

### ***Inhibition of SERCA attenuates CCL2/CCR2-mediated THP-1 cell signalling and function***

The high-affinity SERCA pump is important for sequestering excess levels of cytosolic  $\text{Ca}^{2+}$  and replenishing the ER following agonist-mediated  $\text{Ca}^{2+}$  depletion (Berridge *et al.*, 2000; Clapham, 2007). Although SERCA serves an important role in maintaining  $\text{Ca}^{2+}$  homeostasis, only studies reported by Bizzarri *et al.* (1995) have investigated the requirement of SERCA for efficient CCL2/CCR2-mediated monocyte signalling and function. Studies therefore sought to confirm these findings using the SERCA1/3 inhibitor thapsigargin.

The results of intracellular  $\text{Ca}^{2+}$  studies showed that thapsigargin attenuated CCL2-evoked intracellular  $\text{Ca}^{2+}$  responses in the presence of extracellular  $\text{Ca}^{2+}$  and abolished responses in the absence of extracellular  $\text{Ca}^{2+}$ . These results suggest that SERCA activation is necessary for replenishing the ER during CCL2/CCR2-mediated intracellular  $\text{Ca}^{2+}$  responses. This finding directly contradicts early reports by Sozzani *et al.* (1993) but supports those of Bizzarri *et al.* (1995) whose studies with thapsigargin showed that internal  $\text{Ca}^{2+}$  stores and  $\text{Ca}^{2+}$  influx mechanisms contributed to CCL2-mediated  $\text{Ca}^{2+}$  responses in monocytes. Taken together with other data presented in this thesis, these present findings suggest that CCL2/CCR2-mediated intracellular  $\text{Ca}^{2+}$  responses in monocytes involves an  $\text{IP}_3\text{R}$ -mediated release of  $\text{Ca}^{2+}$  from the ER (and possibly the GA), coupled to a restorative action by SERCA. This hypothesis is also indirectly supported by the fact that addition of thapsigargin to cells increased baseline  $\text{Ca}^{2+}$ . This suggests that thapsigargin renders SERCA unable to maintain ER  $\text{Ca}^{2+}$  thus leading to a leakage and a corresponding  $\text{Ca}^{2+}$  influx (Treiman *et al.*, 1998). However, although the findings of this study indicate a very important discovery, it is important to bear in mind that the results of LDH studies suggested that thapsigargin reduced cell viability, which may have affected the interpretation of the experimental results. Although this finding is disappointing, it agrees with the general hypothesis that cytotoxicity would be expected with thapsigargin, since an impairment of SERCA would render it unable to sequester cytotoxic levels of cytosolic  $\text{Ca}^{2+}$  (Periasamy and Kalyanasundaram, 2007). These latter findings are therefore also very important as they provide an additional depth of understanding of the mechanisms by which intracellular  $\text{Ca}^{2+}$  is maintained by cells.

### ***Inhibition of DAGL attenuates CCL2/CCR2-mediated THP-1 cell signalling and function***

The classical GPCR signalling paradigm predicts that  $\text{PIP}_2$  hydrolysis by PLC yields  $\text{IP}_3$  and the second messenger, DAG. Although DAG is important for the activation of downstream signalling proteins involved in GPCR signalling (Baldanzi, 2014), no previous studies have investigated the requirement of DAG for CCL2/CCR2-mediated monocyte signalling and function. Studies therefore sought to address this gap in knowledge by examining the requirement of DAG through inhibitors of the DAG-metabolising enzymes, DAGL (RHC-80267) and DAGK (R-59-022).

The results of  $\text{Ca}^{2+}$  studies showed that the DAGL inhibitor RHC-80267 attenuated CCL2-evoked intracellular  $\text{Ca}^{2+}$  responses in the presence of extracellular  $\text{Ca}^{2+}$ , but not in the absence of extracellular  $\text{Ca}^{2+}$ . These results suggest a requirement of DAGL for CCL2/CCR2-mediated monocyte signalling, but also indicate that the effects of RHC-80267 are  $\text{Ca}^{2+}$ -dependent. Interestingly, the results of chemotaxis experiments showed that RHC-80267 attenuated THP-1 cell chemotaxis towards CCL2. These data therefore

suggest that DAGL facilitates CCL2/CCR2-mediated monocyte signalling and function, either by limiting DAG availability, or by generating other second messengers. While less is known about DAG, the involvement of DAGL-derived second messengers in CCL2/CCR2-signalling has been well-studied. For example, Kishimoto *et al.* (2004), have shown that monocytes release CCL2 in response to 2-arachidonolyglycerol (2-AG), a product of DAGL. It is possible; therefore, that 2-AG-mediated CCL2 release amplifies CCR2-generated signals. It is also widely accepted that CCL2/CCR2 activation drives monocytes to generate arachidonic acid (AA), a product formed from the hydrolysis of 2-AG by monoacylglycerol lipase (MAGL) (Locati *et al.*, 1994). Given that AA is a precursor for the synthesis of pro-inflammatory thromboxanes and prostaglandins (Smith *et al.*, 1991), pathways downstream of AA might feed into the CCL2/CCR2-axis thereby exacerbating inflammation. However, although these findings indicate a very important discovery, a release of LDH by THP-1 cells exposed to RHC-80267 suggests that this may have resulted in a biased interpretation of these data. An additional note of caution is due here since RHC-80267, at concentrations used for this study, has been shown to inhibit other serine hydrolases such as MAGL, platelet activating factor (PAF) and acetylcholine esterase (AChE) (Hoover *et al.*, 2008). Thus, further experiments with other DAGL inhibitors are required. Despite its exploratory nature, this study offers some insights into the interplay between DAGL and the CCL2/CCR2 axis in monocytes, which might be an important area for future research.

### ***Inhibition of DAGK attenuates CCL2/CCR2- and P2Y<sub>6</sub>-associated THP-1 cell signalling and/or function***

The results of Ca<sup>2+</sup> experiments assessing the requirement of DAG through DAGK showed that CCL2-evoked Ca<sup>2+</sup> responses were almost abolished by R-59-022 in the presence of extracellular Ca<sup>2+</sup>, and significantly attenuated in the absence of extracellular Ca<sup>2+</sup>. These results, indicate a novel requirement of DAGK for CCL2/CCR2-mediated monocyte signalling, but also suggest that the effects of R-59-022 are partially-dependent on Ca<sup>2+</sup>. The findings of this study are also consistent with DAGL studies and point towards the possibility that DAG accumulation attenuates CCL2-evoked Ca<sup>2+</sup> responses. A second interesting observation was that application of R-59-022 transiently increased the baseline Ca<sup>2+</sup> response. A possible explanation for this might be that DAG increased Ca<sup>2+</sup> influx by directly activating TRPC channels (Hofmann *et al.*, 1999).

The results of THP-1 cell chemotaxis studies showed that DAGK inhibition by R-59-022 significantly attenuated CCL2-mediated chemotaxis, where the degree of inhibition with R-59-022 mirrored that seen in Ca<sup>2+</sup> assays. These results are interesting, and suggest that DAGK is required for CCL2/CCR2-mediated monocyte function. However, as with Ca<sup>2+</sup> studies, an alternative explanation for these results might be that DAGK inhibitors

accumulate DAG, which leads to an attenuation of monocyte chemotaxis towards CCL2. Although similar studies have not been performed by others, it is interesting that phosphatidic acid (PA), which is formed by DAGK, and activates PLC (Limatola *et al.*, 1994; Litosch, 2002), has been shown to be secreted by monocytic cells in response to CCL2 (Turner *et al.*, 1996). It is possible, therefore, that PA generated by DAGK amplifies CCL2/CCR2-mediated monocyte signalling and function through PLC. This hypothesis seems plausible given that PA also induces monocyte migration (Zhou *et al.*, 1995). A wider implication to this finding is that CCL2/CCR2-mediated monocyte/macrophage pathologies would be exacerbated by DAGK. However, this hypothesis is disputed by studies showing that DAGK expression is lost upon monocytic cell differentiation to macrophages (Yamada *et al.*, 2003).

It was next hypothesised that DAGK might also be required for P2Y<sub>6</sub>-associated monocyte signalling. The results of THP-1 cell Ca<sup>2+</sup> experiments with R-59-022 suggested that DAGK was also required for P2Y<sub>6</sub>-associated monocyte signalling. This indirectly corroborates the ideas of Scott *et al.* (2013) who found that UDP-activation of P2Y<sub>6</sub>-transfected 1321N1 cells led to a DAGK $\zeta$ - and phospholipase D (PLD)-mediated release of PA. This result indicates an involvement of DAGK in P2Y<sub>6</sub>- and CCR2-mediated monocyte signalling and function. While this is interesting and identifies a point at which P2Y<sub>6</sub> and CCR2 might converge, it may also be that DAGK plays a general role in signalling of all GPCRs. Thus, future studies should seek to examine other chemotactic GPCR-signalling pathways before firm conclusions are drawn.

While the results of this study indicate an important role for DAGK for CCL2/CCR2-mediated monocyte signalling and function, it is important that these results are interpreted with caution since cell viability studies suggested that THP-1 cells exposed to R-59-022 for prolonged periods, released high levels of LDH. A further note of caution is due here since R-59-022 is known to inhibit a number of other kinases (Fedorov *et al.*, 2007), thus further work with better DAGK inhibitors are needed.

### ***Inhibition of PKC attenuates CCL2/CCR2-mediated THP-1 cell signalling***

The classical (cPKC) and novel (nPKC) families of PKC are preferentially activated by DAG (Yang and Kazanietz, 2003). It is possible, therefore, that the inhibitory effects of DAGL and DAGK inhibitors on CCL2/CCR2-mediated monocyte signalling and function reflect an activation of PKC by DAG. The validity of this hypothesis was examined using the PKC inhibitor, GF-109203X.

The results of THP-1 cell Ca<sup>2+</sup> experiments showed that GF-109203X attenuated CCL2-evoked Ca<sup>2+</sup> responses to low concentrations of CCL2, but not to maximal concentrations of CCL2. These findings suggest that activation of PKC is necessary for low-level

CCL2/CCR2 signalling, but not for higher-level signalling. A possible explanation for this might be that a greater level of CCR2 activation promotes a greater turnover of DAG, thereby limiting PKC activation. However, while this hypothesis seems plausible, it is interesting that the present findings differ from Carnevale and Cathcart (2003) whose studies suggested that CCL2-mediated  $\text{Ca}^{2+}$  responses in human monocytes involved PKC $\beta$ . These studies are also interesting because the authors suggest that PKC is indirectly involved in CCL2/CCR2 signalling and is only important for signal-transduction downstream of the immediate calcium signal. This is interesting because, in the present study, PKC inhibition was found to accelerate the decay of CCL2  $\text{Ca}^{2+}$  transients, which suggests that PKC plays a negative role in replenishment of the ER. In support of this, studies by Venkatachalam *et al.* (2003) and Kawasaki *et al.* (2010) have shown that PKC inhibits the SOCE channels TRPC and CRAC, thereby preventing replenishment of the ER. The findings of this study are therefore important as they help us gain a clearer picture of the mechanisms involved in PKC signalling in monocytes.

In experiments addressing the requirement of PKC for CCL2/CCR2-mediated monocyte chemotaxis, it was seen that CCL2-mediated THP-1 cell chemotaxis was unaffected by GF-109203X. This finding contradicts the findings of Carnevale and Cathcart (2003), whose studies showed that GF-109203X or PKC $\beta$ -silencing attenuated CCL2-mediated monocyte chemotaxis. In agreement with Carnevale and Cathcart (2003), other studies have also shown an involvement of PKC isoenzymes in cell polarity and migration (Ng *et al.*, 1999; Larsson, 2006). It may be the case therefore, that the findings of Carnevale and Cathcart (2003) differ from the present study because of differences in the methodologies applied. For example, Carnevale and Cathcart (2003) pre-incubated cells with GF-109203X for 1 hour prior to chemotaxis assays, while the present study did not pre-incubate. Thus, further studies involving a pre-incubation of GF-109203X may be necessary.

While this study may have failed to confirm a requirement of PKC for CCL2/CCR2-mediated monocyte chemotaxis, it nevertheless suggested that monocyte signalling in response to CCL2 is influenced by PKC.

### ***Extracellular nucleotides are required for CCL2/CCR2-mediated THP-1 cell and human PBMC signalling and function***

A considerable amount of the literature has been published on the involvement of purinoceptors in CCL2 release from monocytic cells and monocyte progeny (Cox *et al.*, 2005; Stokes and Surprenant, 2007; Morioka *et al.*, 2013; Garcia *et al.*, 2014; Higgins *et al.*, 2014; Shieh *et al.*, 2014). Although these studies suggest that purinoceptor signalling plays a role in modulating CCL2/CCR2-mediated monocyte signalling and function, the

exact mechanisms by which these pathways crosstalk is still an open question. The present studies therefore sought to address this question using the ecto-nucleotidase, apyrase, which dephosphorylate nucleotides to render them inactive.

The results of  $\text{Ca}^{2+}$  mobilisation experiments showed that apyrase significantly attenuated CCL2-mediated intracellular  $\text{Ca}^{2+}$  responses in THP-1 cells and human PBMCs. These findings are novel and suggest that extracellular nucleotides are required for efficient CCL2/CCR2-mediated monocyte and PBMC signalling. Interestingly, the results of further experiments investigating the requirement for NTPs and NDPs showed that CCL2-mediated  $\text{Ca}^{2+}$  responses were attenuated less by an apyrase isoenzymes with reduced NDPase activity/velocity. This suggests that NDPs are more likely to be required for efficient CCL2-mediated  $\text{Ca}^{2+}$  responses. A second important observation made in these studies was that apyrase caused a dip in the baseline  $\text{Ca}^{2+}$  response. The fact that this effect was less evident in the absence of extracellular  $\text{Ca}^{2+}$  and almost absent in experiments with a lower NDPase apyrase, suggests that NDPs maintain background  $\text{Ca}^{2+}$  homeostasis by releasing intracellular  $\text{Ca}^{2+}$ . This hypothesis differs from prior work reported by this group (Sivaramakrishnan *et al.*, 2012), where the experimental results suggested that ATP played a role in maintaining  $\text{Ca}^{2+}$  homeostasis. A possible explanation for these differences might be that Sivaramakrishnan *et al.* (2012) did not examine the involvement of NDPs on baseline  $\text{Ca}^{2+}$ .

Experiments next examined the requirement of extracellular nucleotides for CCL2/CCR2-mediated monocyte function. The results of chemotaxis experiments showed that apyrase almost abolished CCL2-dependent THP-1 cell chemotaxis but interestingly, potentiated PBMC chemotaxis. A potentiation of PBMC chemotaxis by apyrase was unexpected and may have reflected the heterogeneous nature of PBMCs and the chemotactic effects of nucleotides and nucleosides on different cell types (Chen *et al.*, 2006; Zhang *et al.*, 2006; Myrtek and Idzko, 2007; Kronlage *et al.*, 2010). Although these findings suggest that additional experiments with purified CCR2-expressing monocytes are required, the inhibition of CCL2-mediated THP-1 cell chemotaxis by apyrase is encouraging, because it supports the hypothesis that extracellular nucleotides are required for CCL2/CCR2-mediated monocyte signalling and function. A wider implication of these findings is that ecto-nucleotidases such as NTPDase1 would be therapeutically beneficial for pathologies associated with an excessive trafficking of monocytes towards CCL2, a theory indirectly supported by studies showing that NTPDase1 produces anti-inflammatory and anti-thrombotic effects in cells such as neutrophils and platelets (Enjoji *et al.*, 1999; Hyman *et al.*, 2009; Reutershan *et al.*, 2009). The anti-inflammatory effects of ecto-nucleotidases have also been brought to the fore by APT102, an engineered ADP-selective NTPDase3 that has been shown to prevent thrombus formation and reduce

infarction size in animal models (Moeckel *et al.*, 2014). Using APT102 as a research tool would be therefore be interesting as this would allow enhance our understanding of the involvement of ADP in CCL2/CCR2-mediated monocyte signalling and function.

The results of adhesion experiments showed that apyrase enhanced CCL2-mediated THP-1 cell adhesion to HUVECs. These results conflicted with the findings of chemotaxis and  $\text{Ca}^{2+}$  studies, and suggested that extracellular nucleotide scavenging increased CCL2-mediated monocyte adhesion. Although this finding is disappointing, an alternative explanation for these results may be that apyrase accumulates adenosine, which may facilitate cellular adhesion. However, although this is a possibility and could be tested indirectly with ADA, prior work has shown that ATP and UTP increase monocyte adhesion to endothelial cells by up-regulating VCAM-1 expression (Seye *et al.*, 2003), while adenosine typically inhibits adhesion by down-regulating ICAM-1, VCAM-1 and E-selectin (Takahashi *et al.*, 2007; Hassanian *et al.*, 2014). This suggests that THP-1 cells are likely to respond differently to extracellular nucleotides and nucleosides, and that further studies examining the effects of these on monocyte adhesion are important to conduct before firm conclusions about the findings of this experiment are drawn.

### ***Inhibition of ecto-nucleotidases potentiates CCL2/CCR2-mediated THP-1 cell signalling***

Studies next sought to address whether endogenously active ecto-nucleotidases modulated CCL2/CCR2-mediated monocyte signalling. To address this aim, studies employed the ecto-nucleotidase inhibitors ARL-67156 and POM-1 and tested the effects of these on CCL2-evoked intracellular  $\text{Ca}^{2+}$  responses in THP-1 cells.

The results of  $\text{Ca}^{2+}$  studies showed that ARL-67156 potentiated intracellular  $\text{Ca}^{2+}$  responses evoked by near- $\text{EC}_{50}$  concentrations of CCL2 in the presence of extracellular  $\text{Ca}^{2+}$ , but not in the absence of extracellular  $\text{Ca}^{2+}$ . These findings are interesting because they suggest that  $\text{Ca}^{2+}$ -sensitive ecto-nucleotidases are involved in modulating CCL2/CCR2-mediated  $\text{Ca}^{2+}$  responses in monocytes. An implication of this is the possibility that monocyte sensing of CCL2 is enhanced in environments where ecto-nucleotidase activity is inadequate. However, this hypothesis conflicts with studies showing that monocytes from *ENTPD1* (NTPDase1)-null mice are unable to efficiently transmigrate towards CCL2 and extracellular nucleotides (Goepfert *et al.*, 2001). This suggests that ecto-nucleotidases are needed for monocyte trafficking towards CCL2. It may be the case therefore, that ecto-nucleotidases are required for CCL2/CCR2 signalling, but must be fine-tuned. This is would also support the hypothesis that NDPs are preferentially required for CCL2/CCR2-mediated monocyte signalling.

The results of further  $\text{Ca}^{2+}$  studies with POM-1 showed that high concentrations of this ecto-nucleotidase inhibitor abolished CCL2-evoked  $\text{Ca}^{2+}$  responses. These results were unexpected, and suggested that ecto-nucleotidase inhibition attenuated CCL2/CCR2-mediated monocyte signalling. Additional studies showed that POM-1 abolished  $\text{Ca}^{2+}$  responses evoked by ADP and UDP, and impaired  $\text{Ca}^{2+}$  responses evoked by ATP and UTP, therefore indicating similarities between the effects of POM-1 on NDP- and CCL2-evoked intracellular  $\text{Ca}^{2+}$  responses. While a possible explanation for these findings could be that POM-1 activity leads to a desensitisation/internalisation of NDP and CCL2-sensitive receptors, other studies (Wall *et al.*, 2008) suggest that POM-1 attenuates synaptic transmission independent of its ecto-nucleotidase inhibition. It may be the case; therefore, that POM-1 attenuates CCL2 and NDP  $\text{Ca}^{2+}$  responses through ecto-nucleotidase-independent off-target effects. Given these drawbacks, future studies should use alternative ecto-nucleotidase inhibitors, such as the recently identified NTPDase1 inhibitor, ticlodipine (Lecka *et al.*, 2014).

### ***P1 purinoceptor antagonism does not modulate CCL2/CCR2-mediated THP-1 cell signalling***

To gain a better understanding of the requirement of purinoceptor signalling for CCL2/CCR2-mediated monocyte signalling and function, studies examined the contributions of P1, P2X, and P2Y purinoceptors. Initial studies focused on P1 purinoceptors using the P1 antagonist, CGS-15943.

The results of THP-1 cell  $\text{Ca}^{2+}$  mobilisation experiments showed that CGS-15943 potentiated intracellular  $\text{Ca}^{2+}$  responses evoked by near- $\text{EC}_{20}$  concentrations of CCL2. These data suggest that P1 purinoceptors negatively regulate CCL2/CCR2-mediated monocyte signalling. However, in additional experiments, it was seen that CGS-15943 was unable to recover CCL2-evoked  $\text{Ca}^{2+}$  responses in THP-1 cells treated with apyrase. Furthermore, experimental results showed no modulation of CCL2-evoked intracellular  $\text{Ca}^{2+}$  responses by ADA. These latter findings therefore suggest that P1 purinoceptors are not negative regulators of CCL2/CCR2-mediated monocyte signalling. Although the results of initial experiments suggest that P1 purinoceptors were involved, it may be that CCL2-  $\text{Ca}^{2+}$  responses are potentiated by CGS-15943 through its off-target inhibition of PI3K, which would increase  $\text{Ca}^{2+}$  influx through CRAC channels (Edling *et al.*, 2014). However, a second possible explanation for these results might be that CGS-15943 is unable to distinguish between individual P1 receptors which can produce differential effects in monocytes (Haskó *et al.*, 2007). Future studies should therefore investigate this possibility by using selective P1 antagonists. While this investigation may have failed to suggest an involvement of P1 purinoceptors in CCL2/CCR2-mediated monocyte signalling, it nevertheless demonstrated the importance of P1 purinoceptors.

### ***P2X1, P2X4 and P2X7 antagonism does not modulate CCL2/CCR2-mediated THP-1 cell signalling and function***

Studies next examined the requirement of P2X purinoceptors by testing the effects of antagonists for P2X1 (Ro-0437626), P2X4 (5-BDBD) and P2X7 (A-438079) on THP-1 cell CCL2/CCR2-mediated intracellular Ca<sup>2+</sup> responses and chemotaxis.

The results of Ca<sup>2+</sup> experiments showed that the P2X1 antagonist Ro-0437626 produced a concentration-dependent inhibition of CCL2-evoked intracellular responses in THP-1 cells, but was unable to modulate CCL2-mediated chemotaxis. These results suggested an involvement of P2X1 in CCL2/CCR2-mediated monocyte signalling, but not in function. However, while this indicated a very important discovery, the results of additional selectivity experiments showed that Ro-0437626 was unable to modulate Ca<sup>2+</sup> responses evoked the P2X1 ligand  $\alpha,\beta$ -meATP, suggesting the possibility that P2X1 was either rapidly desensitised (Torres *et al.*, 1998), or not expressed by THP-1 cells at the post-translational level. A further reason for interpreting these data with caution is that Ro-0437626 was used at a concentration which is over 30-fold higher than the reported IC<sub>50</sub> (Jaime-Figueroa *et al.*, 2005) which may have resulted in off-target effects. Moreover, the results of Ca<sup>2+</sup> experiments suggested that Ro-0437626 increased the baseline Ca<sup>2+</sup> response through a Ca<sup>2+</sup> release from internal stores. Although interpreting these data are difficult as a similar result has not been previously demonstrated, it may be that high concentrations of Ro-0437626 produce an off-target effect or that P2X1 receptors negatively couple to Ca<sup>2+</sup> release from internal stores. Although these results are interesting, they have been unable to firmly suggest an association between P2X1 and the CCL2/CCR2 axis in monocytes.

In experiments examining a requirement for P2X4, the results of Ca<sup>2+</sup> experiments showed that the P2X4 antagonist 5-BDBD caused a Ca<sup>2+</sup>-dependent inhibition of CCL2-evoked Ca<sup>2+</sup> responses and slowed their decay. These results suggest that P2X4 receptors are required for CCL2/CCR2-mediated monocyte signalling. However, in cell migration experiments, it was seen that CCL2-mediated THP-1 cell migration was unaffected by 5-BDBD, suggesting that the effects of 5-BDBD on CCL2 Ca<sup>2+</sup> responses did not couple to functional responses. Moreover, in Ca<sup>2+</sup> experiments, it was seen that 5-BDBD increased baseline Ca<sup>2+</sup> levels in the absence of extracellular Ca<sup>2+</sup>. Although a similar result has not been previously demonstrated, it may that a high concentration of 5-BDBD leads to a P2X4-dependent release of Ca<sup>2+</sup> from internal stores. Since no selective P2X4 ligands were available, this hypothesis could not be tested. These studies were therefore unable to confirm a requirement of P2X4 receptors for CCL2/CCR2-mediated monocyte signalling and function, but indicated that the use of more selective approaches to study P2X4 would be an interesting area for future research. Another reason for undertaking this research is

that CCR2 activation is known to increase P2X4 expression and cell-surface trafficking in microglia during neuropathic pain (Toyomitsu *et al.*, 2012), suggesting that both receptors could also engage in similar crosstalk in monocytes.

Although the P2X7 receptor is well-known for its involvement in the release of pro-inflammatory mediators such as IL-1 $\beta$  and IL-18 (Ferrari *et al.*, 1997), its requirement for CCL2/CCR2-mediated monocyte signalling and function has yet to be investigated. Thus, the final studies on P2X purinoceptors examined the requirement of the P2X7 receptor using the P2X7 antagonist, A-438079. The results of THP-1 cell Ca<sup>2+</sup> experiments showed that A-438079 produced a small inhibition of CCL2-evoked intracellular Ca<sup>2+</sup> responses in the presence of extracellular Ca<sup>2+</sup>. This result was considered significant since it supported a requirement of P2X7 for CCL2/CCR2-mediated monocyte signalling. However, the results of chemotaxis experiments showed that THP-1 cell migration towards CCL2 was unaffected by A-438079, suggesting that P2X7 was not required for monocyte migration. Further experiments examining the selectivity of A-438079 for P2X7 showed that BzATP-evoked Ca<sup>2+</sup> responses in THP-1 cells were also unaffected by A-438079. A possible reason for this might be that the effects of A-438079 on BzATP Ca<sup>2+</sup> responses were difficult to detect because P2X1, P2X4, P2X7, P2Y<sub>11</sub>, and P2Y<sub>13</sub> receptors would have also been activated by BzATP (Bianchi *et al.*, 1999; Jarvis and Khakh, 2009). However, although this is a possibility, Nelson *et al.* (2006) have demonstrated in their studies that a similar concentration of A-438079 attenuates BzATP-induced IL-1 $\beta$  release and YoPro-1 uptake in THP-1 cells. Interestingly, P2X7-mediated Ca<sup>2+</sup> influx was not tested by this study, which suggests that it may not be easily detected. Thus, additional studies addressing these issues are recommended. A second reason for pursuing P2X7 receptors further is that P2X7 has been shown to promote CCL2 release in microglia (Shieh *et al.*, 2014), which may suggest an involvement of P2X7 and CCR2 in microglia-associated inflammatory pathologies.

#### ***P2Y<sub>1</sub>, P2Y<sub>11</sub>, P2Y<sub>12</sub>, and P2Y<sub>13</sub> antagonism does not modulate CCL2/CCR2-mediated THP-1 cell signalling and function***

Studies next examined the requirement of P2Y purinoceptors for CCL2/CCR2-mediated monocyte signalling and function. To address this aim, studies examined the effects of antagonists for P2Y<sub>1</sub> (MRS-2179), P2Y<sub>11</sub> (NF-340), P2Y<sub>12</sub> (AR-C-66096), and P2Y<sub>13</sub> (MRS-2211) on CCL2/CCR2-mediated THP-1 cell Ca<sup>2+</sup> responses and chemotaxis.

The results of experiments showed that CCL2/CCR2-mediated THP-1 cell Ca<sup>2+</sup> responses and chemotaxis were not significantly affected by MRS-2179, NF-340, AR-C-66096, and MRS-2211. These results suggested that P2Y<sub>1</sub>, P2Y<sub>11</sub>, P2Y<sub>12</sub>, and P2Y<sub>13</sub> purinoceptors were not required for CCL2/CCR2-mediated monocyte signalling and function. This

finding is important since it suggests that the inhibitory effects of PPADS and apyrase on THP-1 cell CCL2-mediated intracellular  $Ca^{2+}$  responses and chemotaxis are not through an impairment of these receptors. In order to provide additional support for these findings, studies sought evidence that each P2Y antagonist attenuated intracellular  $Ca^{2+}$  responses evoked by preferred ligands.

In experiments for P2Y<sub>1</sub>, ADP-evoked  $Ca^{2+}$  responses were not significantly inhibited by the P2Y<sub>1</sub> antagonist, MRS-2179. Although it is difficult to explain this result, it is possible that P2Y<sub>1</sub> receptors are rapidly desensitised by ADP, making functional responses difficult to detect (Enyoji *et al.*, 1999). Although further  $Ca^{2+}$  studies showed that the P2Y<sub>1</sub>-selective ligand MRS-2365 evoked intracellular  $Ca^{2+}$  responses in THP-1 cells, and that these were potentiated by apyrase, the small magnitude of these responses suggested that P2Y<sub>1</sub> receptors were either rapidly desensitised, or poorly coupled to intracellular  $Ca^{2+}$  release in THP-1 cells. As no prior work has shown an involvement of P2Y<sub>1</sub> receptors in intracellular  $Ca^{2+}$  release from monocytes or monocytic cells, either of these situations are possible. Although this study may have been unable to identify an involvement of P2Y<sub>1</sub> in CCL2/CCR2-mediated monocyte signalling and function, it nevertheless demonstrated a functional presence of P2Y<sub>1</sub> in THP-1 cells, which is a novel finding. Further studies at the post-translational level are therefore recommended to confirm these findings.

The results of  $Ca^{2+}$  experiments for P2Y<sub>11</sub> showed that the P2Y<sub>11</sub> antagonist NF-340, attenuated intracellular  $Ca^{2+}$  responses evoked by ATP in THP-1 cells. Although this result indirectly supported a lack of involvement of P2Y<sub>11</sub> in CCL2/CCR2-mediated monocyte signalling and function, additional experiments showed that NF-340 was unable to modulate  $Ca^{2+}$  responses evoked by the P2Y<sub>1</sub>/P2Y<sub>11</sub> ligand,  $\beta$ -NAD. This result was unexpected and suggests that  $\beta$ -NAD evokes  $Ca^{2+}$  release through P2Y<sub>1</sub> rather than P2Y<sub>11</sub>. However, another possible explanation for this result might be that  $\beta$ -NAD only activates P2Y<sub>11</sub> under inflammatory conditions. This hypothesis supports previous work showing that monocytes only respond to  $\beta$ -NAD following exposure to lipopolysaccharide (Klein *et al.*, 2009). It may be the case, therefore, that P2Y<sub>11</sub> is not readily activated in monocytes. Examining the requirement of P2Y<sub>11</sub> for CCL2/CCR2-mediated monocyte signalling and function under inflammatory conditions would thus be an interesting area for future research.

The results of  $Ca^{2+}$  experiments for P2Y<sub>12</sub> showed that ADP-evoked  $Ca^{2+}$  responses were not significantly affected by the P2Y<sub>12</sub> antagonist, AR-C-66096. Although these results were negative, they tied in with the knowledge that P2Y<sub>12</sub> purinoceptors couple to AC inhibition via  $G_{\alpha_{i/o}}$  (Hollopeter *et al.*, 2001, Savi *et al.*, 2001). However, it is interesting that more recent studies (Bianco *et al.*, 2005; Ceruti *et al.*, 2008) suggest that P2Y<sub>12</sub> receptors couple to intracellular  $Ca^{2+}$  release in microglia. However, a weakness of these studies is

that the results reported by these authors were based on data provided by dual P2Y<sub>12</sub>/P2Y<sub>13</sub> antagonists (AR-C69931MX and Cangrelor), which may have influenced the interpretation of the experimental results. This would potentially explain why no other studies have associated P2Y<sub>12</sub> with intracellular Ca<sup>2+</sup> release. Further research should therefore be done to investigate the effects of AR-C-66096 on ADP-mediated Ca<sup>2+</sup> mobilisation in P2Y<sub>12</sub>-transfected cells. While the present study may have failed to demonstrate a requirement of P2Y<sub>12</sub> for CCL2/CCR2-mediated monocyte signalling and function, it nevertheless provided some insight into P2Y<sub>12</sub> signalling in monocytic cells.

In experiments for P2Y<sub>13</sub>, it was discovered that the P2Y<sub>13</sub> antagonist, MRS-2211 attenuated Ca<sup>2+</sup> responses evoked by ADP. These results tie in with the knowledge that P2Y<sub>13</sub> receptors couple to intracellular Ca<sup>2+</sup> release (Communi *et al.*, 2001; Marteau *et al.*, 2003), but also support the hypothesis that P2Y<sub>13</sub> receptors are not required for CCL2/CCR2-mediated monocyte signalling or function. The results of this study also support the functional presence of P2Y<sub>13</sub> in THP-1 cells, which has not previously been reported. Although other studies have shown that P2Y<sub>13</sub> drives intracellular Ca<sup>2+</sup> release through PLC in microglia (Zeng *et al.*, 2014), similar studies in monocytes and monocytic cells have not been performed. The discovery that THP-1 cells express functional P2Y<sub>13</sub> receptors suggests that these cells may serve as a useful model for investigating P2Y<sub>13</sub>-mediated reverse-cholesterol transport in macrophages (Boeynaems *et al.*, 2010)

### ***P2Y<sub>6</sub> antagonism attenuates CCL2/CCR2-mediated THP-1 cell and human PBMC signalling***

The final chapter in this thesis investigated the requirement of the P2Y<sub>6</sub> purinoceptor for CCL2/CCR2-mediated monocyte signalling and function. Initial studies employed the P2Y<sub>6</sub> antagonist, MRS-2578 and tested its effects on CCL2-evoked intracellular Ca<sup>2+</sup> responses in THP-1 cells and human PBMCs.

The results of these experiments showed that MRS-2578 caused a concentration-dependent inhibition of CCL2-evoked Ca<sup>2+</sup> responses in THP-1 cells and significantly attenuated CCL2-evoked Ca<sup>2+</sup> responses in human PBMCs. These findings supported the results of experiments with apyrase and PPADS, but also importantly indicated a requirement of P2Y<sub>6</sub> for efficient CCL2/CCR2-mediated monocyte signalling. A wider implication of this is that P2Y<sub>6</sub> antagonism *in vivo* would attenuate excessive monocyte trafficking towards CCL2 chemotactic gradients. However, while this indicated a novel and important discovery, the results of experiments showed that MRS-2578 inhibited Ca<sup>2+</sup> responses less in PBMCs than in THP-1 cells. Although this is difficult to explain, it may be that P2Y<sub>6</sub> expression varies between different PBMCs. This seems possible given that prior work has shown that 1 µM MRS-2578 abolishes UDP-mediated IP<sub>3</sub> accumulation in

P2Y<sub>6</sub>-transfected 1321N1 cells, but only halves UDP-evoked Ca<sup>2+</sup> responses in a mixed population of human monocytes (Mamedova *et al.*, 2004; Woszczek *et al.*, 2010). Although this study has been successful in demonstrating crosstalk between P2Y<sub>6</sub> and CCR2, it is important to note that a weakness of this study was that 10 μM MRS-2578 may have antagonised P2Y<sub>1</sub> receptors (Mamedova *et al.*, 2004). Although this may have influenced the interpretation of experimental results, earlier experiments in this thesis were unable to provide firm evidence that THP-1 cells expressed functional P2Y<sub>1</sub> receptors.

Another important finding was that application of MRS-2578 to both cell types increased baseline Ca<sup>2+</sup>. Additional studies in the absence of extracellular Ca<sup>2+</sup> indicated that the effects of MRS-2578 on baseline Ca<sup>2+</sup> involved Ca<sup>2+</sup> influx and a mobilisation from internal stores. This finding is interesting because it suggests that P2Y<sub>6</sub> could be involved in maintaining Ca<sup>2+</sup> homeostasis. Although a similar result has not previously been reported, Bernier *et al.* (2013) have shown through their studies on microglia that P2Y<sub>6</sub> attenuates P2X<sub>4</sub>-mediated Ca<sup>2+</sup> influx, meaning that P2Y<sub>6</sub> could also play a similar role in monocytes. Although this is a possibility, this hypothesis conflicts with data showing a similar elevation of baseline Ca<sup>2+</sup> in the absence of extracellular Ca<sup>2+</sup>. Thus, further work to address the mechanism behind this effect is required.

### ***Dual P2Y<sub>6</sub> and CCR2 antagonism abolishes CCL2/CCR2-mediated THP-1 cell signalling***

Having investigated the requirement of P2Y<sub>6</sub> for CCL2/CCR2-mediated monocyte signalling, this study next asked whether CCL2-evoked intracellular Ca<sup>2+</sup> responses in monocytes involved a co-activation of P2Y<sub>6</sub> and CCR2. The results showed that a co-treatment of THP-1 cells with MRS-2578 and BMS-CCR2-22 abolished CCL2-evoked intracellular Ca<sup>2+</sup> responses. This suggests that CCL2-evoked intracellular Ca<sup>2+</sup> responses in monocytes involves both receptors, but also indicates that dual antagonists of CCR2 and P2Y<sub>6</sub> may be therapeutically beneficial. However, an arguable weakness with this study is that data generated previously in this thesis showed that BMS-CCR2-22 abolished CCL2-evoked intracellular Ca<sup>2+</sup> responses. This essentially means that CCR2 antagonists would be able to regulate monocyte trafficking towards CCL2 without the need for P2Y<sub>6</sub> antagonists. However, as shown by others (Cox *et al.*, 2005; Kim *et al.*, 2011; Zhang *et al.*, 2011), P2Y<sub>6</sub> activation in immune cells and astrocytes is often associated with a release of CCL2, thus highlighting the possibility that CCR2-mediated pathologies are exacerbated by P2Y<sub>6</sub>. This might explain why CCR2 antagonists have lacked clinical efficacy (Bachelier *et al.*, 2014).

## ***P2Y<sub>6</sub> antagonism attenuates CCL2/CCR2-mediated THP-1 cell and human PBMC function***

The findings above suggest that P2Y<sub>6</sub> crosstalk with CCR2 regulates monocyte signalling. It was therefore important to understand the involvement of P2Y<sub>6</sub> in CCL2/CCR2-mediated monocyte function. Studies addressed this aim by testing the effects of MRS-2578 on THP-1 cell and human PBMC chemotaxis, and THP-1 cell adhesion to vascular endothelial cells.

The results of chemotaxis experiments showed that MRS-2578 nearly abolished CCL2-mediated THP-1 cell and PBMC chemotaxis. These results suggest that crosstalk between P2Y<sub>6</sub> and CCR2 is essential for efficient monocyte and PBMC chemotaxis. Although this finding is novel, studies by Zhang *et al.* (2011), have demonstrated that P2Y<sub>6</sub> activation promotes the chemotaxis of RAW264.7-macrophages by inducing the release of CCL2. Cox *et al.* (2005) have also demonstrated the release of CCL2 by U937 monocytic cells in response to UDP. Although these studies differ from the present study, they support the hypothesis that crosstalk between P2Y<sub>6</sub> and CCR2 is important for the signalling and function of monocytes and their progeny. Determining whether CCR2-expressing monocytes release CCL2 in response to P2Y<sub>6</sub> activation would thus represent an interesting research area, as it would enable a greater understanding of how P2Y<sub>6</sub> and CCR2 crosstalk modulates monocyte function.

A second important finding from chemotaxis studies was that the level of inhibition with MRS-2578 mirrored apyrase and PPADS, suggesting that all three compounds attenuated CCL2-mediated cellular chemotaxis through a common pathway. Although these results supported the study hypothesis, the effects of MRS-2578 on PBMCs were unexpected since studies in this thesis showed that apyrase enhanced chemotaxis. These differences are difficult to explain, but might be related to the two different mechanisms by which apyrase and MRS-2578 act (Cohn and Meek, 1957; Mamedova *et al.*, 2004). Further studies to examine the mechanisms by which apyrase and MRS-2578 differentially modulate monocyte chemotaxis are therefore recommended. Despite these discrepancies, the findings of this study indicate that P2Y<sub>6</sub> activation is required for CCL2/CCR2-mediated monocyte signalling and chemotaxis.

The results of adhesion experiments showed that MRS-2578 abolished CCL2/CCR2-mediated THP-1 cell adhesion to both quiescent and TNF $\alpha$ -treated HUVEC monolayers. These findings suggest that P2Y<sub>6</sub> is important for CCL2-mediated monocyte adhesion to the vascular endothelium under homeostatic and inflammatory conditions. Although these findings are novel, it is interesting that other groups also implicate a role for P2Y<sub>6</sub> in vascular inflammation (Bar *et al.*, 2008; Guns *et al.*, 2010; Riegel *et al.*, 2011; Kim *et al.*,

2011; Stachon *et al.*, 2014; Garcia *et al.*, 2014). A key study is that of Riegel *et al.* (2011), in which LPS- or TNF $\alpha$ -challenge of the vascular endothelium led to a selective upregulation of P2Y<sub>6</sub>, VCAM-1 and ICAM-1 expression, and IL-8 release, all of which were markedly attenuated by MRS-2578. More recently, Stachon *et al.* (2014) and Garcia *et al.* (2014) have demonstrated that P2Y<sub>6</sub>-deficient mice exhibit smaller atherosclerotic lesions due to a reduced ability of leukocytes to roll and adhere to vasculature. Garcia *et al.* (2014) have even gone further by showing that P2Y<sub>6</sub>-deficient macrophages secrete less CCL2. In general, therefore, it seems that monocyte chemotaxis and adherence are functions coordinated by P2Y<sub>6</sub> and CCR2. One of the issues that emerge from this is that dual targeting of these receptors may be a more therapeutically efficacious strategy than targeting either receptor alone.

### ***P2Y<sub>6</sub> antagonism attenuates extracellular nucleotide-mediated THP-1 cell signalling***

In an effort to understand the involvement of individual extracellular nucleotides in P2Y<sub>6</sub> activation in monocytes, studies sought to characterise P2Y<sub>6</sub>-mediated Ca<sup>2+</sup> responses using P2Y<sub>6</sub>-stable 1321N1 astrocytoma cells. The results of these experiments suggested that the rank order of potency of extracellular nucleotides (UDP>UTP>ADP>ATP) matched the findings of Communi *et al.* (1996). Moreover, the results of this study suggested that purine and pyrimidine nucleotides were required for P2Y<sub>6</sub> activation in monocytes.

In additional THP-1 cell Ca<sup>2+</sup> experiments, it was discovered that MRS-2578 inhibited Ca<sup>2+</sup> responses evoked by these ligands with a rank order of ADP>UTP>ATP>UDP. Although this suggests that MRS-2578 favours other ligands over UDP, it may be that nucleotide purity, which fluctuated between 95% for ADP, to 99% for ATP, influenced these results. A second possible explanation might be that Ca<sup>2+</sup> responses evoked by UDP in THP-1 cells involved an activation of P2Y<sub>14</sub> and the orphan GPCR, GPR17 (Ciana *et al.*, 2006; Carter *et al.*, 2009; Hamel *et al.*, 2011). Interestingly, further Ca<sup>2+</sup> experiments testing this hypothesis showed that the P2Y<sub>14</sub>/GPR17 ligand UDP-glucose (Ciana *et al.*, 2006; Carter *et al.*, 2009), induced Ca<sup>2+</sup> release from THP-1 cells thereby supporting the hypothesis that these receptors contributed to UDP-evoked Ca<sup>2+</sup> responses in THP-1 cells. This result also supports a functional presence of the P2Y<sub>14</sub> receptor in THP-1 cells, which is a novel finding.

Although this study has been unable to demonstrate that MRS-2578 preferentially impairs UDP-evoked Ca<sup>2+</sup> responses in THP-1 cells, it has demonstrated that purine and pyrimidine extracellular nucleotides are required for P2Y<sub>6</sub> activation in monocytes.

### ***CCL2 and UDP co-application influences THP-1 cell intracellular Ca<sup>2+</sup> responses***

The next study in this thesis set out with the aim of assessing the mechanisms involved in P2Y<sub>6</sub> and CCR2 crosstalk. To address this aim, studies investigated the effects of CCL2 and UDP co-application on THP-1 cell Ca<sup>2+</sup> responses.

The results of this experiment suggested that Ca<sup>2+</sup> responses evoked by UDP/CCL2 were not significantly higher than Ca<sup>2+</sup> responses evoked by CCL2 alone. While this indicated that UDP and CCL2 did not synergistically amplify CCL2 Ca<sup>2+</sup> responses, a slightly higher Ca<sup>2+</sup> response with UDP/CCL2 suggested that additional experiments with a lower concentration of CCL2 were required. In additional Ca<sup>2+</sup> studies examining for crosstalk between P2Y<sub>6</sub> and CCR2, it was seen that the CCR2 antagonist BMS-CCR2-22 did not significantly affect UDP-evoked Ca<sup>2+</sup> responses in THP-1 cells. This finding is important because it suggests that crosstalk between P2Y<sub>6</sub> and CCR2 is unidirectional. A wider implication of this is that antagonists and antibodies targeting CCR2 would be ineffective in modulating monocyte trafficking towards extracellular nucleotides. This is interesting because it provides a possible explanation as to why clinical trials on CCR2 antagonists have proved unsatisfactory (Bachelerie *et al.*, 2014)

Although the findings of this study suggest that further work is required, they also indicate that the relationship between P2Y<sub>6</sub> and CCR2 is unidirectional. This finding may help us to understand how drugs targeting P2Y<sub>6</sub> and CCR2 can be fine-tuned to become effective therapies.

### ***Ecto-nucleotidases attenuate fMLP-FPR-associated THP-1 signalling and function***

The next objective was to examine whether other chemotactic pathways involved in orchestrating monocyte signalling and function required P2Y<sub>6</sub>. To this end, studies tested the effects of apyrase and MRS-2578 on fMLP-FPR-associated THP-1 cell signalling and chemotaxis.

The results of Ca<sup>2+</sup> studies showed that fMLP-FPR-associated Ca<sup>2+</sup> responses were attenuated significantly by apyrase, but not by MRS-2578. Chemotaxis studies mirrored these results, and suggested that P2Y<sub>6</sub> receptors did not modulate monocyte signalling and function by engaging in crosstalk with FPRs. This is important since it suggests that P2Y<sub>6</sub> and CCR2 may form an exclusive pairing. However, the inhibition of fMLP-FPR-associated THP-1 cell signalling and function by apyrase is an interesting finding, and suggests an involvement of other purinoceptors. While further experiments are required to establish this, it is interesting that Chen *et al.* (2006) suggest that A<sub>3</sub> and P2Y<sub>2</sub> purinoceptors guide neutrophil chemotaxis towards fMLP. It is possible; therefore, that A<sub>3</sub> and P2Y<sub>2</sub> play a similar role in monocytes. While these and other purinoceptors are

possible candidates, a lack of involvement of P2Y<sub>6</sub> purinoceptors raises intriguing questions regarding the mechanisms involved in determining its requirement for CCR2 signalling, but not for FPR signalling. Although the reasons for this are unclear, it may be that FPR-mediated extracellular nucleotide release sites are located physically far from P2Y<sub>6</sub>, while CCR2-mediated extracellular nucleotide release sites are in close proximity. However, a second possible explanation for this might be that P2Y<sub>6</sub> and CCR2 form heterodimers. While this is an interesting and novel concept, further work is required to establish this.

Although the findings of these studies indicate that P2Y<sub>6</sub> receptors are not required for fMLP-FPR-associated monocyte signalling and function, they indicate that other purinoceptors may be involved. Understanding whether other purinoceptors crosstalk with FPRs to modulate monocyte signalling and function would thus represent an interesting research area.

### ***P2Y<sub>6</sub> cross-desensitisation of CCR2 attenuates CCL2/CCR2-mediated THP-1 cell signalling***

The findings of this thesis suggest that CCR2-expressing monocytes rely on crosstalk between P2Y<sub>6</sub> and CCR2 for proper guidance towards chemotactic signals transmitted by CCL2. However, as the evidence presented has shown, the relationship between P2Y<sub>6</sub> and CCR2 is unidirectional, indicating that P2Y<sub>6</sub> may functionally regulate CCR2 through the process of cross-(heterologous) desensitisation. Homologous and heterologous desensitisation studies therefore sought to examine this hypothesis by using the P2Y<sub>6</sub> ligands, ADP and UDP.

The results of homologous P2Y<sub>6</sub> desensitisation studies showed that after pre-challenge of THP-1 cells with ADP or UDP, both nucleotides failed to induce a similar Ca<sup>2+</sup> response. This result suggests that P2Y<sub>6</sub> can be desensitised by its ligands ADP and UDP. In cross-desensitisation studies, it was seen that pre-challenge of THP-1 cells with ADP or UDP suppressed subsequent CCL2-evoked Ca<sup>2+</sup> responses. These findings are consistent with MRS-2578 studies, but also suggest that activation of P2Y<sub>6</sub> cross-desensitises CCR2. A wider implication of this is that, in an *in vivo* setting, the capacity of monocytes to traffic in response to CCL2 would be regulated by P2Y<sub>6</sub>, which may serve as an important regulatory mechanism. However, while the findings of this study indicate a very important and novel discovery, they also suggest that reverse agonist studies are required to develop a better understanding of the mechanisms involved in crosstalk between P2Y<sub>6</sub> and CCR2.

## ***P2Y<sub>6</sub> knockdown attenuates CCL2/CCR2-mediated THP-1 cell signalling and function***

To provide further evidence for crosstalk between P2Y<sub>6</sub> and CCR2, studies employed molecular approaches (shRNA) to generate *P2RY6-KD* THP-1 cell lines. Of the five *P2RY6-KD* cell lines generated, four were significantly less responsive to UDP than scrambled THP-1 cells in Ca<sup>2+</sup> studies. However, additional Ca<sup>2+</sup> studies suggested that only the best-performing shRNA from these (358038) displayed an attenuated Ca<sup>2+</sup> response to CCL2. Although it was disappointing that only one *P2RY6-KD* cell line could be taken forward for further studies, qRT-PCR studies were encouraging since they indicated that 358038 cells displayed a 2-fold knockdown in *P2RY6* mRNA expression, but no knockdown in CCR2 mRNA expression. The results of this study are important because they support the hypothesis that P2Y<sub>6</sub> is required for CCL2/CCR2 monocyte signalling.

The results of experiments examining the effects of P2Y<sub>6</sub>-KD on CCL2/CCR2-mediated monocyte chemotaxis showed that 2-fold less P2Y<sub>6</sub>-KD cells migrated towards CCL2 than scrambled cells. This finding agrees with prior observations made in apyrase and MRS-2578 experiments, and is considered important since it suggests that fine-tuning P2Y<sub>6</sub> activation *in vivo* would be therapeutically beneficial as this would attenuate excessive monocyte trafficking towards CCL2.

The results of HUVEC adhesion experiments suggested that CCL2-primed P2Y<sub>6</sub>-KD and scrambled THP-1 cells differed in their capacity to adhere to TNF $\alpha$ -treated HUVEC monolayers. Although both cell types adhered similarly to quiescent HUVECs, it was seen that CCL2-primed P2Y<sub>6</sub>-KD cells adhered significantly less than scrambled cells to TNF $\alpha$ -treated HUVEC monolayers. These findings differed from earlier results showing that MRS-2578 abolished CCL2-mediated THP-1 cell adhesion to quiescent and TNF $\alpha$ -treated HUVEC monolayers. These differences may lie in the fact that MRS-2578 and *P2RY6* shRNA attenuate P2Y<sub>6</sub> by different mechanisms. While 1  $\mu$ M MRS-2578 completely antagonises P2Y<sub>6</sub> responses (Mamedova *et al.*, 2004), *P2RY6* shRNA only partially silences P2Y<sub>6</sub>. This suggests that MRS-2578-treated THP-1 cells would be unable to adhere, but P2Y<sub>6</sub>-KD cells would express enough P2Y<sub>6</sub> to allow some adhesion.

While the results of quiescent experiments suggested that P2Y<sub>6</sub>-KD cells adhered to HUVEC monolayers similarly to scrambled cells, it was interesting that in further experiments, P2Y<sub>6</sub>-KD cells were unable to adhere to TNF $\alpha$ -treated HUVEC monolayers. It may be that, under these conditions, an upregulation of CCR2 and P2Y<sub>6</sub> expression on the endothelium (Weber *et al.*, 1999; Riegel *et al.*, 2011) means that a greater demand is placed on these receptors. This would potentially explain why P2Y<sub>6</sub>-KD cells were unable

to adhere, and why the CCR2 antagonist BMS-CCR2-22 abolished CCL2- and non-CCL2-dependent THP-1 cell adhesion to TNF $\alpha$ -treated HUVEC monolayers. Although several questions remain unanswered at present, it is apparent from the findings of this study that P2Y<sub>6</sub> antagonists or dual CCR2/P2Y<sub>6</sub> antagonists may be therapeutically beneficial.

### ***THP-1 cells challenged with CCL2 release ATP***

The release of ATP is an important mechanism by which cells send danger signals during stress, damage, infection, or hypoxia (Boeynaems, and Communi, 2006; Bours *et al.*, 2006). Many cell types such as immune cells release ATP into their microenvironment in a bid to adjust their functional responses to non-purinoreceptor chemoattractants (Junger, 2011). For example, neutrophils self-regulate their responses to fMLP via autocrine purinoreceptor signalling (Chen *et al.*, 2006; Sumi *et al.*, 2010). Studies therefore examined whether CCR2 and P2Y<sub>6</sub> crosstalk involved a release of extracellular nucleotides.

The results of non-quantitative (HPLC) experiments showed that CCL2 challenge of THP-1 cells resulted in a robust detection of ATP in cell supernatants, while other extracellular nucleotides were difficult to detect. These results, although a little disappointing, suggest that monocytes release ATP upon CCR2 activation, which is a novel finding. Furthermore, these results also support an involvement of ATP in P2Y<sub>6</sub> activation. Given that, ecto-nucleotidases rapidly hydrolyse ATP to ADP (Zimmermann *et al.*, 2012); it may be that ADP also activates P2Y<sub>6</sub>, which would also support the results of apyrase isoenzyme studies showing a greater involvement of NDPs in CCL2 Ca<sup>2+</sup> responses.

The results of quantitative studies suggested that THP-1 cells released 1  $\mu$ M ATP into supernatants following CCL2 challenge. This finding accords with earlier observations, but more importantly, supports prior work (Cox *et al.*, 2005) and data generated in P2Y<sub>6</sub>-stable 1321N1 cells showing that P2Y<sub>6</sub> can be activated by <300 nM ATP. As experiments with P2Y<sub>6</sub>-stable 1321N1 cells also suggested that P2Y<sub>6</sub> could be activated by <300 nM ADP, it may be that ATP release leads to the generation of sufficient levels of ADP for P2Y<sub>6</sub> activation.

Although this finding suggests that monocytes release high amounts of ATP in response to stimuli, it is interesting that other phagocytes such as neutrophils, release higher levels of ATP (3  $\mu$ M) in response to fMLP (Chen *et al.*, 2006). The reason for this is not clear but it might be that neutrophils, which make up the majority of circulating leukocytes, require higher levels of ATP for autocrine and paracrine purinoreceptor signalling (Junger, 2011). However, an alternative explanation may be that the bulk-phase measurements undertaken during this study underestimated the true ATP concentration near the plasma membrane (Praetorius and Leipziger, 2009). This applies not only to ATP, but also to

other extracellular nucleotides. A further study focussing on the concentration of extracellular nucleotides at the plasma membrane is therefore suggested.

### ***THP-1 cells challenged with CCL2 do not release lysosomal enzymes***

Prior work by others has shown that ATP can be stored and released from secretory lysosomes (Zhang *et al.*, 2007; Sivaramakrishnan *et al.*, 2012; Hiasa *et al.*, 2014). However, no previous studies have investigated the source of ATP from monocytes following CCL2 challenge. This study therefore set out to investigate this hypothesis by examining the release of the lysosomal enzyme,  $\beta$ -hexosaminidase in response to CCL2.

The results of experiments showed that THP-1 cells challenged with CCL2 did not release  $\beta$ -hexosaminidase into supernatants. These results were disappointing, but suggested that the levels of  $\beta$ -hexosaminidase released by cells might not have been easily detected using the methodology used. Although these data indicate that monocytes challenged with CCL2 do not release ATP from secretory vesicles containing  $\beta$ -hexosaminidase, it is interesting that microglial cells, which are essentially tissue-resident macrophages, do release  $\beta$ -hexosaminidase in response to CCL2 (Toyomitsu *et al.*, 2012). It is difficult to explain why these differences exist, but it may be that monocytes generally contain less secretory vesicles than macrophages (Cohn and Benson, 1965). However, while this is a valid point, the results of the present study showed that GPN caused a significant release of  $\beta$ -hexosaminidase in THP-1 cells. Sivaramakrishnan *et al.* (2012) have also reported a similar result, but unlike this study, the present study has been unable to demonstrate that  $\beta$ -hexosaminidase release coincides with ATP release. A possible explanation for this may be that ATP and  $\beta$ -hexosaminidase reside in different secretory vesicles, but that the general lysosomotropic and cytotoxic mechanism of GPN (Jadot *et al.*, 1990) led Sivaramakrishnan *et al.* (2012) to believe that ATP and  $\beta$ -hexosaminidase were co-released from the same location. A further study with more focus on the mechanisms involved in ATP secretion is therefore recommended.

## **7.4 Future Directions**

The investigations conducted in this thesis have focussed on deciphering the CCL2/CCR2 axis in monocytes and investigating its modulation by extracellular nucleotides. While several novel hypotheses have been put forward by this research, further work to establish their relevance is required. However, several questions remain unanswered and should be addressed in future investigations in order to understand the mechanisms proposed by this study.

It has been proposed by this research that THP-1 cells and human monocytes exhibit an overlapping expression pattern of mRNA for a number of monocyte markers, CC

chemokines, CC chemokine receptors, and purinoceptors. This study has also assumed that both cell types express mRNA for the enzymes and targets investigated in this study. Determining the expression of these at the post-translational level is therefore required since it would allow a better understanding of the contributions of individual pathways.

The present investigation was unable to investigate the individual contributions of all purinoceptors in CCL2/CCR2 signalling due to a lack of antagonist availability. Addressing the involvement of these receptors in future studies would be useful for determining whether other purinoceptors are involved.

The results of fMLP-FPR studies suggest that other purinoceptors might be involved. Furthermore, a requirement of P2Y<sub>6</sub> for CCL2/CCR2 indicates that other chemotactic pathways may also require P2Y<sub>6</sub>. Understanding the contribution of P2Y<sub>6</sub> and other purinoceptors in other chemotactic pathways would thus represent an interesting area for future research.

It seems clear from this work that the involvement of P2Y<sub>6</sub> in CCL2 release should be investigated further. Experiments addressing this would provide valuable information about the mechanisms involved in P2Y<sub>6</sub> and CCR2 crosstalk. Furthermore, future studies should also investigate the involvement of downstream components such as DAG and PLC in crosstalk studies.

# Appendix : Supplementary Data

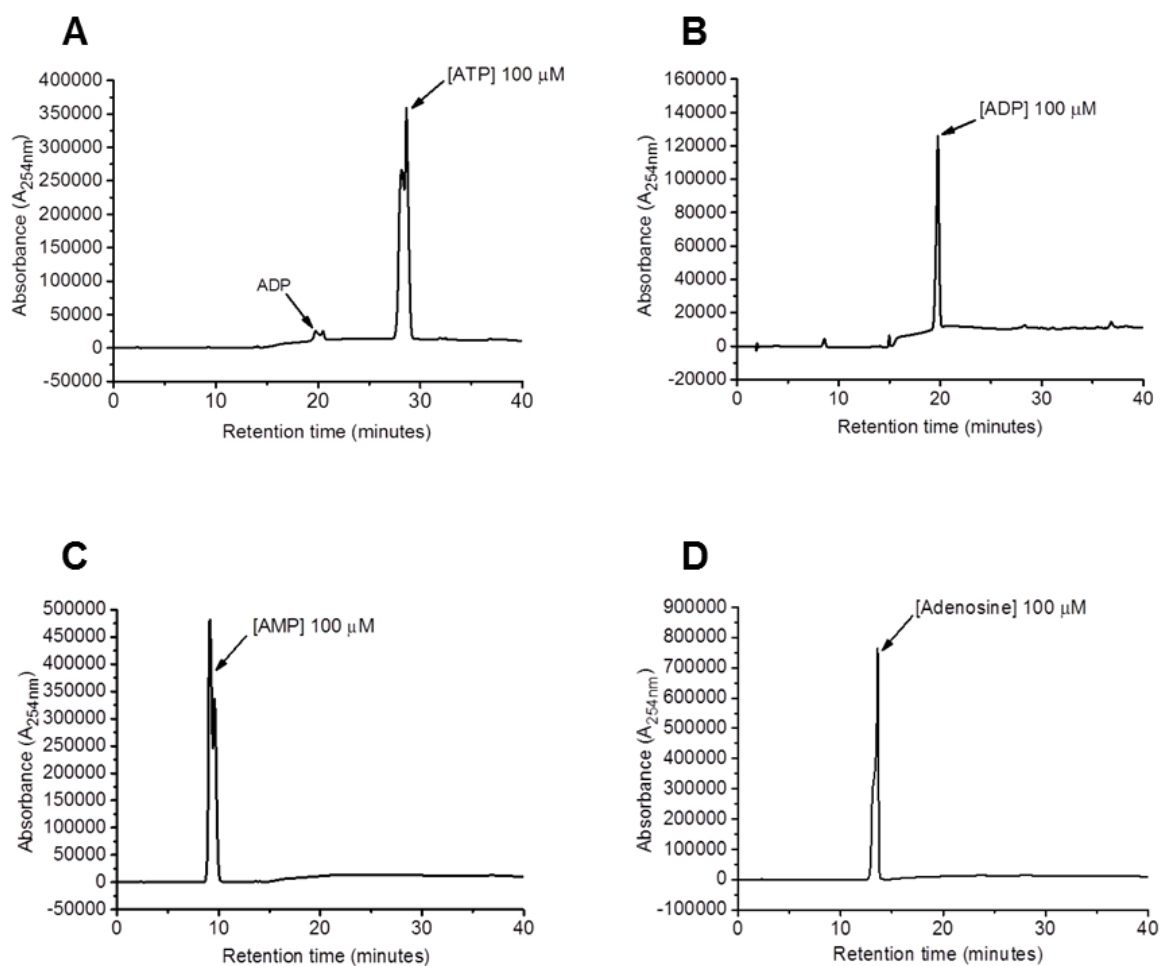


**Figure A1** Detection of adenine nucleotides and nucleosides by ion-pair reverse-phase HPLC

Representative traces showing absorbance ( $A_{254nm}$ ) and retention times of 100  $\mu$ M (A) ATP, (B) ADP, (C) AMP and, (D) adenosine in salt-buffered solution (SBS). Sampling performed immediately after nucleotide and nucleoside addition.

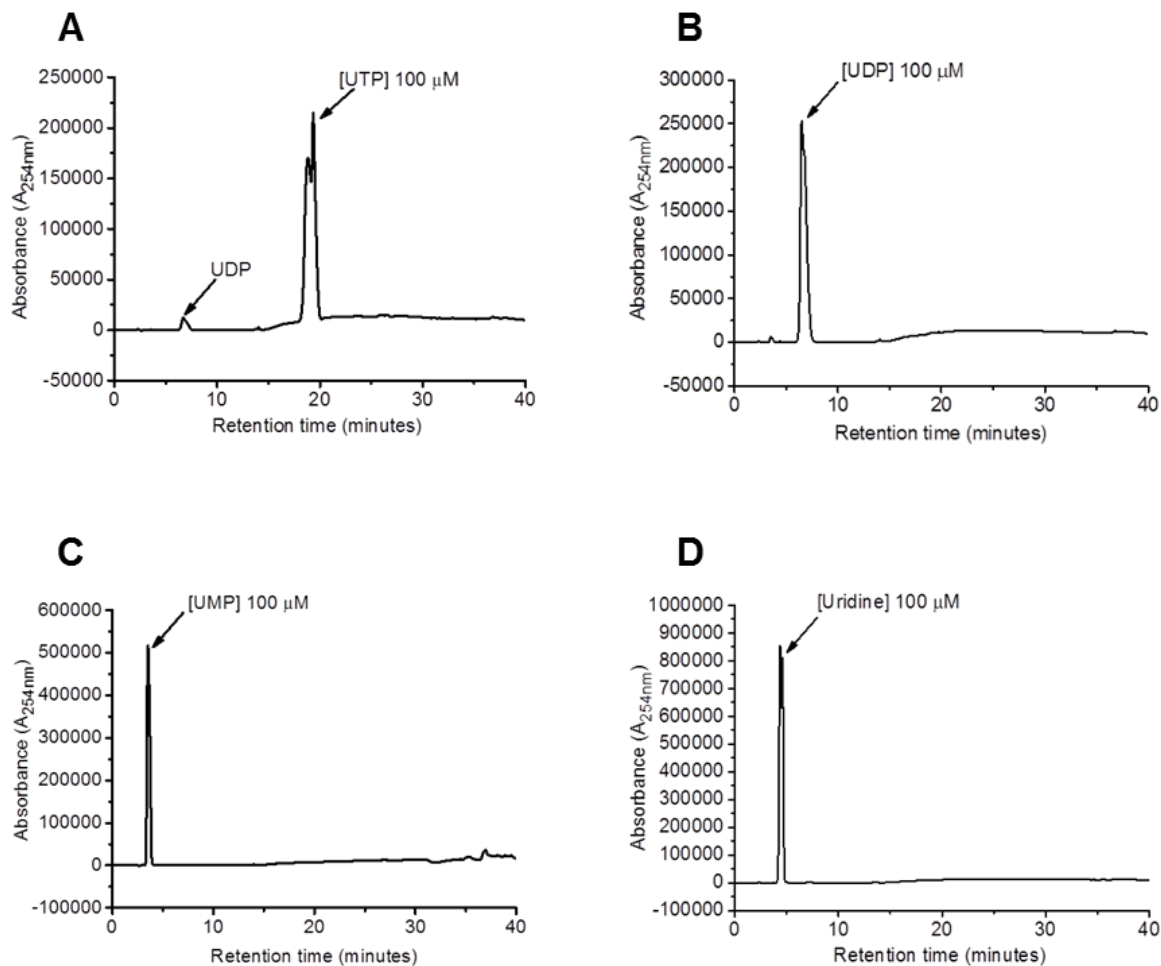


**Figure A2 Detection of uridine nucleotides and nucleoside by ion-pair reverse-phase HPLC**

Representative traces showing absorbance ( $A_{254nm}$ ) and retention times of 100  $\mu$ M (A) UTP, (B) UDP, (C) UMP and, (D) uridine in salt-buffered solution (SBS). Sampling performed immediately after nucleotide and nucleoside addition.

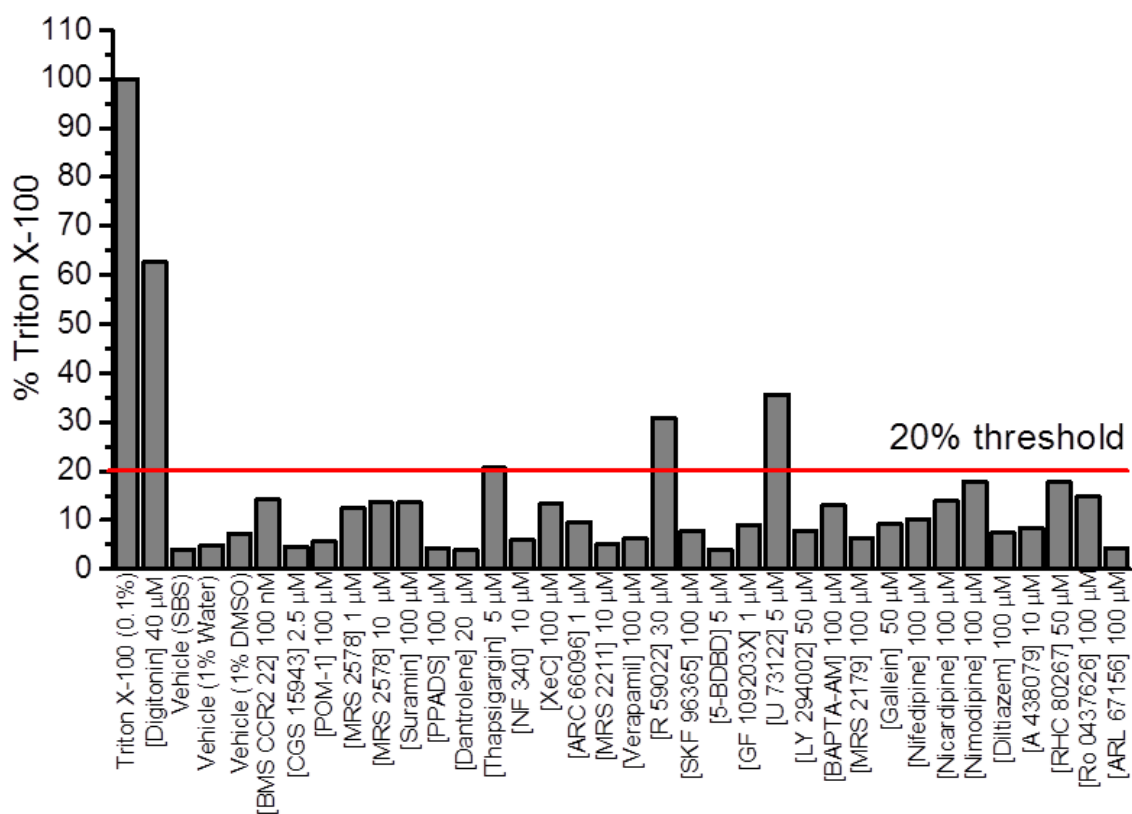


**Figure A3 Effect of compounds on LDH release from THP-1 cells**

Bar chart showing normalised THP-1 cell viability following incubation (2.5 hours) with vehicle (SBS or 1% DMSO) or inhibitors and antagonists at concentrations shown. Loss in cell viability given as a percentage of 0.1% Triton X-100. Acceptable threshold set to 20%. Data represents mean  $\pm$  SEM from n=1 replicate.

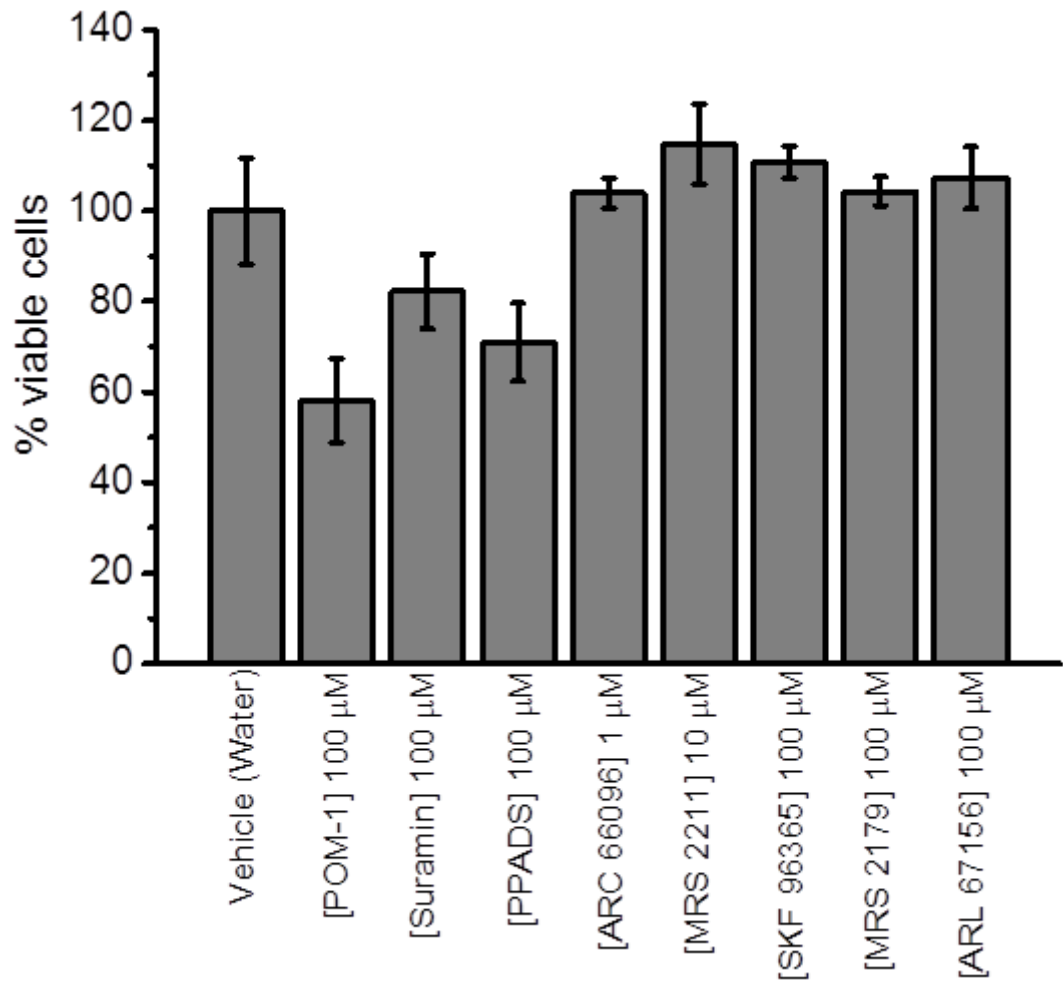


**Figure A4 Effect of water-soluble compounds on THP-1 cell viability**

Bar chart showing normalised THP-1 cell viability following incubation (2.5 hours) with vehicle (water) or inhibitors and antagonists at concentrations shown. Cell viability given as a percentage of vehicle. Data represents mean ± SEM from n=3 replicates

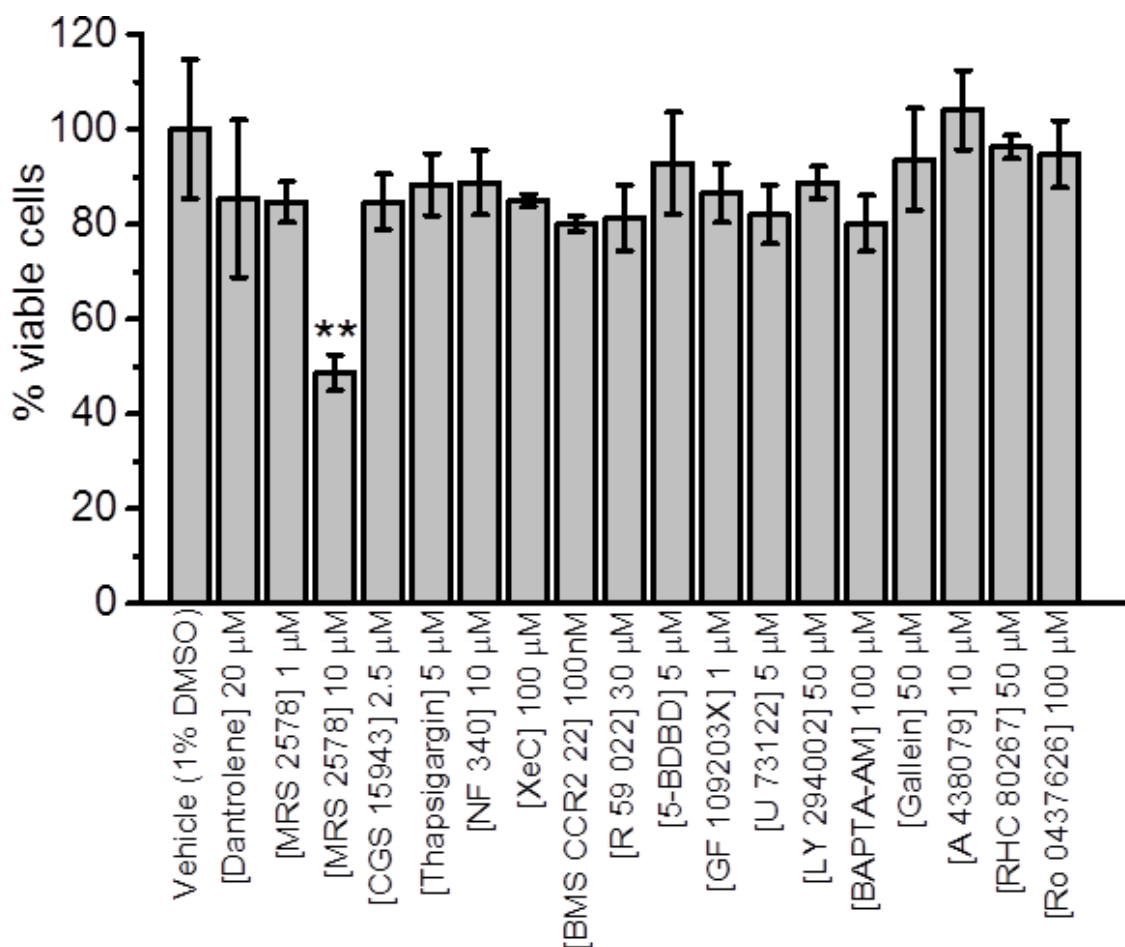


**Figure A5 Effect of DMSO-soluble compounds on THP-1 cell viability**

Bar chart showing normalised THP-1 cell viability following incubation (2.5 hours) with vehicle (DMSO) or inhibitors and antagonists at concentrations shown. Cell viability given as a percentage of vehicle. Data represents mean  $\pm$  SEM from n=3 replicates (\*\*p<0.01, One-way ANOVA with Bonferroni's multiple comparison).

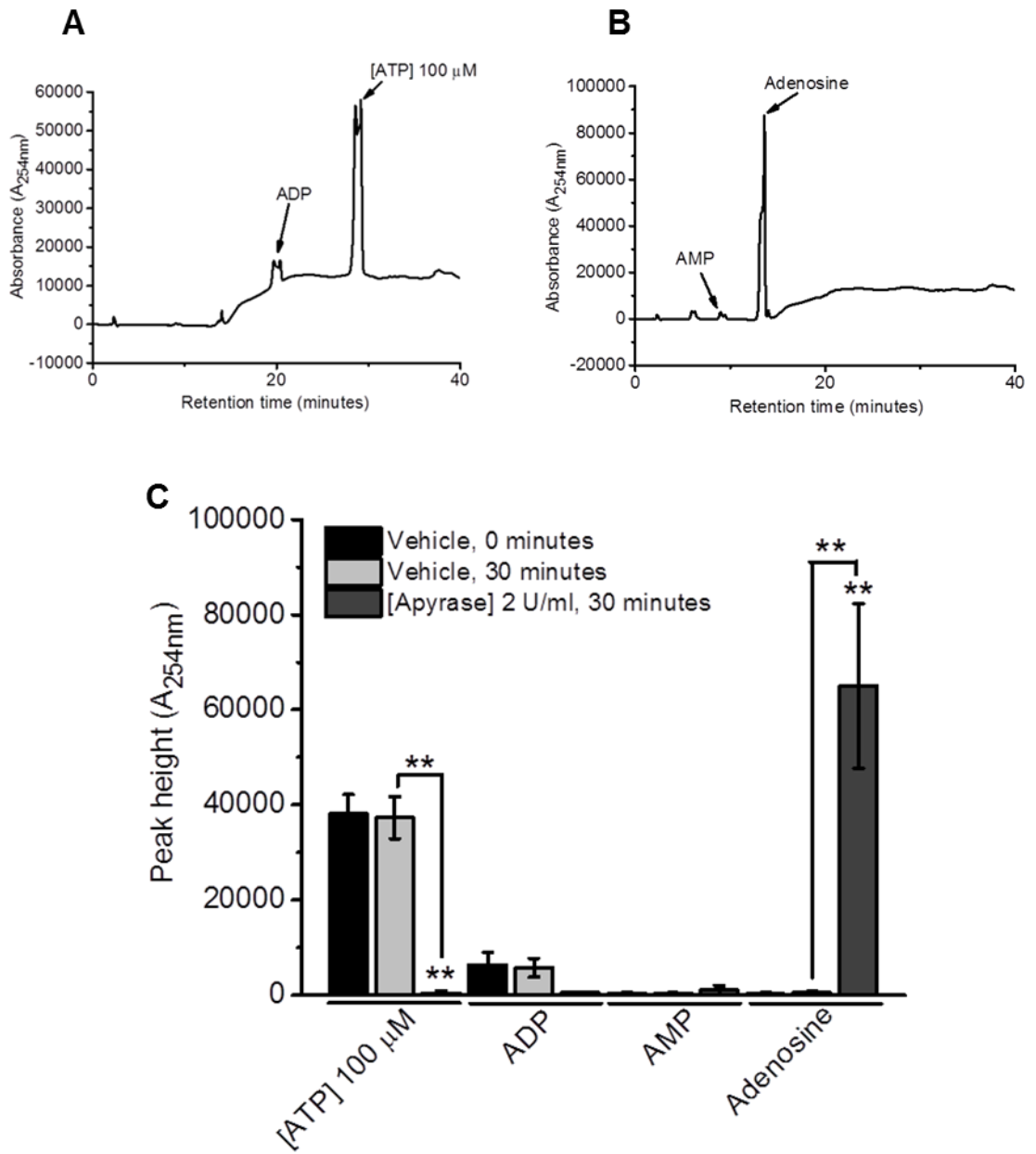


**Figure A6 Effect of apyrase on ATP**

Representative traces showing absorbance ( $A_{254nm}$ ) and retention time for ATP (100  $\mu$ M) at (A) 0 minutes in the presence of vehicle (SBS), and (B) following a 30 minute incubation with apyrase (2U/ml). (C) Bar chart showing peak height (absorbance at  $A_{254nm}$ ) of 100  $\mu$ M ATP and related nucleotides and nucleosides at 0 minutes in the presence of vehicle, and following a 30 minute incubation with vehicle or apyrase (2U/ml). Data represents mean  $\pm$  SEM from n=3 replicates. Asterisks indicate significant changes towards vehicle at 0 minutes (\*\*p<0.01, One-way ANOVA with Bonferroni's multiple comparison).

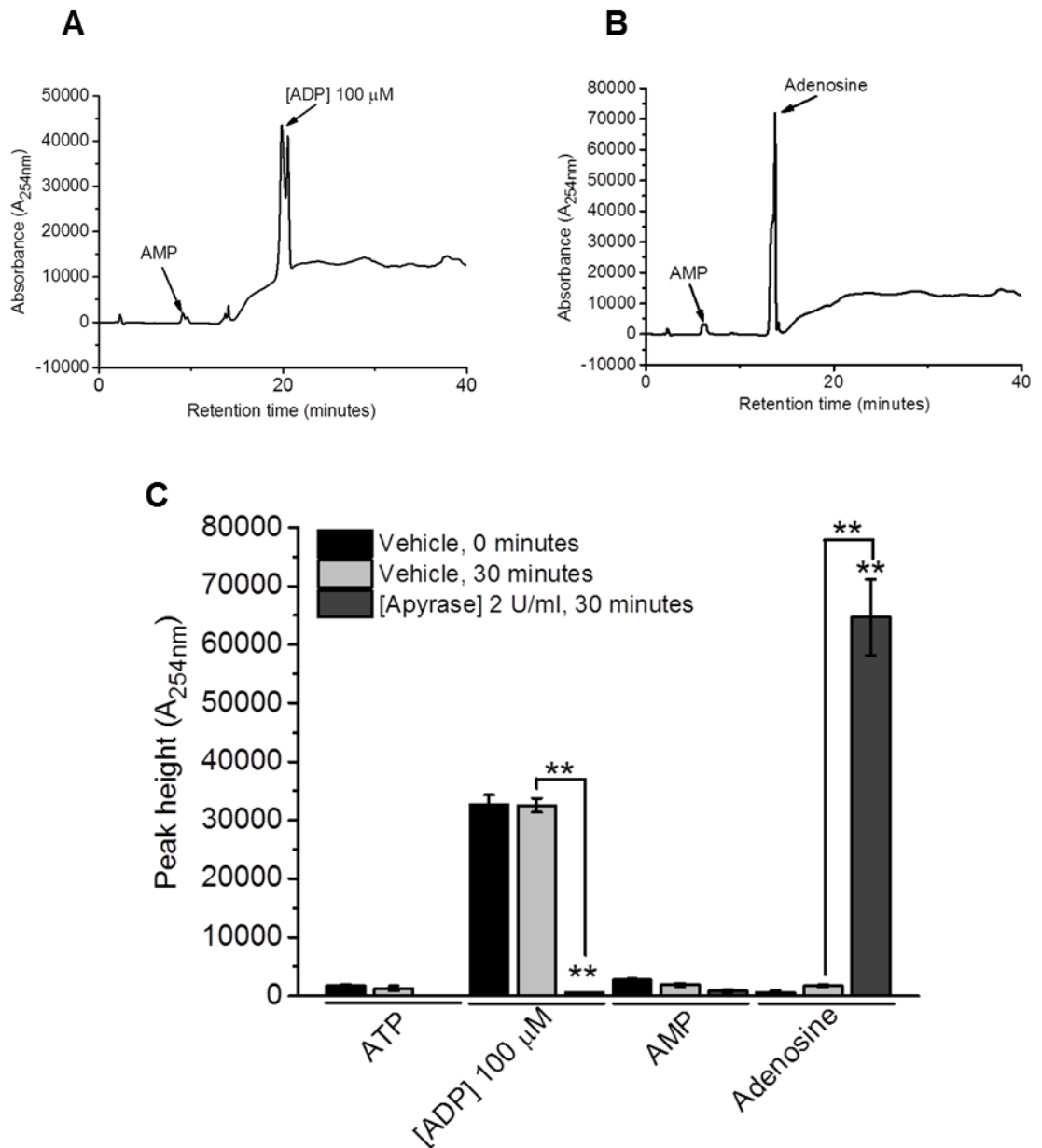


**Figure A7 Effect of apyrase on ADP**

Representative traces showing absorbance ( $A_{254nm}$ ) and retention time for ADP (100  $\mu$ M) at (A) 0 minutes in the presence of vehicle (SBS), and (B) following a 30 minute incubation with apyrase (2U/ml). (C) Bar chart showing peak height (absorbance at  $A_{254nm}$ ) of 100  $\mu$ M ADP and related nucleotides and nucleosides at 0 minutes in the presence of vehicle, and following a 30 minute incubation with vehicle or apyrase (2U/ml). Data represents mean  $\pm$  SEM from n=3 replicates. Asterisks indicate significant changes towards vehicle at 0 minutes (\*\*p<0.01, One-way ANOVA with Bonferroni's multiple comparison).

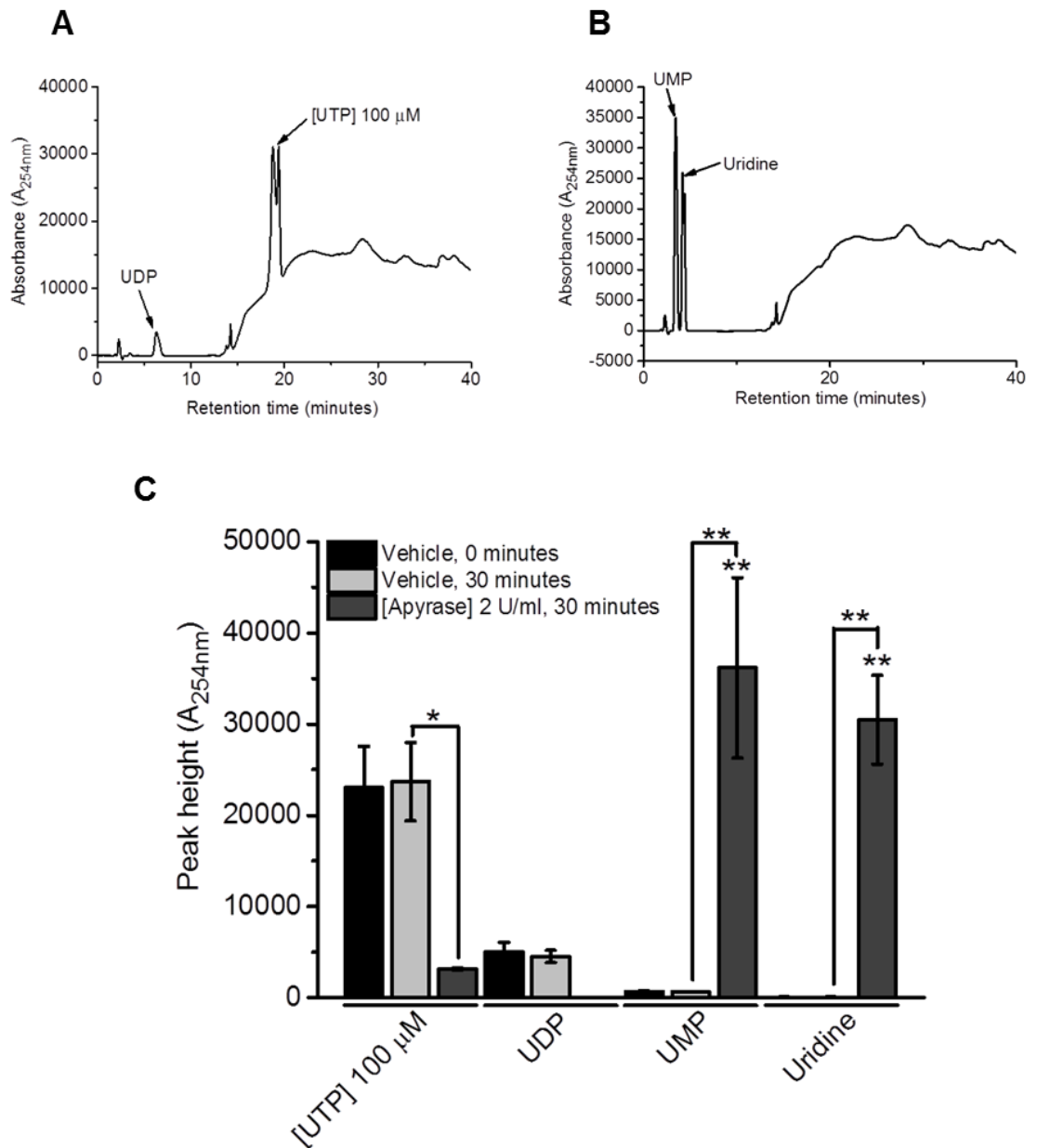


**Figure A8 Effect of apyrase on UTP**

Apyrase treatment reduced levels of UTP in SBS buffer. Representative traces showing absorbance ( $A_{254nm}$ ) and retention time for UTP (100  $\mu$ M) at (A) 0 minutes in the presence of vehicle (SBS), and (B) following a 30 minute incubation with apyrase (2U/ml). (C) Bar chart showing peak height (absorbance at  $A_{254nm}$ ) of 100  $\mu$ M UTP and related nucleotides and nucleosides at 0 minutes in the presence of vehicle, and following a 30 minute incubation with vehicle or apyrase (2U/ml). Data represents mean  $\pm$  SEM from  $n=3$  replicates. Asterisks indicate significant changes towards vehicle at 0 minutes (\*\* $p<0.01$ , \* $p<0.05$ , One-way ANOVA with Bonferroni's multiple comparison).

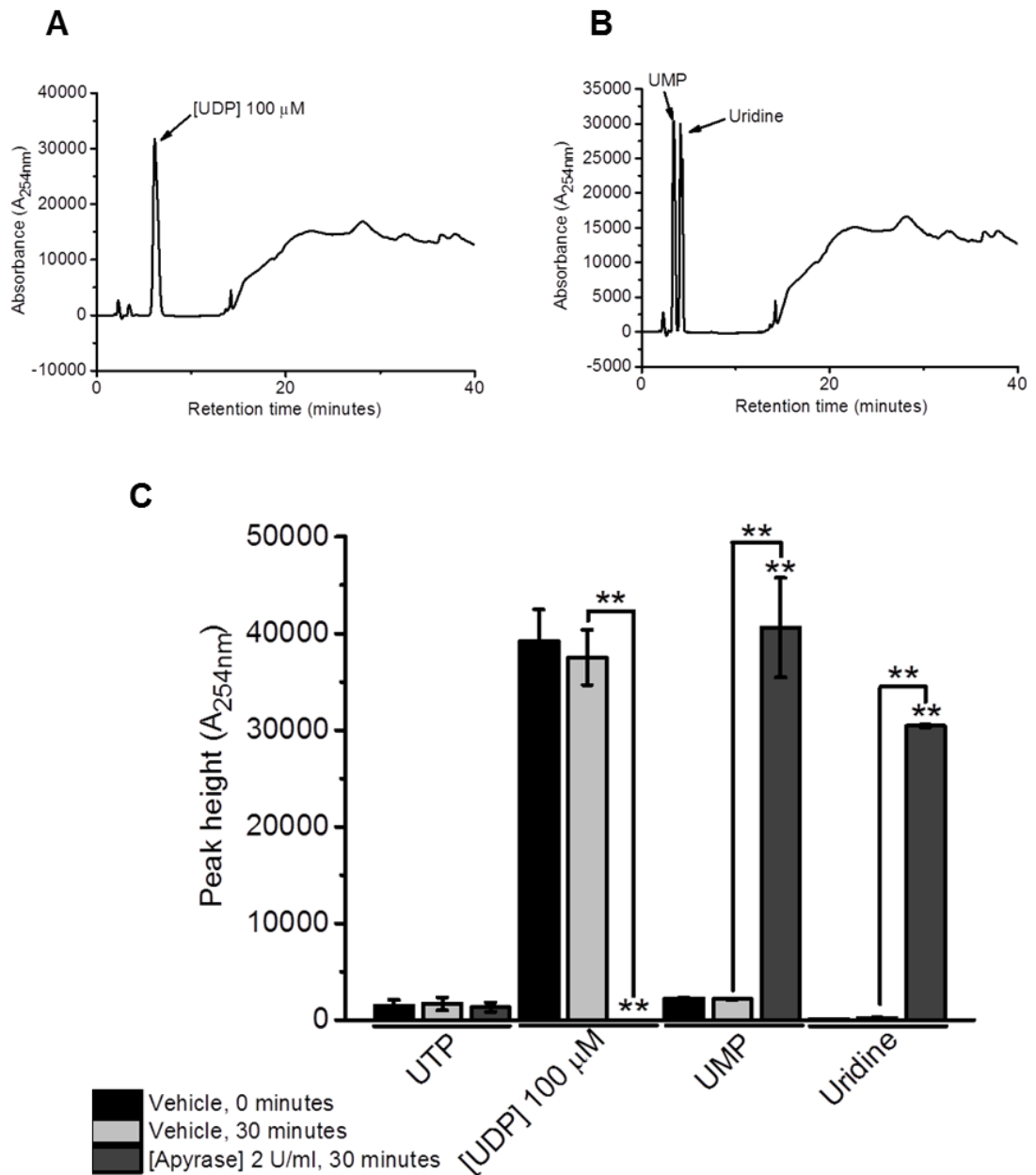


**Figure A9 Effect of apyrase on UDP**

Representative traces showing absorbance ( $A_{254nm}$ ) and retention time for UDP (100  $\mu$ M) at (A) 0 minutes in the presence of vehicle (SBS), and (B) following a 30 minute incubation with apyrase (2U/ml). (C) Bar chart showing peak height (absorbance at  $A_{254nm}$ ) of 100  $\mu$ M UDP and related nucleotides and nucleosides at 0 minutes in the presence of vehicle, and following a 30 minute incubation with vehicle or apyrase (2U/ml). Data represents mean  $\pm$  SEM from n=3 replicates. Asterisks indicate significant changes towards vehicle at 0 minutes (\*\*p<0.01, One-way ANOVA with Bonferroni's multiple comparison).

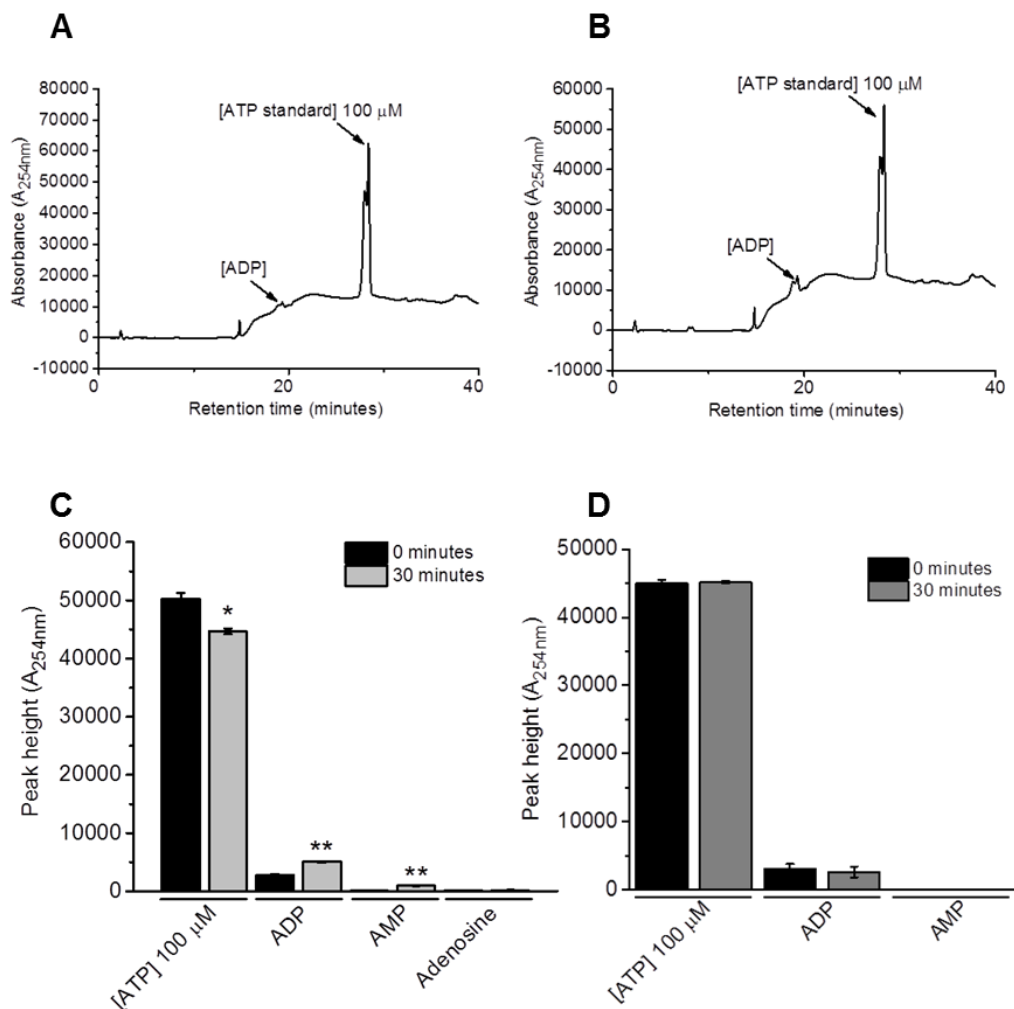


**Figure A10 Hydrolysis of ATP by SBS and THP-1 cells**

Incubation of ATP with THP-1 cells resulted in a reduction in levels of ATP and increase in levels of ADP and AMP. Representative HPLC traces showing ATP and ADP peaks at (A) 0 minutes in SBS and (B), 30 minutes in the presence of THP-1 cells. (C) Bar chart showing mean peak heights for ATP, ADP, AMP and adenosine following incubation of ATP (100  $\mu$ M) for 0 or 30 minutes with THP-1 cells. (D) Bar chart showing mean peak heights for ATP, ADP, AMP and adenosine following incubation of ATP (100  $\mu$ M) for 0 or 30 minutes in the absence of THP-1 cells. Mean peak heights represent mean  $\pm$  SEM for  $n=4$  experiments. Asterisks indicate significant changes towards vehicle at 0 minutes (\* $p<0.05$ , \*\* $p<0.01$ , Students t-test).

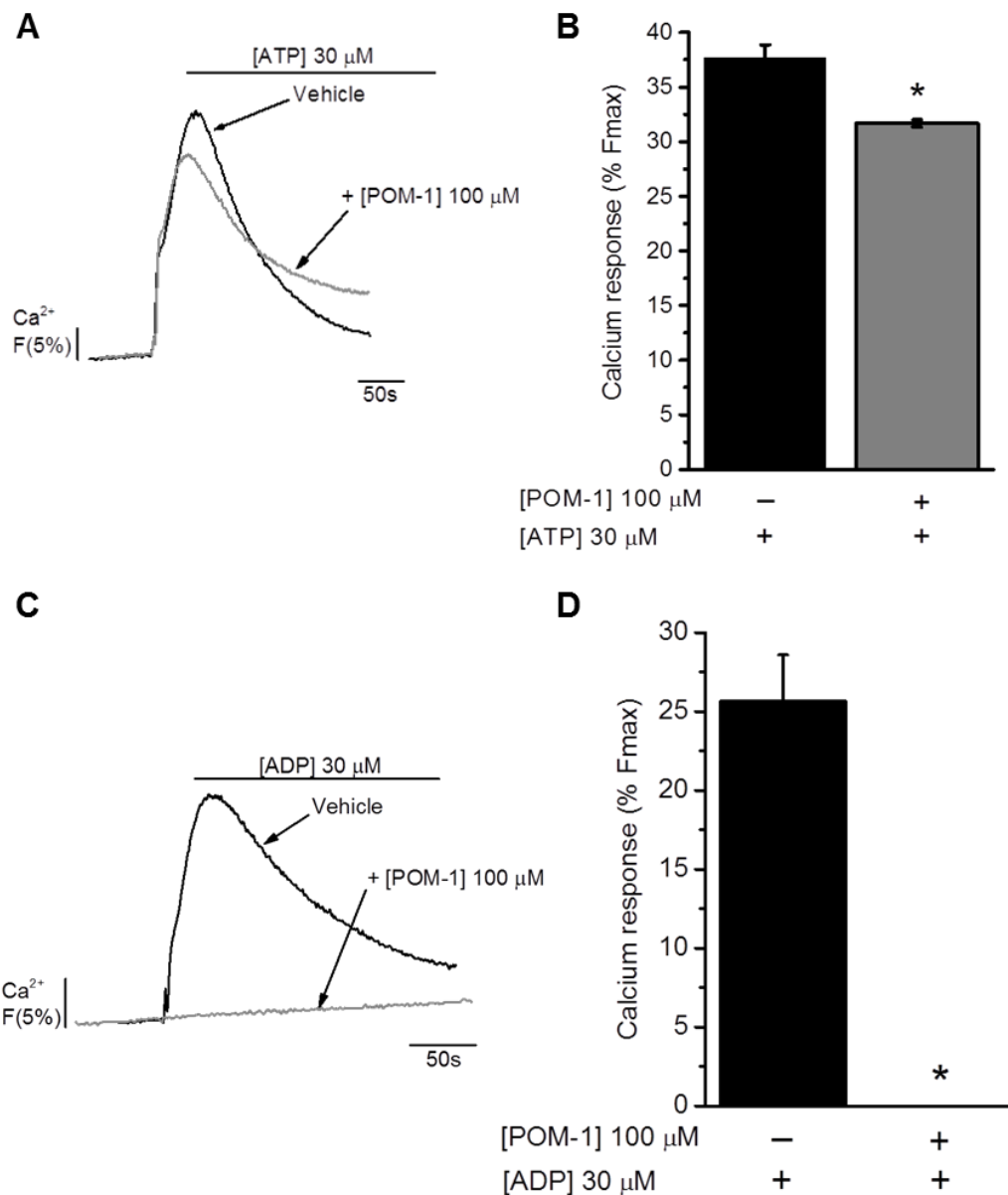


**Figure A11 Effect of POM-1 on ATP- and ADP-evoked Ca<sup>2+</sup> responses in THP-1 cells**

(A) Representative Ca<sup>2+</sup> transients and (B) bar chart showing normalised intracellular Ca<sup>2+</sup> responses to ATP (30  $\mu$ M) in THP-1 cells pre-treated with vehicle (water) or POM-1 (100  $\mu$ M) for 15 minutes. (C) Representative Ca<sup>2+</sup> transients and (D) bar chart showing normalised intracellular Ca<sup>2+</sup> responses to ADP (30  $\mu$ M) in THP-1 cells pre-treated with vehicle (water) or POM-1 (100  $\mu$ M) for 15 minutes. Responses normalised to Ca<sup>2+</sup> signals elicited by 40  $\mu$ M digitonin (%Fmax). Data represents mean  $\pm$  SEM from n=3 replicates. Asterisks indicate significant changes towards vehicle (\*p<0.05, Students t-test).

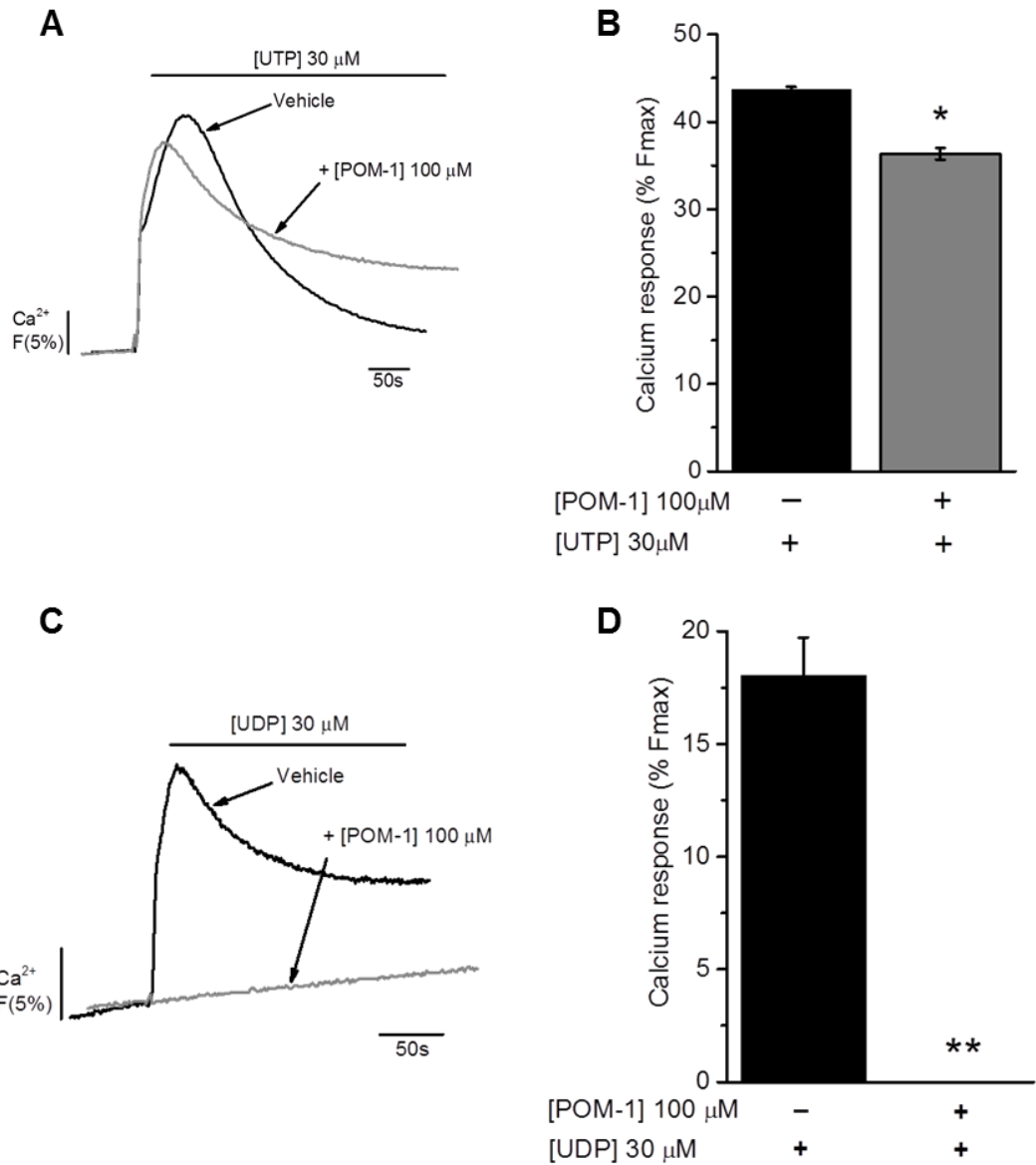


**Figure A12 Effect of POM-1 on UTP- and UDP-evoked Ca<sup>2+</sup> responses in THP-1 cells**

(A) Representative Ca<sup>2+</sup> transients and (B) bar chart showing normalised intracellular Ca<sup>2+</sup> responses to UTP (30  $\mu$ M) in THP-1 cells pre-treated with vehicle (water) or POM-1 (100  $\mu$ M) for 15 minutes. (C) Representative Ca<sup>2+</sup> transients and (D) bar chart showing normalised intracellular Ca<sup>2+</sup> responses to UDP (30  $\mu$ M) in THP-1 cells pre-treated with vehicle (water) or POM-1 (100  $\mu$ M) for 15 minutes. Responses normalised to Ca<sup>2+</sup> signals elicited by 40  $\mu$ M digitonin (%Fmax). Data represents mean  $\pm$  SEM from n=3 replicates. Asterisks indicate significant changes towards vehicle (\*p<0.05, \*\*p<0.01, Students t-test).

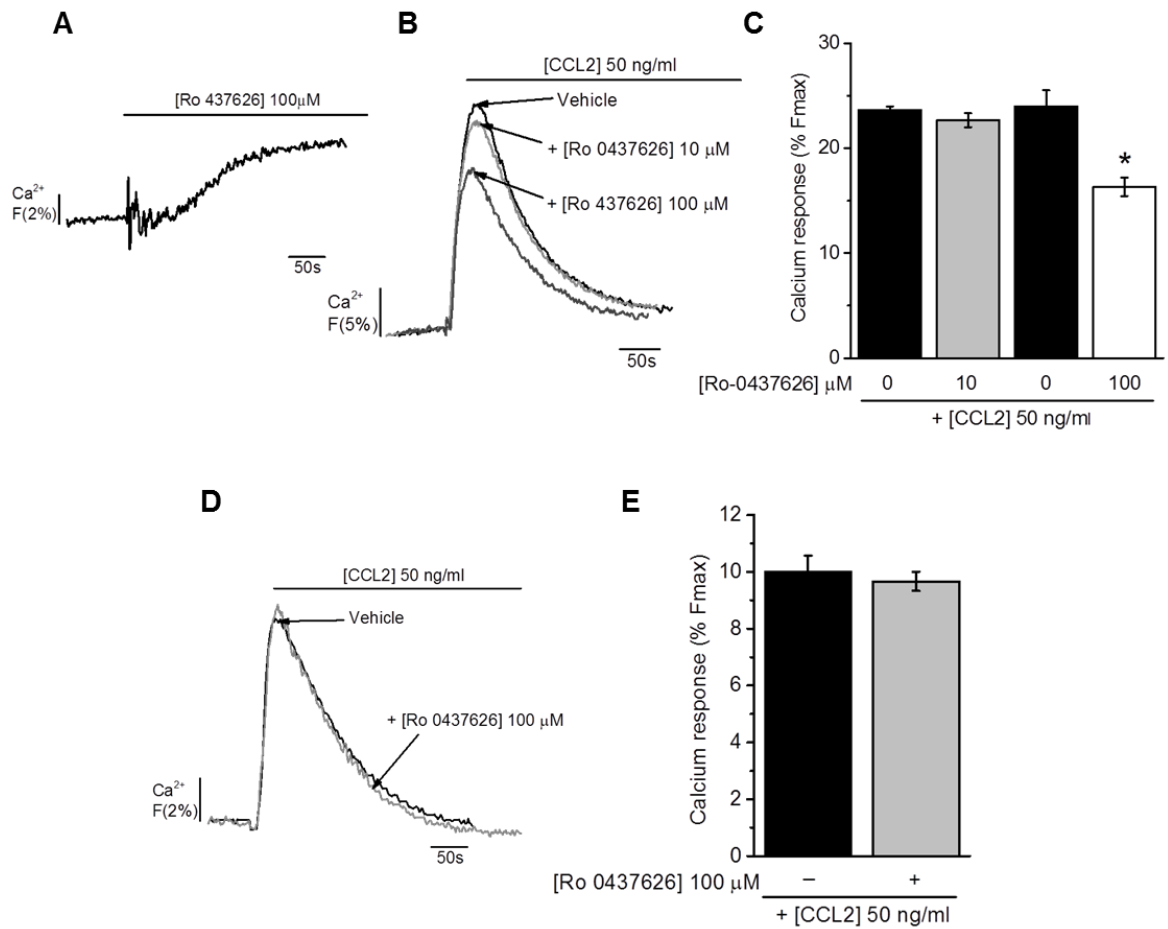


**Figure A13 Effect of Ro-0437626 on CCL2-evoked  $\text{Ca}^{2+}$  responses in THP-1 cells**

(A) Representative trace showing the effect of 100  $\mu\text{M}$  Ro 0437626 on baseline  $\text{Ca}^{2+}$ . (B) Representative  $\text{Ca}^{2+}$  transients and (C) bar chart showing normalised intracellular  $\text{Ca}^{2+}$  responses to CCL2 (50 ng/ml) in THP-1 cells pre-treated with vehicle (DMSO) or Ro-0437626 (10 or 100  $\mu\text{M}$ ), for 15 minutes in the presence of extracellular  $\text{Ca}^{2+}$ . (D) Representative  $\text{Ca}^{2+}$  transients and (E) bar chart showing normalised intracellular  $\text{Ca}^{2+}$  responses to CCL2 (50 ng/ml) in THP-1 cells pre-treated with vehicle (DMSO) or Ro 0437626 (100  $\mu\text{M}$ ), for 15 minutes in the absence of extracellular  $\text{Ca}^{2+}$ . Responses normalised to  $\text{Ca}^{2+}$  signals elicited by 40  $\mu\text{M}$  digitonin (%Fmax). Data represents mean  $\pm$  SEM from  $n=3$  replicates. Asterisks indicate significant changes towards vehicle ( $*p<0.05$ , Students t-test).

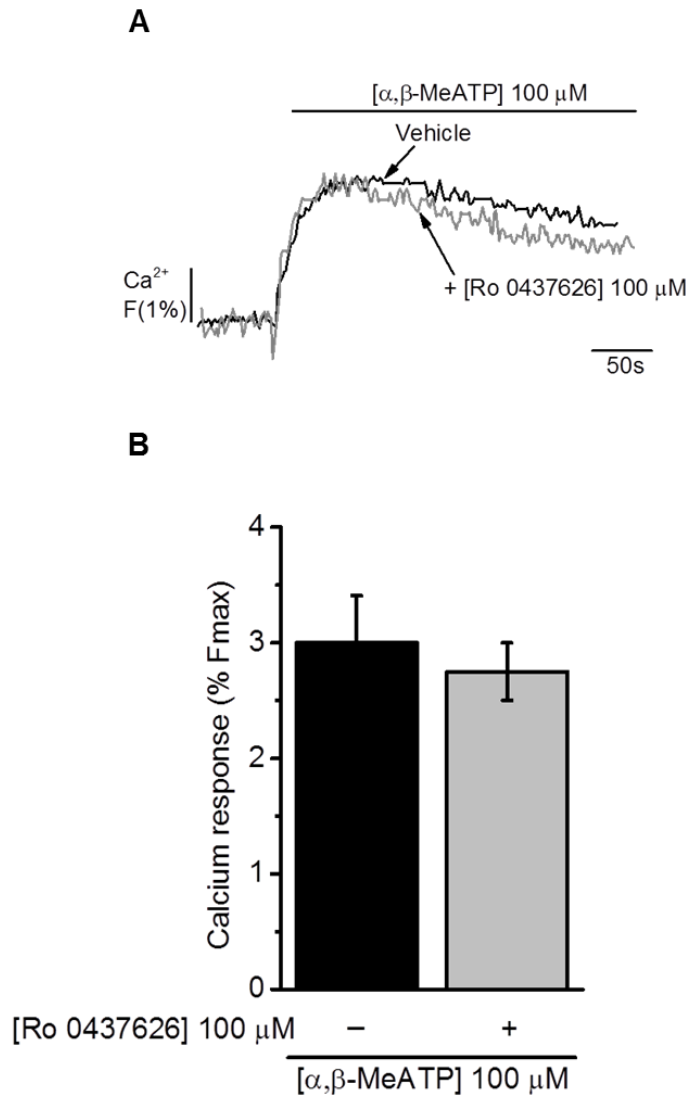


**Figure A14 Effect of Ro-0437626 on  $\alpha,\beta$ -MeATP-evoked  $\text{Ca}^{2+}$  responses in THP-1 cells**

(A) Representative  $\text{Ca}^{2+}$  transients to  $\alpha,\beta$ -MeATP (100  $\mu\text{M}$ ) in THP-1 cells pre-treated with vehicle (DMSO) or Ro 0437626 (100  $\mu\text{M}$ ) for 15 minutes. (B) Bar chart showing normalised intracellular  $\text{Ca}^{2+}$  responses to  $\alpha,\beta$ -MeATP (100  $\mu\text{M}$ ) in THP-1 cells pre-treated with vehicle (DMSO) or Ro 0437626 (100  $\mu\text{M}$ ) for 15 minutes. Responses normalised to  $\text{Ca}^{2+}$  signals elicited by 40  $\mu\text{M}$  digitonin (%Fmax). Data represents mean  $\pm$  SEM from n=3 replicates.

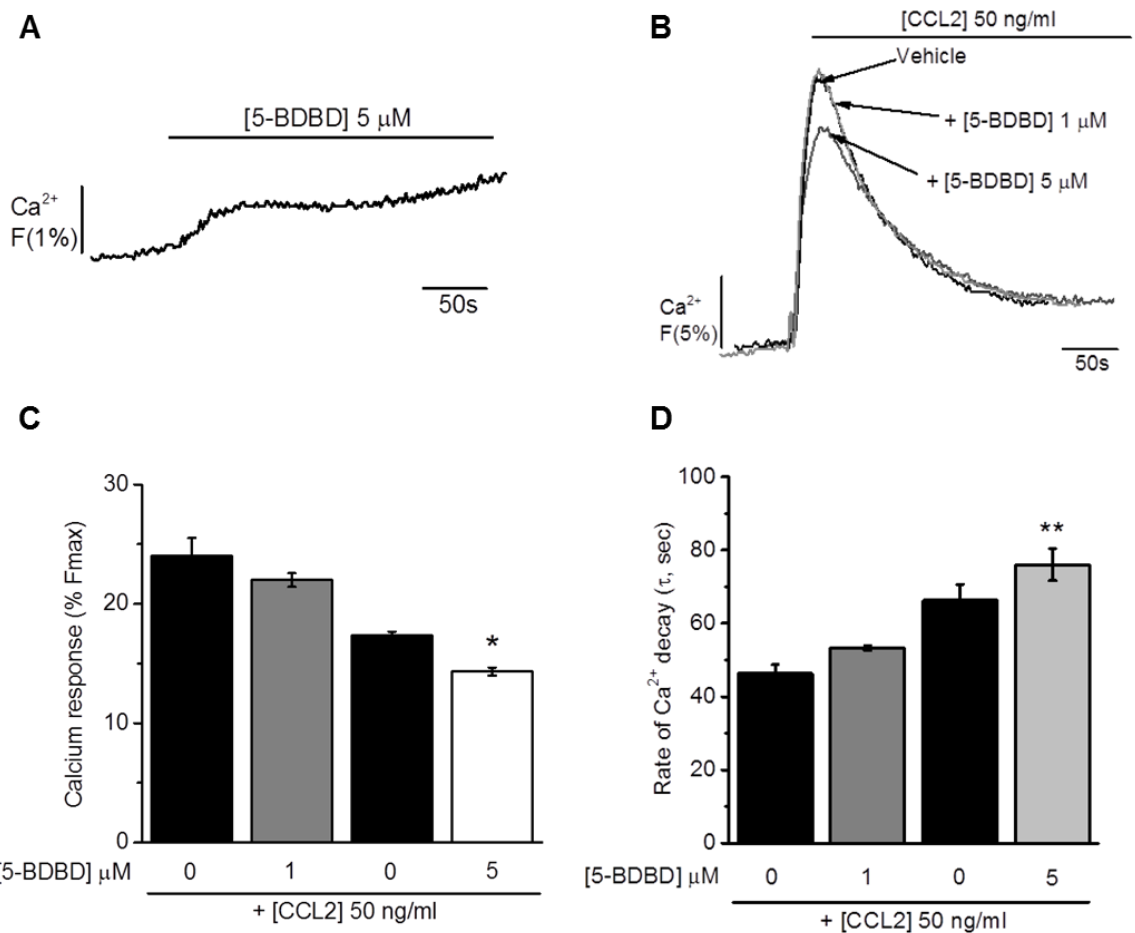


**Figure A15 Effect of 5-BDBD on CCL2-evoked Ca<sup>2+</sup> responses in THP-1 cells**

(A) Representative trace showing the effect of 5  $\mu\text{M}$  5-BDBD on baseline Ca<sup>2+</sup>. (B) Representative Ca<sup>2+</sup> transients and (C) bar chart showing normalised intracellular Ca<sup>2+</sup> responses to CCL2 (50 ng/ml) in THP-1 cells pre-treated with vehicle (DMSO) or 5-BDBD (1 or 5  $\mu\text{M}$ ), for 15 minutes. Responses normalised to Ca<sup>2+</sup> signals elicited by 40  $\mu\text{M}$  digitonin (% Fmax). (D) Bar chart showing Ca<sup>2+</sup> decay rates ( $\tau$ , sec) for Ca<sup>2+</sup> transients to CCL2 (50 ng/ml) in THP-1 cells pre-treated with vehicle (DMSO) or 5-BDBD (1 or 5  $\mu\text{M}$ ), for 15 minutes. Data represents mean  $\pm$  SEM from n=3 replicates. Asterisks indicate significant changes towards vehicle (\*\*p<0.01, \*p<0.05, Students t-test).

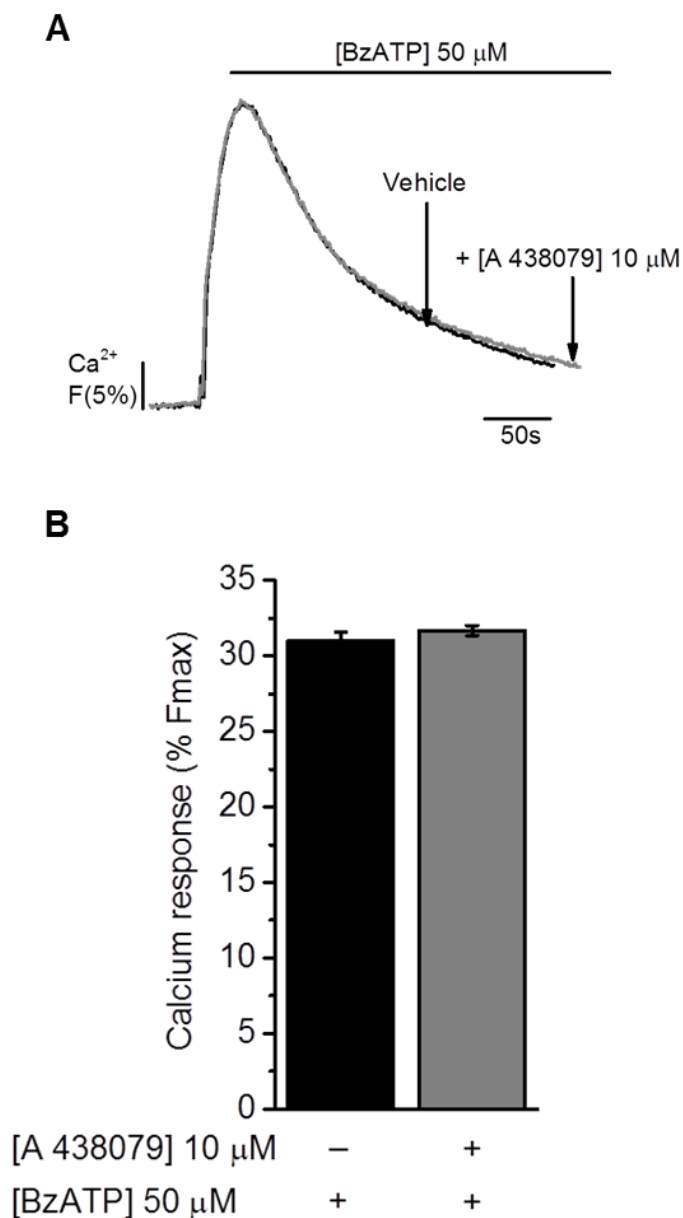


**Figure A16 Effect of A 438079 on BzATP-evoked  $\text{Ca}^{2+}$  responses in THP-1 cells**

(A) Representative  $\text{Ca}^{2+}$  transients to BzATP (50  $\mu\text{M}$ ) in THP-1 cells pre-treated with vehicle (DMSO) or A 438079 (10  $\mu\text{M}$ ) for 15 minutes. (B) Bar chart showing normalised intracellular  $\text{Ca}^{2+}$  responses to BzATP (50  $\mu\text{M}$ ) in THP-1 cells pre-treated with vehicle (DMSO) or A 438079 (10  $\mu\text{M}$ ) for 15 minutes. Responses normalised to  $\text{Ca}^{2+}$  signals elicited by 40  $\mu\text{M}$  digitonin (%Fmax). Data represents mean  $\pm$  SEM from n=3 replicates.

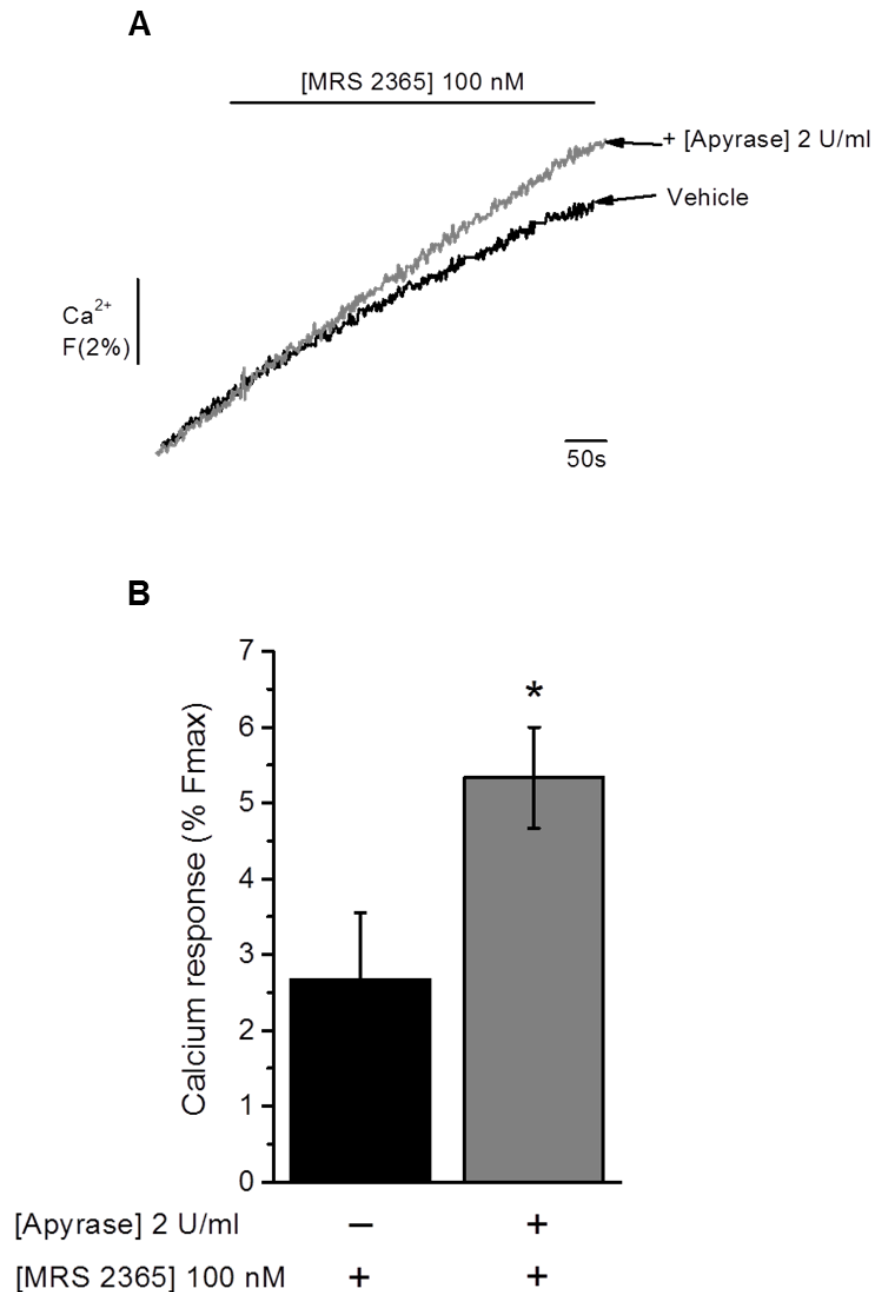


**Figure A17 Effect of apyrase on MRS 2365-evoked Ca<sup>2+</sup> responses in THP-1 cells**

(A) Representative Ca<sup>2+</sup> transients to MRS 2365 (100 nM) in THP-1 cells pre-treated with vehicle (water) or apyrase (2 U/ml) for 10 minutes. (B) Bar chart showing normalised intracellular Ca<sup>2+</sup> responses to MRS 2365 (100 nM) in THP-1 cells pre-treated with vehicle (water) or apyrase (2 U/ml) for 10 minutes. Responses normalised to Ca<sup>2+</sup> signals elicited by 40  $\mu$ M digitonin (%Fmax). Data represents mean  $\pm$  SEM from n=3 replicates. Asterisks indicate significant changes towards vehicle (\*p<0.05, Students t-test).

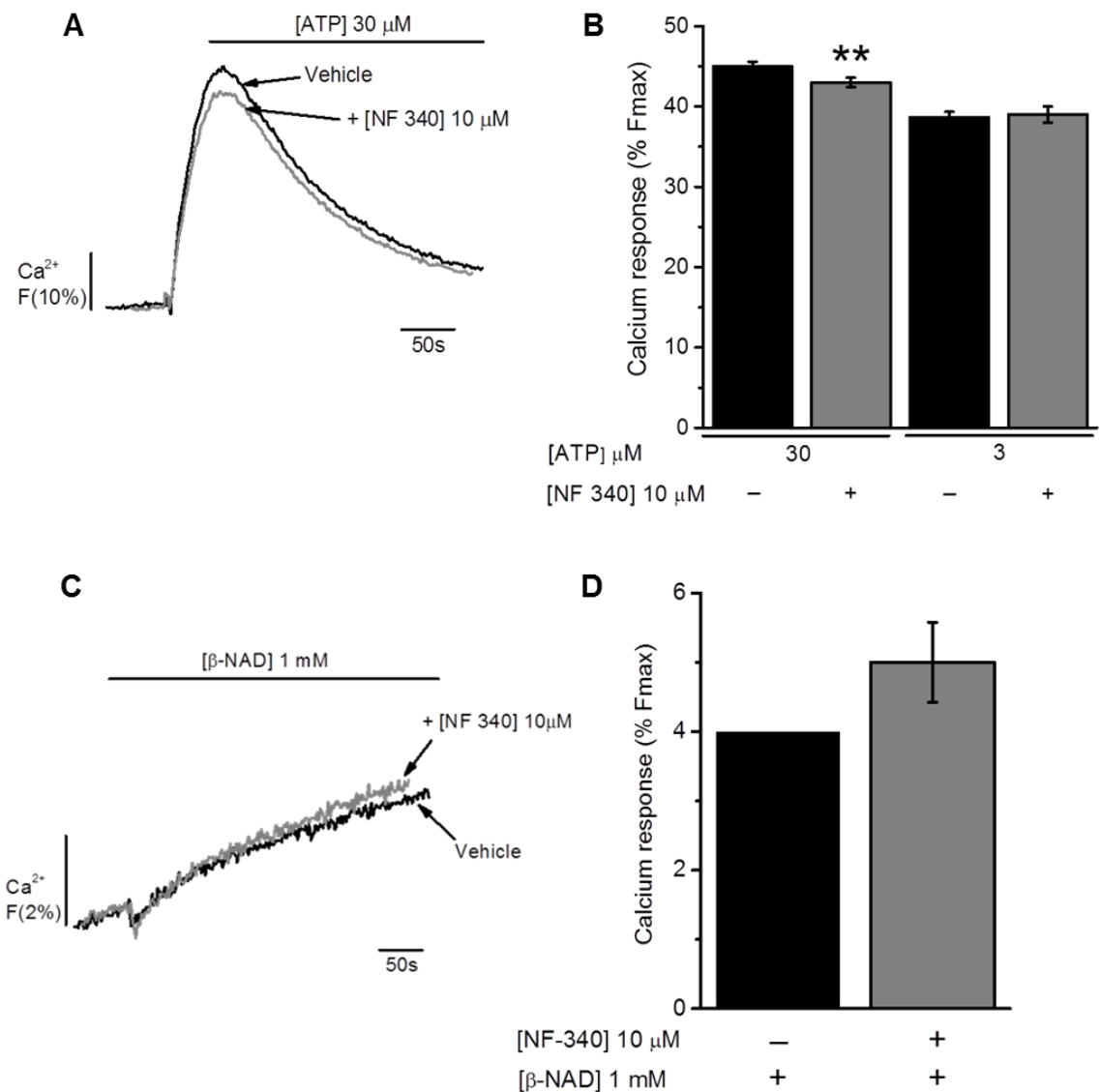


**Figure A18 Effect of NF-340 on ATP- and  $\beta$ NAD-evoked Ca<sup>2+</sup> responses in THP-1 cells**

Representative Ca<sup>2+</sup> transients to (A) ATP (30  $\mu$ M) and (C)  $\beta$ -NAD (1 mM) in THP-1 cells pre-treated with vehicle (DMSO) or NF-340 (10  $\mu$ M) for 15 minutes. Bar chart showing normalised intracellular Ca<sup>2+</sup> responses to (B) ATP (3 and 30  $\mu$ M) and (D)  $\beta$ -NAD (1 mM) in THP-1 cells pre-treated with vehicle (DMSO) or NF 340 (10  $\mu$ M) for 15 minutes. Responses normalised to Ca<sup>2+</sup> signals elicited by 40  $\mu$ M digitonin (%Fmax). Data represents mean  $\pm$  SEM from n=3 replicates. Asterisks indicate significant changes towards vehicle (\*\*p<0.01, Students t-test).

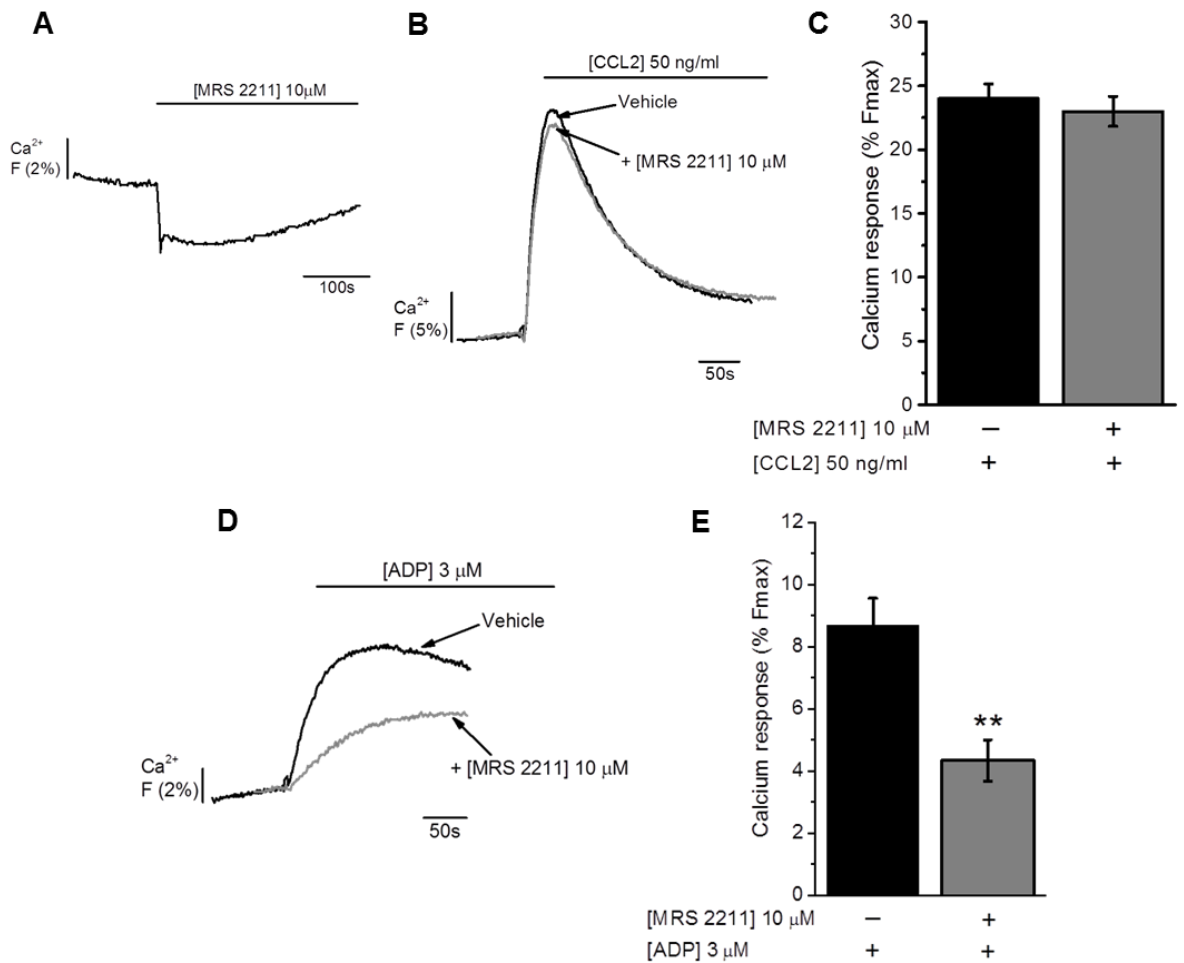


**Figure A19 Effect of MRS-2211 on CCL2- and ADP-evoked  $\text{Ca}^{2+}$  responses in THP-1 cells**

(A) Representative trace showing the effect of MRS-2211 on baseline  $\text{Ca}^{2+}$ . Representative  $\text{Ca}^{2+}$  transients to (B) CCL2 (50 ng/ml) and (D) ADP (3  $\mu\text{M}$ ) in THP-1 cells pre-treated with vehicle (water) or MRS 2211 (10  $\mu\text{M}$ ) for 15 minutes. Bar chart showing normalised intracellular  $\text{Ca}^{2+}$  responses to (C) CCL2 (50 ng/ml) and (E) ADP (3  $\mu\text{M}$ ) in THP-1 cells pre-treated with vehicle (water) or MRS 2211 (10  $\mu\text{M}$ ) for 15 minutes. Responses normalised to  $\text{Ca}^{2+}$  signals elicited by 40  $\mu\text{M}$  digitonin (%Fmax). Data represents mean  $\pm$  SEM from n=3 replicates. Asterisks indicate significant changes towards vehicle (\*\*p<0.01, Students t-test).

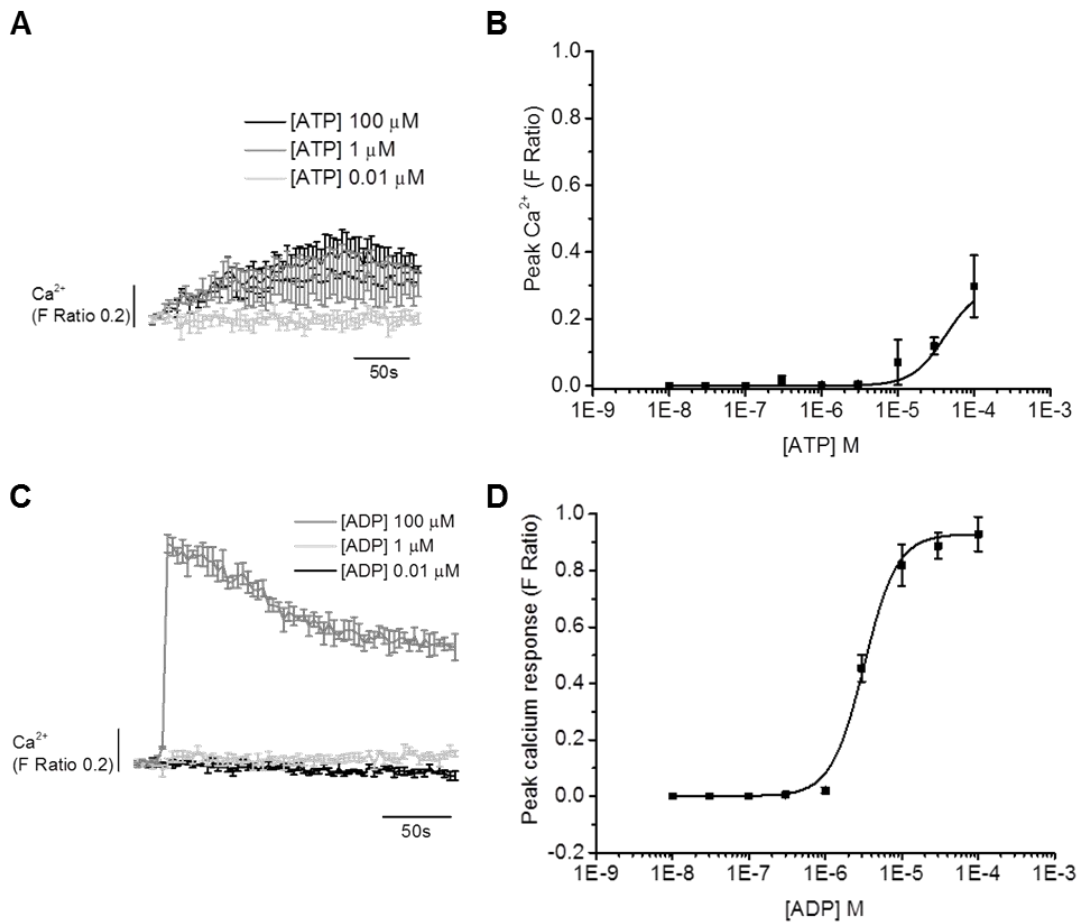


**Figure A20 ATP- and ADP-evoked Ca<sup>2+</sup> responses in P2Y<sub>6</sub>-stable 1321N1 cells**

ATP- and ADP-evoked intracellular Ca<sup>2+</sup> responses in P2Y<sub>6</sub>-stable 1321N1 cells. Representative Ca<sup>2+</sup> transients to (A) ATP (100  $\mu$ M, 1  $\mu$ M and 0.01  $\mu$ M) and (C) ADP (100  $\mu$ M, 1  $\mu$ M and 0.01  $\mu$ M) in P2Y<sub>6</sub>-stable 1321N1 cells. Concentration-response curve showing normalised intracellular Ca<sup>2+</sup> responses to (B) ATP (10 nM – 100  $\mu$ M) and (D) ADP (10 nM – 100  $\mu$ M) in P2Y<sub>6</sub>-transfected 1321N1 cells. Responses normalised to peak Ca<sup>2+</sup> response by subtracting F Ratios for vehicle (SBS) treated cells from F Ratios for ATP- or ADP-treated cells. Data represents mean  $\pm$  SEM from a total of n=9 replicates from n=3 experiments.

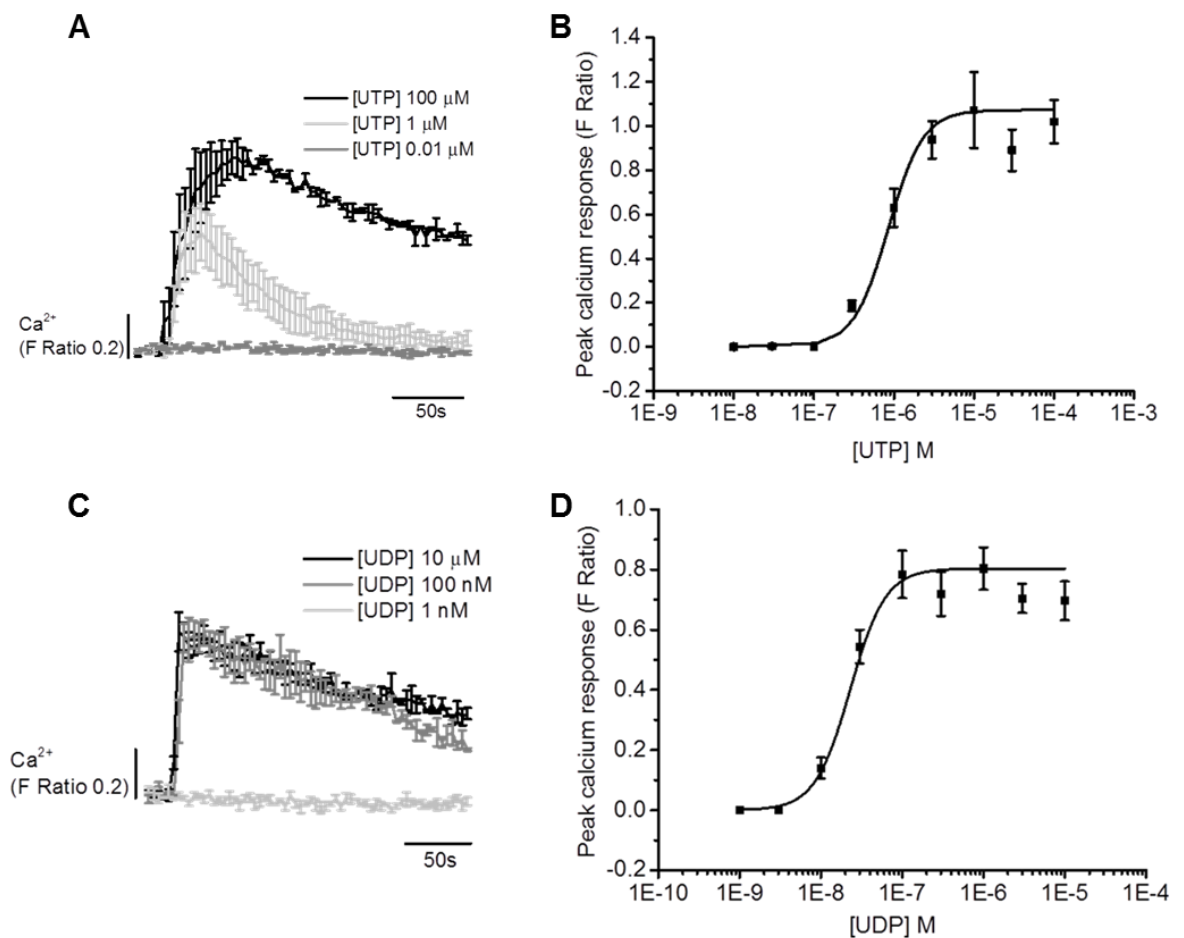


**Figure A21 UTP- and UDP-evoked Ca<sup>2+</sup> responses in P2Y<sub>6</sub>-stable 1321N1 cells**

UTP- and UDP-evoked intracellular Ca<sup>2+</sup> responses in P2Y<sub>6</sub>-stable 1321N1 cells. Representative Ca<sup>2+</sup> transients to (A) UTP (100  $\mu$ M, 1  $\mu$ M and 0.01  $\mu$ M) and (C) UDP (10  $\mu$ M, 100 nM, and 1 nM) in P2Y<sub>6</sub>-stable 1321N1 cells. Concentration-response curve showing normalised intracellular Ca<sup>2+</sup> responses to (B) UTP (10 nM – 100  $\mu$ M) and (D) UDP (1 nM – 10  $\mu$ M) in P2Y<sub>6</sub>-transfected 1321N1 cells. Responses normalised to peak Ca<sup>2+</sup> response by subtracting F Ratios for vehicle (SBS) treated cells from F Ratios for UTP- or UDP-treated cells. Data represents mean  $\pm$  SEM from a total of n=9 replicates from n=3 experiments.

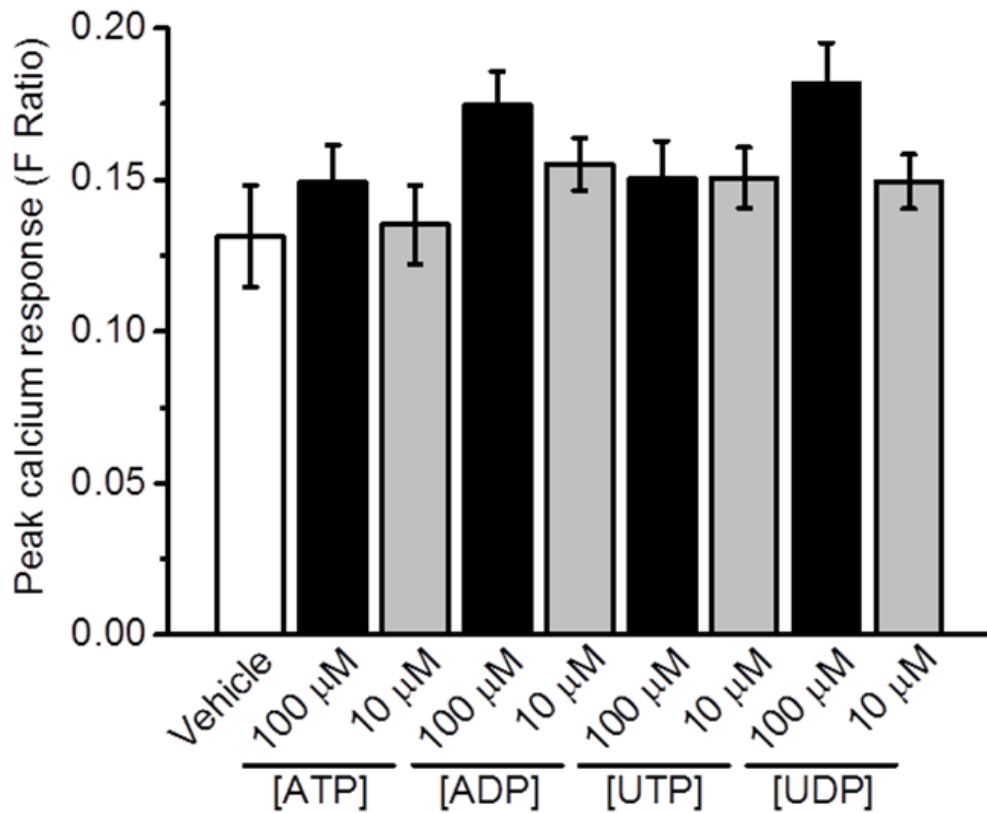


**Figure A22 Extracellular nucleotide-evoked  $\text{Ca}^{2+}$  responses in parental 1321N1 cells**

Extracellular nucleotides (ATP, ADP, UTP and UDP) were unable to evoke intracellular  $\text{Ca}^{2+}$  responses in parental 1321N1 cells. Bar chart showing peak intracellular  $\text{Ca}^{2+}$  responses (F Ratio) in 1321N1 cells challenged with vehicle (SBS) or ATP, ADP, UTP and UDP (10 and 100  $\mu\text{M}$ ). Data represents mean  $\pm$  SEM from a total of n=9 replicates from n=3 experiments.  $p > 0.05$  for all treatments

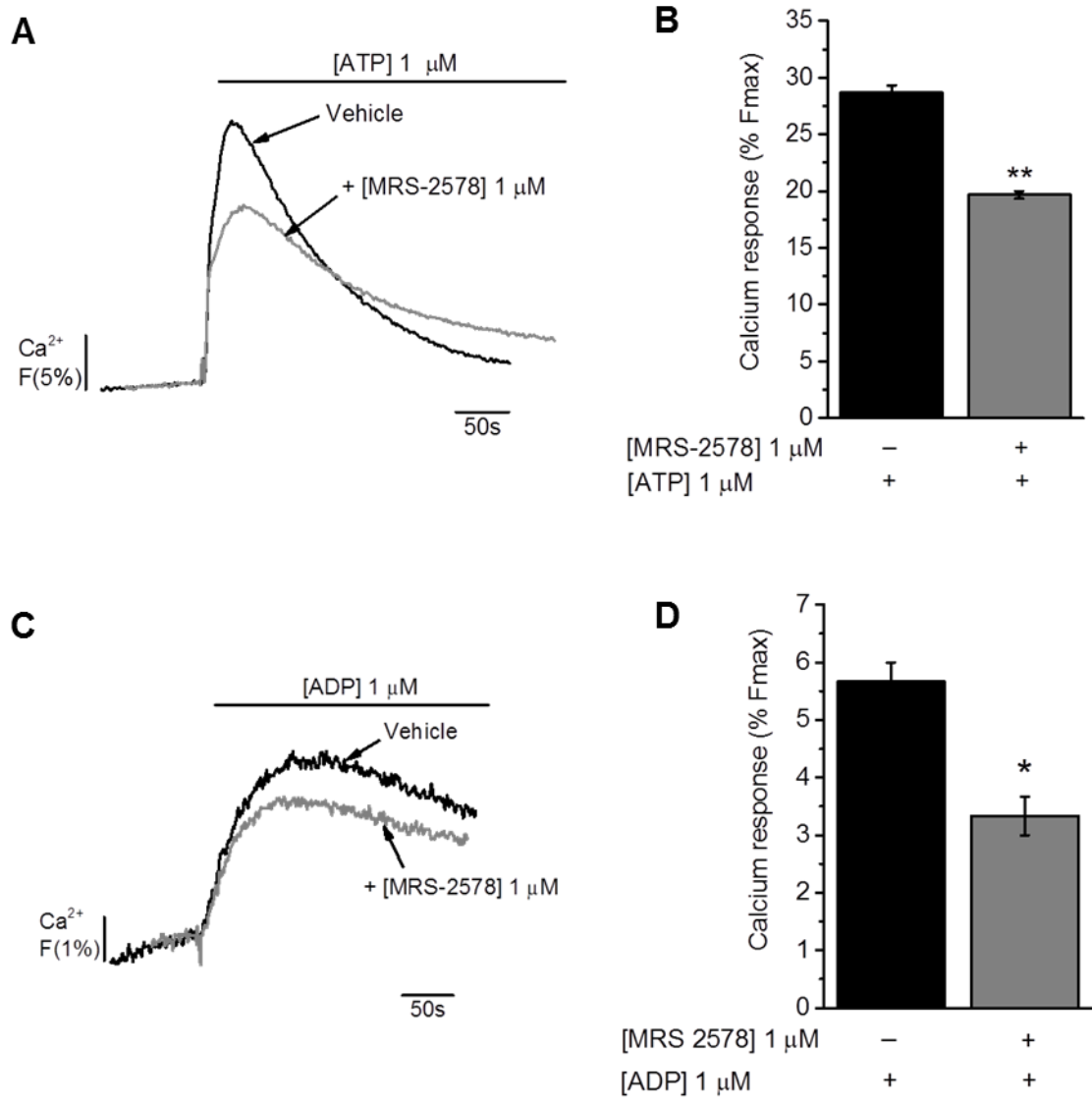


**Figure A23 Effect of MRS-2578 on ATP- and ADP-evoked Ca<sup>2+</sup> responses in THP-1 cells**

Representative Ca<sup>2+</sup> transients to (A) ATP (1  $\mu$ M) and (C) ADP (1  $\mu$ M) in THP-1 cells pre-treated with vehicle (DMSO) or MRS-2578 (1  $\mu$ M) for 15 minutes. Bar chart showing normalised intracellular Ca<sup>2+</sup> responses to (B) ATP (1  $\mu$ M) and (D) ADP (1  $\mu$ M) in THP-1 cells pre-treated with vehicle (DMSO) or MRS-2578 (1  $\mu$ M) for 15 minutes. Responses normalised to Ca<sup>2+</sup> signals elicited by 40  $\mu$ M digitonin (%Fmax). Data represents mean  $\pm$  SEM from n=3 replicates. Asterisks indicate significant changes towards vehicle (\*p<0.05, \*\*p<0.01, Students t-test).

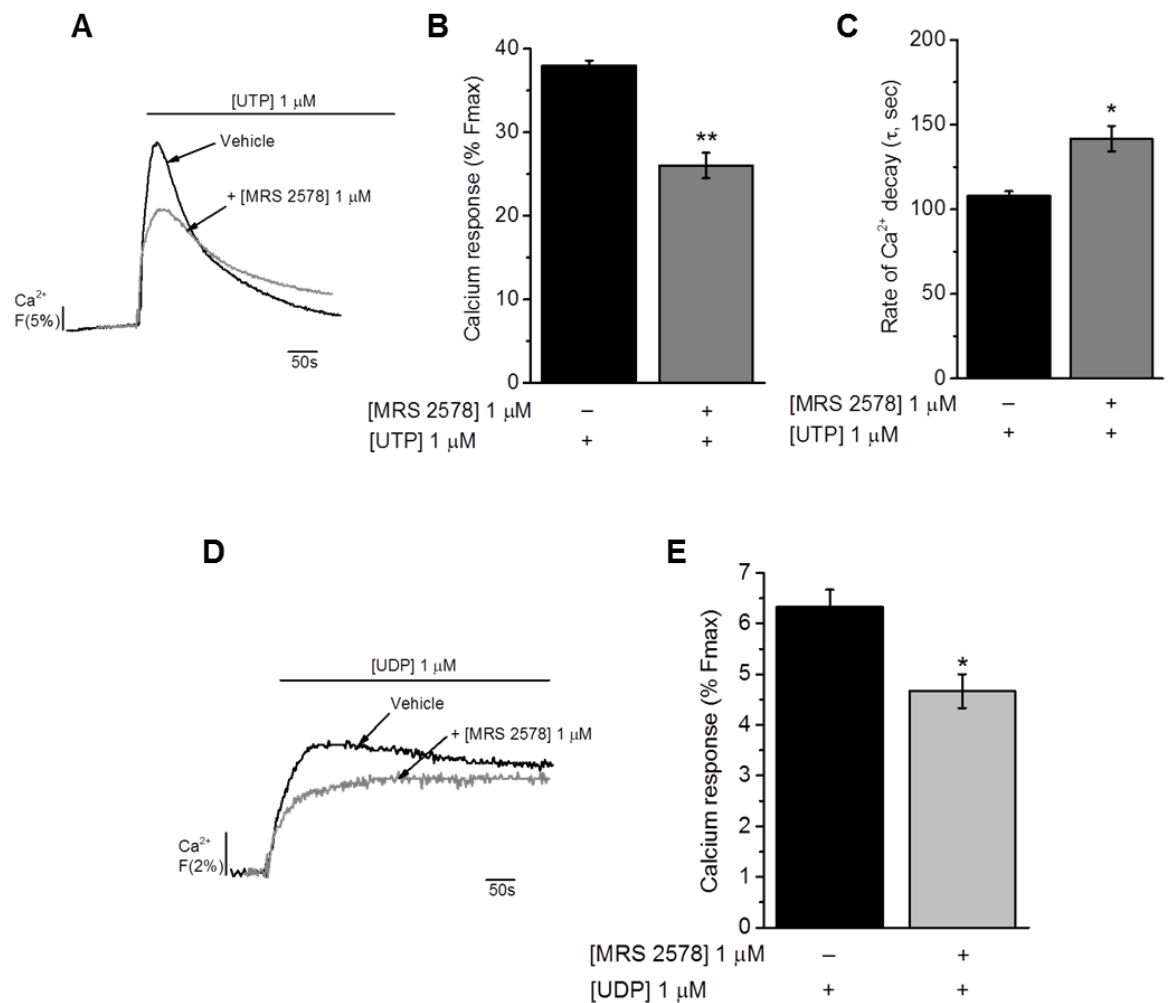


**Figure A24 Effect of MRS-2578 on UTP and UDP-evoked Ca<sup>2+</sup> responses in THP-1 cells**

Representative Ca<sup>2+</sup> transients to (A) UTP (1  $\mu$ M) and (D) UDP (1  $\mu$ M) in THP-1 cells pre-treated with vehicle (DMSO) or MRS-2578 (1  $\mu$ M) for 15 minutes. Bar chart showing normalised intracellular Ca<sup>2+</sup> responses to (B) UTP (1  $\mu$ M) and (E) UDP (1  $\mu$ M) in THP-1 cells pre-treated with vehicle (DMSO) or MRS-2578 (1  $\mu$ M) for 15 minutes. (C) Bar chart showing Ca<sup>2+</sup> decay rates ( $\tau$ , sec) for Ca<sup>2+</sup> transients to UTP (1  $\mu$ M) in THP-1 cells pre-treated with vehicle (DMSO) or MRS-2578 (1  $\mu$ M) for 15 minutes. Responses normalised to Ca<sup>2+</sup> signals elicited by 40  $\mu$ M digitonin (%Fmax). Data represents mean  $\pm$  SEM from n=3 replicates. Asterisks indicate significant changes towards vehicle (\* $p$ <0.05, \*\* $p$ <0.01, Students t-test).

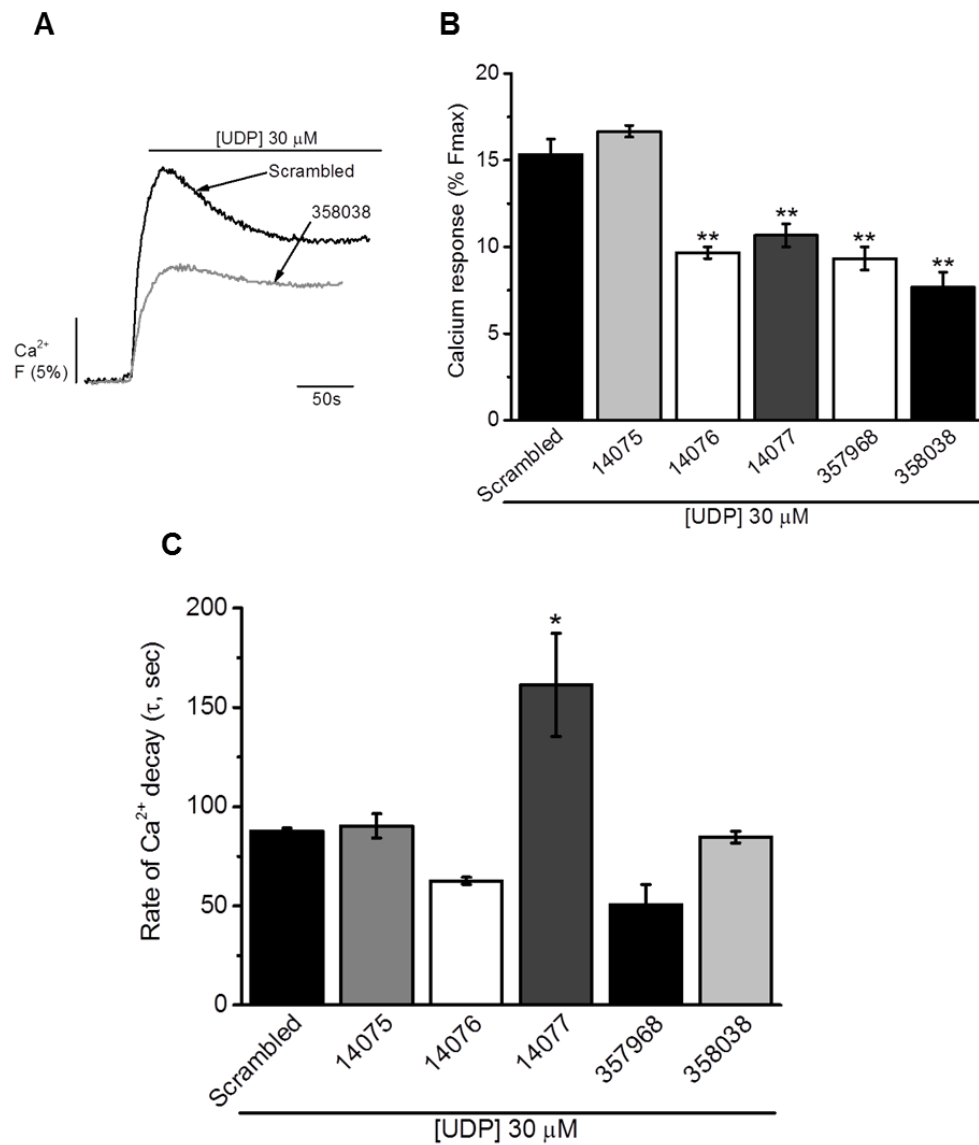


**Figure A25 UDP-evoked Ca<sup>2+</sup> responses in scrambled and *P2RY6*-KD THP-1 cells**

(A) Representative UDP (30  $\mu$ M) Ca<sup>2+</sup> transients in scrambled and 358038 THP-1 cells. (B) Bar chart showing normalised (30  $\mu$ M) UDP-evoked intracellular Ca<sup>2+</sup> responses in THP-1 cells transduced with non-target (scrambled) or *P2YR6*-shRNA sequences 14075, 14076, 14077, 357968 and 358038. (C) Bar chart showing decay rates ( $\tau$ , sec) for UDP (30  $\mu$ M) Ca<sup>2+</sup> transients in THP-1 cells transduced with non-target or *P2YR6*-shRNA sequences. Responses normalised to Ca<sup>2+</sup> signals elicited by 40  $\mu$ M digitonin (%Fmax). Data represents mean  $\pm$  SEM from n=3 paired replicates. Asterisks indicate significant changes towards scrambled (\*p<0.05, \*\*p<0.01, One-way ANOVA with Bonferroni's multiple comparison).

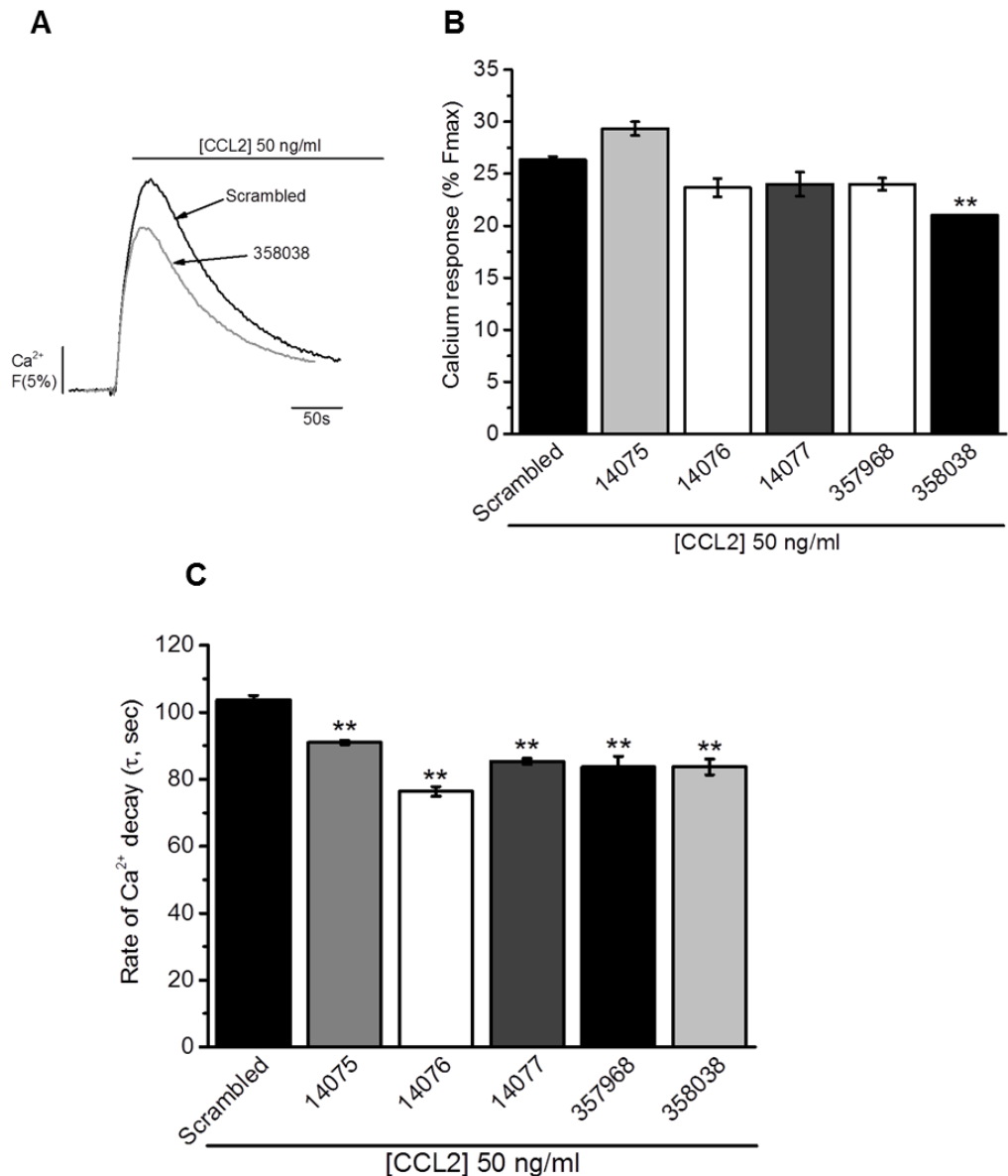


**Figure A26 CCL2-evoked Ca<sup>2+</sup> responses in scrambled and *P2RY6*-KD THP-1 cells**

(A) Representative CCL2 (50 ng/ml) Ca<sup>2+</sup> transients in THP-1 cells transduced with non-target (scrambled) shRNA and *P2RY6*-shRNA 358038. (B) Bar chart showing normalised (50 ng/ml) CCL2-evoked intracellular Ca<sup>2+</sup> responses in THP-1 cells transduced with non-target (scrambled) or *P2RY6*-shRNA sequences 14075, 14076, 14077, 357968 and 358038. (C) Bar chart showing decay rates (τ, sec) for CCL2 (50 ng/ml) Ca<sup>2+</sup> transients in THP-1 cells transduced with non-target or *P2RY6*-shRNA sequences. Responses normalised to Ca<sup>2+</sup> signals elicited by 40 μM digitonin (% Fmax). Data represents mean ± SEM from n=3 replicates. Asterisks indicate significant changes towards scrambled (\*\*p<0.01, One-way ANOVA with Bonferroni's multiple comparison).

# References

---

- Abbadie, C, Lindia, JA, Cumiskey, AM, Peterson, LB, Mudgett, JS, Bayne, EK, Demartino, JA, Macintyre, DE & Forrest, MJ (2003). Impaired neuropathic pain responses in mice lacking the chemokine receptor CCR2. *Proc Natl Acad Sci U S A*, **100**, 7947-52.
- Abbracchio, MP, Burnstock, G, Boeynaems, JM, Barnard, EA, Boyer, JL, Kennedy, C, Knight, GE, Fumagalli, M, Gachet, C, Jacobson, KA & Weisman, GA (2006). International Union of Pharmacology LVIII: update on the P2Y G-protein-coupled nucleotide receptors: from molecular mechanisms and pathophysiology to therapy. *Pharmacol Rev*, **58**, 281-341.
- Akashi, K, Traver, D, Miyamoto, T & Weissman, IL (2000). A clonogenic common myeloid progenitor that gives rise to all myeloid lineages. *Nature*, **404**, 193-7.
- Akeson, AL & Woods, CW (1993). A fluorometric assay for the quantitation of cell adherence to endothelial cells. *J Immunol Methods*, **163**, 181-5.
- Albuquerque, EX, Pereira, EF, Alkondon, M & Rogers, SW (2009). Mammalian nicotinic acetylcholine receptors: from structure to function. *Physiol Rev*, **89**, 73-120.
- Aldo, PB, Craveiro, V, Guller, S & Mor, G (2013). Effect of culture conditions on the phenotype of THP-1 monocyte cell line. *Am J Reprod Immunol*, **70**, 80-6.
- Allen, SJ, Crown, SE & Handel, TM (2007). Chemokine: receptor structure, interactions, and antagonism. *Annu Rev Immunol*, **25**, 787-820.
- Altieri, DC, Wiltse, WL & Edgington, TS (1990). Signal transduction initiated by extracellular nucleotides regulates the high affinity ligand recognition of the adhesive receptor CD11b/CD18. *J Immunol*, **145**, 662-70.
- Anastassiadis, T, Deacon, SW, Devarajan, K, Ma, H & Peterson, JR (2011). Comprehensive assay of kinase catalytic activity reveals features of kinase inhibitor selectivity. *Nat Biotechnol*, **29**, 1039-45.
- Apostolakis, S, Vlata, Z, Vogiatzi, K, Krambovitis, E & Spandidos, DA (2010). Angiotensin II up-regulates CX<sub>3</sub>CR1 expression in THP-1 monocytes: impact on vascular inflammation and atherogenesis. *J Thromb Thrombolysis*, **29**, 443-8.
- Arai, H, Tsou, CL & Charo, IF (1997). Chemotaxis in a lymphocyte cell line transfected with C-C chemokine receptor 2B: evidence that directed migration is mediated by betagamma dimers released by activation of G $\alpha$ hi-coupled receptors. *Proc Natl Acad Sci U S A*, **94**, 14495-9.

Auffray, C, Fogg, D, Garfa, M, Elain, G, Join-Lambert, O, Kayal, S, Sarnacki, S, Cumano, A, Lauvau, G & Geissmann, F (2007). Monitoring of blood vessels and tissues by a population of monocytes with patrolling behavior. *Science*, **317**, 666-70.

Auffray, C, Sieweke, MH & Geissmann, F (2009). Blood monocytes: development, heterogeneity, and relationship with dendritic cells. *Annu Rev Immunol*, **27**, 669-92.

Auwerx, J (1991). The human leukemia cell line, THP-1: a multifaceted model for the study of monocyte-macrophage differentiation. *Experientia*, **47**, 22-31.

Avni, D, Glucksam, Y & Zor, T (2012). The phosphatidylinositol 3-kinase (PI3K) inhibitor LY294002 modulates cytokine expression in macrophages via p50 nuclear factor kappaB inhibition, in a PI3K-independent mechanism. *Biochem Pharmacol*, **83**, 106-14.

Ayyanathan, K, Webbs, TE, Sandhu, AK, Athwal, RS, Barnard, EA & Kunapuli, SP (1996). Cloning and chromosomal localization of the human P2Y<sub>1</sub> purinoceptor. *Biochem Biophys Res Commun*, **218**, 783-8.

Bachelierie, F, Ben-Baruch, A, Burkhardt, AM, Combadiere, C, Farber, JM, Graham, GJ, Horuk, R, Sparre-Ulrich, AH, Locati, M, Luster, AD, Mantovani, A, Matsushima, K, Murphy, PM, Nibbs, R, Nomiyama, H, Power, CA, Proudfoot, AE, Rosenkilde, MM, Rot, A, Sozzani, S, Thelen, M, Yoshie, O & Zlotnik, A (2014). International Union of Basic and Clinical Pharmacology. [corrected]. LXXXIX. Update on the extended family of chemokine receptors and introducing a new nomenclature for atypical chemokine receptors. *Pharmacol Rev*, **66**, 1-79.

Balasubramanian, R, Ruiz De Azua, I, Wess, J & Jacobson, KA (2010). Activation of distinct P2Y receptor subtypes stimulates insulin secretion in MIN6 mouse pancreatic beta cells. *Biochem Pharmacol*, **79**, 1317-26.

Baldanzi, G (2014). Inhibition of diacylglycerol kinases as a physiological way to promote diacylglycerol signaling. *Adv Biol Regul*, **55**, 39-49.

Bao, L, Locovei, S & Dahl, G (2004). Pannexin membrane channels are mechanosensitive conduits for ATP. *FEBS Lett*, **572**, 65-8.

Bar, I, Guns, PJ, Metallo, J, Cammarata, D, Wilkin, F, Boeynants, JM, Bult, H & Robaye, B (2008). Knockout mice reveal a role for P2Y<sub>6</sub> receptor in macrophages, endothelial cells, and vascular smooth muscle cells. *Mol Pharmacol*, **74**, 777-84.

Barrera, NP, Ormond, SJ, Henderson, RM, Murrell-Lagnado, RD & Edwardson, JM (2005). Atomic force microscopy imaging demonstrates that P2X<sub>2</sub> receptors are trimers but that P2X<sub>6</sub> receptor subunits do not oligomerize. *J Biol Chem*, **280**, 10759-65.

- Bartlett, R, Stokes, L & Sluyter, R (2014). The P2X7 receptor channel: recent developments and the use of P2X7 antagonists in models of disease. *Pharmacol Rev*, **66**, 638-75.
- Beekhuizen, H & Van Furth, R (1993). Monocyte adherence to human vascular endothelium. *J Leukoc Biol*, **54**, 363-78.
- Ben Yebdri, F, Kukulski, F, Tremblay, A & Sevigny, J (2009). Concomitant activation of P2Y(2) and P2Y(6) receptors on monocytes is required for TLR1/2-induced neutrophil migration by regulating IL-8 secretion. *Eur J Immunol*, **39**, 2885-94.
- Berchtold, S, Ogilvie, AL, Bogdan, C, Muhl-Zurbes, P, Ogilvie, A, Schuler, G & Steinkasserer, A (1999). Human monocyte derived dendritic cells express functional P2X and P2Y receptors as well as ecto-nucleotidases. *FEBS Lett*, **458**, 424-8.
- Berg, TO, Strømhaug, E, Løvdaal, T, Seglen, O & Berg, T (1994). Use of glycyl-L-phenylalanine 2-naphthylamide, a lysosome-disrupting cathepsin C substrate, to distinguish between lysosomes and prelysosomal endocytic vacuoles, *Biochem J*. **300**(Pt 1):229-36.
- Berlin, C, Bargatze, RF, Campbell, JJ, Von Andrian, UH, Szabo, MC, Hasslen, SR, Nelson, RD, Berg, EL, Erlandsen, SL & Butcher, EC (1995). alpha 4 integrins mediate lymphocyte attachment and rolling under physiologic flow. *Cell*, **80**, 413-22.
- Bernier, LP, Ase, AR, Boue-Grabot, E & Seguela, P (2013). Inhibition of P2X4 function by P2Y<sub>6</sub> UDP receptors in microglia. *Glia*, **61**, 2038-49.
- Berridge, MJ (1983). Rapid accumulation of inositol trisphosphate reveals that agonists hydrolyse polyphosphoinositides instead of phosphatidylinositol. *Biochem J*, **212**, 849-58.
- Berridge, MJ (1993). Inositol trisphosphate and calcium signalling. *Nature*, **361**, 315-25.
- Berridge, MJ (2002). The endoplasmic reticulum: a multifunctional signaling organelle. *Cell Calcium*, **32**, 235-49.
- Berridge, MJ (2009). Inositol trisphosphate and calcium signalling mechanisms. *Biochim Biophys Acta*, **1793**, 933-40.
- Berridge, MJ, Bootman, MD & Roderick, HL (2003). Calcium signalling: dynamics, homeostasis and remodelling. *Nat Rev Mol Cell Biol*, **4**, 517-29.
- Berridge, MJ, Lipp, P & Bootman, MD (2000). The versatility and universality of calcium signalling. *Nat Rev Mol Cell Biol*, **1**, 11-21.

Bianchi, BR, Lynch, KJ, Touma, E, Niforatos, W, Burgard, EC, Alexander, KM, Park, HS, Yu, H, Metzger, R, Kowaluk, E, Jarvis, MF & Van Biesen, T (1999). Pharmacological characterization of recombinant human and rat P2X receptor subtypes. *Eur J Pharmacol*, **376**, 127-38.

Bianchi, ME (2007). DAMPs, PAMPs and alarmins: all we need to know about danger. *J Leukoc Biol*, **81**, 1-5.

Bianco, F, Fumagalli, M, Pravettoni, E, D'ambrosi, N, Volonte, C, Matteoli, M, Abbracchio, MP & Verderio, C (2005). Pathophysiological roles of extracellular nucleotides in glial cells: differential expression of purinergic receptors in resting and activated microglia. *Brain Res Brain Res Rev*, **48**, 144-56.

Bisogno, T, Howell, F, Williams, G, Minassi, A, Cascio, MG, Ligresti, A, Matias, I, Schiano-Moriello, A, Paul, P, Williams, EJ, Gangadharan, U, Hobbs, C, Di Marzo, V & Doherty, P (2003). Cloning of the first sn1-DAG lipases points to the spatial and temporal regulation of endocannabinoid signaling in the brain. *J Cell Biol*, **163**, 463-8.

Bizzarri, C, Bertini, R, Bossu, P, Sozzani, S, Mantovani, A, Van Damme, J, Tagliabue, A & Boraschi, D (1995). Single-cell analysis of macrophage chemotactic protein-1-regulated cytosolic Ca<sup>2+</sup> increase in human adherent monocytes. *Blood*, **86**, 2388-94.

Blank, JL, Brattain, KA & Exton, JH (1992). Activation of cytosolic phosphoinositide phospholipase C by G-protein beta gamma subunits. *J Biol Chem*, **267**, 23069-75.

Blanpain, C, Migeotte, I, Lee, B, Vakili, J, Doranz, BJ, Govaerts, C, Vassart, G, Doms, RW & Parmentier, M (1999). CCR5 binds multiple CC-chemokines: MCP-3 acts as a natural antagonist. *Blood*, **94**, 1899-905.

Bleasdale, JE, Thakur, NR, Gremban, RS, Bundy, GL, Fitzpatrick, FA, Smith, RJ & Bunting, S (1990). Selective inhibition of receptor-coupled phospholipase C-dependent processes in human platelets and polymorphonuclear neutrophils. *J Pharmacol Exp Ther*, **255**, 756-68.

Bodin, P & Burnstock, G (2001). Purinergic signalling: ATP release. *Neurochem Res*, **26**, 959-69.

Bodor, ET, Waldo, GL, Hooks, SB, Corbitt, J, Boyer, JL & Harden, TK (2003). Purification and functional reconstitution of the human P2Y<sub>12</sub> receptor. *Mol Pharmacol*, **64**, 1210-6.

Boeynaems, JM & Communi, D (2006). Modulation of inflammation by extracellular nucleotides. *J Invest Dermatol*, **126**, 943-4.

- Boeynaems, JM & Sirtori, CR (2010). The unexpected roles of extracellular ADP and P2Y(13) receptor in reverse cholesterol transport. *Purinergic Signal*, **6**, 361-3.
- Bonacci, TM, Mathews, JL, Yuan, C, Lehmann, DM, Malik, S, Wu, D, Font, JL, Bidlack, JM & Smrcka, AV (2006). Differential targeting of Gbetagamma-subunit signaling with small molecules. *Science*, **312**, 443-6.
- Bootman, MD, Collins, TJ, Peppiatt, CM, Prothero, LS, Mackenzie, L, De Smet, P, Travers, M, Tovey, SC, Seo, JT, Berridge, MJ, Ciccolini, F & Lipp, P (2001). Calcium signalling--an overview. *Semin Cell Dev Biol*, **12**, 3-10.
- Boring, L, Gosling, J, Cleary, M & Charo, IF (1998). Decreased lesion formation in CCR2<sup>-/-</sup> mice reveals a role for chemokines in the initiation of atherosclerosis. *Nature*, **394**, 894-7.
- Borooah, J, Leback, DH & Walker, PG (1961). Studies on glucosaminidase. 2. Substrates for N-acetyl-beta-glucosaminidase. *Biochem J*, **78**, 106-10.
- Bours, MJ, Swennen, EL, Di Virgilio, F, Cronstein, BN & Dagnelie, PC (2006). Adenosine 5'-triphosphate and adenosine as endogenous signaling molecules in immunity and inflammation. *Pharmacol Ther*, **112**, 358-404.
- Boyer, JL, Mohanram, A, Camaioni, E, Jacobson, KA & Harden, TK (1998). Competitive and selective antagonism of P2Y1 receptors by N6-methyl 2'-deoxyadenosine 3',5'-bisphosphate. *Br J Pharmacol*, **124**, 1-3.
- Boyer, JL, Waldo, GL & Harden, TK (1992). Beta gamma-subunit activation of G-protein-regulated phospholipase C. *J Biol Chem*, **267**, 25451-6.
- Brandt, DR & Ross, EM (1985). GTPase activity of the stimulatory GTP-binding regulatory protein of adenylate cyclase, Gs. Accumulation and turnover of enzyme-nucleotide intermediates. *J Biol Chem*, **260**, 266-72.
- Brake, AJ, Wagenbach, MJ & Julius, D (1994). New structural motif for ligand-gated ion channels defined by an ionotropic ATP receptor. *Nature*, **371**, 519-23.
- Brass, D, Grably, MR, Bronstein-Sitton, N, Gohar, O & Meir, A (2012). Using antibodies against P2Y and P2X receptors in purinergic signaling research. *Purinergic Signal*, **8**, 61-79.
- Bridges, TM & Lindsley, CW (2008). G-protein-coupled receptors: from classical modes of modulation to allosteric mechanisms. *ACS Chem Biol*, **3**, 530-41.

- Brindley, DN, Pilquil, C, Sariahmetoglu, M & Reue, K (2009). Phosphatidate degradation: phosphatidate phosphatases (lipins) and lipid phosphate phosphatases. *Biochim Biophys Acta*, **1791**, 956-61.
- Brini, M & Carafoli, E (2011). The plasma membrane Ca(2)+ ATPase and the plasma membrane sodium calcium exchanger cooperate in the regulation of cell calcium. *Cold Spring Harb Perspect Biol*, **3**.
- Brinson, AE & Harden, TK (2001). Differential regulation of the uridine nucleotide-activated P2Y<sub>4</sub> and P2Y<sub>6</sub> receptors. SER-333 and SER-334 in the carboxyl terminus are involved in agonist-dependent phosphorylation desensitization and internalization of the P2Y<sub>4</sub> receptor. *J Biol Chem*, **276**, 11939-48.
- Brock, C, Schaefer, M, Reusch, HP, Czapalla, C, Michalke, M, Spicher, K, Schultz, G & Nurnberg, B (2003). Roles of G-beta gamma in membrane recruitment and activation of p110 gamma/p101 phosphoinositide 3-kinase gamma. *J Cell Biol*, **160**, 89-99.
- Broussas, M, Cornillet-Lefebvre, P, Potron, G & Nguyen, P (1999). Inhibition of fMLP-triggered respiratory burst of human monocytes by adenosine: involvement of A<sub>3</sub> adenosine receptor. *J Leukoc Biol*, **66**, 495-501.
- Browne, LE (2012). Structure of P2X receptors. *Wiley Interdisciplinary Reviews: Membrane Transport and Signaling*, **1**, 56-69.
- Browne, LE & North, RA (2013). P2X receptor intermediate activation states have altered nucleotide selectivity. *J Neurosci*, **33**, 14801-8.
- Bruckmeier, M, Kuehnl, A, Culmes, M, Pelisek, J & Eckstein, HH (2012). Impact of oxLDL and LPS on C-type natriuretic peptide system is different between THP-1 cells and human peripheral blood monocytic cells. *Cell Physiol Biochem*, **30**, 199-209.
- Bruegel, M, Teupser, D, Haffner, I, Mueller, M & Thiery, J (2006). Statins reduce macrophage inflammatory protein-1alpha expression in human activated monocytes. *Clin Exp Pharmacol Physiol*, **33**, 1144-9.
- Bruhl, H, Cihak, J, Schneider, MA, Plachy, J, Rupp, T, Wenzel, I, Shakarami, M, Milz, S, Ellwart, JW, Stangassinger, M, Schlondorff, D & Mack, M (2004). Dual Role of CCR2 during Initiation and Progression of Collagen-Induced Arthritis: Evidence for Regulatory Activity of CCR2<sup>+</sup> T Cells. *The Journal of Immunology*, **172**, 890-898.
- Bshesh, K, Zhao, B, Spight, D, Biaggioni, I, Feokistov, I, Denenberg, A, Wong, HR & Shanley, TP (2002). The A2A receptor mediates an endogenous regulatory pathway of cytokine expression in THP-1 cells. *J Leukoc Biol*, **72**, 1027-36.

Buchheiser, A, Ebner, A, Burghoff, S, Ding, Z, Romio, M, Viethen, C, Lindecke, A, Kohrer, K, Fischer, JW & Schrader, J (2011). Inactivation of CD73 promotes atherogenesis in apolipoprotein E-deficient mice. *Cardiovasc Res*, **92**, 338-47.

Bunney, TD & Katan, M (2011). PLC regulation: emerging pictures for molecular mechanisms. *Trends Biochem Sci*, **36**, 88-96.

Burns, JC, Friedmann, T, Driever, W, Burrascano, M & Yee, JK (1993). Vesicular stomatitis virus G glycoprotein pseudotyped retroviral vectors: concentration to very high titer and efficient gene transfer into mammalian and nonmammalian cells. *Proc Natl Acad Sci U S A*, **90**, 8033-7.

Burnstock, G (1972). Purinergic nerves. *Pharmacol Rev*, **24**, 509-81.

Burnstock, G (2012). Purinergic signalling: Its unpopular beginning, its acceptance and its exciting future. *Bioessays*, **34**, 218-25.

Burnstock, G & Boeynaems, JM (2014). Purinergic signalling and immune cells. *Purinergic Signal*, **10**, 529-64.

Burnstock, G, Campbell, G, Satchell, D & Smythe, A (1970). Evidence that adenosine triphosphate or a related nucleotide is the transmitter substance released by non-adrenergic inhibitory nerves in the gut. *Br J Pharmacol*, **40**, 668-88.

Burnstock, G & Knight, GE (2004). Cellular distribution and functions of P2 receptor subtypes in different systems. *Int Rev Cytol*, **240**, 31-304.

Caloca, MJ, Wang, H & Kazanietz, MG (2003). Characterization of the Rac-GAP (Rac-GTPase-activating protein) activity of beta2-chimaerin, a 'non-protein kinase C' phorbol ester receptor. *Biochem J*, **375**, 313-21.

Campbell, JJ, Hedrick, J, Zlotnik, A, Siani, MA, Thompson, DA & Butcher, EC (1998). Chemokines and the arrest of lymphocytes rolling under flow conditions. *Science*, **279**, 381-4.

Campwala, H, Sexton, DW, Crossman, DC & Fountain, SJ (2014). P2Y(6) receptor inhibition perturbs CCL2-evoked signalling in human monocytic and peripheral blood mononuclear cells. *J Cell Sci*, **127**, 4964-73.

Canonico, PL, Cronin, MJ & Macleod, RM (1985). Diacylglycerol lipase and pituitary prolactin release in vitro: studies employing RHC 80267. *Life Sci*, **36**, 997-1002.

Cantley, LC (2002). The phosphoinositide 3-kinase pathway. *Science*, **296**, 1655-7.

- Carafoli, E, Tiozzo, R, Lugli, G, Crovetto, F & Kratzing, C (1974). The release of calcium from heart mitochondria by sodium. *J Mol Cell Cardiol*, **6**, 361-71.
- Carlin, Leo m, Stamatiades, Efsthios g, Auffray, C, Hanna, Richard n, Glover, L, Vizcay-Barrena, G, Hedrick, Catherine c, Cook, H t, Diebold, S & Geissmann, F (2013). Nr4a1-Dependent Ly6C<sup>(low)</sup> Monocytes Monitor Endothelial Cells and Orchestrate Their Disposal. *Cell*, **153**, 362-375.
- Carnevale, D & Lembo, G (2012). PI3Kgamma in hypertension: a novel therapeutic target controlling vascular myogenic tone and target organ damage. *Cardiovasc Res*, **95**, 403-8.
- Carnevale, KA & Cathcart, MK (2003). Protein kinase C beta is required for human monocyte chemotaxis to MCP-1. *J Biol Chem*, **278**, 25317-22.
- Carp, H (1982). Mitochondrial N-formylmethionyl proteins as chemoattractants for neutrophils. *J Exp Med*, **155**, 264-75.
- Carrasquero, LM, Delicado, EG, Bustillo, D, Gutierrez-Martin, Y, Artalejo, AR & Miras-Portugal, MT (2009). P2X7 and P2Y<sub>13</sub> purinergic receptors mediate intracellular calcium responses to BzATP in rat cerebellar astrocytes. *J Neurochem*, **110**, 879-89.
- Carter, RL, Fricks, IP, Barrett, MO, Burianek, LE, Zhou, Y, Ko, H, Das, A, Jacobson, KA, Lazarowski, ER & Harden, TK (2009). Quantification of Gi-mediated inhibition of adenylyl cyclase activity reveals that UDP is a potent agonist of the human P2Y<sub>14</sub> receptor. *Mol Pharmacol*, **76**, 1341-8.
- Catterall, WA (2000). Structure and regulation of voltage-gated Ca<sup>2+</sup> channels. *Annu Rev Cell Dev Biol*, **16**, 521-55.
- Ceruti, S, Fumagalli, M, Villa, G, Verderio, C & Abbracchio, MP (2008). Purinoceptor-mediated calcium signaling in primary neuron-glia trigeminal cultures. *Cell Calcium*, **43**, 576-90.
- Chambers, JK (2000). A G Protein-coupled Receptor for UDP-glucose. *Journal of Biological Chemistry*, **275**, 10767-10771.
- Chan, JR, Hyduk, SJ & Cybulsky, MI (2001). Chemoattractants induce a rapid and transient upregulation of monocyte alpha4 integrin affinity for vascular cell adhesion molecule-1 which mediates arrest: an early step in the process of emigration. *J Exp Med*, **193**, 1149-58.
- Chandra, S, Kable, EP, Morrison, GH & Webb, WW (1991). Calcium sequestration in the Golgi apparatus of cultured mammalian cells revealed by laser scanning confocal microscopy and ion microscopy. *J Cell Sci*, **100 (Pt 4)**, 747-52.

Chang, JD, Sukhova, GK, Libby, P, Schwartz, E, Lichtenstein, AH, Field, SJ, Kennedy, C, Madhavarapu, S, Luo, J, Wu, D & Cantley, LC (2007). Deletion of the phosphoinositide 3-kinase p110gamma gene attenuates murine atherosclerosis. *Proc Natl Acad Sci U S A*, **104**, 8077-82.

Chang, K, Hanaoka, K, Kumada, M & Takuwa, Y (1995). Molecular Cloning and Functional Analysis of a Novel P2 Nucleotide Receptor. *Journal of Biological Chemistry*, **270**, 26152-26158.

Charo, IF, Myers, SJ, Herman, A, Franci, C, Connolly, AJ & Coughlin, SR (1994). Molecular cloning and functional expression of two monocyte chemoattractant protein 1 receptors reveals alternative splicing of the carboxyl-terminal tails. *Proc Natl Acad Sci U S A*, **91**, 2752-6.

Chen, Y, Corriden, R, Inoue, Y, Yip, L, Hashiguchi, N, Zinkernagel, A, Nizet, V, Insel, PA & Junger, WG (2006). ATP release guides neutrophil chemotaxis via P2Y<sub>2</sub> and A<sub>3</sub> receptors. *Science*, **314**, 1792-5.

Cherney, RJ, Mo, R, Meyer, DT, Nelson, DJ, Lo, YC, Yang, G, Scherle, PA, Mandlekar, S, Wasserman, ZR, Jezak, H, Solomon, KA, Tebben, AJ, Carter, PH & Decicco, CP (2008). Discovery of disubstituted cyclohexanes as a new class of CC chemokine receptor 2 antagonists. *J Med Chem*, **51**, 721-4.

Chhatriwala, M, Ravi, RG, Patel, RI, Boyer, JL, Jacobson, KA & Harden, TK (2004). Induction of novel agonist selectivity for the ADP-activated P2Y<sub>1</sub> receptor versus the ADP-activated P2Y<sub>12</sub> and P2Y<sub>13</sub> receptors by conformational constraint of an ADP analog. *J Pharmacol Exp Ther*, **311**, 1038-43.

Cho, ML, Yoon, BY, Ju, JH, Jung, YO, Jhun, JY, Park, MK, Park, SH, Cho, CS & Kim, HY (2007). Expression of CCR2A, an isoform of MCP-1 receptor, is increased by MCP-1, CD40 ligand and TGF-beta in fibroblast like synoviocytes of patients with RA. *Exp Mol Med*, **39**, 499-507.

Chomczynski, P & Sacchi, N (1987). Single-step method of RNA isolation by acid guanidinium thiocyanate-phenol-chloroform extraction. *Anal Biochem*, **162**, 156-9.

Chuang, DM & Costa, E (1979). Evidence for internalization of the recognition site of beta-adrenergic receptors during receptor subsensitivity induced by (-)-isoproterenol. *Proc Natl Acad Sci U S A*, **76**, 3024-8.

Ciana, P, Fumagalli, M, Trincavelli, ML, Verderio, C, Rosa, P, Lecca, D, Ferrario, S, Parravicini, C, Capra, V, Gelosa, P, Guerrini, U, Belcredito, S, Cimino, M, Sironi, L, Tremoli, E, Rovati, GE, Martini, C & Abbracchio, MP (2006). The orphan receptor GPR17

- identified as a new dual uracil nucleotides/cysteinyl-leukotrienes receptor. *EMBO J*, **25**, 4615-27.
- Claign, A, Laporte, SA, Caron, MG & Lefkowitz, RJ (2002). Endocytosis of G protein-coupled receptors: roles of G protein-coupled receptor kinases and beta-arrestin proteins. *Prog Neurobiol*, **66**, 61-79.
- Clapham, DE (2007). Calcium signaling. *Cell*, **131**, 1047-58.
- Clark, AJ & Petty, HR (2005). Differential intracellular distributions of inositol trisphosphate and ryanodine receptors within and among hematopoietic cells. *J Histochem Cytochem*, **53**, 913-6.
- Clifford, EE, Martin, KA, Dalal, P, Thomas, R & Dubyak, GR (1997). Stage-specific expression of P2Y receptors, ecto-apyrase, and ecto-5'-nucleotidase in myeloid leukocytes. *Am J Physiol*, **273**, C973-87.
- Coddou, C, Yan, Z, Obsil, T, Huidobro-Toro, JP & Stojilkovic, SS (2011). Activation and regulation of purinergic P2X receptor channels. *Pharmacol Rev*, **63**, 641-83.
- Cohn, M & Meek, GA (1957). The mechanism of hydrolysis of adenosine di- and tri-phosphate catalysed by potato apyrase. *Biochem J*, **66**, 128-30.
- Cohn, ZA & Benson, B (1965). The Differentiation of Mononuclear Phagocytes. Morphology, Cytochemistry, and Biochemistry. *J Exp Med*, **121**, 153-70.
- Colotta, F, Borre, A, Wang, JM, Tattanelli, M, Maddalena, F, Polentarutti, N, Peri, G & Mantovani, A (1992). Expression of a monocyte chemotactic cytokine by human mononuclear phagocytes. *J Immunol*, **148**, 760-5.
- Combadiere, C, Ahuja, SK, Tiffany, HL & Murphy, PM (1996). Cloning and functional expression of CC CKR5, a human monocyte CC chemokine receptor selective for MIP-1(alpha), MIP-1(beta), and RANTES. *J Leukoc Biol*, **60**, 147-52.
- Combadiere, C, Ahuja, SK, Van Damme, J, Tiffany, HL, Gao, JL & Murphy, PM (1995). Monocyte chemoattractant protein-3 is a functional ligand for CC chemokine receptors 1 and 2B. *J Biol Chem*, **270**, 29671-5.
- Communi, D, Gonzalez, NS, Detheux, M, Brezillon, S, Lannoy, V, Parmentier, M & Boeynaems, JM (2001). Identification of a novel human ADP receptor coupled to G(i). *J Biol Chem*, **276**, 41479-85.

Communi, D, Govaerts, C, Parmentier, M & Boeynaems, JM (1997). Cloning of a human purinergic P2Y receptor coupled to phospholipase C and adenylyl cyclase. *J Biol Chem*, **272**, 31969-73.

Communi, D, Parmentier, M & Boeynaems, JM (1996). Cloning, functional expression and tissue distribution of the human P2Y<sub>6</sub> receptor. *Biochem Biophys Res Commun*, **222**, 303-8.

Communi, D, Robaye, B & Boeynaems, JM (1999). Pharmacological characterization of the human P2Y<sub>11</sub> receptor. *Br J Pharmacol*, **128**, 1199-206.

Corriden, R & Insel, PA (2010). Basal release of ATP: an autocrine-paracrine mechanism for cell regulation. *Sci Signal*, **3**, re1.

Corriden, R, Insel, PA & Junger, WG (2007). A novel method using fluorescence microscopy for real-time assessment of ATP release from individual cells. *Am J Physiol Cell Physiol*, **293**, C1420-5.

Cowen, DS, Lazarus, HM, Shurin, SB, Stoll, SE & Dubyak, GR (1989). Extracellular adenosine triphosphate activates calcium mobilization in human phagocytic leukocytes and neutrophil/monocyte progenitor cells. *J Clin Invest*, **83**, 1651-60.

Cox, MA, Gomes, B, Palmer, K, Du, K, Wiekowski, M, Wilburn, B, Petro, M, Chou, CC, Desquitado, C, Schwarz, M, Lunn, C, Lundell, D, Narula, SK, Zavodny, PJ & Jenh, CH (2005). The pyrimidinergic P2Y<sub>6</sub> receptor mediates a novel release of proinflammatory cytokines and chemokines in monocytic cells stimulated with UDP. *Biochem Biophys Res Commun*, **330**, 467-73.

Cros, J, Cagnard, N, Woollard, K, Patey, N, Zhang, SY, Senechal, B, Puel, A, Biswas, SK, Moshous, D, Picard, C, Jais, JP, D'cruz, D, Casanova, JL, Trouillet, C & Geissmann, F (2010). Human CD14<sup>dim</sup> monocytes patrol and sense nucleic acids and viruses via TLR7 and TLR8 receptors. *Immunity*, **33**, 375-86.

Crown, SE, Yu, Y, Sweeney, MD, Leary, JA & Handel, TM (2006). Heterodimerization of CCR2 chemokines and regulation by glycosaminoglycan binding. *J Biol Chem*, **281**, 25438-46.

Daaka, Y, Luttrell, LM & Lefkowitz, RJ (1997). Switching of the coupling of the beta2-adrenergic receptor to different G proteins by protein kinase A. *Nature*, **390**, 88-91.

Dai, XM, Ryan, GR, Hapel, AJ, Dominguez, MG, Russell, RG, Kapp, S, Sylvestre, V & Stanley, ER (2002). Targeted disruption of the mouse colony-stimulating factor 1 receptor

gene results in osteopetrosis, mononuclear phagocyte deficiency, increased primitive progenitor cell frequencies, and reproductive defects. *Blood*, **99**, 111-20.

Daigneault, M, Preston, JA, Marriott, HM, Whyte, MK & Dockrell, DH (2010). The identification of markers of macrophage differentiation in PMA-stimulated THP-1 cells and monocyte-derived macrophages. *PLoS One*, **5**, e8668.

Daugherty, BL, Siciliano, SJ, Demartino, JA, Malkowitz, L, Sirotina, A & Springer, MS (1996). Cloning, expression, and characterization of the human eosinophil eotaxin receptor. *J Exp Med*, **183**, 2349-54.

De Chaffoy De Courcelles, DC, Roevens, P & Van Belle, H (1985). R 59 022, a diacylglycerol kinase inhibitor. Its effect on diacylglycerol and thrombin-induced C kinase activation in the intact platelet. *J Biol Chem*, **260**, 15762-70.

De Smet, P, Parys, JB, Callewaert, G, Weidema, AF, Hill, E, De Smedt, H, Erneux, C, Sorrentino, V & Missiaen, L (1999). Xestospongins C is an equally potent inhibitor of the inositol 1,4,5-trisphosphate receptor and the endoplasmic-reticulum Ca<sup>(2+)</sup> pumps. *Cell Calcium*, **26**, 9-13.

De Stefani, D, Raffaello, A, Teardo, E, Szabo, I & Rizzuto, R (2011). A forty-kilodalton protein of the inner membrane is the mitochondrial calcium uniporter. *Nature*, **476**, 336-40.

Di Virgilio, F (2007). Liaisons dangereuses: P2X(7) and the inflammasome. *Trends Pharmacol Sci*, **28**, 465-72.

Docampo, R & Moreno, SN (2011). Acidocalcisomes. *Cell Calcium*, **50**, 113-9.

Dong, C, Filipeanu, CM, Duvernay, MT & Wu, G (2007). Regulation of G protein-coupled receptor export trafficking. *Biochim Biophys Acta*, **1768**, 853-70.

Donnelly-Roberts, DL, Namovic, MT, Han, P & Jarvis, MF (2009). Mammalian P2X7 receptor pharmacology: comparison of recombinant mouse, rat and human P2X7 receptors. *Br J Pharmacol*, **157**, 1203-14.

Dragan, AI, Pavlovic, R, McGivney, JB, Casas-Finet, JR, Bishop, ES, Strouse, RJ, Schenerman, MA & Geddes, CD (2012). SYBR Green I: fluorescence properties and interaction with DNA. *J Fluoresc*, **22**, 1189-99.

Dubridge, RB, Tang, P, Hsia, HC, Leong, PM, Miller, JH & Calos, MP (1987). Analysis of mutation in human cells by using an Epstein-Barr virus shuttle system. *Mol Cell Biol*, **7**, 379-87.

- Dunn, PM & Blakeley, AG (1988). Suramin: a reversible P2-purinoceptor antagonist in the mouse vas deferens. *Br J Pharmacol*, **93**, 243-5.
- Dupont, G & Goldbeter, A (1993). One-pool model for Ca<sup>2+</sup> oscillations involving Ca<sup>2+</sup> and inositol 1,4,5-trisphosphate as co-agonists for Ca<sup>2+</sup> release. *Cell Calcium*, **14**, 311-22.
- Duvernay, MT, Filipeanu, CM & Wu, G (2005). The regulatory mechanisms of export trafficking of G protein-coupled receptors. *Cell Signal*, **17**, 1457-65.
- Edling, CE, Selvaggi, F, Ghonaim, R, Maffucci, T & Falasca, M (2014). Caffeine and the analog CGS-15943 inhibit cancer cell growth by targeting the phosphoinositide 3-kinase/Akt pathway. *Cancer Biol Ther*, **15**, 524-32.
- Egan, TM & Khakh, BS (2004). Contribution of calcium ions to P2X channel responses. *J Neurosci*, **24**, 3413-20.
- El-Asmar, L, Springael, JY, Ballet, S, Andrieu, EU, Vassart, G & Parmentier, M (2005). Evidence for negative binding cooperativity within CCR5-CCR2b heterodimers. *Mol Pharmacol*, **67**, 460-9.
- Ellgaard, L & Helenius, A (2001). ER quality control: towards an understanding at the molecular level. *Curr Opin Cell Biol*, **13**, 431-7.
- Elliott, MR, Chekeni, FB, Trampont, PC, Lazarowski, ER, Kadl, A, Walk, SF, Park, D, Woodson, RI, Ostankovich, M, Sharma, P, Lysiak, JJ, Harden, TK, Leitinger, N & Ravichandran, KS (2009). Nucleotides released by apoptotic cells act as a find-me signal to promote phagocytic clearance. *Nature*, **461**, 282-6.
- Eltzschig, HK, Eckle, T, Mager, A, Kuper, N, Karcher, C, Weissmuller, T, Boengler, K, Schulz, R, Robson, SC & Colgan, SP (2006). ATP release from activated neutrophils occurs via connexin 43 and modulates adenosine-dependent endothelial cell function. *Circ Res*, **99**, 1100-8.
- Enjyoji, K, Sevigny, J, Lin, Y, Frenette, PS, Christie, PD, Esch, JS, 2nd, Imai, M, Edelberg, JM, Rayburn, H, Lech, M, Beeler, DL, Csizmadia, E, Wagner, DD, Robson, SC & Rosenberg, RD (1999). Targeted disruption of cd39/ATP diphosphohydrolase results in disordered hemostasis and thromboregulation. *Nat Med*, **5**, 1010-7.
- Ennion, S, Hagan, S & Evans, RJ (2000). The role of positively charged amino acids in ATP recognition by human P2X(1) receptors. *J Biol Chem*, **275**, 29361-7.
- Ennion, SJ & Evans, RJ (2002). Conserved cysteine residues in the extracellular loop of the human P2X(1) receptor form disulfide bonds and are involved in receptor trafficking to the cell surface. *Mol Pharmacol*, **61**, 303-11.

Evanko, DS, Thiyagarajan, MM, Siderovski, DP & Wedegaertner, PB (2001). Gbeta gamma isoforms selectively rescue plasma membrane localization and palmitoylation of mutant Galphas and Galphaq. *J Biol Chem*, **276**, 23945-53.

Evans, RJ, Lewis, C, Buell, G, Valera, S, North, RA & Surprenant, A (1995). Pharmacological characterization of heterologously expressed ATP-gated cation channels (P2x purinoceptors). *Mol Pharmacol*, **48**, 178-83.

Fabre, JE, Nguyen, M, Latour, A, Keifer, JA, Audoly, LP, Coffman, TM & Koller, BH (1999). Decreased platelet aggregation, increased bleeding time and resistance to thromboembolism in P2Y<sub>1</sub>-deficient mice. *Nat Med*, **5**, 1199-202.

Falkenburger, BH, Jensen, JB, Dickson, EJ, Suh, BC & Hille, B (2010). Phosphoinositides: lipid regulators of membrane proteins. *J Physiol*, **588**, 3179-85.

Fan, P, Kyaw, H, Su, K, Zeng, Z, Augustus, M, Carter, KC & Li, Y (1998). Cloning and characterization of a novel human chemokine receptor. *Biochem Biophys Res Commun*, **243**, 264-8.

Fantuzzi, L, Borghi, P, Ciolli, V, Pavlakis, G, Belardelli, F & Gessani, S (1999). Loss of CCR2 expression and functional response to monocyte chemotactic protein (MCP-1) during the differentiation of human monocytes: role of secreted MCP-1 in the regulation of the chemotactic response. *Blood*, **94**, 875-83.

Fedorov, O, Marsden, B, Pogacic, V, Rellos, P, Muller, S, Bullock, AN, Schwaller, J, Sundstrom, M & Knapp, S (2007). A systematic interaction map of validated kinase inhibitors with Ser/Thr kinases. *Proc Natl Acad Sci U S A*, **104**, 20523-8.

Ferguson, SS (2001). Evolving concepts in G protein-coupled receptor endocytosis: the role in receptor desensitization and signaling. *Pharmacol Rev*, **53**, 1-24.

Ferguson, SS, Downey, WE, 3rd, Colapietro, AM, Barak, LS, Menard, L & Caron, MG (1996). Role of beta-arrestin in mediating agonist-promoted G protein-coupled receptor internalization. *Science*, **271**, 363-6.

Ferrari, D, Chiozzi, P, Falzoni, S, Dal Susino, M, Melchiorri, L, Baricordi, OR & Di Virgilio, F (1997). Extracellular ATP triggers IL-1 beta release by activating the purinergic P2Z receptor of human macrophages. *J Immunol*, **159**, 1451-8.

Feske, S (2010). CRAC channelopathies. *Pflugers Arch*, **460**, 417-35.

Feske, S, Gwack, Y, Prakriya, M, Srikanth, S, Puppel, SH, Tanasa, B, Hogan, PG, Lewis, RS, Daly, M & Rao, A (2006). A mutation in Orai1 causes immune deficiency by abrogating CRAC channel function. *Nature*, **441**, 179-85.

- Finch, EA, Turner, TJ & Goldin, SM (1991). Calcium as a coagonist of inositol 1,4,5-trisphosphate-induced calcium release. *Science*, **252**, 443-6.
- Fischer, D, Van Der Weyden, MB, Snyderman, R & Kelley, WN (1976). A role for adenosine deaminase in human monocyte maturation. *J Clin Invest*, **58**, 399-407.
- Fischer R, Kalthof B, Rank E, Stelte-Ludwig B, and Wuttke M (2004) Preparation of benzofuro-1,4-diazepin-2-ones as P2X4 receptor antagonists for the treatment of arteriosclerosis and restenosis. DE 10312969A1. 1–14.
- Fleit, HB & Kobasiuk, CD (1991). The human monocyte-like cell line THP-1 expresses Fc gamma RI and Fc gamma RII. *J Leukoc Biol*, **49**, 556-65.
- Flewellen, EH, Nelson, TE, Jones, WP, Arens, JF & Wagner, DL (1983). Dantrolene dose response in awake man: implications for management of malignant hyperthermia. *Anesthesiology*, **59**, 275-80.
- Fogg, DK, Sibon, C, Miled, C, Jung, S, Aucouturier, P, Littman, DR, Cumano, A & Geissmann, F (2006). A clonogenic bone marrow progenitor specific for macrophages and dendritic cells. *Science*, **311**, 83-7.
- Forrester, T (1972). An estimate of adenosine triphosphate release into the venous effluent from exercising human forearm muscle. *J Physiol*, **224**, 611-28.
- Foster, FM, Traer, CJ, Abraham, SM & Fry, MJ (2003). The phosphoinositide (PI)3-kinase family. *J Cell Sci*, **116**, 3037-40.
- Fredholm, BB, Ap, IJ, Jacobson, KA, Klotz, KN & Linden, J (2001). International Union of Pharmacology. XXV. Nomenclature and classification of adenosine receptors. *Pharmacol Rev*, **53**, 527-52.
- Fredholm, BB, Ap, IJ, Jacobson, KA, Linden, J & Muller, CE (2011). International Union of Basic and Clinical Pharmacology. LXXXI. Nomenclature and classification of adenosine receptors--an update. *Pharmacol Rev*, **63**, 1-34.
- Fricks, IP, Carter, RL, Lazarowski, ER & Harden, TK (2009). G<sub>i</sub>-dependent cell signaling responses of the human P2Y<sub>14</sub> receptor in model cell systems. *J Pharmacol Exp Ther*, **330**, 162-8.
- Fukami, K, Inanobe, S, Kanemaru, K & Nakamura, Y (2010). Phospholipase C is a key enzyme regulating intracellular calcium and modulating the phosphoinositide balance. *Prog Lipid Res*, **49**, 429-37.

Gafni, J, Munsch, JA, Lam, TH, Catlin, MC, Costa, LG, Molinski, TF & Pessah, IN (1997). Xestospongins: potent membrane permeable blockers of the inositol 1,4,5-trisphosphate receptor. *Neuron*, **19**, 723-33.

Gainetdinov, RR, Premont, RT, Bohn, LM, Lefkowitz, RJ & Caron, MG (2004). Desensitization of G protein-coupled receptors and neuronal functions. *Annu Rev Neurosci*, **27**, 107-44.

Gancedo, JM (2013). Biological roles of cAMP: variations on a theme in the different kingdoms of life. *Biol Rev Camb Philos Soc*, **88**, 645-68.

Garcia, RA, Yan, M, Search, D, Zhang, R, Carson, NL, Ryan, CS, Smith-Monroy, C, Zheng, J, Chen, J, Kong, Y, Tang, H, Hellings, SE, Wardwell-Swanson, J, Dinchuk, JE, Psaltis, GC, Gordon, DA, Glunz, PW & Gargalovic, PS (2014). P2Y<sub>6</sub> receptor potentiates pro-inflammatory responses in macrophages and exhibits differential roles in atherosclerotic lesion development. *PLoS One*, **9**, e111385.

Garcia-Guzman, M, Soto, F, Gomez-Hernandez, JM, Lund, PE & Stuhmer, W (1997a). Characterization of recombinant human P2X4 receptor reveals pharmacological differences to the rat homologue. *Mol Pharmacol*, **51**, 109-18.

Garcia-Guzman, M, Stühmer, W & Soto, F (1997b). Molecular characterization and pharmacological properties of the human P2X3 purinoceptor. *Molecular Brain Research*, **47**, 59-66.

Garland, SL (2013). Are GPCRs still a source of new targets? *J Biomol Screen*, **18**, 947-66.

Gee, KR, Brown, KA, Chen, WN, Bishop-Stewart, J, Gray, D & Johnson, I (2000). Chemical and physiological characterization of fluo-4 Ca<sup>(2+)</sup>-indicator dyes. *Cell Calcium*, **27**, 97-106.

Geissmann, F, Jung, S & Littman, DR (2003). Blood Monocytes Consist of Two Principal Subsets with Distinct Migratory Properties. *Immunity*, **19**, 71-82.

Geissmann, F, Manz, MG, Jung, S, Sieweke, MH, Merad, M & Ley, K (2010). Development of monocytes, macrophages, and dendritic cells. *Science*, **327**, 656-61.

Gerber, BO, Zanni, MP, Uguccioni, M, Loetscher, M, Mackay, CR, Pichler, WJ, Yawalkar, N, Baggiolini, M & Moser, B (1997). Functional expression of the eotaxin receptor CCR3 in T lymphocytes co-localizing with eosinophils. *Curr Biol*, **7**, 836-43.

Gerszten, RE, Garcia-Zepeda, EA, Lim, YC, Yoshida, M, Ding, HA, Gimbrone, MA, Jr., Luster, AD, Luscinskas, FW & Rosenzweig, A (1999). MCP-1 and IL-8 trigger firm

adhesion of monocytes to vascular endothelium under flow conditions. *Nature*, **398**, 718-23.

Gerwins, P & Fredholm, BB (1992). Stimulation of adenosine A1 receptors and bradykinin receptors, which act via different G proteins, synergistically raises inositol 1,4,5-trisphosphate and intracellular free calcium in DDT1 MF-2 smooth muscle cells. *Proc Natl Acad Sci U S A*, **89**, 7330-4.

Gharbi, SI, Zvelebil, MJ, Shuttleworth, SJ, Hancox, T, Saghir, N, Timms, JF & Waterfield, MD (2007). Exploring the specificity of the PI3K family inhibitor LY294002. *Biochem J*, **404**, 15-21.

Godfrey, RW, Manzi, RM, Jensen, BD & Hoffstein, ST (1988). FMLP-induced arachidonic acid release, phospholipid metabolism, and calcium mobilization in human monocytes. Regulation by cyclic AMP. *Inflammation*, **12**, 223-30.

Goepfert, C, Sundberg, C, Sevigny, J, Enjoji, K, Hoshi, T, Csizmadia, E & Robson, S (2001). Disordered Cellular Migration and Angiogenesis in cd39-Null Mice. *Circulation*, **104**, 3109-3115.

Goodman, OB, Jr., Krupnick, JG, Santini, F, Gurevich, VV, Penn, RB, Gagnon, AW, Keen, JH & Benovic, JL (1996). Beta-arrestin acts as a clathrin adaptor in endocytosis of the beta2-adrenergic receptor. *Nature*, **383**, 447-50.

Gouwy, M, Struyf, S, Leutenez, L, Portner, N, Sozzani, S & Van Damme, J (2014). Chemokines and other GPCR ligands synergize in receptor-mediated migration of monocyte-derived immature and mature dendritic cells. *Immunobiology*, **219**, 218-29.

Gouwy, M, Struyf, S, Noppen, S, Schutyser, E, Springael, JY, Parmentier, M, Proost, P & Van Damme, J (2008). Synergy between coproduced CC and CXC chemokines in monocyte chemotaxis through receptor-mediated events. *Mol Pharmacol*, **74**, 485-95.

Gouwy, M, Struyf, S, Verbeke, H, Put, W, Proost, P, Opdenakker, G & Van Damme, J (2009). CC chemokine ligand-2 synergizes with the nonchemokine G protein-coupled receptor ligand fMLP in monocyte chemotaxis, and it cooperates with the TLR ligand LPS via induction of CXCL8. *J Leukoc Biol*, **86**, 671-80.

Graham, FL, Smiley, J, Russell, WC & Nairn, R (1977). Characteristics of a human cell line transformed by DNA from human adenovirus type 5. *J Gen Virol*, **36**, 59-74.

Grahames, CB, Michel, AD, Chessell, IP & Humphrey, PP (1999). Pharmacological characterization of ATP- and LPS-induced IL-1beta release in human monocytes. *Br J Pharmacol*, **127**, 1915-21.

- Grunewald, JK & Ridley, AJ (2010). CD73 represses pro-inflammatory responses in human endothelial cells. *J Inflamm (Lond)*, **7**, 10.
- Grynkiewicz, G, Poenie, M & Tsien, RY (1985). A new generation of Ca<sup>2+</sup> indicators with greatly improved fluorescence properties. *J Biol Chem*, **260**, 3440-50.
- Gschwendt, M, Dieterich, S, Rennecke, J, Kittstein, W, Mueller, HJ & Johannes, FJ (1996). Inhibition of protein kinase C mu by various inhibitors. Differentiation from protein kinase c isoenzymes. *FEBS Lett*, **392**, 77-80.
- Gu, BJ, Zhang, WY, Bendall, LJ, Chessell, IP, Buell, GN & Wiley, JS (2000). Expression of P2X7 purinoceptors on human lymphocytes and monocytes: evidence for nonfunctional P2X7 receptors. *Am J Physiol Cell Physiol*, **279**: C1189–C1197.
- Gu, L, Okada, Y, Clinton, SK, Gerard, C, Sukhova, GK, Libby, P & Rollins, BJ (1998). Absence of monocyte chemoattractant protein-1 reduces atherosclerosis in low density lipoprotein receptor-deficient mice. *Mol Cell*, **2**, 275-81.
- Guerini, D, Coletto, L & Carafoli, E (2005). Exporting calcium from cells. *Cell Calcium*, **38**, 281-9.
- Guns, PJ, Hendrickx, J, Van Assche, T, Fransen, P & Bult, H (2010). P2Y receptors and atherosclerosis in apolipoprotein E-deficient mice. *Br J Pharmacol*, **159**, 326-36.
- Guo, C, Masin, M, Qureshi, OS & Murrell-Lagnado, RD (2007). Evidence for functional P2X4/P2X7 heteromeric receptors. *Mol Pharmacol*, **72**, 1447-56.
- Hains, MD, Wing, MR, Maddileti, S, Siderovski, DP & Harden, TK (2006). G $\alpha$ <sub>12/13</sub>- and rho-dependent activation of phospholipase C-epsilon by lysophosphatidic acid and thrombin receptors. *Mol Pharmacol*, **69**, 2068-75.
- Hajnóczky, G, Davies, E & Madesh, M (2003). Calcium signaling and apoptosis. *Biochem Biophys Res Commun*, **304**, 445-454.
- Hamel, M, Henault, M, Hyjazie, H, Morin, N, Bayly, C, Skorey, K, Therien, AG, Mancini, J, Brideau, C & Kargman, S (2011). Discovery of novel P2Y<sub>14</sub> agonist and antagonist using conventional and nonconventional methods. *J Biomol Screen*, **16**, 1098-105.
- Hanoune, J & Defer, N (2001). Regulation and role of adenylyl cyclase isoforms. *Annu Rev Pharmacol Toxicol*, **41**, 145-74.
- Harkany, T, Guzman, M, Galve-Roperh, I, Berghuis, P, Devi, LA & Mackie, K (2007). The emerging functions of endocannabinoid signaling during CNS development. *Trends Pharmacol Sci*, **28**, 83-92.

Hashimoto, D, Chow, A, Noizat, C, Teo, P, Beasley, MB, Leboeuf, M, Becker, CD, See, P, Price, J, Lucas, D, Greter, M, Mortha, A, Boyer, SW, Forsberg, EC, Tanaka, M, Van Rooijen, N, Garcia-Sastre, A, Stanley, ER, Ginhoux, F, Frenette, PS & Merad, M (2013). Tissue-resident macrophages self-maintain locally throughout adult life with minimal contribution from circulating monocytes. *Immunity*, **38**, 792-804.

Hasko, G & Pacher, P (2012). Regulation of macrophage function by adenosine. *Arterioscler Thromb Vasc Biol*, **32**, 865-9.

Hasko, G, Pacher, P, Deitch, EA & Vizi, ES (2007). Shaping of monocyte and macrophage function by adenosine receptors. *Pharmacol Ther*, **113**, 264-75.

Hasko, G, Szabo, C, Nemeth, ZH, Kvetan, V, Pastores, SM & Vizi, ES (1996). Adenosine receptor agonists differentially regulate IL-10, TNF-alpha, and nitric oxide production in RAW 264.7 macrophages and in endotoxemic mice. *J Immunol*, **157**, 4634-40.

Hassanian, SM, Dinarvand, P & Rezaie, AR (2014). Adenosine regulates the proinflammatory signaling function of thrombin in endothelial cells. *J Cell Physiol*, **229**, 1292-300.

Hattori, M & Gouaux, E (2012). Molecular mechanism of ATP binding and ion channel activation in P2X receptors. *Nature*, **485**, 207-12.

Hayashi, K & Altman, A (2007). Protein kinase C theta (PKCtheta): a key player in T cell life and death. *Pharmacol Res*, **55**, 537-44.

Hiasa, M, Togawa, N, Miyaji, T, Omote, H, Yamamoto, A & Moriyama, Y (2014). Essential role of vesicular nucleotide transporter in vesicular storage and release of nucleotides in platelets. *Physiol Rep*, **2**.

Higgins, KR, Kovacevic, W & Stokes, L (2014). Nucleotides regulate secretion of the inflammatory chemokine CCL2 from human macrophages and monocytes. *Mediators Inflamm*, **2014**, 293925.

Higuchi, R, Dollinger, G, Walsh, PS & Griffith, R (1992). Simultaneous amplification and detection of specific DNA sequences. *Biotechnology (NY)*, **10**, 413-7.

Hirsch, E (2000). Central Role for G Protein-Coupled Phosphoinositide 3-Kinase  $\gamma$  in Inflammation. *Science*, **287**, 1049-1053.

Hofmann, T, Obukhov, AG, Schaefer, M, Harteneck, C, Gudermann, T & Schultz, G (1999). Direct activation of human TRPC6 and TRPC3 channels by diacylglycerol. *Nature*, **397**, 259-63.

Hollopeter, G, Jantzen, HM, Vincent, D, Li, G, England, L, Ramakrishnan, V, Yang, RB, Nurden, P, Nurden, A, Julius, D & Conley, PB (2001). Identification of the platelet ADP receptor targeted by antithrombotic drugs. *Nature*, **409**, 202-7.

Hoover, HS, Blankman, JL, Niessen, S & Cravatt, BF (2008). Selectivity of inhibitors of endocannabinoid biosynthesis evaluated by activity-based protein profiling. *Bioorg Med Chem Lett*, **18**, 5838-41.

Horowitz, LF, Hirdes, W, Suh, BC, Hilgemann, DW, Mackie, K & Hille, B (2005). Phospholipase C in living cells: activation, inhibition, Ca<sup>2+</sup> requirement, and regulation of M current. *J Gen Physiol*, **126**, 243-62.

Humphreys, BD & Dubyak, GR (1998). Modulation of P2X7 nucleotide receptor expression by pro- and anti-inflammatory stimuli in THP-1 monocytes. *J Leukoc Biol*, **64**, 265-73.

Humphries, RG, Tomlinson, W, Ingall, AH, Cage, PA & Leff, P (1994). FPL 66096: a novel, highly potent and selective antagonist at human platelet P2T-purinoceptors. *Br J Pharmacol*, **113**, 1057-63.

Hyduk, SJ, Chan, JR, Duffy, ST, Chen, M, Peterson, MD, Waddell, TK, Digby, GC, Szaszi, K, Kapus, A & Cybulsky, MI (2007). Phospholipase C, calcium, and calmodulin are critical for alpha4beta1 integrin affinity up-regulation and monocyte arrest triggered by chemoattractants. *Blood*, **109**, 176-84.

Hyman, MC, Petrovic-Djergovic, D, Visovatti, SH, Liao, H, Yanamadala, S, Bouis, D, Su, EJ, Lawrence, DA, Broekman, MJ, Marcus, AJ & Pinsky, DJ (2009). Self-regulation of inflammatory cell trafficking in mice by the leukocyte surface apyrase CD39. *J Clin Invest*, **119**, 1136-49.

Ingersoll, MA, Platt, AM, Potteaux, S & Randolph, GJ (2011). Monocyte trafficking in acute and chronic inflammation. *Trends Immunol*, **32**, 470-7.

Ingersoll, MA, Spanbroek, R, Lottaz, C, Gautier, EL, Frankenberger, M, Hoffmann, R, Lang, R, Haniffa, M, Collin, M, Tacke, F, Habenicht, AJ, Ziegler-Heitbrock, L & Randolph, GJ (2010). Comparison of gene expression profiles between human and mouse monocyte subsets. *Blood*, **115**, e10-9.

Into, T, Fujita, M, Okusawa, T, Hasebe, A, Morita, M & Shibata, KI (2002). Synergic Effects of Mycoplasmal Lipopeptides and Extracellular ATP on Activation of Macrophages. *Infection and Immunity*, **70**, 3586-3591.

- Iwai, M, Michikawa, T, Bosanac, I, Ikura, M & Mikoshiba, K (2007). Molecular basis of the isoform-specific ligand-binding affinity of inositol 1,4,5-trisphosphate receptors. *J Biol Chem*, **282**, 12755-64.
- Izikson, L, Klein, RS, Charo, IF, Weiner, HL & Luster, AD (2000). Resistance to experimental autoimmune encephalomyelitis in mice lacking the CC chemokine receptor (CCR)2. *J Exp Med*, **192**, 1075-80.
- Jackson, CL (2009). Mechanisms of transport through the Golgi complex. *J Cell Sci*, **122**, 443-52.
- Jacobson, KA, Balasubramanian, R, Deflorian, F & Gao, ZG (2012). G protein-coupled adenosine (P1) and P2Y receptors: ligand design and receptor interactions. *Purinergic Signal*, **8**, 419-36.
- Jadot, M, Bielande, V, Beauloye, V, Wattiaux-De Coninck, S & Wattiaux, R (1990). Cytotoxicity and effect of glycyl-D-phenylalanine-2-naphthylamide on lysosomes. *Biochim Biophys Acta*, **1027**, 205-9.
- Jaffe, EA, Nachman, RL, Becker, CG & Minick, CR (1973). Culture of human endothelial cells derived from umbilical veins. Identification by morphologic and immunologic criteria. *J Clin Invest*, **52**, 2745-56.
- Jaime-Figueroa, S, Greenhouse, R, Padilla, F, Dillon, MP, Gever, JR & Ford, AP (2005). Discovery and synthesis of a novel and selective drug-like P2X(1) antagonist. *Bioorg Med Chem Lett*, **15**, 3292-5.
- Janssens, R, Communi, D, Piroton, S, Samson, M, Parmentier, M & Boeynaems, JM (1996). Cloning and tissue distribution of the human P2Y<sub>1</sub> receptor. *Biochem Biophys Res Commun*, **221**, 588-93.
- Jantzen, H-M, Milstone, DS, Gousset, L, Conley, PB & Mortensen, RM (2001). Impaired activation of murine platelets lacking G $\alpha_{i2}$ . *Journal of Clinical Investigation*, **108**, 477-483.
- Jarnagin, K, Grunberger, D, Mulkins, M, Wong, B, Hemmerich, S, Paavola, C, Bloom, A, Bhakta, S, Diehl, F, Freedman, R, Mccarley, D, Polsky, I, Ping-Tsou, A, Kosaka, A & Handel, TM (1999). Identification of surface residues of the monocyte chemotactic protein 1 that affect signaling through the receptor CCR2. *Biochemistry*, **38**, 16167-77.
- Jarvis, MF & Khakh, BS (2009). ATP-gated P2X cation-channels. *Neuropharmacology*, **56**, 208-15.

- Jenkins, SJ, Ruckerl, D, Cook, PC, Jones, LH, Finkelman, FD, Van Rooijen, N, Macdonald, AS & Allen, JE (2011). Local macrophage proliferation, rather than recruitment from the blood, is a signature of TH2 inflammation. *Science*, **332**, 1284-8.
- Jia, T, Serbina, NV, Brandl, K, Zhong, MX, Leiner, IM, Charo, IF & Pamer, EG (2008). Additive Roles for MCP-1 and MCP-3 in CCR2-Mediated Recruitment of Inflammatory Monocytes during *Listeria monocytogenes* Infection. *The Journal of Immunology*, **180**, 6846-6853.
- Jiang, Y, Sakane, F, Kanoh, H & Walsh, JP (2000). Selectivity of the diacylglycerol kinase inhibitor 3-[2-(4-[bis-(4-fluorophenyl)methylene]-1-piperidinyl)ethyl]-2, 3-dihydro-2-thioxo-4(1H)quinazolinone (R59949) among diacylglycerol kinase subtypes. *Biochem Pharmacol*, **59**, 763-72.
- Jin, J, Dasari, VR, Sistare, FD & Kunapuli, SP (1998). Distribution of P2Y receptor subtypes on haematopoietic cells. *Br J Pharmacol*, **123**, 789-94.
- Jin, X, Shepherd, RK, Duling, BR & Linden, J (1997). Inosine binds to A<sub>3</sub> adenosine receptors and stimulates mast cell degranulation. *J Clin Invest*, **100**, 2849-57.
- Johnson, I (2010). *The Molecular Probes Handbook: A Guide to Fluorescent Probes and Labeling Technologies*, 11th Edition, Life Technologies Corporation.
- Johnson, Z, Proudfoot, AE & Handel, TM (2005). Interaction of chemokines and glycosaminoglycans: a new twist in the regulation of chemokine function with opportunities for therapeutic intervention. *Cytokine Growth Factor Rev*, **16**, 625-36.
- Junger, WG (2011). Immune cell regulation by autocrine purinergic signalling. *Nat Rev Immunol*, **11**, 201-12.
- Kaczmarek-Hajek, K, Lorinczi, E, Hausmann, R & Nicke, A (2012). Molecular and functional properties of P2X receptors--recent progress and persisting challenges. *Purinergic Signal*, **8**, 375-417.
- Kadamur, G & Ross, EM (2013). Mammalian phospholipase C. *Annu Rev Physiol*, **75**, 127-54.
- Kaminsky, DE & Rogers, TJ (2008). Suppression of CCL2/MCP-1 and CCL5/RANTES expression by nociceptin in human monocytes. *J Neuroimmune Pharmacol*, **3**, 75-82.
- Karlen, Y, Mcnair, A, Perseguers, S, Mazza, C & Mermod, N (2007). Statistical significance of quantitative PCR. *BMC Bioinformatics*, **8**, 131.

- Katada, T (2012). The inhibitory G protein G(i) identified as pertussis toxin-catalyzed ADP-ribosylation. *Biol Pharm Bull*, **35**, 2103-11.
- Katada, T & Ui, M (1982). ADP ribosylation of the specific membrane protein of C6 cells by islet-activating protein associated with modification of adenylate cyclase activity. *J Biol Chem*, **257**, 7210-6.
- Katso, R, Okkenhaug, K, Ahmadi, K, White, S, Timms, J & Waterfield, MD (2001). Cellular function of phosphoinositide 3-kinases: implications for development, homeostasis, and cancer. *Annu Rev Cell Dev Biol*, **17**, 615-75.
- Kaufmann, A, Musset, B, Limberg, SH, Renigunta, V, Sus, R, Dalpke, AH, Heeg, KM, Robaye, B & Hanley, PJ (2005). "Host tissue damage" signal ATP promotes non-directional migration and negatively regulates toll-like receptor signaling in human monocytes. *J Biol Chem*, **280**, 32459-67.
- Kaufmann, A, Salentin, R, Gemsa, D & Sprenger, H (2001). Increase of CCR1 and CCR5 expression and enhanced functional response to MIP-1 alpha during differentiation of human monocytes to macrophages. *J Leukoc Biol*, **69**, 248-52.
- Kawasaki, T, Ueyama, T, Lange, I, Feske, S & Saito, N (2010). Protein kinase C-induced phosphorylation of Orai1 regulates the intracellular Ca<sup>2+</sup> level via the store-operated Ca<sup>2+</sup> channel. *J Biol Chem*, **285**, 25720-30.
- Kettlun, AM, Uribe, L, Calvo, V, Silva, S, Rivera, J, Mancilla, M, Antonieta, M, Valenzuela & Traverso-Cori, A (1982). Properties of two apyrases from *Solanum tuberosum*. *Phytochemistry*, **21**, 551-558.
- Khakh, BS, Bao, XR, Labarca, C & Lester, HA (1999). Neuronal P2X transmitter-gated cation channels change their ion selectivity in seconds. *Nat Neurosci*, **2**, 322-30.
- Khakh, BS, Burnstock, G, Kennedy, C, King, BF, North, RA, Seguela, P, Voigt, M & Humphrey, PP (2001). International union of pharmacology. XXIV. Current status of the nomenclature and properties of P2X receptors and their subunits. *Pharmacol Rev*, **53**, 107-18.
- Khoa, ND, Montesinos, MC, Reiss, AB, Delano, D, Awadallah, N & Cronstein, BN (2001). Inflammatory Cytokines Regulate Function and Expression of Adenosine A<sub>2A</sub> Receptors in Human Monocytic THP-1 Cells. *The Journal of Immunology*, **167**, 4026-4032.
- Kim, B, Jeong, HK, Kim, JH, Lee, SY, Jou, I & Joe, EH (2011). Uridine 5'-diphosphate induces chemokine expression in microglia and astrocytes through activation of the P2Y<sub>6</sub> receptor. *J Immunol*, **186**, 3701-9.

- Kim, IS, Kim, YS, Jang, SW, Sung, HJ, Han, KH, Na, DS & Ko, J (2004). Differential effects of 9-cis retinoic acid on expression of CC chemokine receptors in human monocytes. *Biochem Pharmacol*, **68**, 611-20.
- Kim, YC, Lee, JS, Sak, K, Marteau, F, Mamedova, L, Boeynaems, JM & Jacobson, KA (2005). Synthesis of pyridoxal phosphate derivatives with antagonist activity at the P2Y<sub>13</sub> receptor. *Biochem Pharmacol*, **70**, 266-74.
- Kirichok, Y, Krapivinsky, G & Clapham, DE (2004). The mitochondrial calcium uniporter is a highly selective ion channel. *Nature*, **427**, 360-4.
- Kishimoto, S, Kobayashi, Y, Oka, S, Gokoh, M, Waku, K & Sugiura, T (2004). 2-Arachidonoylglycerol, an endogenous cannabinoid receptor ligand, induces accelerated production of chemokines in HL-60 cells. *J Biochem*, **135**, 517-24.
- Klein, C, Grahnert, A, Abdelrahman, A, Muller, CE & Hauschildt, S (2009). Extracellular NAD<sup>(+)</sup> induces a rise in [Ca<sup>(2+)</sup>]<sub>i</sub> in activated human monocytes via engagement of P2Y<sub>1</sub> and P2Y<sub>11</sub> receptors. *Cell Calcium*, **46**, 263-72.
- Kobilka, BK (2007). G protein coupled receptor structure and activation. *Biochim Biophys Acta*, **1768**, 794-807.
- Koenderman, L, Buurman, W & Daha, MR (2014). The innate immune response. *Immunol Lett*, **162**, 95-102.
- Kohro, T, Tanaka, T, Murakami, T, Wada, Y, Aburatani, H, Hamakubo, T & Kodama, T (2004). A comparison of differences in the gene expression profiles of phorbol 12-myristate 13-acetate differentiated THP-1 cells and human monocyte-derived macrophage. *J Atheroscler Thromb*, **11**, 88-97.
- Kothandan, G, Gadhe, CG & Cho, SJ (2012). Structural insights from binding poses of CCR2 and CCR5 with clinically important antagonists: a combined in silico study. *PLoS One*, **7**, e32864.
- Kronlage, M, Song, J, Sorokin, L, Isfort, K, Schwerdtle, T, Leipziger, J, Robaye, B, Conley, PB, Kim, HC, Sargin, S, Schon, P, Schwab, A & Hanley, PJ (2010). Autocrine purinergic receptor signaling is essential for macrophage chemotaxis. *Sci Signal*, **3**, ra55.
- Krugmann, S, Hawkins, PT, Pryer, N & Braselmann, S (1999). Characterizing the Interactions between the Two Subunits of the p101/p110gamma Phosphoinositide 3-Kinase and Their Role in the Activation of This Enzyme by Gbeta gamma Subunits. *Journal of Biological Chemistry*, **274**, 17152-17158.

- Krupinski, J, Coussen, F, Bakalyar, HA, Tang, WJ, Feinstein, PG, Orth, K, Slaughter, C, Reed, RR & Gilman, AG (1989). Adenylyl cyclase amino acid sequence: possible channel- or transporter-like structure. *Science*, **244**, 1558-64.
- Kuang, Y, Wu, Y, Jiang, H & Wu, D (1996). Selective G protein coupling by C-C chemokine receptors. *J Biol Chem*, **271**, 3975-8.
- Kukulski, F, Levesque, SA, Lavoie, EG, Lecka, J, Bigonnesse, F, Knowles, AF, Robson, SC, Kirley, TL & Sevigny, J (2005). Comparative hydrolysis of P2 receptor agonists by NTPDases 1, 2, 3 and 8. *Purinergic Signal*, **1**, 193-204.
- Kukulski, F, Levesque, SA & Sevigny, J (2011). Impact of ectoenzymes on p2 and p1 receptor signaling. *Adv Pharmacol*, **61**, 263-99.
- Kurihara, T, Warr, G, Loy, J & Bravo, R (1997). Defects in macrophage recruitment and host defense in mice lacking the CCR2 chemokine receptor. *J Exp Med*, **186**, 1757-62.
- Kuziel, WA, Morgan, SJ, Dawson, TC, Griffin, S, Smithies, O, Ley, K & Maeda, N (1997). Severe reduction in leukocyte adhesion and monocyte extravasation in mice deficient in CC chemokine receptor 2. *Proc Natl Acad Sci U S A*, **94**, 12053-8.
- Lambrecht, G, Friebe, T, Grimm, U, Windscheif, U, Bungardt, E, Hildebrandt, C, Baumert, HG, Spatz-Kumbel, G & Mutschler, E (1992). PPADS, a novel functionally selective antagonist of P2 purinoceptor-mediated responses. *Eur J Pharmacol*, **217**, 217-9.
- Lanner, JT, Georgiou, DK, Joshi, AD & Hamilton, SL (2010). Ryanodine receptors: structure, expression, molecular details, and function in calcium release. *Cold Spring Harb Perspect Biol*, **2**, a003996.
- Larsson, C (2006). Protein kinase C and the regulation of the actin cytoskeleton. *Cell Signal*, **18**, 276-84.
- Lauvau, G, Chorro, L, Spaulding, E & Soudja, SM (2014). Inflammatory monocyte effector mechanisms. *Cell Immunol*, **291**, 32-40.
- Lazarowski, ER, Sesma, JI, Seminario-Vidal, L & Kreda, SM (2011). Molecular mechanisms of purine and pyrimidine nucleotide release. *Adv Pharmacol*, **61**, 221-61.
- Le, KT, Babinski, K & Seguela, P (1998). Central P2X4 and P2X6 channel subunits coassemble into a novel heteromeric ATP receptor. *J Neurosci*, **18**, 7152-9.
- Lê, K-T, Paquet, M, Nouel, D, Babinski, K & Séguéla, P (1997). Primary structure and expression of a naturally truncated human P2X ATP receptor subunit from brain and immune system. *FEBS Lett*, **418**, 195-199.

- Lecka, J, Fausther, M, Kunzli, B & Sevigny, J (2014). Ticlopidine in its prodrug form is a selective inhibitor of human NTPDase1. *Mediators Inflamm*, **2014**, 547480.
- Lee, JS, Yang, EJ & Kim, IS (2009). The roles of MCP-1 and protein kinase C delta activation in human eosinophilic leukemia EoL-1 cells. *Cytokine*, **48**, 186-95.
- Leff, P (1995). The two-state model of receptor activation. *Trends Pharmacol Sci*, **16**, 89-97.
- Leifert, WR, Aloia, AL, Bucco, O & McMurchie, EJ (2005). GPCR-induced dissociation of G-protein subunits in early stage signal transduction. *Mol Membr Biol*, **22**, 507-17.
- Léon, C, Hechler, B, Vial, C, Leray, C, Cazenave, J-P & Gachet, C (1997). The P2Y<sub>1</sub> receptor is an ADP receptor antagonized by ATP and expressed in platelets and megakaryoblastic cells. *FEBS Lett*, **403**, 26-30.
- Levesque, SA, Lavoie, EG, Lecka, J, Bigonnesse, F & Sevigny, J (2007). Specificity of the ecto-ATPase inhibitor ARL-67156 on human and mouse ectonucleotidases. *Br J Pharmacol*, **152**, 141-50.
- Le Vraux, V, Chen, YL, Masson, I, De Sousa, M, Giroud, JP, Florentin, I & Chauvelot-Moachon, L (1993). Inhibition of human monocyte TNF production by adenosine receptor agonists. *Life Sci*, **52**, 1917-24.
- Ley, K, Laudanna, C, Cybulsky, MI & Nourshargh, S (2007). Getting to the site of inflammation: the leukocyte adhesion cascade updated. *Nat Rev Immunol*, **7**, 678-89.
- Li, J & Fountain, SJ (2012). Fluvastatin suppresses native and recombinant human P2X<sub>4</sub> receptor function. *Purinergic Signal*, **8**, 311-6.
- Li, Z, Jiang, H, Xie, W, Zhang, Z, Smrcka, AV & Wu, D (2000). Roles of PLC-beta2 and -beta3 and PI3Kgamma in chemoattractant-mediated signal transduction. *Science*, **287**, 1046-9.
- Limatola, C, Schaap, D, Moolenaar, WH & Van Blitterswijk, WJ (1994). Phosphatidic acid activation of protein kinase C-zeta overexpressed in COS cells: comparison with other protein kinase C isoforms and other acidic lipids. *Biochem J*, **304 ( Pt 3)**, 1001-8.
- Liou, J, Kim, ML, Heo, WD, Jones, JT, Myers, JW, Ferrell, JE, Jr. & Meyer, T (2005). STIM is a Ca<sup>2+</sup> sensor essential for Ca<sup>2+</sup>-store-depletion-triggered Ca<sup>2+</sup> influx. *Curr Biol*, **15**, 1235-41.
- Litosch, I (2002). Phosphatidic acid modulates G protein regulation of phospholipase C-beta1 activity in membranes. *Cell Signal*, **14**, 259-63.

- Locati, M, Zhou, D, Luini, W, Evangelista, V, Mantovani, A & Sozzani, S (1994). Rapid induction of arachidonic acid release by monocyte chemotactic protein-1 and related chemokines. Role of Ca<sup>2+</sup> influx, synergism with platelet-activating factor and significance for chemotaxis. *J Biol Chem*, **269**, 4746-53.
- Lock, K, Zhang, J, Lu, J, Lee, SH & Crocker, PR (2004). Expression of CD33-related siglecs on human mononuclear phagocytes, monocyte-derived dendritic cells and plasmacytoid dendritic cells. *Immunobiology*, **209**, 199-207.
- Loetscher, P, Seitz, M, Baggiolini, M & Moser, B (1996). Interleukin-2 regulates CC chemokine receptor expression and chemotactic responsiveness in T lymphocytes. *J Exp Med*, **184**, 569-77.
- Lu, J, Honczarenko, M & Sloan, SR (2004). Independent expression of the two paralogous CCL4 genes in monocytes and B lymphocytes. *Immunogenetics*, **55**, 706-11.
- Lustig, KD, Conklin, BR, Herzmark, P, Taussig, R & Bourne, HR (1993). Type II adenylyl cyclase integrates coincident signals from Gs, Gi, and Gq. *J Biol Chem*, **268**, 13900-5.
- Lynch, KJ, Touma, E, Niforatos, W, Kage, KL, Burgard, EC, Van Biesen, T, Kowaluk, EA & Jarvis, MF (1999). Molecular and functional characterization of human P2X(2) receptors. *Mol Pharmacol*, **56**, 1171-81.
- Maier, R, Glatz, A, Mosbacher, J & Bilbe, G (1997). Cloning of P2Y<sub>6</sub> cDNAs and identification of a pseudogene: comparison of P2Y receptor subtype expression in bone and brain tissues. *Biochem Biophys Res Commun*, **240**, 298-302.
- Malmsjo, M, Hou, M, Pendergast, W, Erlinge, D & Edvinsson, L (2003). Potent P2Y<sub>6</sub> receptor mediated contractions in human cerebral arteries. *BMC Pharmacol*, **3**, 4.
- Mamedova, LK, Joshi, BV, Gao, ZG, Von Kugelgen, I & Jacobson, KA (2004). Diisothiocyanate derivatives as potent, insurmountable antagonists of P2Y<sub>6</sub> nucleotide receptors. *Biochem Pharmacol*, **67**, 1763-70.
- Marchand, A, Abi-Gerges, A, Saliba, Y, Merlet, E & Lompre, AM (2012). Calcium signaling in vascular smooth muscle cells: from physiology to pathology. *Adv Exp Med Biol*, **740**, 795-810.
- Margeta-Mitrovic, M, Jan, YN & Jan, LY (2000). A trafficking checkpoint controls GABA(B) receptor heterodimerization. *Neuron*, **27**, 97-106.

Marteau, F, Le Poul, E, Communi, D, Communi, D, Labouret, C, Savi, P, Boeynaems, JM & Gonzalez, NS (2003). Pharmacological characterization of the human P2Y<sub>13</sub> receptor. *Mol Pharmacol*, **64**, 104-12.

Martin, P, Villares, R, Rodriguez-Mascarenhas, S, Zaballos, A, Leitges, M, Kovac, J, Sizing, I, Rennert, P, Marquez, G, Martinez, AC, Diaz-Meco, MT & Moscat, J (2005). Control of T helper 2 cell function and allergic airway inflammation by PKCzeta. *Proc Natl Acad Sci U S A*, **102**, 9866-71.

Martinelli, R, Sabroe, I, Larosa, G, Williams, TJ & Pease, JE (2001). The CC chemokine eotaxin (CCL11) is a partial agonist of CC chemokine receptor 2b. *J Biol Chem*, **276**, 42957-64.

Martinez, FO & Gordon, S (2014). The M1 and M2 paradigm of macrophage activation: time for reassessment. *F1000Prime Rep*, **6**, 13.

Martiny-Baron, G, Kazanietz, MG, Mischak, H, Blumberg, PM, Kochs, G, Hug, H, Marme, D & Schachtele, C (1993). Selective inhibition of protein kinase C isozymes by the indolocarbazole Go 6976. *J Biol Chem*, **268**, 9194-7.

Mason, MJ, Mayer, B & Hymel, LJ (1993). Inhibition of Ca<sup>2+</sup> transport pathways in thymic lymphocytes by econazole, miconazole, and SKF 96365. *Am J Physiol*, **264**, C654-62.

Matyash, M, Matyash, V, Nolte, C, Sorrentino, V & Kettenmann, H (2002). Requirement of functional ryanodine receptor type 3 for astrocyte migration. *FASEB J*, **16**, 84-6.

Meis, S, Hamacher, A, Hongwiset, D, Marzian, C, Wiese, M, Eckstein, N, Royer, HD, Communi, D, Boeynaems, JM, Hausmann, R, Schmalzing, G & Kassack, MU (2010). NF546 [4,4'-(carbonylbis(imino-3,1-phenylene-carbonylimino-3,1-(4-methyl-phenylene)-carbonylimino))-bis(1,3-xylene-alpha,alpha'-diphosphonic acid) tetrasodium salt] is a non-nucleotide P2Y<sub>11</sub> agonist and stimulates release of interleukin-8 from human monocyte-derived dendritic cells. *J Pharmacol Exp Ther*, **332**, 238-47.

Mellado, M, Rodriguez-Frade, JM, Vila-Coro, AJ, Fernandez, S, Martin De Ana, A, Jones, DR, Toran, JL & Martinez, AC (2001). Chemokine receptor homo- or heterodimerization activates distinct signaling pathways. *EMBO J*, **20**, 2497-507.

Mellor, EA, Maekawa, A, Austen, KF & Boyce, JA (2001). Cysteinyl leukotriene receptor 1 is also a pyrimidinergic receptor and is expressed by human mast cells. *Proc Natl Acad Sci U S A*, **98**, 7964-9.

Merida, I, Avila-Flores, A & Merino, E (2008). Diacylglycerol kinases: at the hub of cell signalling. *Biochem J*, **409**, 1-18.

Merrill, JT, Shen, C, Schreiber, D, Coffey, D, Zakharenko, O, Fisher, R, Lahita, RG, Salmon, J & Cronstein, BN (1997). Adenosine A1 receptor promotion of multinucleated giant cell formation by human monocytes: a mechanism for methotrexate-induced nodulosis in rheumatoid arthritis. *Arthritis Rheum*, **40**, 1308-15.

Merritt, JE, Armstrong, WP, Benham, CD, Hallam, TJ, Jacob, R, Jaxa-Chamiec, A, Leigh, BK, McCarthy, SA, Moores, KE & Rink, TJ (1990). SK&F 96365, a novel inhibitor of receptor-mediated calcium entry. *Biochem J*, **271**, 515-22.

Meusser, B, Hirsch, C, Jarosch, E & Sommer, T (2005). ERAD: the long road to destruction. *Nat Cell Biol*, **7**, 766-72.

Migeotte, I, Franssen, JD, Goriely, S, Willems, F & Parmentier, M (2002). Distribution and regulation of expression of the putative human chemokine receptor HCR in leukocyte populations. *Eur J Immunol*, **32**, 494-501.

Mitchell, KJ, Lai, FA & Rutter, GA (2003). Ryanodine receptor type I and nicotinic acid adenine dinucleotide phosphate receptors mediate Ca<sup>2+</sup> release from insulin-containing vesicles in living pancreatic beta-cells (MIN6). *J Biol Chem*, **278**, 11057-64.

Moeckel, D, Jeong, SS, Sun, X, Broekman, MJ, Nguyen, A, Drosopoulos, JH, Marcus, AJ, Robson, SC, Chen, R & Abendschein, D (2014). Optimizing human apyrase to treat arterial thrombosis and limit reperfusion injury without increasing bleeding risk. *Sci Transl Med*, **6**, 248ra105.

Moffat, J, Grueneberg, DA, Yang, X, Kim, SY, Kloepfer, AM, Hinkle, G, Piquani, B, Eisenhaure, TM, Luo, B, Grenier, JK, Carpenter, AE, Foo, SY, Stewart, SA, Stockwell, BR, Hacohen, N, Hahn, WC, Lander, ES, Sabatini, DM & Root, DE (2006). A lentiviral RNAi library for human and mouse genes applied to an arrayed viral high-content screen. *Cell*, **124**, 1283-98.

Montecclaro, FS & Charo, IF (1996). The Amino-terminal Extracellular Domain of the MCP-1 Receptor, but Not the RANTES/MIP-1 Receptor, Confers Chemokine Selectivity: EVIDENCE FOR A TWO-STEP MECHANISM FOR MCP-1 RECEPTOR ACTIVATION. *Journal of Biological Chemistry*, **271**, 19084-19092.

Moore, DJ, Chambers, JK, Wahlin, JP, Tan, KB, Moore, GB, Jenkins, O, Emson, PC & Murdock, PR (2001). Expression pattern of human P2Y receptor subtypes: a quantitative reverse transcription-polymerase chain reaction study. *Biochim Biophys Acta*, **1521**, 107-19.

Moreschi, I, Bruzzone, S, Nicholas, RA, Fruscione, F, Sturla, L, Benvenuto, F, Usai, C, Meis, S, Kassack, MU, Zocchi, E & De Flora, A (2006). Extracellular NAD<sup>+</sup> is an agonist

- of the human P2Y<sub>11</sub> purinergic receptor in human granulocytes. *J Biol Chem*, **281**, 31419-29.
- Morioka, N, Tokuhara, M, Harano, S, Nakamura, Y, Hisaoka-Nakashima, K & Nakata, Y (2013). The activation of P2Y<sub>6</sub> receptor in cultured spinal microglia induces the production of CCL2 through the MAP kinases-NF-kappaB pathway. *Neuropharmacology*, **75**, 116-25.
- Morrow, GB, Nicholas, RA & Kennedy, C (2014). UTP is not a biased agonist at human P2Y receptors. *Purinergic Signal*, **12**, 12.
- Moyano Cardaba, C, Jacques, RO, Barrett, JE, Hassell, KM, Kavanagh, A, Remington, FC, Tse, T & Mueller, A (2012). CCL3 induced migration occurs independently of intracellular calcium release. *Biochem Biophys Res Commun*, **418**, 17-21.
- Muller, CE, Iqbal, J, Baqi, Y, Zimmermann, H, Rollich, A & Stephan, H (2006). Polyoxometalates--a new class of potent ecto-nucleoside triphosphate diphosphohydrolase (NTPDase) inhibitors. *Bioorg Med Chem Lett*, **16**, 5943-7.
- Muller, G, Kerkhoff, C, Hankowitz, J, Pataki, M, Kovacs, E, Lackner, KJ & Schmitz, G (1993). Effects of purinergic agents on human mononuclear phagocytes are differentiation dependent. Implications for atherogenesis. *Arterioscler Thromb*, **13**, 1317-26.
- Muller, T, Bayer, H, Myrtek, D, Ferrari, D, Sorichter, S, Ziegenhagen, MW, Zissel, G, Virchow, JC, Jr., Luttmann, W, Norgauer, J, Di Virgilio, F & Idzko, M (2005). The P2Y<sub>14</sub> receptor of airway epithelial cells: coupling to intracellular Ca<sup>2+</sup> and IL-8 secretion. *Am J Respir Cell Mol Biol*, **33**, 601-9.
- Munro, R, Ressler, R, Stone, M, Gessner, G, Jarvis, MF & Saltzman, A (1998). Differential expression of adenosine A<sub>2A</sub> and A<sub>2B</sub> receptor subtypes on myeloid U937 and THP-1 cells: Adenosine A<sub>2B</sub> receptor activation selectively stimulates cAMP formation and inhibition of TNF $\alpha$  release in THP-1 cells. *Drug Development Research*, **44**, 41-47.
- Murchison, D & Griffith, WH (2000). Mitochondria buffer non-toxic calcium loads and release calcium through the mitochondrial permeability transition pore and sodium/calcium exchanger in rat basal forebrain neurons. *Brain Res*, **854**, 139-51.
- Myers, SJ, Wong, LM & Charo, IF (1995). Signal transduction and ligand specificity of the human monocyte chemoattractant protein-1 receptor in transfected embryonic kidney cells. *J Biol Chem*, **270**, 5786-92.
- Myrtek, D & Idzko, M (2007). Chemotactic activity of extracellular nucleotides on human immune cells. *Purinergic Signal*, **3**, 5-11.

Nelson, DW, Gregg, RJ, Kort, ME, Perez-Medrano, A, Voight, EA, Wang, Y, Grayson, G, Namovic, MT, Donnelly-Roberts, DL, Niforatos, W, Honore, P, Jarvis, MF, Faltynek, CR & Carroll, WA (2006). Structure-activity relationship studies on a series of novel, substituted 1-benzyl-5-phenyltetrazole P2X7 antagonists. *J Med Chem*, **49**, 3659-66.

Neote, K, Digregorio, D, Mak, JY, Horuk, R & Schall, TJ (1993). Molecular cloning, functional expression, and signaling characteristics of a C-C chemokine receptor. *Cell*, **72**, 415-25.

Nepomuceno, RR, Henschen-Edman, AH, Burgess, WH & Tenner, AJ (1997). cDNA Cloning and Primary Structure Analysis of C1qRP, the Human C1q/MBL/SPA Receptor That Mediates Enhanced Phagocytosis In Vitro. *Immunity*, **6**, 119-129.

Neptune, ER & Bourne, HR (1997). Receptors induce chemotaxis by releasing the betagamma subunit of Gi, not by activating Gq or Gs. *Proc Natl Acad Sci U S A*, **94**, 14489-94.

Ng, T, Shima, D, Squire, A, Bastiaens, PI, Gschmeissner, S, Humphries, MJ & Parker, PJ (1999). PKC $\alpha$  regulates beta1 integrin-dependent cell motility through association and control of integrin traffic. *EMBO J*, **18**, 3909-23.

Nicke, A, Kerschensteiner, D & Soto, F (2005). Biochemical and functional evidence for heteromeric assembly of P2X1 and P2X4 subunits. *J Neurochem*, **92**, 925-33.

Nishida, M, Sato, Y, Uemura, A, Narita, Y, Tozaki-Saitoh, H, Nakaya, M, Ide, T, Suzuki, K, Inoue, K, Nagao, T & Kurose, H (2008). P2Y<sub>6</sub> receptor-G $\alpha$ <sub>12/13</sub> signalling in cardiomyocytes triggers pressure overload-induced cardiac fibrosis. *EMBO J*, **27**, 3104-15.

Niyadurupola, N, Sidaway, P, Osborne, A, Broadway, DC & Sanderson, J (2011). The development of human organotypic retinal cultures (HORCs) to study retinal neurodegeneration. *Br J Ophthalmol*, **95**, 720-6.

Nomura, N, Miyajima, N, Sazuka, T, Tanaka, A, Kawarabayasi, Y, Sato, S, Nagase, T, Seki, N, Ishikawa, K & Tabata, S (1994). Prediction of the coding sequences of unidentified human genes. I. The coding sequences of 40 new genes (KIAA0001-KIAA0040) deduced by analysis of randomly sampled cDNA clones from human immature myeloid cell line KG-1. *DNA Res*, **1**, 27-35.

North, RA (2002). Molecular physiology of P2X receptors. *Physiol Rev*, **82**, 1013-67.

- Oestreich, JH, Ferraris, SP, Steinhubl, SR & Akers, WS (2013). Pharmacodynamic interplay of the P2Y(1), P2Y(12), and TxA(2) pathways in platelets: the potential of triple antiplatelet therapy with P2Y(1) receptor antagonism. *Thromb Res*, **131**, e64-70.
- Ohura, K, Katona, IM, Wahl, LM, Chenoweth, DE & Wahl, SM (1987). Co-expression of chemotactic ligand receptors on human peripheral blood monocytes. *J Immunol*, **138**, 2633-9.
- Olszak, IT, Poznansky, MC, Evans, RH, Olson, D, Kos, C, Pollak, MR, Brown, EM & Scadden, DT (2000). Extracellular calcium elicits a chemokinetic response from monocytes in vitro and in vivo. *J Clin Invest*, **105**, 1299-305.
- Ongini, E, Dionisotti, S, Gessi, S, Irenius, E & Fredholm, BB (1999). Comparison of CGS-15943, ZM-241385 and SCH-58261 as antagonists at human adenosine receptors. *Naunyn Schmiedebergs Arch Pharmacol*, **359**, 7-10.
- Palczewski, K (2000). Crystal Structure of Rhodopsin: A G Protein-Coupled Receptor. *Science*, **289**, 739-745.
- Pamer, EG (2004). Immune responses to *Listeria monocytogenes*. *Nat Rev Immunol*, **4**, 812-23.
- Parekh, AB & Putney, JW, Jr. (2005). Store-operated calcium channels. *Physiol Rev*, **85**, 757-810.
- Parkin, J & Cohen, B (2001). An overview of the immune system. *The Lancet*, **357**, 1777-1789.
- Parys, JB & De Smedt, H (2012). Inositol 1,4,5-trisphosphate and its receptors. *Adv Exp Med Biol*, **740**, 255-79.
- Passlick, B, Flieger, D & Ziegler-Heitbrock, HW (1989). Identification and characterization of a novel monocyte subpopulation in human peripheral blood. *Blood*, **74**, 2527-34.
- Patel, S & Docampo, R (2010). Acidic calcium stores open for business: expanding the potential for intracellular Ca<sup>2+</sup> signaling. *Trends Cell Biol*, **20**, 277-86.
- Patel, S, Joseph, SK & Thomas, AP (1999). Molecular properties of inositol 1,4,5-trisphosphate receptors. *Cell Calcium*, **25**, 247-64.
- Patel, S, Marchant, J & Brailoiu, E (2010). Two-pore channels: Regulation by NAADP and customized roles in triggering calcium signals. *Cell Calcium*, **47**, 480-90.
- Periasamy, M & Kalyanasundaram, A (2007). SERCA pump isoforms: their role in calcium transport and disease. *Muscle Nerve*, **35**, 430-42.

- Phillips, RJ, Lutz, M & Premack, B (2005). Differential signaling mechanisms regulate expression of CC chemokine receptor-2 during monocyte maturation. *J Inflamm (Lond)*, **2**, 14.
- Pidlaoan, LV, Jin, J, Sandhu, AK, Athwal, RS & Kunapuli, SP (1997). Colocalization of P2Y<sub>2</sub> and P2Y<sub>6</sub> receptor genes at human chromosome 11q13.3-14.1. *Somat Cell Mol Genet*, **23**, 291-6.
- Pierce, KL, Premont, RT & Lefkowitz, RJ (2002). Seven-transmembrane receptors. *Nat Rev Mol Cell Biol*, **3**, 639-50.
- Piirainen, H, Ashok, Y, Nanekar, RT & Jaakola, VP (2011). Structural features of adenosine receptors: from crystal to function. *Biochim Biophys Acta*, **1808**, 1233-44.
- Pilling, D, Fan, T, Huang, D, Kaul, B & Gomer, RH (2009). Identification of markers that distinguish monocyte-derived fibrocytes from monocytes, macrophages, and fibroblasts. *PLoS One*, **4**, e7475.
- Pinton, P, Pozzan, T & Rizzuto, R (1998). The Golgi apparatus is an inositol 1,4,5-trisphosphate-sensitive Ca<sup>2+</sup> store, with functional properties distinct from those of the endoplasmic reticulum. *EMBO J*, **17**, 5298-308.
- Pitcher, JA, Freedman, NJ & Lefkowitz, RJ (1998). G protein-coupled receptor kinases. *Annu Rev Biochem*, **67**, 653-92.
- Polentarutti, N, Allavena, P, Bianchi, G, Giardina, G, Basile, A, Sozzani, S, Mantovani, A & Introna, M (1997). IL-2-regulated expression of the monocyte chemotactic protein-1 receptor (CCR2) in human NK cells: characterization of a predominant 3.4-kilobase transcript containing CCR2B and CCR2A sequences. *J Immunol*, **158**, 2689-94.
- Pontén, JaN & Macintyre, EH (1968). Long-term culture of normal and neoplastic glia. *Acta Pathologica Microbiologica Scandinavica*, **74**, 465-486.
- Powis, G, Seewald, MJ, Gratas, C, Melder, D, Riebow, J & Modest, EJ (1992). Selective inhibition of phosphatidylinositol phospholipase C by cytotoxic ether lipid analogues. *Cancer Res*, **52**, 2835-40.
- Praetorius, HA & Leipziger, J (2009). ATP release from non-excitable cells. *Purinergic Signal*, **5**, 433-46.
- Prakriya, M, Feske, S, Gwack, Y, Srikanth, S, Rao, A & Hogan, PG (2006). Orai1 is an essential pore subunit of the CRAC channel. *Nature*, **443**, 230-3.

- Putney, JW, Jr., Broad, LM, Braun, FJ, Lievremont, JP & Bird, GS (2001). Mechanisms of capacitative calcium entry. *J Cell Sci*, **114**, 2223-9.
- Qi, AD, Kennedy, C, Harden, TK & Nicholas, RA (2001). Differential coupling of the human P2Y(11) receptor to phospholipase C and adenylyl cyclase. *Br J Pharmacol*, **132**, 318-26.
- Qin, Z (2012). The use of THP-1 cells as a model for mimicking the function and regulation of monocytes and macrophages in the vasculature. *Atherosclerosis*, **221**, 2-11.
- Raffaello, A, De Stefani, D & Rizzuto, R (2012). The mitochondrial Ca<sup>(2+)</sup> uniporter. *Cell Calcium*, **52**, 16-21.
- Ralevic, V & Burnstock, G (1990). Postjunctional synergism of noradrenaline and adenosine 5'-triphosphate in the mesenteric arterial bed of the rat. *Eur J Pharmacol*, **175**, 291-9.
- Raman, D, Sobolik-Delmaire, T & Richmond, A (2011). Chemokines in health and disease. *Exp Cell Res*, **317**, 575-89.
- Rameh, LE, Rhee, SG, Spokes, K, Kazlauskas, A, Cantley, LC & Cantley, LG (1998). Phosphoinositide 3-kinase regulates phospholipase Cgamma-mediated calcium signaling. *J Biol Chem*, **273**, 23750-7.
- Randolph, GJ, Inaba, K, Robbiani, DF, Steinman, RM & Muller, WA (1999). Differentiation of phagocytic monocytes into lymph node dendritic cells in vivo. *Immunity*, **11**, 753-61.
- Rasmussen, SG, Devree, BT, Zou, Y, Kruse, AC, Chung, KY, Kobilka, TS, Thian, FS, Chae, PS, Pardon, E, Calinski, D, Mathiesen, JM, Shah, ST, Lyons, JA, Caffrey, M, Gellman, SH, Steyaert, J, Skiniotis, G, Weis, WI, Sunahara, RK & Kobilka, BK (2011). Crystal structure of the beta2 adrenergic receptor-Gs protein complex. *Nature*, **477**, 549-55.
- Rassendren, F, Buell, GN, Virginio, C, Collo, G, North, RA & Surprenant, A (1997). The Permeabilizing ATP Receptor, P2X7: CLONING AND EXPRESSION OF A HUMAN cDNA. *Journal of Biological Chemistry*, **272**, 5482-5486.
- Resendiz, JC, Feng, S, Ji, G, Francis, KA, Berndt, MC & Kroll, MH (2003). Purinergic P2Y12 receptor blockade inhibits shear-induced platelet phosphatidylinositol 3-kinase activation. *Mol Pharmacol*, **63**, 639-45.
- Reutershan, J, Vollmer, I, Stark, S, Wagner, R, Ngamsri, KC & Eltzschig, HK (2009). Adenosine and inflammation: CD39 and CD73 are critical mediators in LPS-induced PMN trafficking into the lungs. *FASEB J*, **23**, 473-82.

Riegel, AK, Faigle, M, Zug, S, Rosenberger, P, Robaye, B, Boeynaems, JM, Idzko, M & Eltzschig, HK (2011). Selective induction of endothelial P2Y<sub>6</sub> nucleotide receptor promotes vascular inflammation. *Blood*, **117**, 2548-55.

Roach, TI, Rebres, RA, Fraser, ID, Decamp, DL, Lin, KM, Sternweis, PC, Simon, MI & Seaman, WE (2008). Signaling and cross-talk by C5a and UDP in macrophages selectively use PLCbeta3 to regulate intracellular free calcium. *J Biol Chem*, **283**, 17351-61.

Robaye, B, Boeynaems, JM & Communi, D (1997). Slow desensitization of the human P2Y<sub>6</sub> receptor. *Eur J Pharmacol*, **329**, 231-6.

Robson, SC, Sevigny, J & Zimmermann, H (2006). The E-NTPDase family of ectonucleotidases: Structure function relationships and pathophysiological significance. *Purinergic Signal*, **2**, 409-30.

Rodriguez-Frade, JM, Vila-Coro, AJ, De Ana, AM, Albar, JP, Martinez, AC & Mellado, M (1999). The chemokine monocyte chemoattractant protein-1 induces functional responses through dimerization of its receptor CCR2. *Proc Natl Acad Sci U S A*, **96**, 3628-33.

Rollins, BJ (1997). Chemokines. *Blood*, **90**, 909-28.

Roos, J, Digregorio, PJ, Yeromin, AV, Ohlsen, K, Lioudyno, M, Zhang, S, Safrina, O, Kozak, JA, Wagner, SL, Cahalan, MD, Velicelebi, G & Stauderman, KA (2005). STIM1, an essential and conserved component of store-operated Ca<sup>2+</sup> channel function. *J Cell Biol*, **169**, 435-45.

Ross, EM & Wilkie, TM (2000). GTPase-activating proteins for heterotrimeric G proteins: regulators of G protein signaling (RGS) and RGS-like proteins. *Annu Rev Biochem*, **69**, 795-827.

Sagara, Y & Inesi, G (1991). Inhibition of the sarcoplasmic reticulum Ca<sup>2+</sup> transport ATPase by thapsigargin at subnanomolar concentrations. *J Biol Chem*, **266**, 13503-6.

Sajjadi, FG, Takabayashi, K, Foster, AC, Domingo, RC & Firestein, GS (1996). Inhibition of TNF-alpha expression by adenosine: role of A3 adenosine receptors. *J Immunol*, **156**, 3435-42.

Saleem, H, Tovey, SC, Molinski, TF & Taylor, CW (2014). Interactions of antagonists with subtypes of inositol 1,4,5-trisphosphate (IP<sub>3</sub>) receptor. *Br J Pharmacol*, **171**, 3298-312.

Samson, M, Soularue, P, Vassart, G & Parmentier, M (1996). The genes encoding the human CC-chemokine receptors CC-CKR1 to CC-CKR5 (CMKBR1-CMKBR5) are clustered in the p21.3-p24 region of chromosome 3. *Genomics*, **36**, 522-6.

- Samstein, M, Schreiber, HA, Leiner, IM, Susac, B, Glickman, MS & Pamer, EG (2013). Essential yet limited role for CCR2(+) inflammatory monocytes during Mycobacterium tuberculosis-specific T cell priming. *Elife*, **2**, e01086.
- Sanders, SK, Crean, SM, Boxer, PA, Kellner, D, Larosa, GJ & Hunt, SW, 3rd (2000). Functional differences between monocyte chemotactic protein-1 receptor A and monocyte chemotactic protein-1 receptor B expressed in a Jurkat T cell. *J Immunol*, **165**, 4877-83.
- Savi, P, Labouret, C, Delesque, N, Guette, F, Lupker, J & Herbert, JM (2001). P2y(12), a new platelet ADP receptor, target of clopidogrel. *Biochem Biophys Res Commun*, **283**, 379-83.
- Schachter, JB & Harden, TK (1997). An examination of deoxyadenosine 5'(alpha-thio)triphosphate as a ligand to define P2Y receptors and its selectivity as a low potency partial agonist of the P2Y<sub>1</sub> receptor. *Br J Pharmacol*, **121**, 338-44.
- Schenkel, AR, Mamdouh, Z & Muller, WA (2004). Locomotion of monocytes on endothelium is a critical step during extravasation. *Nat Immunol*, **5**, 393-400.
- Schertler, GF, Villa, C & Henderson, R (1993). Projection structure of rhodopsin. *Nature*, **362**, 770-2.
- Schildberger, A, Rossmanith, E, Eichhorn, T, Strassl, K & Weber, V (2013). Monocytes, peripheral blood mononuclear cells, and THP-1 cells exhibit different cytokine expression patterns following stimulation with lipopolysaccharide. *Mediators Inflamm*, **2013**, 697972.
- Schmutz, C, Cartwright, A, Williams, H, Haworth, O, Williams, JH, Filer, A, Salmon, M, Buckley, CD & Middleton, J (2010). Monocytes/macrophages express chemokine receptor CCR9 in rheumatoid arthritis and CCL25 stimulates their differentiation. *Arthritis Res Ther*, **12**, R161.
- Scott, SA, Xiang, Y, Mathews, TP, Cho, HP, Myers, DS, Armstrong, MD, Tallman, KA, O'reilly, MC, Lindsley, CW & Brown, HA (2013). Regulation of phospholipase D activity and phosphatidic acid production after purinergic (P2Y<sub>6</sub>) receptor stimulation. *J Biol Chem*, **288**, 20477-87.
- Selvaraj, P, Harishankar, M, Singh, B, Banurekha, VV & Jawahar, MS (2012). Effect of vitamin D3 on chemokine expression in pulmonary tuberculosis. *Cytokine*, **60**, 212-9.
- Serbina, NV, Jia, T, Hohl, TM & Pamer, EG (2008). Monocyte-mediated defense against microbial pathogens. *Annu Rev Immunol*, **26**, 421-52.

Serbina, NV, Kuziel, W, Flavell, R, Akira, S, Rollins, B & Pamer, EG (2003a). Sequential MyD88-independent and -dependent activation of innate immune responses to intracellular bacterial infection. *Immunity*, **19**, 891-901.

Serbina, NV, Salazar-Mather, TP, Biron, CA, Kuziel, WA & Pamer, EG (2003b). TNF/iNOS-Producing Dendritic Cells Mediate Innate Immune Defense against Bacterial Infection. *Immunity*, **19**, 59-70.

Serbina, NV & Pamer, EG (2006). Monocyte emigration from bone marrow during bacterial infection requires signals mediated by chemokine receptor CCR2. *Nat Immunol*, **7**, 311-7.

Seye, CI, Yu, N, Jain, R, Kong, Q, Minor, T, Newton, J, Erb, L, Gonzalez, FA & Weisman, GA (2003). The P2Y2 nucleotide receptor mediates UTP-induced vascular cell adhesion molecule-1 expression in coronary artery endothelial cells. *J Biol Chem*, **278**, 24960-5.

Shi, C, Jia, T, Mendez-Ferrer, S, Hohl, TM, Serbina, NV, Lipuma, L, Leiner, I, Li, MO, Frenette, PS & Pamer, EG (2011). Bone marrow mesenchymal stem and progenitor cells induce monocyte emigration in response to circulating toll-like receptor ligands. *Immunity*, **34**, 590-601.

Shi, C, Velazquez, P, Hohl, TM, Leiner, I, Dustin, ML & Pamer, EG (2010). Monocyte trafficking to hepatic sites of bacterial infection is chemokine independent and directed by focal intercellular adhesion molecule-1 expression. *J Immunol*, **184**, 6266-74.

Shieh, CH, Heinrich, A, Serchov, T, Van Calker, D & Biber, K (2014). P2X7-dependent, but differentially regulated release of IL-6, CCL2, and TNF-alpha in cultured mouse microglia. *Glia*, **62**, 592-607.

Showell, HJ, Freer, RJ, Zigmond, SH, Schiffmann, E, Aswanikumar, S, Corcoran, B & Becker, EL (1976). The structure-activity relations of synthetic peptides as chemotactic factors and inducers of lysosomal secretion for neutrophils. *J Exp Med*, **143**, 1154-69.

Shyy, YJ, Wickham, LL, Hagan, JP, Hsieh, HJ, Hu, YL, Telian, SH, Valente, AJ, Sung, KL & Chien, S (1993). Human monocyte colony-stimulating factor stimulates the gene expression of monocyte chemotactic protein-1 and increases the adhesion of monocytes to endothelial monolayers. *J Clin Invest*, **92**, 1745-51.

Singh, A, Hildebrand, ME, Garcia, E & Snutch, TP (2010). The transient receptor potential channel antagonist SKF96365 is a potent blocker of low-voltage-activated T-type calcium channels. *Br J Pharmacol*, **160**, 1464-75.

Sivaramakrishnan, V, Bidula, S, Campwala, H, Katikaneni, D & Fountain, SJ (2012). Constitutive lysosome exocytosis releases ATP and engages P2Y receptors in human monocytes. *J Cell Sci*, **125**, 4567-75.

Skelton, L, Cooper, M, Murphy, M & Platt, A (2003). Human immature monocyte-derived dendritic cells express the G protein-coupled receptor GPR105 (KIAA0001, P2Y14) and increase intracellular calcium in response to its agonist, uridine diphosphoglucose. *J Immunol*, **171**, 1941-9.

Smith, WL, Marnett, LJ & Dewitt, DL (1991). Prostaglandin and thromboxane biosynthesis. *Pharmacol Ther*, **49**, 153-79.

Smrcka, AV (2008). G protein betagamma subunits: central mediators of G protein-coupled receptor signaling. *Cell Mol Life Sci*, **65**, 2191-214.

Smrcka, AV & Sternweis, PC (1993). Regulation of purified subtypes of phosphatidylinositol-specific phospholipase C beta by G protein alpha and beta gamma subunits. *J Biol Chem*, **268**, 9667-74.

Somers, GR, Hammet, F, Woollatt, E, Richards, RI, Southey, MC & Venter, DJ (1997). Chromosomal localization of the human P2y6 purinoceptor gene and phylogenetic analysis of the P2y purinoceptor family. *Genomics*, **44**, 127-30.

Southey, MC, Hammet, F, Hutchins, AM, Paidhungat, M, Somers, GR & Venter, DJ (1996). Molecular cloning and sequencing of a novel human P2 nucleotide receptor. *Biochim Biophys Acta*, **1309**, 77-80.

Sozzani, S, Locati, M, Zhou, D, Rieppi, M, Luini, W, Lamorte, G, Bianchi, G, Polentarutti, N, Allavena, P & Mantovani, A (1995). Receptors, signal transduction, and spectrum of action of monocyte chemotactic protein-1 and related chemokines. *J Leukoc Biol*, **57**, 788-94.

Sozzani, S, Luini, W, Borsatti, A, Polentarutti, N, Zhou, D, Piemonti, L, D'amico, G, Power, CA, Wells, TN, Gobbi, M, Allavena, P & Mantovani, A (1997). Receptor expression and responsiveness of human dendritic cells to a defined set of CC and CXC chemokines. *J Immunol*, **159**, 1993-2000.

Sozzani, S, Molino, M, Locati, M, Luini, W, Cerletti, C, Vecchi, A & Mantovani, A (1993). Receptor-activated calcium influx in human monocytes exposed to monocyte chemotactic protein-1 and related cytokines. *J Immunol*, **150**, 1544-53.

Sozzani, S, Zhou, D, Locati, M, Rieppi, M, Proost, P, Magazin, M, Vita, N, Van Damme, J & Mantovani, A (1994). Receptors and transduction pathways for monocyte chemotactic

- protein-2 and monocyte chemotactic protein-3. Similarities and differences with MCP-1. *J Immunol*, **152**, 3615-22.
- Stachon, P, Peikert, A, Michel, NA, Hergeth, S, Marchini, T, Wolf, D, Dufner, B, Hoppe, N, Ayata, CK, Grimm, M, Cicko, S, Schulte, L, Reinohl, J, Von Zur Muhlen, C, Bode, C, Idzko, M & Zirlik, A (2014). P2Y<sub>6</sub> deficiency limits vascular inflammation and atherosclerosis in mice. *Arterioscler Thromb Vasc Biol*, **34**, 2237-45.
- Stokes, L & Surprenant, A (2007). Purinergic P2Y<sub>2</sub> receptors induce increased MCP-1/CCL2 synthesis and release from rat alveolar and peritoneal macrophages. *J Immunol*, **179**, 6016-23.
- Streb, H, Irvine, RF, Berridge, MJ & Schulz, I (1983). Release of Ca<sup>2+</sup> from a nonmitochondrial intracellular store in pancreatic acinar cells by inositol-1,4,5-trisphosphate. *Nature*, **306**, 67-9.
- Stubbs, VE, Power, C & Patel, KD (2010). Regulation of eotaxin-3/CCL26 expression in human monocytic cells. *Immunology*, **130**, 74-82.
- Suadicani, SO, Brosnan, CF & Scemes, E (2006). P2X7 receptors mediate ATP release and amplification of astrocytic intercellular Ca<sup>2+</sup> signaling. *J Neurosci*, **26**, 1378-85.
- Sumi, Y, Woehrle, T, Chen, Y, Yao, Y, Li, A & Junger, WG (2010). Adrenergic receptor activation involves ATP release and feedback through purinergic receptors. *Am J Physiol Cell Physiol*, 299, C1118-26.
- Sunahara, RK & Taussig, R (2002). Isoforms of mammalian adenylyl cyclase: multiplicities of signaling. *Mol Interv*, **2**, 168-84.
- Sunderkotter, C, Nikolic, T, Dillon, MJ, Van Rooijen, N, Stehling, M, Drevets, DA & Leenen, PJM (2004). Subpopulations of Mouse Blood Monocytes Differ in Maturation Stage and Inflammatory Response. *The Journal of Immunology*, **172**, 4410-4417.
- Surprenant, A, Rassendren, F, Kawashima, E, North, RA & Buell, G (1996). The cytolytic P2Z receptor for extracellular ATP identified as a P2X receptor (P2X7). *Science*, **272**, 735-8.
- Sutherland, CA & Amin, D (1982). Relative activities of rat and dog platelet phospholipase A<sub>2</sub> and diglyceride lipase. Selective inhibition of diglyceride lipase by RHC-80267. *J Biol Chem*, **257**, 14006-10.
- Suzuki, A, Yamanaka, T, Hirose, T, Manabe, N, Mizuno, K, Shimizu, M, Akimoto, K, Izumi, Y, Ohnishi, T & Ohno, S (2001). Atypical protein kinase C is involved in the evolutionarily

conserved par protein complex and plays a critical role in establishing epithelia-specific junctional structures. *J Cell Biol*, **152**, 1183-96.

Suzuki, Y, Inoue, T & Ra, C (2010). L-type  $Ca^{2+}$  channels: a new player in the regulation of  $Ca^{2+}$  signaling, cell activation and cell survival in immune cells. *Mol Immunol*, **47**, 640-8.

Swirski, FK, Nahrendorf, M, Etzrodt, M, Wildgruber, M, Cortez-Retamozo, V, Panizzi, P, Figueiredo, JL, Kohler, RH, Chudnovskiy, A, Waterman, P, Aikawa, E, Mempel, TR, Libby, P, Weissleder, R & Pittet, MJ (2009). Identification of splenic reservoir monocytes and their deployment to inflammatory sites. *Science*, **325**, 612-6.

Szabo, C, Scott, GS, Virag, L, Egnaczyk, G, Salzman, AL, Shanley, TP & Hasko, G (1998). Suppression of macrophage inflammatory protein (MIP)-1alpha production and collagen-induced arthritis by adenosine receptor agonists. *Br J Pharmacol*, **125**, 379-87.

Tacke, F, Alvarez, D, Kaplan, TJ, Jakubzick, C, Spanbroek, R, Llodra, J, Garin, A, Liu, J, Mack, M, Van Rooijen, N, Lira, SA, Habenicht, AJ & Randolph, GJ (2007). Monocyte subsets differentially employ CCR2, CCR5, and CX<sub>3</sub>CR1 to accumulate within atherosclerotic plaques. *J Clin Invest*, **117**, 185-94.

Takahashi, HK, Iwagaki, H, Hamano, R, Wake, H, Kanke, T, Liu, K, Yoshino, T, Tanaka, N & Nishibori, M (2007). Effects of adenosine on adhesion molecule expression and cytokine production in human PBMC depend on the receptor subtype activated. *Br J Pharmacol*, **150**, 816-22.

Terashima, Y, Onai, N, Murai, M, Enomoto, M, Poonpiriya, V, Hamada, T, Motomura, K, Suwa, M, Ezaki, T, Haga, T, Kanegasaki, S & Matsushima, K (2005). Pivotal function for cytoplasmic protein FROUNT in CCR2-mediated monocyte chemotaxis. *Nat Immunol*, **6**, 827-35.

Thastrup, O, Cullen, PJ, Drobak, BK, Hanley, MR & Dawson, AP (1990). Thapsigargin, a tumor promoter, discharges intracellular  $Ca^{2+}$  stores by specific inhibition of the endoplasmic reticulum  $Ca^{2+}$ -ATPase. *Proc Natl Acad Sci U S A*, **87**, 2466-70.

Thiele, A, Kronstein, R, Wetzelsch, A, Gerth, A, Nieber, K & Hauschildt, S (2004). Regulation of Adenosine Receptor Subtypes during Cultivation of Human Monocytes: Role of Receptors in Preventing Lipopolysaccharide-Triggered Respiratory Burst. *Infection and Immunity*, **72**, 1349-1357.

Torres, GE, Egan, TM & Voigt, MM (1999). Hetero-oligomeric Assembly of P2X Receptor Subunits: SPECIFICITIES EXIST WITH REGARD TO POSSIBLE PARTNERS. *Journal of Biological Chemistry*, **274**, 6653-6659.

Torres, GE, Haines, WR, Egan, TM & Voigt, MM (1998). Co-expression of P2X1 and P2X5 receptor subunits reveals a novel ATP-gated ion channel. *Mol Pharmacol*, **54**, 989-93.

Toullec, D, Pianetti, P, Coste, H, Bellevergue, P, Grand-Perret, T, Ajakane, M, Baudet, V, Boissin, P, Boursier, E, Loriolle, F & Et Al. (1991). The bisindolylmaleimide GF-109203X is a potent and selective inhibitor of protein kinase C. *J Biol Chem*, **266**, 15771-81.

Townson, DH & Liptak, AR (2003). Chemokines in the corpus luteum: implications of leukocyte chemotaxis. *Reprod Biol Endocrinol*, **1**, 94.

Toyomitsu, E, Tsuda, M, Yamashita, T, Tozaki-Saitoh, H, Tanaka, Y & Inoue, K (2012). CCL2 promotes P2X4 receptor trafficking to the cell surface of microglia. *Purinergic Signal*, **8**, 301-10.

Treiman, M, Caspersen, C & Christensen, SB (1998). A tool coming of age: thapsigargin as an inhibitor of sarco-endoplasmic reticulum Ca<sup>2+</sup>-ATPases. *Trends Pharmacol Sci*, **19**, 131-5.

Tsai, F-C, Seki, A, Yang, HW, Hayer, A, Carrasco, S, Malmersjö, S & Meyer, T (2014). A polarized Ca<sup>2+</sup>, diacylglycerol and STIM1 signalling system regulates directed cell migration. *Nat Cell Biol*, **16**, 133-144.

Tsien, RY (1980). New calcium indicators and buffers with high selectivity against magnesium and protons: design, synthesis, and properties of prototype structures. *Biochemistry*, **19**, 2396-404.

Tsien, RY (1981). A non-disruptive technique for loading calcium buffers and indicators into cells. *Nature*, **290**, 527-8.

Tsou, CL, Peters, W, Si, Y, Slaymaker, S, Aslanian, AM, Weisberg, SP, Mack, M & Charo, IF (2007). Critical roles for CCR2 and MCP-3 in monocyte mobilization from bone marrow and recruitment to inflammatory sites. *J Clin Invest*, **117**, 902-9.

Tsuchiya, S, Yamabe, M, Yamaguchi, Y, Kobayashi, Y, Konno, T & Tada, K (1980). Establishment and characterization of a human acute monocytic leukemia cell line (THP-1). *Int J Cancer*, **26**, 171-6.

Tsuda, M, Masuda, T, Tozaki-Saitoh, H & Inoue, K (2013). P2X4 receptors and neuropathic pain. *Front Cell Neurosci*, **7**, 191.

Turner, SJ, Domin, J, Waterfield, MD, Ward, SG & Westwick, J (1998). The CC chemokine monocyte chemoattractant peptide-1 activates both the class I p85/p110 phosphatidylinositol 3-kinase and the class II PI3K-C2alpha. *J Biol Chem*, **273**, 25987-95.

- Turner, SJ, Ward, SG, Mckinnon, M & Westwick, J (1996). Stimulation of signal transduction pathways by MCP-1 in human monocytes and THP-1 cells. *Biochem Soc Trans*, **24**, 69S.
- Ulmann, L, Hirbec, H & Rassendren, F (2010). P2X4 receptors mediate PGE2 release by tissue-resident macrophages and initiate inflammatory pain. *EMBO J*, **29**, 2290-300.
- Valera, S, Hussy, N, Evans, RJ, Adami, N, North, RA, Surprenant, A & Buell, G (1994). A new class of ligand-gated ion channel defined by P2x receptor for extracellular ATP. *Nature*, **371**, 516-9.
- Van Coillie, E, Van Damme, J & Opdenakker, G (1999). The MCP/eotaxin subfamily of CC chemokines. *Cytokine Growth Factor Rev*, **10**, 61-86.
- Van Furth, R, Cohn, ZA, Hirsch, JG, Humphrey, JH, Spector, WG & Langevoort, HL (1972). The mononuclear phagocyte system: a new classification of macrophages, monocytes, and their precursor cells. *Bull World Health Organ*, **46**, 845-52.
- Van Furth, R & Sluiter, W (1986). Distribution of blood monocytes between a marginating and a circulating pool. *J Exp Med*, **163**, 474-9.
- Van Petegem, F (2012). Ryanodine receptors: structure and function. *J Biol Chem*, **287**, 31624-32.
- Vanoevelen, J, Raeymaekers, L, Dode, L, Parys, JB, De Smedt, H, Callewaert, G, Wuytack, F & Missiaen, L (2005). Cytosolic Ca<sup>2+</sup> signals depending on the functional state of the Golgi in HeLa cells. *Cell Calcium*, **38**, 489-95.
- Venkatachalam, K, Zheng, F & Gill, DL (2003). Regulation of canonical transient receptor potential (TRPC) channel function by diacylglycerol and protein kinase C. *J Biol Chem*, **278**, 29031-40.
- Vetter, I (2012). Development and optimization of FLIPR high throughput calcium assays for ion channels and GPCRs. *Adv Exp Med Biol*, **740**, 45-82.
- Vieira, RP, Muller, T, Grimm, M, Von Gernler, V, Vetter, B, Durk, T, Cicko, S, Ayata, CK, Sorichter, S, Robaye, B, Zeiser, R, Ferrari, D, Kirschbaum, A, Zissel, G, Virchow, JC, Boeynaems, JM & Idzko, M (2011). Purinergic receptor type 6 contributes to airway inflammation and remodeling in experimental allergic airway inflammation. *Am J Respir Crit Care Med*, **184**, 215-23.
- Vlahos, CJ, Matter, WF, Hui, KY & Brown, RF (1994). A specific inhibitor of phosphatidylinositol 3-kinase, 2-(4-morpholinyl)-8-phenyl-4H-1-benzopyran-4-one (LY-294002). *J Biol Chem*, **269**, 5241-8.

- Volpe, S, Thelen, S, Pertel, T, Lohse, MJ & Thelen, M (2010). Polarization of migrating monocytic cells is independent of PI3-kinase activity. *PLoS One*, **5**, e10159.
- Von Hundelshausen, P, Weber, KS, Huo, Y, Proudfoot, AE, Nelson, PJ, Ley, K & Weber, C (2001). RANTES deposition by platelets triggers monocyte arrest on inflamed and atherosclerotic endothelium. *Circulation*, **103**, 1772-7.
- Von Kugelgen, I (2006). Pharmacological profiles of cloned mammalian P2Y-receptor subtypes. *Pharmacol Ther*, **110**, 415-32.
- Von Kugelgen, I (2008). Pharmacology of mammalian P2X- and P2Y-receptors. . *Biotrend Reviews*, **no.3/9**.
- Waldo, GL, Corbitt, J, Boyer, JL, Ravi, G, Kim, HS, Ji, XD, Lacy, J, Jacobson, KA & Harden, TK (2002). Quantitation of the P2Y(1) receptor with a high affinity radiolabeled antagonist. *Mol Pharmacol*, **62**, 1249-57.
- Waldo, GL & Harden, TK (2004). Agonist binding and Gq-stimulating activities of the purified human P2Y1 receptor. *Mol Pharmacol*, **65**, 426-36.
- Wall, MJ, Wigmore, G, Lopatar, J, Frenguelli, BG & Dale, N (2008). The novel NTPDase inhibitor sodium polyoxotungstate (POM-1) inhibits ATP breakdown but also blocks central synaptic transmission, an action independent of NTPDase inhibition. *Neuropharmacology*, **55**, 1251-8.
- Wang, F, Herzmark, P, Weiner, OD, Srinivasan, S, Servant, G & Bourne, HR (2002). Lipid products of PI(3)Ks maintain persistent cell polarity and directed motility in neutrophils. *Nat Cell Biol*, **4**, 513-8.
- Wang, L, Jacobsen, SE, Bengtsson, A & Erlinge, D (2004). P2 receptor mRNA expression profiles in human lymphocytes, monocytes and CD34<sup>+</sup> stem and progenitor cells. *BMC Immunol*, **5**, 16.
- Wang, T, Pentylala, S, Rebecchi, MJ & Scarlata, S (1999). Differential association of the pleckstrin homology domains of phospholipases C-beta 1, C-beta 2, and C-delta 1 with lipid bilayers and the beta gamma subunits of heterotrimeric G proteins. *Biochemistry*, **38**, 1517-24.
- Wantha, S, Alard, JE, Megens, RT, Van Der Does, AM, Doring, Y, Drechsler, M, Pham, CT, Wang, MW, Wang, JM, Gallo, RL, Von Hundelshausen, P, Lindbom, L, Hackeng, T, Weber, C & Soehnlein, O (2013). Neutrophil-derived cathelicidin promotes adhesion of classical monocytes. *Circ Res*, **112**, 792-801.

- Warny, M, Aboudola, S, Robson, SC, Sevigny, J, Communi, D, Soltoff, SP & Kelly, CP (2001). P2Y(6) nucleotide receptor mediates monocyte interleukin-8 production in response to UDP or lipopolysaccharide. *J Biol Chem*, **276**, 26051-6.
- Weber, C, Belge, KU, Von Hundelshausen, P, Draude, G, Steppich, B, Mack, M, Frankenberger, M, Weber, KS & Ziegler-Heitbrock, HW (2000). Differential chemokine receptor expression and function in human monocyte subpopulations. *J Leukoc Biol*, **67**, 699-704.
- Weber, KSC, Nelson, PJ, Grone, HJ & Weber, C (1999). Expression of CCR2 by Endothelial Cells : Implications for MCP-1 Mediated Wound Injury Repair and In Vivo Inflammatory Activation of Endothelium. *Arterioscler Thromb Vasc Biol*, **19**, 2085-2093.
- Wei, C, Wang, X, Chen, M, Ouyang, K, Song, LS & Cheng, H (2009). Calcium flickers steer cell migration. *Nature*, **457**, 901-5.
- Werry, TD, Wilkinson, GF & Willars, GB (2003). Mechanisms of cross-talk between G-protein-coupled receptors resulting in enhanced release of intracellular  $Ca^{2+}$ . *Biochem J*, **374**, 281-96.
- Wettschureck, N & Offermanns, S (2005). Mammalian G proteins and their cell type specific functions. *Physiol Rev*, **85**, 1159-204.
- White, PJ, Webb, TE & Boarder, MR (2003). Characterization of a  $Ca^{2+}$  response to both UTP and ATP at human P2Y<sub>11</sub> receptors: evidence for agonist-specific signaling. *Mol Pharmacol*, **63**, 1356-63.
- Wiginton, DA, Kaplan, DJ, States, JC, Akeson, AL, Perme, CM, Bilyk, IJ, Vaughn, AJ, Lattier, DL & Hutton, JJ (1986). Complete sequence and structure of the gene for human adenosine deaminase. *Biochemistry*, **25**, 8234-8244.
- Wihlborg, AK, Balogh, J, Wang, L, Borna, C, Dou, Y, Joshi, BV, Lazarowski, E, Jacobson, KA, Arner, A & Erlinge, D (2006). Positive inotropic effects by uridine triphosphate (UTP) and uridine diphosphate (UDP) via P2Y<sub>2</sub> and P2Y<sub>6</sub> receptors on cardiomyocytes and release of UTP in man during myocardial infarction. *Circ Res*, **98**, 970-6.
- Wijeyeratne, YD & Heptinstall, S (2011). Anti-platelet therapy: ADP receptor antagonists. *Br J Clin Pharmacol*, **72**, 647-57.
- Williams, DB (2006). Beyond lectins: the calnexin/calreticulin chaperone system of the endoplasmic reticulum. *J Cell Sci*, **119**, 615-23.

- Williams, M, Francis, J, Ghai, G, Braunwalder, A, Psychoyos, S, Stone, GA & Cash, WD (1987). Biochemical characterization of the triazoloquinazoline, CGS-15943, a novel, non-xanthine adenosine antagonist. *J Pharmacol Exp Ther*, **241**, 415-20.
- Wong, AM, Chow, AW, Au, SC, Wong, CC & Ko, WH (2009). Apical versus basolateral P2Y(6) receptor-mediated Cl(-) secretion in immortalized bronchial epithelia. *Am J Respir Cell Mol Biol*, **40**, 733-45.
- Wong, LM, Myers, SJ, Tsou, CL, Gosling, J, Arai, H & Charo, IF (1997). Organization and differential expression of the human monocyte chemoattractant protein 1 receptor gene. Evidence for the role of the carboxyl-terminal tail in receptor trafficking. *J Biol Chem*, **272**, 1038-45.
- Woollard, KJ & Geissmann, F (2010). Monocytes in atherosclerosis: subsets and functions. *Nat Rev Cardiol*, **7**, 77-86.
- Woszczek, G, Chen, LY, Alsaaty, S, Nagineni, S & Shelhamer, JH (2010). Concentration-dependent noncysteinyl leukotriene type 1 receptor-mediated inhibitory activity of leukotriene receptor antagonists. *J Immunol*, **184**, 2219-25.
- Wuytack, F, Raeymaekers, L & Missiaen, L (2002). Molecular physiology of the SERCA and SPCA pumps. *Cell Calcium*, **32**, 279-305.
- Yamada, K, Sakane, F, Imai, S-I, Tsushima, S, Murakami, T & Kanoh, H (2003). Regulatory role of diacylglycerol kinase  $\gamma$  in macrophage differentiation of leukemia cells. *Biochem Biophys Res Commun*, **305**, 101-107.
- Yamagami, S, Tokuda, Y, Ishii, K, Tanaka, H & Endo, N (1994). cDNA cloning and functional expression of a human monocyte chemoattractant protein 1 receptor. *Biochem Biophys Res Commun*, **202**, 1156-62.
- Yanez, M, Gil-Longo, J & Campos-Toimil, M (2012). Calcium binding proteins. *Adv Exp Med Biol*, **740**, 461-82.
- Yang, C & Kazanietz, MG (2003). Divergence and complexities in DAG signaling: looking beyond PKC. *Trends Pharmacol Sci*, **24**, 602-8.
- Yang, YR, Follo, MY, Cocco, L & Suh, PG (2013). The physiological roles of primary phospholipase C. *Adv Biol Regul*, **53**, 232-41.
- Yang, J, Zhang, L, Yu, C, Yang, XF & Wang, H (2014). Monocyte and macrophage differentiation: circulation inflammatory monocyte as biomarker for inflammatory diseases. *Biomark Res*, **2**, 1.

- Yasaka, T, Boxer, LA & Baehner, RL (1982). Monocyte aggregation and superoxide anion release in response to formyl-methionyl-leucyl-phenylalanine (FMLP) and platelet-activating factor (PAF). *J Immunol*, **128**, 1939-44.
- Ye, RD, Boulay, F, Wang, JM, Dahlgren, C, Gerard, C, Parmentier, M, Serhan, CN & Murphy, PM (2009). International Union of Basic and Clinical Pharmacology. LXXIII. Nomenclature for the formyl peptide receptor (FPR) family. *Pharmacol Rev*, **61**, 119-61.
- Yegutkin, GG (2008). Nucleotide- and nucleoside-converting ectoenzymes: Important modulators of purinergic signalling cascade. *Biochim Biophys Acta*, **1783**, 673-94.
- Yona, S & Jung, S (2010). Monocytes: subsets, origins, fates and functions. *Curr Opin Hematol*, **17**, 53-9.
- Yona, S, Kim, KW, Wolf, Y, Mildner, A, Varol, D, Breker, M, Strauss-Ayali, D, Viukov, S, Guillemins, M, Misharin, A, Hume, DA, Perlman, H, Malissen, B, Zelzer, E & Jung, S (2013). Fate mapping reveals origins and dynamics of monocytes and tissue macrophages under homeostasis. *Immunity*, **38**, 79-91.
- Yoshimura, T, Yuhki, N, Moore, SK, Appella, E, Lerman, MI & Leonard, EJ (1989). Human monocyte chemoattractant protein-1 (MCP-1). Full-length cDNA cloning, expression in mitogen-stimulated blood mononuclear leukocytes, and sequence similarity to mouse competence gene JE. *FEBS Lett*, **244**, 487-93.
- Yu, Y, Sweeney, MD, Saad, OM & Leary, JA (2006). Potential inhibitors of chemokine function: analysis of noncovalent complexes of CC chemokine and small polyanionic molecules by ESI FT-ICR mass spectrometry. *J Am Soc Mass Spectrom*, **17**, 524-35.
- Zavialov, AV & Engstrom, A (2005). Human ADA2 belongs to a new family of growth factors with adenosine deaminase activity. *Biochem J*, **391**, 51-7.
- Zeng, J, Wang, G, Liu, X, Wang, C, Tian, H, Liu, A, Jin, H, Luo, X & Chen, Y (2014). P2Y<sub>13</sub> receptor-mediated rapid increase in intracellular calcium induced by ADP in cultured dorsal spinal cord microglia. *Neurochem Res*, **39**, 2240-50.
- Zhang, F, Jin, S, Yi, F & Li, PL (2009). TRP-ML1 functions as a lysosomal NAADP-sensitive Ca<sup>2+</sup> release channel in coronary arterial myocytes. *J Cell Mol Med*, **13**, 3174-85.
- Zhang, FL, Luo, L, Gustafson, E, Lachowicz, J, Smith, M, Qiao, X, Liu, YH, Chen, G, Pramanik, B, Laz, TM, Palmer, K, Bayne, M & Monsma, FJ, Jr. (2001). ADP is the cognate ligand for the orphan G protein-coupled receptor SP1999. *J Biol Chem*, **276**, 8608-15.

Zhang, FL, Luo, L, Gustafson, E, Palmer, K, Qiao, X, Fan, X, Yang, S, Laz, TM, Bayne, M & Monsma, F, Jr. (2002). P2Y(13): identification and characterization of a novel Galphai-coupled ADP receptor from human and mouse. *J Pharmacol Exp Ther*, **301**, 705-13.

Zhang, N, Yang, D, Dong, H, Chen, Q, Dimitrova, DI, Rogers, TJ, Sitkovsky, M & Oppenheim, JJ (2006). Adenosine A2a receptors induce heterologous desensitization of chemokine receptors. *Blood*, **108**, 38-44.

Zhang, Z, Chen, G, Zhou, W, Song, A, Xu, T, Luo, Q, Wang, W, Gu, XS & Duan, S (2007). Regulated ATP release from astrocytes through lysosome exocytosis. *Nat Cell Biol*, **9**, 945-53.

Zhang, Z, Wang, Z, Ren, H, Yue, M, Huang, K, Gu, H, Liu, M, Du, B & Qian, M (2011). P2Y(6) agonist uridine 5'-diphosphate promotes host defense against bacterial infection via monocyte chemoattractant protein-1-mediated monocytes/macrophages recruitment. *J Immunol*, **186**, 5376-87.

Zhang, K, Zhang, J, Gao, ZG, Zhang, D, Zhu, L, Han, GW, Moss, SM, Paoletta, S, Kiselev, E, Lu, W, Fenalti, G, Zhang, W, Muller, CE, Yang, H, Jiang, H, Cherezov, V, Katritch, V, Jacobson, KA, Stevens, RC, Wu, B & Zhao, Q (2014). Structure of the human P2Y12 receptor in complex with an antithrombotic drug. *Nature*, **509**, 115-8.

Zhang, D, Gao, Z-G, Zhang, K, Kiselev, E, Crane, S, Wang, J, Paoletta, S, Yi, C, Ma, L, Zhang, W, Han, GW, Liu, H, Cherezov, V, Katritch, V, Jiang, H, Stevens, RC, Jacobson, KA, Zhao, Q & Wu, B (2015). Two disparate ligand-binding sites in the human P2Y1 receptor. *Nature*, **520**, 317-321.

Zhao, F, Li, P, Chen, SR, Louis, CF & Fruen, BR (2001). Dantrolene inhibition of ryanodine receptor Ca<sup>2+</sup> release channels. Molecular mechanism and isoform selectivity. *J Biol Chem*, **276**, 13810-6.

Zhou, D, Luini, W, Bernasconi, S, Diomedea, L, Salmona, M, Mantovani, A & Sozzani, S (1995). Phosphatidic Acid and Lysophosphatidic Acid Induce Haptotactic Migration of Human Monocytes. *Journal of Biological Chemistry*, **270**, 25549-25556.

Ziegler-Heitbrock, L (2007). The CD14<sup>+</sup> CD16<sup>+</sup> blood monocytes: their role in infection and inflammation. *J Leukoc Biol*, **81**, 584-92.

Ziegler-Heitbrock, L, Ancuta, P, Crowe, S, Dalod, M, Grau, V, Hart, DN, Leenen, PJ, Liu, YJ, Macpherson, G, Randolph, GJ, Scherberich, J, Schmitz, J, Shortman, K, Sozzani, S, Strobl, H, Zembala, M, Austyn, JM & Lutz, MB (2010). Nomenclature of monocytes and dendritic cells in blood. *Blood*, **116**, e74-80.

Zimmermann, H, Zebisch, M & Strater, N (2012). Cellular function and molecular structure of ecto-nucleotidases. *Purinergic Signal*, **8**, 437-502.

Zlotnik, A & Yoshie, O (2000). Chemokines: a new classification system and their role in immunity. *Immunity*, **12**, 121-7.

Zufferey, R, Nagy, D, Mandel, RJ, Naldini, L & Trono, D (1997). Multiply attenuated lentiviral vector achieves efficient gene delivery in vivo. *Nat Biotech*, **15**, 871-875.

Zweemer, AJ, Toraskar, J, Heitman, LH & Ap, IJ (2014). Bias in chemokine receptor signalling. *Trends Immunol*, **35**, 243-52.